EXTENDED ABSTRACTS
The 19th Himalaya-Karakoram-Tibet Workshop

10-12 July, 2004
Niseko Higashiyama Prince Hotel
Niseko, Hokkaido, Japan

Guest Editors

Kazunori ARITA

Pitambar GAUTAM

Lalu Prasad PAUDEL

Youichiro TAKADA

Teiji WATANABE

The 19th Himalaya-Karakoram-Tibet Workshop

including a special session on

Uplift of Himalaya-Tibet Region and Asian Monsoon:
Interactions among Tectonic Events, Climatic Changes and Biotic Responses during Late Tertiary to Recent Times

Co-hosted by

The Organizing Committee of
The 19th HIMALAYA-KARAKORAM-TIBET WORKSHOP

The 21st Century Center of Excellence (COE) Program on
"Neo-Science of Natural History – Origin and Evolution of Natural Diversity"
Hokkaido University

The 21st Century Center of Excellence (COE) Program on
"Dynamics of the Sun-Earth-Life Interactive System"
Nagoya University

Division of Earth and Planetary Sciences,
Graduate School of Science, Hokkaido University

Sponsored by

International Lithosphere Program (ILP)
Hokkaido Prefecture, Japan
Niseko Town, Japan
Tokyo Geographical Society
Geological Society of Japan
Japan Association for Quaternary Research
Tectonic Research Group of Japan
Kajima Foundation, Tokyo
Hokkaido Geotechnical Consultants Association, Sapporo
Hakusan Corporation, Fuchu, Tokyo
Kao Foundation for Arts and Sciences, Tokyo
Tethys Society, Sapporo
Confectionary *Kinotoya,* Sapporo
Shugakuso Outdoor Equipment, Sapporo
JEOL Ltd, Akishima, Tokyo

Preface

The Himalaya-Karakoram-Tibet (HKT) region, well known as "the roof of the world," embraces the highest elevations and the greatest relief on earth. The formation and uplift of the HKT region during the Cenozoic was a crucial event in the geological evolution of our planet and its major rivers support more than two-thirds of the world's human population.

In geoscientific terms, the HKT region is important in two ways. First, it serves as a natural laboratory for study of the composition, structure and formational process of the continental crust. The area today occupied by the Tibetan Plateau was the focus of subduction-related magmatism before the collision of India with Eurasia. After the collision, continental deformation led to the formation of the earth's thickest crust beneath Tibet. Early in this process the Karakoram-Kohistan area was at the island-arc stage of formation and now is the site of ultra-high-pressure rocks. The Himalaya, a foreland fold-thrust belt with metamorphic core, formed along the northern margin of the Indian continent after the collision. It exhibits the effects of thrust tectonics resulting in rapid uplift – most dramatically, an unrivalled array of the eight-thousand-meter giants. The highest section extends more than halfway into the troposphere and exerts a major influence on the global atmospheric circulation. In order to develop future global climatic scenarios it is necessary to understand: (i) the timing, underlying causes, and mechanism of the uplift; (ii) the monsoon climate, its time of initiation and manner of evolution; and (iii) the relationship between the two.

The HKT region is a natural laboratory where one can observe the diversity of both geological and biological phenomena, a thorough understanding of which is vital for the development of rational resource-use policies.

The HKT Workshops, since their inception in 1985, have become an important forum for sharing scientific knowledge and experience. The present workshop, held in Japan, will include a special session on "Uplift of the Himalaya-Tibet region and the Asian Monsoon: Interactions among Tectonic Events, Climatic Change and Biotic Responses during Late Tertiary to Recent Times".

Despite its distance from the HKT region, Japan is an appropriate venue for the workshops. The northern side of Japan, facing the Japan Sea, experiences some of the world's highest annual snowfall. The Japanese monsoon (*tsuyu*) occurs in June. Thanks to the water derived from snowmelt, together with the accompanying rainfall during the *tsuyu*, Japan has evolved a remarkable form of rice cultivation. It was the uplift of the HKT region that was essential to this development, which in the old days was called a *toyo-ashihara-no-mizuho-no-kuni* (literally, "beautiful country of rice"). If the HKT region in its present form did not exist, Japan probably would have no monsoon and conditions would be very different from those of today.

This special issue of the *Himalayan Journal of Sciences* contains one hundred and thirty-six abstracts. One hundred and fifty scholars from fourteen countries have pre-registered for the Workshop. It is our hope that all the participants will take advantage of this meeting to express their views, listen to the opinions of others, and exchange scientific knowledge.

The Organizing Committee would like to express its sincere thanks to the many organizations and enterprises that provided financial support and facilitated the participation of many scholars from the HKT region (China, India, Nepal, Pakistan) and Japan (especially graduate students from abroad). Twenty-one participants received registration grants and sixteen received grants covering registration and full or partial travel expenses. Furthermore, special gratitude is expressed to Prof. Arvind K. Jain for his assistance in evaluating the abstracts, to Prof. Mitsuhiro Nakagawa for his generous offer to lead an excursion to the active volcanic area of Mt. Usu, and to Mr. Takahiro Tajima for managing the HKT19 homepage.

Members of the Organizing Committee
of the 19th Himalaya-Karakoram-Tibet Workshop:

Kazunori ARITA (Hokkaido University)
Kazuhisa CHIKITA (Hokkaido University)
Pitambar GAUTAM (Hokkaido University)
Shuji IIWATA (Tokyo Metropolitan University)
Takashi NAKATA (Hiroshima University)
Hiroshi NISHI (Hokkaido University)
Harutaka SAKAI (Kyushu University)
Tetsuya SAKAI (Shimane University)
Teiji WATANABE (Hokkaido University)

Editorial Policy

Himalayan Journal of Sciences (ISSN 1727 5210) is a peer-reviewed multi-disciplinary journal published twice yearly. HJS focuses on biodiversity, natural resource management, ecology and environment, and other fields related to Himalayan conservation, and development. HJS invites authors to communicate their knowledge and uncertainties from all the sciences.

HJS publishes works in the following genres:
i)   **Research papers**: report on original research
ii)   **Review papers:** thorough account of current developments and trajectories in any field covered in the journal
iii) **Articles**: narrowly-focused account of a current development in any field covered in the journal
iv)   **Editorial**: opinionated essay on an issue of public interest
v)   **Essay**: similar to editorial but longer and more comprehensive; may include tables and figures
vi)   **Commentary and Correspondence**: persuasive and informed commentary on any topical issues or on articles published in prior issues of the journal
vii) **Policy**: critical review of some topic of high public interest, hybrid of essay and review article, with the basis of highly valid facts and figures
viii) **Resource review**: evaluation of books, websites, CDs, etc. pertinent to the scope of HJS
ix)   **Publication preview**: description/epitome of the forthcoming important books
x)   **Calender**: notice of forthcoming conferences, seminars, workshops, and other events related to science and the Himalayas.

Permission

Acknowledgments

Special Acknowledgments

Notice

This is a special issue of the Himalayan Journal of Sciences, containing extended abstracts of papers to be presented at the 19th Himalaya-Karakoram-Tibet Workshop to be held in Niseko, Japan, July 10-12, 2004. The issue was produced by guest editors and its contents have not been subjected to peer review.

extended abstracts

➤

extended abstracts (continued)

miscellaneous

Climate change in East and Central Asia associated with the uplift of the Tibetan Plateau–A simulation with the MRI coupled atmosphere-ocean GCM

Manabu Abe†*, Tetsuzo Yasunari‡ and Akio Kitoh§

† Graduate School of Environmental Studies, Nagoya University, Nagoya, 464-8601, JAPAN
‡ Hydrospheric Atmospheric Research Center, Nagoya University, Nagoya, 464-8601, JAPAN
§ Meteorological Research Institute, Tsukuba, 305-0052, JAPAN

* To whom correspondence should be addressed. E-mail: mabe@hyarc.nagoya-u.ac.jp

The Tibetan plateau has significant roles in the formation of the Asian monsoon circulation. The effect of the Tibetan plateau on the Asian monsoon circulation has been investigated using the atmospheric general circulation model (AGCM) (e.g., Hahn and Manabe 1975, An et al. 2001). Also, Broccoli and Manabe (1992) investigated the role of the Tibetan plateau on the formation of the mid-latitude dry climate in Central Asia, using AGCM. In their study, while the moist climate is formed in South and East Asia, the dry climate appears in the northwest of the Tibetan plateau due to its existence. Thus, their result makes us recognize that the Tibetan plateau does not affect the climate only in moist climate, such as South and East Asia, but also in dry climate, such as Central Asia. Further, because the oceanic changes associated with the uplift of the large-scale orography, which is shown in Abe et al. (2003, 2004), affects the climate in Asia, changes in the oceanic circulation should be considered in the experiments to study the effect of the orography on formation of the climate. In order to investigate the climate change due to the progressive uplift of the large-scale orography, an experiment considering changes in the oceanic circulation was conducted using the Meteorological Research Institute (MRI) coupled atmosphere–ocean general circulation model I (CGCM-I). In this presentation, the climate change in East and Central Asia is focused on.

Our experiment has six runs, and in the runs which, individually, were called M0, M2, M4, M6, M8, and M, six different elevations of the global mountain, which are 0, 20, 40, 60, 80, and 100% of the present standard mountain height, were used, respectively. Land-sea distribution is the same in all runs. All the runs were integrated for 50 years, separately, and the data for the last 30 years (21-50) were used in our analyses. The MRI CGCM-I is the global grid model. Horizontal resolution of atmospheric part of the CGCM is 5° in longitude and 4° in latitude, and the vertical is 15 layers. The oceanic part has nonuniform meridional resolution ranging from 0.5 to 2.0°, with a finer grid in the tropics, fixed zonal resolution of 2.5°, and 21 layers vertically. The original model predicts sea ice concentration and thickness, but for our experiments fixed monthly sea ice conditions based on observations, were prescribed for all the runs.

In summer (June, July and August), the southwesterlies at low-level from South through East Asia are enhanced with the uplift of the Tibetan Plateau, and the region of the great precipitation in moist Asia also migrates into the interior of the land. At the upper level in the troposphere, the anticyclonic circulation appears over the Tibetan Plateau and become stronger, as the Tibetan plateau becomes higher. The summer precipitation in East Asia increases gradually from M0 to M8, because the moisture transported by the southwesterlies increases, but the increase from M8 to M is not found. These increased rates are larger in the lower stages from M0 to M6 than the higher stages from M6 to M (Abe et al. 2003). These changes are also related to the enhancement of the subtropical high over the North Pacific with the uplift of the global orography, and the region of great precipitation in East Asia moves into the interior as the subtropical high expands into the East Asia. Further, because the moisture transported from the western Pacific is also increases due to the enhancement of the trade wind and the warm pool in the western Pacific appears with the uplift of the Tibetan plateau (Abe et al. 2004), these influences should be connected with the summer monsoon climate in Southeast and East Asia. Kitoh (2004) conducted the same experiment using the new MRI coupled GCM (MRI CGCM-II). His study shows the appearance of the Baiu-front over around Japan associated with the uplift of the Tibetan plateau, which is related to the appearance of the warm pool in the western Pacific and the increase in moisture transported from western Pacific. In winter (December, January, and February), the westerlies in M0 in East Asia change to the northwesterlies in M due to the uplift of the Tibetan plateau, although the wind velocity shows small change.
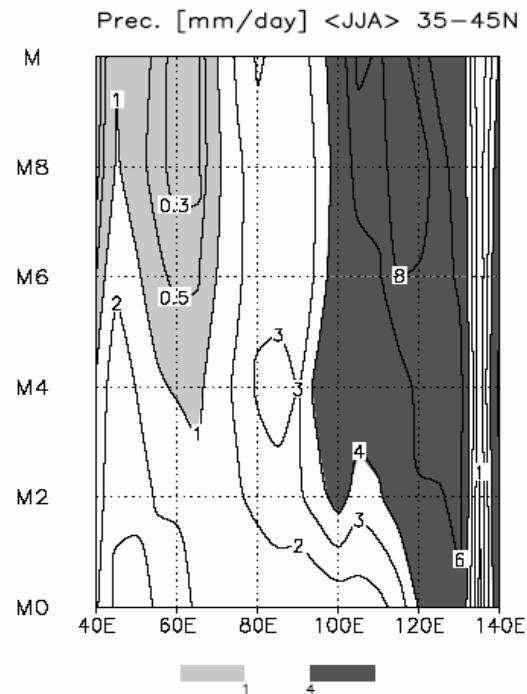
FIGURE 1. The changes in summer precipitation, averaged 35˚-45˚N, with the uplift of the Tibetan plateau. Unit is mm per day.

Dry climate region is found the west of the Tibetan plateau in the lower stages (M2 and M4). In the higher stages, the dry climate expanded clearly to the northwest of the Tibetan plateau and Central Asia. In Central Asia, summer precipitation in Central Asia decreases gradually with the uplift of the Tibetan plateau and that below 1 mm day^{-1} appears in M4 (**Figure 1**). The region of great precipitation in East Asia expands significantly to the interior of the land in the lower stages from M0 to M4. From M4 to M6, however, retreat of the expansion of the greater precipitation region is found, as shown in **Figure 1**. In the higher stages from M6 to M, the precipitation decreases gradually. Further, no expansion of the greater precipitation region to Central Asia is found as if the appearance of the dry climate region begins to prevent the greater precipitation region in East Asia from expanding west, although precipitation in East Asia increases.

References

Abe M, A Kitoh and T Yasunari. 2003. An evolution of the Asian summer monsoon associated with mountain uplift –simulation with the MRI atmosphere-ocean coupled GCM-. *J Meteor Soc Japan* **81**: 909-33

Abe M, T Yasunari and A Kitoh. 2004. Effects of large-scale orography on the coupled atmosphere-ocean system in the tropical Indian and Pacific oceans in boreal summer. *J Meteor Soc Japan* **82**: 745-59

An Z–S, JE Kutzbach, WL Prell and SC Porter. 2001. Evolution of Asian monsoon and phased uplift on the Himalayan-Tibetan plateau since late Miocene times. *Nature* **41:** 62-6

Broccoli AJ and S Manabe. 1992. The effects of orography on middle latitude northern hemisphere dry climate. *J Climate* **5**: 1181-201

Hahn DG and S Manabe. 1975. The role of mountains in the south Asian monsoon circulation. *J Atmos Sci* **77**: 1515-41

Kitoh A. 2004. Effects of mountain uplift on East Asian summer climate investigated by a coupled atmosphere-ocean GCM. *J Climate* **17**: 783-802

Collisional emplacement history of the Naga-Andaman ophiolites and the position of the eastern Indian suture

Subhrangsu K Acharyya

Department of Geological Sciences, Jadavpur University, Kolkata 700032, INDIA

For correspondence, E-mail: skacharyya@yahoo.com

Late Mesozoic to early Eocene ophiolites and associated rocks occur in two parallel north-south trending belts along the eastern margin of the Indian plate (Anon 1977, 1986). The presence of glaucophane and jadeite bearing schists in the ophiolite mélange indicate involvement of subduction process. The eastern belt passes through central Myanmar, Sumatra and Java, and broadly coincides with a zone of gravity high resulting from steeply dipping mafic-ultramafic rocks. The ophiolitic rocks in the eastern belt are often intruded by the Mid Cretaceous and younger plutons of the Central-Burmese magmatic arc and are also covered by younger rocks to the south. Geological details are less known from this belt. It possibly denotes the loci of the collision zone developed along the eastern and western margins of a Central Burmese micro-continent during its respective sutering with the Sino-Burman and the Indian blocks (**Figure 1**). In contrast, the western belt, which passes through the Indo-Burmese Range (Nagaland and Manipur states, India, Chin Hills and Arakan Yoma in Myanmar) and Andaman Island Arc (India), similar assemblage of ophiolites and associated rocks occur as rootless, subhorizontal bodies tectonically overriding the Eocene-Oligocene flyschoid sequence. This belt is flanked to the east by a negative gravity anomaly zone. These ophiolitic rocks are inferred to represent a westward propagated nappe from the eastern belt, which represents the suture during the late Oligocene terminal collision of the Indian and the Burmese continents (Sengupta et al. 1990).

In the northern parts of Central Burmese magmatic arc, adjacent jade mine belt and upper defiles of the Irrawadi river, narrow belts of mafic-ultramafic rocks and cherts, and metamorphic rocks like mica schist, graphitic schist, kyanite schist and Triassic turbidites occur in complex structural association. These rocks are intruded by mid Cretaceous granodiorite-tonalite plutons and unconformably overlain by shallow marine Albian limestone (Anon 1986, Mitchell 1993). Early Eocene debris flow is also recorded with serpentinite and other clasts. These ophiolites and Triassic turbidites were possibly accreted at a west dipping subduction zone due to closure of a small ocean basin separating a Central Burma micro-continent and the Sino-Burmese continent (**Figure 1a-b**). The plutons intruding the accretionary prism were possibly generated by an east dipping subduction beneath the collided Burmese continents (**Figure 1b**).

Similar assemblage of ophiolitic rocks, and clastics with ophiolitic and metamorphic rocks are recorded from the Naga Hills and Andaman Islands of the western belt (Acharyya et al. 1990, Acharyya 1997). Continent derived Triassic turbidites override Mt. Victoria basement dome and in turn are overridden by the ophiolites in the eastern parts of the Chin Hills (Mitchell 1993), whereas Triassic elements occur within the Eocene olistostromes in Andaman (Acharyya 1997). Eocene conglomerate beds with granodiorite and dacite clasts overlie the ophiolites and Albian limestone along the eastern margin of the Chin Hills (Mitchell 1993). In Naga Hills, the accreted ophiolites and their cover are overthrust by metamorphic rocks comprising micaschists, garnet-micaschists, gneisses, which at places are unconformably overlain by mid Cretaceous continental arkosic quartzite and limestone. Smaller bodies of metamorphic rocks occur in the ophiolites from Andaman (Acharyya et al. 1990).

The mid Eocene age of ophiolite-derived and plagioclase bearing clastic rocks occurring in places as unconformable cover on the western belt ophiolite slices, especially from Naga Hills and at places in Andaman Islands, marks the minimum accretion age of these ophiolites (**Figure 1d-e**). The olistostromal units juxtaposed to and tectonically underlying the ophiolites is a trench deposit containing olistoliths of various sizes and ages. The youngest olistoliths of mid Eocene age represent the age of trench sediments. The age of these two contrasting sedimentary facies marks the beginning of a second phase of subduction-related ophiolite accretion just prior to mid Eocene (Acharyya et al. 1990). Several Eocene dioritic intrusives and related volcanic rocks from the Sino-Burmese range east of inferred suture confirm location of this subduction zone. The chemistry of basalts, associated shallow marine limestone, and the fauna indicate that Maastrichtian and Palaeocene seamounts were important constituents of the subducting ocean crust (Sengupta et al. 1990). Clipped off parts of seamounts together with slices from ocean floor were accreted at the leading margin of the overriding Sino-Burmese continent to the east (**Figure 1d-e**). Continued subduction brought the Indian and the Sino-Burmese blocks closer to each other. During this period, which spanned parts of the Eocene and the Oligocene, uninterrupted flysch sediments were deposited on the margin of the Indian continental block towards the west. With closure of the ocean, the Indian and Sino-Burmese continental blocks collided along a suture, which was located along the eastern belt ophiolites; the late Oligocene pronounced unconformity marks the time of terminal collision (Acharyya et al. 1990). Gently dipping ophiolitic slices, their cover, together with the metamorphic basement of the overriding continent and olistostromal trench rocks, were thrust westward from the suture as nappes (**Figure 1f-g**). Although the components of both ophiolite belts are similar, the presence of late Cretaceous – early Eocene ophiolites has not yet been established from the eastern belt. These rocks may be tectonically concealed or truncated. The floor sediments, the nappe rocks as well as the younger Neogene sediments in the western belt were subsequently co-folded. Mitchell (1993), on the other hand, postulated that the eastern belt ophiolites were overthrust from the Indo-Burmese Range eastward, which lacks factual support.

Ophiolite occurrences in the Andaman Islands, belonging to the western belt, are generally linked with active subduction west of the island arc. The accreted ophiolites from this belt, however, already existed as tectonised on-land features during mid Eocene and thus much before the initiation of late Miocene subduction and opening of the Andaman Sea (cf. Curray et al. 1982). It is inferred that in the north, the collision occurred between the Sino-Burmese and the main Indian continent

(**Figure 1d-f**), whereas, in the south, it occurred between the Sino-Burmese and a small continental fragment that was separated from the main Indian continent by parts of the Indian Ocean (**Figure 1e-g**). As a result, a new subduction regime and active Andaman-Java trench developed along the western margin of continental fragment in the southern sector after the Late Oligocene terminal collision (**Figure 1i**).

References

Acharyya SK. 1997. Stratigraphy and tectonic history reconstruction of the Indo-Burma-Andaman mobile belt. *Ind J Geol* **69**: 211-234

Acharyya SK, KK Ray and S Sengupta. 1990. Tectonics of the ophiolite belt from Naga Hills and Andaman Islands, India. *Proc Ind Acad Sci (Earth Planet Sci)* **99**: 187-199

Anon. 1977. *Geological map of the Socialistic Republic of the Union of Burma,* 1:1M. Burma: Earth Sciences Research Division, Govt. of Burma.

Anon. 1986. Geology of Nagaland ophiolite. *Geol Surv Ind Mem* **119**: 113 p

Curray JR, FJ Emmel, DG Moore and RW Raitt. 1982. Structure, tectonics and geological history of the northeast Indian Ocean. In: Nairn AEM and FG Stehli (eds), The Ocean Basins and Margins, Vol 6: *The Indian Ocean.* New York: Plenum Press. p 399-450

Mitchell AHG. 1993. Cretaceous-Cenozoic tectonic events in the western Myanmar (Burma) - Assam region. *J Geol Soc Lond* **150**: 1089-102

Sengupta S, KK Ray, SK Acharyya and JB deSmeth. 1990. Nature of ophiolite occurrences along the eastern margin of the Indian plate and their tectonic significance. *Geology* **18**: 439-442
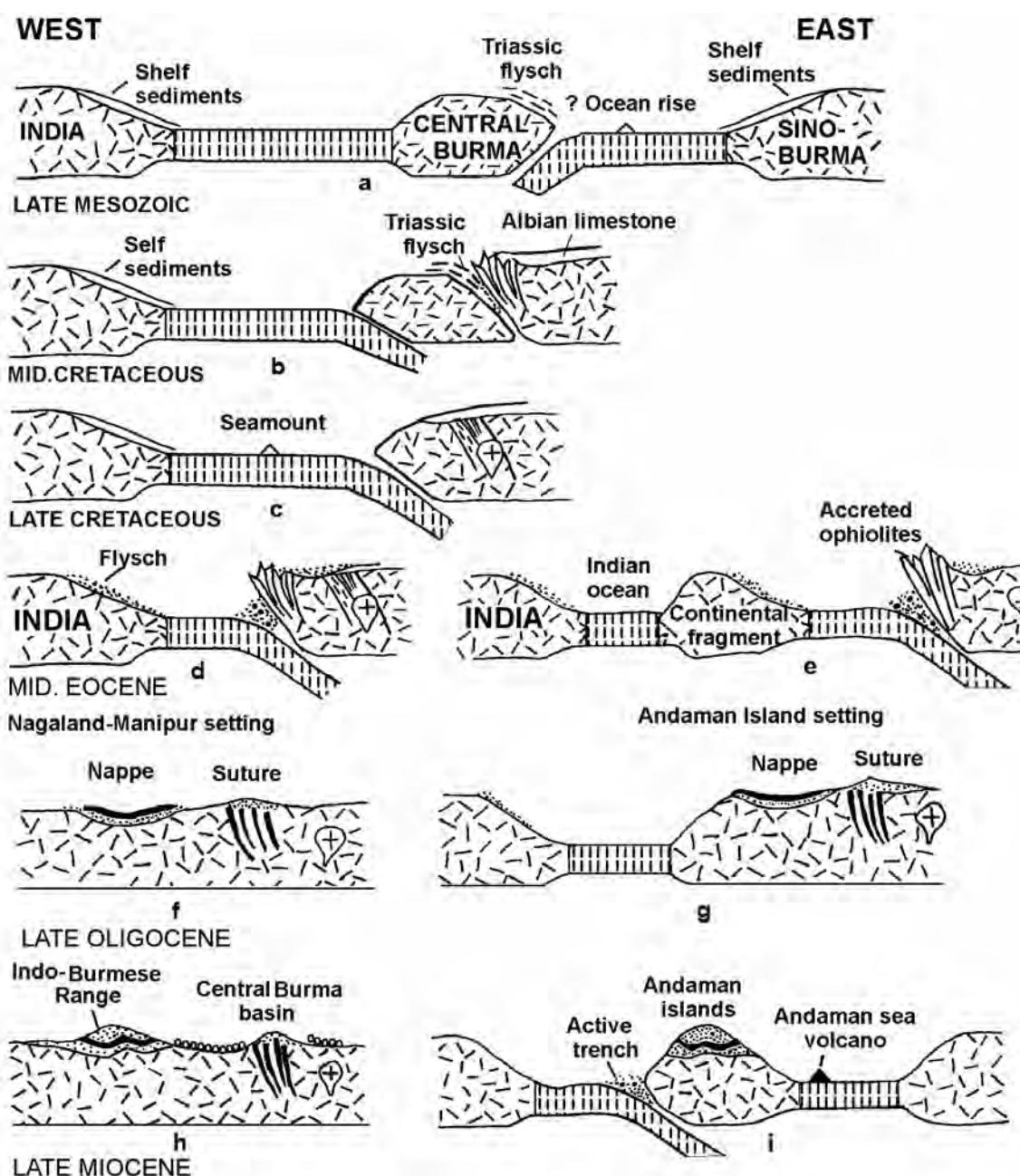
FIGURE 1. Schematic diagram showing successively closed oceanic basins relative to Indian and Sino-Burmese continents

Debris flow disaster in Larcha, upper Bhotekoshi Valley, central Nepal

Danda P Adhikari†* and Satoshi Koshimizu‡

† JSPS Research fellow, Earth Science Division, Yamanashi Institute of Environmental Sciences, 5597-1, Kenmarubi, Kamiyoshida,
  Fujiyoshida, Yamanashi 403-0005, JAPAN
  Permanent Address: Department of Geology, Tri-Chandra Multiple Campus, Tribhuvan University, PO Box 13644, Kathmandu,
  NEPAL
‡ Earth Science Division, Yamanashi Institute of Environmental Sciences, 5597-1, Kenmarubi, Kamiyoshida, Fujiyoshida,
  Yamanashi 403-0005, JAPAN

* To whom correspondence should be addressed. E-mail: adhikaridp@hotmail.com

In the Himalayas, damage, destruction, and casualties related to landslide and debris flow are common phenomena, especially during the monsoon period. This fact was tragically illustrated at 11:30 pm on 22 July 1996 when Larcha, situated at km-109 milestone of the Arniko Highway, upper Bhotekoshi Valley experienced an unprecedented debris flow down poured by the Bhairabkunda Stream (BKS). Geologically, Larcha is almost at the northern edge of the Lesser Himalaya close to the Main Central Thrust (MCT) zone in central Nepal. Out of the 22 business and residential houses located at the disaster site, 13 along the highway sides and 3 from the terrace were swept away, 2 were partially damaged (**Figure 1a and b**); and 54 residents on their beds were killed in a matter of a few minutes. The debris surge also washed out 5 water mills, one temple, 150 m of road stretch and a highway bridge over the BKS, and destroyed crops and agricultural lands. Apart from the loss of life and damage to the infrastructures and properties, human suffering was tremendously high and the mountain environment was deteriorated at an alarming rate. Despite the severity of the event, this area did not experience heavy rainfall for the past two weeks; but continual rainfall of small intensity had been observed from the beginning of July. This case study, in one hand, furnishes an example of how disastrous can be a small event at the base of steep mountain slope if settled underestimating the natural process, and on the other hand, it provides basis for questioning the widely held concept of debris flow can occur only during high intensity precipitation.

The Bhotekoshi valley is characterized by chronically unstable slopes composed of very thick unconsolidated soil cover. The BKS, one of the right tributaries of the Bhotekoshi River with an average slope of 30% drains a basin (25.25 km²) underlain by both the Lesser Himalayan and the Higher Himalayan rocks, allowing source rock composition to be the controlled variable to understand the source of the debris generation. The lower reaches of the basin is very steep as compared to the upper part, and in Larcha area the BKS follows the regional trend of the strike. The basin has either unstable dip slopes mantled by discontinuous thick surficial deposit or vertical cliff. The lower mountain slopes have extensive talus cones and relict colluvial veneers with deep erosional gullies and slump scars. Rock fall chutes are common along the wall of the cliff and bouldery loose sagging mass blanket the torrent embankment below bedrock cliff.

Bhairab Kunda Glacier Lake located at an altitude of 4467 m in the Higher Himalaya supplies head water for the 10 km long BKS. Glacier lakes in the Himalayas are retreating fast in alarming rates and there were several cases of Glacier Lake Outburst Flood (GLOF) in the second half of the past century in the territory of Nepal. As the main source of the stream is glacier lake, which, including most part of the catchment area, is generally invisible and inaccessible during monsoon period, media then linked the event to the GLOF. This study provided a basis for questioning the then widely held concept of GLOF.

Because no one observed the event, our knowledge of it is based on indirect evidence and inference together with survivors' account and our experience to the area. Monsoon rain contributed to incipient instabilities and the stream undercutting further enhanced the instabilities along the embankments. As a result, plane rock failure occurred on the phyllite beds at the notch of a 50 m high waterfall at about 400 m upstream from the bridge site; this in turn removed support for the overlying and adjacent soil mass. Soil sliding and slumping propagated rapidly up the slope so that a large volume of materials began to move almost simultaneously like a 'slope-clearing event'. Detached rock blocks blocked the stream flow for a short time and a large volume of debris was mobilized from the side masses. By any mechanism, eventually the dam breached the narrow outlet and the surge of debris overwhelmed the small settlement along the Arniko Highway (**Figure 1a and b**) and mixed into the Bhotekoshi River. According to the survivors' account, the Larcha area experienced a threatening noise from the bouncing of boulders and ground shaking as if it was stricken by a strong earthquake.

Material transformation into debris flow was promoted by the lack of sorting and the presence of silt and clay, both of which significantly lowered the soil permeability. Reduced permeability cause pore water to be trapped, increasing hydrostatic pressure, adding strength to the interstitial fluid phase, and decreasing shear strength of soil. Maximum flow depth was estimated from the elevation of mud lines on the valley wall that ranged from 7-9 m. Some of the largest blocks transported in the debris front measure $10 \times 6.8 \times 6.6$ m³, $10.5 \times 5.5 \times 3$ m³, $8.6 \times 6.7 \times 3.7$ m³, $8.5 \times 4.3 \times 2.5$ m³, and $7.5 \times 6.5 \times 5.7$ m³. The debris deposited as a fan measuring 400 m long, 30-150 m wide and 2-7 m thick with an average slope of 10°. Total volume of the materials up to the high flood level was estimated to be 175,200 m³, and the actual volume deposited on the fan was about 106,800 m³ spreading over 26,000 m² before channel erosion began.

Based on petrographic composition and size of individual fragment, the debris flow deposit was easily discernible into three segments with a blocky front. The materials were predominantly of the Lesser Himalayan origin, ruling out the possibility of GLOF although some Higher Himalayan materials were observed as reworked material, transported not from above the middle reaches of the catchment. Tree ring counting on trunks deposited on the debris fan yielded ages from 60 to 65 years, which probably indicates the recurrence interval of debris flow of the equal or smaller magnitude.
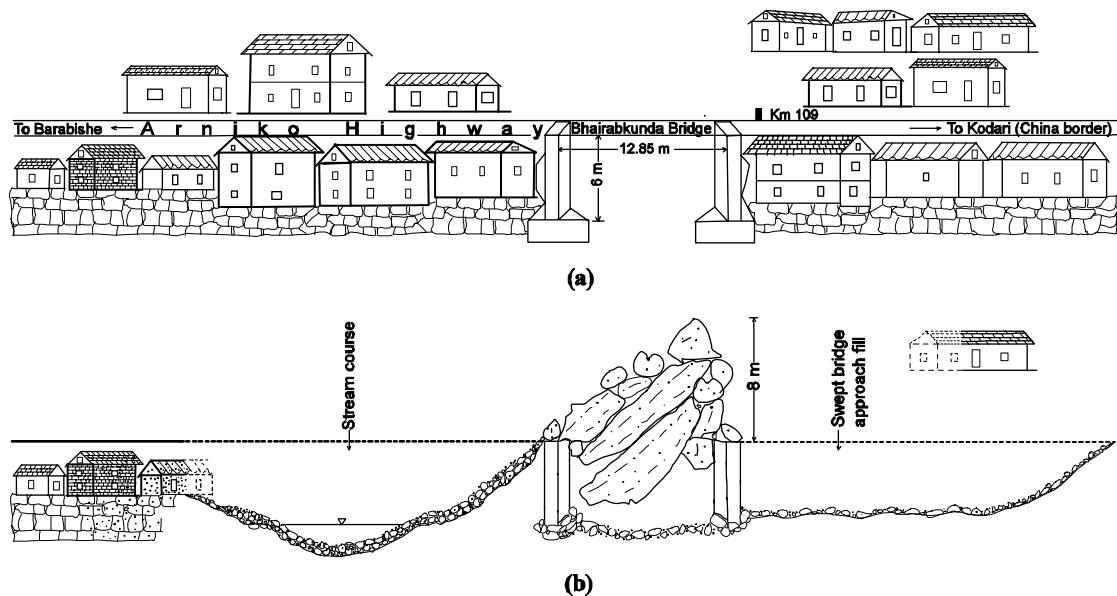
FIGURE 1. Schematic map of the settlement along the highway sides at Larcha: (a) before (based on old photographs and field knowledge) and (b) after the disaster

Preliminary Results from the Yala-Xiangbo Leucogranite Dome, SE Tibet

Amos B Aikman†*, T Mark Harrison† and Ding Lin‡

† Research School of Earth Sciences, The Australian National University, Canberra, ACT 0200, AUSTRALIA
‡ Institute of Geology and Geophysics, Chinese Academy of Sciences, 100029, Beijing, CHINA

* To whom correspondence should be addressed. E-mail: amos.aikman@anu.edu.au

The Yala-Xiangbo Leucogranite dome is situated in southeastern Tibet, ~60 km south of the Indus-Tsangpo Suture, and is broadly similar in style, position and age to other North Himalayan domes. The area comprises ~25 km² aerial exposure of predominantly coarse-grained micaceous leucogranite, emplaced into garnet-mica and graphitic schists. Penetrative fabrics associated with emplacement of the leucogranite dip broadly away from the core, whereas stretching lineations appear to be oriented approximately N-S, similar to those seen in the Kangmar Dome (Lee et. al. 2001). Preliminary thermochronological data indicate that the leucogranites were emplaced at ca. 18 Ma, and cooled through the muscovite closure window at ca. 13.5 Ma. Microstructural analysis suggests that formation of penetrative fabrics was frequently associated with a period of growth and recrystallisation. Relative to fabric formation, initiation of this growth event occurred progressively later with increasing structural height, suggesting upward migration of a thermal anomaly. Thermometric analysis indicates peak temperatures in surrounding schists were above 500 °C even several kilometres structural section from the core of the dome. Preliminary studies on zircons from the Yala-Xiangbo Leucogranite show several populations that are significantly younger than those found in the Greater Himalaya and could represent southward migration of Tibetan middle-crustal material by ductile flow (e.g. Beaumont et. al. 2001, 2004, Jamieson et. al. 2004). Alternatively, they may be attributed to reworking of underthrusted components of the former Gandese Arc.

References

Beaumont C, RA Jamieson, MH Nguyen and B Lee. 2001. Himalayan tectonics explained by extrusion of a low-viscosity channel coupled to focused surface denudation. *Nature* **414**: 738-742

Beaumont C, RA Jamieson, MH Nguyen and S Medvedev. 2004. Crustal channel flows: 1. Numerical models with applications to the tectonics of the Himalayan-Tibetan Orogen. *Journal of Geophysical Research* [in press]

Jamieson RA, C Beaumont, S Medvedev and MH Nguyen. 2004. Crustal channel flows: 2. Numerical models with implications for metamorphism in the Himalayan-Tibetan Orogen. *Journal of Geophysical Research* [in press]

Lee J, BR Hacker, WS Dinklage, Y Wang, P Gans, A Calvert, JL Wan, W Chen, AE Blythe and W McLelland. 2000. Evolution of the Kangmar Dome, southern Tibet: Structural, petrologic and thermochronologic constraints. *Tectonics* **19**: 872-895

The Malashan metamorphic complex in southern Tibet: Dominantly top-to-the north deformation and intrusive origin of its associated granites

Mutsuki Aoya†*, Simon R Wallis†, Tetsuo Kawakami‡, Jeffrey Lee§ and Yu Wang¶

† Department of Earth and Planetary Sciences, Graduate School of Environmental Studies, Nagoya University, Nagoya, 464-8602, JAPAN
‡ Department of Earth Sciences, Faculty of Education, Okayama University, Okayama, 700-8530, JAPAN
§ Department of Geological Sciences, Central Washington University, Ellensburg, WA 98926, USA
¶ Department of Geology, China University of Geosciences, Beijing, 100083, CHINA

* To whom correspondence should be addressed. E-mail: f030402r@mbox.nagoya-u.ac.jp

The kinematics of deformation associated with the formation of the south Tibetan metamorphic domes has important implication for the distribution of extensional (top-to-the north) tectonic regime represented by the STDS (South Tibetan Detachment System, **Figure 1**). However, this deformation has not been well-documented. Even for the Kangmar dome (**Figure 1**), the most accessible and well-documented metamorphic dome, two contrasting views exist about the kinematic nature of the associated deformation: (i) dominantly top-to-the north shear (Chen et al. 1990); and (ii) bulk pure shear reflected by a combination of top-to the north and top-to the south senses of shear in the northern and the southern parts of the dome, respectively (Lee et al. 2000). A second important point to be assessed is the origin of the granitic cores to the metamorphic domes. In the Kangmar dome the granite is thought to represent part of the basement root complex and not an intrusion during the Himalayan orogeny (Chen et al. 1990, Lee et al. 2000). To obtain new insights into these issues and to compare our new results with the Kangmar examples, structural and geochemical studies were carried in a metamorphosed region of Malashan area, located about 400 km west of the Kangmar dome (**Figure 1**).

Granite bodies and associated metamorphism

The Malashan area in southern Tibet is located within the so-called Tethyan Himalayan sequence on the north of the STDS (**Figure 1**). The area contains three two-mica granite bodies: Malashan, Cuobu and Paiku granites. Their surrounding lithologies are mainly calc-schists with minor amounts of pelitic-psammitic schists. In the pelitic schists close to the granite bodies, garnet+staurolite+biotite assemblages are developed representing intermediate-pressure metamorphism similar to that seen in the Kangmar dome. In addition, pelitic schists from the area adjacent to the Cuobu and Paiku granites contain andalusite (Burg et al. 1984).

Deformation phases and their distribution

The dominant foliation developed in the schists surrounding the granite bodies is broadly horizontal and is defined as D2 foliation. An earlier deformation phase, D1, is defined by the foliation folded by D2 folds. The D2 stretching lineation, mainly defined by the alignment of pyrite fragments in calc-schists, is dominantly oriented N-S to NE-SW. In addition, D2 foliation is, on the whole, most strongly developed in the region adjacent to the granite bodies and becomes less strongly developed with increasing distance from the granite bodies. These features are strikingly similar to those of D2 recognized for the Kangmar dome (Chen et al. 1990, Lee et al. 2000).

Kinematic indicators and shear senses

The following kinematic indicators are used to determine the sense of shear for the D2 deformation: (i) asymmetry of quartz-rich lenses in calc-schist; (ii) asymmetry of porphyroclasts such as pyrite in calc schist; (iii) vein sets representing shortening and stretching quarters of bulk strain; (iv) shear bands (S-C' fabric); and (v) opening direction of foliation boudinage that is oblique to stretching lineation. Especially the last indicator (oblique boudin neck) is widely applicable for the calc-schist of the Malashan area. The results show that with only few exceptions the sense of shear in the Malashan area is the top-to-the north.

Origin of granite bodies

The outer marginal zone of the Malashan granite is strongly affected by D2 deformation as in the case of the Kangmar dome. In contrast, the orientation distribution of biotite grains shows that the Cuobu granite is relatively less deformed. Other observations are: (i) the Cuobu granite has dykes originating from the main body and cross-cutting the surrounding D2 foliation; (ii) the Cuobu granite is associated with formation of andalusite and skarn in the adjacent metasediments; and (iii) the andalusite schist and skarn are moderately affected by the D2 deformation. These observations indicate that the Cuobu granite is an intrusive body that was emplaced during the later stages of the D2 deformation. On the other hand, geochemical studies for the Malashan and Cuobu granite show that these bodies have strikingly similar bulk chemical compositions suggesting that they are derived from the same type of original magma. Taking this into account the Malashan granite can also be interpreted as an intrusive body, but the much stronger D2 deformation suggests its emplacement was earlier.

Implications

The Malashan granite and its associated metamorphism and deformation show many similarities with the Kangmar dome. It is, therefore, possible to consider that the region around the Malashan granite forms a metamorphic dome similar to the Kangmar dome. However, the following conclusions of this study bear incompatibility with previous studies for the Kangmar dome: (i) The D2 deformation around the Malashan dome is associated with dominantly top-to-the north sense of shear; and (ii) the Malashan granite is interpreted as an intrusive body formed during the Himalayan orogeny. These results suggest that the formation mechanism of the south Tibetan metamorphic domes may need to be reevaluated.

References

Burchfiel BC, Z Chen, KV Hodges, Y Liu, LH Royden, C Deng and J Xu. 1992. The south Tibetan detachment system, Himalayan orogen: Extension contemporaneous with and parallel to shortening in a collisional mountain belt. *Geol Soc Am Special Paper* **269**: 1-41

Burg JP, M Guiraud, GM Chen and GC Li. 1984. Himalayan metamorphism and deformations in the North Himalayan Belt (southern Tibet, China). *Earth and Planetary Science Letters* **69**: 391-400

Chen Z, Y Liu, KV Hodges, BC Burchfiel, LH Royden and C Deng. 1990. The Kangmar dome: A metamorphic core complex in southern Xizang (Tibet). *Science* **250**: 1552-6

Lee J, BR Hacker, WS Dinklage, Y Wang, P Gans, A Calvert, JL Wan, W Chen, AE Blythe and W McClelland. 2000. Evolution of Kangmar Dome, southern Tibet: Structural, petrologic, and thermochronologic constraints. *Tectonics* **19**: 872-95
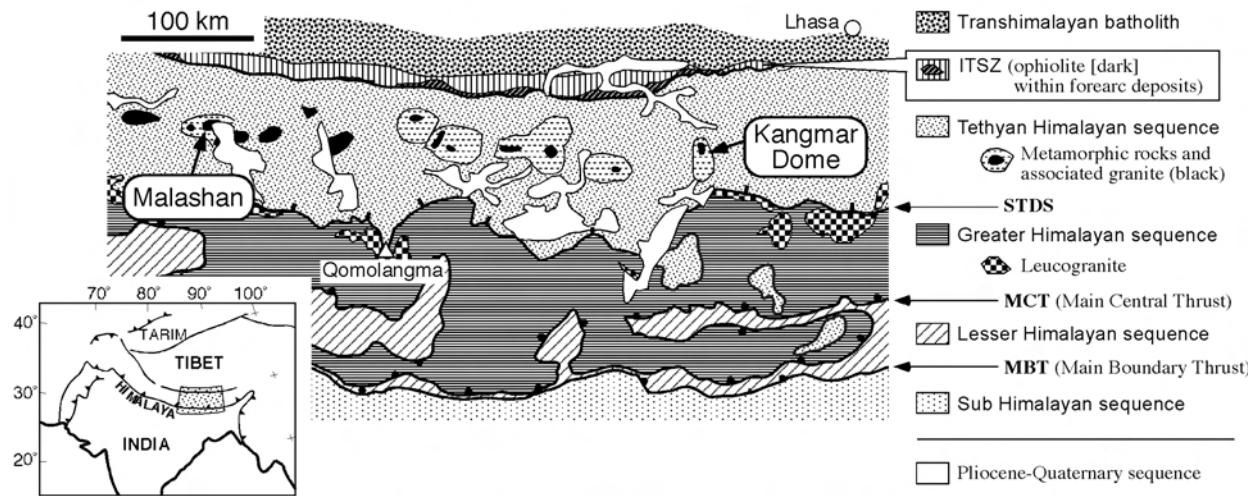
FIGURE 1. Tectonic map of southern Tibet with locality of the Malashan area (modified from Burchfiel et al. 1992)

Palaeoenvironmental events and cycles at the southern front of the Tibetan Plateau during the Pleistocene: A record from lake sediments

Erwin Appel†*, Srinivasa R Goddu†, Shouyun Hu‡, Xiangdong Yang†, Suming Wang‡, Yaeko Igarashi§ and Pitambar Gautam¶

† *Institute for Geosciences, University of Tuebingen, Sigwartstrasse 10, 72076 Tuebingen, GERMANY*
‡ *Nanjing Institute of Geography and Limnology, Chinese Academy of Sciences, 73 East Beijing Rd, Nanjing 210008, CHINA*
§ *Department of Geology and Mineralogy, Hokkaido University, Sapporo 060, JAPAN*
¶ *Central Department of Geology, Tribhuvan University, Kathmandu, NEPAL (now at 21st Century COE Program for Neo-science of Natural History, Faculty of Science, Hokkaido University, Sapporo 060-0810, JAPAN)*

* *To whom correspondence should be addressed. E-mail: erwin.appel@uni-tuebingen.de*

Lake sediments provide high resolution palaeoenviromental archives. In and around the Himalayan region there are numerous lacustrine deposits formed during the last ca. 40 ka. However, there are only few such basins covering almost the complete Pleistocene. These are the Karewa basin (Kashmir, India), Kathmandu basin (central Nepal) and Heqing basin (Yunnan, China). They span over a distance of about 2000 km and are therefore suitable targets to search for synchronous climatic or tectonic events significant for a large region south of the Tibetan Plateau. Karewa sediments cover the Pleistocene until to about 200 ka. They were studied mainly during the eighties of the last century, but due to political instability of the Kashmir region research stopped since then. In the Kathmandu basin early work was done by Yoshida and Igarashi (1984). During recent years drill-cores from the center of the basin were studied (Sakai et al. 2001 and this volume) providing a far more continuous record. Our own work focuses on a continuous succession of fine-grained almost uniform lacustrine sediments from a 168 m-drill-core in the Heqing basin and a 120 m long section of the Lukundol Fm in the Kathmandu basin **(Figure 1)**. This core spans a period of 0.05 to 1.00 ka.

The most remarkable feature of the Heqing core is the record of both, orbital cyclicities and regional events. Cyclicities are observed along the entire succession in the carbonate content as well as in the carbonate-free concentration of magnetic minerals. Spectral analysis reveal dominant power in a cycle, which according to dating results (radiocarbon, magnetostratigraphy) is about 100 ka and thus seems to be controlled by eccentricity. Despite solar radiation is only weakly influenced by eccentricity a 100 ka variation is also dominating the marine oxygen isotope curve of the Late Pleistocene. The carbonate content of the Heqing sediments is extremely high (between 20-80%) and most likely stems from erosion of limestones in the catchment area. However, the mechanism of carbonate variation is not clear in detail. Probably it is related to climatically driven changes in the catchment area, i.e. conditions of weathering, erosion and transport. Changes of mineral magnetic concentration are likely due to low temperature oxidation (LTO) of magnetite resulting in maghemite formation. With increasing degree of weathering more maghemite is formed, which further converts to hematite under more extreme conditions. The magnetic concentration signal decreases with progressing degree of maghemite formation. Time series of carbonate content and magnetic concentration show a non-linear phase shift varying between in-phase and anticorrelated, which indicates that the control mechanism of the magnetic concentration signal is non-unique. This could explain why the precession cycle is well represented in the carbonate spectrum but insignificant in the spectra of magnetic concentration parameters.

The pollen record of Heqing shows no cyclic behaviour. However, it indicates the prevalence of strong temperate-humid and cold-dry periods documented by increased *Tsuga* and reduced total tree pollen, respectively. Magnetic mineralogy also provides indications for climatic events. The highest degree of alteration by LTO can be expected during extreme temperate-humid conditions. It results in a tendency towards an increased ratio of ARM/SIRM (due to a decrease of the effective magnetic grain size by maghemite formation) and a lower S-ratio (due to formation of hematite). Temperate-humid phases in the Heqing core (based on *Tsuga* and supported by ARM/SIRM and S-ratio) can be identified at 990-960 ka (strong indication), 800-780 ka (moderate), 690-670 ka (strong), 630-620 ka (moderate), 580-570 (moderate), 530-520 ka (weak), 450-420 (strong), 360-340 (strong), 215-200 (weak) and 65-35 ka (strong). Especially the event at 450-420 ka is interesting as it could provide a high-resolution record of oxygen isotope stage 11. The transition of glacial stage 12 to interglacial stage 11 represents the highest-amplitude deglacial warming within the past 5 Myr, it cannot be solely explained by Milankovitch forcing mechanisms, and is considered to be of particular importance in terms of understanding present global warming (Droxler et al. 1999). In the lower and middle part of the Heqing core the temperate-humid events seem to be related to the global oxygen isotope curve. In contrary, this is not the case in the upper part (above the event at 360-340 ka, which probably represents stage 9). Data show no indication for the last interglacial stage 5. Furthermore,
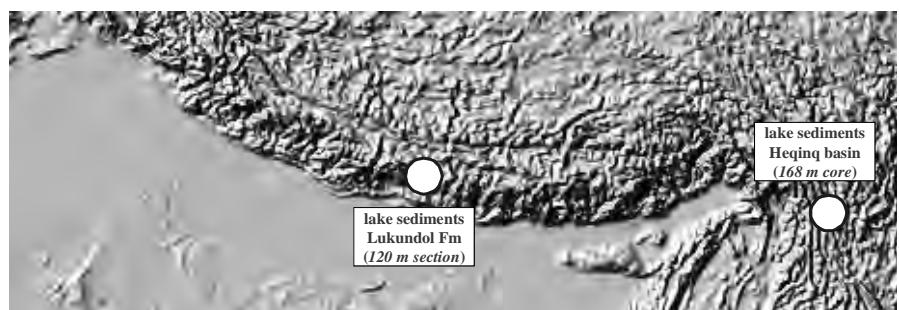
FIGURE 1. Locations of the studied lacustrine sequences in Heqing basin and Kathmandu basin

a strong cold-dry period indicated at 160-110 ka and the temperate-humid period at 65-35 ka do not match with the global climate evolution. They probably reflect regionally controlled climatic features. The later phase of the 65-35 temperate-humid period coincides with the formation of many lakes in the Himalayan and Tibetan region at 40-30 ka, which is attributed to neotectonic activity in the Himalaya (Kotlia et al. 2000) and intensification of Indian monsoon with distinctly higher temperatures and higher precipitation on the Tibetan Plateau (Shi et al. 2001). The most dramatic event seen in the sedimentary record of Heqing is the found at about 65 m (420 ka) where several properties (sedimentation rate, grain size, magnetic mineralogy) reflect a distinct transition of environmental conditions in the region. This fits with the observation that in the lower and middle part the pollen record can be related to the global oxgen isotope curve whereas this is not the case in the upper part. It is interesting that this transition occurred during the time after high-amplitude warming of stage 11 followed by a period without significant temperate-humid phases. We may speculate that changes in the realm of the Tibetan Plateau caused or at least influenced the transition at 65 m. It should be also mentioned that there is a slight indication for a further earlier but less clear transition in the sedimentation regime at around 700 ka (change of sedimentation rate and wavelet power spectrum).

A further study section (ca. 120 m) on outcrops of the Lukundol Formation in the southern Kathmandu basin comprises an age of probably 0.7 to 1.8 Ma overlapping in part with the Heqing core. Observed characteristic features are far less significant than for the Heqing core due to non-uniform and discontinuous sedimentation. The topmost 10 m interval shows a clearly different pattern of anisotropy of magnetic susceptibility than in the succession below. This indicates a change in the sedimentation regime contemporaneous with the temperate-

humid period at 800-780 ka of the Heqing core. Thick gravel beds were deposited during the preceding ca. 200 kyr and a dry period is evident at these times. Before 1.0 Ma humid climate prevailed with changes of warm and cool conditions.

The Heqing core has revealed interesting new aspects about the palaeoenvironmental evolution in the Indian monsoon region southeast of the Tibetan Plateau (**Figure 2**). It still bears a large potential for further high resolution analyses. On the other hand the results from Kathmandu basin has clearly shown the limited use of outcrop studies. A more suitable database to compare with the Heqing core can be expected from the Japanese drilling project in the center of the Kathmandu basin. Availability of drillhole-based Pleistocene records from these two areas should stimulate our Indian collegues to initiate a lake sediment drilling project in the Karewa basin of Kashmir.

References

Droxler AW, R Poor and L Burckle. 1999. Data on past climate warmth may lead to better model of warm future. *EOS* **80(26)**: 289-290

Kotlia BS, C Sharama, MS Bhalla, G Rajagopalan, K Subrahmanyam, A Bhattacharyya and KS Valdiya. 2000. Palaeoclimatic conditions in the LatePleistocene Wadda Lake, eastern Kumaun Himalaya (India). *Palaeogeography Palaeoclimatology Palaeoecology* **162**: 105-118

Sakai H, R Fujii, Y Kuwahara Y, BN Upreti and SD Shrestha. 2001. Core drilling of the basin-fill sediments in the Kathmandu Valley for palaeoclimate study: preliminary results. *J Nepal Geol Soc* **25** (Spec. Issue): 9-18

Shi Y, G Yu, X Liu, B Li and T Yao. 2001. Reconstruction of the 30-40 ka BP enhanced Indian Monsoon climate based on geological records from the Tibetan Plateau. *Palaeogeography Palaeoclimatology Palaeoecology* **169**: 69-83

Yoshida M and Y Igarashi. 1984. Neogene to Quarternary lacustrine sediments in the southern Kathmandu Valley, Nepal. *J Nepal Geol Soc* **4** (Spec. Issue): 73-100
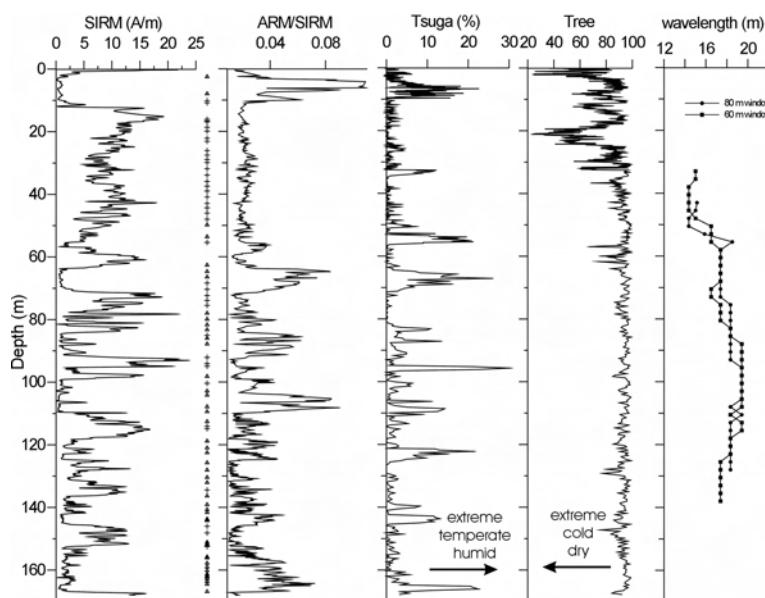
FIGURE 2. Results of Heqing core. Saturation isothermal magnetization (SIRM), ratio of anhysteretic remanent magnetization (ARM) to SIRM, pollen data (*Tsuga* and total tree) and wavelength of main spectral peak of carbonate variation. Crosses and triangles along ARM/SIRM column denotes magnetic mineralogy (crosses: magnetite + maghemite, triangles: maghemite only)

Phylogeny and biogeography of the lucanid beetles of the tribe Aesalini (Insecta, Coleoptera, Lucanidae), with special reference to the effect of Himalayan uplift as the vicariance event

Kunio Araya

Graduate School of Social and Cultural Studies, Kyushu University, Ropponmatsu 4-2-1, Chuo-ku, Fukuoka, 810-8560 JAPAN

For correspondence, E-mail: arayarcb@mbox.nc.kyushu-u.ac.jp

The lucanid tribe Aesalini (Insecta, Coleoptera, Lucanidae) consists of the three genera, *Aesalus* Fabricius, 1801, *Lucanobium* Howden et Lawrence, 1974 and *Echinoaesalus* Zelenka, 1993 (Krajcik, 2001). Of these, the genus *Aesalus* includes more than 10 species from both the Old and New Worlds, while *Lucanobium* is containing two species from South America (Araya and Yoshitomi, 2003). The genus *Echinoaesalus* has most recently been erected based on the Indonesian species, *E. jaechi* Zelenka, 1993, and afterwards, all the Southeast Asian species which had belonged to the genus *Aesalus* were moved to the genus *Echinoaesalus* (Araya et al. 1998, Zelenka 1994). In the present study, phylogenetic relationships among 22 species of the tribe Aesalini (including the genera *Aesalus*, *Echinoaesalus* and *Lucanobium*) are analyzed based on the adult morphologies (a total of 36 characters).

The resultant phylogeny demonstrates that the Aesalini is composed of two major lineages, northern Aesalini and southern Aesalini lineages. The northern Aesalini lineage is composed of three major lines: a Palearctic *Aesalus* line (containing *A. scarabaeoides* from Europe, *A. ulanoskii* from Caucasus and *A. asiaticus* from Japan), African *Aesalus* line (*Aesalus* sp. from Zaire) and a Chinese *Aesalus* line (containing *A. imanishii* from Taiwan and *A. sichuanensis* from West China). The southern Aesalini lineage contains two major lines: a Himalayan *Aesalus* and a tropical Aesalini line. The former line consists of *A. himalayicus* complex and the latter consists of two major groups: a bristly tropical Aesalini group (containing *A. satoi* from Laos, Neotropical *Aesalus* members and southeast Asian *E. matsuii* complex) and a clumpy Aesalini group (containing Neotropical *Lucanobium* and southeast Asian *E. timidus- hidakai* subgroup).
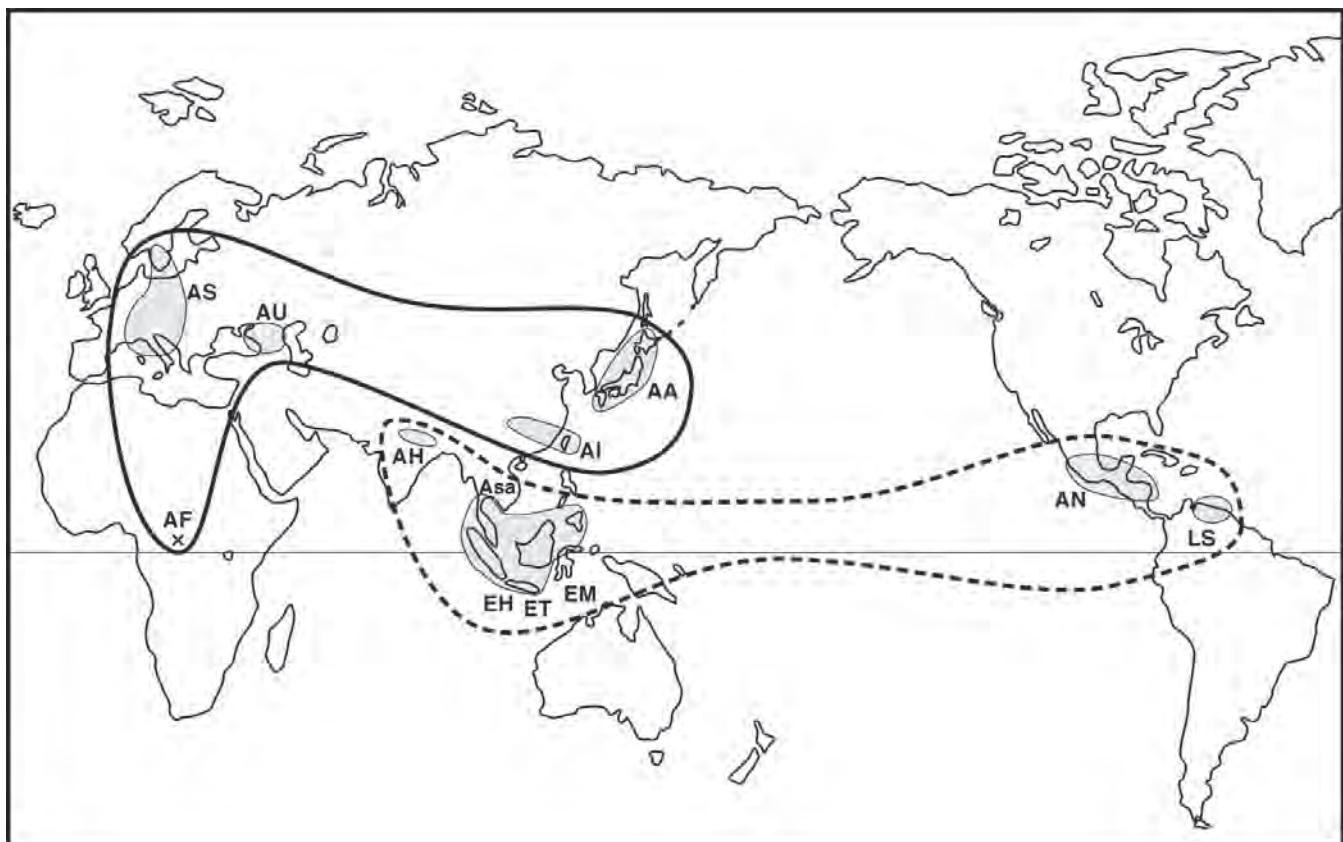
FIGURE 1. Map showing the distribution of the tribe Aesalini. AS=*A. scarabaeoides*, AU=*A. ulanowskii*, AA=*A. asiaticus*, AH=*A. himalayicus* complex, AI=*A. imanishii* complex, Asa=A. satoi, AN=*A. neotropicalis* complex, LS=*L. squamosum* complex, EM= *E.matsuii* complex, ET=*E. timidus* complex and EH=*E. hidakai* complex

The inferred phylogenetic patterns among the members of Aesalini indicated that the *A. himalayicus* complex and the *A. imanishii* complex, both of which showed relic distributions in the Asian Continent, retained the most ancestral character states in the northern Aesalini and the southern Aesalini lineages, respectively. Further, recently a fossil genus, *Cretaesalus* Nikolajev, 1993, belonging to the subfamily Aesalinae was described from the upper Cretaceous stratum of Kazakhstan. Based on these paleontological and neontological information, it is suggested that the ancestor of Aesalini originated in the Eurasian Continent, possibly around the Himalayas, and that Himalayan uplift, the great vicariance event against dispersal and gene flow, may strongly effect on the initial divergence between two major lineages, northern Aesalini and southern Aesalini lineages. In the southern Aesalini lineage, the Himalayan *Aesalus* line and the tropical Aesalini line were separated in the Oriental Region. In the tropical Aesalini line, the bristly and clumpy Aesalini groups were separated in Southeast Asia. Thereafter, both the ancestor of *Lucanobium* in the clumpy Aesalini groups and the ancestor of *A. neotropicalis* complex migrated from the Old World to the New World through the Bering Land Bridge like tapirs (Mammalia, Perissodactyla).

References

Araya K, Yoshitomi H. 2003. Discovery of the lucanid genus Aesalus (Coleoptera) in the Indochina region, with description of a new species. *Spec Bull Jpn Soc Coleopterol Tokyo* (**6**): 189-199

Araya K, Tanaka M & Bartolozzi L. 1998. Taxonomic review of the genus *Aesalus* (Coleoptera: Lucanidae) in the Himalayas. *European J Entomol* **95**: 407-416

Krajcik M. 2001. *Lucanidae of the world, Catalogue Part I. Checklist of the stag beetles of the world* (Coleoptera: Lucanidae). Czech, 2001: 108 p

Nikolajev GV. 1993. Nahodka grebenchatousogo zhuka (Coleoptera, Lucanidae) v verkhnem mele Kazakhstana. *Selevinia 1993*(**1**): 89-92

Zelenka W. 1994. Zwei neue Echinoaesalus-Arten aus Sostasien (Coleoptera, Lucanidae). *Z Arbgem Oster Ent* **46** (1/2): 56-61

Plio-Pleistocene rapid uplift process of the Nepal Himalaya revealed from fission-track ages

Kazunori Arita†* and Hiroto Ohira‡

† Department of Earth and Planetary Sciences, Graduate School of Science, Hokkaido University, Sapporo, 060-0810, JAPAN
‡ Department of Geosciences, Interdisciplinary Faculty of Science and Technology, Shimane University, Matsue, 690-8504, JAPAN

* To whom correspondence should be addressed. E-mail: arita@ep.sci.hokudai.ac.jp

The Nepal Himalaya has been a fold-and-thrust belt in the northern margin of the Indian continent after the India-Eurasia collision during the Eocene time. It is characterized by a series of foreland-propagating thrusts with an out-of-sequence thrust in the northern part of the Lesser Himalaya. Among these thrusts which splay of from a major mid-crustal subhorizontal décollement (Main Detachment Fault or Main Himalayan Thrust), the Main Central Thrust zone, along which the Higher Himalayan crystallines in the north are thrust over the Lesser Himalayan sediments in the south, is the most important one in the Himalayan tectonic evolution (Schelling and Arita 1991, Zhao et al. 1993).

Abundant geological and geomorphological evidences have suggested that the Himalayan uplift began in the Tethys Himalaya, which is situated to the north of the present crest line of the Higher Himalaya in the Miocene; the uplift then shifted southward with time and was finally accelerated in the Higher Himalaya since the Late Pliocene (Arita and Ganzawa 1997). Such a southward migration of the uplift process through time is attributed principally to the southward shifting of a series of the thrusts splays from the décollement. Radiometric age data indicate that the Higher Himalaya has uplifted more rapidly since the Late Pliocene. The fission-tack age data, however, show that the recent rapid uplift of the Higher Himalaya (6 mm/y during the last 1.2 ma) is not related with the activity of the Main Central Thrust zone but is most likely caused by activity of the out-of-sequence thrusting (Arita and Ganzawa 1997, Arita et al. 1997).

In central Nepal the Kathmandu nappe consisting of the Higher Himalayan crystallines and the overlying Tethyan sediments extends southward covering the Lesser Himalayan sediments and forming a reverse Ω shape. An out-of-sequence thrust cuts the Higher Himalayan crystallines and the underlying Main Central Thrust zone in a narrow part to the north of Kathmandu basin (**Figure 1**). The Gosainkund Lekh (range) of nearly 5, 500 m in altitude between the out-of-sequence thrust and the Langtang Valley in the north is composed mainly of sillimanite-kyanite-garnet gneisses and granitic gneisses of the Higher Himalayan crystallines. We did fission-track dating on zircons from nine samples of these gneisses (**Figure 1**). The ages range from 1.5±0.1 Ma (1, 525 m in elevation) to 2.8±0.2 Ma (5, 045 m) (**Figure 2**) and they are almost similar to those from the Annapurna area (1.2 Ma to 2.3 Ma: Arita and Ganzawa 1997). One of the samples dated comes from mylonitic augen gneiss in the Main Central Thrust zone (**no. 9 in Figure 1**) which is equivalent to so-called Ulleri-type augen gneiss in the Annapurna area of central Nepal. The relationship between ages and elevations of sampled locality shows notable contrast between the northern slope and the southern slope of the Gosainkund Lekh. The ages of samples from the northern side increase linearly with increase in the elevation of sampled sites and show an average exhumation

rate of 2.7 mm/y. This rate is significantly higher than that in the Annapurna area (0.9 mm/y). On the other hand, southern side yields almost identical ages between 2.5±0.2 Ma and 2.8±0.2 Ma regardless of sample elevation despite the large distance covered by the samples 1 to 6 (**Figure 2**).

These data suggest that the rocks on the southern side of the Gasainkund Lekh passed evenly the depth of closure temperature of zircon around 2.6 Ma, and then the northern part of the southern side (the highest part of the Gosainkund Lekh) and the northern side uplifted more rapidly and steadily than the southern part. The uplift of the area from the highest part of the Gosainkund Lekh northward resulted probably from the subsurface antiformal structure due to ramping in a depth caused by northward advancement of the Indian mid-crustal wedge sandwiched between the overlying out-of-sequence thrust and the underlying Main Detachment Fault (**Figure 3**).

As shown in **Figure 2** samples 6 to 9 plot linearly although the Upper Main Central Thrust is located between samples 8 and 9. This suggests that the Upper Main Central Thrust has been inactive from 1.5 Ma onward. Takagi et al. (2003) observed that a northeastward brittle extensional movement of the Main Central Thrust zone overprinted the southward ductile thrust
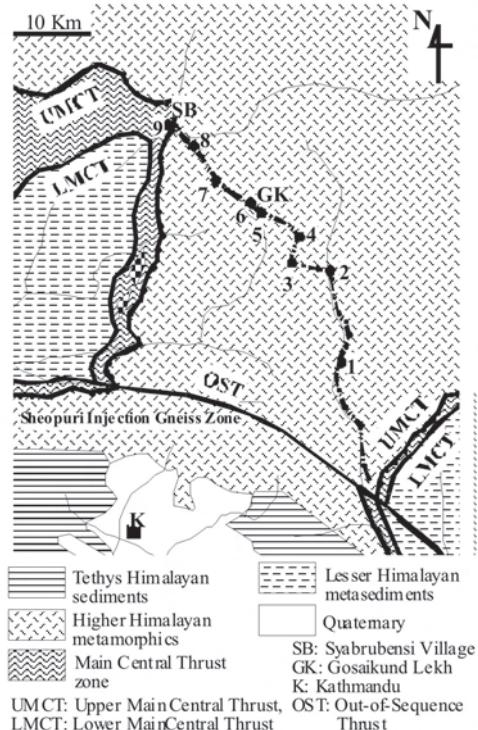
FIGURE 1. Geological division of the Gosaikund Lekh area in central Nepal and sample localities (1-9) for fission-tack dating

movement in the Syabrubensi area (**SB in Figure 1**). They assumed the age of the northward normal faulting to be 3-2 Ma. Hence, our data are consistent with their interpretation.

References

Arita K and Y Ganzawa. 1997. Thrust tectonics and uplift of the Nepal Himalaya revealed from Fission-track ages. *Journal of Geography* **106**(2): 156-167

Arita K, RD Dallmeyer and A Takasu. 1997. Tectonothermal volution of the Lesser Himalaya, Nepal: constraints from $^{40}Ar/^{39}Ar$ ages from the Ka from the Kathmandu nappe. *The Island Arc* **6**: 372-384

Schelling D and K Arita. 1991. Thrust tectonics, crustal shortening, and the structure of the far-eastern Nepal Himalaya. *Tectonics* **10**: 851-862

Takagi H, K Arita, T Sawaguchi, K Kobayashi and D Awaji. 2003. Kinematic history of the Main Central Thrust zone in the Langtang area, Nepal. *Tectonophysics* **366**: 151-163

Zhao WJ, KD Nelson and Project INDEPTH Team. 1993. Deep seismic reflection evidence for continental underthrusting beneath southern Tibet. *Nature* **366**: 557-559
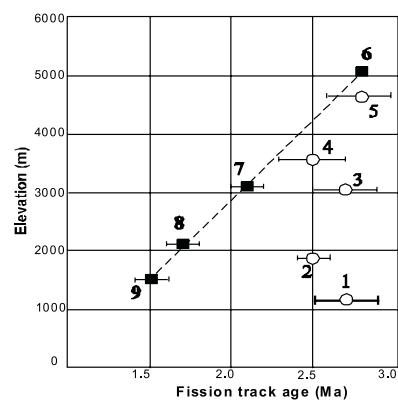
FIGURE 2. Relationship between fission track age and sample elevation. Sample localities are shown in Figure 1
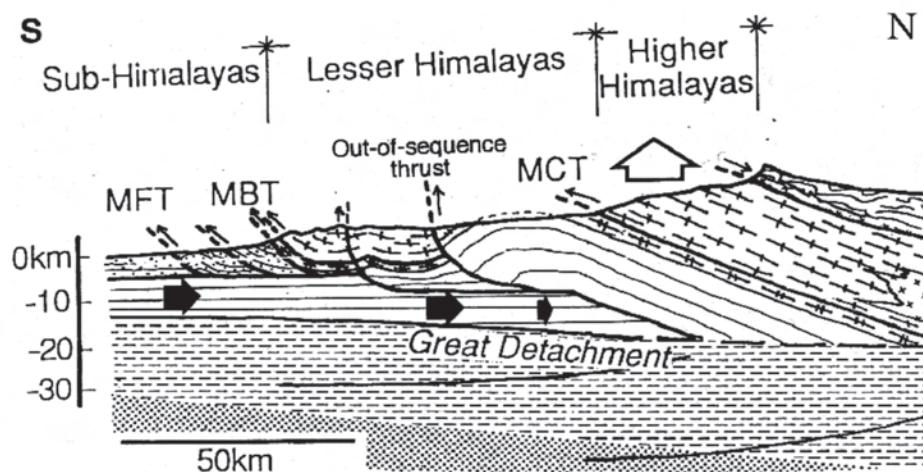
FIGURE 3. Schematic cross-section of the Nepal Himalaya showing recent rapid uplift of the area north of the out-of-sequence thrust (Higher Himalaya) caused by ramping of the thrust and the resultant crustal antiform due to rushing of brittle Indian mid-crustal wedge

Paleoclimate of the Nepal Himalayas during the Last Glacial: Reconstructing from glacial equilibrium-line altitude

Katsuhiko Asahi* and Teiji Watanabe

Graduate School of Environmental Earth Science, Hokkaido University, Sapporo, 060-0810, JAPAN

* To whom correspondence should be addressed. E-mail: asahi@wwwgeo.ees.hokudai.ac.jp

Himalayas could be characterized by the existence of the glaciers which lies higher than about 5200 m in altitude. In the Ice age, glaciers covered vast area rather than those of the present, and many of the high altitude regions in the Nepal Himalayas have been glacierized earlier. Glacial landforms indicate the existence of the past glaciation, and the limits of glacier extent may suggest paleoclimatic conditions. As widely known-well, the Nepal Himalayas experiences a strong summer monsoon environments, and monsoon precipitation plays an important role in glacier accumulation and fluctuation. And a study about the past glaciation can reveal the monsoon fluctuations in the Himalayas. However, in western Nepal, the amount of winter precipitation, which delivered by the westerlies, should be considered for the glaciation. The western Nepal Himalayas are particularly an important region because they make the junction between the westward summer monsoon and eastward winter westerlies along the southern flank of the great Himalayas. Hence a comparative study on glaciation limit between eastern and western Nepal will lead to understand the relative importance of the monsoon and westerlies during the Last Glacial.

Glacial equilibrium-line altitude (ELA) is the elevation where the accumulation and ablation of the glacier is balanced. This is generally regarded as the snowline altitude on glacier and therefore, it is an appropriate indicator for glaciation and local climate. Where modern glaciers exist, the lowering altitude of ELA can be used as a high resolution proxy of air temperature and precipitation changes. This study addresses on the ELA of the present glaciers in eastern and western Nepal, comparing with that of the last Glacial ones. The aim of this study is to speculate on the climatic change during the global Last Glacial Maximum (LGM). The study sites were the Kanchenjunga and Khumbu Himals in eastern Nepal and Chandi and Api Himals in western Nepal (**Figure 1**).

The present ELA of each glacier was identified by the surface topography of glacier using the latest aerial photo interpretation. ELAs during the global LGM were estimated by the maximum elevation of lateral moraines (MELM) method as described in Dahl and Nesje (1992). In this study, at first, geomorphic maps of glacial landforms were delineated using aerial photographs throughout each region. Successive moraine development designates reiterated glaciations. Stratigraphical relationship and the configuration of these moraines, however, discriminate only those formed during the global LGM. Numerical dating data were inferred from OSL age by Richards et al. (2000) and cosmogenic radionuclide age by Finkel et al. (2003) in the Khumbu Himal and OSL age by Tsukamoto et al. (2002) in the Kanchenjunga Himal. Several methods have been adopted in order to estimate past ELA. However, reconstructed ELA during the LGM is commonly overestimated in the Himalayas due to the steep topography and the influence of blown snow. In this study, the distinguished higher altitudes of the MELM were selected to estimate the ELAs during the LGM.

It can demonstrate the minimum amount of ELA depression and it implies paleoclimate practically rather than previous studies.

In **Figure 2**, smaller points and the solid regression lines denote the present ELAs both in eastern and western Nepal. Latitudinal profiles of equilibrium-line display steep gradients in both regions, as a result of the reduction in precipitation by monsoon humid wind blow into the high Himalayas (Müller 1980). Meanwhile glaciers are mainly maintained by sources of summer monsoon moisture. Monsoon vapors were brought as rainfall or snowfall depending on the altitude. Then ELAs at the southern margin in both regions would be subject to the summer air temperature. This is the typical feature of the ELA under the strong summer monsoon environment.

During the global LGM period, the latitudinal ELA profiles show same southward inclination tendency. They suggest that monsoon precipitation is likely to be ruling resource of glacier accumulation. The Nepal Himalayas, hence, were under summer monsoon environment during the LGM as today, even if the monsoon was weakened. Some paleoenvironmental studies suggest a weakening or even a possible loss of the Indian summer monsoon during the LGM. Glaciers were extended, however, by monsoon precipitation and cooling air temperature. In eastern Nepal, the inclination of equilibrium-line enhanced southward (**Figure 2B**), interpreted as a consequence of the decreased precipitation northward and arid condition toward Tibet. In contrast, in western Nepal, glacial equilibrium-line inclined southward equally as today (**Figure 2A**). Therefore western Nepal is expected to belong under similar climatic condition, even though summer precipitation was decreased. Winter precipitation delivered by mid-latitude westerlies, possibly sifted farther to the south and was enhanced. It affected the glacier maintenance in western Nepal. In this way, relative climatic enhancement or weakening between monsoon and westerlies controlled the style and timing of glaciations in the Nepal Himalayas.
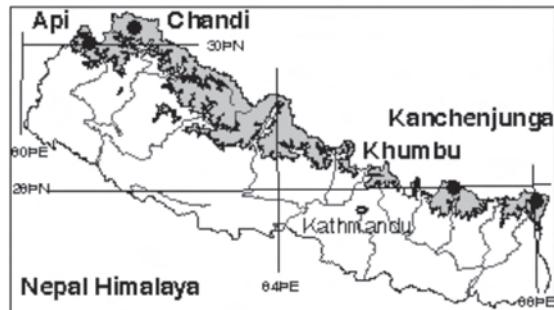
FIGURE 1. Location of the study area in the Nepal Himalayas
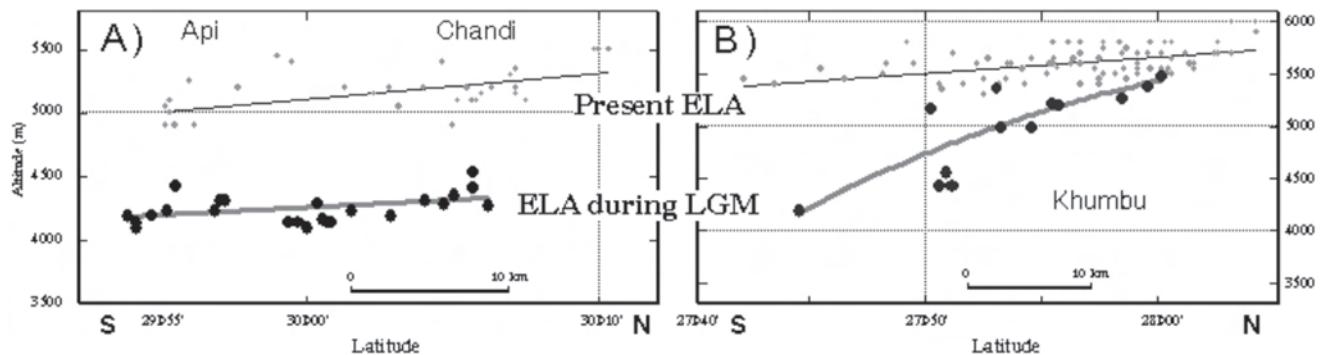
FIGURE 2. Latitudinal profiles of glacial equilibrium-line altitudes (ELAs) of the present and the global LGM in the southern flank of the Nepal Himalayas. A) Api and Chandi Himals from western Nepal, B) Khumbu Himal from eastern Nepal

References

Müller F.1980. Present and late Pleistocene equilibrium line altitudes in the Mt Everest region – an application of the glacier inventory. *IAHS Pub* **126**: 75-94

Dahl SO and A Nesje. 1992. Paleoclimatic implications based on equilibrium-line altitude depressions of reconstructed Younger Dryas and Holocene cirque glaciers in inner Nordfjord, western Norway. *Paleogeog, Paleoclim, Paleoeco* **94**: 87-97

Richards BMW, DI Benn, LA Owen, EJ Rhodes and JQ Spencer. 2000. Timing of late Quaternary glaciations south of Mount Everest in the Khumbu Himal, Nepal. *Geol Soc Am Bull* **112**: 1621-32

Finkel RC, LA Owen, PL Barnard and MW Caffee. 2003. Beryllium-10 dating of Mount Everest moraines indicates a strong monsoon influence and glacial synchroneity throughout the Himalaya. *Geology* **31**: 561-4

Tsukamoto S, K Asahi, T Watanabe and WJ Rink. 2002. Timing of past glaciations in Kanchenjunga Himal, Nepal by optically stimulated luminescence dating of tills. *Quarter Inter* **97/98**: 57-67

Renewed tectonic extrusion of high-grade metamorphic rocks in the MCT footwall since Late Miocene (Sutlej Valley, India)

Vincent Baudraz†*, Jean-Claude Vannay†, Elizabeth Catlos‡, Mike Cosca†, and Torsten Vennemann†

† Institut de Minéralogie et Géochimie, Université de Lausanne, CH-1015 Lausanne, SWITZERLAND
‡ School of Geology, Oklahoma State University, Stillwater, OK, 74078, USA

* To whom correspondence should be addressed. E-mail: vincent.baudraz@img.unil.ch

The metamorphic crystalline core of the Himalaya is classically considered to be composed of a single tectonic unit, the High Himalayan Crystalline Sequence (HHCS), thrusted during Early Miocene over the low-grade sediments of the Lesser Himalaya along the Main Central Thrust (MCT). However, recent geochronological data from the MCT footwall (e.g., Catlos et al. 2002) indicate high-temperature protracted tectono-thermal activity up to Pliocene in the frontal part of the orogen, from Eastern Nepal to Garhwal (India). Further to the west, in the Sutlej Valley area (Himachal Pradesh, India), the metamorphic crystalline core is composed of two lithotectonic units, the High Himalayan Crystalline Sequence and the Lesser Himalayan Crystalline Sequence (LHCS). The latter crops out within a large-scale antiformal tectonic window called the Larji-Kullu-Rampur Window. Both units show inverted metamorphic field gradients. New oxygen isotope thermometry combined with multiple equilibrium thermobarometry constrains the temperature and pressure field gradients for the LHCS. The 2.5 km thick, mylonitic schists forming the lowermost part of the unit show inverted temperature and pressure profiles, increasing upsection from about 520 °C at 6.0 kbars to about 600 °C at 8.6 kbars. These data,

together with the ubiquitous top-to-the-south sense of shear indicators associated to the mylonitic deformation, suggest that the metamorphic isograds were passively sheared and inverted during the extrusion of the unit. Above the mylonitic zone of the LHCS, the temperature profile flattens at about 620 to 650 °C, whereas the pressure shows a marked decrease from about 8.6 to 6.5 kbars. These data are consistent with two different scenarios:

1) After having reached a maximum burial depth of about 30 km, the LHCS unit initially experienced a temperature increase during the beginning of its extrusion, as a consequence of the relaxation of the deflected isotherms. As a function of their position in the unit, mineral assemblages recorded conditions corresponding to different periods of the thrusting/extrusion history.

2) Peak metamorphic conditions were reached contemporaneously in the whole unit and peak isotherms were strongly inverted. Both pressure and temperature gradients were subsequently deformed by a heterogeneous simple shear flow such as proposed in the channel flow model by Grujic et al. (1996). A combination of the two proposed scenarios is conceivable as they are not mutually exclusive.
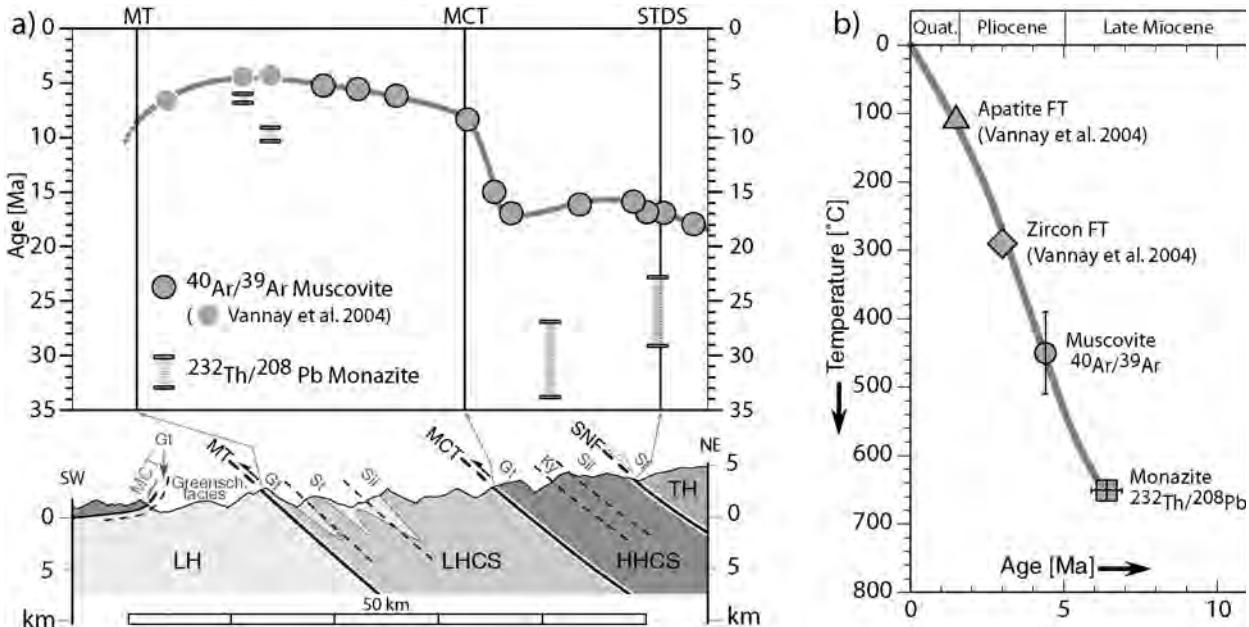
FIGURE 1. (a) Monazite crystallization ages and muscovite cooling ages from the Himalayan crystalline core in the Sutlej Valley, showing the distinct evolutions of both units. The monazite crystallization ages indicate a temperature peak after 6.4 Ma in the LHCS and are in agreement with a temperature peak after ~ 23 Ma in the HHCS. (b) Cooling history of the LHCS unit, characterized by an average cooling rate of about 100 °C/Ma, which corresponds to an extrusion rate of about 8 mm/year along the Munsiari Thrust.

In situ Th-Pb monazite ages from both units constrain the timing of the kinematic evolution of the Himalayan crystalline core. In the HHCS unit, multiple spot analyses from individual matrix monazite grains yielded ages ranging from ~34 to ~23 Ma. These ages are interpreted as representing episodic growth during prograde metamorphism. It is unlikely that the grains suffered any Pb loss because of the very low Pb diffusivities in monazites (Cherniak et al. 2003), their P-T-path, and their size. In the lower part of the underlying LHCS, monazite crystals included in garnet have an age of 9.8±0.3 Ma (MSWD=0.4), whereas a younger age of 6.4±0.5 Ma has been measured for a crystal included in staurolite. These ages are interpreted as crystallization ages related to prograde metamorphism. Matrix monazite grains from the upper orthogneissic part of the LHCS, whose granitic protolith has an age of 1.84 Ga (Miller et al. 2000), yielded variable ages ranging from ~1090 to 11 Ma. These ages are interpreted as mixed ages of inherited magmatic cores and metamorphic growth domains.

The new thermobarometric and geochronological data, together with systematic ^{40}Ar/^{39}Ar muscovite cooling ages across both units, allow us to reconstruct the tectono-thermal evolution of the active Himalayan front since the Eocene. In contrast to the HHCS that experienced Early Miocene peak metamorphic conditions followed by Early to Middle Miocene rapid exhumation along the MCT, the LHCS underwent Late Miocene peak metamorphic conditions followed by rapid exhumation along the Munsiari Thrust. The LHCS testifies to renewed and still active tectonic extrusion of high-grade metamorphic rocks, linked to on-going prograding deformation in the frontal parts of the Himalayan orogen.

References

Catlos E, TM Harrison, CE Manning, M Grove, SM Rai, MS Hubbard and BN Upreti. 2002. Records of the evolution of the Himalayan orogen from in situ Th-Pb ion microprobe dating of monazite: Eastern Nepal and western Garhwal. *J Asian Earth Sci* **20**(5): 459-79

Cherniak DJ, EB Watson, M Grove and TM Harrison. 2003. Pb diffusion in monazite: A combined RBS/SIMS study. *Geoch et Cosmoch Act* **68**(4): 829-40

Grujic D, M Casey, C Davidson, LS Hollister, R Kundig, T Pavlis, and S Schmid . 1996. Ductile extrusion of the Higher Himalayan Crystalline in Bhutan: Evidence from quartz microfabrics. *Tectonophysics* **260**(1): 21-43

Miller C, U Klötzli, W Frank, M Thöni, and B Grasemann. 2000. Proterozoic crustal evolution in the NW Himalaya (India) as recorded by circa 1.80 Ga mafic and 1.84 Ga granitic magmatism. *Precambrian Res* **103**: 191-206

Cenozoic tectonics of Central Asia: Basement control

Michael M Buslov

United Institute of Geology, Geophysics and Mineralogy, Siberian Branch - Russian Academy of Science, Novosibirsk, RUSSIA, and Hokkaido University, Sapporo, JAPAN

For correspondence, E-mail: misha@uiggm.nsc.ru, mmbuslov@museum.hokudai.ac.jp

The Paleozoic mosaic-block structure of the Central Asia folded area is formed by isometrically outlined Precambrian microcontinents (Tarim, Tadjik, Issyk-Kul, Junggar, Tuva-Mongolian etc.) surrounded by Paleozoic accretion-collision zones and Late Paleozoic-Early Mesozoic transverse strike-slip faults. The complicated structure of the crust in Central Asia has a strong impact on the distribution of strain induced by the India-Eurasia collision. Most implications are based on the study of reactivated ancient faults (Avouac and Tapponnier 1993). The Cenozoic tectonics of Central Asia strongly inherited the fabric acquired from the pre-Cenozoic evolution: the microcontinents comprising Precambrian-Paleozoic metamorphic and magmatic rocks having lens shape and surrounded by thick zones of Late Paleozoic strike-slip deformation. For a long time during the Cenozoic, the deformation was mainly affecting the zone surrounding the microcontinentes. By now the deformation has resulted in a system of compressed mountain ranges around the microcontinent (**Figure 1**). Precambrian microcontinents are overlapped by Meso-Cenozoic sediments and remained homogenous structure. These homogenous structures in Central Asia were uplifted as a far-field effect of orogeny associated with India-Eurasia convergence. The Cenozoic deformation and modern earthquakes (M> 6) are found to be concentrate around microcontinent edges (Buslov et al. 2003).

Northward propagation of deformation front away from the Himalayan collision zone is suggested by systematic northward rejuvenation of mountains and intramontane basins. This model can be outlined in the following manner:

1. The Eocene initial collision phase (52-35 Ma) in which India collided with Asia, the rise of Pamir plateau, anticlockwise rotation of the Tadjik and Tien-Shan blocks (Thomas et al. 2002).

2. The Oligocene Pamir collision phases (35-20 Ma) during which India thrusts under the Himalaya and Tibet, resulting in the rotation of the latter, and thrusting of the Pamir on the Tadjik microcontinent, anticlockwise rotation of the Tadjik and Tien-Shan blocks, first stage of reactivation of the accretion-collision zones and strike-slip faults around the various Precambrian microcontinents.

3. The Neogene-Quaternary Himalayan thrusting phases (last 20 Ma) in which India is thrusting under the Himalaya and Tibet, peak of Main Central Thrust (MCT) activity, subsidence of the Tarim and Tadjik depressions, Tarim and Tadjik microcontinentes started thrusting under the Tien-Shan, the rise of the South Tien Shan (after 20 Ma), reactivation of accretion-collision zones and strike-slip faults around the Issyk-Kul, Junggar and Tuva-Mongolian microcontinents (after 10 Ma), rise of the North Tien-Shan (peak activity at 10 and 3 Ma) and Altai areas (after 6 Ma, peak activity at 3 Ma). Intensive tectonic activity continued in the Late Pleistocene-Holocene resulting in the formation of the present high-mountain relief of Central Asia.

Figure 1 demonstrates the tectonic scheme of Central Asia with triangle-like peaks of compressed mountain ranges divided by sedimentary depressions including the Tarim ramp basin, Junggar and Inner-Altai semi-ramp basins. Triangle or rhomb-shaped depressions and horsts tend to the NW front of the Tien Shan-Junggar system: (1) the Zaysan, Junggar, Alakol, Chu, Issyk-Kul, Fergana basins, (2) the Saur, western Kyrgyz and Kuramin horsts. The largest oil-bearing basins in the Turan, Tarim, Turfan, Junggar, and Zaysan depressions evolved as intermountain depressions since the Permian-Triassic, mainly in the Late Jurassic-Early Cretaceous. After the Late Cretaceous-Paleogene stage of regional tectonic stabilization, the Neogene-Quaternary stage of active tectonics and sedimentation began. In the Eocene an epicontinental sea existed and was located in the Fergana, Afghan-Tadjik and western Tarim depression. Sea-beach sediments accumulated in the Issyk-Kul depression. Uplifting took place in the territory of the present axial zones of the Himalayas, Karakoram, Hindukush, South Tien Shan, and Pamirs resulting in denudation. Locally, the depressions were filled with molasse. Orogenesis in the Pamirs and South Tien Shan was accompanied by the accumulation of Late Oligocene coarse-clastic continental red sediments. In the Miocene the landscape of the Pamirs and South Tien Shan was dominated by uplifts of up to 3 km elevation and interlying troughs. In the Pliocene climatic cooling was responsible for the change of red molasse to gray molasse as the elevation of uplifts reached 4-5 km. In the Quaternary the further uplifting of the Pamirs caused the development of a typical glacial landscape. Miocene uplifting of the Pamirs and Southern Tien Shan was accompanied by molasse depositing in the Fergana, Afghan-Tadjik, Issyk-Kul and other depressions. In the Late Pliocene-Middle Pleistocene a thick series (over 1.5 km) of alluvial pebble-stone deposits formed. At that time, the faults were reactivated mainly as strike-slip faults or reverse faults.

Deformation of SW Altai (Zaysan basin) began in the late Eocene, after a widespread Late Cretaceous-Pleistocene period of erosion and peneplanation. The paleogeographic environment in the Zaysan basin changed from a marginal sea during the Late Cretaceous-Pleistocene, to an intracontinental lake in the Late Eocene-Early Oligocene. Movement of the Junggar microcontinent and rotation of the Tuva-Mongolian microcontinent induced regional uplift of the Altai Mountains. The structure of the Altai Mountains is interpreted as a result of the reactivation of Paleozoic accretion-collision zones and faults between the Junggar and Tuva-Mongolian microcontinents (Dobretsov et al. 1996, Buslov et al. 1999). The faults were reactivated mainly as strike-slip faults or reverse faults. The Junggar microcontinent subsided beneath the Altai together with the Zaysan basin. This induced several tectonic phases recorded along the margin of the Zaysan depression: Middle Eocene (40-35 Ma), Middle Oligocene (30-25 Ma), and Late Miocene-Pliocene (6-3 Ma). In the Chuya depression (at the NE-margin of the Altai and Tuva-Mongolian microcontinent) tectonic pulses occurred in the Late Oligocene (28-23 Ma) and Late Pliocene - Early Pleistocene (3-2 Ma). Periods of relaxation between the tectonic phases are recorded by lacustrine

carbonaceous clay sedimentation in extensional setting during the Lower-Middle Miocene in the Zaysan basin and the Upper Miocene in the Chuya basin. In the Middle Eocene, the SW-area of the Altai uplift formed in the frontal part of the Junggar microcontinent. In the Late Pliocene, deformation reached the NE-margin of Altai.

The Altai range has a modern block structure, with flat plateaus separated by thrusts and oblique-reverse faults. The most contrasting deformation took place around Altai and resulted in the formation of conjugated grabens, ramps and horsts. In the Middle Miocene, the northern part of the Junggar basin subsided northward, turning the Zaysan depression into a half-graben. In the Upper Miocene, the graben of the Chuya depression formed. The Altai area was fragmented into alternating mountains ranges and intramontane depressions starting in the Late Pliocene - Early Pleistocene.

References

Avouac JP and P Tapponnier. 1993. Kinematic model of active deformation in Central Asia. *Geophys Res Lett* **20**: 895-898

Buslov. MM, VS Zykin, IS Novikov and D Delvaux. 1999. Cenozoic history of the Chuya depression (Gorny Altai): Structure and Geodynamics. *Russian Geol Geophys* **40**(12): 1687-1701

Buslov MM, J Klerkx, K Abdarakhmatov, D Delvaux, Yu Batalev., OA Kuchai, B Dehandschutter, and A Muraliev. 2003. Resent strike-slip deformation of the northern Tien-Shan. In: F Stori, RE Holdsworth and F Salvini. (eds). *Intraplate strike-slip deformation belts. Geol Soc London. Spec Publ* **210**: 53-64

Dobretsov NL, MM Buslov, D Delvaux, NA Berzin and VD Ermikov. 1996. Meso- and Cenozoic tectonics of the Central Asian mountain belt: effects of lithospheric plate interaction and mantle plumes. *Int Geol Review* **38**: 430-466

Thomas JC, R Lanza, A Kazansky, V Zykin, N Semakov, D Mitrokhin and D Delvaux. 2002. Paleomagnetic study of Cenozoic sediments from the Zaisan basin (SE Kazakhstan) and the Chuya depression (Siberian Altai): tectonic implications for central Asia. *Tectonophysics* **351**: 119-137
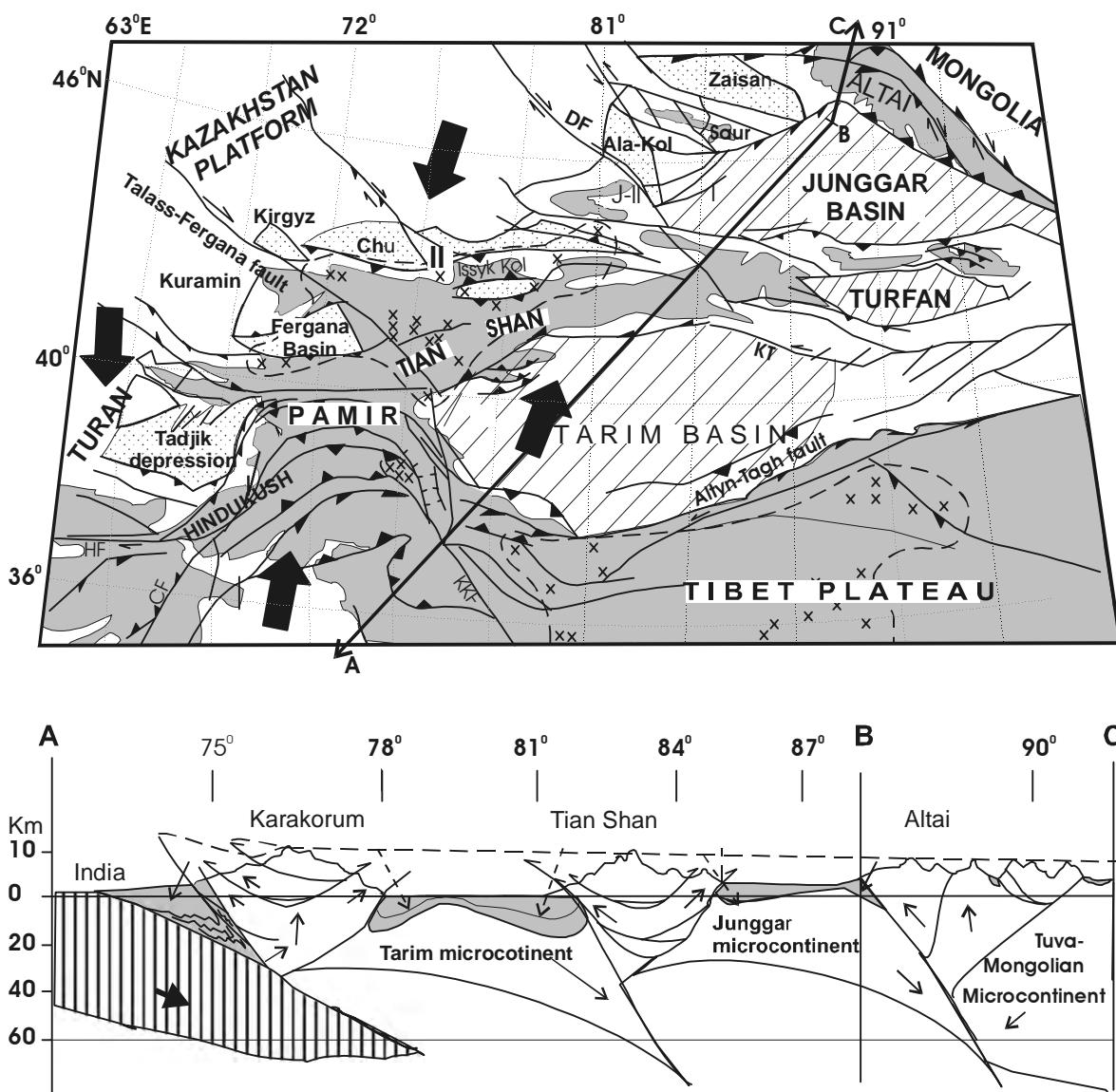
FIGURE 1. Tectonic scheme and cross-section of the Central Asia. Diagonal crosses show the localities of mantle plume basalts. Thick arrows show the main direction of compression. Schematic cross-section from the India continent to the Altai mountain range (line ABC). Vertical stretching shows the Indian plate crust, dots-sediments. Grey tone show the mountain range (more 2000 m) on tectonic scheme and the sediment basin on the cross-section

Cenozoic tectonics and geodynamic evolution of the Tien Shan mountain belt as response to India-Eurasia convergence

Michael M Buslov†‡*, Johan De Grave§¶ and Elena A Bataleva#

† United Institute of Geology, Geophysics & Mineralogy, Siberian Branch-Russian Academy of Science, Novosibirsk, RUSSIA
‡ Hokkaido University, Sapporo, JAPAN
§ Department of Mineralogy & Petrology, University of Gent, Gent, BELGIUM
¶ Department of Geological & Environmental Sciences, Stanford University, Stanford, USA
# United Institute of High Temperatures RAS, Bishkek, KYRGYZSTAN

* To whom correspondence should be addressed. E-mail: misha@uiggm.nsc.ru

The present-day structure of the Tien Shan mountains consists out of roughly E-W trending, high mountain ranges (exceeding 7000 m), alternating with (near) parallel sedimentary basins. The Tien Shan is situated in Central Asia at the boundary between the active orogenic structures of the northern Tarim plate and the stable Kazakhstan platform (**Figure 1**). The structural pattern of the Tien Shan indicates a complex Cenozoic deformational history with a current N-S shortening rate of 10-15 mm/yr in the southern Tien Shan and 2-6 mm/yr in the northern Tien Shan. Moreover, shortening vectors from the northern and southern Tien Shan are oriented along different directions. These different shortening rates and orientations can be explained by the presence of the Precambrian Issyk-Kul microcontinent embedded in the northern Tien Shan region. The mosaic-block structure of the Tien Shan mountains is shaped by isometrically outlined Precambrian microcontinents (Tarim and Issyk-Kul) surrounded by Paleozoic island arcs and accretionary prisms that are dissected by Late Paleozoic-Early Mesozoic strike-slip faults. This complex structure of the Central Asian crust has a strong impact on the distribution of strain induced by the ongoing India-Eurasia convergence. In this study we investigate the relationships between the Cenozoic structure of the Tien Shan, reactivation of inherited faults, and interaction of rigid Precambrian microcontinents in the relatively mobile accretionary-collision belts (Buslov et al. 2003).

Northward propagation of the deformation front away from the Himalayan collision zone towards intracontinental Central Asia is suggested by systematic northward rejuvenation of mountain ranges and intramontane basins (Dobretsov et al. 1995). The model for this northward propagation may be described as follows: (1) India thrusting under Tibet, resulting in the uplift and rotation of the latter (35 to 20 Ma); (2) subsidence of the Tarim depression, Tarim under-thrusting the Tien Shan, rise of the southern Tien Shan (20 to 11 Ma); (3) reactivation of pre-existing structures around and within the Issyk-Kul microcontinent (10 to 3 Ma); (4) rise of the northern Tien Shan (peak at 3-2 Ma).

Apatite fission track thermochronology performed on crystalline basement rocks from the western and northern Issyk-Kul basin showed that a first acceleration of rock uplift and denudation affected the northern Tien Shan starting between 20 and 10 Ma ago, and a second acceleration occurred after 3 Ma ago. The latter is also expressed in the stratigraphy by a marked change in sedimentary environment in the Late Pliocene-Early Pleistocene, by thick sequences of coarse conglomerates, sedimentary gaps and tectonic unconformities. In the Paleogene, more than 3 km of lacustrine sediments were deposited in the subsiding basin. The onset of uplift of the southern Tien Shan started in the Neogene, when clastic and proluvial sediments, transported from the rising southern ranges

were deposited in the basin. In this stage, the basin was much larger and more elongated than at present. It was probably controlled by ENE trending faults.

The thrusting of the Tarim plate under the southern Tien Shan results in the shortening of the upper crust at rates of <10-15 mm/yr, whereas India moves northward at 50 mm/yr (Abdrakhmatov et al. 2001). A part of the strain may have been accommodated within viscoelastic layers in the middle crust of the Tien Shan. Seismic and magneto-telluric studies show clear tectonic layering of the Tien Shan lithosphere, with several nearly horizontal viscoelastic layers. The lower layer is underthrust northward underneath the northern Tien Shan as indicated by seismic data (**Figure 1b**). Tectonic layering of the lithosphere beneath the southern Tien Shan is possibly related to the rotation and underplating of the Tarim plate and indentation of its basement into the middle crust of the southern Tien Shan. This caused high-rate slip and failure in the upper crust to depths of 20-30 km (Sabitova and Adamova 2001). Wave-guide lenses are found in the upper crust at a depth of 10-20 km north of the Pamir thrust sheets. Oblique wave-guide layers connect the horizontal layers. A clear change of the wave-guide is present along an EW profile at 42°N (**profile II-II in Figure 1**): its southern extremity is located 15 km shallower than the northern one. These thick wave-guides are absent beneath the Fergana depression and adjacent flats. Magneto-telluric studies in the Tien Shan (Rybin et al. 2001) also indicate the presence of the abovementioned layers and lenses with a high electric conductivity. Profile II-II shows the position of the low seismic wave area (seismic data) and high conductivity layers (magneto-telluric data). There is a good correlation between the results obtained by the different methods. A 15-25 km thick layer is located at a depth of 35-50 km to the north of 42°N and at a depth of 20-35 km to the south of 42 °N. Oblique wave-guides mark the southern border of the Issyk-Kul microcontinent (Buslov et al. 2003).

The upper crustal strain has been mainly controlled by the Issyk-Kul microcontinent. This lens-shaped microcontinent is surrounded by vast shear zones that have been involved in the tectonic activity during most of the Cenozoic. During the Quaternary the strain has propagated as far as the central part of the Issyk-Kul basin. Activity in the northern Tien Shan reached its peak in the Pliocene-Early Quaternary and resulted in the formation of the present-day topography and strong deformation of the Issyk-Kul basement and its Cenozoic cover. The strike of regional compression changed from NW-SE in the Late Miocene to N-S in the Pliocene-Early Quaternary. Both the southern and northern margins of the microcontinent were gradually deformed and uplifted, hence reducing the area of deposition in the basin. Due to thrusting of the northern and southern margins, the basin morphology at both the western

and eastern end can be described as full-ramp structures. Underthrusting of Tarim along the southern Tien Shan resulted in segmentation of the southern margin of the Issyk-Kul microcontinent into several blocks separated by oblique thrusts and strike-slip faults. Strike-slip along the Chon-Kemin fault resulted in thrusting and reverse faulting along the northern margin of the microcontinent. The most important active tectonic movements affecting the Issyk-Kul region today are sinistral strike-slip motions along the Chon-Kemin, Chon-Aksu, Pred-Kungei, North Issyk-Kul and South Issyk-Kul faults. Strike-slip faulting probably was responsible for the formation of a pull-apart structure in the central part of the basin.

References

Abdrakhmatov KE, R Weldon, S Thompson, D Burbank, CH Rubin, M Miller and P Molnar. 2001. Origin, direction, and rate of modern compression of the central Tien Shan (Kyrgyzstan). *Russian Geology and Geophysics* **42**(11-12): 1585-1609

Buslov MM, J Klerkx, K Abdarakhmatov, D Delvaux, VY Batalev, OA Kuchai, D Dehandschutter and A Muraliev. 2003. Recent strike-slip deformation of the northern Tien-Shan. In: Stori F, RE Holdsworth and F Salvini (eds). *Intraplate strike-slip deformation belts*. Geological Society. London. Special Publication **210**: 53-64

Dobretsov NL, MM Buslov, D Delvaux, NA Berzin and VD Ermikov. 1996. Meso- and Cenozoic tectonics of the Central Asian mountain belt: effects of lithospheric plate interaction and mantle plumes. *International Geology Review* **38**: 430-466

Sabitova TM and AA Adamova. 2001. Seismic tomography study of the Tien Shan crust: (results, problems, and prospects). *Russian Geology and Geophysics* **42**(11-12): 1543-1553

Rybin AK, VY Batalev, PV Il'ichev and GG Shchelochkov. 2001. Magnetotelluric and magnetovariational studies of the Kyrgyz Tien Shan. *Russian Geology and Geophysics* **42**(11-12): 1566-1573

FIGURE 1. (a) Tectonic scheme of the Tien Shan Mountains. (b) Geophysical profiles within the study area (see a for location)

Deformation features of the Higher Himalayan Crystallines in Western Bhutan during exhumation

Rodolfo Carosi†, Chiara Montomoli†*, Dario Visonà‡

† Dipartimento di Scienze della Terra & Istituto di Geoscienze e Georisorse, via S.Maria 53, 56126 Pisa, ITALY
‡ Dipartimento di Mineralogia e Petrologia & Istituto di Geoscienze e Georisorse , c.so Garibaldi 37, 35122 Padova, ITALY

* To whom corresspondence should be addressed. E-mail: montomoli@dst.unipi.it

The superposition of the three main tectonic units building up the core of the Himalayan chain (Lesser Himalaya, Higher Himalayan Crystallines and Tibetan Sedimentary Sequence) have been recognized and mapped also in the Bhutan Himalaya (Gansser 1983, Bhargava 1995, Grujic et al. 1996, 2002, Davidson et al. 1997). Among the main units also the main tectonic discontinuitis, such as the southward thrusting MCT and the northward faulting STDS, have been detected. The HHC, bounded by the nearly coeval MCT and STDS (Hodges et al. 1992), has been interpreted as an extruding wedge (Burchfield et al. 1992, Hodges et al. 1992). Main models regarding the extrusion of the HHC propose a major component of simple shear near the boundaries of the wedge while a pure shear component could accomodate deformation in its central portion (Grasemann et al. 1999, Grujic et al. 2002).

Our work focused in western Bhutan where structural analyses have been performed mainly in the HHC, expecially in its central and upper portion cropping out North of Thimpu. Well developed extensional shear zones have been recognized in gneiss and subordinately in leucogranites. Shear zones strike NE-SW and dip toward the South. Kinematic indicators mainly represented by shear band cleavages and mica fishes point out a top-to-the-SW sense of shear. Microstructural analyses highlight the main metamorphic minerals are deformed by the extensional shear zones while deformation mechanism show ductile up to brittle conditions of deformation. These shear zones could accomodate the pure shear component of deformation expected to be localized in the core of the extruding wedge. Moving upward, at the boundary between HHC and TSS, the extensional deformation of the STDS is localized along a ductile shear zone at the base of the Chekha Formation in the TSS (Grujic et al. 1996). Our meso and microstructural data pointed out some similarities between the lower part of the Checka formation and the North Col formation cropping out in the Everest area and in western Nepal (Carosi et al. 1998).

References

Bhargava ON.1995. *The Bhutan Himalaya: a geological account*. Geol. Survey of India, special publ, 245 p

Burchfield BC, Z Chen, KV Hodges, Y Liu, L Royden, C Deng and J Xu. 1992. The South Tibetan Detachment system, Himalayan Orogen. Extension contemporaneous with and parallel to shortening in a collisional mountain belt. *Geological Society of America, Special paper* **269**: 1-41

Carosi R, B Lombardo, G Molli, G Musumeci and PC Pertusati. 1988. The South Tibetan Detachment system in the Rongbuck valley, Everest region. Deformation features and geological implications. *J Asian Earth Sci* **16**: 299-311

Davidson C, D Grujic, LH Hollister and S Schmid. 1997. Metamorphic reactions related to decompression and synkinematic intrusion of leucogranite, Hih Himalayan Crystallines. *Bhutan. J Met Geol* **15**: 593-612

Gansser A. 1983. *Geology of the Bhutan Himalaya*. Birkhauser Verlag, Basel. 181p

Graseman B, H Fritz and JC Vannay. 1999. Quantitative kinematic flow analyses from the Main Central Thrust Zone (NW Himalaya, India): implications for a deceleratimg strain path and the extrusion of orogenic wedges. *J Struct Geol* **21**: 837-853

Gruijc D, M Casey, C Davidson, LS Hollister, R Kundig, T Pavlis and S Schmid. 1996. Ductile extrusion of the Higher Himalayan Crystalline in Bhutan: evidence from quartz microfabrics. *Tectonophysics* **260**: 21-43

Gruijc D, LS Hollister, R Parrish.2002. Himalayanmetamorphic sequence as an orogenic channel: insight from Bhutan. *Earth and Planet Sci Letters* **198**: 177-191

Hodges KV, BC Burchfiel, LH Royden, Z Chen and Y Liu. 1992. The metamorphic signature of contemporaneous extension and shortening in the central Himalayan orogen: data from the Nyalam transect, southern Tibet. *J Metamorphic Geol* **11**: 721-737

Structural data from lower Dolpo (western Nepal)

Rodolfo Carosi†, Chiara Montomoli†* and Dario Visonà‡

† Dipartimento di Scienze della Terra & Istituto di Geoscienze e Georisorse, via S.Maria 53, 56126 Pisa, ITALY
‡ Dipartimento di Mineralogia e Petrologia & Istituto di Geoscienze e Georisorse , c.so Garibaldi 37, 35122 Padova, ITALY

* To whom correspondence should be addressed. E-mail: montomoli@dst.unipi.it

Structural investigation in Lower Dolpo (Western Nepal) led to recognize the main tectonic setting of the area. A NE-SW structural transect confirms the presence of the three main tectonic units building up the chain that from bottom to top are represented by the Lesser Himalaya (LH), the Higher Himalayan Crystalline (HHC) and the Tibetan Zone (TZ). Different metamorphic and structural evolution have been recognized along the study transect in the TZ and in the HHC. The TZ is characterized by two main deformation phases both developed under a low-grade metamorphic facies of metamorphism. An increase of both metamorphism and deformation has been detected moving across the TZ approaching towards the lower HHC.

The HHC has been deformed under amphibolite facies metamorphism and the main fabric is represented by an S_2 mylonitic schistosity. It is worth noting the occurrence of a ductile shear zone in the middle part of the HHC (Tojem shear zone) with a top to the south sense of shear. It divides the HHC in two units. The main differences between the two units are the presence of sillimanite developed after the main Barrovian minerals and leucogranite bodies in the upper unit. The Higher Himalayan Cryistalline has been interpreted as an extruding wedge of crystalline rocks bounded by the MCT at the base and by the STDS at the top (Burchfiel et al. 1992, Hodges et al. 1992, Graseman et al. 1999, Gruijc et al. 1996, 2002).

By the way even if the STDS has been traced for several hundred kilometers along the Himalayan chain, in this area the contact is reported to be transitional (Fuchs and Frank 1970, Fuchs 1977). In the study area the two tectonic units get in touch through a thick sequence of carbonatic rocks and our data point out the presence of a metamorphic jump passing from the upper TZ to the lower HHC. The biotite-bearing marbles of the metapelite sequence of the TZ get in contact with the underlying diopside- and forsterite-bearing marbles of the sillimanite-bearing metapelite sequence of the HHC. In addition in the TZ the strain increases towards the boundary between HHC and TZ and the deformation mechanisms change from pressure solution to crystalline plasticity going down from Ordovician limestones to the marbles of the "Dhaulagiri Limestone". The contact zone is characterized by asymmetric folds and kinematic indicators with a top-to-the NE vergence, connected to a down-to-the NE tectonic transport. On the basis of these features we regard the boundary between HHC and TZ as a high strain extensional zone, linked to the STDS.

References

Burchfield BC, Z Chen, KV Hodges, Y Liu, L Royden, C Deng and J Xu. 1992. The South Tibetan Detachment system, Himalayan Orogen. Extension contemporaneous with and parallel to shortening in a collisional mountain belt. *Geological Society of America, Special paper* **269**: 1-41

Fuchs G and W Frank. 1970. The geology of West Nepal between the rivers Kali Gandaki and Thulo Bheri. *Jahr der Geol Bund Wien* **18**: 1-103

Fuchs G. 1977. The geology of the Karnali and Dolpo regions, Western Nepal. *Jahr der Geol Bund Wien* **120**: 165-217

Grujic D, L Hollister and R Parrish. 2002. Himalayan metamorphic sequence as an orogenic channel: insight from Bhutan. *Earth and Planet Sci Letters* **198**: 177-191

Graseman B, H Fritz and JC Vannay. 1999. Quantitative kinematic flow analyses from the Main Central Thrust Zone (NW Himalaya, India): implications for a deceleratimg strain path and the extrusion of orogenic wedges. *J Struct Geol* **21**: 837-853

Gruijc D, M Casey, C Davidson, LS Hollister, R Kundig, T Pavlis and Schmid. 1996. Ductile extrusion of the Higher Himalayan Crystalline in Bhutan: evidence from quartz microfabrics. *Tectonophysics* **260**: 21-43

Gruijc D, LS Hollister and R Parrish.2002. Himalayanmetamorphic sequence as an orogenic channel: insight from Bhutan. *Earth and Planet Sci Letters* **198**: 177-191

Hodges KV, BC Burchfiel, LH Royden, Z Chen and Y Liu. 1992. The metamorphic signature of contemporaneous extension and shortening in the central Himalayan orogen: data from the Nyalam transect, southern Tibet. *J Metamorphic Geol* **11**: 721-737

Testing Models of MCT Reactivation vs. Duplex Formation in the Kumuan and Garwhal Himalaya, India

Julien Célérier*, T Mark Harrison and William J Dunlap

Research School of Earth Sciences, The Australian National University, Canberra, ACT 0200, AUSTRALIA

* To whom correspondence should be addressed. E-mail: julien.celerier@anu.edu.au

We present preliminary results of the thermochronologic, microstructural and metamorphic evolution of the Kumaun and Garhwal Himalaya in the vicinity of the Alaknanda and Bhagarathi rivers, northern India. Samples of quartzite, schist and gneiss were collected from the Lesser Himalayan and Greater Himalayan sequences to explore the sequence of thrusting. We find that within the duplex of Lesser Himalayan rocks (Srivastava and Mitra, 1994), microstructures suggest that temperatures (and/or strain rates) during deformation did not vary significantly in the transport direction. Thermometric estimates from carbonaceous material are consistent with this observation. In contrast, the upper Lesser Himalayan sequence and MCT zone show strong gradients in quartz microstructure, metamorphic grade, thermal structure and age of textural development, with extensive reworking of earlier kyanite grade fabrics. In order to assess the conditions and sequence of thrusting, within and beneath the MCT zone, a series of thermochronologic measurements (40Ar/ 39Ar) on fabric-forming white micas have been made as well as a suite of thermometric analyses on carbonaceous material. Preliminary results indicate that thrust sheets immediately below the MCT zone cooled through the muscovite closure temperature as late as 4 Ma. Thermometric analyses on adjacent samples indicate peak metamorphic temperatures of 550°C. Lesser Himalayan quartzites up to 30 km south of the MCT record Ar/Ar ages of ~20 Ma and peak temperatures in the vicinity of 300°C. Work aimed at understanding the significance of these early results in the context of activity along the MCT is ongoing.

References

Srivastava, Pand Mitra G. 1994. Thrust geometries and deep structure of the outer and Lesser Himalaya, Kumaon and Garhwal (India); implications for evolution of the Himalayan fold-and-thrust belt: *Tectonics*, v. 13, p. 89-109

Numerical simulation of fault development in fold-and-thrust belt of Nepal Himalaya

D Chamlagain* and D Hayashi

Department of Physics and Earth Sciences, University of the Ryukyus, Nishihara, Okinawa, 903-0213, JAPAN

* To whom correspondence should be addressed. E-mail: dchamlagain@hotmail.com

The Himalaya, a fold-and-thrust belt on the northern margin of the Indian continent, is characterized by a series of foreland propagating thrust system. From north to south these are: the Main Central Thrust (MCT), the Main Boundary Thrust (MBT) and the Main Frontal Thrust (MFT) (Schelling and Arita 1991). These intracrustal thrusts are splay thrusts of the Main Himalayan Thrust (MHT), which marks the underthrusting of Indian lithosphere beneath the Himalayas and Tibet. Geodetic and microseismic data have revealed stress accumulation due to mid-crustal ramp, which acts as a geometrical asperity during interseismic period. The stress state and seismicity in the Himalaya is largely influenced by the nature and geometry of MHT. Further, structural and seismic data show segmentation and variation in geometry of the MHT in Nepal Himalaya. It is well understood that neotectonics and present-day seismicity of the Himalaya are largely controlled by its activity. Thus, it is essential to gain better understanding of deformation along different structural sections of Nepal Himalaya.

In the present study, we examined the state of stress in eastern, central and western Nepal Himalaya using 2D elastic finite element method under plane strain condition. We chose three structural cross-sections from east (Schelling and Arita 1991), central (Upreti and Le Fort 1999) and western (Upreti and Le Fort 1999) Nepal Himalaya. Detailed analysis of the medium-scale seismicity has shown the existence of several distinct clusters in eastern, central and western Nepal (Pandey et al. 1999). The projection of events on structural cross-sections reveals rounded shape in central Nepal where center is located at flat-ramp transition whereas in western Nepal cluster is elongated and nearly horizontal. The structural cross-sections used by our simulation represent these clusters as microseismic zones.

This study mainly focuses on applications of numerical modelling technique and the finite element method to compute stresses and faults as a function of rock layer properties, convergent displacement and boundary condition in the convergent tectonic environment of Nepal Himalaya. However, interpretation of the simulated models remains ambiguous to some extent because of the limitations of elastic modelling. Despite its limitations, our models still allow us comparison with geological, microseismic and geophysical data. The results of this simulation are compared with three cross-sections of eastern, central and western Nepal by using recordings of neotectonics and microseimicity of the area. The stress distribution pattern shows similarity in magnitude and orientation in east, central and western Nepal Himalaya. Compressive state of the stress is found in all models. The magnitude of principal stresses mainly depends upon rock layer properties and applied convergent displacement. With increasing convergent displacement, the magnitude of σ_1 increases and its axis rotates towards horizontal resulting thrust fault.

Failure analysis demonstrates realistic fault patterns on the profiles of Nepal Himalaya. We have successfully computed several active faults at their proper locations, which corresponds the field observations. Active faults both normal and thrust types are predicted in Lesser Himalaya, Siwalik and the frontal part of MFT. All models predict faulting to initiate at depth and to transmit to surface with increasing convergent displacement and finally propagate towards south. This is consistent with the sequence of thrust development in Himalayan fold-and-thrust belt. The distribution of simulated faults seems to associate with the major thrusts e.g. MBT and MFT forming north dipping imbricated zone as revealed by field study (e.g. Nakata 1989). For eastern and central Nepal, the simulated fault pattern is similar but for western Nepal thrust fault emerges in shallow depth under the same convergent displacement suggesting difference in geometry of MHT and convergence displacement. Moreover, we observed faults around the mid-crustal ramp, which shows the active nature of MHT. It could be attributed to interseismic stress accumulation around the flat-ramp-flat region. Thus, our models clearly indicate that present-day tectonic activities are mainly concentrated around the mid-crustal ramp, MBT and MFT of the fold-and-thrust belt of Nepal Himalaya.

References

Nakata T. 1989. Active faults of the Himalaya of India and Nepal. *Geol Soc Amer Spec Paper* **232**: 243-263

Pandey MR, RP Tandukar, JP Avouac, J Lave and J P Massot. 1995. Interseismic strain accumulation on the Himalayan crustal ramp (Nepal). *Geophys Res Lett* **22**: 751-754

Schelling, D and K Arita. 1991. Thrust tectonics, crustal shortening, and the structure of the far eastern Nepal Himalaya. *Tectonics* **10(5)**: 851-862

Upreti BN and P Le Fort. 1999. Lesser Himalayan crystalline nappes of Nepal: problems of their origin. In Macfarlane, A, R B Sorkhabi, and J Quade (eds) *Himalaya and Tibet: Mountain Roots to Mountains top*, *Geol Soc Amer Spec Paper* **328**, 225-238

Miocene collision-related conglomerates near Dazhuqu and Xigaze, Yarlung Tsangpo suture zone, Tibet

Angel On Kee Chan†*, Jonathan C Aitchison†, Badengzhu‡ and Lan Hui†

† Tibet Reseach Group, Department of Earth Sciences, James Lee Bldg., University of Hong Kong, Pokfulam Road, Hong Kong SAR, CHINA
‡ Geological Team No. 2, Tibet Geological Survey, Lhasa, Tibet, CHINA

* To whom correspondence should be addressed. E-mail: chanangel@hkusua.hku.hk

The conglomeratic Dazhuqu and Qiuwu formations are correlative units associated with the Gangrinboche facies of southern Tibet. Rocks of this facies crop out for >2000 km along the strike of Yarlung Tsangpo suture zone from west of Mt Kailas (81°E) to east of Namche Barwa (95°E). As these predominantly coarse clastic rocks record tectonic activity associated with the collision between India and Eurasia their detailed study should further clarify our understanding of this event.

Dazhuqu and Qiuwu are the local names used in mapping near the towns of Xigaze and Dazhuqu. The lowermost conglomerates of these units rest unconformably on an eroded surface of Lhasa terrane rocks. This surface locally has considerable relief. Dazhuqu and Qiuwu formations are both characterized by south-dipping strata. They lie in the footwall of a major north-directed thrust fault of regional extent, which places the hanging wall of Xigaze terrane rocks above them.

Clastic detritus within the formations is sourced from all terranes nearby. Clasts include porphyritic volcanic rocks from the Lhasa terrane; gabbro, serpentinite and ultramafics from the Dazhuqu terrane; green and red cherts from the Bainang terrane; and distal continental margin sedimentary rocks from the Indian terrane. Clasts immediately above the basal unconformity are predominantly derived from the Lhasa terrane. The dominant source of detrital clasts exhibits a gradual change up-section from the north (the Lhasa terrane) to the south of the suture zone (the Indian and other nearby terranes) (Aitchison et al. 2002). This indicates that the conglomeratic succession records tectonic, or otherwise, induced changes in relief during the time of its deposition. Lower Cretaceous radiolarians from red chert clasts fingerprint one of the source terranes.

We report the discovery of tuffaceous layers interbedded within the Dazhuqu Formation as a significant result from this study. These pyroclastic deposits are associated with a magmatic suite, which also intrudes the conglomerates. Earlier works have dated these intrusions and used their age as a constraint on the minimum age of the conglomerates along the suture. The discovery of these tuffs within the conglomerates obviously provides a direct constraint on the timing of their deposition and places further constraints on the timing of collision-related events.

References

Aitchison JC, AM Davis, Badengzhu and H Luo. 2002. New constraints on the India-Asia collision: The Lower Miocene Gangrinboche conglomerates, Yarlung Tsangpo suture zone, SE Tibet. J *Asian Earth Sci* **21**: 253-256

Presence of two plume-related volcanic events along the Indian northern passive margin evidenced by the geochemistry of the Carboniferous Baralacha La dykes, the Permian Panjal traps and the Drakkar Po phonolites

F Chauvet†, H Lapierre†, D Bosch‡, F Bussy§, JC Vannay§, GH Mascle†*, P Brunet¶, J Cotten# and F Keller†

† Department of Mineralogy and Petrology, University of Gent, 281/S8 Krijgslaan, 9000 Gent, BELGIUM
‡ UMR-CNRS 5568, Place Bataillon, F. 34095 Montpellier
§ BFSH2, UNIL, CH-1O15, Lausanne
¶ UMR-CNRS 5563, 38 rue des 36 Ponts, F. 31400 Toulouse
 # UMR-CNRS 6538, Place Nicolas Copernic, F. 29380 Plouzané

* To whom correspondence should be addressed. E-mail: gmascle@ujf-grenoble.fr

The built-up of the Himalayan Ranges is related to the collision of the Indian and Asian plates which occurred 52 Ma ago. Subduction-related magmatism developed, south of the Tibet block while the Indian northern margin remained passive. During the collision, the Indian northern margin was dismembered in several tectonic units, caught between the High Himalayan Cristalline domain and the Indus-Zangbo suture. These tectonic units are largely exposed in the Zanskar, Spiti and Upper Lahul areas in north-western Himalayas.

The pre-rift units consist of platform-type detric sediments ranging in age from the Late Precambrian up to the mid to late Permian; they are characterized by four magmatic events, i.e., the Cambrian to Ordovician granites, the Baralacha La Carboniferous basaltic dykes, the Yunam Early Permian intrusives and the Middle Permian Panjal traps. The latter are related to the Neotethys opening. In the Indus-Zangbo suture, blocks of Late Permian phonolites associated with reefal limestones represent the remnants of the oceanic basin neighbouring the northern Indian passive margin.

The Lower Carboniferous Baralacha La basaltic dykes emplaced along transtensional faults that never affected the "pre-rift units" younger than Early Carboniferous. The basalts exhibit tholeiitic and alkaline affinities. The tholeiites are TiO_2-poor, moderately enriched in light rare earth elements (LREE) $(La/Yb)_N$<2.9), and display Nb(La/Nb=1.5) and Ta negative and Th positive anomalies. The alkali basalts, compared to the tholeiites, have higher TiO_2, rare earth and incompatible trace element contents and LREE enrichments $(3.5<(La/Yb)_N<5.2)$. The Nb and Ta negative anomaly is not systematically present in the alkali basalts. The Nd (+2.3<eNd<-1.3) and Pb isotope compositions of the Baralacha La basalts suggest that they were derived from the partial melting of an enriched OIB mantle source, characterized by an HIMU component, and contaminated by the lower continental crust. The Baralacha La dyke swarms represent the remnants of an early rifting event of the northern Indian passive margin.

Major and trace element analyses show that the Permian Panjal traps exhibit features of continental tholeiites: low TiO_2 contents (<1.6%), LREE enrichments and Nb and Ta negative anomalies (1.25<La/Nb<1.8). The initial Nd and Pb ratios show that the Panjal traps derived from an enriched OIB-type mantle source $(-1.5<e(Nd)_i<+0.8)$, contaminated by the upper continental crust (high Pb/Pb ratios, low $e(Nd)_i$ values). The Drakkar Po phonolites derived from melting of an enriched OIB mantle source $(+4<e(Nd)_i<+6)$ but are devoid of crustal contamination.

Remnants of volcanic suites related to the Neotethys opening are found also in the Hawasina nappes and Saih Hatat tectonic window, exposed in the Oman Ranges. The basalts of the Hawasina basin exhibit tholeiitic and alkaline affinities and derived from the mixing of depleted and enriched mantle sources without crustal contamination. In contrast, the low $e(Nd)_i$ values and the initial Pb isotopic ratios indicate that the enriched mantle source of the mafic lavas erupted on the Arabian platform (Saih Hatat) have features consistent with contamination by the lower crust. Thus, the Permian mafic lavas related to the Neotethys opening exhibit features typical of within-plate volcanism. Continental crust is involved solely in the genesis of the volcanics erupted on the Indian and Arabian margins. According to the palinspatic maps for Permian times, the Indian plate was close to the Arabian plate. This geographic layout and the similarities of the mantle sources of the Permian volcanics emplaced on the northern Gondwana margin and in the Neotethyan basin suggest the presence of a wide igneous province (2000 to 3000 km long). The latter could be linked to the melting of a large plume (Tethyan plume) or to activity of some smaller hot spots.

Sedimentation of the Jianggalesayi basin and its response to the unroofing history of the Altyn Tagh, northern Tibetan Plateau

Zhengle Chen*, Xiaofeng Wang, Jian Liu, Xuanhua Chen, Zhiming Sun and Junling Pei

Institute of Geomechanics, Chinese Academy of Geological Sciences, Beijing 100081,PR CHINA

* To whom correspondence should be addressed. E-mail: chenzhengle@263.net

....

The uplift of the Tibetan plateau is one of the most prominent geological event of the past 50 Ma. However, the timing and range of the uplift are still poorly constrained, and little attention has been given to the elevation history of mountains in northern plateau (Sobel and Trevor 1997, Zheng et al. 2000). In this study, we present new evidence from the sedimentation in the foreland basin to discuss the exhumation history of the Altyn Tagh in the northern Tibetan plateau.

Geological setting

The Jianggeleshayi basin is located on the northwestern edge of the Altyn Tagh, one of northwestern boundary mountains of the plateau. More than 3 km in thick Mesozoic to Cenozoic sedimentary rocks are continuously exposed in this foreland basin along the northwestern side of the northern Altyn Tagh fault (Cowgill et al. 2000). These Mesozoic to Cenozoic rocks can be divided into seven segments, including Jurassic Ye'erqiang Formation, Cretaceous Kezilesu Formation, Early Tertiary Kumugeliemu Formation, Oligocene to Miocene Wuqia Formation, Pliocene Atushi Formation, Early Pleistocene Xiyu Formation and Middle Pleistocene Wusu Formation according to the geological map of the Xinjiang BGMR (1993). A gently plunging anticline, the Jianggalesayi anticline is composed of these sedimentary units with Jurassic in the core, and is unconformably overlain by Middle Pleistocene Wusu conglomerate. Jianggeleshayi normal- and strike-slip fault cuts through the northwestern side of the fold (Cowgill et al. 2000). Field measurement of these sedimentary units in the northwestern side of the Jianggeleshayi normal fault was firstly completed in 2000 and about 200 samples were collected. More than 700 Cenozoic paleomagnetic samples were collected again to date the Cenozoic rocks in the summer of 2003.

Sedimentary features

The Jurassic Ye'erqiang Formation is composed of colorful fluvial and lacustrine coal-bearing sediments, which are mostly grey to dark, and brown sandstones interbedded with mudstones. The Cretaceous Kezilesu Formation is mainly composed of brown-grey sandstones with a few mudstones and conglomerates in bottom, full of calcite nodule, and mostly sand and mud as cement, showing alluvial fan and lacustrine sedimentary features. The Early Tertiary (Paleocene to Eocene) Kumugeliemu Formation is alluvial fan deposit, and composed of red to brown sandstones and conglomerates interbededd with mud-bearing sandstones and mudstones. The Wuqia Formation can be divided into two parts. The lower part is mainly composed of grey to red sandstones and siltstones. The upper one is mostly composed of gray conglomerates interbedded with mud-sandstones, behaving as a kind of fluvial deposits. The Atushi Formation is composed mainly of pluvial-circle sediments, having grey to brown conglomerates at the bottom and changing upwards into sandstones and mudstones. The Xiyu Formation is mainly composed of grey thick-bedded cobblestones with a few sandstone lenticular bodies, characterized by a rapid accumulated feature. The Wusu Formation is composed of fluvial terrace conglomerates.

Field measurements of ratio of conglomerate units in stratigraphic layer show a rapid increase of the ratio occurred in the lower part of the Wuqia Formation. The lower part of the section is dominated by fine-grain sandstone or siltstone, while the upper one is dominantly composed of coarse-grained conglomerates. If we suggest a stable sedimentary velocity in a geological time-period and take 35 Ma and 5 Ma as the beginning and end ages of the sedimentation of the Wuqia Formation (because the paleomagnetic data are still in the lab), the boundary age of the lower part with the upper should be ca. 25 Ma. And according to the thickness of the stratigraphic units, sedimentary velocities could be calculated out: 4.8m/Ma during the Cretaceous, 12m/Ma during the Paleocene to Eocene, 19.7m/Ma during the Oligocene to Miocene, 180.9m/Ma during the Pliocene, and 651.9m/Ma during the Early Pleistocene.

Composition of detritus in sandstone and conglomerate clast

44 samples are selected to analyze the composition of detritus in sandstone by point-counting of more than 300 grains per thin section. Overall, sandstone samples are quartzolithic arenites (Qm=55, F=20, Lt=25). However, lithic fragments (Lt) are less than 20% in sandstone from the Kezilesu(K) to Wuqia Formation and larger than 20% in sandstones from the uppermost part of the Wuqia Formation, while monocrystalline and polycrystalline quartz fragments (Qt=Qm+Qp) decrease from >50 into <50 at the same time. The rapid decrease of volcanic lithic fragments (Lv) occurred between the lower part and upper part of the Wuqia Formation (from 8 down to 5). The metamorphic lithic fragments (Lm), dominated by metamorphic-sedimentary lithic grains, increase from the bottom of the upper Wuqia Formation, and reach its peak at the uppermost part of the Quqia Formation(33). They are also major kind of detritus in sandstone of the Atushi Formation, but Lm is usually less than 5 in Xiyu Formation. Sedimentary lithic fragments (Ls) begin to increase in the uppermost part of the Wuqia Formation and become the dominant composition in Early Quaternary Xiyu conglomerate.

47 sites for point counting analysis of clast composition in conglomerate were completed in the field in 2003. The results show that clast composition in conglomerate is dominated by metamorphic rocks. The content is usually larger than 60%. sedimentary clast and is mainly composed of limestones. The rapid increase of its content occurred in the bottom of the Atushi Formation. The granitic clast is usually less than 10% in content and a few clast is sour or basic volcanic rocks in this section. The ecologite clasts can only be found in the Middle Pleistocene Wusu Formation.

Unroofing history of the Altyn Tagh

The sedimentary features in the Altyg Tagh basin together with point counting analyses of detritus in sandstone and conglomerate indicate the change of its paleogeomorgraphy as the main resource of sediments in this basin and thus the exhumation and uplifting history of the mountain. Paleozoic bimodal volcanic assemblage was firstly eroded during Cretaceous to Early Tertiary. During early Miocene, rapid uplift of mountains for the first time resulted in the exhumation of the Upper and Middle Proterozoic basement. Secondary rapid uplift began in the Late Miocene, while the fastest uplift of the mountains occurred since Late Pliocene. This has resulted in the exposition and erosion of the middle and lower part of the Proterozoic and Archean rocks. Deeply buried basement rocks such as ecologite began to be eroded till the Middle Pleistocene. This result is fairly consistent with our previous suggestions of the uplifting of the Altyn Tagh, especially the rapid uplift of the Altyn Tagh and rapid strike slip faulting of the Altyn Tagh fault at ca. 8 Ma, as has been indicated by fission track dating method of apatites, and the changes in values of $\delta^{18}O$ and $\delta^{13}C$ in carbonate cements from the same strata in this basin (Chen et al. 2002).

References

Chen ZL, XF Wang, XH Feng, CQ Wang, XH Chen, and J Liu. 2002. New evidence from stable isotope for the uplift of mountains in northern edge of the Qinghai-Tibetan plateau. *Sciences in China (B)*, **32(Suppl.)**:1-10

Cowgill E, A Yin, XF Wang, and Q Zhang. 2000. Is the North Altyn fault part of a strike-slip duplex along the Altyn Tagh fault system?. *Geology* **28(2)**: 255-258.

Sobel ER, and AD Trevor. 1997. Thrusting and exhumation around the margins of the western Tarim basin during the India-Asia collision. *J Geoph Res*, **102(B3)**: 5043-5063

Xinjiang BGMR(Xinjiang Bureau of Geology and Mineral Resources). 1993. *Geologic history of the Xinjiang Uygur Autonomous Region*. Beijing: Geological Publishing House, 681 p.

Zheng HB, C Powell, and ZS An. 2000. Pliocene uplift of the northern Tibetan Plateau. *Geology*, **28(8)**:715-718

The exhumation rate of Dabie orogen: Evidence from garnet diffusion zoning

Hao Cheng†*, Daogong Chen‡, and Etienne Deloule§

† School of Ocean and Earth Science, Tongji University, Shanghai, PR CHINA
‡ School of Earth and Space Sciences, University of Scicence and Technology of China, Hefei, PR CHINA
§ CRPG-CNRS, Nancy, FRANCE

* To whom correspondence should be addressed. E-mail: chenghao@mail.tongji.edu.cn

Dabie-Sulu terrain is a joint suture formed by Triassic collision between the northern margin of Yangtze craton with southern margin of Sino-Korean craton. Coesite and diamond-bearing eclogites and other UHP/HP rocks have been discovered there, and it is thought to be the largest HP-UHP terrain all over the world. From north to south, Dabie terrain is separated into four different petro-tectonic unites by two NW and EW trend fault systems: the Northern Huaiyan, Northern Dabie metamorphic complex, Southern Dabie UHP metamorphic belt and Susong metamorphic complex (Liou et al. 1995). Okay (1993) divided Southern Dabie into northern hot eclogite and southern cold eclogite zone based on metamorphic temperature and pressure. Coesite-bearing hot eclogite has higher PT as to 640⁰C and 27-40 kbar and cold eclogite has lower PT as to 580-635⁰C and 20-24 kbar, which contain no coesite and underwent only HP metamorphism (Carswell et al. 1997). Sulu HP-UHP terrain is believed as the eastern extension of Dabie terrain translated by Tanlu fault. Our samples were collected from this orogen, which are Bixiling (BXL) eclogites, the largest coesite-bearing garnet peridotite-eclogite complex in Southern Dabie UHP terrain; JInheqiao(JHQ) eclogites is in south side of Bixiling eclogite; Qinglongshan (QLS) eclogite is in Southern end of Sulu terrain,Donghai; Huangzhen (HZ) eclogites locate at the boundary between Southern Dabie UHP terrain and Susong HP terrain in Taihu, which is cold eclogite. Raobazhai (RBZ) eclogite is an ultramafic-eclogite complex, Nothern Dabie metamorphic zone. It has granlulite regression after elcogite peak metamorphism. Huangtuling (HTL) granulite and acidic granulite from Luotian Hubei belongs to west part of Northern Dabie Terrain, the core of Luotian complex. Except for HTL granulite, the above five rocks are believed to be involved in Triassic HP-UHP metamorphism.

Based on diffusion theory we analyzed garnet zoning for these six HP-UHP metamorphic rocks from Dabie and modeled these different diffusion zoning, followed the methods by Duchene et al. (1998), Lommis et al. (1975), Perchuk et al. (2002), Lasaga (1983) and Ganguly et al. (2000). The estimated peak metamorphic temperature and pressure, and calculated cooling rate from different diffusion models for garnets are described in **Figure 1**. Since the meaning lowest temperature for Fe, Mg ion exchange between garnet and other

minerals is around 500⁰C, the cooling rate obtained by garnet diffusion usually means its average values for duration from peak metamorphic temperature to about 500⁰C. From **Figure 1** we can see that the cooling rate for BXL eclogite was more than 20⁰C/Ma at beginning, and it has decreased to less than 10⁰C/Ma with time at 500⁰C; JHQ eclogite shows similar zoning pattern with BXL eclogite and its average cooling at rate of about 20-30⁰C/Ma within 10 Ma duration; Garnet modeling for QLS eclogite reveals a faster than 20⁰C/Ma cooling rate. The cooling rate for Dabie and Sulu UHP hot eclogites is comparable. HZ eclogite showed that the adjustment of zoning lasted 20 Ma at an average cooling rate of 8⁰C/Ma after peak temperature. The special zoning for RBZ eclogite was caused by new formed component across a tiny crack diffusion adjustment with the previous garnet parts. The result shows it cooled down to 700⁰C at rate of about 25⁰C/Ma, similar to that of hot eclogite at initial cooling. HTL granulite, different from eclogite, exhumed up to mid-low crust with isothermal depression(ITD) after peak granulite metamorphism and stay
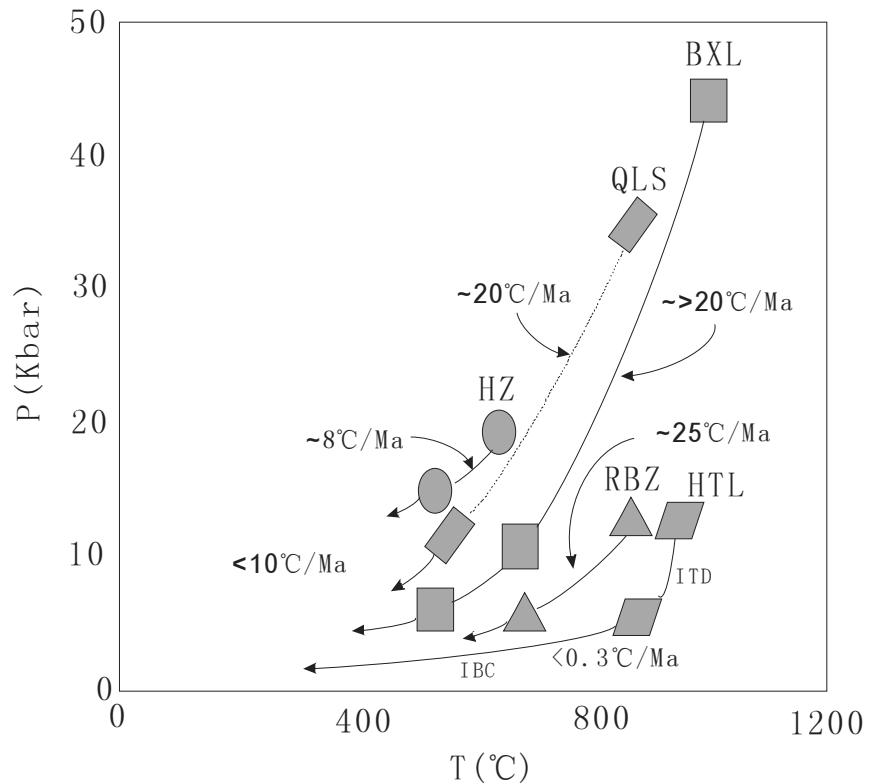
FIGURE 1. Cooling rate of eclogites from Dabie orogen

there for quite long and then its cooling was very slow as to less than 0.3⁰C/Ma without pressure decreasing (IBC) until its exposure to surface by erosion. The rock was not involved in deep subduction unit.

Cooling and exhumation of Dabie orogen rocks by using age data also have very large variations by geochronology. Hacker et al. (2000) obtained an average vertical exhumation rate larger than 2 km/Ma for Dabie-Hongan terrain; Ayers et al. (2002) calculated exhumation rate of 7.1-8.0 km/Ma for Maowu eclogite and only 1.0 km/Ma for Shuanghe UHP rock. Li et al. (2000) released a cooling of 40⁰C/Ma for Shuanghe slate. Based on garnet diffusion kinetics data we acquired approximately similar cooling rates for different petro-tectonic unit of Dabie-Sulu orogen. It is indicated that HP-UHP rocks from Southern Dabie, Northern Dabie and Sulu belong to a coherent orogenic terrain and are product within one episodic event. Even at above 500⁰C, the cooling rate of eclogite is still keep such a process from fast to slow. According to age data of HZ eclogite, we calculated average exhumation of 1.5 km/Ma. Obviously, the obtained cooling and exhumation rate is similar to that of Hacker et al. (2000) for Dabie-Sulu and Ayers et al. (2002) for Shuanghe, but not for Maowu. Compared to Alps and Kazakstan UHP rocks, most of Dabie-Sulu data show relative slower cooling and exhumation rates. Different cooling and uplift reflect different exhumation mechanism, like plate break off, buoyancy and fast erosion. If the exhumation for Dabie rocks is definitely distinguished from that of Alps and Kazakstan, then their tectonic evolution should be different. Study on exhumation rate by modelling of garnet diffusion zoning and geochronology could and should be comparable and complement as well as validate each other.

References

Carswell D, O'P Brien, and R Wilson. 1997. Thermobarometry of phengite-bearing eclogites in the Dabie mountains of central China. *J. Metamor Geol* **15**: 239-252

Duchêne S, S Albarede, and J Lardeaux. 1998. Mineral zoning and exhumation history in the Munchberg eclogites (Bohemia). *Amer J Sci.* **298**: 30-59

Ganguly J, S Dasgupta, and W Cheng. 2000. Exhumation history of a section of the Sikkim Himalayas, India: records in the metamorphic mineral equilibris and compositional zoning in garnet. *Earth Planet Sci Lett* **183**: 471-486

Lasaga AC, SM Richardson, and HD Holland. 1977. The mathematics of cation diffusion and exchange between silicate minerals during retrograde metamorphism . In: Saxena S K.,Bhattacharji, (eds) *Energetics of Geological Processes*. Springer,Berlin. 353-388

Liou JG, and R Zhang. 1995. Significance of ultrahigh-P talc-bearing eclogites assembles. *Mineral Mag* **59**: 93-102

The expansion mechanism of Himalayan supraglacial lakes: Observations and modelling

KA Chikita

Division of Earth and Planetary Sciences, Graduate School of Science, Hokkaido University, Sapporo, 060-0810, JAPAN

For correspondence, E-mail: chikita@ep.sci.hokudai.ac.jp

In 1950's, due to the glacial retreat, supraglacial ponds started to appear on tongues of glaciers in the Himalayas, and have so far been expanding to the extent of moraine-dammed lakes with ca. 1 km² in surface area. Since 1960's, the glacial lake outburst flood (GLOF) has occurred once per three years on average by the collapse of end moraine (Yamada 1998). Three moraine-dammed lakes (Tsho Rolpa and Imja, Nepal and Lugge, Bhutan) were hydrodynamically examined in the past, in order to clarify the expansion mechanism (Chikita et al. 1999, Chikita et al. 2000, Sakai et al. 2000, Yamada et al. 2004).

Figure 1a-c shows the location of Tsho Rolpa and Imja Lakes in Nepal and observation sites on the bathymetric maps. Tsho Rolpa (4580 m asl) is 3100 m long and 450 m wide (surface area, 1.39 km²) and 131 m deep at maximum in 1994, which has been expanding from a supraglacial pond of 0.23 km² in area (Kadota 1994) (Figure 1c). Imja (5010 m asl) appeared as some ponds of 200 m×50 m scale in 1960's, and is 1200 m long, 450 m wide and 92 m deep at maximum in 1992 (Yamada and Sharma 1993) (Figure 1b).

I explored physical conditions of Tsho Rolpa Lake in May - June 1996 and Imja Lake in July 1997. Figure 2 shows longitudinal distributions of water temperature and turbidity and resultant water density. Here, water density is expressed by "density residue" ó, defined by $\sigma = (\rho_{TCP} - 1000) \times 10$, where ρ_{TCP} is bulk density, a function of water temperature T, suspended sediment concentration (SSC) C and water pressure P. Water turbidity (ppm) measured was converted into SSC (mg/l) by using significant correlations ($r^2 = 0.66$ to 0.89) between turbidity and SSC. As a result, Tsho Rolpa has a wind-mixed layer ca. 25 m thick below the surface with nearly uniform SSC and density, while Imja does not have such a mixed layer. The wind-mixed layer is formed by wind-forced vertical mixing and wind-driven currents during the leeward setup of surface water. A difference of the spatial distributions between the two lakes suggests that wind velocity over Tsho Rolpa is much higher than that over Imja Lake. Meanwhile, wind velocity measured near or over the end moraine (site M in Figure 1) is not so different between the two lakes, indicating a diurnal valley wind of 2 to 8 m/s (northwest and west winds in Tsho Rolpa and Imja, respectively) and a nocturnal mountain wind of 0 to 2 m/s. The wind velocity is likely controlled by the topography of end moraine; a top of the end moraine upwind of Imja Lake is higher by 10 to 20 m than the lake level, while that of Tsho Rolpa Lake is almost leveled to the lake surface. It should be noted that in Tsho Rolpa, turbid meltwater inflows at the base of the glacier front, and produces a turbid layer near the bottom. This indicates the occurrence of sediment-laden underflow, originating from near the glacier front. The lake-water temperature ranges from 2 to 8 °C, thus giving water density of 999.85 to 1000.00 kg/m³ for clear water under 1 atm. Water density is thus always more than 1000 kg/m³ at SSC of more than 300 mg/l, since the density of suspended sediment is 2760 kg/m³. Hence, lake water density is controlled by SSC rather than temperature, since dissolved solids are negligible at less than 0.1 mg/l. The spatial patterns of SSC in Figure 2 is thus similar to those of ó. In Imja Lake, there is no bottom layer of high SSC. Thus, neither turbid meltwater inflow nor sediment-laden underflow is produced (Figure 2b). Time series of flow velocity and water temperature were obtained at 25.4 m in depth at site A of Tsho Rolpa Lake (Figure 3). It is seen that when a valley wind blows on daytime, lake currents prevail in the upwind direction with declining temperature. This indicates that return flow occurred to compensate for the leeward water transfer by the upper wind-driven currents. The decline of water temperature shows the upwelling of the lower cold water by the uplift of the pycnocline at ca. 25 m depth (Figure 2a). Thus, a nodal line (black circle in Figure 4) exists on the pycnocline uplake of site A (white circle in Figure 4) during the leeward setup.

A conceptual model of hydrodynamics in Tsho Rolpa is shown in Figure 4. Strong valley winds diurnally blow along the apse line of the lake, and produce wind-driven currents and return flow (vertical water circulation). Meanwhile, turbid
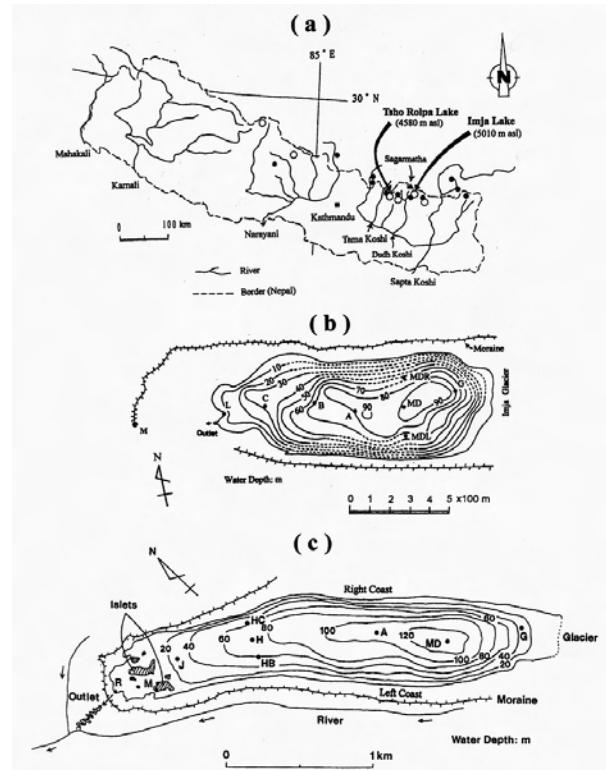
FIGURE 1. (a) Index map of Nepal with locations of lakes studied. The bathymetry and observation sites are given for (b) Imja and (c) Tsho Rolpa Lake. A weather station is at site M in (b) and (c)
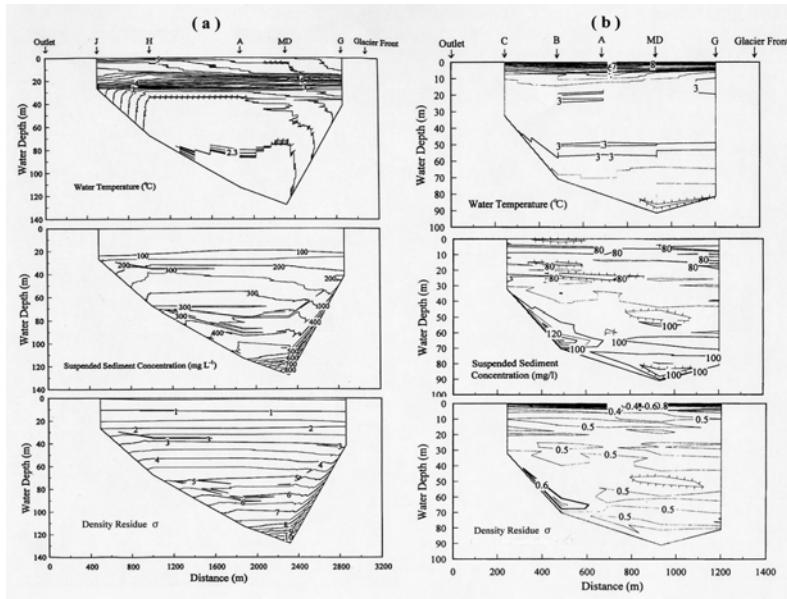
FIGURE 2. Longitudinal distributions of water temperature, suspended sediment concentration (SSC) and density residue in (a) Tsho Rolpa and (b) Imja Lakes
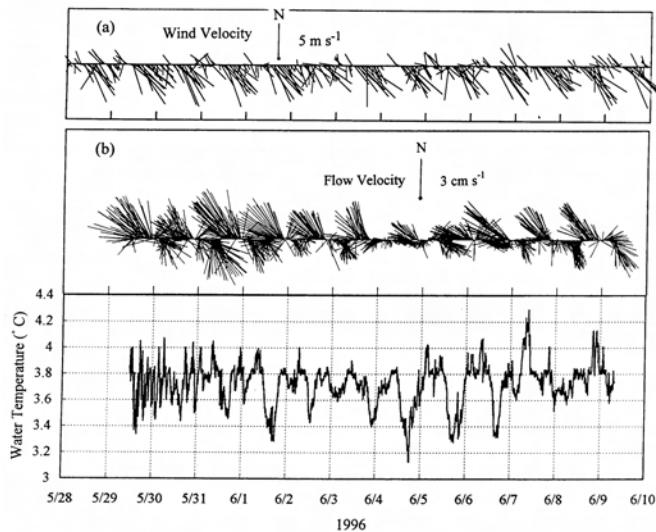
FIGURE 3. Temporal variations of (a) wind velocity at site M and (b) flow velocity and water temperature at site A (25.4 m deep) (see Figure 1 for location)
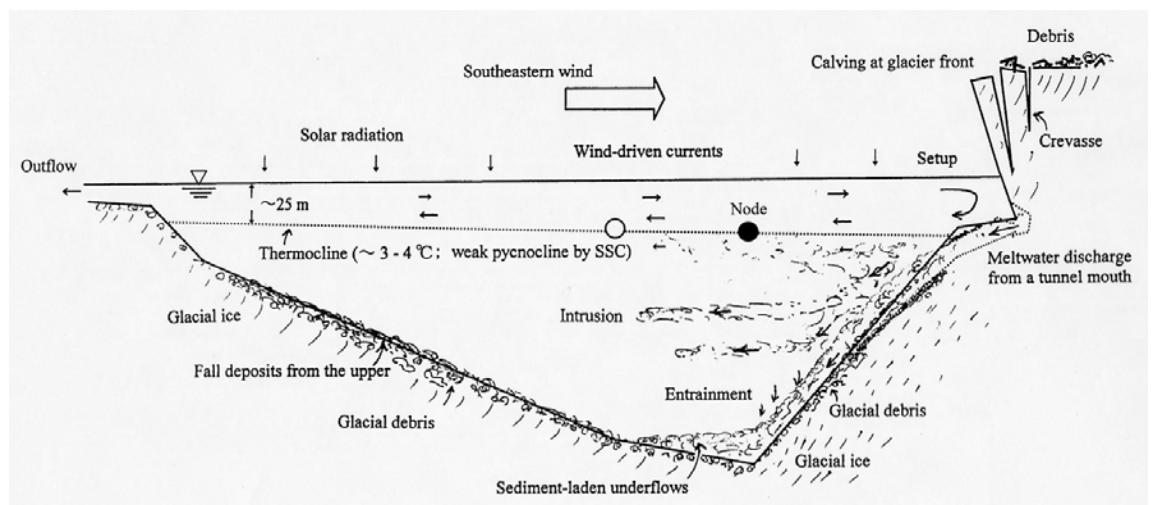
meltwater inflow initiates sediment-laden underflow near the glacier front, which establishes the inner density structure by bifurcation into turbid interflows and consequently limits the vertical wind circulation to the upper layer. The vertical water circulation exalts the ice melt at the base of the glacier front and induces calving at the glacier front, since the radiation-heated surface water is transported toward the glacier front by the wind-driven currents, and then the water cooled by the ice melt is moved toward the outlet by return flow. For Imja Lake, a vertical mixing is probably very weak because of the weakness of wind over lake. The heat transfer within the lake could occur throughout the depths because of the weak density stratification (**Figure 3b**).

3D numerical simulation of wind velocity over glacial lakes was performed, in order to know how the topography of end moraine affects a wind system over lakes. A 3D topographic model around Tsho Rolpa Lake is shown in **Figure 5**. This is set in a calculation domain of x×y×z = 7000m×2000m×400m in size. The topography was made by using a topographic map of 1/50000 scale made in 1997 and considering results of topographic surveys in the past. The glacier front and side moraine's top are 30 m high and 70 m high, respectively above the lake surface of x×y = 3100m×400m (or 1200m ×400m) in size. The height of end moraine above the lake surface was given at 0 m or 20 m. The water depth of the lake is constant at 50 m. Constant wind velocity of 5 m/s was given as the typical velocity of a valley wind (**Figure 3a**). Standard air pressure is 0.6 atm and air density is 0.75 kg/m³, considering highly mountainous conditions. I solved the equations of momentum and continuum under steady state by the finite difference method, in order to get air pressure P and wind velocity (u, v, w). The grid number is x × y × z = 65 × 50 × 44. Each calculation was continued until wind velocity at a point far from the topographic model reached to ca. 5 m/s.

Calculated results are shown as wind vectors at 2 m above the lake surface in **Figure 6**. The 2-m wind velocity ranges from 4.4 to 4.8 m/s for the

FIGURE 4. Conceptual of hydrodynamics in Tsho Rolpa Lake

lake model 3100 m long with the end moraine's top leveled to the lake surface, but 2.6 to 3.0 m/s for that 1200 m long (Figure 6ab). A decrease of fetch (leeward lake length) thus tends to decrease the wind velocity all over the surface. On the other hand, the wind velocity ranged over 1.1 to 3.2 m/s for the model 3100 m long with the end moraine's top 20 m higher than the surface, and over 2.1 to 2.6 m/s in a water area within 1200 m downwind of end moraine (Figure 6c). The topography of end moraine can thus affect greatly a wind-velocity distribution over lake. These calculated results suggest that the weak wind mixing in Imja Lake is due to the topographic feature of the plane end moraine ca. 10 to 20 m higher than the lake surface, in addition to the relatively short fetch.

As a next step, hydrodynamics in Tsho Rolpa (**Figure 4**) will be reproduced by 3D numerical simulation. Moreover, the lake expansion by the melt of glacier ice in contact with the lake basin will be reproduced similarly, in order to clarify the lake expansion mechanism.

FIGURE 5. Topographic model around Tsho Rolpa Lake for numerical simulation

References

Chikita K, J Jha and T Yamada. 1999. Hydrodynamics of a supraglacial lake and its effect on the basin expansion: Tsho Rolpa, Rolwaling Valley, Nepal Himalaya. *Arctic, Antarctic and Alpine Research* **31**(1): 58-70

Chikita K, SP Joshi, J Jha and H Hasegawa. 2000: Hydrological and thermal regimes in a supraglacial lake: Imja, Khumbu, Nepal Himalaya. *Hydrological Sciences Journal* **45**(4): 507-21

Chikita K, J Jha and T Yamada. 2001: Sedimentary effects on the expansion of a Himalayan supraglacial lake. *Global and Planetary Change* **28**: 23-34

Kadota T 1994. Report for the filed investigation on the Tsho Rolpa glacier lake, Rolwaling Valley, February 1993-June 1994. *WECS Report*, N551.489 KAD, 26pp

Sakai A, K Chikita and T Yamada. 2000. Expansion of a moraine-dammed glacial lake, Tsho Rolpa, in Rolwaling Himal. *Limnology and Oceanography* **45**(6): 1401-08

Yamada T. 1998. *Glacier Lake and its outburst flood in the Nepal Himalaya*. Monograph no. 1, Data Center for Glacier Research, Japanese Society of Snow and Ice, 96pp

Yamada T and CK Sharma. 1993. Glacier lakes and outburst floods in the Nepal Himalaya. *Snow and Glacier Hydrology* (Proceedings of the Kathmandu Symposium, November 1992), *IAHS Publication* no. 218: 319-30

Yamada T, N Naito, S Kohshima, H Fushimi, F Nakazawa, T Segawa, J Uetake, R Suzuki, N Sato, Karma, IK Chhetri, L Gyenden, H Yabuki and K Chikita. 2004. Outline of 2002 – research activities on glaciers and glacier lakes in Lunana region , Bhutan Himalayas. *Bulletin of Glaciological Research* **21**: 79-90

FIGURE 6. Calculated wind velocity at 2 m above the lake surface for lake models (a) 3100 m long and (b) 1200 m long with leveled to lake surface, and (c) 3100 m long with end moraine's top at 20 m above the surface

Intracontinental deformation in central Asia: Distant effects of India – Eurasia convergence revealed by apatite fission-track thermochronology

Johan De Grave†‡*, Michael M Buslov§ and Peter Van Den Haute†

† Department of Mineralogy & Petrology, University of Gent, 281/S8 Krijgslaan, 9000 Gent, BELGIUM
‡ Department of Geological & Environmental Sciences, Stanford University, Stanford, USA
§ United Institute of Geology, Geophysics & Mineralogy, Siberian Branch - Russian Academy of Science, Novosibirsk, RUSSIA

* To whom correspondence should be addressed. E-mail: johan.degrave@ugent.be, jdegrave@pangea.stanford.edu

During the Paleozoic Central Asia was the site of large-scale continental growth and accretion around the Siberian craton. By the Late Permian much of Eurasia had been assembled and formed part of the Pangean supercontinent. In Central Asia the Paleozoic basement is characterized by a complex mosaic architecture with various composing blocks mainly bound by large strike-slip faults (Sengör et al. 1993). In the Late Paleozoic and Mesozoic these faults were repeatedly reactivated (Buslov et al. 2003).

After Early Mesozoic break-up of Pangea the southern rim of Eurasia was again characterized by convergent tectonics. In eastern Asia, convergence between the amalgamated Siberian and the composite North China-Mongolian continents led to closure of the Mongol-Okhotsk Ocean. This ocean was closed in a scissors-like manner from west to east in the Jurassic to Early Cretaceous and gave rise to the Mongol-Okhotsk orogeny. To the southwest, closure of the Tethyan basin first led to accretion of several smaller units (e.g., Farah, Karakoram, Pamir, Qiangtang, Lhasa, Indochina) onto the southern, active Eurasian margin in the Late Triassic, Jurassic and Early Cretaceous. These events jointly contributed to the Cimmerian orogeny. Further closure of the Neotethys eventually culminated in the massive India-Eurasia continent-continent collision at the Meso-Cenozoic transition.

Ongoing convergence and indentation of India into Eurasia dominated the Cenozoic tectonic evolution of Asia (**Figure 1**). Strike-slip tectonics and lateral escape of crustal blocks along major shear zones (e.g. Ailao Shan-Red River system) was a key mechanism for accommodating penetration of India into Eurasia during much of the Oligocene. Thrusting, crustal thickening and uplift of the Himalayas and the Tibetan Plateau became an important factor since the Early to Mid-Miocene. A third essential effect of continued convergence between both continents is the reactivation of the inherited structural fabric in the continental interior of Central Asia, far from the active plate boundaries, since the Middle to Late Miocene.

In order to test this model of current deformation in Central Asia and to constrain the timeframe, we performed apatite fission-track (AFT) analyses on crystalline rocks from both the Kyrgyz Tien Shan Mountains and the South Siberian Altai-Sayan Mountains in Central Asia (De Grave and Van Den Haute 2002, De Grave 2003) (**Figure 1**). In the Tien Shan the main sampled area is the Paleozoic basement of the Lake Issyk-Kul region in northeastern Kyrgyzstan. Most samples were collected along elevation profiles in the Kungey and Terzkey ranges. These ranges are primarily formed by Ordovician granitoids and are thrust upon the northern and southern margins of the Cenozoic intramontane Issyk-Kul basin. In the Altai-Sayan Mountains, samples originate from four key regions. The majority of the apatites were collected in the Paleozoic basement rocks of the Plio-Pleistocene Teletskoye graben (northern Siberian Altai-Sayan). Other sample localities include the Chulyshman Plateau,

and the Paleozoic basement of the Cenozoic Chuya-Kurai and Dzhulukul basins.

AFT age and length data from a total of about 75 samples were obtained (around 50 from the Altai-Sayan and 25 from the Tien Shan Mountains). Thermal history models for the studied regions were reconstructed using the AFTSolve modelling software (Ketcham et al. 2000). These models, generally reveal a three-stage cooling history throughout the investigated area, confirming and constraining the Meso-Cenozoic tectonic evolution portrayed above (**Figure 1**).

The modelled t,T-paths show a first stage of Jurassic to Late Cretaceous cooling in both the Tien Shan and Altai-Sayan regions. For the Tien Shan (Issyk-Kul area) the cooling spans much of the Jurassic, until the Early Cretaceous (~180-110 Ma). We attribute this cooling to the denudation of the Issyk-Kul basement associated with tectonic activity during the Cimmerian orogeny. At that time the active southern Eurasian margin, to the (south)west of the current Tien Shan, was the site of accretion and collision of the tectonic units building the present Tethyan belt that ranges from the Hindu Kush (west) to Indochina in the east (**Figure 1**). At the cessation of Mesozoic cooling, the studied rocks in the Issyk-Kul basement reached upper apatite-Partial Annealing Zone (APAZ) temperatures. A Late Jurassic-Mid Cretaceous cooling (~150-80 Ma) also affected all studied rocks in the Altai-Sayan region and brought them to upper APAZ temperatures as well. Considering a normal geothermal gradient of 25 to 30°C/km, the modelled AFT thermal histories indicate the rocks had been brought from below 4 km in the crust to depths of around 2 to 2.5 km after the Mesozoic denudation. In the case of the Altai-Sayan, the cooling is also interpreted as denudation associated with a phase of tectonic uplift. This uplift is thought to be a far-field effect of the major continent-continent collision of amalgamated Siberia with the composite North-China/Mongolia continent. This was a consequence of oblique closure of the Mongol-Okhotsk Ocean that existed between both landmasses. This oblique or scissors-like closure acted from west to east and initially affected the area in West Mongolia, just east of the present Altai orogen.

After the Mesozoic, near-horizontal modelled t,T-paths prevail during the Late Cretaceous and Paleogene and reflect a period of tectonic quiescence and peneplanation throughout Central Asia. Both the thermal history models for the Tien Shan and Altai-Sayan regions exhibit this period of stability. Remnants of this vast Central Asian peneplain have been described from the Tien Shan all the way to the Baikal area. At the end of this period, before onset of rapid Late Cenozoic cooling, most of the investigated apatites remained at upper APAZ temperatures or seem to have just reached lower AFT retention temperatures. This long period of APAZ-residence is corroborated by the thermal signature in the AFT lengths and their frequency distributions. Low mean track lengths (~11 to 14 µm) and negatively skewed distributions are exhibited by all samples.

The present neotectonic reactivation of intracontinental Central Asia is shown by a new cooling stage described by the AFT thermal history models. The models obtained from the Tien Shan apatites exhibit this feature from ~15-10 Ma onwards; while for the Altai-Sayan samples this youngest stage is only seen during the last ~5 Ma. We interpret this young cooling down to ambient surface temperatures as the result of exhumation of the studied rocks to their present outcrop positions.

These observations suggest that reactivation and deformation in the interior of the Eurasian continent is gradually propagating northward through Central Asia since the Miocene as a distant effect of the ongoing indentation of India into Eurasia. Intracontinental, mainly transpressional, reactivation in Central Asia seems to follow an inherited structural pattern. The Mesozoic orogenic belts act as precursors to the Cenozoic and active mountain belts, while the ancestral Mesozoic belts in their turn were built along the inherited Paleozoic structural basement fabric. These multiphased Central Asian structures were rejuvenated in the Mesozoic as far-field effects of the orogeny and accretion acting on the distant continental margins, much in similar fashion as the ongoing India/Eurasia convergence is inducing deformation in the region today.

Our data shows that India/Eurasia convergence is partly accommodated by a northward propagation of deformation though intracontinental Central Asia via inherited large-scale structures. This deformation resulted in transpressional mountain building and roughly 2 km of denudation of the northern Kyrgyz Tien Shan Mountains since the Middle to Late Miocene. Deformation reached the Altai-Sayan area in southern Siberia significantly later. Since the earliest Pliocene this area also underwent about 2 km of denudation. Ongoing research in the vast area of the southern Tien Shan to the East Sayan, near the southwestern edges of the Baikal riftzone, is being carried out to refine and complete this image. Apart from AFT, other low-temperature thermochronometers (U-Th/He and $^{40}Ar/^{39}Ar$) will be applied in this study.

Also, our data suggests that the mechanism of far-field tectonic reactivation of discrete mobile belts cross-cutting the interior of Central Asia is not solely constrained to the Cenozoic framework of India/Eurasia collision. During the Mesozoic the area was subjected to similar reactivation in analogous tectonic regimes linked to continued accretion of the Eurasian continent.

References

Buslov MM, T Watanabe, LV Smirnova, I Fujiwara, K Iwata, J De Grave, NN Semakov, AV Travin, AP Kiryanova and DA Kokh. 2003. Role of strike-slip faults in Late Paleozoic-Early Mesozoic tectonics and geodynamics of the Altai-Sayan and East Kazakhstan folded zone. *Russian Geology and Geophysics* **44**(1-2): 49-75

De Grave J. 2003. *Apatite fission-track thermochronology of the Altai Mountains (South Siberia, Russia) and the Tien Shan Mountains (Kyrgyzstan): relevance to Mesozoic tectonics and denudation in Central Asia* [PhD dissertation]. University of Gent, 289 p

De Grave J and P Van Den Haute. Denudation and cooling of the Lake Teletskoye region in the Altai Mountains (South Siberia) as revealed by apatite fission-track thermochronology. *Tectonophysics*, **349**: 145-159

Ketcham RA, RA Donelick, MB Donelick. 2000. AFTSolve: A program for multi-kinetic modeling of apatite fission-track data. *Geological Materials Research* **2**(1): 1-32

Sengör AMC, BA Natalin and VS Burtman. 1993. Evolution of the Altaid tectonic collage and Palaeozoic crustal growth in Eurasia. *Nature* **364**: 299-307
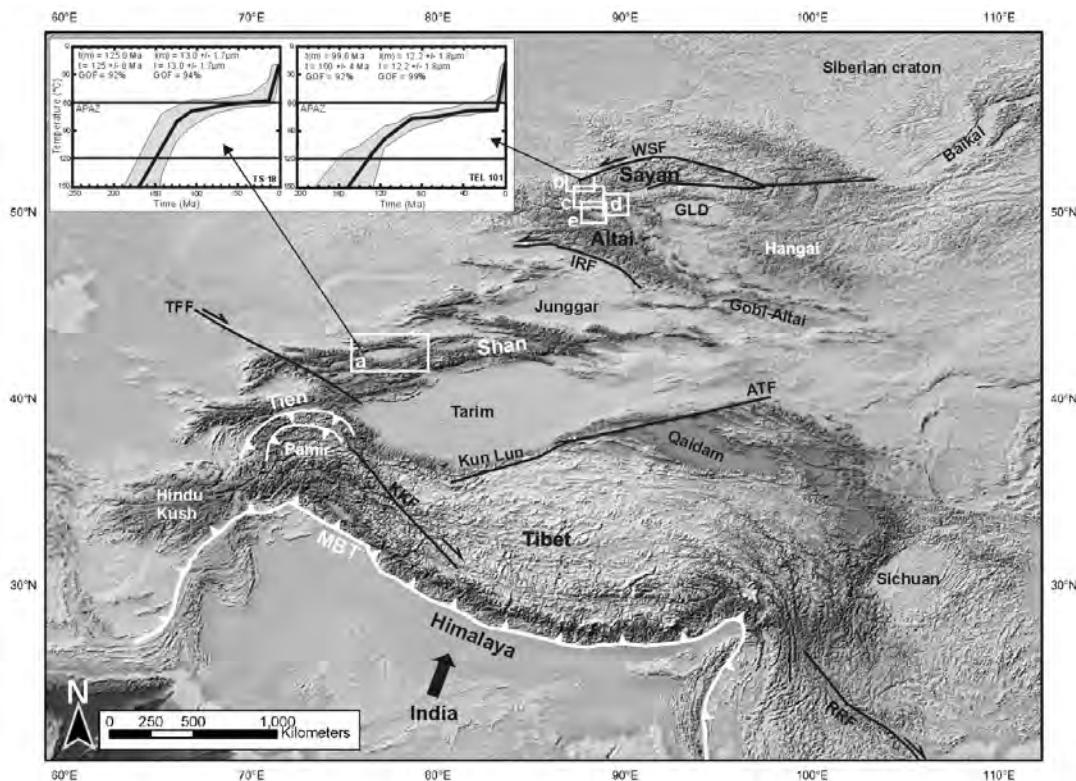
FIGURE 1. DTM of Central Asia indicating major tectonic and structural features: ATF = Altyn Tagh Fault, GLD = (Mongolian) Great Lakes Depression, IRF = Irtysh Fault, KKF = Karakoram Fault, MBT = Main Boundary Thrust, RRF = Red River Fault, TFF = Talas-Fergana Fault, WSF = West Sayan Fault. Sample areas for our AFT research are delineated by the boxes. Tien Shan Mountains: (a) Issyk-Kul basin, Altai-Sayan Mountains: (b) Teletskoye graben, (c) Chulyshman plateau, (d) Dzhulukul basin, (e) Chuya-Kurai basin. The inset in the upper left shows an AFT thermal history model of a representative sample for the Tien Shan (TS18) and the Altai-Sayan region (TEL101). Modelled (m) and measured AFT ages (t) and mean lengths (l) are indicated.

A comparison of Main Central Thrust and other Himalayan fault systems from central and west Nepal with some two-dimensional stress fields

Megh R Dhital

Central Department of Geology, Tribhuvan University, Kirtipur, Kathmandu, NEPAL

For correspondence, E-mail: mrdhital@wlink.com.np

Like the entire Himalayan range, the Main Central Thrust (MCT) in central and west Nepal constituted a single sheet, which was subsequently eroded away giving rise to various klippe and windows. Detailed field mapping in central and west Nepal revealed that the MCT is a sharp thrust fault along which there has been a movement of more than 80 km. As a rule, in this area the hanging wall of the MCT includes sillimanite-grade rocks in the inner belt and garnet-grade rocks in the outer belt. The MCT overrides the Lesser Himalayan rocks, whose grade of metamorphism also decreases from the inner to outer belt. On the other hand, the hanging wall of the MCT frequently contains a zone of retrograde (inverted) metamorphism at the base followed by a zone of prograde (normal) metamorphism towards the top, whereas the footwall always reveals a prograde (inverted) metamorphism towards the inner belt.

Though inverted metamorphism in the footwall is generally attributed to the MCT, such a relationship is inconsistent with the present field observations. For example, in the Melamchi Khola area to NE of Kathmandu at Majhitar the hanging wall of the MCT contains sillimanite-gneiss, which overrides the Benighat Slates and Dunga Quartzite of the Lesser Himalayan footwall. Similarly, in the Mahesh Khola – Belkhu area to SW of Kathmandu, the MCT also contains sillimanite gneisses and migmatites which rest over slates and phyllites of the Lesser Himalaya. But along the strike of the MCT, grade of metamorphism of the hanging wall decreases substantially towards SW to the garnet grade whereas the footwall rocks remain almost unaffected. On the other hand, in the inner belt of the Barpak area, the footwall rocks have undergone a wide zone of inverted metamorphism up to the kyanite grade.

Around Kathmandu, the MCT is folded to form the Mahabharat Synclinorium, where the augen gneisses are confined to the periphery of the Synclinorium and granites occupy only the core zone. This fact as well as the presence of
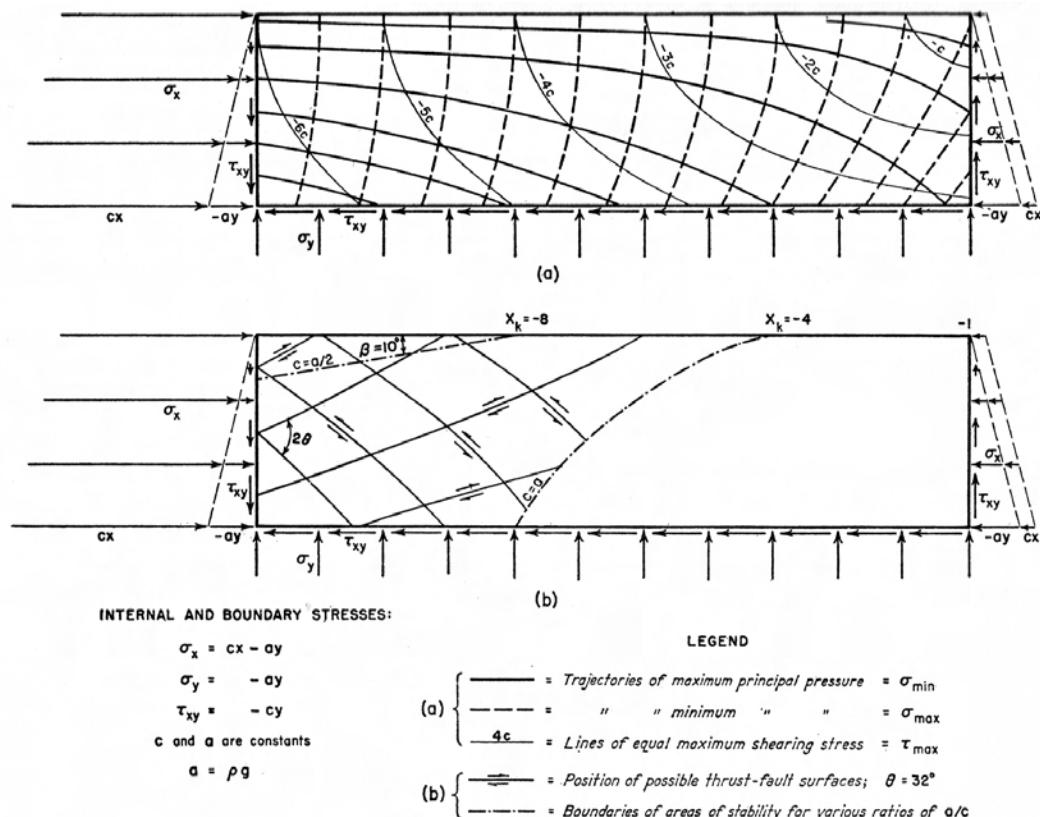
FIGURE 1. Supplementary stress system consisting of superimposed horizontal pressure constant with depth and with constant lateral gradient (Hafner 1951). Note that the trajectories of maximum principal compressive stress (principal pressure) are converging towards the top left, indicating an increase in their magnitude

xenoliths of schist and quartzite in them together with their identical mineral composition clearly point out to the igneous origin of the augen gneisses, most probably derived from the same type of granites. In the Lima Khola area of west Nepal, the MCT forms a small klippe of garnetiferous schist and quartzite, and it is the continuation of the Mahabharat Synclinorium. Hence, there were remarkable tectonic movements after the emplacement of the MCT in central and west Nepal.

Imbricate faults prevail in the Siwaliks and the Lesser Himalaya of Nepal. Though they frequently dip to the north, some of them also dip to the south, forming back thrusts. Such back thrusts were mapped in the Siwaliks of west Nepal and the Lesser Himalayan rocks of the Kusma – Syangja area. Most of the imbricate faults in the Lesser Himalaya formed duplexes in the past and were subsequently exposed after erosion of their roof thrust.

Hafner (1951) obtained an exact solution of stress fields using simple polynomials that satisfy the biharmonic equations for Airy's stress function. He determined the stress distribution to explain fault orientations in a two-dimensional, isotropic, continuous, elastic, and static body taking a variety of horizontal compressive or shear stresses expected in the earth's crust as boundary conditions for the bodies, and predicted the fault types in the earth's crust (**Figure 1**). On the other hand, Sanford (1959) studied the stresses in a uniform upper layer caused by movements of the basement. He also obtained an exact solution on the elastic theory and derived the stress fields (**Figure 2**).

The similarity between the predicted fault system based on Hafner's stress field and the Himalayan faults like the MCT and other faults in the Lesser Himalaya and Siwaliks is remarkable (**Figure 1**). The theoretically predicted listric faults closely resemble the foreland- as well as hinterland- vergent imbricate thrusts. On the other hand, the compressive principal stress trajectories converge (implying their increasing magnitude) towards the top left and so does the average shear stress. This process could ultimately be responsible for the inverted metamorphism in the Himalayas. In these circumstances, thrusting along the MCT and the prograde inverted metamorphism could be two independent phenomena, whereas the retrograde inverted metamorphism is probably related to the movement along the MCT.

Since there is no evidence of South Tibetan Detachment system and other normal faults in the outer Higher Himalayan belt, it is clear that the fault post-dated the MCT. One of the explanations of the extensional tectonics in the Trans Himalayan range could be due to the subsequent uplift of the basement. In this regard, Sanford's stress field (**Figure 2**) can successfully explain such a phenomenon.

References

Hafner W 1951. Stress distributions and faulting. *Geol Soc Amer Bull* **62**: 373-398

Sanford, AR 1959. Analytical and experimental study of simple geologic structures. *Geol Soc Amer Bull* **70**: 19-52
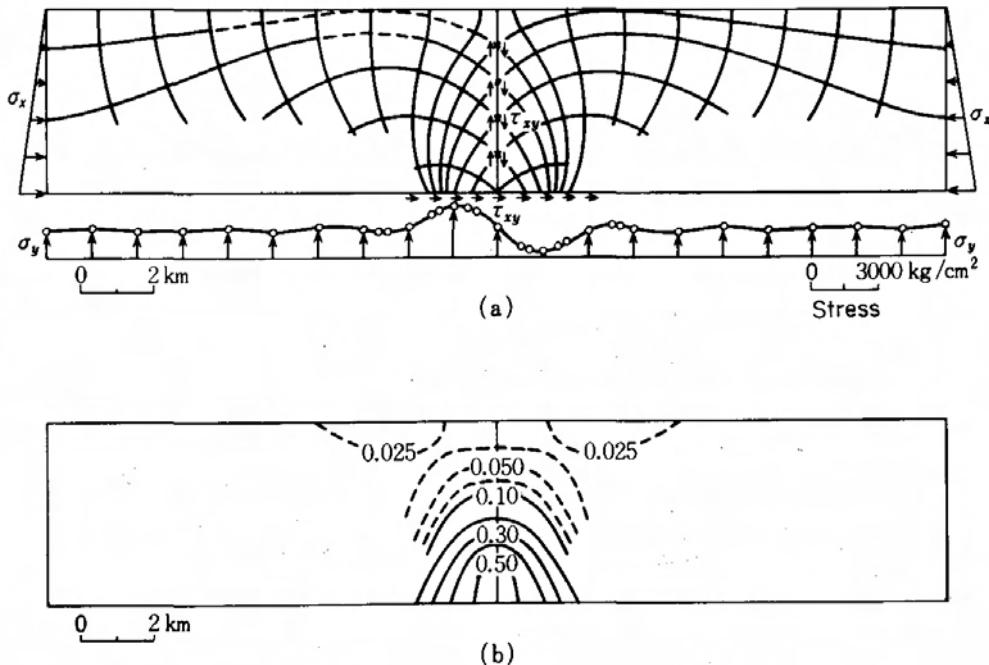
FIGURE 2. Stress field generated inside elastic layer resulting from step-like displacement in the basement. (a) Stress distribution (solid line: compression, broken line: tension). (b) Distortional strain energy distribution. Units in kg/cm^2 (Sanford 1959)

Petrogenesis of basalts for Sangxiu Formation in the central segment from Tethyan Himalayas: Plume-lithosphere interaction

Zhu Dicheng†*, Pan Guitang†, Mo Xuanxue‡, Liao Zhongli†, Wang Liquan†, Jiang Xinsheng† and Zhao Zhidan‡

† *Chengdu Institute of Geology and Mineral Resources, Chengdu, 610082, CHINA*
‡ *China University of Geosciences, Beijing, 100083, CHINA*

* *To whom correspondence should be addressed. E-mail: cdzdc@cgs.gov.cn*

Sangxiu Formation, which is only distributed in the Yangzuoyong Tso area (south to Lhasa, **Figure 1b**), is a special stratum unit that is mainly characterized by volcanic interlayers. Tectonically, it is located in the eastern part of central segment of Tethyan Himalayas, and paleogeography belongs to the northern margin of Greater India. Here one finds not only the southern transitional part of space-time framework of the central-eastern Yarlung Zangbo ophiolitic mélange zone, but also the supposedly the extended end-point of Ninetyeast Ridge (**Figure 1a**). The age of the Sangxiu Fm is from Late Jurassic to Early Cretaceous, which is constrained by fossils, though precise isotopic age of basaltic magmatic effusion is not known at present. Regionally, the Rajmahal traps on eastern Indian margin are explained by the consequences of early activity of the Kerguelen hotspot (Kent et al. 2002), and the track of Kerguelen hotspot since 120 Ma was interpreted from Rajmahal traps via Ninetyeast Ridge to the Kerguelen hotspot (O'Neill et al. 2003). If the early volcanic activity of the Kerguelen hotspot is extended much farther to the north and northeast, can this hotspot influence the volcanic activity in Tethyan Himalayas– the northern margin of Greater India during Late Jurassic to Early Cretaceous?

The goal of this paper is to show our recent work on the geochemical and isotopic compositions and to discuss the characteristics of magmatic source, especially to shed light on the petrogenetic processes and to suggest a possible genetic relationship with Kerguelen hotspot in the light of systemically petrological and geochemical data (including REE, incompatible trace element and isotopic data) for basalts from Sangxiu Fm in Tethyan Himalayas.

Stratigraphy and petrography

The underlying stratum of Sangxiu Fm is the Late Jurassic Weimei Fm., which is mainly consists of quartz sandstones and dark grey argillaceous rocks with high content of quartz, shallow water ripple marks and relic fossils, is thought to the sedimentary records of shore-shallow sea (Jiang et al. 2003). The overlying stratum is the Early Cretaceous Jiabula Fm. that is characterized by accumulates of collapse and turbid sediments. The lower parts of Sangxiu Fm are mainly composed of apogrites, conglomerates, the middle parts are mainly basalts and shales gripped, and the upper parts are aleuritic shales and calcipulverite lens gripped. The massive, amygdaloidal, pillow basalts can be observed in different outcrops.

The phenocrysts (about 5-10%) in basalts are mainly consist of plagioclase and pyroxene, which have experienced variable degree of alteration and metamorphism, however, the original textures appear to have been preserved; the plagioclase ground-mass also underwent partly alteration; the accessory mineral assemblages include ilmenite, titanite and magnetite.

Geochemistry

The significant features of basalts from Sangxiu Fm. are characterized by high contents of TiO_2, FeO and P_2O_5 (averages are 3.46%, 7.76%, 0.51% respectively) that are similar to the OIB in Hawaiian, and low content of MgO (average is only 4.64%) indicating an evolved magma. Using the immobile trace element discrimination diagram ($Nb/Y-Zr/TiO_2$, Winchester and Floyd, 1977) confirms that the basalts of Sangxiu Fm belong to alkaline basalt.
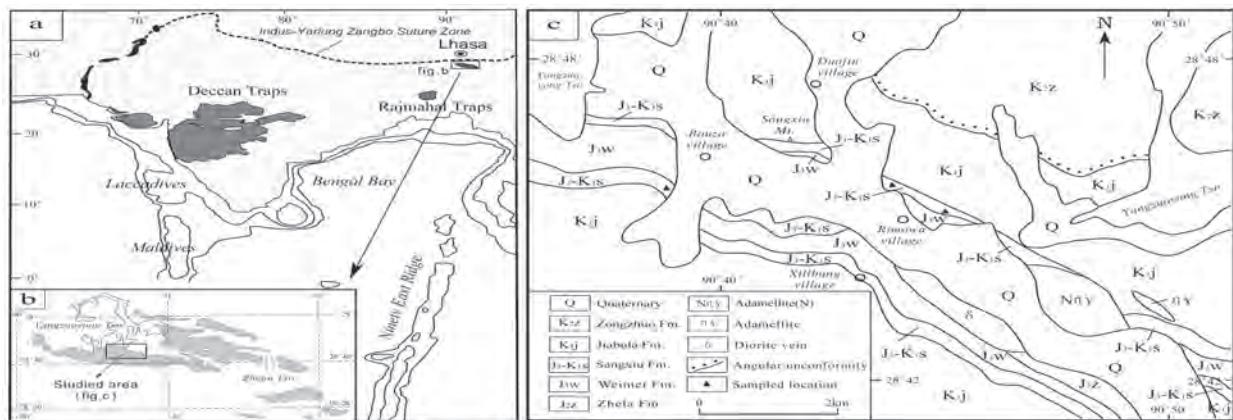
FIGURE 1. Geological distribution map for basalts from Sangxiu Formation in the central segment of Tethyan Himalayas. a. Tectonic location (modified from Mahoney et al. 2002). b. Distributions (after Pan Gui-tang et al. 2004, in press). c. Geological map for studied area (Regional Geological report (1: 250, 000) for Luoza County, 2003, unpublished)

Geochemically, the basalts are characterized by high contents of total REE ($\sum$REE$_{aver}$=213.99$\times$10-6), enriched in LREE [(La/Yb)$_{Naver}$=8.42~10.15] and in HFSE [Nb$_{aver.}$, Zr$_{aver.}$ are 35.58$\times10^{-6}$, 352$\times10^{-6}$ respectively], as well as in some LILE (Ba, Th etc.). All of these characteristics together with high ratios of Ti/Y (578.71~753.96), Zr/Y (10.2~10.98), indicating a similarity with OIB. On the other hand, the basalts show lower abundances of compatible elements (such as of Cr$_{aver}$, Yb$_{aver}$ are only 3.32$\times10^{-6}$ and 2.86$\times10^{-6}$ respectively), indicating a fractional crystallization and/or garnet remains in source. The markedly characteristics of the basalts are characterized by high Sr, low Nd isotopic compositions, the age-corrected (150Ma assumed) of isotopic compositions of basalts for Sangxiu Fm are ranging between 0.707331 and 0.709889 for ^{87}Sr/^{86}Sr, between 0.512364 and 0.512554 for ^{143}Nd/^{144}Nd respectively.

Basalts from Sangxiu Fm are more enriched in LREE and HFSE than those of tholeiites in Rajmahal and Hawaiian, which further confirm that these basalts are alkaline series. The other important features among the alkaline basalt patterns relative to the N-MORB pattern are depletions in Y, Yb and some of Rb, and are enrichments in LILEs (especially in Ba, Th) and HFSEs. In general, these two kinds of patterns are not only largely parallel to the OIB in Hawaiian and Kerguelen, but also are similar to Rajmahal alkaline basalts, they are all plot within the field of Emeishan basalts, suggesting that the basalts of Sangxiu Fm. are most likely derived from OIB-type magma that are similar to Hawaiian and other plume-derived record.

The discrimination plots indicate that the alkaline basalts were derived from melts generated in continental margin rift environment, in agreement with the underlying stratum that was thought to the sedimentary records of shore-shallow sea.

Petrogenesis
Identification of OIB-type component
Apart from the REE and trace element patterns of basalts for Sangxiu Fm indicate that these basalts are petrogenetically related to the OIB-type magma, the following evidences further confirm that the melts are derived from OIB-type mantle source:

(i) The La/Nb-La, Nb/Th-Nb, Sm/Eu-La/Yb and Tb/Yb-La/Yb diagrams are believed to the effectively diagrams to identify the characteristics of magmatic source (Li Shuguang 1993, Xu Xue-yi et al. 2003), basalts from Sangxiu Fm. are all clusteringly plot within OIB field on these diagrams, showing the source of magma has a clear similarity with OIB.

(ii) From the fuzzy cluster analyzed diagram of incompatible trace element ratios (i.e. Zr/Nb, La/Nb, Ba/Nb, Ba/Th, Rb/Nb, Th/Nb, Th/La, Ba/La) for Sangxiu Fm basalts, hotspot/plume-basalts and major geochemical reservoirs, we can conclude that these basalts are akin to the hotspot-type magma inferred from the larger distance of cluster with Hawaiian basalts, Kerguelen OIBs and Ninetyeast Ridge basalts than that of N-MORB and crust.

(iii) Furthermore, a widely accepted concept is that the isotopic ratio of Nd is insusceptible to alteration during metamorphism and magmatic evolution processes, the Nd isotopic composition represents the characteristics of magmatic source. The depleted Nd isotopic ratios of basalts for Sangxiu Fm are close to one of the OIB-type end members (EMI) also indicating an affiliation with deep mantle materials.

Lithospheric component
How to explain the high initial Sr isotopic composition for basalts from Sangxiu Fm? Four factors need to be considered we think:

a. *crustal contamination*; b. *alteration by seawater*; c. *degree of partial melting*; d. *contributions from lithospheric mantle*. Due to the crustal contamination has been eliminated by trace element indicators, the best way to interpret the high initial Sr isotopic compositions for these basalts would ascribe to the results of alteration by seawater, lower degree of partial melting and contamination of lithospheric mantle materials inferred from alkaline basalt with pillow structure and low initial ratio of Nd isotope of basalt from Sangxiu Fm. The imprints from lithospheric mantle can also be identified by the (Th/Ta)$_{PM}$-(La/Nb)$_{PM}$, (Th/Nb)$_{PM}$-Nb/U and Nb/Th-Ti/Yb diagrams, together with the fuzzy cluster of incompatible trace element ratios analyzed diagram that shows a fairly large distance of cluster with lithospheric mantle. In Ce/Y-Zr/Nb diagram, the basalts of Sangxiu Fm fall between depleted garnet lherzolite (GD) and primitive garnet lherzolite (GP) non-modal fractional melting curves (Deniel C, 1998). Integrated with the high ratios of Ce/Yb (=25.70~31.82), as well as the considerable fractionation between LREE and HREE, further confirm that the alkaline basalts of Sangxiu Fm are related to low degree of partial melting of melts from lithospheric mantle.

As discussed previously, trace element and Sr-Nd isotopic ratios provide the clearly evidences for these basalts derived from the OIB-type mantle and lithospheric mantle source. Therefore, a model of plume-lithosphere interaction is attractive for basalts from Sangxiu Fm. The basalts are interpreted as the products of lower degree of partial melting within the mixed magmas that may have formed as a result of the infiltration of plume-derived melts into the base of lithosphere, which indicating a process of plume-lithosphere interaction.

Relationship to Kerguelen hotspot
Geochemically, the characteristics of basalts from Sangxiu Fm are similar to those from Rajmahal basalts in eastern India, Ninetyeast Ridge and Kerguelen hotspot in Indian Ocean, whereas the isotopic composition of these basalts are significantly far from the fields of basalts from the Tethys and Yarlung Zangbo. Combined with the tectonic location of basalts from Sangxiu Fm, it would be relatively straightforward to explain the similar geochemical characteristics between basalts for Sangxiu Fm from the Tethyan Himalayas and basalts from the eastern Indian (Rajmahal Traps), the Ninetyeast Ridge and the Kerguelen hotspot in Indian Ocean were the consequences of interaction between the early activity of Kerguelen hotspot and lithosphere of northern margin of Greater India.

Conclusions
Basalts of Sangxiu Fm in the central segment of Tethyan Himalayas have similar geochemical characteristics to OIB, trace element and Sr-Nd isotopic ratios provide the clearly evidences for these basalts derived from the OIB-type mantle and lithospheric mantle source. The basalts are interpreted as the products of lower degree of partial melting within the mixed magmas that may have formed as a result of the infiltration of plume-derived melts into the base of lithosphere. It would be a consequence of the interaction between early activity of Kerguelen hotspot and lithosphere in northern margin of Greater India.

References

Jiang X, Y Yan and G Pan. 2004. Sedimentary environment of the Late Jurassic Weimei Formation in the southern Tibetan Tethys. *Geol Bull China* **22**(11-12): 900-907 (in Chinese with English abstract)

Kent RW, MS Pringle, and RD Müller. 2002. ^{40}Ar/^{39}Ar Geochronology of the Rajmahal Basalts, India, and their Relationship to the Kerguelen Plateau. *J Petro* **43**(7):1141-1153

Li S. 1993. Ba-Nb-Th-La diagrams used to identify tectonic environments of ophiolite. *Acta Petrologic Sinica* **9**(2): 146-157 (in Chinese with English abstract)

O'Neill C, D Müller and B Steinberger. 2003. Geodynamic implications of moving Indian Ocean hotspots. *Earth Planet Sci Lett* **215**(1): 151-168

Xu X, L Xia and Z Xia. 2003. Geochemistry and genesis of Cretaceous-Paleogene basalts from the Tuoyun Basin, southwest Tianshan mountains [J]. *Geochimica* **32**(6): 551-560 (in Chinese with English abstract)

Linzizong Volcanic Rocks in Linzhou of Tibet: A Volcanic Petrologic Assemblage in Continental Collision Environment

Guochen Dong*, Xuanxue Mo, Zhidan Zhao, Liang Wang and Su Zhao

Earth Sciences and Land Resources School, China University of Geosciences (Beijing), 29 Xueyuan Road, Haidian District, 100083 Beijing, CHINA

* To whom correspondence should be addressed. E-mail: guochdong@263.ent

Cenozoic Linzizong volcanic rocks, originally named as Linzhou volcanic basin, southern Tibet, are widely spread in Gangdese magmatic belt and unconformably overlain by the late Mesozoic sedimentary sequences. These consist of a set of potassic moderate to acid volcanic rocks including the basaltic andesite, andesite, dacite, trachyandesite, shoshonite, rhyolite and their related pyroclastic rocks with interlayers of sedimentary rocks, which can be divided into 3 categories: Dianzhong Formation, Nianbo Formation and Pana Formation. Based on petrology and geochemistry, K_2O and Al_2O_3 contents in volcanic rocks increase from bottom to top, changing from potassic to highly potassic field in K_2O-Na_2O diagram, and from sub-aluminous to peraluminous. It tends to evolve to acid from moderate and develops huge thick pyroclastic flows in the upper part, responding significantly to the thickening of the crust in the later stage. The volcanic rocks are enriched relatively in Cs, Rb, K, U and deplete Ta, Nb, Ti, Sr, Ba and P. Spider diagrams and REE pattern of the Linzizong volcanic rocks show similar characteristics with post-collisional highly potassic volcanic rocks in the Gangdese magmatic belt. $^{40}Ar/^{39}Ar$ isotopic isotopic dating has constrained the age of formation at 43.93-64.43 Ma for the Linzizong volcanic rocks, in which Dianzhong Fm formed during 61.45-64.43 Ma, Nianbo Fm. 54.07-50 Ma and Pana Fm 43.93- 48.72Ma. The strata across the unconformity were tremendously different in sedimentary facies and structural deformation, implying a major tectonic event. The formation of the unconformity was constrained by $^{40}Ar/^{39}Ar$ age (~65 Ma) of the basal andesite of Linzizong volcanic strata. In combination with evidence from the temporal evolution and spatial distribution of igneous rocks in Tibetan Plateau, and the stratigraphical and paleontological evidences in southern Tibet that documented dramatic change in sedimentary facies and microfuna content across the Cretaceous-Tertiary (K/T) boundary, it is concluded that the collision between India and Eurasia continents was most likely initiated at ~K/T boundary time and that Linzizong volcanic rocks, as volcanic assemblage produced during continental collision to post-collision, were recoding the transitional process from beginning of the collision to post-collision between Indian and Eurasian continents during Paleocene to Eocene (65-40 Ma). While the volcanic rocks formed in early stage, it had fingerprints of continental margin-arc settings, those in middle and late stages reflected environments of intra-continental convergence and crust thickening.

Refenences

Xuanxue Mo, Jinfu Deng, and Chonghe Zhao. 2003. Response of the volcanism to the India-Asia collision. *Earth Science Frontiers* **10** (3): 135-148

Mo X, Z Zhao, and S Zhao. 2002. Evidence for timing of the initiation of India -Asia collision from igneous rocks in Tibet [J]. *EOS Trans*, **83** (47)

Mo X, J Deng, and Z Zhao. 2003. Volcanic records of India-Asia collision and post-collision processes. *Proc. EGS-AGU-EUG Joint Assembly (Nice)* [C]., 263.

Dong Guochen, Xuanxue Mo, and Zhidan Zhao. In press. A New Study on the Stratigraphy Sequences of Linzizong Volcanic Rocks in Linzhou Basin, Tibet. *Geol Bull China*

Miller, C, R Schuster, and U Kloetzli. 1999. Post-collisional potassic and ultrapotassic magmatism in SW Tibet; geochemical and Sr-Nd-Pb-O isotopic constraints for mantle source characteristics and petrogenesis. *J Petrol* **40**(9): 1399-1424

Younger hanging wall rocks along the Vaikrita Thrust of the High Himalaya: A model based on inversion tectonics

Ashok K Dubey* and Surendra S Bhakuni

Wadia Institute of Himalayan Geology, 33 General Mahadev Singh Road, Dehra Dun - 248 001, INDIA

* *To whom correspondence should be addressed. E-mail: akdubey@rediffmail.com*

The High Himalayan rocks are divided into two main units, Munsiari Formation and Vaikrita Group. A geochronological study by Ahmad et al. (2000) revealed that the rocks of the Munsiari Formation, consisting of mainly granite gneisses have ε_{Nd} values from -23 to -28 similar to the Lesser Himalayan rocks occurring in the footwall of the Munsiari Thrust whereas the metasedimentary rocks of the Vaikrita Group show ε_{Nd} values from -14 to -19. The Sr isotope study revealed that the Vaikrita Group shows partial equilibration at 500 Ma and the Munsiari Group has undergone Sr isotope homogenization at 1800 Ma. In absence of marker horizons, displacements along the Munsiari and Vaikrita thrusts are still a matter of speculation. However, the Munsiari rocks occur as klippen in the Lesser Himalaya and the klippe to fenster method reveals that the maximum displacement along the klippen thrust in the Simla klippe is of the order of ~ 40 km (Dubey and Bhat 1991). On the contrary, the trace of the Vaikrita Thrust is linear with occasional curves at oblique thrust ramps. Moreover, the Vaikrita Thrust has a weak geomorphic expression, which does not allow its mapping by satellite imagery. Mylonitization of the Vaikrita rocks can only be seen at the base but kyanite is uniformly distributed throughout the rock. The constituent minerals are coarse grained (size, 1-2 mm). In sharp contrast to these properties the constituent minerals of the Munsiari rocks are fine to medium grained (size, <1mm), kyanite is occasionally present in small pockets, and mylonitization is a common feature throughout the sequence. Class 2 and Class 3 fold patterns are typical of Vaikrita rocks indicating ductile deformation whereas the Munsiari rocks exhibit mostly Class 1C folds characteristic of deformation at comparatively upper levels of the Earth's crust. Prominent stretching mineral lineation and presence of sheath folds suggest greater shear strain in the Munsiari rocks.

The metamorphic episodes in the area can be broadly classified into two: (i) pre-Himalayan metamorphism, and (ii) Tertiary Himalayan metamorphism. The pre-Himalayan metamorphism is now well established in several parts of the Himalaya. For example, a metamorphic event, prior to the emplacement of the early Palaeozoic granitoids was recognized in the SE Zanskar (NW Himalaya) by Pognante et al. (1990). The mineral assemblage indicated high T and high P conditions of crystallization (T = 750 ± 50⁰C; P = 12.0 ± 0.5 kbar). The Vaikrita rocks underwent a higher grade of metamorphism (lower granulite facies) as compared to the Munsiari rocks and the

metamorphic reconstitution took place at a depth of ~30 km (Valdiya et al. 1999). The pre-Himalayan metamorphism was higher in metamorphic grade than the younger Himalayan metamorphism (Arita 1983).

Different phases of the Himalayan metamorphism are now known (Hodges and Silverberg 1988). The first Himalayan metamorphism was associated with the initial collision between India and Eurasia and the subsequent metamorphism was related to thrusting along the MCT. The second metamorphic event (i.e. Himalayan) occurred at similar or lower T and at lower P. The rocks show a normal metamorphism decreasing upward in metamorphic grade toward the overlying Tethyan sediments (Arita 1983).

The present study in the Garhwal-Kumaun High Himalaya help in understanding the occurrence of the younger hanging wall Vaikrita Group above the older footwall Munsiari Formation along the Vaikrita Thrust. The phenomenon is explained by an inversion tectonics based model where normal faulting and metamorphism was followed by thrusting characterized by displacement amount less than the displacement during the early normal faulting. The study takes into account the simple shear strains associated with the piggy back sequence of thrusting and pure shear strains associated with folding to explain the present structural set-up of the region.

References

Ahmad T, N Harris, M Bickle, H Chapman, J Bunbury and C Prince. 2000. Isotopic constraints on the structural relationships between the Lesser Himalayan Series and the High Himalayan Crystalline Series, Garhwal Himalaya. *Bull Geol Soc Amer* **112**: 467-477

Arita, K. 1983. Origin of the inverted metamorphism of the Lower Himalayas, Central Nepal. *Tectonophysics* **95**: 43-60

Dubey, AK and MI Bhat. 1991. Structural evolution of the Simla area, NW Himalayas: Implications for crustal thickening. *J Southeast Asian Earth Sci* **6**: 41-53

Hodges KV and DS Silverberg. 1988. Thermal evolution of the greater Himalaya, Garhwal, India. *Tectonics* **7**: 583-600

Pognante, U, D Castelli, P Benna, G Genivese, F Oberli, M Meier and S Tonarini. 1990. The crystalline units of the High Himalayas in the Lahul-Zanskar region (north-west India): Metamorphic-tectonic history and geochronology of the collided and imbricated Indian plate. *Geol Mag* **127**: 101-116

Valdiya, KS, SK Paul, T Chandra, SS Bhakuni and RC Upadhyay. 1999. Tectonic and lithological characterization of Himadri (Great Himalaya) between Kali and Yamuna rivers, Central Himalaya. *Himal Geol* **20**: 1-17

Out-of-sequence thrusting in Himalaya: Modification of wedge extrusion and channel flow models

CS Dubey†*, BK Sharma†, EJ Catlos‡ and RA Marston‡

† Department of Geology, University of Delhi, Delhi-110 007, INDIA
‡ School of Geology, Oklahoma State University, Stillwater, Oklahoma, USA

* To whom correspondence should be addressed. Email: csdubey@yahoo.com

....

Recent seismic events in the Lesser Himalayas between the Main Central Thrust (MCT) and Main Boundary Thrust (MBT) have brought to light the importance of paleoslip along structures in controlling mass movement in the area, as evidenced by several devastating landslides and major earthquake in 1991. In Uttarkashi region MCT shear zone can be divided into three different thrusts i.e. MCT-I (Vaikrita thrust), MCT-II (Munsiari/ Jutogh Thrust), MCT-III (Chail/Ramgarh Thrust). The rocks present between Munsiari Thrust in Bhatwari area and Ramgarh/ Chail thrust near Sainj (Garhwal Himalaya) depict very young in situ monazites ages varying from 6-1 Ma (Catlos et al. 2003). The younger ages and the geometry of the MCT-III reveal this thrust to be an out-of-sequence thrust reactivating the MCT-II, i.e., the Munsiari Thrust.

Schelling and Arita (1991) and Pandey and Virdi (2004) have also observed such relationships in Nepal and Himachal Pradesh respectively. MCT-III is a high angle reverse thrust fault at Sainj and it extends in the Sarhan-Jhakri area (Himachal Pradesh) where monazite dates obtained are as young as 3.4 Ma. This Thrust is also observed as high angle reverse Fault at Pachekhani mines, Rorathang and Ranpo in Sikkim. These relationships may have implications on the high seismic activity in the Himalaya at regional scale between MCT-I (Vaikrita thrust) and MBT due to an out of sequence thrust reactivating older thrusts in the hinterland affecting the break in slope, probably affecting the climate change as reflected in the stable isotopes from the Lesser Himalaya (Hodges et al. 2004). Occurrences of such out-of-sequence thrusts have been known (at several other locations near the STD, MCT-I and MCT-III and above MBT (Grujic et al. 2002; Catlos et al. 2003). Out-of-Sequence thrusts and related Neotectonic activity clearly depicts that the channel flow model and wedge extrusion models need modifications in the light of above. A modified model based on the data from the Lesser Himalayan region from East to West will be discussed.

References

Catlos EJ, CS Dubey, RA Marston and TM Harisson. 2003. Moving mountains: Reactivation of the Himalayan Main Central Thrust at 4 Ma Bhagirathi river, NW India. *Geol Soc Am Paper # 60243*, Seatle meeting, USA

Grujic D, LS Hollister and RR Parrish. 2002. Himalayan metamorphic sequence as an orogenic channel: insight from Bhutan. *Earth Planet Sci Lett*, 198; 177-191

Pandey AK, HK Sachan and NS Virdi. 2004 Exhumation history of a shear zone constrained by Microstructural and fluid inclusion techniques: an example from the Satluj valley, NW Himalaya, India, *Jour Asian Earth Sc* 23: 391-406

Schelling D and K Arita. 1991. Thrust tectonics, crustal shortening, and the structure of the far-eastern Nepal Himalayas. *Tectonics* 10: 851-862

Hodges KV, C Wobus, K Ruhl, T Schildgen and K Whipple. 2004. Quaternary deformation, river steepening, and heavy precipitation at the front of the Higher Himalayan ranges. *Earth Planet Sci Lett* 220: 379-389

The tectonometamorphic evolution of the Alpine metamorphic belt of the Central Pamir

MS Dufour†* and Yu V Miller‡

† *Geological Faculty, St. Petersburg State University, St.Petersburg, Universitetskaya nab. 7/9, 199034, RUSSIA*
‡ *Institute of Precambrian Geology and Geochronology, Russian Academy of Science, St. Petersburg 199034, RUSSIA*

* *To whom correspondence should be addressed. E-mail: dufourms@rambler.ru*

The Alpine fold zone of the Central Pamir forms an arc elongated in sublatitudinal direction between the Hercynians of the Northern Pamir and the Cimmerians of the Southern Pamir. Its structure was formed in Oligocene-Miocene as a result of the collision of continental masses of the Northern Pamir –Kunlun and the Southern Pamir-Karakoram after closing of the oceanic or suboceanic floor basin (Dufour 2000).

The Alpine zonal metamorphic belt of the kyanite-sillimanite type (more correctly, of the intermediate type of the high pressure) including series of domes (thermal anticlines) can be traced along the Central Pamir. Cores of domes include migmatites and remobilized bodies of the Early Paleozoic gneisses and granites as the Kangmar dome in the Southern Tibet does. The sequence of endogenic processes forms tectonometamorphic cycle (Miller 1982, Miller and Dufour 2000) which includes two stages. Structural forms of the first stage are represented by parallel bedding flow or nappe structural parageneses, reflecting increase in temperature and decrease in viscosity of rocks. The second stage includes linear folding, systems of fractures and faults and other structures, reflecting gradual transition from plastic to brittle deformations in accordance with the decrease of temperature and increase of the rock viscosity. The correlation of metamorphic and metasomatic processes and the igneous activity with the sequentially generating structural forms provides a possibility to produce an unified scale of the development of endogenic processes.

1. The first stage of the tectonometamorphic cycle. Tectonic processes began with the formation of nappes and the displacement of masses of gabbros and pyroxenites. Then the rapid increase of the PT conditions till the maximum of T = ab. 700 °C, P = 7-7,5 kbar was achieved. In central parts of thermal anticlines a parallel bedding schistosity S_1 and locally small lying isoclinal folds F_1 were formed.

Processes of the high temperature metamorphism started resulting in formation of migmatites and small parallel bedded pegmatitic veins. These processes were followed by the Na metasomatism and attendant Fe-Mg metasomatism and then subtraction by leaching. The S_1 schistosity was folded by small folds F_2. Then large to gigantic lying isoclinal folds F_3 with the amplitude of some km evolved. They deformed all deposits of the Central Pamir irrespective of the metamorphic degree. These folds have long normal limbs and short overturned limbs sheared by overthrusts. The S_3 schistosity evolved parallel their axial planes. Large bodies of pegmatites occur in these slackening zones.

The front of metamorphism spread in the periphery of thermal anticlines after the formation of F_3 folds. Therefore the S_3 schistosity is the first one here. Thus the maximum metamorphic recrystallization at these places attributes to the end of the first stage or the beginning of the second stage of the tectonometamorphic cycle.

2. The second stage of the tectonometamorphic cycle. This stage is characterized by the gradual decrease of temperature and the drop of pressure till ab. 4 kbar. At this stage mainly large linear upright, sometimes overturned folds were superimposed on all earlier structures. NE striking F_4 folds and NW strike F_5 folds are recognized. The decompression caused the development of the andalusite-sillimanite type metamorphism and the formation of syenite and granite masses, miarolitic pegmatites and aplite veins. Systems of fractures and faults were generated as a result of the decrease of temperature and consequently of the rock plasticity. Late bodies of basic rocks were formed. The generation of systems of tectonic nappes and gravitational faults then continued after processes of metamorphism were ceased.

References

Dufour MS. 2000. The Central Pamir – an Alpine collision zone [abstract]. In: *15th Himalaya-Karakoram-Tibet Workshop. Volume of abstracts*. Beijing

Miller YV. 1982. *Tectonometamorphic cycles* (in Russian). Leningrad: Nauka. 160 p.

Miller YV and MS Dufour. 2000. Tectonometamorphic cycles in different geodynamic conditions. *J China Univ Geosciences* 11(4): 383-91

When the Kunlun fault began its left-lateral strike-slip faulting in the northern Tibet: Evidence from cumulative offsets of basement rocks and geomorphic features

Bihong Fu* and Yasuo Awata

Active Fault Research Center, National Institute of Advanced Industrial Science and Technology (AIST), 1-1-1 Higashi, Tsukuba 305-8567, JAPAN

* *To whom correspondence should be addressed. E-mail: bihongfu-fu@aist.go.jp*

The E-W to WNW-ESE striking Kunlun fault, extending about 1600 km-long (between 86ºE to 105ºE), is one of large strike-slip faults in northern Tibet, China. As a major strike-slip fault, it plays an important role in the extrusion of the Tibetan plateau in accommodating northeastward shortening caused by India-Eurasia convergence. However, initiation time of left-lateral strike-slip faulting of the Kunlun fault is still largely debated, ranging from the late Eocene (34 Ma) to early Quaternary (2 Ma). It is well known that the growth of fault-bounded geologic structures and geomorphic features accumulate over time as a result of repeated large seismic events. Active strike-slip faulting causes a variety of geomorphic features, including linear valleys, offset streams, shutter ridges, sag ponds and pressure ridges. Offset or displaced stream channels and basement rocks are common characteristics developed along active strike-slip faults. Offset basement rocks and geomorphic features along the Kunlun fault are analyzed based on analysis of satellite remote sensing images and field tectono-geomorphic observations. These results indicate that stream channels at various scales show systematic sinistral offset along the Kusai Lake segement of the Kunlun fault zone. Largest cumulative offset of basement rocks is about 55 km in the Kusai Lake segment. Similarly, a series of pull-apart basins, such as the Kusai Lake, Xiugou, Alag Lake and Tusuo Lake pull-apart basins with ~40 to 60 km long and ~8 to 10 km wide developed along the Kunlun fault zone, which formed at releasing bend or extensional step-over as a result of long-term geomorphic development. In addition, restored geomorphic features, such as large-scale pull-apart grabens and pressure ridges developed along the splaying fault of the Kunlun fault system, also show about 30 km cumulative offset.

The 14 November 2001 Mw 7.8 (Ms 8.1) Central Kunlun earthquake produced a 400-km-long surface rupture zone. It is the longest rupture zone produced by a single intracontinental earthquake ever reported worldwide. This earthquake has also produced large coseismic left-lateral strike-slip displacements or offsets of typical geomorphic markers, such as small gullies, stream channel banks, and edges of alluvial fans, terraces as well as modern moraines as we observed in the field survey, generally ranging from 3-8 m. The ^{14}C dating data imply that the latest seismic event before the 2001 Mw 7.8 Central Kunlun earthquake occurred at 430 ± 50 yr B.P. near the Kunlun Pass in the Kunsai Lake segment. We estimate an average slip rate of 10 ± 2 mm/yr based on typical 4-5 m offset and 430 ± 50 yr recurrence interval of large earthquake. Similarly, we can calculate an apparent slip rate of 10± 1 mm/yr based on 275 ± 15 m lateral offset of stream channels and fluvial fans occurred about 27 500 yr B.P. to the east of the Kunlun Pass. Previous studies also inferred an average slip rate of 11.5 ± 2.0 mm/yr based on cosmogenic age dating data and terrace riser offsets along the Xidatan-Dongdatan and Dongxi-Anyemaqin segments during the Late Quaternary. Therefore, we can estimate that the Kunlun fault likely began the left-lateral strike-slip faulting at 5 ± 0.5 Ma based on total 55 km displacement and a long-term average strike-slip rate 10 ± 1.5 mm/yr. Therefore, this study provides an acceptable timing constraint on initiation of left-lateral strike-slip faulting of the Kunlun fault zone.

References

Avouac JP and P Tapponnier. 1993. Kinematic model of active deformation in central Asia. *Geophy Res Lett* **20**: 895-898

Aydin A and A Nur. 1982. Evolution of pull-apart basins and their scale independence. *Tectonics* **1**: 91-105

Fu B and A Lin. 2003. Spatial distribution of the surface rupture zone associated with the 2001 Ms 8.1 Central Kunlun earthquake, northern Tibet, revealed by satellite remote sensing data. *Int J Remote Sensing* **24**: 2191-2198

Jolivet M, M Brunel, D Seward, Z Xu, J Yang, J Malavieille, F Roger, A Lereloup, N Arnaud and C Wu. 2003, Neogene extension and volcanism in the Kunlun Fault zone, northern Tibet: New constraints on the age of the Kunlun Fault. *Tectonics* **22(5)**: 1052, doi: 10.1029/2002TC001428.

Lin A. B Fu, J Guo, Q Zeng, G Dang, W He and Y Zhao. 2002. Co-seismic strike-slip and rupture length produced by the 2001 Ms 8.1 Central Kunlun earthquake. *Science* **296**: 2015-2017

Van der Woerd J, P Tapponnier, FJ Ryerson, AS Meriaux, B Meyer, Y Gaudemer, RC Finkel, MW Caffee, G Zhao, and Z Xu. 2002. Uniform postglacial slip- rate along the central 600 km of the Kunlun fault (Tibet), from ^{26}Al, ^{10}Be, and ^{14}C dating of riser offsets, and climatic origin of the regional morphology. *Geophys J Int* **148**: 356-388

Fluctuation of Indian monsoon during the last glacial period revealed by pollen analysis of Kathmandu Basin sediments, Nepal Himalaya

Rie Fujii†*, Harutaka Sakai‡ and Norio Miyoshi†

† Faculty of Science, Okayama University of Science, Ridaicho 1-1 Okayama, 700-0005, JAPAN
‡ Department of Earth Sciences, Kyushu University, Ropponmatsu 4-2-1, Fukuoka, 810-8560, JAPAN

* To whom correspondence should be addressed. E-mail: rfuji@chem.ous.ac.jp, riezof28@yahoo.co.jp

Palynological and sedimentorogical studies of a 218-m-long core taken from the Kathmandu Basin by Paleo-Kathmandu Lake Project have revealed continuous record of paleoclimatic changes in the valley during the last 750 ka (Fujii et al. 2004 and Maki et al. 2004). This is the first report on the continuous terrestrial climatic record in South Asia. In this paper, we report millennial-scale climatic changes in the valley from 50 ka to 12 ka, and attempt to compare the result with the glaciation in the Himalaya and the ice cores in both Greeanland and Antarctica.

The Kathmandu basin-fill sediments consist of the late Pliocene to Pleistocene thick fluvio-lacustrine sediments. The 218-m-long core was obtained at Rabibhawan in the western central part of the Kathmand Valley. The core is lithologically divided into three parts (Sakai et al. 2001): 1) 15 m thick gravelly mud at the basal part (Bagmati Formation), 2) 187 m thick clayey and muddy sediments in the middle (Kalimati Formation), 3) 9 m thick sand bed at the top (Patan Formation). On the basis of magnetostratigraphic study and AMS ^{14}C dating, ages of the core

have been estimated to range from ca. 750 to 12 ka. We carried out pollen analysis for the samples obtained at 1 m intervals from the 218-m-long core, in order to clarify the outline of a paleoclimatic changes (Fujii et al. 2004, Maki et al. 2004), and then reconstructed millennial-scale climatic changes from 50 to 12 ka using samples taken at 10 cm intervals for the top part of the core (45 m in length).

The pollen diagram of 218-m-long core is characterized by predominance of *Quercus*, which attains 30~80% of the arboreal pollen, and by dominance of *Pinus*, *Castanopsis*, *Alnus*, *Betula* and *Carpinus*. Gramineae, *Artemisia* and Chenopodiaceae were predominant in non-arboreal pollen. The pollen diagram was divided into 19 pollen zones, on the basis of pollen assemblages and fluctuation of ratio of arboreal and non-arboreal pollen (Fujii et al. 2004, Maki et al. 2004). According to Fujii et al. (2004) and Maki et al. (2004), a paleoclimatic curve obtained from the Kathmandu Basin sediments well-corresponds to $\delta^{18}O$ curve ranging from MIS 2 to MIS 19. In addition, paleoclimatic record
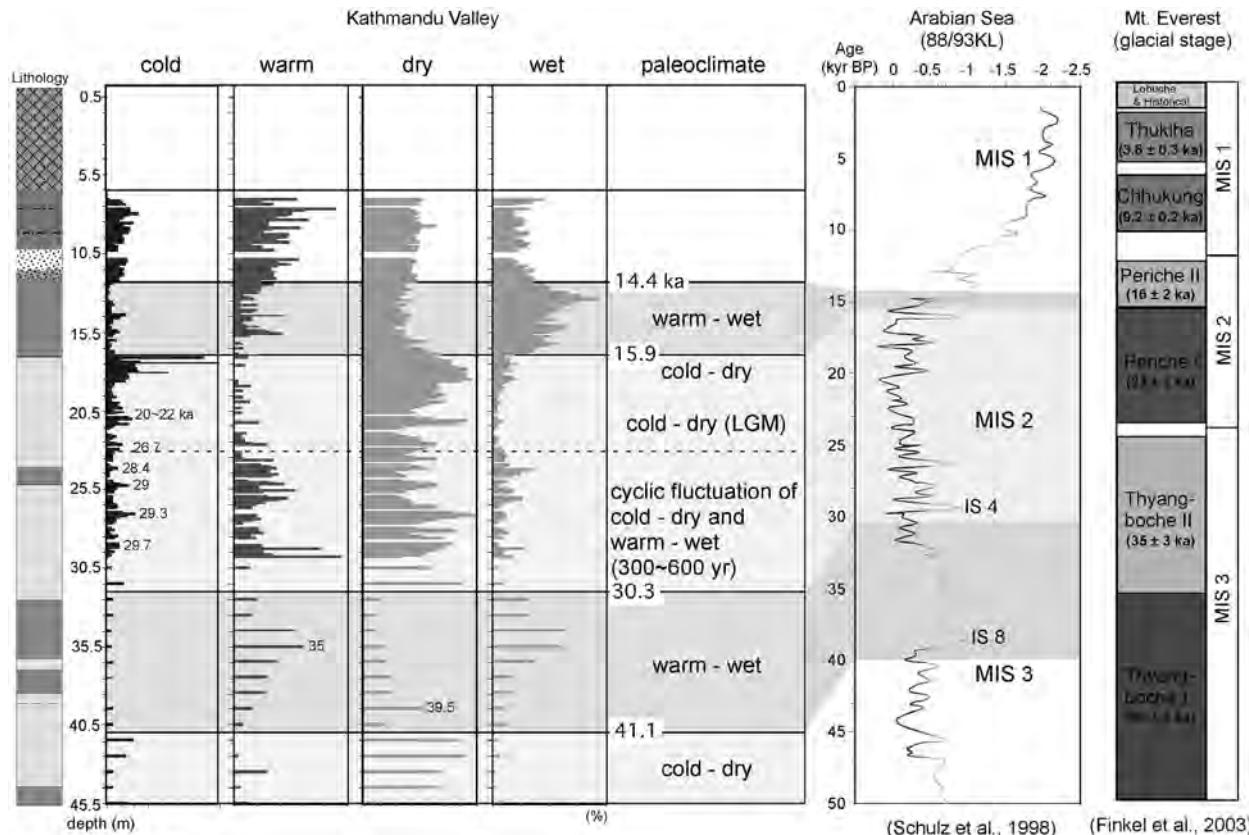
FIGURE 1. Comparison of paleoclimatic records in the Kathmandu Basin with $\delta^{18}O$ variation curve in the Arabian Sea and timing of expansion of glaciers in the Everest area. Paleoclimatic records are based on assemblage of representative fossil-pollen.

in the valley is divided into two parts at boundary between MIS 8 (pollen zone 10) and MIS 9 (pollen zone 11), judging from drastic changes of numbers of pollen concentration: the lower part is three to four times larger than the upper part. Moreover, interglacial periods of MIS 11 and MIS 13 were warmer-and-wetter climate, in comparison with interglacial periods from MIS 2 to MIS 19. A pollen diagram of the topmost 45 m in depth range after MIS 4, and is generally characterized by lower number of pollen concentration and low ratio of pollen indicating warm-temperate climate like as *Castanopsis* and *Mallotus*.

As a result of pollen analysis at 10 cm intervals, we could have reconstructed paleocliamtic changes in 100 year intervals from 50 ka to 12 ka, and then divide paleoclimatic record in the valley into five stages : 1) before ca. 41 ka, it was cold-and-dry climate, 2) from ca. 41 to 30 ka, the climate became warm-and-wet, especially around ca. 35 ka, it was warmest-and-wettest climate, 3) from ca. 30 to 26.7 ka, the climate was characterized by fluctuation of cold-dry and warm-wet at 300~600 yr intervals, 4) from ca. 26.7 to 16 ka, cold-and-dry climate was prevailed. Especially it was coldest in ca. 20~22 ka, which corresponds to the last glacial maximum, 5) from ca. 16 to 14.4 ka, the climate became warm-and-wet gradually.

We compared the climatic records in the Kathmandu Valley with timing of expansion of glaciers in the Everest area during the last glacial period from ca. 50 to 12 ka (**Figure 1**). Frinkel et al. (2003) reported that extensive glaciation occurred three times in the Everest area : 1) Thangboche II (35±3 ka), 2) Periche I (23±3 ka), 3) Periche II (16±2 ka). In Periche II stage (16±2 ka), the Kathmandu Valley had a cold-and-dry climate, which is characterized by abrupt increase of *Pinus* and non-arboreal pollen as Gramineae. Periche I (23±3 ka) corresponds to the last glacial maximum in the Kathmandu Valley, which is characterized by increase of *Picea*. During the stage of Thangboche II (35 ± 3 ka), warm-and-wet climate prevailed in Kathmandu. Increase of precipitation under warm climate in Kathmandu around 35 ka suggest strength of the Indian summer monsoon, which must have brought about heavy snow fall in the Everest area and following extensive glaciation.

Method of pollen analysis

Fossil pollen and spores were extracted from the muddy samples by 10% KOH-ZnCl$_2$ (s.g. 1.85)-acetolysis method. Microfossils of the treated material were mounted in glycerol on a glass slide. I counted until the two rules where the arboreal pollen (AP) is over 200 grains and the total pollen is over 500 grains for each sample were filled. In the pollen diagram, percentage for each genus of AP was calculated on the basis of the sum of the AP. The percentage for each genus of NAP (non-arboreal pollen: herb pollen and fern spore) was calculated based on the total sum of pollen and spores.

We inferred paleoclimatic changes on the basis of interrelationship between present distribution of vegetation and vertical climatic zonation in the Kathmandu Valley and surrounded mountains. For the purpose of inference of paleoclimate, we used the following genera as climatic indexes: *Pinus, Tsuga, Picea and Abies* for cold climate, *Quercus* and *Castanopsis* for warm climate, *Alnus, Betula, Carpinus* for wet climate and Gramineae, *Artemisia* and Chenopodiaceae for dry climate.

References

Fujii R, T Maki, H Sakai and N Miyoshi. 2004. Paleoclimatic changes during the last ca. 750 kyr recorded in the Kathmandu Valley, central Himalaya. Proceedings of XI International Palynological Congress, *Polen*.

Maki T, R Fujii, H Umeda, H Sakai, Y Hase and K Shichi. 2004. Paleovegetation and paleoclimate in the Kathmandu Valley and Lake Baikal during the late Quaternary. Proceedings of XI International Palynological Congress, *Polen*.

Sakai H, R Fujii, Y Kuwahara, BN Upreti and SD Shresta. 2001. Core drilling of the basin-fill sediments in the Kathmandu Valley for paleoclimatic study: preliminaly results. *Journal of Nepal Geological Society Special Issue* **25**: 9-18

Finkel RC, LA Owen, PL Barnard and MW Caffee. 2003. Beryllium-10 dating of Mount Everest moraines indicate a strong monsoon influence and glacial synchroneity throughout the Himalaya. *Geology* **31** (6): 561-564

Schulz H, UV Rad and H Erlenkeuser. 1998. Correlation between Arabian Sea and and climate oscillations of the past 110,000 years. *Nature* **393**: 54-57

Effects of global warming on Asian lakes from viewpoints of water resources and environmental change

H Fushimi

The University of Shiga Prefecture, School of Environmental Science, 2400 Hassakacho, Hikone 522-8533 JAPAN

For correspondence, E-mail: fushimi@ses.usp.ac.jp

Lakes in the Himalayas and Tibetan plateau

Due to the global warming, the recent fluctuations of glaciers and lakes in the Nepal and Bhutan Himalayas are extremely immense and the region faces more natural disasters including the glacial lake outburst flood. There is a need to create a new management system for the rational use of water resources taking into account the recent changes in glacial as well as limnological phenomena.

The Himalayas and Tibetan plateau will face the shortage of glacier-fed water resources due to the shrinkage of glacier as well as permafrost ice bodies in the late period of the 21st century, and the decrease in glacial melt-water will tend to exacerbate drought phenomena in the catchment areas of the mighty rivers, such as Rivers Yellow, Yangtze, Mekong, Ganges and Indus, especially during the dry season in areas with the rapid population growth dependent on water resources from the glaciers and permafrost layers in the Himalayas and Tibetan plateau.

Lake Hovsgol in Mongolia

The water level of Lake Hovsgol in Mongolia has risen 60 cm during the past 20 years, so that the surrounding forests, pastures and the lakeshore town have been inundating year by year. Three causes of the water level rise could be noticed as follows: 1) the formation of a natural dam at the southern end of the lake caused by the sedimentation of sand and gravel which were transported from the tributary river at the time of heavy rain, 2) the thaw of permafrost around the lake where the ground temperature becomes higher with increases of the incoming radiation due to deforestation owing to the anthropogenic expansion of pasturage and forest fire, and 3) the thaw of permafrost caused by the global warming.

Here, we would like to suggest as the short-term countermeasure that the natural dam should be dredged to prevent the inundation, because it can be estimated to lower 30 cm of the water level by the dredging of only 500 m^3. As the mid-term countermove, it is important to improve the anthropogenic land-use for preventing the expansion of pasturage and forest fire. Finally, as the long-term issue, we hope to solve the global warming with the international cooperation by monitoring the natural environmental changes of Lake Hovsgol.

Lake Biwa in Japan

It is reported that an average air temperature will increase by 1.5 to 3.5 degrees Celsius by the 2030's due to the global warming. If the increase in average air temperature is 1.5 degrees Celsius, the amount of snow cover would not exceed 1 billion tons, which is the average amount of snow cover in Lake Biwa basin, unless the precipitation exceeds more than 20 %. When the average air temperature rises by 3.5 degrees Celsius, the amount of snow cover would significantly decrease to 0.6 billion tons even if the precipitation exceeds by 20%.

When the amount of snow cover is more than 1 billion tons, the lowest dissolved oxygen concentration in the deep layer of Lake Biwa increases due to the density current of the oxygen-rich snowmelt. However, the dissolved oxygen concentration rapidly decreases, when the amount of snow cover is less than 1 billion tons. The global warming will significantly decrease the amount of snow cover in Lake Biwa basin and the dissolved oxygen concentration in the deep layer of the lake, so it leads to further enhancement of eutrophication in the 21st century.

New significant advances of regional geological survey in the blank regions of Qinghai-Xizang Plateau

Zhai Gangyi

Bureau of China Geological Survey, Beijing, 100037, CHINA

For correspondence, E-mail: zgangyi@mail.cgs.gov.cn

Qinghai-Xizang Plateau provides an unparalleled opportunity to study the Tethyan evolution and the continental dynamics in which continents respond to subduction of slabs and collisional orogenesis. Many projects are mainly placed on this "key testing site" by geologists from all over the world. The main parts of Qinghai-Xizang Plateau are always the blank regions in the geological maps of large to intermediate scales of the mainland of China. Since 1999, approximately 1000 geologists from 32 geological survey institutes and scientific research academies are called for by the Bureau of China Geological Survey to conduct geological mapping in the blank regions of Qinghai-Xizang Plateau in an unparalleled fashion.

The blank regions not covered by geological survey in Qinghai-Xizang Plateau are up to 1.45×10^6 km^2, which account for 60% of the total area of Qinghai-Xizang Plateau. They have been subdivided into 110 maps of regional geological survey at a scale of 1: 250, 000. Mapping of more than two third of the blank regions was completed by the end of last year. Significant progress has been made as evidenced from a large volume of new and important data obtained from the regional geological survey (Bureau of China Geological Survey, 2004a, 2004b, 2004c). These data are extensive and effective for interpretation and re-evaluation of the geological problems that are related to the formation and evolution of Qinghai-Xizang Plateau.

Discoveries and identifications of a series of ophiolitic mélange zones, main faults and important regional discontinuities offer new, important information to reconstruct the tectonic framework and evolutional history in Qinghai-Xizang Plateau. The significant findings in Yarlung Zangbo ophiolitic mélange zone are T_{2-3}, T_3-J_1 radiolarian assemblages from argillaceous-siliceous rock in Tangga, Pomulong, and T_{2-3} radiolarian assemblages from siliceous rock in Zedang. An ophiolitic mélange zone called Shiquanhe-Namu Co-Jiali was identified in Gangdise. Identification of Hongliugou-Lapeiquan ophiolitic zone, Apa-Mangya ophiolitic zone (Cambrian-Ordovician) in A'erjin region and Qimayute-Qimantage ophiolitic zone (Cambrian-Ordovician), Yanbishan-Xiangyangshan ophiolitic zone (Ordovician-Carboniferous), Subashi-Muzitage ophiolitic zone (Carboniferous-Permian) in Kunlun mountain region enables reconstruction a clear evolutional history for the northern Qinghai-Xizang Plateau. Furthermore, Recognition of significant regional angular unconformities in Himalayas (Ordovician / metamorphic basement), Gangdise (P_3/ P_2, and T_3/P_3, J_{1-2}/P_3 etc.) and Qiangtang (T_3/J_2) clearly show the evidences of orogenesis in different regions of Qinghai-Xizang Plateau (Wang et al. 2004).

The findings of a great deal of fossils provide the most important constraints for the stratigraphic framework, tectonic paleogeography and evolutionary history of Qinghai-Xizang Plateau. These kinds of data contain relatively continuous marine sedimentary records in the Himalayas and Gangdise, the mixed biota of the cool water biota with warmer water biota in the Upper Permian stratum of Gangdise, the Ordovician hornstones in Qiangtang basin, the cool water biota with single channels in Jinyuhu area of northern Qinghai-Xizang Plateau, the Early Triassic conodonts, the Late Permian and Late Triassic pollens and spores in Bayankala Group etc.

A series of significant volcanic interlayers, abundant high-quality isotopic ages of high-pressure metamorphic rocks, and magmatic rocks provide reliable chronological constraints in assessing the tectonic evolutional history of Tethys. Eleven volcanic interlayers that are mainly characterized by intermediate-basic from Permian to Cretaceous in Tethyan Himalayas (Zhu et al. 2004) and the Late Paleozoic volcanic interlayers are mainly composed of basalt, andesite, dacite, and rhyodacite in Gangdise (Wang et al. 2004) provide possibilities to study the continental breakup of northern margin of Gondwana and the tectonic evolution of Gangdise in the Late Paleozoic. The findings of basic granulites in Yadong, central segment of Higher Himalayas (zircon SHRIMP ages distributed at 1.99 Ga±0.03 Ga, 29.5 Ma±0.4 Ma, 17.6 Ma±0.3 Ma), the 525 Ma ~ 553 Ma crystalline ages of granite from rock suite of Namche Barwa, and the granodiorite with huge phenocrysts (concordant age of zircon is 217.1±3.4 Ma) from Gangdise, together with the leucitic phonolites, high-K lithophysa rhyolites (48 Ma) from Yangbajing, hornblende aegirite augitic syenite (15.8 Ma) from the western Gangdise, as well as the granulite, eclogite, and the granitic gneiss (zircon SHRIMP age is 856 Ma±12 Ma) from the complex of A'erjinshan, are very much important for understanding the tectonic evolution of the Tethys zone and Qinghai-Xizang Plateau.

The abundant and useful information on new findings of numbers of mineral resources are valuable for the regional economic development. More than 500 deposits and mineralized spots have been found in the process of regional geological survey. A significant number of these newly found mineralizations serve as potential large-scale and super large-scale deposits. In addition, 9 major mineralization belts of polymetals including Cu, Fe, Pb, Zn, and Ag also have been recognized.

A large dataset obtained newly on Cenozoic tectonics and Quaternary sedimentary records of terrestrial and lacustrine facies is valuable to study the collisional behavior, the process of uplift and the environmental evolution for the Qinghai-Xizang Plateau. The angular unconformities between Dazhuka and Lamayejia Formations in southern margin of Gangdise, the Zu'erkenwulashan (Ez) and Tuotuohe (Et) Formation in northern Qinghai-Xizang Plateau yield information that is useful for evaluation of collisional behavior of the continent-continent type. Thirty eight levels of lacustrine terraces from the northern bank of Peiku Co and 153.95 m thick sedimentary record of glacial lacustrine facies from Paixiang-Yusong in eastern Tibet show characteristics of Barrier Lakes. While the sedimentary records such as 119 m higher than the lake level from Zabuyechaka-Taruo Co-Xueli Co-Kongqie Co, as well as the 130-140 m higher than the lake level from peri-Namu Co indicate that there was a huge paleo-lake (the area exceeded 10×10^4 km^2) in the late Pleistocene

in the northern Tibetan Plateau. The five terraces of continental river from Nuomuhong in the northern Qinghai-Xizang Plateau provide significant information in order to understand the climate change and the uplift of Plateau.

A lot of cultural relics provide important opportunities to study the culture of paleo-humanity in Qinghai-Xizang Plateau. Five activity relics of paleo-humanity (including 390 stone implements and also pottery fragments) from Zadong, Qiongguo, Saga, Dajia Co in Himalayas, and 3 stone implements, 1 tooth of large animal from Kumu'ewulazi in eastern Kunlunshan have been found. These data show the history of paleo-humanity activity at about 7~4 KaB.P. and 10 KaB.P. in Qinghai-Xizang Plateau.

Under the deployment of Bureau of China Geological Survey, the new version of geological map of Qinghai-Xizang Plateau and its adjacent regions (25º to 40º N latitudes, 72º to 106º E longitudes) at 1:1,500,000 scale was completed. This was accomplished through the use of the knowledge and experience of mapping of Chinese as well as foreign geologists on geological phenomena in Qinghai-Xizang Plateau gathered during the last two decades. Of special importance were the new data gathered during the geological surveying at 1:250, 000 scale in the blank regions of Qinghai-Xizang Plateau. This new version geological map is essential graphic guide for the researchers from all over the world for carrying out research on geology and other related scientific fields on Qinghai-Xizang Plateau.

References

Bureau of China Geological Survey. 2004a. The results and advances of regional geological survey in Himalayas. In: Special issue on the first group of results in 1:250 000 geological mapping in the Qinghai-Tibet Plateau, *Geological Bulletin of China* **23**(1): 27-39 (in Chinese)

Bureau of China Geological Survey. 2004b. The results and advances of regional geological survey in Gangdise. In: Special issue on the first group of results in 1:250 000 geological mapping in the Qinghai-Tibet Plateau, *Geological Bulletin of China* **23**(1), 45-60 (in Chinese)

Bureau of China Geological Survey. 2004c. The results and advances of regional geological survey in A'erjin-Kunlun mountain. In: Special issue on the first group of results in 1:250 000 geological mapping in the Qinghai-Tibet Plateau, *Geological Bulletin of China* **23**(1): 68-96 (in Chinese)

Wang L, D Zhu and G Pan. 2004. Primary Results and Progress of Regional Geological Survey (1:250, 000): the South of Qinghai-Tibet Plateau. *Geological Bulletin of China* **23**(6), in press (in Chinese with English abstract).

Zhu D, G Pan, X Mo X and others. 2004. The volcanic activities in the central segment of Tethyan Himalayas from Permian to Cretaceous (I): Distributions and Significances. *Geological Bulletin of China* **23**(5), in press (in Chinese with English abstract)

Land cover change in Himalaya with special reference to forest disturbance: A case of Bharse area, Lesser Himalaya, West Central Nepal

Chinta Mani Gautam* and Teiji Watanabe

Graduate School of Environmental Earth Science, Division of Geoscience, Hokkaido University, JAPAN

* To whom correspondence should be addressed, E-mail: cgautam@ees.hokudai.ac.jp

The status of forests in Nepal is often expressed in terms of the extent of deforestation (World Bank 1978, Bishop 1990, UNEP 2001). However, in case of the hill forests extraction of timber, lopped for firewood and foliage, litter collection and grazing degrade forest structure and create land cover types that are intermediate between intact and cleared forests. Such forests which are supplying the basic needs of local people and continuing their existence help to protect biodiversity that existed locally for a long time. This study refers such an intermediate type of forest to as disturbed forest. The term 'degradation' has been used for the loss of biomass from the forest floor with undesired effects on the forest structure. The disturbance caused by extraction of timber, lopping for firewood and foliage, litter collection and grazing etc. are referred to as anthropogenic disturbance.

The aim of this study was to quantify the land cover change between 1958 and 2002, using topographical maps (1958), aerial photographs (1992) and field observation in 2002 in the Bharse area, Gulmi district, western Nepal. Five managed forest plots, within the area, which remained virtually unchanged during the period were selected to measure the disturbance intensity and species diversity indices for trees. We believe that both intensity of disturbance and diversity indices for trees should differ despite the forest cover remained unchanged. Therefore, we determined the disturbance intensity (DI) and analyzed the diversity indices for tree species of each selected forest to evaluate the influence of human disturbance in the forest floor.

Land cover change during 1958-2002 was analysed in the same area using Geographical Information System as an analytical tool. Seventy-five circular plots belonging to five forests; Thaple (TL), Raniban (RB), Lurung Bhitta (LB), Chiureko Lek (CL) and Raiker (RK) were sampled to measure the disturbance intensity and diversity indices. Each plot covered 50 m² area, In each plot, floristic composition (total number of woody species), stand structure (density, species type and diameter at breast height (DBH) at 1.3 meter height (for stands with diameter greater than 5 cm) and succession (number of tree species less than 5 cm DBH and height greater than 50 cm) were measured. Further, the number of stumps, the number of trees lopped for firewood (tree with at least one cut branch exceeding 5 cm diameter), and foliage were counted in each plot to determine the cutting disturbance intensity. The DBH of removed trees was calculated from stump height and diameter at cut point (Khatry-Chhetry and Fowler 1996). Each species encountered was identified at first by local name in the field and the botanical name was identified at the National Herbarium Center, Godavari, Kathmandu. Evidence of grazing in each sample plot was determined from the presence of cattle, dung, browsing, trampling and grazing traces.

To determine the DI from the cutting pressure, three variables were calculated as proportions; (a) proportion of removed basal area, (b) proportion of removed trees and (c) proportion of lopped trees. The weights were subjectively assigned based upon the relative contribution for the removed ground biomass loss from the forest and their effects on forest structure and composition (Khatry-Chhetry 1997, Acharya 1999). The removed basal area is strongly correlated with the removed biomass, so, it is considered to be important (W = 0.50). Lopping for firewood and foliage represents the smallest loss of biomass amount and its effect is quite small among the selected variables of this study. So it was assigned the lowest value (W = 0.1666) (Khatry-Chhetry 1997).

$$\mathbf{DI} = \sum_{i=1}^{n}(DVi * Wi)$$

Where,
DVi = ith disturbance variable
Wi = Assigned weight for ith variable

The cutting disturbance intensity is a relative index of a weighted additive form (Oat 1978) with a theoretical range of zero (no disturbance) to one (maximum disturbance).

Grazing intensity was determined from the qualitative data observed during the field work. Evidence of grazing in each plot was determined from the presence of cattle, dung, browsing, trampling and grazing traces, ranking 0%, 25%, 50%, 75% and 100%. The rank percentage of grazing was changed to the percentage of grazing area in the forest level dividing the sum of rank of each forest by the total number of sampled plots of the same forest.

The different indices of species diversity, i.e., species richness (number of species per unit area), evenness (distribution of abundances among the species) and diversity index were calculated for succession and trees in five forests (Margalef 1958, Shannon and Weaver 1949, Simpson 1949), which are the most commonly used measures of diversity indices by ecologists.

The forest land increased by 3.31 km² (33%) whereas agriculture and shrub lands decreased by 1.21 km² (19%) and 2.14 km², respectively, between 1958 and 1992. The shrub land increased by 0.85 km² (16%) whereas agriculture and forest lands decreased by 0.80 km² (16%) and 0.04 km² (<1%), respectively, between 1992 and 2002. The other types of land cover (landslides and water bodies) occupied minimal area (<0.2%) of the Bharse area for periods 1958, 1992 and 2002.

Among the five forests, the highest cutting disturbance intensity of 0.141 was determined in forest TL whereas the lowest value of 0.049 was found for forest RB. Forest RK occupies second highest position according to DI having a value of 0.10. The forest LB and CL have quite similar values of 0.053 and 0.058 of DI, respectively.

Grazing evidence was found only for CL, RB and TL. Almost all parts of forest TL has been affected form the cattle grazing having highest value of 58% followed by forest RB, 48%. Only 20% area of forest CL was affected from the grazing practices.

TABLE 1. Pattern of species diversity in studied forests for trees (> 5 cm DBH) arranged according to increasing level of cutting disturbance

Diversity indices	Forests				
	RB	LB	CL	RK	TL
Species richness	3.67	3.10	2.60	2.64	1.99
Shannon Weaver's Index	2.36	2.39	2.18	2.26	1.93
Simpson's diversity	0.85	0.89	0.85	0.87	0.81
Evenness (Shannon Weaver's)	0.76	0.84	0.82	0.83	0.81

Note: LB, Lurung Bhitta; CL, Chiureko Lek; RB, Raniban; RK, Raiker; TL, Thaple

TABLE 2. Pattern of species diversity in studied forests for succession of tree species (> 5 cm DBH) arranged according to increasing level of grazing disturbance

Diversity indices	Forests				
	LB	RK	CL	RB	TL
Species richness	3.54	2.83	2.52	2.87	1.55
Shannon Weaver's Index	2.43	2.56	2.35	2.33	1.86
Simpson's diversity	0.88	0.90	0.87	0.0.87	0.83
Evenness (Shannon Weaver's)	0.81	0.90	0.89	0.80	0.85

Note: LB, Lurung Bhitta; CL, Chiureko Lek; RB, Raniban; RK, Raiker; TL, Thaple

The studied forests of Bharse area have relatively low disturbance as compared to the surrounding area of Kathmandu valley (Acharya 1999, Khatry-Chhetry 1997). Such differences are probably due to effective forest management practices of the local inhabitants and increased forest cover in private land between 1958 and 1992. Hence, effective management practices are crucial in order to reduce the disturbance intensities.

According to field data, on disturbance intensity and the types of disturbances, which were collected during the fieldwork, the five forest patches were categorized as affected by illegal timber extraction (LB), illegal timber extraction and grazing (CL), illegal timber extraction and opening for grazing (RB), opening for timber extraction (RK), and opening for both grazing and timber extraction (TL). The different indices of species diversity of vegetation for succession and trees were calculated for each forest patch to know the influence of cutting and grazing intensity on the forest floor.

The species richness for trees (> 5 cm DBH) decreases with increasing cutting disturbance (Table 1). However, no effects were seen from cutting for succession (< 5 cm DBH) compared to the value of trees (> 5 cm DBH) in respective forest patch (Tables 1 and 2). Species richness and diversity of Shannon-Weaver index were found high for succession compared to the values of trees for forests accessible to cutting (RK and LB). The above indices were low for forests opened for grazing (RB), and cutting and grazing (TL). Diversity indices for succession were high in the forest affected by cutting (RK).

The diversity indices indicate a poor regeneration of species in the forests used heavily for cattle grazing, whereas no such effects were seen for forests affected by cutting.

References

Acharya B. 1999. *Forest Bio-diversity Assessment: A Spatial Analysis of Tree Species Diversity of Nepal*. Netherland, ITC (International Institute for Aerospace Survey and Earth Science). 199 p

Bishop BC. 1990. *Karnali Under Stress: Livelihood Strategies and Seasonal Rhythms in a Changing Nepal Himalaya*. Chicago, The University of Chicago: 460 p

Kairo JG, F Dahdouh-Guebas, PO Gwada, C Ochieng and N Koedam. 2002. Regeneration status of Mangrove forests in Mida Creek, Kenya: a compromised or secured future? *Ambio* **31**(7): 562-568

Khatry-Chhetry DB. 1997. *The ecology of warm-temperature forests in the central Himalayas across a human-induced disturbance gradient*. Natural Resources and Environment. (PhD Thesis) Michigan University, Michigan. 253 p

Khatry-Chhetry DB and GW Fowler. 1996. Estimating diameter at breast height and basal diameter of trees from stump measurements in Nepal's lower temperate broad leaved forests. *Forest Ecology and Management* **84**: 177-186

Margalef R. 1958. Information theory in ecology. *General Systematics* **3**: 36-71

Oat WR. 1978. Environment Indices: *Theory and Practice*. An Arbor, An Arbor Science, Michigan

Shannon CE and W Weaver. 1949. *The Mathematical Theory of Communication*. Urbana, University of Illinois Press, Illinois. 144 p

Simpson EH. 1949. *Measurement of diversity*. Nature **163**: 688

World Bank. 1978. *Nepal staff projects reports and appraisal of the Community Forestry Development and Training Projects*. Washington DC

Integration of magnetic properties and heavy metal chemistry to quantify environmental pollution in urban soils, Kathmandu, Nepal

Pitambar Gautam†[*], Ulrich Blaha‡ and Erwin Appel‡

† COE Neo-science of Natural History, Graduate School of Science, Hokkaido University, Sapporo 060-0810, JAPAN
‡ Institute of Geosciences, University of Tuebingen, Sigwartstrasse 10, D-72076 Tuebingen, GERMANY

* To whom correspondence should be addressed. E-mail: p-gautam@nature.sci.hokudai.ac.jp

The state of environment of the Kathmandu valley has been deteriorating due to various causative factors such as the traffic pollution dominant in the urban area, industrial activities including the cement factory, emissions from the traditional brick-kilns scattered throughout the Kathmandu valley, probably biomass burning and other factors that are not adequately known. Hence, it is important to recognize the major sources of the pollution, the share of each of these sources and also characterization of the type of pollution and quantification of the degree of pollution in space and monitoring so as to reveal the changes with time.

In order to characterize and quantify the degree of pollution we have been carrying out measurements of rockmagnetic properties (magnetic susceptibility, susceptibility vs. temperature characteristics, isothermal remanent magnetization (IRM) acquired stepwise at 18-20 steps up to 2.5 T DC pulse field) and chemical analyses on heavy metals (Cd, Co, Cr, Cu, Fe, Mn, Ni, Pb, Zn) by atomic absorption spectrometry of a variety of material (dust-loaded leaves of road-side trees, road dust and soils from decimetric to metric vertical sections etc.). The effectiveness of chemical analyses and magnetic methods in such studies has been well established (Devkota 2001, Gautam et al. 2004). Here we describe these properties for soils and describe the use of the pollution index based on selected heavy metals to compare the soil sections from sites variously affected by urban pollution and also the application of susceptibility or IRM as proxy parameters to rapidly characterize the soils.

A study of soils from vertical profiles from more than a dozen sites scattered in Kathmandu, and Kirtipur reveals that the mass-specific magnetic susceptibility (MS) fluctuates by three orders of magnitude. MS can be used to broadly categorize the soil intervals such as 'normal' (MS$<10 \times 10^{-8}$ m^3 kg^{-1}), 'moderately magnetic' ($10–100 \times 10^{-8}$ m^3 kg^{-1}), and 'highly magnetic' (MS $>100 \times 10^{-8}$ m^3 kg^{-1}). Except for thin Fe-oxide-enriched layers within the soil profile, soils far from road and industrial sites belong to the 'normal' category (e.g., the paddy field in Kirtipur, site K in **Figure 1**). In soils in close proximity to a road corridor, MS is highest at several cm depth and it remains at 'highly magnetic' level within the upper 20 cm interval after which it decreases with depth through 'moderately magnetic' level reaching to 'normal' at ca. 40 cm depths (i.e., east of Rani Pokhari and Exhibition ground, sites Hx7 and Hx8, respectively, shown in the **Figure 1**). The upper parts of soil profiles in city parks (i.e., Ratna Park, Balaju) exhibit MS within 'moderately magnetic' levels. SIRM is contributed mostly by three components of distinct median acquisition fields (B$_{1/2}$): soft (B$_{1/2}$ = 30 mT; magnetite-like phase), intermediate (160 mT) and hard (600 mT; hematite). In 'normal' intervals, soft and intermediate components contribute to 90% of SIRM. Within 'highly or moderately magnetic' soils, the contribution of soft

and intermediate components seems to decrease with depth (e.g., from ca. 90% near the surface to 70% at 30 cm) in favor of the hard component. Susceptibility (logarithmic) variably correlates with heavy metals. We observe a very good positive correlation with all metals at Rani Pokhari (Hx7). However, for the Ratna Park (Hx3) there is very good positive correlation of MS and SIRM with Zn, Pb and Cu but poor and even negative correlation with Fe (Mn), Cr, Ni and Co (**Figure 2**). These data suggest that the use of MS for estimating heavy element content in urban soils of Kathmandu needs to be considered locally.

Our analysis of several soil profiles reveals that the contents of so-called 'urban elements' represented by Pb, Zn and Cu can be collectively used to compare the level of pollution among the sites. This is demonstrated in **Figure 3** in the example of 3 profiles which belong to Ratna Park, Balaju and Kirtipur, respectively. The contents of 3 metals are used to calculate the Tomlinson pollution load index (PLI) (Angulo 1996), which represents the number of times by which the heavy metal concentration in soils at particular horizon exceeds the background concentration (Chan et al. 2001). It is obvious from **Figure 3** that the PLI variation is very well reflected by variation of susceptibility and SIRM with depth and therefore the latter can be used as proxy of the former.
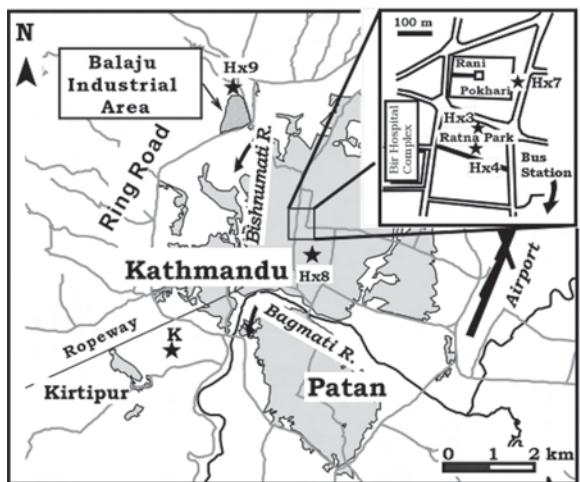
FIGURE 1. Schematic map of the Kathmandu urban area (lightly shaded) showing several soil coring sites (Hx*n*, and K, denoted by stars) which are the objects of investigation for magnetic properties and heavy metal chemistry
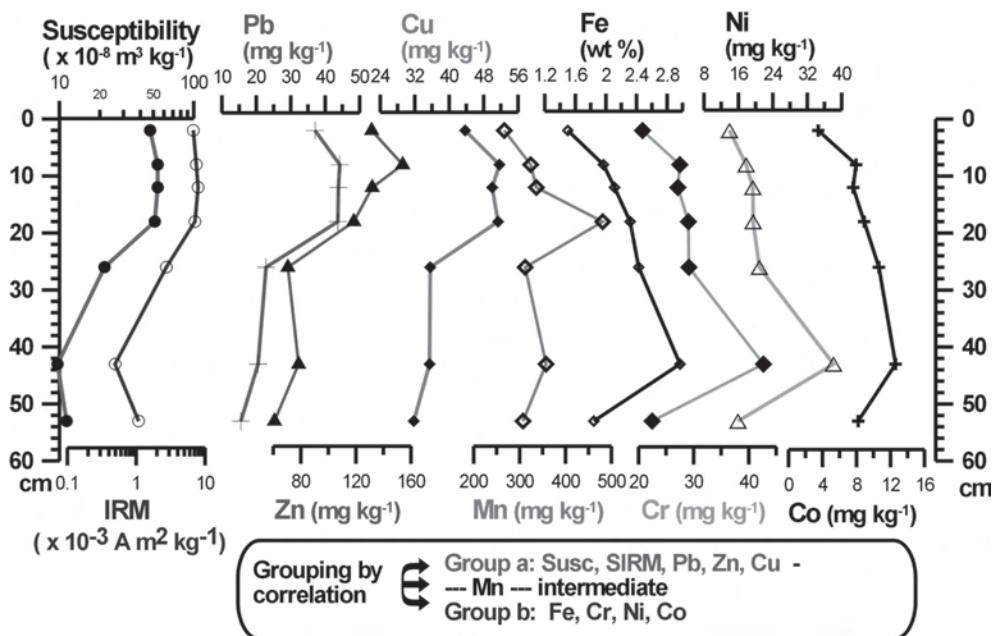
FIGURE 2. Downhole plots of magnetic parameters (susceptibility and isothermal remanences) and heavy metal contents in vertical soil profiles from Ratna park situated in the city center
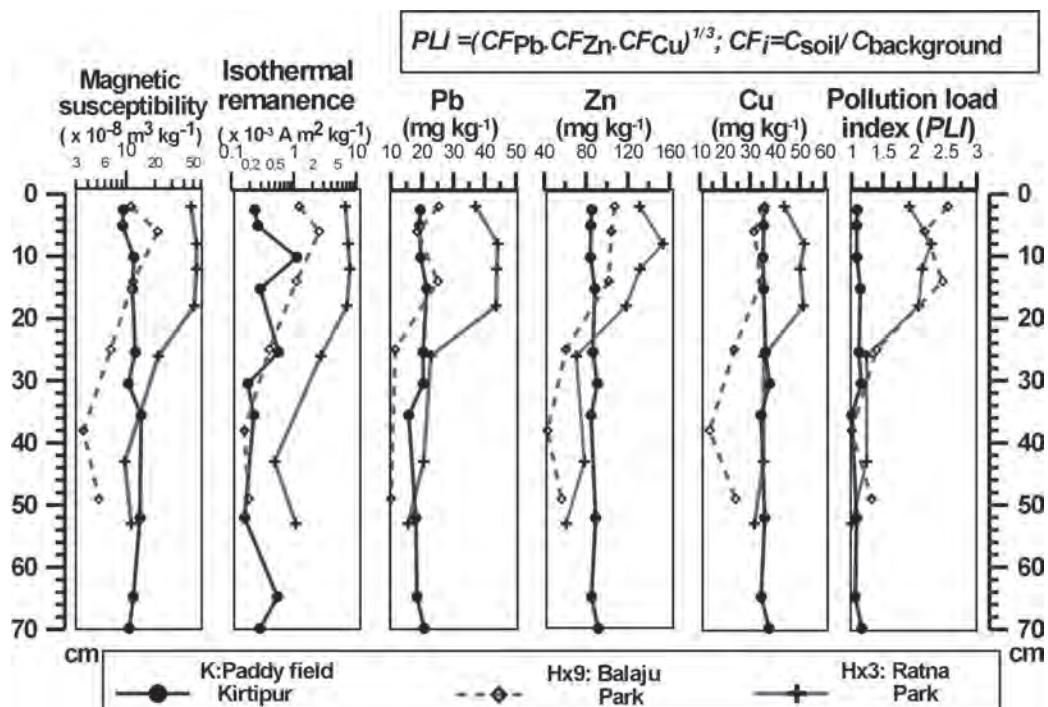
FIGURE 3. Comparison of the magnetic parameters and the pollution load index (PLI) based on the contents of 'urban elements' in 3 sites which are variously affected by urban pollution. Note the very good correlation between the magnetic properties and the PLI justifying the use of the former as proxy parameters

References

Angulo E. 1996. The Tomlinson pollution load index applied to heavy metal 'Mussel-Watch' data: a useful index to assess coastal pollution. *Science of the Total Environme*nt **187**: 19-56

Chan LS, SL Ng, AM Davis, WWS Yim and CH Yeung. 2001. Magnetic properties and heavy-metal contents of contaminated seabed sediments of Penny's Bay, Hong Kong. *Marine Pollution Bulletin* **42**(7):569-83

Devkota D. 2001. Total and extractable (mobilizable and mobile) heavy metals in the Bagmati river sediment of Kathmandu, Nepal. *Journal of the Environment* **6**(7): 34-51

Gautam P, U Blaha, E Appel and G Neupane. 2004. Environmental magnetic approach towards the quantification of pollution in Kathmandu urban area, Nepal. *Physics and Chemistry of the Earth* (in press)

Initial uplift of the Tibetan Plateau and environmental implications

Xiaohong Ge†, Shoumai Ren‡§ *, Yongjiang Liu† and Lixiang Ma¶

† College of Earth Sciences, Jilin University, Changchun, 130061, CHINA
‡ Institute of Geomechanics, Chinese Academy of Geological Sciences, Beijing, 100081, CHINA
§ Strategic Research Center for Oil and Gas Resources, Ministry of Land & Resources, Beijing, 100034, CHINA
¶ Institute of Graduates, China University of Geosciences, Wuhan, 430074, CHINA

* To whom correspondence should be addressed. E-mail: realshaw@vip.sina.com

When did the Tibetan plateau uplift firstly? This is an attentive question to all geologists who are studying on the Himalayan structure. Aitchison et al. (2002) discovered the Oligocene-Early Miocene radiolarite silicon rock and the Lower Miocene Gangrinboche conglomerates along the Yarlung-Tsangpo suture zone, which provided a significant evidence to postpone by nearly 20 Ma the closure time of Tethys ocean along the Yarlung-Tsangpo suture belt. They also suggested that the real collision between Indian and Eurasian plate happened between 30 Ma to 25 Ma ago, unlike the previous supposition as 50 Ma (Patriat and Achache 1984). Therefore, we are sure that the initial uplift of the Tibetan plateau should have occurred in the Early Miocene period. This is also consistent with the results we got from the Qaidam basin recently.

Many profiles, which cross the Qaidam basin and East Kunlun Mountains, indicate that sedimentary center of the Qaidam basin was around Yiliping region in the central basin in Paleocene-Oligocene period, with the characteristics of diminishing depression. Grain size analyses of the related formation sediments and rather lower sedimentary rate indicate that the basin was in an extension tectonic setting at that time, then the Miocene basin area was reduced apparently, and the sedimentary rate was increased suddenly around 25 Ma ago. A foreland depression existed in front of the Paleo-Kunlun Mountains, which implies that the regional uplift happened in the whole Qaidam basin during the Mid-Miocene epoch and was eroded subsequently. The large-scale distribution of the angular unconformity between Xia Youshashan Formation and Shang Youshashan Formation, which is marked as T2' reflect layer in seismic profile, on the basin margin can provide the evidence for this raising procedure. This raising of compression in Qaidam basin about 25-22 Ma ago is actually the first uplift of the Tibetan plateau. The appearance of the loess in the adjacent region of Tibetan plateau around 22 Myr ago (Guo et al. 2002), the pre-Miocene thrust fold in the Qiangtang basin in the northern Tibet, the Lower Miocene conglomeratic molasses along the Yarlung-Tsangpo suture zone on the southern margin of the Lhasa terrane (Aitchison et al. 2002), the potassic lavas in western Tibet over the past 20 Myr (Chung et al. 1998, Turner et al. 1993) and the changes of sedimentary-tectonic setting and biological characters in northwestern China, are the symbols of the initial uplift of the Tibetan plateau.

The research results of Aitchison et al. (2002) could reasonably explained the geological background of the appearance of the arc-continent collision fossil-structure belt and Gangdess porphyritic copper ore deposit on both side of the Yarlung-Tsangpo suture belt, this suggests that the Yarlung-Tsangpo and Gangdess belts located on the anterior border of the arc-continent/arc-arc collision during the Paleo-Asian plate colliding to Tethys ocean plate, it is similar to the position of the present Japan-Taiwan- Philippine island arc around the west Pacific Ocean, while the hinterland, the region from the western China to Kazakstan, was in the tectonic surrounding similar to the eastern Asian plate. Large-scale peneplanation and pangeo-basin were developed at that time. Therefore, similar as Qaidam basin, the Tarim basin, Junggar basin, Tu-ha basin, and Hexi Corridor are not foreland or compression basins, and are likely the dishing depressions under the stretch environment during the Eocene-Oligocene period. The relative lower sedimentary rates in those basins during the Paleocene and the latitudinal circulation of the subtropical paleo-climate zone in western China also support above ideas.

References

Aitchison JC, AM Davis, B Zhu and H Luo. 2002. New constraints on the India-Asia collision: the Lower Miocene Gangrinboche conglomerates, Yarlung Tsangpo suture zone, SE Tibet. *Journal of Asian Earth Sciences* **21**: 521-263

Chung SL, CH Lo, TY Lee, YQ Zhang, YW Xie, XH Li, KL Wang and PL Wang. 1998. Diachronous uplift of the Tibetan plateau starting 40 Myr ago. *Nature* **394:** 769-773

Guo ZT, WF Ruddiman, QZ Hao, HB0Wu, YS Qiao, RX Zhu, SZ Peng, JJ Wei, BY Yuan and TS Liu. 2002. Onset of Asian desertification by 22 Myr ago inferred from loess deposits in China. *Nature* **416:** 159-163

Patriat P and J Achache. 1984. India-Eurasia collision chronology has implications for crustal shortening and driving mechanism of plates. *Nature* **311:** 615-621

Turner S, C Hawkesworth, JQ Liu, N Rogers, S Kelley and P Calsteren. 1993. Timing of Tibetan uplift constrained by analysis of volcanic rocks. *Nature* **364:** 50-54

Study of geo-hydrological processes and assessment of hazard and risk in the Banganga Watershed, Nepal

Motilal Ghimire

Central Department of Geography, Tribhuvan University, Kirtipur, Kathmandu, NEPAL

For correspondence. E-mail: motilal@wlink.com.np

Present study attempts to assess the nature of geo-hydrological hazards and risk in the Banganga watershed (27.69 to 27.75º N and 83.07 to 83.32º E) in the western Nepal vis-à-vis the watershed's terrain, climatic geomorphic and socio-economic characteristics/processes. It also attempts to identify the hazard and risk areas based on the terrain relationship to the landslides incorporating the sites of gully and bank erosion, river shifting and flooding.

The information about the geo-hydrological events and their impacts, and the socio-economic characteristics of the watershed has been obtained from Participatory Rural Approach (PRA) and Rural Rapid Appraisal (RRA) methods. Similarly Geographic Information System (GIS) and the remote sensing techniques, the state-of-the art has been used for analysing the watershed terrain and assessing the hazard and risk. Topographic maps (1:25,000) prepared by the Topographic Survey Department in 1993 and the geological map (1:50,000) prepared by the Department of Mines and Geology in 1978, and the aerial photographs of 1978/79 and 1990 (1:50,000) produced by the Topographic Survey Department and the imageries obtained from Landsat Thematic Mapper (TM), 1998 were used for interpreting and analysing topography, drainage, geology and structure, geo-hydrological processes, and landuse/land cover changes. Substantial field verification of the map and photo/imagery interpretation and observation/measurements including the PRA/RRA survey was carried out in October 1999.

The Banganga watershed (**Figure 1**) characterises the steep slopes (average slope 28º), narrow valley, steeper channel course (5.7º for the Banganga River and 6.7º for the Dhungre River), and fragile geology (the Siwaliks of Neogene age) occupy the southern half of the watershed. The remaining area beyond the Main Boundary Thrust is made of the Precambrian to Eocene Lesser Himalayan rocks comprising slate, shale, limestone, dolomite, sandstone and quartzite; these rocks are highly fractured consisting about three sets of joints (Aryal 1978). These factors have contributed to frequent slope movement and intense erosion processes during the heavy rainfall in monsoon. This is evidenced by widespread landslide scars, gully development, badland topography and large scale sedimentation in the narrow valleys. The topographic and geomorphic features reflect the marginality and susceptibility of the environment in terms of productivity and human habitat. The growing population pressure (3.5% annual growth of households over the last 20 years) has been pressurizing the marginal ecosystem of the area. The expansion of the cultivated land (between 1954-1998, the cultivated land has increased by 2250 hectares i.e. 85%) on the steep slopes (71% increase in agricultural land on slopes of 15-35º) either encroaching the forest area or shrub or grassland is evidence to this. The economy is characterised by the traditional agriculture of low productivity which has resulted in food shortage to more than 70 % of the households. Due to adverse economic condition, the people of the watersheds are highly vulnerable to the geo-hydrological disasters caused by the landslides, gully erosion, bankcutting, river course shifting, debris torrents and flood.

In the watershed, active landslides have widely varying dimensions (up to 400 m long and wide up to 250 m) and they are generally clustered. The chance of occurrence (Boots and Gettis 1988) of a new landslide within the distance of 500 m from any existing slide is 0.5 and that with 800 m is 1.0. The sediments produced by landslides alone contribute to 14 kg/m²/year. Potentially unstable slopes were found in steep slopes, relatively high relief, in areas underlain by the shale and soft Siwalik sediments near to the lineaments and in the surface slope perpendicular or opposite to the dip direction of the bedding planes. Interestingly the slope movement phenomenon is high in the forest than in the cultivated land. The natural factors seem to have played predominant role in causing slope failures. The debris flows raise the bed level and lead to change in the river course on several reaches causing damage to agricultural land. Inundation is only during the rare high magnitude flood events and is limited to lower fan of Banganga River. The instantaneous impact of landslides and gully erosion is limited to not more than 2 km downstream.

The socio-economic significance of the hazard in the watershed is considerably high. There has been a significant loss of agricultural land and other infrastructure during the extreme geo-hydrological events. These events commonly recur at 10 years interval. The 24 hour maximum rainfall analysis shows that the recurrence interval of landslide triggering extreme rainfall, i.e. above 150 mm (Starkel 1972), in most meteorological stations around the watershed is about 5 years (Department of Hydrology and Meteorology 1975-98). This indicates that the potential threat from geo-hydrological disaster is quite frequent and risk is expected to increase with the growth of population and expansion of infrastructures.

The geo-hydrological hazard map (Varnes 1984, UNDRO 1991) (**Figure 1**) generated by GIS based bivariate statistical method (ILWIS 1997) has displayed high degree of reliability as overwhelming number of active and old landslides scars occur on high and very high hazard zone. This highly instable zone seems to be trending along the MBT. The hazard assessment shows that about 8% of the agricultural land is in high hazard areas. Similarly, 111 houses are located in the areas of high hazard and 211 houses in moderately high hazard areas and the rest 2152 (85.9 %) houses in the safe areas. And the risk map (UNDRO 1991) generated by combining the hazard map and the vulnerability map shows the 13% of area is under high risk.

The statistical relationship between the terrain parameters and landslide density is important for the development of the methodology for hazard zonation in the areas like the Banganga watershed where the landslides causing factors are widely varied and complex and are not well understood. The GIS and remote sensing technology has been successfully applied in the study. These techniques have been used for generating and analysing several terrain parameters and geo-hydrological hazard and risk
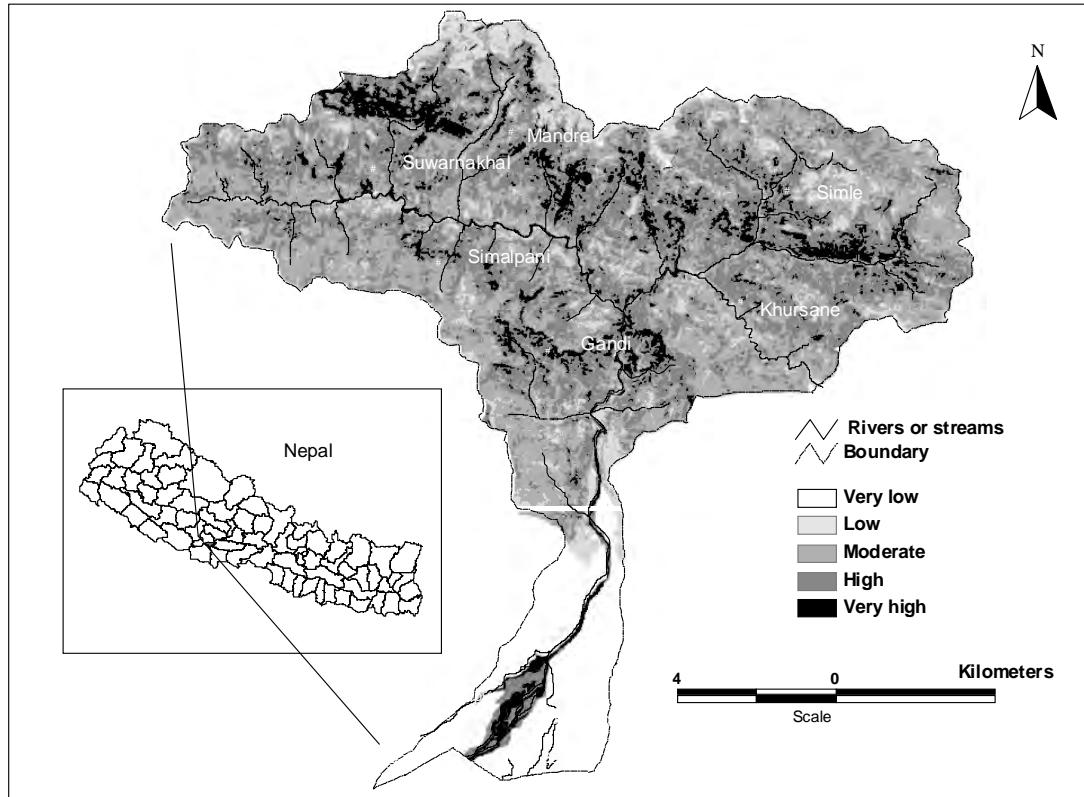
FIGURE 1. Geo-hydrological hazard map, the Banganga Watershed, western Nepal

assessment of the watershed. However, there is a scope to improve the result by using the imageries of higher resolution, and inclusion of more hazard parameters not used in the present study.

References

Aryal RK. 1978. *Geological map of Lumbini Zone.* Unpublished map and report submitted to the Department of Mines and Geology, Lainchaur, Kathmandu, Nepal

Boots BN and A Gettis. 1988. Analysing the spatial distributions of drumlins: a two mosaic approach. *Jour Glaciology* **6**: 717-36

Department of Hydrology and Meteorology. 1975-1998. Climatic records of Nepal. DHM, Kathmandu.

Starkel L. 1972. The role of catestrophic rainfall in the shaping of the relief of the lower Himalaya (Darjeeling Hills). *Geographia Polonica* **21**: 103-147

Survey Department, His Majesty's Government of Nepal. 1993. *Topographic maps of Lumbini Zone.* Produced in cooperation with the Japan International Cooperation Agency (JICA), 5 sheets: 098-05, 06, 07, 010, and 011)

The Integrated Land and Water Information System. *ILWIS 1997 User's Guide.* ILWIS Department, International Institute for Aerospace Survey and Earth Science Enschede, The Netherlands. p 419-420

UNDRO Office of the United Nations Disaster Relief Co-ordinator. 1991. *Mitigation natural disasters: phenomena, effects and options.* A manual for policy makers and planners, United Nations, New York, 164 p

Varnes DJ. 1984. *Landslide hazard zonation: a review of principles and practices.* Commision on Land slides of the IAEG, UNESCO, Natural Hazards No. 3. 66 p

Cyclicities and clusters in the lacustrine sequence of Heqing basin (SW China): Its use for dating and palaeoenvironmental reconstruction

Srinivasa R Goddu†*, Shouyun Hu‡ and Erwin Appel†

† Institut for Geosciences, University of Tuebingen, Sigwartstrasse 10, 72076 Tuebingen, GERMANY
‡ Nanjing Institute of Geography and Limnology, Chinese Academy of Sciences, 73 East Beijing Rd, Nanjing 210008, CHINA

* To whom correspondence should be addressed. E-mail: srinivasa.rao@uni-tuebingen.de

Heqing basin is situated in Yunnan province (SW China), at the southeastern margin of the Himalayan-Tibetan Plateau area. This region is suitable to study the evolution of the southwest monsoon and to identify regional tectonic events. A 168 m drill-core comprising a continuous succession of fine-grained almost uniform lacustrine sediments was recovered from the center of the basin. A High-resolution data set of palaeoenvironmental proxies is available from this core (Yang et al. 2000, Hu et al. subm.). The present study uses time series analysis and multivariate statistics to interpret these data and also uses spectral analysis in combination with magnetostratigraphy and radiometric dating to provide an optimum age frame.

Time series analysis on carbonate content and magnetic concentration parameters (χ: susceptibility, SIRM: saturation isothermal magnetization, ARM: anhysteretic remanent magnetization) show a remarkable cyclicity with a predominating spectral peak at about 15-20 m (wavelength domain). There are two clear age markers, i.e. a ^{14}C-age of 51.6 ka at a depth of 7.3 m and the Brunhes-Matuyama boundary at a depth of 141.5 m. They indicate that the dominating wavelength represents an eccentricity cycle. Spectral analysis with sliding windows (different window lengths of 40-80 m) reveal a variation of this main spectral peak changing from 18.5 m in the lower part (> 65 m depth) to 14.5 m in the upper part (<65 m depth). Using tie points from ^{14}C dating (7.3 m), Blake event (16.3-17.5 m), discrete change of sedimentation rate at 65 m (calculated from spectral data of sliding windows), Brunhes-Matuyama boundary (141.5 m) and magnetic polarity transition related to top of Jaramillo (167.0 m), a tuned age model is obtained by cubic spline interpolation. This tuned age model dates the cores from 1,001 to 5 ka. It results in a significant Milankovitch spectrum for whole-core carbonate data showing the 95-kyr eccentricity, obliquity (41 kyr) and precession (23 and 19 kyr). Spectral results of magnetic concentration parameters also show eccentricity and obliquity, but not precession. Alternative depth-to-age transfer functions were tested, i.e., a linear model (tie point ^{14}C age), a cyclostratigraphic model (using bandpass-filtered carbonate data corresponding to 95-kyr eccentricity cycles) and correlation of carbonate variation to the marine oxygen isotope curve. However, none of these approaches result in a Milankovitch spectrum of whole-core carbonate data comparably significant as for the tuned age model.

According to the spectral results the core clearly shows a control of global palaeoclimatic variations. To identify a trend through time the spectral power was further analyzed by wavelet transform of carbonate and susceptibility (χ). From the wavelet power spectra it is evident that eccentricity was mostly predominant within the period of 750-300 ka, whereas obliquity and precession were strongest between 700-500 ka. Correlation coefficients (R) of carbonate and χ were determined for depth intervals of different lengths (2.5 m to 15 m). Negative correlation dominates within depths of 50-150 m, whereas positive correlation is observed below 150 m and also dominates above 50 m. Surprisingly, R-values of small depth intervals (2.5 and 3.5 m) show a cyclic behaviour with clear obliquity and precssion peaks. This striking result might be explained by a mixed and varying global and regional control of carbonate and χ. It seems that variation of magnetic concentration is dependent on both, magnetic mineral content and dilution by carbonate, with different contribution at different times. The change of sedimentation rate at about 65 m (and probably also in the lower part of the core) clearly points to a regional effect. Mineral magnetic indicators, i.e. ARM/SIRM-ratio and S-ratio, and pollen data (showing no cyclic behaviour) also are evidence of a regional influence.

The regional palaeoenvironmental changes can be better reconstructed by multivariate statistics applying fuzzy c-means cluster analysis. The most significant result could be obtained with a 3-cluster solution including magnetic data (ARM/SIRM, χ) carbonate content, and pollen concentration (*tsuga* and total tree). The parameter selection is based on analysis of Euclidean linkage distances (dendrogram analysis) and can be also well explained by their meaning. Carbonate and χ represent a global effect, however with different regional influence (shown by R-values). ARM/SIRM is an indicator for grain size variations which are probably caused by alteration of magnetite to maghemite (weathering during warmer and more humid conditions). Values of χ are also dependent on this magneto-mineralogical alteration. Tsuga documents temperate-humid phases and total tree is indicative for extreme cold-dry conditions (maghemitization leading to lower magnetic concentration). The resulting cluster probabilities confirm the subdivision of the core into three parts, i.e. below about 120 m (ca 700 ka), 120-65 m and above 65 m (ca 420 ka). Further subdivision and interpretations in terms of palaeoclimate are presented by Appel et al. (this volume).

References

Yang X, S Wang, G Tong and X Jiang. 2000. Vegetational and climatic responses to tectonic uplift in the Heqing Basin of Yunnan Province during the past 1.0 Ma. *Acta Micropaleontologica Sinica* **17(2)**: 207-217

Hu S, SR Goddu, E Appel, K Verosub, X Yang and S Wang. Submitted. Palaeoclimatic changes over the past one million years derived from lacustrine sediments of Heqing basin (Yunnan, China). *Quarternary Int.*

Cretaceous isochron ages of K-Ar system in the UHP metamorphic rocks of the Tso Morari dome, western Himalaya, India

Chitaro Gouzu†*, Tetsumaru Itaya‡ and Talat Ahmad§

† Graduate School of Science and Technology, Kobe University, Kobe 1-1 Rokkodai-cho, Nada, Kobe 657-8501, JAPAN
  Present address: Hiruzen Institute for Geology & Chronology, 161-1 Sai, Okayama 703-8248, JAPAN
‡ Research Institute of Natural Sciences, Okayama University of Science, 1-1 Ridai-cho, Okayama 700-0005, JAPAN
§ Wadia Institute of Himalayan Geology, 33, G.M.S. Road, Dehradun 248001, INDIA

* To whom correspondence should be addressed. E-mail: gouzu@geohiruzen.co.jp

Ultrahigh-pressure metamorphic (UHPM) rocks occur commonly in continent-continent collision type orogenic belts and their mineral assemblages indicate the formation at the depth of 100 km and more. Since Chopin (1984), the geology and petrology of the UHPM rocks have been studied well to estimate their P-T histories at ca. 20 localities in the world. However, the geochronological approaches to estimate time of events, especially exhumation, are still not well successful. In UHPM rocks and the associated high-pressure metamorphic (HPM) rocks of many metamorphic sequences, discordant K-Ar and Ar/Ar age relations have been reported, probably caused by the excess ^{40}Ar. To reveal exhumation history of UHPM rocks, phengite and paragonite, separated from UHPM rocks from the Tso Morari dome (TMD), western Himalaya, India, are analyzed with K-Ar and Ar/Ar methods.

The authors applied an isochron method to the UHPM rocks of which the host lithologies were continental materials having potential excess ^{40}Ar. Then petrology and geochronology of UHPM rocks from Tso Morari dome (50 km x 100 km), western Himalaya, India were examined. The lithology, which is thought to be margin of Indian continent, consists of eclogites, and basic and pelitic schists, which are closely associated with each other. Recently, Sachan et al. (2001) discovered coesite from an eclogite block. The authors collected the three types of rocks from an area (ca. 20 km x 15 km) of the Tso Morari dome where coesite has been found, and calcschist and basic schist from the adjacent Indus suture zone, which is the boundary between Eurasian and Indian continents. Eclogite having Grt+Omp+Ca-amp+Czo+Phn+Rtl±Pg±Chl±Cc occurs only in the core of meter-scale mafic rock lenses, which were intercalated with the pelitic schists. This suggests that the coexisted mafic and pelitic rocks have suffered the UHPM and the same P-T-t history. The smaller mafic lenses and pelitic rocks were heavily retrograded and have mineral assemblages of Ca-Amp+Czo+Bt+Chl+Ab+Cc+Tnt ±Phn±Grt (relict)±Rtl and Qtz+Phn+Ab+Tnt+Zrn±Pg±Chl± Grt±Bt±Ap±Czo±Kfs±Cc, respectively.

Examined were the representative samples collected from eclogites (TM810 and TM214), basic schists (TM702, TM1006) and peltic schists (TM205, TM706, TM1003, TM1012, TM1015, TM1207 and TM1209), and from calcshists (TM1401 and TM1402). Eclogite sample TM214 has pseudomorph of coesite as inclusion of garnet. Phengites are common in eclogites and pelitic schists which sometimes have paragonite. The basic schists, which have sometimes biotite, contain rarely phengite and paragonite. Phengites have significantly different chemistry between the eclogite and pelitic schists, being due to difference of bulk chemistry of rocks. Phengites in pelitic schists show variable Si/Al and Na/K ratios in a thin section and even in a
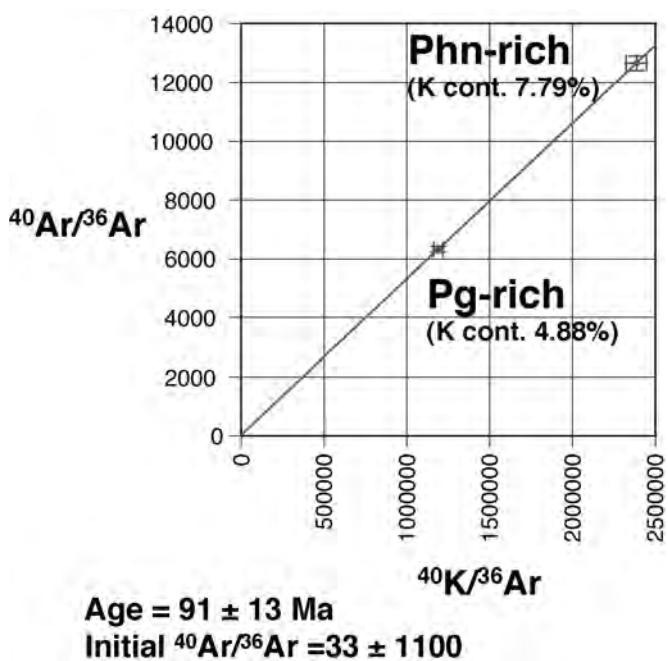
FIGURE 1. Isochron diagram and calculated age using data obtained from K-analyses of two different mineral fractions collected from a pelitic schist (TM205)

single crystal, which indicating retrograde metamorphism. Biotites are homogeneous. K-Ar analyses were carried out on phengite (50 to 87 Ma) from pelitic schists and biotite (96 and 134 Ma) from the basic schists in the Tso Morari dome, indicating variety of ages. Phengites from calcshists in the Indus suture zone were 40 and 43 Ma. Pelitic schist TM205 has paragonite and phengite, giving 84 Ma in paragonite - phengite mixture (K=4.9 wt. %) and 85 Ma in phengite rich fraction (K=7.8 wt. %). The isochron age using the two data sets is 91±13 Ma. Eclogite TM810 having phengite and paragonite were analyzed by laser probe Ar/Ar method. Ar/Ar step-heating analyses using single phengite crystal showed the age spectra having 130 to 170 Ma fractions and with a plateau of 132 Ma defined by 80% of total gas released. Ar/Ar spot dating results using a thin section were 124 and 145 Ma from phengites, and 77 and 155 Ma from paragonites. The isochron age using the four data sets is 143±34 Ma with an initial ratio of 166±110, and the age using the two data sets, which have relatively small errors in age and diagram, is 111±53 Ma with an initial ratio of 736±830.

The Tso Morari dome has also been studied with other chronological methods, giving a Lu-Hf mineral age of 55±12 Ma (De Sigoyer et al. 2000), a Sm-Nd mineral age of 55±7 Ma (De Sigoyer et al. 2000) and a SHRIMP U-Pb zircon age of 48±1 Ma (Leech et al. 2003) as the timing of eclogite-facies metamorphism. These previous ages are consistent with phengite K-Ar phengite ages of the calcschists from the Indus suture zone. Their ages may not be the timing of UHPM because they do not have any feature of UHPM for the geochronological system and the ages are inconsistent with the isochron age from the eclogite (111 and 143 Ma) and from the pelitic schist (91 Ma).

References

Chopin C. 1984. Coesite and pure pyrope in high-grade blueschists of the western Alps: a first record and some consequences. *Contrib Mineral Petrol* **86**:107-118

De Sigoyer J, V Chavagnac, J Blichert-Toft, I Villa, B Luais, S Guillot, M Cosca and G Mascle. 2000. Dating the Indian continental subduction and collisional thickening in the northwest Himalaya: Multichronology of the Tso Morari eclogites. *Geology* **28**: 487-490

Leech M, S Singh, AK Jain and RM Manickavasagam. 2003. New U-Pb SHRIMP ages for the UHP Tso-Morari crystallines, eastern Ladakh, India. 2003 GSA abstract no. 260-24

Sachan HK, BK Mukherjee, Y Ogasawara, S Maruyama, AK Pandey, A Muko, N Yoshioka and H Ishida. 2001. Discovery of coesite from Indian Himalaya: consequences on Himalayan tectonics. *UHPM Workshop 2001 at Waseda University abstract*, 124-128

Himalayan ultrahigh pressure rocks and warped Indian subduction plane

Stéphane Guillot*, Anne Replumaz and Pierre Strzerzynski

Laboratoire de Sciences de la Terre, CNRS UMR 5570, Ecole Normale Supérieure de Lyon et Université Claude Bernard, 2 rue Dubois 69622 Villeurbanne, FRANCE

* To whom correspondence should be addressed. E-mail: Stephane.Guillot@univ-lyon1.fr

In this paper, we will use the knowledge of ultrahigh-pressure (UHP) metamorphic evolution as independent data to constraint the geometry and reconstruct the tectonic evolution of the early stage of the India-Asia collision.

The two UHP units recognized in NW Himalaya (Kaghan in Pakistan and Tso Morari in India) belong to distal parts of the continental Indian margin subducted between 55 and 45 Ma at a minimum depth of 100 km (e.g. Guillot et al. 2003 for review), evolving simultaneously during the early Himalayan evolution. They are interpreted as the signature of the early subduction of the Indian continental plate at the Paleocene-Eocene boundary. The metamorphic conditions are synthesized in Table 1 for both units. Even if similar protoliths are involved and both UHP units record the same maximum depth of about 100 km, some differences in P-T-t conditions may be emphasized. Firstly, the temperature of the metamorphism peak is significantly lower than a minimum of 100°C in the Tso Morari unit suggesting that the subduction rate is higher (Peacock 1992) in the Eastern part. Secondly, the western Kaghan unit seems to be involved in the subduction zone 4 Ma (~ 53 Ma) after the Eastern Tso Morari unit (~ 57 Ma). The later implication of the Kaghan unit in the subduction zone is related to its greater internal localization on the Indian margin, which, combined with a lower subduction rate, induce a higher temperature peak.

As the UHP units are buried and exhumed along the subduction plane (e.g. Chemenda et al. 2000), the dip angle of the subduction plane can be deduced from the geometry of the subduction and the timing of the processes. The sinus of dip angle is equal to the amount of vertical displacement (D) during an interval of time, divided by the amount of Indian plate subduction during the same time interval (H). Those two data are independently measured, D from the exhumed rocks, H from the motion of the Indian plate.

Guillot et al. (2003) demonstrated that the paleomagnetic data tracing the motion of India with respect to Eurasia can be fitted by an exponential law, allowing to numerically estimate the amount of north-south India-Asia convergence. The amount of vertical displacement (D) is simply evaluated by the combination of the barometric and geochronologic estimates on the UHP units. Combining those 2 independent data set (results in **Table 1**), it is possible to deduce that, during burial of both units, the dip angle of subduction was relatively high (30-40°), indeed much higher than previously estimated on both sides of the Western Syntaxis. During their exhumation, the dip of the subduction angle westward increased from 9°, for the Tso Morari unit, to 25-45°, for the Kaghan unit, as observed today.

As demonstrated by Klootwijk et al. (1992) and Guillot et al. (2003) the onset of India-Asia contact occurred between 57 and 55 Ma. The onset of Tso Morari subduction is closer to 57 Ma, which is the age related to the distal part of the Indian margin. The maximum depth reached by the Tso Morari unit is estimated to 100 km, and associated with a minimum age of 54 Ma. Thus the interval of time between the initiation of the burial of the unit, that could be approximated by the initiation of the subduction and the maximum depth reached, which is the maximum duration for the burial, is of 9 Ma. Considering an average subduction rate of 7 cm/yr between 55 and 50 Ma, this allows us to estimate the dip of the subduction angle between 57 and 54 Ma at a minimum of 30° (**Table 1**). Kaneko et al. (2003) proposed that the onset of subduction of the Kaghan unit is about 55 Ma with an India-Asia convergence rate of 4.5 cm/yr. This gives a time-integrated dip of the subduction angle of 14 to 19° from 55 to 46 Ma. However, as previously discussed, the average Indian subduction rate between 55 Ma and 50 was higher (7 cm/yr), and moreover, the dip of the subduction angle was probably closer to 35° rather than 14-19°. This suggests the time span necessary for the Kaghan UHP unit to reach the depth of 50 km, before 50 ± 1 Ma, is less than 2 Myr. Thus, the Kaghan UHP unit was probably involved in the subduction zone after 53 Ma rather than 55 Ma or 57 Ma as for the Tso Morari unit.

We estimate that during the burial of both units the dip angle of subduction was quite steep (30-40°), and much steeper than previously estimated (14-19° according to Kaneko et al. 2003). The steep dip angle deduced from both UHP unit for the early Indian plate subduction, close to the oceanic subduction angle, is compatible with modelling of Chemenda et al. (2000), suggesting that the Indian plate was initially attached to the already subducted Tethyan oceanic plate. This corresponds to the subduction of the thinned continental lithosphere, with the same geometry as for the oceanic subduction. In contrast, during the exhumation of the UHP units, the dip of the subduction angle seems to evolve differently for the eastern and western units. In the eastern part, we estimate from the Tso Morari unit that the subduction plane dips gently around 9°. This value is similar to the estimated dip of the present Moho and MHT between the Himalayan foreland and southern Tibet (Nelson et al. 1996). This result is also compatible with the conclusion of Chemenda et al. (2000) showing that the near frontal subduction of the buoyant Indian plate allows the subduction plane to straighten up beneath the Southern Tibet. Moreover, an early break-off of the Indian plate between 50 and 45 Ma has been probably evidenced East of the Western Syntaxis and would have actively participated to the straightening up of the subducted Indian plate (Chemenda

TABLE 1. Pressure temperature time path evolution of the UHP Kaghan and Tso Morari unit with the velocity and dip estimates

Kaghan unit					
Facies	Pressure	Temperature	Age	Velocity	Dip angle
HP	~ 15 Kbar	~ 350 °C	50 ± 1 Ma	$\Rightarrow$ 12 mm/yr	$\Rightarrow$ **35 ± 13°**
UHP	30 ± 2 Kbar	770 ± 50 °C	46 ± 0.7 Ma	$\Rightarrow$ 20 mm/yr	$\Rightarrow$ **45 ± 15°**
Amph	11 ± 1 Kbar	650 ± 50°C	43 ± 1 Ma	$\Rightarrow$ 7 mm/yr	$\Rightarrow$ **25 ± 9°**
Greenschist	~ 4 Kbar	~ 500 °C	~ 40 Ma		
Tso Morari unit					
Facies	Pressure	Temperature	Age	Velocity	Dip angle
HP	10 ± 1 Kbar	470 ± 10°C	> 55 Ma		$\Rightarrow$ **>30°***
UHP	~ 28 Kbar	~ 650 °C	55-54 Ma	$\Rightarrow$ 8 mm/yr	$\Rightarrow$ **9 ± 4°**
Amph	9 ± 3 Kbar	630 ± 50°C	47 ± 2 Ma	$\Rightarrow$ 3 mm/yr	$\Rightarrow$ **9 ± 3°**
Greenschist	~ 3 Kbar	250 ± 50°C	40 ± 2 Ma		

* This dip angle estimate is explained in the abstract
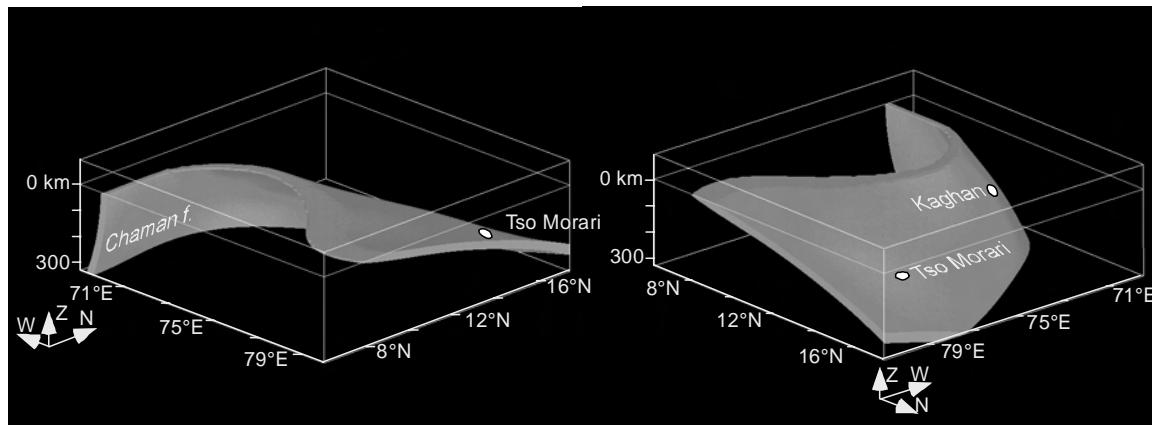
FIGURE 1. 3D models of the NW Himalaya localizing the UHP units between 55 and 50 Ma. The warped geometry of the Indian subduction plane defines, at the surface, the contour of the Western Syntaxis

et al. 2000; Kohn and Parkinson 2004). West of the Western Syntaxis, the high dip angle of subduction (30-40°) seems to persist till 40 Ma. In this area, the Indian plate is quenched towards the West by the Chaman fault. We can thus reconstruct a 3D image of the early collision slab, showing the dip change recorded by the Tso Morari unit, and the warping of the west syntaxis by the Chaman fault (**Figure 1**).

References

Chemenda AI, JP Burg and M Mattauer. 2000. Evolutionary model of the Himalaya-Tibet system: geopoem based on new modelling, geological and geophysical data. *Earth and Planetary Science Letters*, **174**: 397-409

Guillot S, E Garzanti, D Baratoux, D Marquer, G Mahéo and J de Sigoyer. 2003. Reconstructing the total shortening history of the NW Himalaya: *Geochem. Geophys. Geosyst* **4**(1): XXXX, doi:10.1029/2002GC000484

Kaneko Y, I Katayama, H Yamamoto, K Misawa, M Ishikawa, HU Rehman, AB Kausar and K Shiraishi. 2003. Timing of Himalayan ultrahigh-pressure metamorphism: sinking rate and subduction angle of the Indian continental crust beneath Asia: Journal of Metamorphic Geology, **21**: 589-599

Klootwijk CT, JS Gee, JW Peirce, GM Smith and PL McFadden. 1992. An early India-Asia contact: paleomagnetic constraints from Ninetyeast Ridge, ODP Leg 121, *Geology*, **20**: 395-398

Nelson KD, W Zhao, LD Brown, J Kuo, J Che, X Liu, SL Klempere, Y Makovsky, R Meissner, J Mechie, R Kind, F Wenzel, J Ni, J Nabelek, C Leshou, H Tan, W Wei, AG Jones, J Booker, M Unsworth, WSF Kidd, M Hauck, D Alsdorf, A Ross, M Cogan, C Wu, E Sandvol and M Edwards. 1996. Partially Molten Middle Crust Beneath Southern Tibet: Synthesis of Project INDEPTH Results.: *Science* **274**: 1684-1696

Palaeozoic metallogeny in Tethyan Black Mountain Basin, Bhutan Himalaya and its regional implication

Anupendu Gupta

Ex Geological Survey Of India, BB 45/3, Salt Lake, Kolkata 700064, INDIA

For correspondence, E-mail: anupendu@yahoo.com

Several isolated domains of Tethyan Palaeozoic sediments occur within the central crystalline complex of Bhutan Himalaya. The Black Mountain Group in central Bhutan represents one such sediment dominated ensemble of Tethyan affinity, which occupies about 6000 sq km area and rests unconformably on the Precambrian basement (**Figure 1**, inset). On the basis of fossil finds the age range of the sequence is considered to be Lower Ordovician to Devonian (Chaturvedi et al 1983 a, b). The sequence begins with Early Ordovician cross bedded orthoquartzite and polimictic conglomerate of Nake Chu Formation and represents a proximal facies deposit in shallow water shelf condition. This is followed upwards by the thick interbanded sequence of Middle to Upper Ordovician Mane Ting Formation comprising quartz wacke and rudites (debri flow deposit), psammopelites, carbon phyllite (black shale), minor metavolcanics of andesitic composition, and stratabound manganoan siderite bands hosting copper sulphide mineralisation. The uppermost Wachila Formation, composed dominantly of carbonate lithofacies was deposited in a deep water setting during Silurian and most of Devonian period.

The sediments of Mane Ting Formation, which host the copper deposit at Gongkhola - Nobji Chu reflects intermittent basinal instability caused by tectno- magmatic impulses as depicted by the development of debri flow units at various stratigraphic levels and minor volcanics (Bandyopadhyay and Gupta 1990). In contrast to this there were periods of quiescence marked by deposition of thinly laminated black shale. The formational strike of lithounits in the deposit is NE-SW with average dip of 55 - 65° towards NW and the ore bodies show overall conformity with this attitude.

The rocks of the area display a low grade of metamorphism and at least two deformative episodes. The earliest fold deformation is most widely recorded in the pelites and psammopelites as mesoscopic inclined to reclined folds on bedding with strong development of axial plane schistosity.

The siderite hosted ore bodies are best developed along the interface of contrasting lithounits, carbon phyllite (black shale) in the hangwall and lithic wacke (often rudaceous) in the footwall, and display conformable disposition with respect to the country rock. Several ore zones with varying persistence, width and sulphide concentration have been located along different tectono-stratigraphic levels. The most prominent ore body occurs along the southern contact of the main carbon phyllite horizon, extending for more then 5 km with local breaks (**Figure 1**). The average width of the main ore body is about 10 m, the subsidiery mineralised bands measure upto 1 to 3 m. The principal sulphide assemblege in association with sideritic rock is composed of chalcopyrite, pyrrhotite, pyrite, arsenopyrite, galena and sphalerite. Chalcopyrite or pyrrhotite mostly dominates other sulphides. All the sulphide phases are seen to coexist showing mutual boundary relationship, mutual embayment and mutual inclusion. Pyrrhotite displays significant poligonisation with the development of straight boundary and triple point. Twining is also evident in both

pyrrhotite and chalcopyrite. The textural features in general indicate static recrystallization of the sulphides.

Besides the mostly chalcopyrite dominant sulphide assemblage in siderite host, very fine dissemination and streaks of pyrite and pyrrhotite parallel to the thin bedding laminates are noted in the carbonaceous phyllite. This bedding- controlled mineralization evidently represents the common syngenetic/ diagenetic phase of sulphide mineralization. Another conspicuous mode of mineralization, as noted in the calcareous wacke and quartzite, is depicted by pyrrhotite streaks and blebs strongly oriented parallel to the dominant schistosity, displaying sulphide schistosity at places.

While considering the genetic aspects of the deposit it may be seen that there are multiple phases of sulphide mineralization in the area, viz. (a) syngenetic sedimentary/diagenetic iron sulphide in black shale, (b) pre-metamorphic (possibly diagenetic) iron sulphide in wacke, and (c) copper sulphide within or in close association with manganoan siderite. It is evident that siderite provides the basic control on the localisation of the principal phase of copper sulphide mineralization in this deposit and the ore mineral emplacement is broadly coeval or marginally post-dates the formation of coarsely crystalline siderite gangue. While looking into the possible processes leading to the formation of siderite gangue, in order to understand the genesis of associated main sulphide phase, it is observed that viable genetic processes are: (a) direct sedimentary deposition followed by remobilization, (b) diagenetic segregation along favourable strata followed by remobilization, (c) hydrothermal epigenetic emplacement in tectono - metamorphic stage. The other theoritical possibility of sideritic rock being a carbonatitic intrusion may be discarded in view of unfavourable tectonic set up, absence of characteristic petrological suite and mineral indicators, and low abundance of Zr, Nb and Sr. There is no direct evidence in form of internal sedimentary structures to support the concept of purely sedimentary origin of the siderite bed. However, close proximity of the debri flow deposits and volcanic components with sulphidic siderite does indicate an unstable basinal condition which could trigger sudden physico-chemical changes to cause deposition of iron carbonate aided by metallic additives from volcanic exhalative source, following the major destabilising impulses in an unstable slope succession. Another equally tenable genetic process could be diagenetic segregation of crystalline sideriti rock along energised litho contacts and other similar surfaces, giving rise to more or less stratabound disposition. The process of recrystallization and remobilization could continue up to early tectonic stage, thereby resulting in local discordant and transgressive features. The same diagenetic-epigenetic process could be responsible for the emplacement of silica and sulphides within the carbonate host. This may be followed by processes of reconstitution and remobilization over a protracted time span from late diagenetic to early tectono-metamorphic stage. The entire process could be governed by a low to moderate temperature hydrodynamic system, the ore
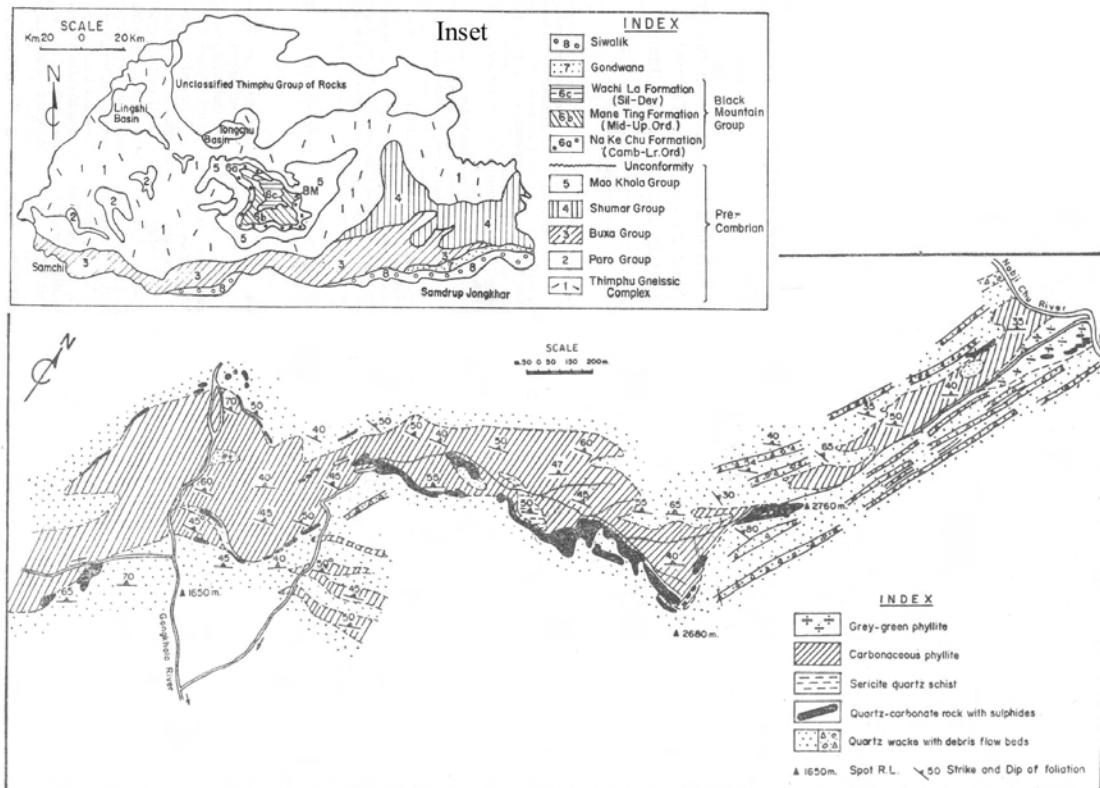
FIGURE 1. Geological map of Gongkhola-Nobji Chu area, Tongsa district, Bhutan. Inset: Simplifiedgeological map of Bhutan showing location of Black Mountain Basin (BM)

forming fluids and nutrients derived from sediments themselves and thermal component derived from deformative processes. However, the possible role of an hydrodynamic system set up by exhalative source may also be considered in this model in conjunction with diagenetic recrystallization.The concept of entirely external source for copper sulphides in both the above models is to a great extent weakened by the fact that the volcanic components themselves do not show any significant metal concentration and these are far insignificant in proportion compared to the siderite hosted sulphide body. As such, a combination of sedimentary and diagenetic processes for the initial deposition of carbonate followed by its recrystallization, local segregation along favoured domains, emplacement of silica and copper sulphides by a diagenetic/epigenetic hydrodynamic system and some amount of later remobilization during tectono-metamorphic stage may, thus, be regarded as the most viable ore genetic model for the deposit (Gupta and Bandyopadhyay 2000).

The copper deposit at Gongkhola, though of limited economic potentiality (about 2.5 mt ore reserve with 1.56% cu), is by far the best located in the Himalaya. The unique geological setting of the deposit and the mode of mineralization may, however, provide definite clue for similar occurrences elsewhere in the Himalayan belt. The fossiliferous Palaeozoic sequences of Tethyan affinity are recognised in many parts of this belt, which should be regarded as first order potential milieu, followed by search and identification of the suitable sedimentary packages, possible signatures of basin instability during sedimentation due to tectono-magmatic impulses and evidences of low to moderate temperature diagenetic/epithermal hydrodynamic activity. In the northeastern parts of Bhutan, Palaeozoic sequences similar to the Black Mountain Group were located which extends more prominently into the northwestern territory of Arunachal Pradesh, India. It is felt that the regional implication of the deposiit at Gongkhola would deserve due attention and serious follow-up.

References

Bandyopadhyay BK and A Gupta.1990. Submarine debri-flow deposits from Ordovician Mane Ting Formation in Tethyan Black Mountain Basin, Central Bhutan. *Ind J Geol* **36**: 277-289

Chaturvedi RK, SN Mishra and VV Mulay. 1983a. On fossiliferous Ordovician rocks of Black Mountain region, Bhutan Himalaya and their significance in stratigraphic correlation. *Rec Geol Surv India* **113** (2): 35-47

Chaturvedi RK, SN Mishra and VV Mulay. 1983b. On the Tethyan Palaeozoic sequence of Black Mountain region, Central Bhutan. *Him Geol* **11:** 224-249

Gupta A and BK Bandyopadhyay. 2000. Siderite hosted copper sulphide mineralization in Palaeozoic sequence of east Himalaya, Bhutan. *Abstract vol, IGC-2000*

Timing and processes of Himalayan and Tibetan uplift

T Mark Harrison†* and An Yin‡

† Research School of Earth Sciences, The Australian National University, Canberra, A.C.T. 0200, AUSTRALIA
‡ Department of Earth and Space Sciences and IGPP, UCLA, Los Angeles, CA 90095 USA

* To whom correspondence should be addressed. E-mail: Director.RSES@anu.edu.au

Numerical simulations indicate that major climate change can be triggered by the appearance of a mountain belt or the uplift of a large region. There is accumulating evidence that the appearance of a high and extensive Himalayan-Tibetan mountain system significantly influenced Neogene climate (Hahn and Manabe 1975). Although long appreciated as the best modern example of a continental collision orogen, our knowledge of the uplift history of the Indo-Asian collision is only now coming into focus due in part to the still relatively blunt instruments we have at our disposal for determining elevation histories.

Models advanced to explain the evolution of the present distribution of crust within the Indo-Asian orogen include those that predict wholesale uplift (mantle delamination, delayed under-plating), progressive growth (Indian under-thrusting, Asian under-thrusting, continental injection), lateral responses (orogenic collapse, horizontal extrusion), and inheritance of an elevated terrane (multiple collision, intra-arc thickening). Investigations of the timing and magnitude of deformation in Tibet and surrounding regions provide some constraints on the crustal thickening and elevation histories that help select among these models. However, the pattern of crustal displacements in response to the collision is inconsistent with most permutations of these single mechanisms but instead requires a specific, time-dependent transfer among several of these processes, often with multiple mechanisms operating simultaneously. The parameters that appear most important in dictating which mechanisms are dominant at any one time are: the location and geometry of pre-existing lithospheric weakness, the distribution of topography before and during the collision, the geometry of the indenter and extruded blocks, the magnitude of boundary stresses, and the age of the lithosphere (Kong et al. 1997).

The Tibetan Plateau began to form locally in response to the collision of the Lhasa block with southern Asia during the Early Cretaceous, particularly in central and southern Tibet. For example, this event is well-documented in the northern Lhasa block where a fold and thrust belt developed between 144–110 Ma and remained substantially elevated until the onset of the collision of India with Asia. The >1400 km of N-S shortening absorbed by the Himalayan-Tibetan orogen since the onset of collision at ~70 Ma is manifested in two ways: 1) discrete thrust belts with relatively narrow zones of contraction or regional decollement (e.g., MCT, Qimen Tagh-North Kunlun thrust system), and 2) distributed shortening over a wide region involving basement rocks (e.g., Nan Shan and western Kunlun thrust belts). This crustal shortening began synchronously in the early Paleogene in the Tethyan and Eo-Himalaya and in the Nan Shan, some 1400 km to the north suggesting that the plateau began to be constructed between the northern margin of India and the Qilian suture zone simultaneously, and not through sequential propagation from south to north. Paleozoic and Mesozoic tectonic histories have exerted strong control on the Cenozoic strain distribution and history during development of the plateau (e.g., Cenozoic thrust belts developed along pre-

existing sutures; the Triassic flysch complex is spatially correlated with Cenozoic volcanism and thrusting; basement-involved thrusts in the Nan Shan and Kunlun Shan follow pre-Cenozoic tectonic belts.

Evidence in the form of deformation and clastic sediment production indicates that the Nan Shan and Fenghuo Shan regions of northern Tibet were actively uplifting at about 45–32 Ma. Possibly in response to this thickening, the left-lateral Red River fault initiated at ca. 35 Ma permitting the eastward extrusion of Indochina until ~17 Ma. This had the effect of reducing the rate of crustal thickening in Tibet, perhaps by accommodating as much as one-half of Indo-Asian convergence during the Oligocene (37–24 Ma). Thin-skinned thrusting was occurring in the Tethyan Himalaya throughout the Paleogene while cover rocks on the northern margin of the Indian shield experienced significant crustal thickening. Although little crustal thickening of Tibet within fold and thrust belts can be documented for the Eo-oligocene (58–24 Ma), mass balance considerations all but require that channeled flow in the ductile lower crust (e.g., Zhao and Morgan 1985) has continuously thickened the crust, uniformly raising much of Tibet to between 1 and 3 km in elevation.

Thus by the beginning of the Late Oligocene, a relatively low Tibetan Plateau (except, perhaps, along the collision zone between the Lhasa and Qiangtang blocks) was likely in existence while the Tethyan Himalaya was topographically subdued and the proto-Himalayan range was shedding little sediment. At ca. 28 Ma, crustal thickening began in southern Tibet along the Gangdese Thrust, moving southward to the Himalaya shortly thereafter in a series of south-directed thrusts which appear to be splays of the same decollement. We can infer the magnitude of this surface uplift from estimates of the amount of crustal shortening and denudation. We think it likely that the Main Central Thrust (MCT) decollement is responsible for generating the 24–9 Ma Himalayan leucogranites which suggests an Early Miocene age for the initial phase of MCT fault activity. This general pattern of propagation toward the foreland was interrupted by the north-directed Renbu Zedong Thrust which was active in southern Tibet between 19–11 Ma. Extension in the High Himalaya along the South Tibetan Detachment System occurred concurrently with slip on the MCT and RZT. The Tien Shan thrusts and thickening in the western Kun Lun were also initiated during the Early Miocene (~20 Ma). By ca. 20 Ma, the Gangdese Shan, Tethyan Himalaya, and High Himalaya were now likely a significant climatic barrier, with an average elevation of perhaps 4–5 km, behind which stood a large but still relatively subdued Tibetan Plateau. At this point, thickening deformation jumped the Tarim basin to the Tien Shan.

Thickening in northwest Tibet, apparently related to transtension along the Altyn Tagh fault, began during the middle Miocene (~15 Ma). Subsequent to Middle Miocene initiation of the Main Boundary Thrust, a broad zone of deformation beneath the MCT fault was active between 10–4 Ma producing the classic Himalayan inverted metamorphic sequences. Recognizing the

juxtaposition of hanging wall gneisses partially melted at ca. 22 Ma and young (ca. 11-3 Ma), lower grade footwall rocks across this tectonically telescoped section renders unnecessary appeals for high shear stress during faulting in order to create the leucogranite melts (e.g., England et al. 1992).

By ~9 Ma, the Tibetan Plateau had attained an average elevation of approximately 5 km and began to differentially extend E-W in a set of N-S trending graben. Although the entire plateau is in extension, these features are particularly well-developed in southern Tibet, perhaps because of accretion of India to southern Asia leading to higher extensional strains.

The discrete changes we infer in the manner in which continuous Indo-Asian convergence was accommodated over the past ca. 70 Ma provides a cautionary tale against interpreting episodic phenomena in the geological record in terms of discontinuous processes, particularly in light of the growing appreciation that complex physical systems driven by structureless inputs can exhibit highly intermittent dynamics. Perhaps the clearest lesson emerging from our study of the Indo-Asian collision is that the continental lithosphere's complex history and geometry exerts a powerful control on continuous plate convergence being manifested in the geological record as episodic phenomena.

References

England P, P Le Fort, P Molnar and A Pêcher. 1992. Heat sources for Tertiary metamorphism and anatexis in the Annapurna–Manaslu region, Central Nepal. *J Geophys Res* **97**: 2107–28

Hahn DG and S Manabe. 1975. The role of mountains in the south Asia monsoon circulation. *J Atmos Sci* **32**: 1515–1541

Kong X, A Yin and TM Harrison. 1997. Evaluating the role of pre–existing weakness and topographic distributions in the Indo–Asian collision by use of a thin–shell numerical model. *Geology* **25**: 527–30

Zhao W and WJ Morgan. 1985. Uplift of the Tibetan Plateau. *Tectonics* **4**: 359–69

Reconstruction of environmental and climatic changes in the Paleo-Kathmandu Lake during the last 700 ka: An approach from fossil-diatom study

Tatsuya Hayashi†*, Harutaka Sakai†, Yoshihiro Tanimura‡, Hideo Sakai§, Wataru Yahagi§ and Masao Uchida¶

† Department of Earth Sciences, Kyushu University, Ropponmatsu, Fukuoka, 810-8560, JAPAN
‡ Department of Geology, National Science Museum, Tokyo 169-0073, JAPAN
§ Department of Earth Sciences, Toyama University, Gohuku, Toyama, 930-8555 JAPAN
¶ Japan Marine Science and Technology Center, Yokosuka, 237-0061 JAPAN

* To whom correspondence should be addressed. E-mail: cs501034@scs.kyushu-u.ac.jp

Terrestrial paleoclimatic and paleoenvironmental records on the Indian monsoon are extremely limited, though many investigations have been done on the deep-sea sediments in the Indian Ocean during the last few decades. In order to clarify the terrestrial monsoonal climatic records during the Quaternary, we undertook core-drilling of the basin-fill sediments of the Kathmandu Valley, which is located under Indian monsoon zone. In this paper, we attempt to reconstruct the environmental changes of the Pakeo-Kathmandu Lake, on the basis of studies on the fossil-diatom collected from a 218-m-long core drilled at Rabibhawan, western central part of Kathmandu.

Except the uppermost thin cover of fluvial sediments (Patan Formation), the core is continuous and mainly composed of muddy lacustrine sediments (Kalimati Formation) containing abundant fossil-diatoms, which document ecological responses to climatic and environmental changes (Sakai 2001, Hayashi et al. 2002). Mud samples were collected at 50 cm interval from 7 to 45.5 m in depth and at 2 m interval from 47.5 to 218 m in depth. We identified each species and counted the number of valves by means of a scanning electron microscope (JSM-5600) at x5,000 magnification, because dominant species in the RB-core are very small, ranging from 5 to 30 μm. For each sample, at least 300 diatom valves were counted.

On the basis of relative abundance and the number of principal diatoms, eight fossil zones and three subzones in zone 2 were defined in the Kalimati Formation (**Figure 1**). Zone 8 at the basal part is characterized by variety of diatom assemblages and relatively low number of diatom valves, which reflect marsh or very shallow-water environments. Based on water-level indicators (ratio of planktonic diatoms to benthic diatoms and frequency of genus *Aulacoseira*), the water-level seems to have deepened gradually from zone 8 to zone 7, and retained deep condition from zone 6 to zone 4. Zones 6 to 4 are characterized by monodominance of *Cyclotella*: *Cyclotella* sp.1 is a characteristic in zone 5, and *Cyclotella* sp.2 is in zone 6 and zone 4. Number of their valves is very abundant. On the other hand, in zone 3 and zone 2, there are several dominant species and number of total diatom valves decreases. Furthermore, ratio of planktonic diatoms to benthic diatoms periodically rises and

falls, which probably indicates water-level fluctuations. Especially in zone 2A, fluvial and marsh environments were expanded in marginal area of the lake, because relative abundance and number of *Staurosira construens* and *Pseudostaurosira brevistriata*, indicative species for marsh environment, become high. In zone 1, ratio of planktonic diatoms increases, which indicates the water-level rose again. But after zone 1, number of total diatom valves drastically reduces. It demonstrates that the lake was drained during a short period at about 12 ka.

Comparison of environmental changes of the Paleo-Kathmandu Lake with $\delta^{18}O$ record from a core MD900963 collected in the Indian Ocean (Bassinot et al. 1994) for the past 630 ka, shows that the water-level of the Paleo-Kathmandu Lake seems to have fallen at glacial age (MIS 14, 10, 8, 6, 2). We recognized following five major events expressed by high ratio of benthic diatoms, which indicate lowering of water-level. According to the time-scale derived from paleomagnetic study and AMS ^{14}C dating of the core, the following stages correspond to marine isotope stages (MIS) from MIS 14 to MIS 2.

> Zone 5 ~ zone 4 = MIS 14
> Early stage of zone 3 = MIS 10
> Later stage of zone 3 = MIS 8
> Later stage of zone 2C = MIS 6
> Later stage of zone 2A = MIS 2

It is likely that these environmental changes of the Paleo-Kathmandu Lake mainly caused by fluctuations of Indian monsoon related to global climatic changes (glacial-interglacial cycle).

References

Bassinot FC, LD Labeyrie, E Vincent, X Quidelleur, NJ Shackleton and Y Lancelot. 1994. The astronomical theory of climate and the age of the Brunhes-Matuyama magnetic reversal. *Earth Planet Sci Lett* **126**: 91-108

Hayashi T, Y Tanimura and H Sakai. 2002. A preliminary report on the study of fossil diatoms in the drilled core from the Paleo-Kathmandu Lake. *Chikyu Monthly* **24**: 359-362

Sakai H. 2001. Stratigraphic division and sedimentary facies of the Kathmandu Basin Group, central Nepal. *J Nepal Geol Soc* **25**: 19-32
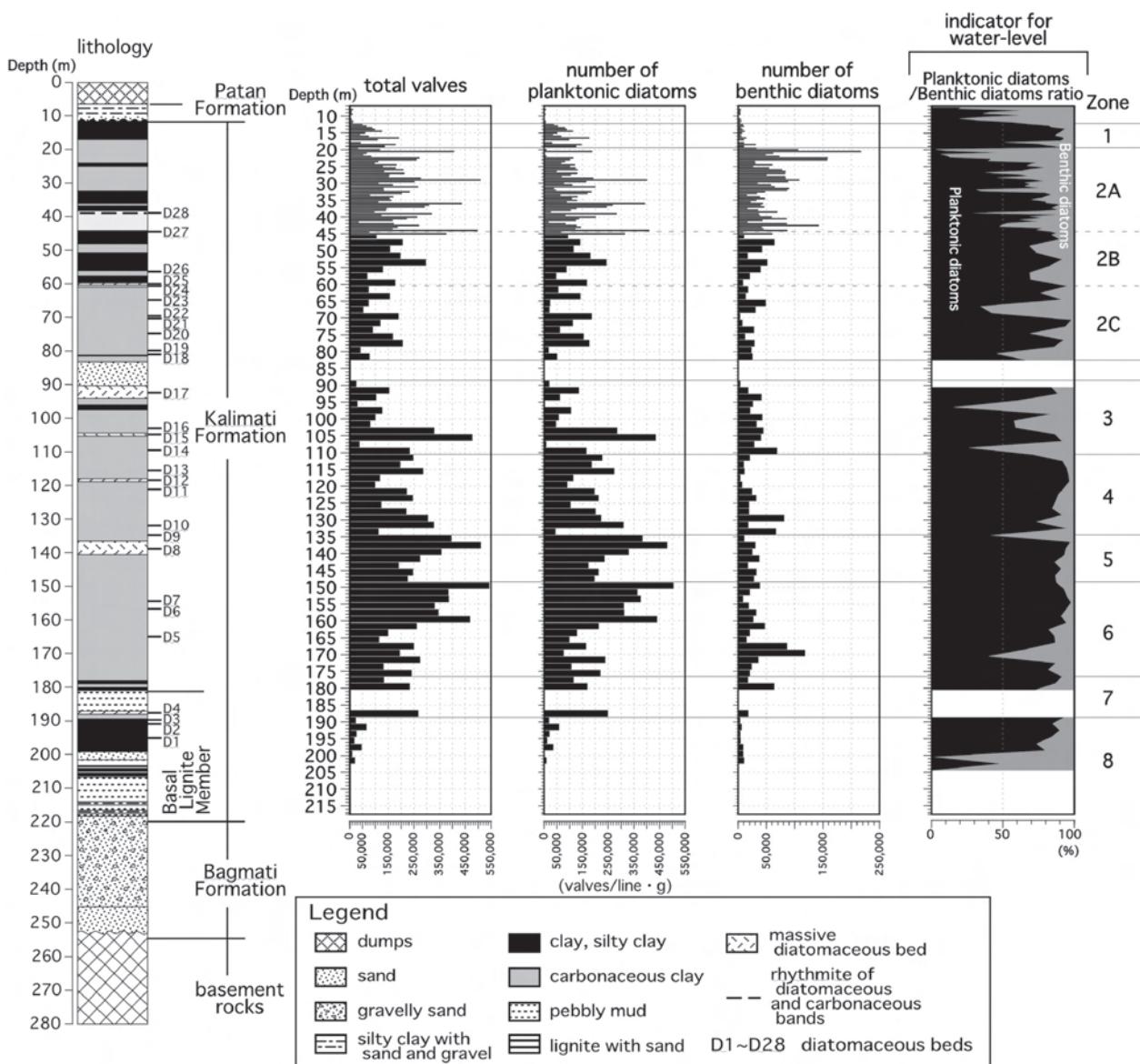
FIGURE 1. Histograms of number of total valves and ratio of planktonic diatoms to benthic diatoms. Lithostratigraphy of RB-core is shown on the left

The record of climate and uplift in the palaeo-Ganga plain: A way to decipher the interactions between climate and tectonics

Pascale Huyghe†*, Jean-Louis Mugnier‡ , Ananta P Gajurel§ and Christian France-Lanord¶

† LGCA Grenoble University, FRANCE
‡ LGCA CNRS, FRANCE
§ Tri-Chandra College, Tribuvan University, Kathmandu, NEPAL
¶ CRPG Nancy, FRANCE

* To whom correspondence should be addressed. E-mail: huyghe@ujf-grenoble.fr

Foreland basin sediments provide a record of the tectonic and climatic processes that control the morphologic evolution of mountain belts, through their sedimentological, geochemical and geophysical characteristics. The Siwalik continental molasses were deposited in the Tertiary Himalayan foreland basin. These sediments represent the record of more than 15 Ma of Himalayan denudation. They consist of fluvial deposits strongly influenced by the Neogene tectonics of the mountain belt. Also the climatic changes that affected the area are recorded in them. A multidisciplinary study has been conducted in the Siwaliks of Nepal in order to decipher the interactions between climate and tectonics.

Analysis of the tectonic-sediment relationships to estimate shortening velocity

From growth structures and reworked Middle Siwalik blocks, the timing of the Siwalik Thrusts has been specified: it is found to be 1.8-2.4 Ma for the initiation of the Main Frontal Thrust (MFT) and 2.4-3 Ma for the Main Dun Thrust (MDT). From balanced cross-sections through the Siwalik belt it has been shown that the shortening rate is greater than 17 mm/yr. A comparison between global positioning system (GPS) studies, shortening rate inferred from the uplift of Holocene terraces above the thrust and balanced cross-sections through the Lesser Himalaya suggests that the shortening rate is constant over the different periods of time and close to 19 mm/yr (Mugnier et al. 2003).

In summary, the convergence rate in Himalaya may be considered as constant since ~11 Ma and possibly 20 Ma.

Analysis of the geometry of the foreland basin as a marker of the Himalayan thrust wedge evolution

Geometry of foreland basins is primarily controlled by subsidence and provides a data set fairly independent from climate evolution. We analysed major erosion surfaces and migration of the sedimentary sequences between 20 and 0 Ma from seismic reflection profiles and logs of the Ganga basin and field data on the Siwalik belt. Three main periods may be distinguished as given below:

0-2 Ma: No major migration is detected for both the southward edge of the post-Siwalik sequences and the location of the most external Himalayan thrust. As the shortening rate is constant, the width of the belt must have narrowed. The altitude remained nearly constant as it is affected by strong erosion (~2.5 mm, from Galy and France-Lanord 2001) that balances the solid advection.

2-13 Ma: Siwalik sequences (s.s.) migrated southwards with speed varying from 10 to 16 mm/yr close to the shortening rate (Lyon-Caen and Molnar, 1985). This suggests that the whole geometry of the Himalaya-Ganga basin system has been translated above the Indian Plate and the altitude of the belt has remained fairly constant.

13-20 Ma: no southward migration of the Ganga basin may be observed but a major erosion affected the pre-13 Ma deposits. Back-stripping of magneto-stratigraphic sections permitted to reconstruct the evolution of subsidence and calculate the curvature of the Indian lithosphere (Lyon-Caen et Molnar 1983). From 17 to 13 Ma erosion affected temporarily large area of the foreland basin, and a northward migration of the peripheric bulge is inferred.

We propose that a continental slab separated from the Indian lithosphere prior to 13 Ma. It would have induced an uplift of the Himalayan belt over a > 100 km width.

In summary there is no large scale relief changes since 13 Ma, but a major uplift occurred in Himalaya between 20-13 Ma.

Analysis of the filling of the Tertiary foreland basin

Facies analysis, geochemistry and clay mineralogy studies have been realized to detect and characterize the events recorded by the Siwalik molasses. Our analysis mainly focuses on sections which have been accurately dated by magnetostratigraphy (Gautam and Roesler 1999): Karnali section, Surai section and Tinau section, respectively located in Western, Middle West and Central Nepal.

Oxygen and carbon isotopes of gastropods

Mollusca fossils (10 to 2 Ma) were collected from clayey and sandy lithologies representing channel and floodplain sediments of the paleo-Ganga plain. The isotopic data of fossil shells show:

i) a sudden increase in $\delta^{13}C$ values at 5 Ma with values varying between -12‰ and -6‰ prior to 5 Ma to values varying between -4‰ and +2‰. This increase in $\delta^{13}C$ values corresponds to the change of carbon isotopic composition of rivers induced by the expansion of C4-plants. This expansion is also well documented by pedogenic carbonates or by teeth of mammals in the Siwaliks (Quade et al. 1995).

ii) the high variability of oxygen isotopic data with values ranging from -16 to -2 ‰ PDB. The upper limit (~-2‰) is present since 10 Ma suggesting confined environment with possible evaporation of water for biogenic carbonate accretion. The lower limit of oxygen isotopic data varies with time. Prior to 5 Ma, one third of the values range between -11 and -15‰ while between 5 and 1 Ma, a unique sample among 25 has a $\delta^{18}O$ value of -12‰. These data therefore imply that prior to 5 Ma, the river waters in the Gangetic plain could reach very low $\delta^{18}O$ values or that temperatures were much higher than during 5 Ma to 1 Ma period. A temperature control is not realistic; therefore these

results suggest that prior to 5 Ma, rivers waters could have reached much lower isotopic composition than the present-day range for the Ganga (-6 and -10‰). Such conditions could derive from higher elevation of the Himalayan watershed relative to present.

Sedimentary facies and clay mineralogy
i) Facies analysis has been used to characterize the major changes of the Siwalik fluvial system.

ii) $\varepsilon_{Nd}(0)$ was used as a source indicator as the sharp contrast in $\varepsilon_{Nd}(0)$ between the juxtaposed crustal terranes in the Himalayas provides the possibility to identify sediment provenance and detect large-scale tectonic evolution of the belt (Huyghe et al. 2001).

iii) When source rocks are constant, clay mineralogy is considered as a weathering indicator.

Combining these three data sets, it is shown that the major changes evidenced in the Western Siwalik of Nepal from a meandering to a braided system and from a sandy braided system to debris-flow-dominated braided system were linked to the uplift and/or migration of the major Himalayan thrust system (constant weathering indicators, similar fluvial changes not synchronous from one section to the other one). The fluvial change recorded at 6.4±0.5 Ma from a deep sandy braided river system to a shallow sandy river system would rather have a climatic origin as shown by the constant source marker and the quasi-simultaneity of its occurrence over more than (600 x 100) km^2. As the sediment accumulation rate has not significantly changed (Gautam and Rosler 1999), this change of fluvial style could be due to an increase of the bed-load of the river in relation with a change of water discharge that would either diminish or be controlled by seasonality.

Conclusions
Both the characteristics of the deposits and the geometry of the Siwalik molassic sequences show that this part of the Himalayan foreland basin mainly follows a classic steady state evolution controlled by the continuous convergence in the Himalayan belt.

Nonetheless, events of different origins occurred and are detected in the foreland basin:
-A lithospheric event before 13 Ma
-Crustal-scale tectonic events
o Initiation of motion along the Lesser Himalaya Thrust System around 11 Ma;
o Initiation of motion along the thrust system of the Siwalik domain (MFT, MDT and inner Siwalik thrusts)
-A major climatic event superimposed after 7 Ma, as recorded by different markers.

From this timing inferred from the Siwalik record, it is suggested that the huge relief of Himalaya has enhanced on its southern flank the effect of the south-east Asian monsoon strengthening from 7 Ma. Nonetheless no direct feed-back has been found between tectonic evolution of the Himalayan belt and climate at a larger scale than the Himalaya; the relief of Himalaya predates by several Myrs the main south-east Asian monsoon strengthening, and there is no direct correlation between tectonic events and climatic events.

References

Galy A and C France-Lanord. 2001. Higher erosion rates in the Himalaya: Geochemical constraints on riverine fluxes. *Geology* **29**: 23-26

Gautam P and W Roesler. 1999. Depositional Chronology and fabric of Siwalik group sediments in Central Nepal from magnetostratigraphy and Magnetic anisotropy, *in* Le Fort, P., and B.N. Upreti, eds., Geology of the Nepal Himalayas: recent advances: *Journal of Asian Earth Sciences*, Special issue **17**:659-82

Huyghe P, A Galy, J-L Mugnier and C France-Lanord. 2001. Propagation of the thrust system and erosion in the Lesser Himalaya: Geochemical and sedimentological evidence. *Geology* **29**: 1007-10

Lyon-Caen H and P Molnar. 1985. Gravity anomalies, flexure of the Indian plate, and the structure, support and evolution of the Himalaya and Ganga basin, *Tectonics* **4**: 513-38

Mugnier JL, P Huyghe, P Leturmy and Jouanne F. 2003. Episodicity and rates of thrust sheet motion in Himalaya (Western Nepal), in "Thrust Tectonics and Hydrocarbon Systems", Mc Clay, eds, *AAPG Mem.* **82***: 1-24.* SPI Publisher Services, 11147 Air Park road, Suite 4. Ashland, VA 23005

Quade J, JML Cater, TP Ojha, J Adam and TM Harrison. 1995. Late Miocene environmental change in Nepal and the northern Indian subcontinent: Stable isotopic evidence from paleosols. *GSA Bulletin* **107** (12): 1381-97

Isotopic study of the Himalayan metamorphic rocks in the far-eastern Nepal

Takeshi Imayama* and Kazunori Arita

Department of Earth and Planetary Sciences, Graduate School of Science, Hokkaido University, Sapporo, JAPAN

* To whom correspondence should be addressed. E-mail: imayama@ep.sci.hokudai.ac.jp

Previous studies have documented that Sr-Nd and U-Pb zircon isotopic compositions are different between the Lesser Himalayan and the Higher Himalayan metamorphic rocks in Nepal, India, and Pakistan (Parrish and Hodges 1996, Ahmad et al. 2000). However, not much attention was paid to the metamorphic rocks of Main Central Thrust (MCT) zone. We report the result of Sr-Nd isotopic studies in the Higher Himalayan zone, the Lesser Himalayan zone and the MCT zone in far-eastern Nepal.

Far-eastern Nepal (Kangchenjunga-Taplejung-Ilam region) comprises three distinct tectonic units: the Higher Himalaya, the Lesser Himalaya and the Sub-Himalaya (Shelling and Arita 1991). Each of these tectonic units is a fault-bound tectonic package. The Higher Himalayan metamorphic rocks consist of medium- to high-grade paragneisses and orthogneisses. The Lesser Himalayan metamorphic rocks comprise primarily meta-sandstones with intercalations of phyllites and meta-quarzites. The Ilam Nappe is composed of the Higher Himalayan metamorphic rocks. It is a geologically siginificant unit in far-eastern Nepal. The Ilam Nappe with no overlying the Tethyan sedimentary rocks has been thrust over the Lesser Himalayan thrust package along the MCT zone up to near the Sub-Himalaya zone in the south.

The MCT zone is a ductile-brittle zone with a thickness of less than 1 km to several km. The upper boundary of the MCT zone is known as the Upper MCT (UMCT) and the lower one as the Lower MCT (LMCT). The lithology of the MCT zone is characterized by mylonitic augen gneiss, biotite-muscovite-chlorite phyllite with S-shaped garnet and graphitic phyllite. Compositions and zoning patterns of garnets can be discriminated between the MCT zone and the Higher Himalaya.

Information on the tectonic disposition prior to the Himalayan orogeny of the geologic units juxtaposed by the MCT is important for understanding the crustal shortening and changes of thermal structure due to the MCT activity. In general, the Higher Himalayan sequence has been considered to be Indian basement in origin, and the Lesser Himalayan sequence has been deposited on the northern margin of the Indian continent in the Precambrian times. However, the Higher Himalayan sequence in the Langtang area, central Nepal yields zircon U-Pb ages of 0.8 to 1.0 Ga, implying a sedimentary provenance of the Late Proterozoic. On the other hand, the Lesser Himalayan sequence contains 1.8 to 2.6 Ga zircons. Therefore, it was proposed that the Higher Himalayan sequence is metasedimentary rocks that were originally deposited north of continental margin than the Lesser Himalayan sequence (Parrish and Hodges 1996). Furthermore, Nd isotope data are useful in

distinguishing between Higher Himalayan and Lesser Himalayan zones (Ahmad et al. 2000). These data show that the ε_{Nd} values for t=1000 Ma in the Higher Himalayan are –10 to –3, whereas these of the Lesser Himalayan are –17 to –7. We have recalculated ε_{Nd} values at 1000 Ma as this time corresponds to a "Grenville" thermal event in the Himalayas.

17 Samples in the far-eastern Nepal were collected from the Lesser Himalayan, the Higher Himalayan and the MCT zones by the tectonostratigrapic units (**Figure 1**). The isotopic work presented in this study follows on the structural and petrological studies of Schelling and Arita (1991). In study area the ε_{Nd} values for t=1000 Ma from rocks of the Higher Himalaya and the Lesser Himalaya are almost within the range of the previous data except for the Tamar Khola Granite. The ε_{Nd} values for t=1000 Ma obtained are –10 to –2 in the Higher Himalaya and –17 to –15 in the Lesser Himalaya. The Tamar Khola Granite has the ε_{Nd} value for t=1000 Ma of –11 and the high $^{147}Sm/^{144}Nd$. Most samples from the MCT zone have the middle ε_{Nd} values for t=1000 Ma (–15 to –11) of the samples from Higher Himalaya and Lesser Himalaya (**Figure 2a**). Similarly, the $^{87}Sr/^{86}Sr$ values obtained from the MCT zone show the values between those of Higher Himalayan and Lesser Himalayan zones although a few rocks units of Lesser Himalaya have very high $^{87}Sr/^{86}Sr$ values (**Figure 2b**).

These data may serve to strengthen the opinion that the Higher Himalayan sequence is not Indian basement in origin. Further, these data may suggest that the rocks of the MCT zone fill a gap between the Higher and Lesser Himalayan sequence although Sm-Nd isotopic signiture from them indicate that they had different sediment sources area. Finally, both the Higher and the Lesser Himalayan sequence, including the rocks of the MCT zone between them, may represent thick clastic successions deposited on the north of the thinned continental margin of the Indian basement.

References

Ahmad T, N Harris, M Bickle, H Chapman, J Bunbury and C Prince. 2000. Isotopic constraints on the structural relationships between the Lesser Himalaya Series and the High Himalayan Crystalline Series, Garhwal Himalaya. *GSA Bulletin* **112**(3): 467-77

Parrish RR and KVHodges. 1996. Isotopic constrains on the age and provenance of the Lesser and Greater Himalayan sequences, Nepalese Himalaya. *GSA Bulletin* **108**(7): 904-911

Paudel LP and K Arita. 2002. Locating the Main Central Thrust in central Nepal using lithologic, microstructual and metamorphic criteria. *Journal of Nepal Geological Society* **26**: 561-584

Schelling D and K Arita. 1991. Thrust tectonics, central shortening, and the structure of the far-eastern Nepal Himalaya. *Tectonics* **10**(5): 851-862
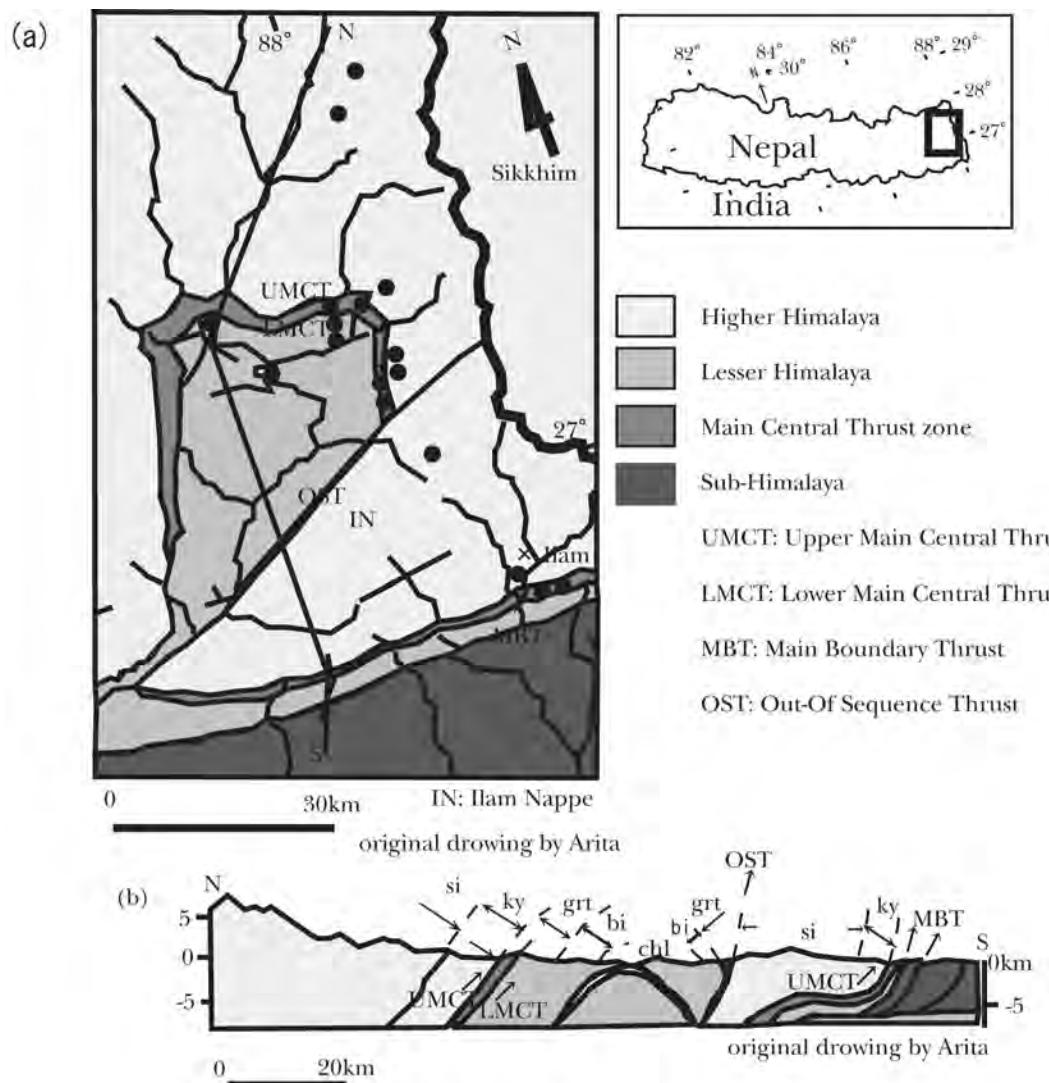
FIGURE 1. Geologic map (a) and cross section (b) of the far-eastern Nepal with sample locations
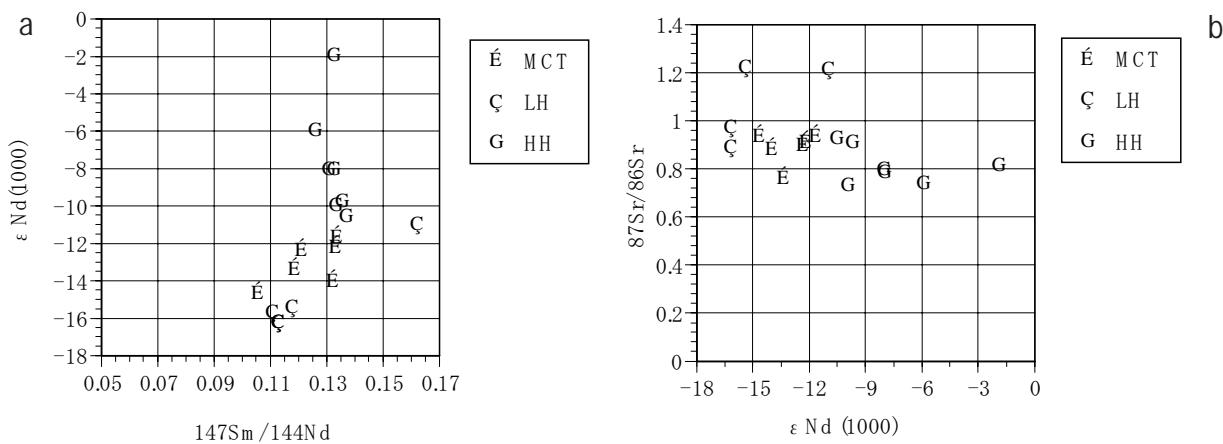
FIGURE 2. ε_{Nd} values for = 1000 Ma vs. ^{147}Sm/^{144}Nd (a) and ^{87}Sr/^{86}Sr vs. ε_{Nd} values for t=1000 Ma (b) for Far-eastern samples

Ice-dammed lakes in the Hindukush-Karakoram Mountains (Pakistan): Geomorphological impacts of outbursts floods in the Karambar valley

Lasafam Iturrizaga

Earth Surface Processes Research Group, School of Earth Sciences and Geography, Keele University, UK

For correspondence, E-mail: liturri@gwdg.de

Glacial outburst floods have played a prominent role in shaping of the Hindukush-Karakoram landscape. In the Karambar valley occurred in the last two centuries some of the most devastating glacial floods in this mountain range. The glacier dams were caused by tributary glaciers located at an height between 2800 m and 3750 m with potential lake volumes amounting up to 300–500 mill. m³. Up to date, only the Karambar glacier was considered as the origin of these flood events. However, more detailed investigations showed that seven more glaciers could have dammed the main valley in historical times (**Figure 1, Plates 1, 2, 3, 4**). At least five of them have definitely formed lakes in the 19th and 20th century. The dense concentration of eight glacier dams along a horizontal distance of only 32 km results in a complex interfingering from lake basins and flooded valley sections. In the individual flood events were involved probably almost synchronously the drainage of at least two lakes. Disastrous flood events were registered in the years 1844, 1861, 1865, 1893, 1895 and 1905. The reconstructed Karambar flood chronology, including five glacier outbursts before 1900, represents with a time period of 150 years one the longest record for this region. On the basis of the formation of glacier dams and glacial lakes conclusions can be drawn in respect to glacier oscillations and especially to the timing of the decline of the *Little Ice Age* in the Hindukush-Karakoram. In 1905, glacier lake outbursts are also reported from the Khurdopin-/Yuskhin Gardan glaciers in the Shimshal valley (Iturrizaga 1994, 1997) and from the Kilchik glacier in the Shyok valley.

The abundant occurrence of unconsolidated sediments in form of mud flow cones and slope moraines manteling the valley flanks caused a high sediment load and enhanced its erosion potential. The up to 100 m high erosion cliffs of the sediment cones, wash limits along the slopes and longitudinal bars in the gravel floors are main characteristics of the flood landscape. Lacustrine sediments are scarcely deposited due to the short sedimentation time of those temporary ice-dammed lakes or they are removed by later flood events. Secondary lake formation in consequence of blockages of the ice- and mud-loaden flood masses in the narrower valley sections occurred at Matram
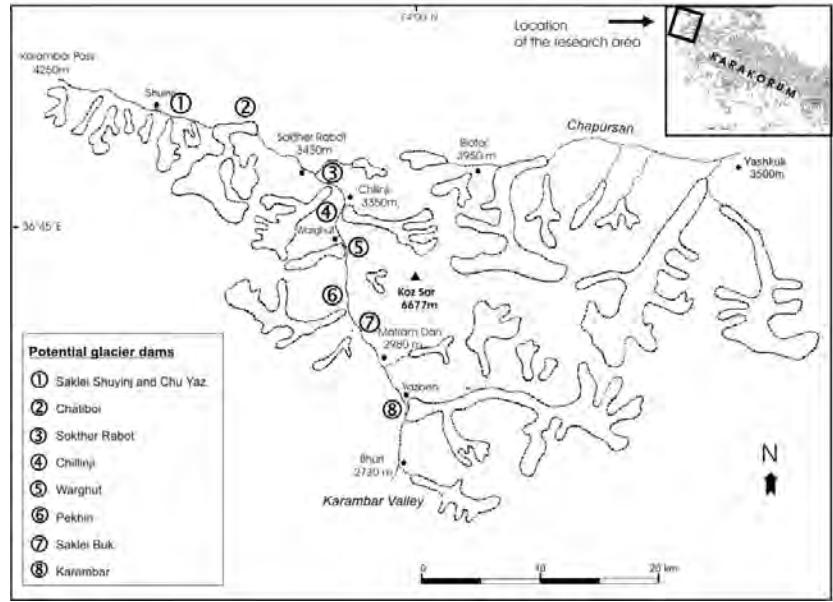
FIGURE 1. The research area: Glacier dams in the Karambar valley
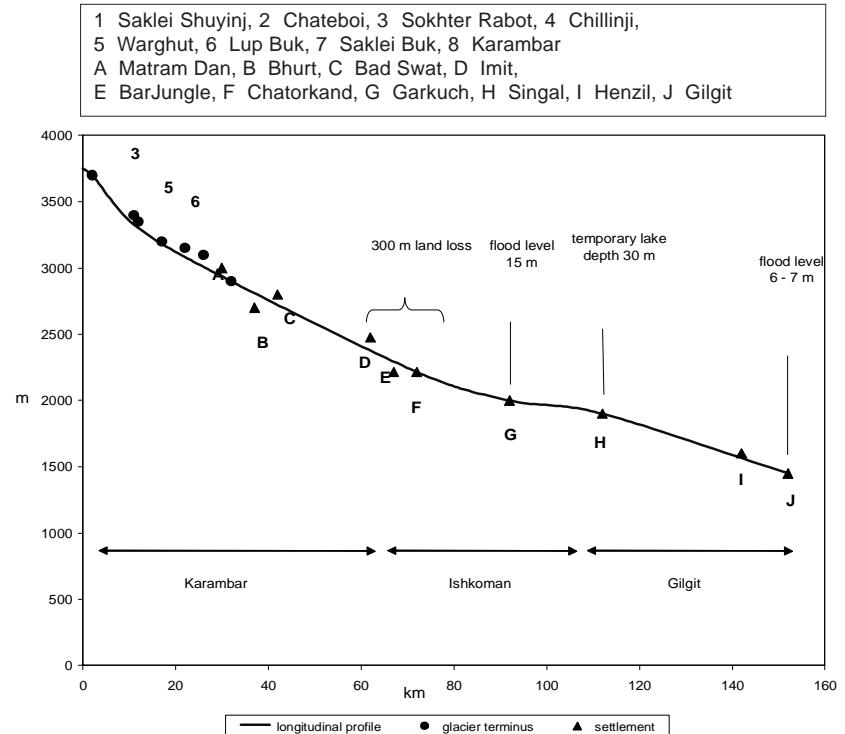
FIGURE 2. Longitudinal profile along Ishkkoman –Karambar – Gilgit valleys

PLATES 1 AND 2. Chateboi glacier dam. PLATE 3. Chillinji glacier dam. PLATE 4. Warghut glacier dam

Das, Bad Swat, Imit, Bar Jungle, Chatorkand and Singal and lasted for several days.

Downvalley from the glacier dams, the Karambar and Gilgit valleys are densely populated. On the basis of settlement losses and eye witness reports the extent, erosion rates and characteristics of the 1905 flood event can be reconstructed. The horizontal range of the flood is documented as far as Gilgit, almost 160 km far away from its origin (**Figure 2**). The flood level in Gilgit was still as high as 6 m. Up to 300 m broad sediment strips were eroded at the settlement areas. In order to warn the villagers living downstream, the Karambar people established an early fire-warning system (*Puberanch*) from Matram Das down to Gilgit until 1905, which was also sucessfully operated in the flood-affected Shimshal valley (Iturrizaga 2004).

The highest glacial dam was produced by the Saklei Shuyinj glacier, a short and inconspicuous hanging glacier, which is nowadays not even visible from the main valley. In 1911, it had formed in combination with a roche moutonée a barrier (cf. Stein 1928), which lied inside the the former Chateboi lake basin. A glacier advance could have easily triggered an lake outurst. One of the latest glacier lakes occurred in 1990 at the Warghut glacier, which also blocked the valley in 1909 (**Plate 4**).

The Chateboi glacier presently blocks the Karambar valley over a distance of 2 km (**Plates 1 and 2**). The Karambar river drains subglacially and small lakes are occasionally impounded. Slight changes in the glacier interior and its subglacial

environment could therefore again produce a large-sized lake. Additionally a minor decrease in snowline depression could also result in several glacier dams in the Karambar valley. A future flood event would have disastrous impacts to the human infrastructure as the settlement areas expanded to the flood plains in the last decades. Also mudflows have dammed temporarily the Karambar valley (Hewitt 1998), especially at Matram Dan (2800 m) and pose nowadays a permanent threat to the villagers. The landslide-induced deposits and terraces are closely interfingered with the glacial lake outburst sediments.

References

Hewitt K. 1998. Himalayan Indus Streams in the Holocene: Glacier-, and Landslide-"Interrupted" Fluvial Systems. In: Stellrecht I (ed.), *Karakorum–Hindukush–Himalaya: Dynamics of Change. Part I, Culture Area Karakorum*, Scientific Studies 4,1, p.3-28.

Iturrizaga, L. 1994. *Das Naturgefahrenpotential der Talschaft Shimshal, NW-Karakorum*. Unpublished diploma thesis. University of Göttingen. 2 volumes, 210 p

Iturrizaga, L. 1997. The Valley of Shimshal–A Geographical Portrait of a Remote High Mountain Settlement And Its Pastures with reference to environmental habitat conditions in the North West Karakorum. In: Kuhle M (ed.): *GeoJournal, Tibet and High Asia* IV, 42, 2/3, 305-328

Iturrizaga, L. (in press). New observations on glacier lake outbursts in the Shimshal valley. *J Asian Earth Sciences*

Stein, A. 1928. *Innermost Asia. Detailed Report of Explorations in Central Asia, Kan-Su and Eastern Iran*. Oxford at the Clarendon Press

When did the metamorphic nappe cover the Lesser Himalayan authochton? An approach from study on thermal history of Proterozoic granitic rocks and Miocene fluvial sediments

Hideki Iwano†*, Harutaka Sakai‡, Tohru Danhara†, Yutaka Takigami§ and Santa Man Rai¶

† Kyoto Fission - Track Co. Ltd., Kyoto, 603-8832, JAPAN
‡ Department of Earth Sciences, Kyushu University, Ropponmatsu, Fukuoka, 810-8560, JAPAN
§ Kanto Gakuen University, Gunma, 373-8515, JAPAN
¶ Department of Geology, Tri-Chandra Campus, Tribhuvan University, Kathmandu, NEPAL

* To whom correspondence should be addressed. E-mail: kyoto-ft@mb.neweb.ne.jp

The timing of exhumation of the Higher Himalaya Crystalline (HHC) is well dated in the Nepal Himalaya by dating of various metamorphic minerals of the MCT zone and the Higher Himalayan Crystalline. Previous studies indicate that rapid exhumation of the HHC occurred at around 25 to 13 Ma, and reactivation of the MCT occurred in Pliocene at 6 to 3 Ma. Exhumation of the HHC gave rise to southward advancement of crystalline nappe (Lesser Himalayan Crystalline: LHC) which tectonically covered the Lesser Himalayan authochthon over 100 km. However, it is not well understood when and how did the metamorphic nappe cover the authochton and when did the metamorphic nappe reach southern margin of the Lesser Himalaya just to the north of the Main Boundary Thrust (MBT).

In order to solve these problems, we have started investigation of thermal history of the Lesser Himalayan autochthon and overlying low-grade metamorphic nappe in western and eastern Nepal Himalaya. This is the first report on the $^{40}Ar/^{39}Ar$ and fission-track dating of the granitic rocks in the LHC and underlying Dumri Formation of Miocene fluvial sediments in the far eastern and eastern Nepal.

We collected granitic rocks and their mylonitized rocks in the Lesser Himalayan Crystalline at three different tectonic positions along a NNW-SSE section connecting Taplejung and Ilam: (1) the north of Taplejung, (2) SW of Taplejung within the Taplejung tectonic window, (3) SW of Ilam just to the north of the MBT (**Figure 1** and **2**). Ar-Ar dating of biotite of garnet-biotite-muscovite gneiss in the Higher Himalayan Crystalline shows an isochron age of about 28 Ma, and that of muscovite shows isochron and plateau (880-1120 ºC) ages of about 11 Ma. Ar-Ar dating of biotite from augen gneiss in the LHC within the Taprejung tectonic window shows two isochrone ages: about 25 Ma (500-760 ºC) and 22Ma (920-1200 ºC), and that of muscovite shows a plateau age (1020-1100ºC) of about 15 Ma.

F.T. dating of zircon and apatite indicate 2.0±0.4 Ma (Ap) age for from 1.6 Ga Kabeli Khola Granite, 4.6±0.4 Ma (Zr) and 2.5±0.3 Ma (Ap) ages for 16~14 Ga mylonitized granite just to the north of the Kabeli Khola (Takigami et al. 2003), and 5.5±0.3 Ma (Zr) and 2.6±0.4 Ma (Ap) ages for micaceous schist of their country rock (location shown in Figure 2).

A mylonitized granitic sheet at southern end of the Lesser Himalaya near MBT in Ilam yields the F.T. ages of 12.5±0.4 Ma (Zr) and 1.8±0.4 Ma, (Ap) respectively. The western extension of the mylonitic granite sheet to the south of Dhankuta yields the F.T. ages of 8.9±0.3 Ma (Zr) and 7.2±0.8 Ma (Ap).

The Dumri Formation comprising of pre-Siwalik fluvial beds are narrowly distributed along the southern margin of the Lesser Himalaya just to the north of the MBT, around a village Tribeni (**Figures 1, 2**). The Miocene fluvial sediments of about 1 km thick is tectonically overlain by the LHC, and the upper part of them are weakly metamorphosed, ranging more than 300 m in thickness. In the Dumri sandstone, metamorphic muscovite was formed along the foliation plane, and its crystallinity increased upwards. Fission-track of detrital zircon grains in the upper part are reset by heating probably due to thermal effect from overlying low-grade metamorphic nappe with sheets of mylonitic granite. However, in the middle part of the Dumri Formation, fission-track of detrital zircon has been partially reset, and that of the lower part has never been reset. It means thermal effect is stronger in the upper part, just beneath the nappe. This is the same type of inverted metamorphism reported from the Dumri Formation in the Karnali Klippe area, western Nepal (Sakai et al. 1999).

One of the detrital zircon and apatite grains from the uppermost part of the Dumri Formation show fission-track ages of 13.6±0.6 Ma (Zr) and 4.6±0.6 Ma (Ap). A mylonitic granite sheet to the south of Dhankuta yielded the F.T. ages of 8.9±0.3 (Zr) and 7.2±0.8 (Ap), and its western extension to the north of Tribeni indicates the F.T. ages of 9.2±0.7 Ma (Zr) and 8.5±1.0 Ma (Ap).

These results suggest that the crystalline nappe has covered the Lesser Himalayan autochthon by 14 Ma and affected thermally (350±50 ºC) the uppermost part of the autochthon. In the middle part of the Lesser Himalaya, temperature of LHC was kept about 240~300 ºC till the earliest Pliocene around 5 Ma, and cooled down about 130±30 ºC by the latest Pliocene around 2.5~2 Ma. The cooling rate in the frontal part of the LHC seems to have been much higher than the middle part, and the temperature at the frontal part decreased up to 130±30 ºC by the late Miocene around 8~7 Ma.

References

Sakai H, Y Takigami, Y Nakamuta and H Nomura. 1991. Inverted metamorphism in the Pre-Siwalik foreland basin sediments beneath the crystalline nappe, western Nepal Himalaya. *J Asian Earth Sciences* **17**: 727-739

Takigami Y, H Sakai and Y Orihashi. 2002. 1.5-1.7 Ga rocks discovered from the Lesser Himalaya and Siwalik belt: 40Ar-39Ar ages and their significances in the evolution of the Himalayan orogen. *Gechim. Cosmochim. Acta* **66** (S1): A762

Upreti BN. 1999. An overview of the stratigraphy and tectonics of the Nepal Himalaya. *Journal of Asian Earth Sciences* **17**: 577-606
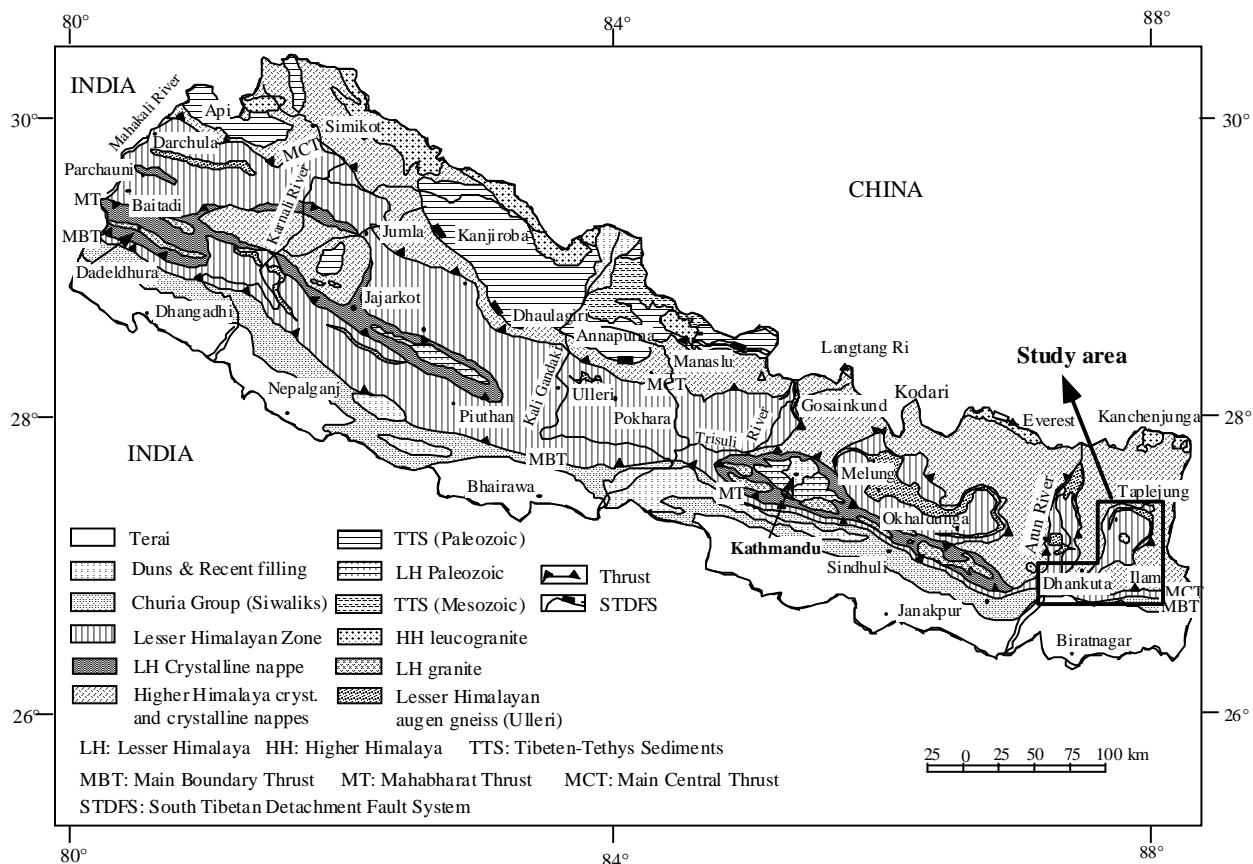
FIGURE 1. Geological outline map of the Nepal Himalaya after Upreti (1999)
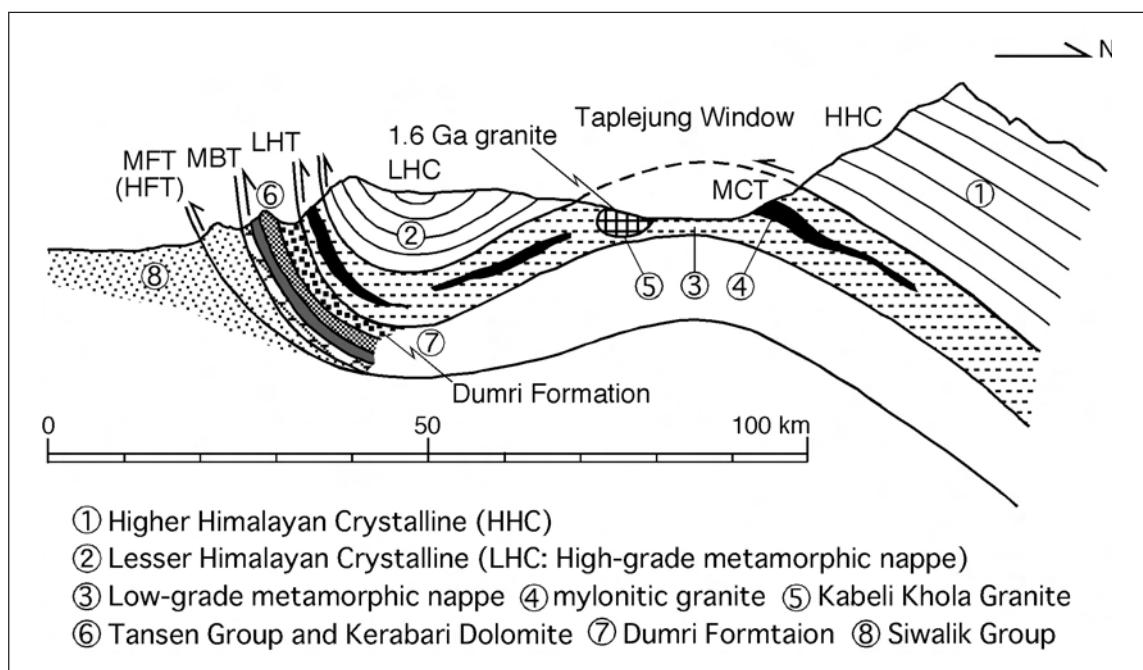
FIGURE 2. Schematic geological cross-section of far eastern Nepal, central Himalaya

Glacial goemorphology in the Lunana area in the Bhutan Himalaya: Moraine stages, glacial lakes, and rock glaciers

Shuji Iwata†*, Karma‡, Yutaka Ageta§, Akiko Sakai§, Chiyuki Narama§ and Nozomu Naito¶

† Department of Geography, Tokyo Metropolitan University, Tokyo,192-0397 JAPAN
‡ Geological Survey of Bhutan, PO Box 173, Thimphu,, BHUTAN
§ Graduate School of Environmental Studies, Nagoya University, Chikusa, Nagoya, 464-8601 JAPAN
¶ Faculty of Environmental Studies,Hiroshima Institute of Technology, Hiroshima, 731-5193 JAPAN

* To whom correspondence should be addressed. E-mail address: iwata-s@comp.metro-u.ac.jp

Although the first report by Augusto Gansser with beautiful photographs on the glacial lakes in Lunana of the Bhutan Himalayas attracted considerable attention in the 1970s (Gansser 1970), the Lunana area was left by any scientific research for many years after the Gansser's visit. In 1994, as per Gansser's prediction, a glacial lake outburst flood (GLOF) occurred in the Lunana area and killed over 20 persons in the downstream area. The Bhutanese Government and scientists started monitoring and scientific researches of glaciers, glacial lakes, and related phenomenon in the Lunana area from 1995. The Bhutan-Japan Joint Research on the Assessment of GLOF started research from 1998 and continues at present. The present authors took part in the project. In this paper, they present analyses and discussion on the timing and extent of glacial fluctuations for selected glaciers, risk of some glacial lakes and permafrost and related phenomena and importance of these phenomenon in the Lunana area.

The Lunana area is a basin with the altitudes of 4300-4500 m between the main Himalayan divide and mountains and plateau with 5000-5500 m in altitudes to the south. **Figure 1** shows moraines, glaciers, and glacial lakes around Thanza village in the eastern part of the Lunana basin. Contemporary glaciers are common on the main divide of the Bhutan Himalayas to the north of Lunana. The large glaciers are located in the Lunana basin, while smaller glaciers are on plateaus that stretch to the south from the Lunana basin. Moraines in the Thanza Village area, Lunana, constitute three distinct stages with contrasts of spatial situations and volume of moraines, and surface features such as clasts, soils, and vegetation. These three stages correlate with some glacial stages in the Khumbu Himal, eastern Nepal, using morphostratigraphic criteria (Iwata 1976). Dates of moraines in the Khumbu Himal (Richards et al. 2000) provide a tentative chronological sequence of these three stages. Valley glaciers in Lunana expanded during the following periods: (1) the Raphsthreng Stages related to the Little Ice Age and late Holocene glacial advances, (2) the Tenchey Stages represent the Late Glacial and/or early Holocene glacial advances, (3) the Lunana Stages are coincident with the Last Glacial period.

00GLOF events have been common phenomena in the Lunana area in the past 50 years, and have been accelerated in the recent years. Field observations and investigation by map and satellite images indicate that most supraglacial lakes tend to connect each other and grow up to a large lake rapidly, and some moraine-dammed lakes were formed and rapidly expanded after the 1970s due to retreating and/or melting of glaciers (**Figure 2**). Rates of the glacial lake expansion vary with individual lakes. The largest mean annual rate is 160 m year^{-1} for Lugge Tsho between 1988 and 1993. Ageta et al. (2000) concluded that the mean annual expansion rates fall within a range of 30-35 m year^{-1}. Assessment on occurrence of triggers, impact to the lakes, and vulnerability of moraine-dams suggests that there are at least 3 potential dangerous glacial lakes in the Lunana area. Dangerous glacial lakes are Lugge Tsho, Raphsthreng Tsho, and Thorthomi Tsho in eastern Lunana. Since these three glacial lakes still contain a large volume of water, and are bounded each other and interact sensitively through water flux and erosion. Constant and regular monitoring of glaciers and glacial lakes are urgently required to prepare necessary mitigation activities.

Rock glaciers and periglacial features exist in many places in Lunana. The distribution of active periglacial rock glaciers suggests that the lower limit of discontinuous permafrost is at 4800 m on north-facing slopes and at 5000 m on south- to east-facing slopes. Results of automatic weather-station measurements suggest that mean annual air temperatures at the lower limits of the permafrost zone are -1.1 °C at 5000 m and +0.1 °C at 4800 m. Some periglacial features, such as earth hummocks, debris islands, and rubble and block slopes indicate that the periglacial environment in the Bhutan Himalayas is very similar to that of the Khumbu Himal in eastern Nepal.

The equilibrium line altitudes of glaciers (ELAs) and lower limit of discontinuous permafrost in the Lunana area are lower than those in eastern Nepal. This lower expansion of these boundaries may be caused by much precipitation and diminished solar radiation in summer due to the monsoon bad weather during monsoon season. Glacier terminus and moraine dams that form glacial lakes in the Lunana basin are situated at around 4400 m. These elevations are about 1000 m lower than those in Khumbu, eastern Nepal, and are apparently at lower altitudes than the lower limit of discontinuous permafrost. This suggests that the melting rates of glaciers are higher rates than that in Khumbu and ice core of moraine dams melts soon after glacier retreat. The vulnerability of the ice-cored moraines in Lunana is greater than those in Khumbu.

References

Ageta Y, S Iwata, H Yabuki, N Naito, A Sakai, C Narama and Karma. 2000. Expansion of glacier lakes in recent decades in the Bhutan Himalayas. In: Nakawo M, CF Raymond and A Fountain (eds): Debris-Covered Glaciers (Proceedings of a workshop held at Seattle, Washington, USA, September 2000). IAHS Publ. no. 246: 165-75

Gansser A. 1970. Lunana: the peaks, glaciers and lakes of northern Bhutan. The Mountain World 1968/69: 117-31

Iwata S. 1976. Late Pleistocene and Holocene moraines in the Sagarmath (Everest) region, Khumbu Himal. Seppyo. *Japanese Journal of Snow and Ice Special Issue* **38**: 109-114

Richards BWM, DI Benn, LA Owen, EJ Rhodes and JQ Spencer. 2000. Timing of late Quaternary glaciations south of Mount Everest in the Khumbu Himal, Nepal. *Geological Society of America, Bulletin* **112**: 1621-1632
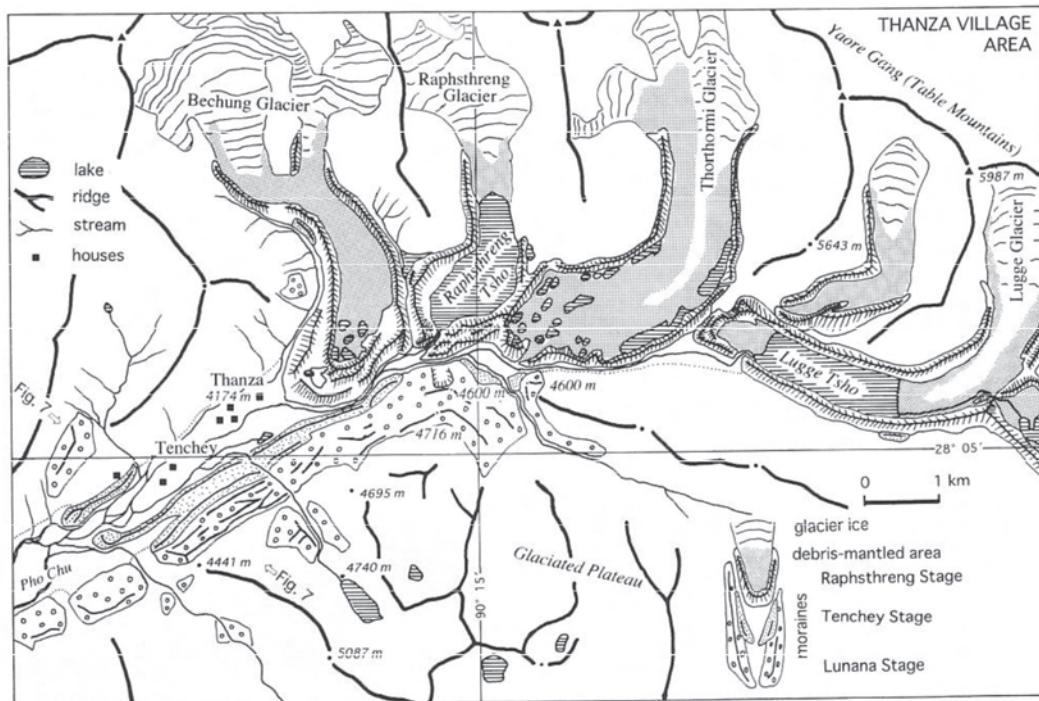
FIGURE 1. Geomorphological map of the area around Thanza Village (4170 m asl) in the eastern part of the Lunana basin, northern Bhutan
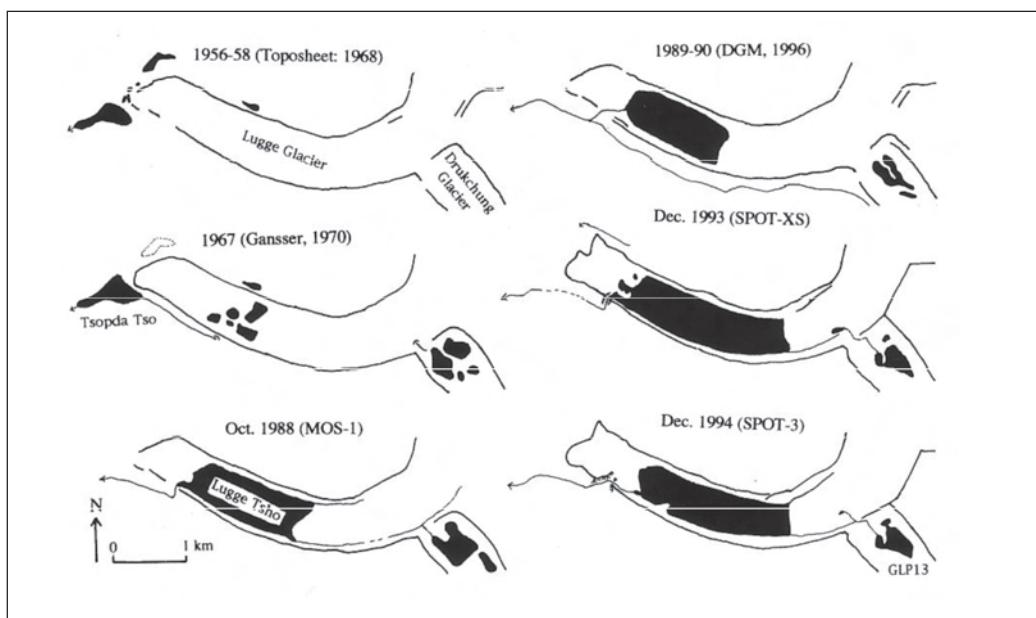
FIGURE 2. Expansion of Lugge Tsho (Lake), Tsopda Tsho, and Drucchung in the Lunana area, Bhutan Himalaya (Ageta et al. 2000)

Zoned ultramafic intrusions of the Chilas Complex in Kohistan (NE Pakistan): Mantle diapers and km-scale melt conduits in extending island arcs

O Jagoutz†*, J-P Burg†, E Jagoutz‡, O Müntener§, T Pettke† and P Ulmer†

† Department of Earth Sciences ETH Zürich, 8092 Zürich, SWITZERLAND
‡ Max-Planck Institut für Chemie, Postfach 3060, D-55020 Mainz, GERMANY
§ Geological Institute, University of Neuchâtel, SWITZERLAND

* To whom correspondence should be addressed. E-mail: jagoutz@erdw.ethz.ch

The Kohistan terrane in NE Pakistan is a fossil oceanic island arc that was trapped during the Himalayan orogeny between the colliding Indian and Asian plates. The Chilas Complex is reported to be the largest ($300 \times 30\,km^2$) mafic-ultramafic intrusion into this paleo-arc. From field and geochemical evidences, the Chilas Complex is regarded to have emplaced during intra-arc rifting. It is subdivided into homogeneous gabbro/gabbronorite enclosing zoned mafic-ultramafic units (UMA). We present field, Sr and Nd isotope measurements and mineral major (EMP) and trace element (La-ICPMS) analyses to evaluate the complicated relationships between the gabbronorite and the UMA.

Field observation gives evidence for upward flow of the UMA with respect to the layered gabbroic sequence. In map view the UMA units have a dike-like shape and are in line, along strike, with hornblendite pegmatites. Across strike the UMA dike-like bodies have a 5-10 km periodicity.

The gabbro, which displays a predominantly magmatic fabric, is composed of plagioclase, clinopyroxene, spinel and amphibole (grain size ~0.5 cm). Appearance of orthopyroxene defines gradual changes into gabbronorite towards the steep contacts with UMA. The UMA are dominantly dunites composed of olivine and spinel. Field observations reveal two settings for associated amphibole-bearing lherzolites. Some are relictual into dunite. The others result from infiltration of a basaltic melt reacting with dunite. Pyroxenites at the contact with the gabbronorite are ultimate products of these reactions. The basaltic melts infiltrating the UMA are parental to the gabbro/gabbronorite.

Preliminary Sr and Nd isotopic data indicate a common, slightly depleted reservoir for both the gabbro/gabbronorite and the UMA. A Sm-Nd whole rock clinopyroxene-plagioclase isochrone yields an "age" of 102 ± 15 Ma, older than the reported ca. 85 Ma crystallization age of the Chilas Complex. In effect, the orthopyroxene isotopic chemistry indicates that the Sm-Nd system has been disturbed by a recent event. Laser-ablation ICPMS trace element mineral analyses have a discrete subduction signature in both UMA and gabbro/ gabbronorite rocks. However, the melt calculated for equilibrium with clinopyroxene has a strong affinity with MORB.

Field, petrological and geochemical data are in accordance with melts derived from a shallow mantle and subsequent fractional crystallization at 6-7 kbars. Melts percolated amphibole-bearing lherzolites to produce dunites and feed the Chilas gabbro/gabbronorite; later cooling triggered new reactions between melts and olivine to produce reactional lherzolites. Accordingly, the Chilas UMA are interpreted as rising mantle diapirs channeling magmas parental to the surrounding gabbro/gabbronorites.

SHRIMP U-Pb zircon ages from Trans–Himalayan Ladakh Batholith and its exhumation using fission track zircon–apatite ages

AK Jain†*, Rajeev Kumar†, Sandeep Singh†, Nand Lal‡ and ME Barley§

† Department of Earth Sciences, Indian Institute of Technology Roorkee, Roorkee-247667, INDIA
‡ Department of Earth Sciences, Kurukshetra University, Kurukshetra – 132 119, INDIA
§ Centre for Global Metallogeny, School of Earth and Geographical Science, The University of Western Australia, 35 Stirling Highway, Crawley, WA 6009, AUSTRALIA

* To whom correspondence should be addressed. E-mail: akj_rke@yahoo.co.in, himalfes@iitr.ernet.in

SHRIMP U–Pb zircon ages from the Trans–Himalayan Ladakh Batholith provide better constraint on the crystallization of this important calc–alkaline Andean–type pluton between 60.1±0.9 Ma and 58.4±1.0 Ma beneath the southern leading edge of the Eurasian Plate due to partial melting of mantle as a consequence of northward subduction of the Neo–Tethyan oceanic lithosphere. These ages have been obtained from two widely–spaced bodies–the older one from granodiorite on the northern face of the batholith along Kharu–Chang La section near Tsoltak, while slightly younger diorite phase has been dated from Igu village near Upshi. No older cores have been observed in the CL images, therefore Ladakh Batholith represents crystallization of an I–type granitoid. When these ages are analyzed with the available Rb–Sr whole rock isochron age of 60±1 Ma of the Shey granite and 60±3 Ma U–Pb zircon concordia age from Leh, it is evident that the southernmost edge of the Eurasian Plate has witnessed extensive plutonism ~60 Ma.

In addition, fission track dating of zircon and apatite has been carried out along 3 important profiles of the Ladakh Batholith: Leh–Khardung La, Kharu–Chang La and Lyoma–Hanle sections. Two zircon ages from the Chang La section are 41.73±2.28 Ma and 43.37±3.36 Ma, while one sample from Lyoma–Hanle section yields a much younger age of 31.71±2.68 Ma.

30 FT apatite samples from the Ladakh Batholith provide a very good constraint on its exhumation at low temperature (~110 °C). The oldest apatite ages have been encountered from highest uplifted parts of the batholith and are 23.07±1.10 Ma from Khardung La (5440 m), and 25.35±2.57 Ma from Chang La (5301 m), while youngest ages are 11.79±1.10 Ma (4038 m), 9.21±0.87 Ma (3732 m) in these two corresponding sections. Weighted mean FT ages from these sections are 14.93±0.32 Ma, 17.38±0.33 Ma and 14.33±0.32 Ma along Lyoma–Hanle section. Elevation profiles of the former two sections from 10 FT apatite samples each yield exhumation rates of 0.11 mm/a for Khardung La between 23 Ma and 12 Ma and 0.09 mm/a for the Chang La section between 25 Ma and 9 Ma.

SHRIMP U–Pb zircon and FT zircon and apatite data have been critically analyzed with the available and reliable other geochronological data set from the Ladakh Bahtolith to decipher its exhumation rates since its crystallization ~60 Ma. The Ladakh Batholith witnessed extremely fast exhumation of about 3.75mm/yr during 45 Ma ([40]Ar/[39]Ar hornblende) and 42 Ma (FT zircon), which follows a moderate exhumation of 0.55 mm/yr between 60 Ma and 45 Ma. It has witnessed much slower exhumation at 0.10 mm/yr since 25 Ma.

Variable exhumation rates within the Ladakh Batholith have been interpreted due to subduction of the Indian continental lithosphere to depth of about 100 km where it had witnessed UHP metamorphism ~53 Ma and its subsequent exhumation, which has resulted in the piggy-back ride of the Ladakh Batholith to its present heights.

The Jijal Complex in the roots of the Kohistan island arc in the northwest Himalaya of Pakistan revisited

M Qasim Jan†* and Barry L Weaver‡

† Department of Geology, University of Peshawar, Peshawar, PAKISTAN
‡ School of Geology and Geophysics, University of Oklahoma, OK730911, USA

* To whom correspondence should be addressed. E-mail: mqjan@yahoo.com

The Kohistan Magmatic arc started building during the Early Cretaceous as an intra-oceanic island arc thousands of kilometers to the south of its present position. It was welded to the Karakoram plate along the Shyok suture during the mid-Cretaceous, after which it became an Andean-type continental margin. Collision with India along the Indus suture occurred during the Early Eocene. The Kohistan arc exposes a complete section across the crust and consists of a range of variably metamorphosed plutonic, volcanic, and subordinate sedimentary rocks.

The lower crust in Kohistan is represented by a series of mafic to ultramafic rocks. These include the granulite facies metamorphosed Jijal complex, which covers 150 sq km area of the southern fringe of the arc along the Indus River. Relics of similar rocks in amphibolites also occur 35 km to the southwest, north of Shangla. The southern (structurally lower) part of the Jijal complex in the hanging wall of the Indus suture comprises chromite-layered dunites, peridotites, and pyroxenites. These pass upwards into garnet-bearing ultramafic and mafic granulites. The transition zone contains pyroxenites (±Grt) or peridotites showing the development of garnet at the interface of plagioclase and opaque oxide /olivine.

The main bulk of the granulites is represented by the assemblage Grt+Px+Pl+Qtz+Rt±Hbl. These rocks are mostly homogeneous, but locally well-layered. In addition to the principal assemblage, the layers comprise garnet pyroxenites (Cpx ± Opx ± Hbl), garnetites (±Cpx±Pl±Hbl), and meta-anorthosites represented by the assemblages Pl+Grt+Cpx+Scp and (Zo+Grt±Cpx±Hbl±Qtz). The northern part of the complex contains relics of gabbronorites/pyroxene granulites (Pl+Opx+Cpx+Hbl+Ilm+Mag) protolith. The garnet granulites here invade the protolith in networks of veins and patches that appear to have formed along joints and fractures due to release of H2O during compression (increasing load pressure and temperature). Field data, combined with petrographic study and mineral analysis, suggest the following reaction for the transformation: Pl(An45)+Opx(En62)+Cpx(Mg 33.8, Fe 18.6, Ca 47.6; Al_2O_3 7.2%, Na_2O 1.8%)+Prg=Pl(An48)+Grt(Mg 31.7, Fe 44.9, Ca 23.4)+Cpx(Mg 37.7, Fe 13.0, Ca 49.2; Al_2O_3 5.6%, Na_2O 1.6%)+Rt+Qtz. Jan et al. (1997) and Yamamoto and Yoshino (1998) showed that this transformation was isochemical for major elements. Further XRF data (Table 1) show that apart from a loss in soda, the major and trace elements remained immobile during the pyroxene-granulite to garnet granulite transition. When normalized to primordial mantle values, the analyses of the mafic granulites display island arc signatures (**Figure 1**).

The garnet granulites contain pods and elongated bodies (rarely exceeding a few tens of meters across) of hornblendites (commonly with Grt±Cpx), garnetites (±Cpx±Pl±Hbl), and pyroxenites (±Grt±Hbl). These are scattered throughout, but are
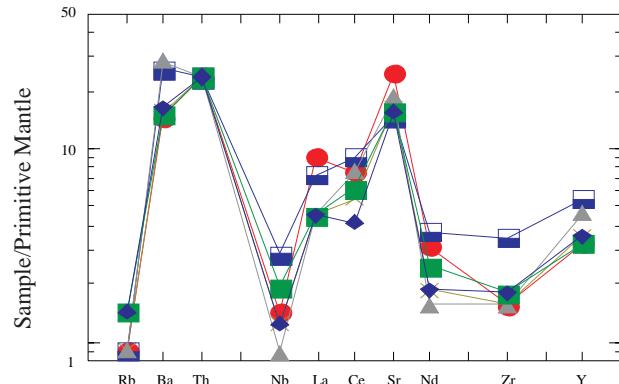
FIGURE 1. Mantle normalized analyses of the granulites

TABLE 1. XRF Analyses of Gabbronorite relic (1) and garnet granulite derivative (2)

	1	2		1	2
SiO_2	49.63	50.43	Zn	75	78
TiO_2	0.78	0.77	V	247	269
Al_2O_3	18.05	18.59	Zr	15	15
FeO	11.56	11.59	Nb	0.7	1.1
MnO	0.17	0.17	Rb	<1	<1
MgO	5.47	5.45	Sr	275	278
CaO	11.49	11.32	Ba	84	77
Na_2O	2.65	1.47	Th	<2	<2
K_2O	0.17	0.15	Pb	3.6	3.4
P_2O_5	0.05	0.05	La	<3	<3
Cr	29	29	Ce	6	9
Ni	12	10	Nd	3	4
Cu	30	24	Y	12	11

particularly common in the southern part of the granulite terrain. It seems that the garnetites are metamorphosed intrusions of troctolite, allivalite, and olivine gabbros in the noritic hosts, a situation similar to that of the Chilas complex. Some of the hornblendites are intimately associated with the garnetites and there are local gradations between the two. Instead of proposing an origin by replacement (metasomatism), however, it is thought

that they may also be magmatic intrusions (Yamamoto and Yoshino 1998), similar to those of Tora Tigga complex, 130 km to the southwest. Yamamoto and Nakamura (2000) have reported a younger Sm-Nd metamorphic age (83 Ma) for the garnet hornblendites than for the garnet granulites (96-90 Ma). But these dates have to be taken cautiously. The granulites, garnetites, garnet hornblendites, and Grt+Cpx+Hbl veins in the latter yield similar PT estimates (750-900 °C, 11-15 kbar; Jan and Howie 1981, Yamamoto 1993). It is likely that all these bodies were emplaced before the peak metamorphic conditions of the high-pressure granulite facies were attained in the deep levels of the thickened arc. It is tempting to postulate that the thickening is related to collision along the Shyok suture, which resulted in overthrusting of the Karakoram plate onto the Kohistan arc. But the timing of this collision is poorly constrained and presumed to have occurred between 75 and 100 Ma ago. Therefore, alternate hypotheses for crustal thickening (dragging down of the complex along the Main Mantle Thrust; imbrication and thrusting in the frontal arc; continued magmatism) should not be summarily discarded.

During cooling and uplift, the Jijal complex was locally hydrated, especially in shear zones and along fractures. This resulted in the development of a range of amphibolite facies and greenschist facies assemblages. These include Ky+Zo+Pg+Crn (after meta-anorthosites), and Hbl±Pl±Grt±Ep±Pg and Act+Chl+Ep+Ab (after mafic rocks).

References

Jan MQ and RA Howie. 1981. The mineralogy and geochemistry of the metamorphosed basic and ultrabasic rocks of the Jijal complex, Kohistan, NW Pakistan. *J Petrol* **22**: 85-126

Jan MQ, BL Weaver and BF Windley. 1997. Summarised petrology of the garnet granulites of the Jijal complex, Kohistan Himalaya. *Abs 3rd Pak Geol Cong Peshawar*: 29-30

Yamamoto H. 1993. Contrasting metamorphic P-T paths of the Kohistan granulites and tectonics of the western Himalaya. *J Geol Soc London* **150**: 843-856

Yamamoto H and E Nakamura. 2000. Timing of magmatic and metamorphic events in the Jijal complex of the Kohistan arc deduced from Sm-Nd dating of mafic granulites. In: Khan MA, PJ Treloar, MP Searle and MQ Jan (eds) Tectonics of the Nanga Parbat Syntaxis and the Western Himalaya. *Geol Soc London Spec Publ* **170**: 313-319

Yamamoto H and T Yoshino. 1998. Superposition of replacements in the mafic granulites of the Jijal complex of the Kohistan arc, northern Pakistan: dehydration and rehydration within deep arc crust. *Lithos* **43**: 219-234

Geothermobarometry of the Dudatoli-Almora Crystallines, Garhwal, Kumaun Lesser Himalaya

Tejender N Jowhar

Wadia Insitute of Himalayan Geology, 33 GMS Road, Dehra Dun 248 001, INDIA

For correspondence, E-mail: tnjowhar@rediffmail.com

The Garhwal and Kumaun regions of the Himalaya in Uttaranchal State of India are critical areas for studying the typical characteristics of the Himalayan fold-and-thrust belt, in contrast to the areas in close proximity of the northeast and northwest Himalayan syntaxes, where complications arise due to strike-slip faulting. In this region, the Lesser Himalaya is characterized by the occurrence of many crystalline bodies of varying dimensions, of which synformally disposed Dudatoli-Almora Crystalline Zone (ACZ) is the largest. Dudatoli-Almora Crystallines (also called Almora Klippen) constitutes one of the most important tectonic units in the Garhwal-Kumaun Lesser Himalaya and it is the remnant of a large thrust sheet nappe that moved southward from the Higher Himalayan Crystalline Zone, to rest over the Lesser Himalayan Volcano-Sedimentary belt. The Almora klippen consists of amphibolite grade metapelites, quartzites, augen gneisses and granites belonging to the Precambrian Almora Group. At places, the greenschist grade metapelites of the Precambrian Ramgarh Group (Chails) occur underneath the Almora Group, forming a series of lower klippen.

The North Almora Thrust (NAT) marks the northern boundary of the Almora klippen, its southern margin is bound by the South Almora Thrust (SAT). The metamorphic sequence of the Almora Klippen exhibits regional metamorphism of Barrovian type, which increases progressively upward in the sequence from peripheral part to the central part of the synform. In Champawat and Almora areas the metamorphism is largely restricted to the chlorite, biotite and garnet zones; however, in the Dudatoli-Bungidhar regions, the metamorphic grade reaches upto staurolite-kyanite and biotite-sillimanite zones.

The EPMA data on garnet, biotite, muscovite and plagioclase were obtained on twenty samples collected from Chamoli, Pauri and Almora districts of Garhwal and Kumaun Himalaya by utilizing JEOL-8600 M super microprobe. In the rim of garnet, (X_{Mg}/X_{Fe}) varies from 0.053 to 0.297, $X_{Almandine}$ varies from 0.488 to 0.780 and (Ca+Mn)/(Ca+Mn+Fe+Mg) varies from 0.065 to 0.423. In the core of garnet, (X_{Mg}/X_{Fe}) varies from 0.030 to 0.279, $X_{Almandine}$ varies from 0.487 to 0.753 and (Ca+Mn)/(Ca+Mn+Fe+Mg) varies from 0.118 to 0.461. Ti in garnets is significantly low, in the rim it varies from 0.004 to 0.012 and in cores 0.008 to 0.115. In the rim of biotites, (X_{Mg}/X_{Fe}) varies from 0.513 to 2.245, $(Al^{VI}+Ti)/(Al^{VI}+Ti+Fe+Mg)$ varies from 0.142 to 0.204 and $X_{Phlogopite}$ from 0.270 to 0.579. In the core of biotites, (X_{Mg}/X_{Fe}) varies from 0.547 to 2.198, $(Al^{VI}+Ti)/(Al^{VI}+Ti+Fe+Mg)$ varies from 0.125 to 0.216 and $X_{Phlogopite}$ from 0.277 to 0.581. In all the samples from Dudatoli-Almora crystallines (Ca+Mn)/(Ca+Mn+Fe+Mg) in garnets exceeds value of 0.2 or $(Al^{VI}+Ti)/(Al^{VI}+Ti+Fe+Mg)$ in biotite exceeds value of 0.15. P-T estimates have been done on the Dudatoli-Almora Crystallines in order to place quantitative constraints on the conditions attained during the regional metamorphism. P-T calculations were carried out using computer programs BGT (Jowhar 1999), GPT (Reche and Martinez 1996), TWQ (Berman 1991), WEBINVEQ (Gordon 1998). GPT computer program (Reche and Martinez, 1996) was used for simultaneous solution of P and T. For P estimation garnet-plagioclase-muscovite-biotite-quartz geobarometer and for T estimation various models of garnet-biotite geothermometer were utilized. It is interpreted that in Dudatoli-Almora Crystallines T varies from 500 to 650 ºC and P from 6 to 8 kbar. Spatial distribution of data indicates inverted metamorphism.

References

Berman RG. 1991. Thermobarometry using multiequilibrium calculations: a new technique with petrologic applications. *Canadian Mineralogist* **29**: 833-855

Gordon TM. 1998. WEBINVEQ Thermobarometry: An experiment in providing interactive scientific software on the World Wide web. *Computers & Geosciences* **24**(1): 43-49

Jowhar TN. 1999. BGT: A FORTRAN 77 computer program for biotite-garnet geothermometry. *Computers & Geosciences* **25**: 609-620

Reche J and FJ Martinez. 1996. GPT: An EXCEL spreadsheet for thermobarometric calculations in metapelitic rocks. *Computers and Geosciences* **25**: 775-784

Spatial and frequency distributions of triclinisity of K-feldspar in augen gneisses and related granitic rocks in the Nepal Himalayas

Takashi Kano

Department of Earth Sciences, Yamaguchi University, 1677-1 Yoshida, Yamaguchi 753-8512, JAPAN

For correspondence, E-mail: kano@yamaguchi-u.ac.jp

Triclinicity (obliquity and/or △-value) has been well known as the mineralogical term indicating the ordering degree of K-feldspar, and defined as △=12.5 (d13-1-d131) by Goldsmith and Laves (1954). Since then, it has been considered as a petrological indicator for the thermal history of granitic rocks. The factor controlling triclinicity in natural rocks is variable and different from case by case, but the most basic factors are the temperature of formation or the temperature of recrystallization and cooling rate of the rocks and /or the influence of hydrothermal fluids (Parsons and Brown, 1984). The aim of this study is to obtain information for the thermal history of granitic rocks in the Himalayas from the frequency and spatial distributions of triclinicity. More than 600 grains of K-feldspar collected from different types of augen gneisses and related granitic rocks in the Nepal Himalayas were X-rayed by powder method in this study.

Mode of occurrence of granitic rocks carrying K-feldspar in the Himalayas

Granitic rocks carrying K-feldspar in the Himalayas are exposed mainly in three zones from north to south; the higher Himalayas, the MCT zone and the Mahabharat Range (Ohta and Akiba, 1973). They have characteristic lithological nature in each. The occurrence of granitic rocks in the higher Himalayas is recognized in three types. One is tourmaline granites occurred in the High Himalayan Range intruding into both the Tibetan Tethys sediments and Himalayan gneisses. They form intrusive bodies and/or small veinlets in Himalayan gneisses. The Manaslu granite and Makalu granite are the typical examples of large intrusives (Le Fort 1981). The granites have typical S-type nature and considered to be the product of crustal anatexis derived from basement gneisses at the Tertiary orogeny. The second type is the Himalayan gneiss its self. The neighbor of the tourmaline granites, the gneiss is highly migmatitic with rheomorphic appearance consisting of K-feldspar, plagioclase, biotite, garnet, kyanite or sillimanaite and tourmaline. The third type is the higher Himalayan augen gneiss, some of which include remarkably large K-feldspar single crystals reaching 50cm in diameter.

Granitic rocks in the MCT-zone occur as augen gneiss too and are associated with mylonitic and cataclastic rocks. The augen gneiss in the MCT-zone is exposed in narrow bands of several 10 centimeters to several 10 meters in thickness intercalated concordantly in the low to middle grade metamorphic rocks derived from the Midland metasediments. The zone of augen gneiss is traceable through whole areas along the MCT zone with swell and pinch structure. In the part of east and west Nepal Himalayas, the zone of augen gneiss form lenticular bodies of several kilometers thick. The outer part of the body is highly sheared into blastomylonitic, but porphyritic appearance still remains in the inner core, and hence, the origin of augen gneiss is defined as a porphyritic granite intruded along the thrust sheet dipping low angle (Kano 1984). The Sheopuri zone flinging the northern border of the Kathmandu basin is the other intrusive zone of granitic and gneissic rocks associated with augen gneiss.

Granitic rocks in the Mahabharat Range are exposed also in several lenticular bodies elongated in the E-W direction (the general trend of the Mahabharat zone) with several to ten-several kilometers in short axis of the body. This granitic body is generally composed of porphyritic granite or partly massive granite in the inner core, and is grade into augen gneiss to blastomylonite toward the outer part of the body. These occurrences are similar to those of the augen gneiss in the MCT-zone, although the general dips of the elongated (flattened) body is high angle in the Mahabharat Range. The radiometric agse of these granitic bodies are, however, early Paleozoic, and do not indicate the Himalayan orogeny.

Measurement of triclinicity and 131 peak patterns

K-feldspar in augen gneisses and porphyritic granites is separated by hand picking and examined in grain by grain. Powdered samples are X-rayed using Cu-Kα, 2θ=29° to 31°, 0.25°/min. In most case, △-value of K-feldspar could not be exactly determined due to the broad peak patterns of X-ray diffractions on the intermediate state, particularly in the case of RD (randomly disordered) feldspar. In this study, ten types of 131 peak patterns were used to describe the crystalline states of K-feldspar for triclinicity, namely from Type 1 indicated nearly =0 to Type 9 nearly maximum ordering with △=1.0. The results of measurements are listed in histograms for several rock types in different regions.

Frequency distribution of triclinicity (131 peak patterns) of K-feldspar

K-feldspar in higher Himalayan gneisses and granitic rocks including tourmaline granites has mostly high ordered peak patterns of maximum microcline (△= nearly 1.0), and orthoclase (△= nearly 0) is subordinate or rather rare. K-feldspar of granitic and gneissic rocks in the Sheopuri zone shows a similar frequency distribution with that in the higher Himalayan gneiss zone.

K-feldspar of augen gneisses in the MCT-zone is characteristic in occurrences of wide ranges of triclinicity from △= nearly 0 to nearly 1.0, and particularly broad peak patterns indicating the intermediate state between orthoclase and maximum microcline. The broadness of X-ray diffraction is shown on a single grain in its self indicating the RD feldspar. In several examples, which are not rare, the coexistence of quite different states of feldspar grains is distinct even in a hand specimen, such as of △= 0, △= 1.0, △= 0.5 (intermediate microcline), RD feldspar and albite megacrysts in same size of K-feldspar. K-feldspar in the Maharabhat Range has also similar characteristics with those of the augen gneiss in the MCT-zone in the central Nepal Himalayas.

The frequency distribution of triclinicity is different from the area to area in the MCT-zone among the east, central and

west Nepal Himalayas. The distribution in the east Nepal Himalayas is bimodal consisting of orthoclase and microcline, and rather predominated in orthoclase ($\triangle$= nearly 0) than microcline. On the other hand, K-feldspar in the central Nepal Himalayas is most frequent in the intermediate microcline or RD feldspar. The distribution in the west Nepal Himalayas is also similar with that in the east Nepal Himalayas (more predominated in intermediate type than in the east Nepal Himalayas).

Concluding remarks

The spatial and frequency distributions of K-feldspar crystalline state estimated by X-ray diffraction patterns is characteristic both in rock types and from the area to area. This may suggest the difference of cooling histories of granitic rocks in the Himalayas. There has been an expectation that recrystallization under deformation operate to transform K-feldspar to low microcline from high temperature state, but the results were quite unexpected.

The augen gneiss in the MCT-zone is a kind of sheared granite intruding along the thrust sheet, however, K-feldspar is not always low microcline, but also it remains intermediate to rather high temperature forms. This augen gneiss contains albite megacrysts as an isolated mineral phase. These occurrences may indicate that the granitic magma was comparatively low temperature at the intrusion (but higher than the orthoclase stable temperature), and then quickly solidified and cooled to remain high form. On the other hand, tourmaline granites and gneisses in the higher Himalayas, which are expected to carry high temperature type K-feldspar, are predominated in low microcline. This may be the result of crystallization of K-feldspar under the influence of fluids and slower cooling than the MCT zone.

References

Goldsmith JR and F Laves. 1954. The microcline-sanidine stability relations. *Geochim Cosmochim Acta* **5**: 1-19.

Kano T. 1984. Occurrences of augen gneisses in the Nepal Himalayas. J. Nepal Geol. Soc. Spec Vol **4**: 121-139

Le Fort P. 1981. Manaslu leucogranite: A collision signature of the Himalayas, a model for its genesis and emplacement. *J Geophys Res* **86**: 10545-10568

Parsons I and WL Brown. 1984. Feldspars and the thermal history of igneous rocks. In: WL Brown (ed), *Feldspars and feldspathoids*, *NATO ASI Series*. 317-371

Ohta Y and C Akiba (ed) 1973. *Geology of the Nepal Himalayas*. Saikon shuppann, Tokyo. 286p

Trace and Rare-Earth Elements distribution patterns of rocks of Chilas Complex and Kamila Amphibolites, Kohistan Arc, North Pakistan

Allah B Kausar†*, Hiroshi Yamamoto‡, Kazuya Kubo§, Yutaka Takahashi§, Masumi U Mikoshiba§ and Hafiz U Rehman†‡

† Geoscience Laboratory, Geological Survey of Pakistan, Shahzad Town, Islamabad 44000, PAKISTAN
‡ Department of Earth and Environmental Sciences, Faculty of Science, Kagoshima University, Kagoshima, JAPAN
§ National Institute of Advanced Industrial Science and Technology, Geological Survey of Japan, Tsukuba 305-8567, JAPAN

* To whom correspondence should be addressed. E-mail: kausar_20001@yahoo.com

....

The Kohistan Arc is situated in the northwestern part of Pakistan and formed during subduction in the Tethys Ocean between the Indian and Asian continental plates (Tahirkheli 1979). From north to south, the interior of the Kohistan arc comprises Jurassic to Cretaceous sedimentary rocks called Yasin Group followed by a sequence of arc type volcanic rocks called the Rakaposhi Volcanics. The southern margin of the Rakoposhi Volcanics is bounded by large-scale granitic plutons called the Kohistan Batholith, which are intruded by huge volumes of noritic gabbros (Chilas Complex) during a phase of intra-arc rifting and mantle upwelling (Treloar et al. 1996), which indicates a change of the tectonic framework with opening of a backarc like that behind the Mariana Arc. The rock assemblages of the Chilas Complex are more or less deformed, exhibiting foliation and ductile shear zones at places with a geochemical trend between tholeiitic and calc-alkaline compositions (Khan et al. 1993). The southern margin of the Chilas Complex consists of imbricated and variously metamorphosed gabbros, diorites, granodiorites, granites and metavolcanics called the Kamila Amphibolites with a tholeiitic geochemical trend. In the south, the Kamila Amphibolites are separated from the Jijal Complex by a shear zone, the Pattan fault. The southern margin of the Jijal Complex is bounded by the Main Mantle Thrust (MMT), where the Kohistan Arc is juxtaposed against Indian continental crust. Not surprisingly, there has been much interest in and debate about the origin of these juxtaposed and diverse magamtic complexes of the Kohistan Arc.

Basically, the Chilas Complex is composed of two distinct rock associations: 1) the Main Facies Zone (MFZ), formally known as gabbro-norite association, and 2) Thak Gah Ultramafic-Mafic Association (TGUM), formally known as Ultramafic-Mafic-Anorthosite Association (UMA). Genetic relationship between these MFZ and TGUM and the origin of their magmas are still uncertain, although many geological and petrological aspects on the Chilas Complex have been discussed by many workers (e.g. Khan et al. 1989).

The TGUM is composed mainly of ultramafic (dunites, wehrlite, websterite) and mafic (gabbros, gabbronorites, anorthosites etc) sequences. The rock assemblages of MFZ include a wide range from gabbronorites to trondhjemites, with the main lithologies typically being gabbros and diorites. The Kamila Amphibolites is also a composite body, predominantly consisting of amphibolites, with subordinate hornblendites, hornblende gneisses, diorites, gabbros, plagiogranites, metavolcanics and minor metasediments. According to field and petrographic characteristics, the rock assemblages of Kamila Amphibolites are classified into "fine-grained metavolcanics; referred herein as Group-1"; which are intruded by "coarse-grained plutonic rocks, referred herein as Group-2".

The present study is focused on the trace and rare earth element (REE) geochemistry of an extensive sampling of the major rock types of the Chilas Complex and the Kamila Amphibolites. The geochemistry of the trace and REE provides a sensitive and powerful petrogenetic tool that, integrated with the existing information on the batholith, is used to provide insights into sources, generation and evolution of the batholithic magmas.

The field, petrographic and geochemical data suggest that the various rock types from MFZ and Group-2 of the Kamila Amphibolites are linked through fractional crystallization and evidence for common parentage includes a close spatial and temporal association, systematic variations in mode and mineralogy, and progression through time towards more evolved compositions. The dissimilarities between the rock assemblages of the Group-1 of Kamila Amphibolites and Group-2 and MFZ are illustrated by comparison of their major and trace elements characteristics. In particular, the rocks belonging to Group-1 differ from the rocks of Group-2 and MFZ in having relatively low SiO_2, Al_2O_3, P_2O_3 and Na_2O contents, and higher MgO, FeO, CaO and TiO_2. Trace element distinctions of Group-1 relative to Group-2 include lower abundances of most incompatible elements (particularly Ba, Rb and Sr), lower $(La/Sm)_N$ and $(La/Yb)_N$ ratios, and higher abundances of transitional elements. Two chemically distinct groups can also be recognized on the basis of N-MORB-normalized spidergrams, excluding alkali (K, Rb) and alkaline earth (Sr, Ba) elements. The patterns representing rocks of Group-2 and MFZ do not differ significantly and are remarkably parallel, with only minor crossing of these elements; and the part of the pattern from Ta to Yb lies parallel to but slightly lower than MORB, presumably reflecting the pre-subduction characteristics of the mantle wedge. In contrast, Rb, Ba, Th and K are enriched above this level. A marked depletion at Nb and Ta is a characteristic of island arc tholeiitic magmas.

The Group-1, fine-grained metavolcanics are different from the rocks of Group-2 and MFZ in their MORB-normalized element patterns. The most striking difference is the relative enrichment in HFSE particularly in Ti, Ta and Nb in Group-1 relative to Group-2 and MFZ. By comparison with Group-2 and MFZ, rocks of Group-1 show no negative Ta-anomaly, and very small negative Nb-anomaly, and part of the curve from Th to Gd also discriminates these rocks from the Group-2 and MFZ. The difference in trace element contents and patterns supports the conclusion that the rocks of Group-1 and MFZ are not the deformed protolith of other plutonic rocks of the Kamila Amphibolites and Chilas Complex. On the contrary, these metavolcanic basic rocks are genetically related among themselves and the similar REE distribution in these rocks suggests that all these rocks have a common source region, but show a greater influence of an N-MORB source with possible contribution of a less depleted mantle source.

The result of this study further suggests that many of the basic assemblages from the MFZ and Group-2 may be the

products of cumulus enrichment processes and the crux of the argument relies on their REE data. In common with many island arc suites, magmas from the Chilas Complex and Group-2 of Kamila Amphibolites have variable Eu anomalies. The positive to negative Eu anomalies in the REE profiles for the basic to more evolved rocks indicate that fractionation has taken place during magma evolution. More basic magmas, with less than 53 wt % SiO_2 have positive anomalies indicative of accumulation of more plagioclase than is lost due to crystal settling. The flat profile, as shown by some samples suggests that Eu gained by plagioclase settling into it compensated Eu loss by plagioclase fractionation. Similarly, the study of Hakesworth et al. (1977) of the Scotia arc shows similar REE distribution.

The main conclusion that can be reached on the basis of geochemical studies is that there is a bimodality of compositions, Group-1 having clear MORB affinities, the Group-2 and MFZ clear island-arc affinities. We would suggest that the complex-metavolcanic amphibolite association of the Kamila Amphibolites, and similar units occurring elsewhere in the Kamila Amphibolites, having N-type MORB affinity and may represent fragments of pre-existing oceanic crust. But the assemblages of the metaplutonic rocks of the MFZ and Kamila Amphibolites from the study area differ significantly from MORB by a characteristic over-abundance of LILE over other incompatible elements such as REE or HFSE and pronounced

depletion in Ta and Nb. We relate this to an original tectonic setting of southern Kohistan above the Tethyan actively subducting plate to the north. Fluids enriched in water-soluble LILE are released from the subducting slab by dehydration of OH-bearing minerals inhomogeneously impregnating the overlying mantle wedge, the actual source region of these rocks. Therefore, the mantle-derived heat and material contributed of the rock assemblages of the metaplutonics of the Kamila Amphibolites and MFZ of the Chilas Complex.

References

Tahirkheli RAK. 1979. Geology of Kohistan, and adjoining Eurasian and Indo-Pakistan continents, Pakistan. *University Peshawar Geological Bulletin* **11**: p 1-30

Treloar PJ, MG Petterson, MQ Jan and MA Sullivan. 1996. A re-evaluation of the stratigraphy and evolution of the Kohistan arc sequences, Pakistan Himalaya: implications for magmatic and tectonic arc-building processes. *J Geol Soc Lond* **153**: p 681-93

Khan MA, MQ Jan, BF Windley, J Tarney and MF Thirwall. 1989. The Chilas mafic-ultramafic igneous complex; the root of the Kohistan Island Arc in the Himalaya of northern Pakistan. In: Malinconico LL and RJ Lillie (eds), *Tectonics of the Western Himalayas*. Geological Society of America, Special Paper **232**: p 75-93

Hakesworth CJ, RK O'Nions, RJ Pankhrust, OJ Hamilton and NM Evenson. 1977. A geochemical study of island arc and back-arc tholeiites from the Scotia Sea. *Earth Planetary Science Lett* **36**: 253-262

Structure and crustal shortening of the Subhimalayan fold and thrust belt, western Arunachal Pradesh, NE India

Thomas K Kelty†*, An Yin‡, and CS Dubey§

† Department of Geological Sciences, California State University, Long Beach, California 90840-3902, USA
‡ Department of Earth and Space Sciences and Institute of Geophysics and Planetary Physics, University of California, Los Angeles, CA 90095-1567, USA
§ Department of Geology, University of Delhi, Delhi 110007, INDIA

* To whom correspondence should be addressed. E-mail: tkelty@csulb.edu

The Subhimalayan fold and thrust belt of western Arunachal Pradesh (AP) includes Miocene and younger sedimentary rocks that comprise northward dipping thrust sheets, structurally below the Main Boundary Thrust (MBT) and above the Main Frontal Thrust (MFT). Balanced cross sections are constructed at various locations along a 100-km segment of the AP Subhimalayan fold and thrust belt. Comparison of these sections reveals structural configurations that are remarkably consistent perpendicular and parallel to the fold and thrust belt. Three regionally significant faults are developed from north to south and are the: (1) MBT, (2) Tipi Thrust and (3) MFT. These faults are subparallel and strike approximately E-W for 200 km from the eastern Bhutan/India border to the Dikrang River, where the strike changes to N50°E and continues NE to eastern syntaxsis.

There are four lithostratigraphic units in the AP Subhimalayan fold and thrust belt, between the MBT and MFT. From oldest to youngest, the consist of the Kimi, Dafla, Subansiri, and Kimin Formations. The Dafla and Subansiri Formations are equivalent to the Middle Siwalik (Kumar 1997). The Kimin and Kimi Formations are equivalent to the Upper and Lower Siwalik, respectively (Kumar 1997). There are no early Miocene lithostratigraphic equivalents in AP to the Murree Formation, Pakistan, the Kasauli and Dagshai Formations, northern India, and the Dumri Fm, Nepal (Kumar 1997).

Within the AP Subhimalayan zone the structures can be lumped into two tectonostratigraphic units: (1) the MFT-Tipi Thrust unit and (2) the MBT-Tipi Thrust unit. The structures of the fold and thrust belt between the MFT and Tipi Thrust in most locations consists of a northerly dipping (10° to 30°) monocline consisting of the Subansiri and Kimin Formations. This part of the fold and thrust belt is interpreted to be the hanging wall flat above the MFT. There are also large folds developed between the Tipi Thrust and MFT. For example, in the Dikrang river valley, a 20-km-long plunging anticline is interpreted to be a fault bend fold above a ramp in the MFT. The tectonostratigraphic unit bounded by the MBT and Tipi Thrust consists exclusively of Dafla Formation that dips northward between 20° to 60°. The Subansiri and Kimin Formations have not been observed in the hanging wall of the Tipi Thrust in AP. No ramp anticlines are developed on top of the Tipi Thrust, which cuts upsection through approximately 4.5 km of the Neogene sedimentary rocks. The Tipi Thrust is interpreted to flatten into a decollement that is regionally extensive and located at the base-Neogene unconformity. The decollement is developed in the AP Subhimalayan zone over a distance of at least 300 km. There is evidence of structurally analogous fault to the Tipi Thrust described in the Subhimalayan fold and thrust belt of Nepal (1000 km to the west). In Nepal, several thrusts place Lower and Middle Siwalik on top of Upper Siwalik. DeCelles et al. (2001) identified a thrust between the MBT and MFT in western Nepal. In central Nepal, Lave and Avouac (2000) describe the Main Dun Thrust. In eastern Nepal, Schelling and Arita (1991) document the Dabmai Thrust. All of these thrust faults are structurally analogous to the Tipi Thrust. It is not being proposed here that the Tipi fault is traceable for 1000 km to Nepal. In fact it is uncertain if an equivalent to the Tipi Thrust has been identified in the Subhimalayan zone of Bhutan. However, it is likely that the same stratigraphically controlled, regional decollement exists at the base of the Siwalik or top of pre-Tertiary basement in Nepal and AP. The depth to the detachment in both Nepal and western part of AP is approximately 5 km.

The restored balanced cross sections are used to estimate the amount of shortening within the AP Subhimalayan fold and thrust belt. The regional dip and depth of basement for these cross sections is based on seismic sections and aeromagnetic data interpreted by Kumar (1997). The minimum shortening between the MFT and Tipi Thrust is about 6 km. The minimum shortening between the MBT and Tipi Thrust is also approximately 6 km. Thus, the total minimum shortening across the Subhimalayan zone is approximately 12 km. This interpretation includes a dramatic four-fold stratigraphic thickening of the Dafla Formation across the Tipi Thrust. Structural thickening caused by fault imbrication is an alternative interpretation to an increase in stratigraphic thickness of the Dafla Formation. This imbricate system has the geometry of a leading imbricate fan. The alternative structural interpretation increases the estimate of shortening to maximum of 30 km between the MBT and MFT.

Because the Kimin Formation is truncated by the Tipi Thrust and MFT, deformation must have occurred in the Subhimalayan fold and thrust belt since 1.5 Ma. Given the minimum estimate of shortening (stratigraphic thickening) of 12 km, the minimum-shortening rate is 8 mm/yr. If the Dafla Formation has been structurally thickened the shortening rate could be as high as 20 mm/yr. Powers et al. (1998) determined shortening rates of 6-16 mm/yr for the Subhimalayan zone in NW India.

References

DeCelles P, DM Robinson, J Quade, TP Ojha, CN Garzione, P Copeland and BN Upreti. 2001. Stratigraphy, structure, and tectonic evolution of the Himalayan fold-thrust belt in western Nepal. *Tectonics* 20(4): 487-509

Kumar G. 1997. *Geology of Arunachal Pradesh*. Bangalore: Geological Society of India. 217 p

Lave J and JP Avouac. 2000. Active fold of fluvial terraces across the Siwaliks Hills, Himalayas of central Nepal. *Journal of Geophysical Research* 105(B3): 5735-70

Powers PM, RJ Lillie and RS Yeats. 1998. Structure and shortening of the Kangra and Dehra Dun reentrants, Sub-Himalaya, India. *Geological Society of America Bulletin* 110(8): 1010-27

Schelling D and K Arita. 1991. Thrust tectonics, crustal shortening, and the structure of the far-eastern Nepal Himalaya. *Tectonics* 10(5): 851-62

Waziristan Ophiolite: A back-arc basin caught in continental collision, Waziristan, NW Pakistan

Said Rahim Khan†*, M Qasim Jan‡, Tahseenullah Khan† and M Asif Khan§

† Geoscience Laboratory, Geological Survey of Pakistan, Shahzad Town, Islamabad, PAKISTAN
‡ Department of Geology, University of Peshawar, Peshawar, PAKISTAN
§ National Centre of Excellence in Geology, University of Peshawar, Peshawar, PAKISTAN

* To whom correspondence should be addressed. E-mail: srk1953@yahoo.com

....

The western margin of the Indian plate is a classical example of continent-continent collision. The Afghanistan-Kabul-India continental blocks are here welded to each other by a network of sutures defined by the occurrence of ophiolites. The Waziristan Ophiolite (WO) is one of a series of ophiolites sandwiched between the western margin of the Indian plate and Afghanistan block. It is highly dismembered, but contains all the segments of an ideal ophiolite suite. It can be internally divided into three nappes which, from east to west, are: Vezhda Sar nappe, comprising entirely of pillow basalts; Boya nappe, a tectonic melange with an intact ophiolite section in the basal part at Mami Rogha; and Datta Khel nappe, consisting of sheeted dykes with variable proportions of other components.

The intact ophiolite section consists of 1) basal ultramafics followed upward by 2) isotropic gabbros, and 3) pillow basalts, intercalated with and capped by pelagic sediments (chert, shale, limestone) (Figure 1). Isolated mafic dykes (doleritic), characterised by chilled margins, intrude all types of ophiolitic rocks, except the pillow basalts of Vezhda Sar nappe. Trondhjemites mostly intrude the ultramafics and rarely gabbroic rocks. Layered gabbros, missing in the ophiolite section, are sporadically distributed as fault-bounded blocks in the two western nappes.

The ophiolite is thrust eastwards onto the Indian plate sediments, rather than beneath these sediments as reported. Regionally, the Main Waziristan Thrust (MWT) trends north-south and dips towards west. Local changes in the trend of the MWT (from N-S to E-W) and dip (W to N) occurs north of Boya-Mohammad Khel, which have been effected by later east-west trending strike-slip faults. Additional field data like the intact ophiolite section with base towards east and top towards west, and deposition of the Tertiary sediments on top of the ophiolite to the west, clearly support overthrusting of the ophiolite onto the sediments of the Indian plate to the east.

Radiolarian fauna (Tithonian-Valanginian) suggests Late Jurassic or older age for the formation of the WO. The presence of tectonic blocks of Campanian limestone (Parh Group) in the melange and coupling of the ophiolite with Maastrichtian shale suggest post Maastrichtian, most probably Palaeocene, emplacement of the ophiolite. A sequence of Early Eocene to Middle Eocene sediments unconformably overlying the WO, supports the Palaeocene emplacement of the ophiolite.

On the multi-element variation diagram, the geochemical data sets of the Waziristan ophiolitic rocks, display similar patterns, as would be expected in comagmatic rocks. Higher LILE/HFSE ratios and slight or no depletion of Nb characterise these rocks. The HFSE display a flat pattern similar to mid-ocean ridge basalt, whereas the LILE, particularly Rb and Ba, mark prominent positive spikes. The wide compositional variation of the ophiolitic rocks (volcanics: basalt to rhyolite, dykes: basalt to andesite, gabbros: gabbro to gabbro-diorite), with transitional characteristics between MORB and IAT, negates origin of the ophiolite in a typical mid-ocean ridge environment. A fore-arc origin for the ophiolite cannot be advocated due to absence of rocks typical of fore-arcs, particularly bonninites which are common in active fore-arcs of the present day, e. g., Mariana. However, strong negative Nb anomaly characteristic of island-arc rock suites is also not found in these rocks. This raises the possibility that these rocks might have originated in a back-arc basin setting. The high LILE/HFSE ratios in these rocks suggest that crustal components along subduction zone were added to the overlying mantle by rising fluids. The back arc basin setting is suggested by several chemical traits of the ophiolitic rocks: 1) transitional chemistry between MORB and island arc rocks, 2) enrichment in LILE (such as Ba, Rb) and depletion in HFSE (such as Zr or Nb), low negative Nb anomaly, and lower MgO than MORB glasses. It is concluded that the Waziristan ophiolitic rocks are comagmatic and probably owe their origin to a back-arc basin or supra-subduction zone setting.

FIGURE 1. A schematic litho - stratigraphic column of the Waziristan Ophiolite at Mami Rogha. The dykes are not according to scale

Back-Arc Basin Rocks in the Kohistan Arc Terrane, Northwestern Himalaya, Pakistan

Tahseenullah Khan†*, Mamoru Murata‡, and Hiraoki Ozawa‡

† Geoscience Laboratory, Geological Survey of Pakistan, Shahzad Town, Islamabad, PAKISTAN
‡ Department of Geosciences, Faculty of Science, Naruto University of Education, Tokushima, JAPAN

* To whom correspondence should be addressed. E-mail: bangash1444@hotmail.com

The Majne area lies west of Gilgit in Kar Gah valley that represents the middle part of the Kohistan arc terrane. This arc is accreted to the Karakoram continental plate along the Shyok suture and subsequently obducted onto the Indian continental plate along the Indus suture. The arc contains volcanic, plutonic and sedimentary rocks, which are variably deformed and metamorphosed. The main rock units of the arc include the Kamila amphibolites, the Chilas mafic-ultramafic complex and the Jaglot, Chalt and Yasin groups. The Kohistan batholith intrudes all rock formations except Kamila amphibolites.

Our main interest is in the Jaglot group, which occupies the east central part of the arc terrane and includes from bottom to top, (i) the Gilgit formation, (ii) the Gashu-confluence volcanics, and (iii) the Thelichi formation.

Based on field observation and petrological study, we re-evaluate stratigraphy of the Thelichi formation and report for the first time doleritic and basaltic dykes and gabbros. The NW-SE trending dykes unit is about 100-500 m wide and 15 km long and composed entirely of dykes. The width of these dykes is not constant and ranges from about 10 cm to 5 m. In the dykes unit, the doleritic dykes are split and intruded by younger basaltic dykes. A 2 m wide volcanic breccia zone is present in the upper part of the dykes unit, which is overlain by the Thelichi formation comprising bedded chert, phyllite, greenschist volcaniclastics, meta-greywacke, marble (meta-micritic limestone), conglomerates and the turbidites (pebbly slate, silty and sandy quartzite). The meta-sedimentary rocks of the Thelichi formation are frequently intruded by the doleritic, basaltic, and dacitic to rhyolitic dykes (minor).

The gabbroic unit is about 50-100 m wide. Its northwest and southeast extension has not been marked due to rugged topography and inaccessibility. The gabbro at the base is characterized by layered structure transitional into the overlying isotropic gabbro. The gabbro contains diopsidic-augite and plagioclase as primary minerals. The dykes unit and the individual dykes intruding the Thelichi formation comprise mainly hornblende (altered from augite), augite (relics and grains; ophitic to sub-ophitic), titaniferous augite (relics), chlorite, epidote, sphene, ilmenite and titanomagnetite.

Geochemical studies show that the dykes are basaltic in composition and characterized by high TiO_2, Na_2O and Fe_2O_3 and low K_2O. They show wide range in MgO in spite of restricted SiO_2 contents. High TiO_2, Na_2O and Fe_2O_3, and low K_2O characterize the gabbros also. The n-MORB-normalized plot shows slight depletion in HFSE for the comparatively less fractionated dykes
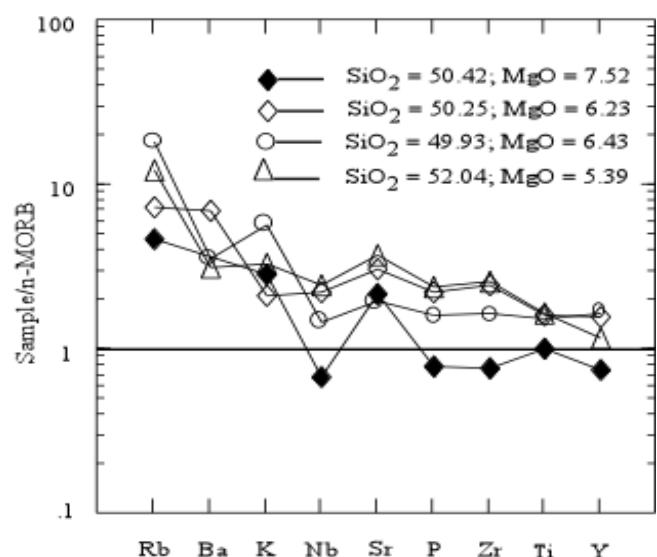
FIGURE 1. The n-MORB-normalized pattern for dykes of Majne area, Kohistan arc terrane, North Pakistan

with negative Nb anomaly in sample with SiO2 = 50.42 wt.% and MgO = 7.52 wt.% (**Figure 1**). The rest of the dykes show enrichment in both the LIL and the HFS elements. The Zr/Nb ratio of all the dykes falls in the range of 33-36 exhibiting n-MORB characteristics.

The enrichment in minor, trace and rare-earth elements and the linear trends of major and trace elements in entire dykes unit suggest that they are genetically coherent to a common MORB magma source possibly by high degree 20-30% of partial melting for the initial melt, followed possibly by low degree of partial melting and/or accompanied by fractional crystallization at low pressure. The evolved and/or fractionated dykes may also demonstrate geochemistry of crust contaminated MORB(?). The initial MORB source melt seems to have subduction component as depicted by negative Nb anomaly in one of the dyke sample. It is to be noted that MORB- and island-arc types geochemical features are characteristic of back-arc basin basalts. We, therefore, conclude that the Majne rocks represent ocean floor of back-arc or marginal basin, formed due to extension.

Origin of dunite of the Sapat Complex, Himalaya, North Pakistan

Tahseenullah Khan†*, Mamoru Murata‡, Hiraoki Ozawa‡, and Allah B Kausar†

† Geoscience Laboratory, Geological Survey of Pakistan, Shahzad Town, Islamabad, PAKISTAN
‡ Department of Geosciences, Faculty of Science, Naruto University of Education, Tokushima, JAPAN

* To whom correspondence should be addressed. E-mail: bangash1444@hotmail.com

The geotectonic framework of northern part of Pakistan involves intra-oceanic Kohistan arc formation in early Cretaceous time, its accretion to the Karakoram plate along the Shyok suture some 85-102 Ma ago and subsequent obduction onto the higher Himalayas of the Indian plate along the Indus suture about 55 Ma ago. The investigated area lies in the upper Kaghan valley of the North West Frontier Province of Pakistan, which is traversed by Indus suture or Main Mantle Thrust (MMT). The Indus suture comprises ophiolite and ophiolitic mélange, exposed at several places in northwestern Himalayas that includes Shangla, Mingora and Malakand ophiolite and ophiolitic melange, and further towards south the Waziristan, Muslim Bagh-Bela ophiolites and towards east Nidar ophiolite in Ladakh, India.

The Sapat area is characterized by rocks of the Indian plate, which has tectonic contact with mafic-ultramafic rocks of the Sapat complex. Our main interest is in the Sapat complex where high quality peridot (gem olivine) occurs. The Sapat complex is distinguished by peridot-bearing dunite and serpentinite at the base, followed by the ultramafic cumulates and layered to isotropic gabbros and metavolcanics of basaltic composition. Talc carbonate lenses and greenschist are incorporated as tectonic mélange within the phyllitic schists of the underlying Indian continental plate. The peridot-bearing dunite is homogeneous and sheared and traversed by numerous joints and fractures, along which gem-quality peridot mineralization has taken place. Other minerals associated with peridot are clinochrysotile, antigorite, talc and magnetite. The dunite contains mainly olivine, and serpentine along fractures. It also contains well-developed chrome spinel grains as accessory mineral. Besides, altered chrome spinel grains are also noticed in the rock. Olivine and chrome spinel of dunite were analyzed with EPMA, showing the forsterite content of olivine ranging between Fo_{91-94}, and Mg# (0.41), Cr# (0.72) and Fe^{3+}# (0.05) at average, Cr_2O_3 (51.62-53.99 wt.%) and Al_2O_3 (7.89-14.83 wt.%) in chrome spinel.

In Cr_2O_3- Al_2O_3 diagram, the chrome spinel data plots in mantle array field, which indicates that the dunite has mantle origin (**Figure 1**). Plotting on TiO_2-Cr# of chrome spinel, this dunite seems to be the end member for fore-arc peridotite with Cr# (>0.7), which in turn lies close and/or overlaps the fields of Izu-Bonin-Mariana boninite and the Lau Basin depleted arc basalt, some transitional to boninites (**Figure 2**). This infers that the dunite of the Sapat complex might have formed in a supra-subduction zone tectonic setting of fore-arc affinity. As evident from field and mineral chemistry data, it is further inferred that the Sapat mafic-ultramafic complex does not represent base of the Kohistan island arc as described previously but typifies an ophiolite sequence along the Indus suture between the Kohistan island arc and the Indian continental plate, and marks same zone along which other ophiolite sequences are exposed in Pakistan and India.
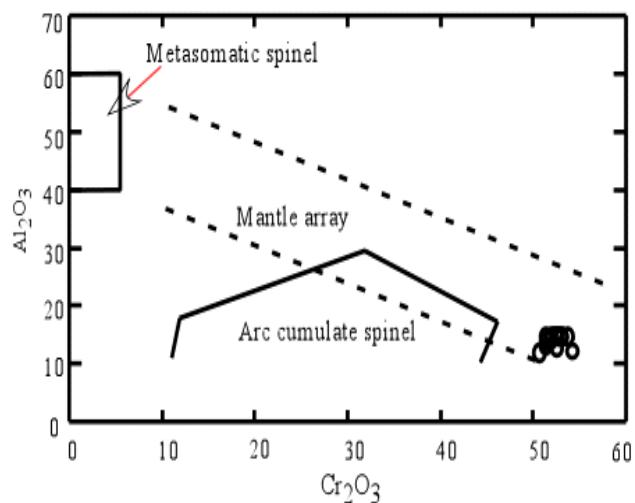
FIGURE 1. Al_2O_3-Cr_2O_3 diagram for chrome spinel and chromite samples from Sapat dunite and serpentinized dunite
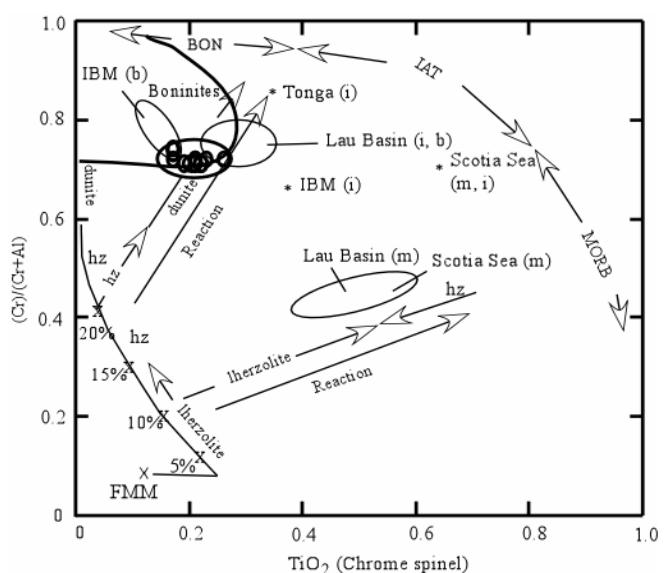
FIGURE 2. Plot of Cr# (Cr/Cr+Al) against TiO_2 in chrome spinel for the dunite of Sapat mafic-ultramafic complex. Symbols: IBM, Izu-Bonin Mariana System; BON, boninites; IAT, island arc tholeiites; MORB, mid ocean ridge basalts; hz, harzbergite; i, island arc; m, MORB; b, boninites; FMM, fertile MORB mantle.

Landslide and debris flow in the Himalayas: A case study of the Madi Watershed in Nepal

Narendra R Khanal†* and Teiji Watanabe‡

† Central Department of Geography, Tribhuvan University, Kirtipur, Kathmandu, NEPAL
‡ Laboratory of Geoecology, Graduate School of Environmental Earth Science, Hokkaido University, Sapporo 060-0810, JAPAN

* To whom correspondence should be addressed. E-mail: nrkhanal@geo07.ees.hokudai.ac.jp

Landslides, debris flow and other forms of mass wasting are common in mountain areas. These are the main geomorphic processes which are responsible for the transformation of landforms not only the mountain slopes but also the valleys, plains and river channels far downstream. Such transformation because of frequent occurrences of landslides and debris flow is very pronounced in the Himalayas with high energy environment due to active tectonics, rugged topography with very high relief and highly concentrated monsoon precipitation. Moreover, high density of both human and livestock population and consequent change in land use and land cover have caused further intensification of the processes of landslide and debris flow occurrence. The loss of life and properties from landslide, debris flow and flood has been increasing and the livelihood options of mountain people have been threatening.

This paper aims to discuss i) temporal and spatial distribution of landslide and debris flow ii) its causes iii) dynamics in terms of stability and iv) vulnerability and mitigation issues. This is a case study done in the Madi watershed. Major sources of information for this study are air photographs taken in different periods – 1956/58, 1972, 1979 and 1996 and discussions with local people. Field verification of the information derived after the interpretation of air photographs and group discussions in many places in the watershed were carried out during field work in 1999/2000.

The Madi watershed with an area of 1123 sq km and population of about 0.2 million is located in the Western Development Region of Nepal. The altitude of the watershed ranges from 307 m in the south to 7937 m in the north encompassing three major physiographic regions – the middle mountain, the high mountain and the high Himalaya. It comprises three major geological formations – the Lesser Himalayan meta-sediments in the south, the Higher Himalayan crystalline and Tibetan sedimentary Tethys sediment in the north. The Lesser Himalayan consists of intensely folded meta-sedimentary rocks whereas the Higher Himalayan crystalline consists of Precambrian high grade metamorphic rocks. The Main Central Thrust (MCT) crosses in the east-west direction in the central part of the watershed. The topography is very rugged. Gently sloping land ($< 5^0$) comprises only 9 percent of the total basin area followed by moderately to steeply sloping ($5-30^0$) mountain terrain and very steeply sloping ($> 30^0$) mountain terrain with rock headwalls. The average annual precipitation ranges from 1795 mm in the south to 3743 mm in the northwest. The average number of rainy days is between 130-180 days per year. More than 70 percent of the total precipitation occurs in four summer months (June-September). Daily precipitation with more than 100 mm, which causes slope instability (Caine and Mool 1982), occurs frequently in the watershed. The area is inhabited by more than 16 ethnic groups. The livelihood of most of people is based on natural resources and agriculture is the main occupation.

TABLE 1. Area covered by air photographs (sq km) and number and density (no/100 sq km) of landslide and debris flow scars in different periods in the Madi watershed

Year	Area	Total number	New	Active/ reactivated	Density
1956/58	998.1	236	na	236	23.6
1972	481.0	18	5	13	3.7
1979	744.5	5	1	4	0.7
1996	1123.5	25	15	10	2.2

FIGURE 1. Distribution of landslide and debris flow scars in the Madi watershed

A total of 236 active landslide and debris flow scars were identified in air photographs taken in 1956/58, 18 in 1972, 5 in 1979 and 25 in 1996 in the Madi watershed. Direct comparison of the number of landslide and debris flow scars for this watershed is not possible due to unavailability of air photographs covering the whole watershed for all the periods. In order to compare the results, density of landslide and debris flow scars has been calculated and presented in **Table 1**. The density of landslide and debris flow scars declined from about 24 per 100 sq km in 1956/58 to 4 in 1972, one in 1979 and 2 in 1996. These landslide and debris flow scars were concentrated mainly in five localities namely Siklesh, Saimarang, Bhujung, Karapu and Jita area (**Figure 1**).

Large numbers of landslide and debris flow scars were initiated in between 1948-1955 in many parts of the watershed due to heavy precipitation though the volume and intensity of those events were not recorded. Rivers were blocked for few hours by the logs and sediment several times particularly at the confluence point of two major rivers and narrow sections of the channel resulting drastic change in the morphology of both the channels and flood plains even far downstream areas during this period. Many of the landslide and debris flow scars identified in photographs taken in 1956/58 were small and shallow. Initiation of many small and shallow landslide and debris flow scars during and after highly localized heavy precipitation events like in the Madi watershed in between 1948-1955 has also been reported from other areas of Nepal in recent years (Manandhar and Khanal 1988, Dhital et al. 1993, Upreti and Dhital 1983, Khanal 1998). Some of the landslide and debris flow scars were initiated during the earthquake of 1934 and some were initiated later along the MCT. Many of them are located between 500 and 2500 m in altitudes, on southern aspect and shrub land. Some of them are located in remote areas far from human settlement affecting down stream landforms and hydrology. A few on upper slopes were initiated even in winter period (Feb-March) due to the melting snow and ice. Factors such as tectonic activities, climate, topography, river hydrology and land use/land cover play important role in the initiation and enlargement of landslide and debris flow scar in the watershed.

Many of the small and shallow landslide and debris flow scars were stabilized in a few years after their occurrence. Many of them were stabilized naturally and some of them were stabilized through the efforts of local community. However, large landslide and even the small one located along the gullies and river course are expanded and reactivated from time to time. Out of a total of 25 landslide and debris flow scars identified in air photographs taken in 1996, 10 were initiated before 1956/58 and remaining 15 were occurred between 1979 and 1996.

Landslide and debris flow events in between 1948-55 damaged large area of agricultural land and threatened many settlements in the watershed. As a result large scale outmigration took place from those areas which were affected most by landslides and floods. The damages from landslide, debris flow and flood events during this period remained very high not only in this watershed but in many parts of the country. As a response,

the government started resettlement program in the Inner Terai and Terai regions of Nepal for families severely affected by landslide and debris flow immediately after the events of 1948-55. The loss of life and properties from landslide and debris flow remained very high also in 1976, 1983 and 1998 in this watershed. One landslide and debris flow at Paire swept away 90 people including hotel owners and travelers rested there in 1976. Landslide and debris flow of 1983 killed seven people at Tandrang Taksar and that of 1998 displaced many families at Saimarang.

Human settlements in the watershed have been threatened due to reactivation and enlargement of old landslides. Six major settlements are in immediate danger from active landslide. Some of these landslides were very small at the initial stage and could be controlled through local efforts. But now some of them are very big and it is beyond the capability of local people to control them and the only way to reduce the loss is to abandon the area. The landslide initiated before 1954 in Taprang was reactivated in 1979. It is being enlarged every year threatening the livelihood options of more than 305 families residing in Taprang. Many families have already been migrated to other places due to danger of landslide. Similar situation is found in other areas such as Chautha, Saimarang, Bhoje and Gobinderi in the Madi watershed.

Though local people are aware about the problem of landslide still landslide control and management activities in organized way have not received priority yet. Moreover, the community based natural resource management and disaster mitigation systems of the past have been eroding. As a result, the vulnerability of life and properties in the area has been increasing. It requires effective landslide and debris flow control activities in an organized way with active participation of local people in order to minimize the loss of life and properties. These community based institutions should be strengthened with provision of training and other necessary supports.

References
Caine N and PK Mool. 1982. Landslides in the Kolpu Khola drainage, middle mountains, Nepal. *Mountain Research and Development* **2**(2): 157-173

Dhital M, N Khanal and KB Thapa.1993. *The role of extreme weather events, mass movements, and land use changes in increasing natural hazards.* A report of the preliminary field assessment and workshop on causes of the recent damage incurred in south-central Nepal (July 19-20, 1993), Kathmandu: ICIMOD

Khanal NR. 1998. *Study of landslide and flood affected area in Syangja and Rupandehi districts of Nepal. A* report submitted to Mountain Natural Resources' Division, International Centre for Integrated Mountain Development (ICIMOD), Kathmandu, Nepal

Manandhar IN and NR Khanal. 1988. *Study on landscape processes with special reference to landslides in Lele watershed, Central Nepal.* A report submitted to Research Division, Tribhuvan University, Kathmandu, Nepal

Upreti BN and MR Dhital. 1996. *Landslide Studies and Management in Nepal.* Kathmandu: ICIMOD

Comparative morphotectonics in the Himalayan foreland and the forearc of Southwest Japan

Kazuo Kimura

Naruto University of Education, 772-8502, JAPAN

For correspondence, E-mail: kkazz@naruto-u.ac.jp

The Southwest Japan, which is developed along a subduction boundary, is not a typical island arc. It has rich granitoid and crystalline, poor active volcano, thick upper crust and so on. These geophysical characteristics are in common with a collision mountain range such as the Himalayas. Geodetic surveying and seismology in SW Japan are ahead with those in the Himalayas. On the other hand, the Himalayan front that is a subaerial plate boundary has advantage for geologic and geomorphic studies. Therefore, comparative studies in the two boundaries aid to clarify their active tectonics by recovering the deficiency of each other.

Reflecting crustal thickness and shortening rate, the Himalayas is about twice larger in relief energy and far shorter in topographic wavelength than the SW Japan arc. In a seismotectonic sense of the boundary fault, the arc is divided into proto-thrust zone, imbricate thrust zone, multi-decollement zone, and earthquake thrust zone (Kagami et al. 1983). Morphostructural similarity in the Himalayas and the SW Japan is obvious as close to the plate boundaries. The proto-thrust zone is just on the plate boundary and is filling up with thick sediments. These characteristics are in common with the Ganges foredeep. Geostructure and morphology on the imbricate thrust zone is similar to those of the Sub-Himalaya. Both areas are deformation fronts with relatively low relief, and consist of Neogene-Quarternary deposits, which are sliced by imbricate thrusts in piggyback sequence. In a sense of lithostrigraphy, the area above the multi-decollement zone can not correlate to the Lesser Himalaya directly. However, nappe structure and its related crustal processes in the Lesser Himalaya resemble the development of the multi-decollement. In addition, its geomorphic pattern composed of the Mahabharat Range and the midland depression also corresponds to a series of outer ridges (Tosa-bae etc.) and forearc basins (Muroto trough etc.) on the decollement zone. The area above the earthquake thrust zone forms steep slope from the Muroto Trough to the Shikoku Island. Relief energy of the slope is the largest in the SW Japan arc. Though there is rare similarity in lithostratigraphy, south face of the Higher Himalaya may equivalent to the slope on the earthquake thrust zone by its remarkable topographic gap.

The above mentioned meso-scale morphotectonic features, which are over 10 km in topographic wavelength, are essentially formed by stable slip of flat-lying boundary faults. A dislocation model (Kimura and Komatsubara 2000) can reproduce it. In this model, ridges and basins and of the Himalayan foreland are mainly simulated by slip on thrust ramps branched off from the decollement. Also, slip on the decollement may be considered. Its topographic profile is in accord with the interseismic (post-seismic) crustal movement. On the other hand, remarkable uplift by the 1905 Kangra earthquake, which is considered to be a huge inter-plate earthquake, was observed along topographic depressions in the sub-Himalaya (Yeats and Lillie 1991). This is simulated chiefly by rupture on the decollement beneath the Lesser to Higher Himalayas. These facts show that coseismic crustal movement is less effective to form morphotectonic sequence of the Himalayas. Similar trend is known in the SW Japan Arc. For example, seismic uplift by the 1946 Nankai earthquake (M 8.0) was only observed on the south margin of the Shikoku Island (Ohmori 1978) that is topographic depression in front of the pre-Neogene prism.

Regardless, seismic slip by inter-plate earthquake occurs beneath a frontal margin of a pre-Neogene accretionary wedge, which forms as a steep topographic gap. It means that implications of the next inter-plate earthquake are hidden in the Lesser Himalaya to the southern slope of the Higher Himalaya. Intensive research of seismology and geodesy should be focused to these zones. In addition, the areas above the earthquake thrust zone and their backarc side, there are minor active faults, which are causes of intra-plate earthquakes. Though the earthquakes are relatively small and their recurrent interval are usually over 10^3 years, they must be care as secondary important seismic hazards. Their behavior can be clarified by geomorphic and trenching survey.

References

Kagami H, S Shiono and A Taira. 1983. Plate subdution and formation of accretionary prism in the Nankai trough. *Kagaku (Science)* **53**: 429-438 (*in Japanese*)

Kimura, K. and T. Komatsubara. 2000. Is the Himalayan Frontal Fault a source of the great earthquakes? *Chikyu Monthly (Gekkan Chikyu)* 28: p 54-60 (*in Japanese*)

Ohmori H 1978. Relief structure of the Japanese mountains and their stages in geomorphic development. *Bulletin of Department of Geography, the University of Tokyo* **10**: 31-85

Yeats RS and RJ Lillie. 1991. Contemporary tectonics of the Himalayan Frontal Fault system: folds, blind thrusts, and the 1905 Kangra earthquake. *Journal of Structural Geology* **13**: 215-225

Glacial lakes and its expansion in the north-central Bhutan and Kulha Kangri massif, Eastern Himalaya

Jiro Komori†*, Syuji Iwata†, Deo Raji Gurung‡ and Hironori Yabuki§

† Department of Geography, Tokyo Metropolitan University, Tokyo,192-0397, JAPAN
‡ Department of Geology and Mines, Ministry of Trade and Industry, PO Box 173, Thimphu, BHUTAN
§ Frontier Observational Research System for Global Change, Kanagawa, 236-0001, JAPAN

* To whom correspondence should be addressed. E-mail: jkomori@comp.metro-u.ac.jp

A great number of the glacial lakes have appeared in many mountain areas of the world during the last half-century due to global warming. Severe floods have been caused by frequent outbursts from the glacial lakes. These glacial lake outburst floods (GLOF) have also occurred in the Himalayan mountains (e.g., Vuichard and Zimmermann 1987, Xu and Feng 1994), including Bhutan Himalaya. The last outburst flood in Bhutan, which originated from Lugge Glacial Lake in October 1994, caused damage to property along the river with the loss of more than 20 lives (Watanabe and Rothacher 1996). Hence, investigation of the glacial lakes is necessary for disaster prevention in Bhutan and the downstream region. Geological Survey of Bhutan (1999) and Mool et al. (2001) made the inventory of the glaciers and glacial lakes in Bhutan. Ageta et al. (2000) and Komori et al. (2003) obtained the expansion records of the lakes in Bhutan. However, much remains to be established about the spatial and temporal variation of glacial lakes not only in Bhutan but also the other Himalayan mountains. The present study revealed the current condition of glacial lakes and its secular variations during the last 45 years.

Study area and method
The study area is focused in the north-central Bhutan and Kulha Kangri massif, border region of Tibet which are the headwater of Chamkhar Chhu (river) and Kuri Chhu (lat. 27º59'-28º24' N, long. 90º28'-91º10' E), the upper streams of the Manas river system. Distribution and development history of the lakes is revealed from detail tracing by the image-editing program (Deneba Canvas 9), using digitized two CORONA satellite imagery (about 10 m digitized resolution, taken in 1967 and 1968), two Landsat satellite imagery (normal resolution of 30 m, taken in 1990 and 2000) and three SPOT satellite imagery (nominal resolution of 10 - 20 m, taken in 1991, 1993 and 2001). The Indian toposheets (1:50,000 in scale, based on aerial photographs taken in 1956 and 1958) and the Soviet toposheets (1:200,000 in scale, based on aerial photographs taken from 1972 to 1974) were used for geometric correction. The field investigation in Chamkhar Chhu was carried out in late September 2002, with the cooperation of the Geological Survey of Bhutan.

Results and discussion
More than twenty glacial lakes, located on the surface or front of the glacier in the headwater of Chamkhar Chhu and Kuri Chhu are recognized. In particular, detail observation was carried out for 19 potentially hazardous lakes which are large and expanding water area, and showing dangerous situation. The observation provided important and previously unknown information. The serial number of hazardous lakes in Chamkhar Chhu and Kuri Chhu basin were given as CGL-1, 2, 3, and KGL-1, 2, 3, tentatively. The summarized features of these lakes as follows:

(1) Lake area: Maximum area of hazardous lakes is 1.70 km^2 (KGL-13, **Figure 1**). Besides, three lakes area are over 1 km^2.

(2) Expansion rate: **Figure 2** showing the expansion rate of the lake area in the southern and northern side of the Himalaya. The largest expanding lake in Chamkhar Chhu and Kuri Chhu basin shows highly expansion rates of 0.027 km^2/y (CGL-6, Chamkhar glacial lake) and 0.025 km^2/y (KGL-13), respectively.
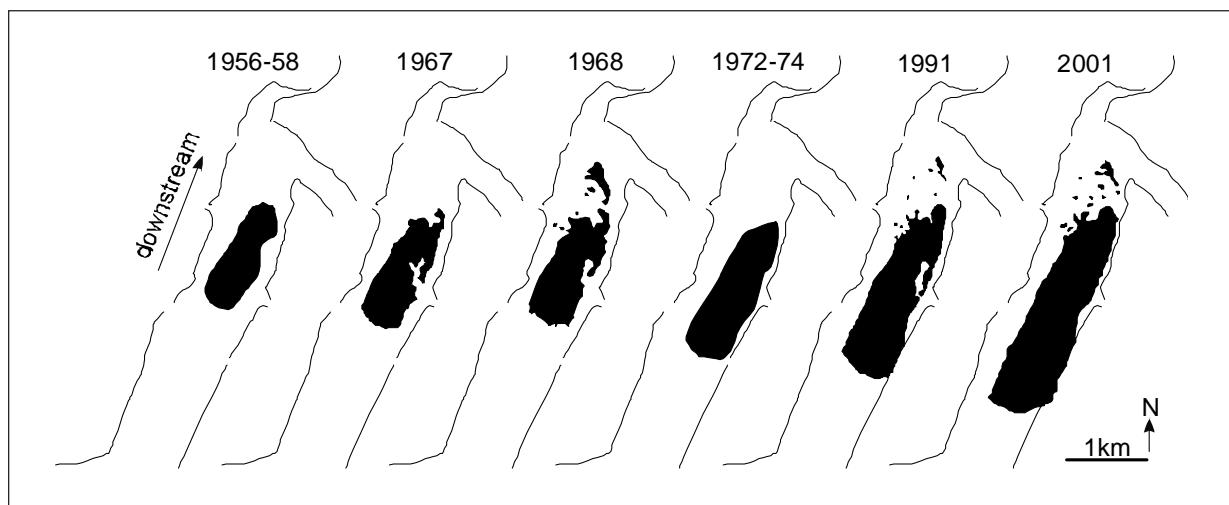
Figure 1. Area variation of KGL-13 from 1956-58 to 2001. Outer solid line is the outline of the glacier
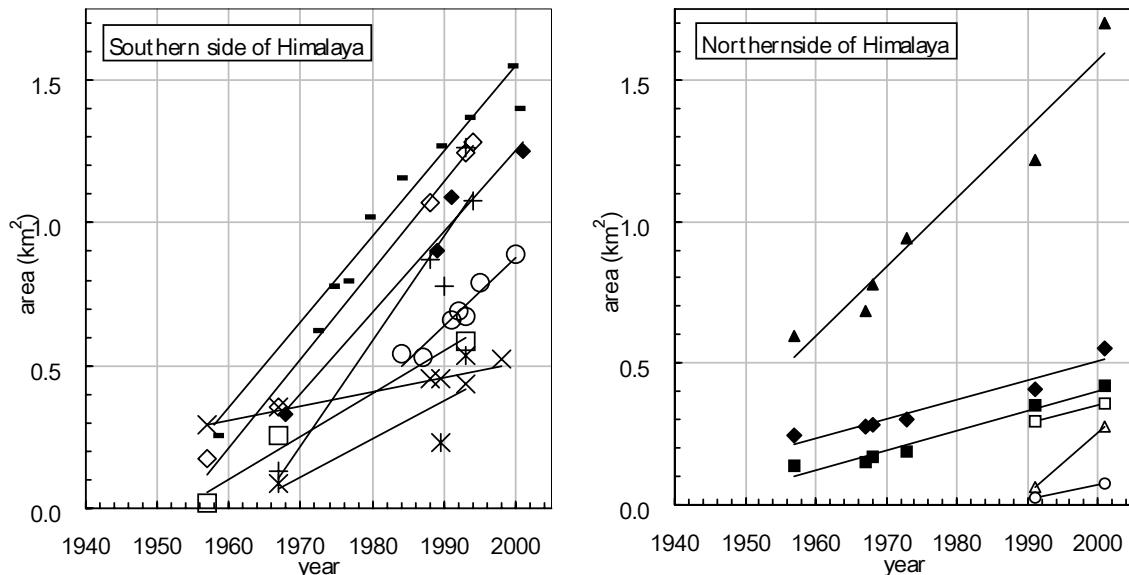
FIGURE 2. Expansion rate of the glacier

The highest rate of 0.037 km²/y are calculate from Lugge glacial lake. On the other hand, some small lakes and supraglacial ponds show low expansion rate of up to 1 km²/y. The expansion rates of the northern side are relatively slower than the other side. Some expansion rate of latter period is higher than early period.

(3) Topographical feature: These lakes are classified as the moraine dammed proglacial lake and supraglacial lake (or ponds). Most expansion has advanced at the upper end of the lakes which is contact part between the water area and ice cliff of glacial ice.

Extrapolation of the expansion rate indicates that the initial water area of the southern side of the Himalaya appeared in the 1950s to early 1960s. On the contrary, the emergent year of lakes at the northern side of the Himalaya vary about from 1940s to early 1990s. The differentiation of the expansion rate and emergent year are caused by differences of meteorological and topographical condition at both side of Himalaya mountains. In addition, increasing the expansion rate and appearance the initial water area at the northern side (KGL-11 and KGL-10) in the late 1980s to early 1990s suggests that the enhanced global warming closely affected the glacial lake forming. In the presentation, we will incidentally exhibit the some types of lake expansion and one of the evidence of GLOF occurrence before 1967.

References

Ageta Y, S Iwata, H Yabuki, N Naito, A Sakai, C Narama and Karma. 2000. Expansion of glacier lakes in recent decades in the Bhutan Himalayas. Proceedings of the Seattle Workshop, 2000; Debris-Covered Glaciers. IAHS, Publication no. **264**: 165-175

Geological Survey of Bhutan. 1999. *Glaciers and Glacier Lakes in Bhutan.* Geological Survey of Bhutan. 83 p

Komori J, DR Gurung, S Iwata and H Yabuki. 2003. Variation and lake expansion of Chubda Glacier, Bhutan Himalayas, during the last 35 years. *Bulletin of Glaciological Research* **21**: 49-55

Mool PK, D Wangda, SR Bajrachaya, DR Gurung and SP Joshi. 2001. *Inventory of glaciers, glacial lakes and glacial lake outburst floods, Bhutan.* ICIMOD, Kathmandu. 247 p

Vuichard D and M Zimmermann. 1987. The 1985 catastrophic drainage of a moraine-dammed lake, Khumbu Himal, Nepal: case and consequences. *Mountain Research and Development* **7**: 91-110

Watanabe T and D Rothacher. 1996. The 1994 Lugge Tsho glacial lake outburst flood, Bhutan Himalaya. *Mountain Research and Development* **16**: 77-81

Xu D and Q Feng. 1994. Dangerous glacier lakes and their outburst features in the Tibetan Himalayas. *Bulletin of Glacier Research* **12**: 1-8

Yabuki H. 2003. Investigation for expansion of Imja glacier lake using satellite images. Meeting report of the Joint Research Program of the Institute of Low Temperature Science, Hokkaido University, 24-30 (In Japanese)

Yamada T. 1998. *Glacier lake and its outburst flood in the Nepal Himalaya.* Monograph No. 1, March 1998 Data Center for Glacier Research, Japanese Society of Snow and Ice. 96 p

FIGURE 2. Expansion rate of the glacier

Right: in the southern side of the Himalaya. -:Tsho Rolpa, ○ : Imja lake, ◇ : Raphsthreng, + : Lugge, * : Thorthomi, □ : Wackey, × : Mouzom, ● : Chubda

Left: in the northern side of the Himalaya. ▲ : KGL-13, ◆ : KGL-9, ■ : KGL-12, △ : KGL-11, ○ : KGL-10, □ :KGL-12

The plots of Fig 2-b and Chubda glacial lake are based on this study. Tsho Rolpa and Imja were reffered form Yamada et al.(1998) and Yabuki (2003), respectively. The othe data are digitized and measured from the figures in Ageta et al. (2000).

Tectonics and climate for the last ca. 35,000 years in the Kumaun Himalaya, India

BS Kotlia

Department of Geology, Kumaun University, Nainital, 263 002, INDIA

For correspondence, E-mail: bskotlia@yahoo.com

The Kumaun Lesser Himalayan terrain is defined by very active intracrustal thrusts where the strain progressively builds up due to horizontal compression. A number of thrusts/faults parallel or oblique to the intracrustal boundary thrusts were reactivated in the Late Pleistocene. The neotectonic movements along the main and associated faults are manifest in the pronounced geomorphic rejuvenation of the landscape such as off-setting of the country rocks, formation and dislocation of terraces and colluvial cones, deposition of unsorted huge gravels and debris flows, structurally-controlled meandering, triangular fault facets, fault scarps and steel waterfalls. The resultant stream ponding culminated in the formation of lakes behind recently uplifted blocks upstream of the active faults. Very recently, our group has discovered a number of such tectonic lakes in the Kumaun Himalaya, represented by 10-13 m thick succession of clays and carbonaceous muds.

We suggest that the Kumaun Himalaya experienced four major tectonic events at ca. 35 ka, 22-21 ka, 10 ka and 1.5-1.3 ka BP. These events were responsible either for formation of lakes or closure of some of the existing ones. Four minor magnetic reversals are detected in the palaeolake profiles at ca. 35 ka, 28-25 ka. 22-21 ka and 8 ka BP. This is the first report of the minor reversals in the lacustrine systems of the Indian sub-continent.

Using a variety of multidisciplinary techniques, e.g., chronological, isotopes, clay mineralogy, elemental analysis and pollen spectra, following climatic events are obtained for the Kumaun Himalaya. Climatic amelioration (ca. 34.3-32.2 ka BP), short spell of aridity (32.2-31.3 ka BP), warm and moist conditions (31.3-30.0 ka BP), cool/arid climate (30.0-28.9 ka BP), warm/humid conditions (28.9-27.4 ka BP), aridity (27.4-26.8 ka BP), humid/moist conditions (26.8-25.3 ka BP), semi-arid conditions (25.3-24.5 ka BP), humid conditions (24.5-22.4 ka BP), aridity (22.4-21.7 ka BP), humid conditions (21.7-20.0 ka BP), arid conditions (20.0-18.0 ka BP), semi-arid conditions (18.0-17.0 ka BP), arid climate (17.0-15.2 ka BP), humid phase (7.3-4.2 ka BP) and aridity from ca. 4 ka BP onwards. **Figure 1** shows high resolution climatic changes between ca. 31 and 22 ka BP.
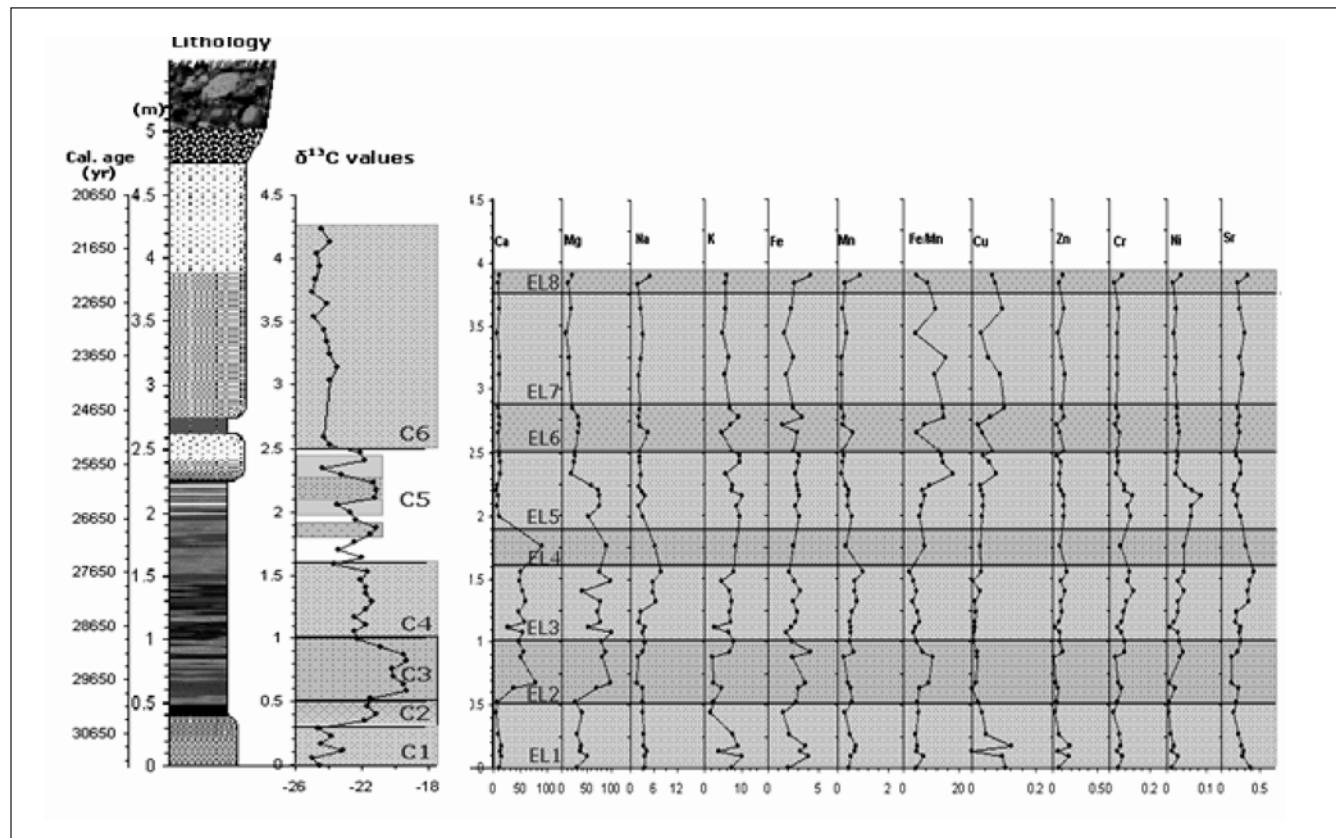
FIGURE 1. Climatic changes between ca. 31 and 22 ka BP in the Dulam area, Kumaun Lesser Himalaya, India

Glacial Geomorphology and Ice Ages in Tibet and surrounding mountains

Matthias Kuhle

Geography and High Mountain Geomorphology; Geographical Institut, University of Göttingen, Goldschmidtstr. 5, D-37077 Göttingen, GERMANY

For correspondence, E-mail: mkuhle@gwdg.de

Evidence for an ice sheet covering Tibet during the Last Glacial Maximum (LGM: stage 3-2) means a radical rethinking about glaciation in the Northern Hemisphere. The ice sheet's subtropical latitude, vast size (2.4 million km²) and high elevation (~6000 m asl) (**Figure 2**) caused a substantial, albedo-induced cooling of the Earth's atmosphere and the disruption of summer monsoon circulation. The uplift of Tibet and the reaching of specific threshold values of plateau elevation being synchronous with the onset of the ice ages at ~2.8 Ma B.P. and their intensification from ~1 Ma B.P. onwards, a causal link between these factors seems likely.

During 35 campaigns of field investigations (**Figure 1**), the ice-age inland glaciation of Tibet has been reconstructed on the basis of classical glacigenic forms of erosion and accumulation as well as on its accompanying sediments and the arrangement of the positions. Absolute datings obtained by different methods classify this glaciation as being from the LGM. With the help of 13 climate measuring stations, radiation and radiation balance measurements have been carried out between 3300 and 6650 m asl in Tibet. They indicate that the subtropical global radiation reaches its highest energies on the High Plateau, thus making Tibet today's most important heating surface of the atmosphere. At glacial times 70% of those energies were reflected into space by the snow and firn of the 2.4 million km² extended glacier area covering the upland. As a result, 32% of the entire global cooling during the ice ages, determined by the albedo, was brought about by this area– now the most significant cooling surface. The uplift of Tibet to a high altitude about 2.8 Ma ago, coincides with the commencement of the Quaternary Ice Ages. When the Plateau was lifted above the snowline (=ELA) and glaciated, this cooling effect gave rise to the global depression of the snowline and to the first Ice Age. The interglacial periods are explained by the glacial-isostatic lowering of Tibet by 650 m, having the effect that the initial Tibet ice, which had evoked the build-up of the much more extended lowland ices, could completely melt away in a period of positive radiation anomalies. The next ice age begins, when – because of the glacial-isostatic reveres uplift – the surface of the Plateau has again reached the snowline. This explains, why

1: 1973, 1974   2: 1976, 1977, 1995, 1998, 2000, 2002   3: 1981, 1998   4: 1982, 2003   5: 1984   6: 1986   7: 1987, 1992, 1995, 2000   8: 1988   9: 1988/89
10: 1989   11: 1991   12: 1991   13: 1984, 1991   14: 1986, 1992   15: 1992   16: 1993   17: 1993, 1996   18: 1993, 2004   19: 1994   20: 1994/95, 2000   21: 1995
22: 1995   23: 1996   24: 1997   25: 1998   26: 1999   27: 1999, 2000   28: 2000   29: 2000   30: 2002   31: 2004   Draft: M. Kuhle (2004)
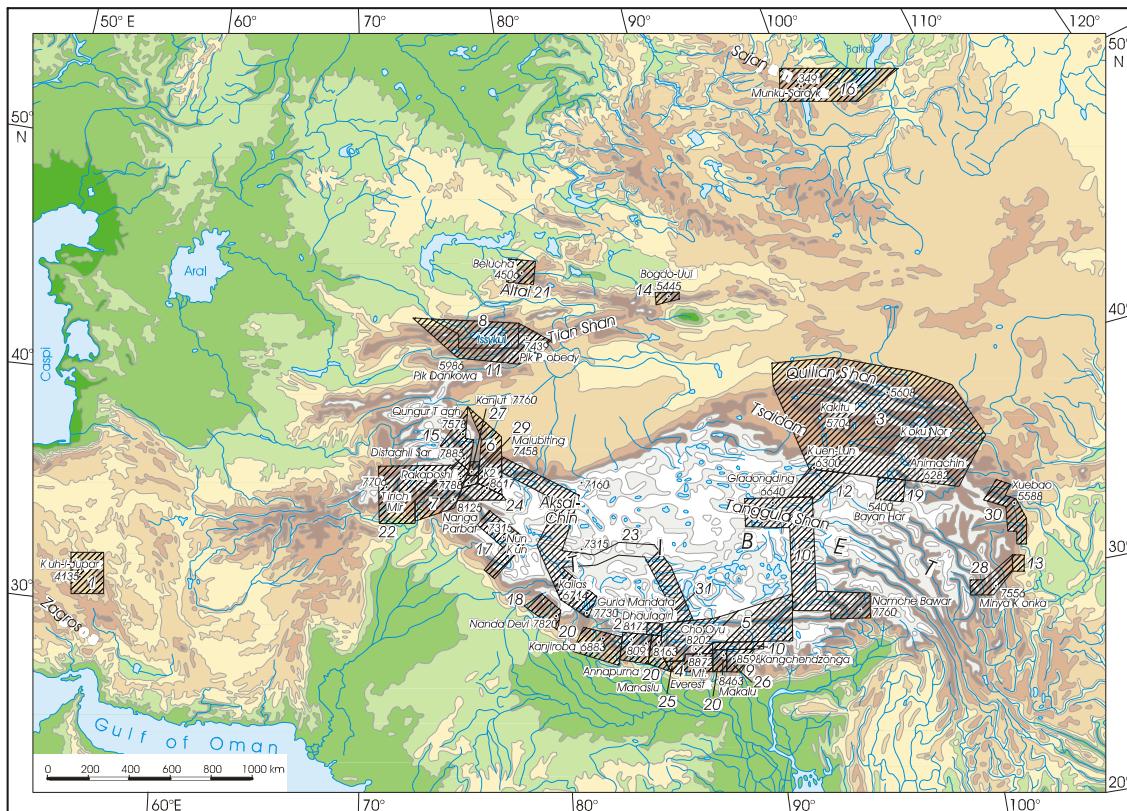
FIGURE 1. The areas in Tibet and High Asia under investigation by the author since 1973

the orbital variations (MILANKOVIC- theory 1941) could only have a modifying effect on the Quaternary climate dynamic, but were not primarily time-giving: as long as Tibet does not glaciate automatically by rising above the snowline, the depression in temperature is not sufficient for initiating a worldwide ice age; if Tibet is glaciated, but not yet lowered isostatically, a warming-up by 4°C might be able to cause an important loss in surface but no deglaciation, so that its cooling effect remains in a maximum intensity. Only a glaciation of the Plateau lowered by isostasy, can be removed through a sufficiently strong warming phase, so that interglacial climate conditions are prevailing until a renewed uplift of Tibet sets in up to the altitude of glaciation. The chronology of a Tibetan glaciation since ~2.8 Ma B.P. and its intensification since ~1 Ma B.P. has been confirmed by the weakening of the summer monsoon and the intensification of the Asian winter monsoon respectively, which have been evidenced by marine sediment drillings and loess records. Altogether in High Asia at least 13 further glacier positions have been evidenced, including an oldest Riá-position (pre-last High Glacial maximum). They concern a lowest Wurmian ice margin position (Stage 3-2) with ELA-depressions from 1100 to 1300 m,

4 to 6 Late Glacial ice margin positions with ELA-depressions from 1100 to 700 m, 3 neoglacial ice margin positions with ELA-depressions from 300 to 80 m and 6 historical ice margin positions including the current glacier margin with only insignificant snowline depressions of less than 80 m. The geomorphological observation of the moraines in the field was confirmed by more than 1000 petrographical, granulometrical and morphoscopical analyses of sediment samples. All absolute datings were younger than 47 Ka.

References

Kuhle M. 1998. Reconstruction of the 2.4 Million km² Late Pleistocene ice sheet on the Tibetan Plateau and its impact on the global climate. *Quater Int* **45/46:** 71-108 (additional Figures in: **47/48**, 173-182)

Kuhle M. 2002. A relief-specific model of the ice age on the basis of uplift-controlled glacier areas in Tibet and the corresponding albedo increase as well as their positiv climatological feedback by means of the global radiation geometry. *Climate Res* **20**:1-7

Kuhle M. 2003. New geomorphological indicators of a former Tibetan ice sheet in the central and notheastern part of the high plateau.- *Zeitschrift Geomorph N.F.* Suppl.-Vol. **130**: 75-97

Milankovic M. 1941. Kanon der Erdbestrahlung. Belgrad
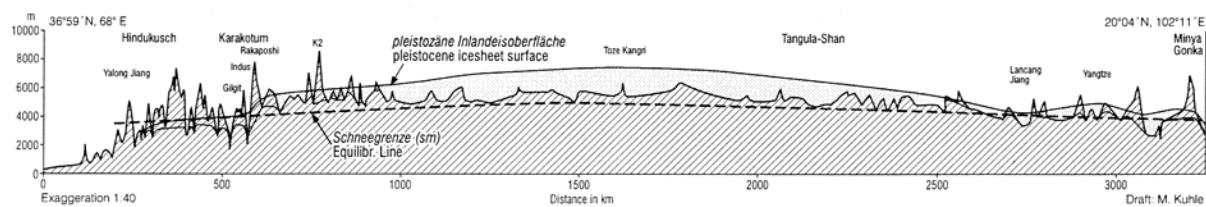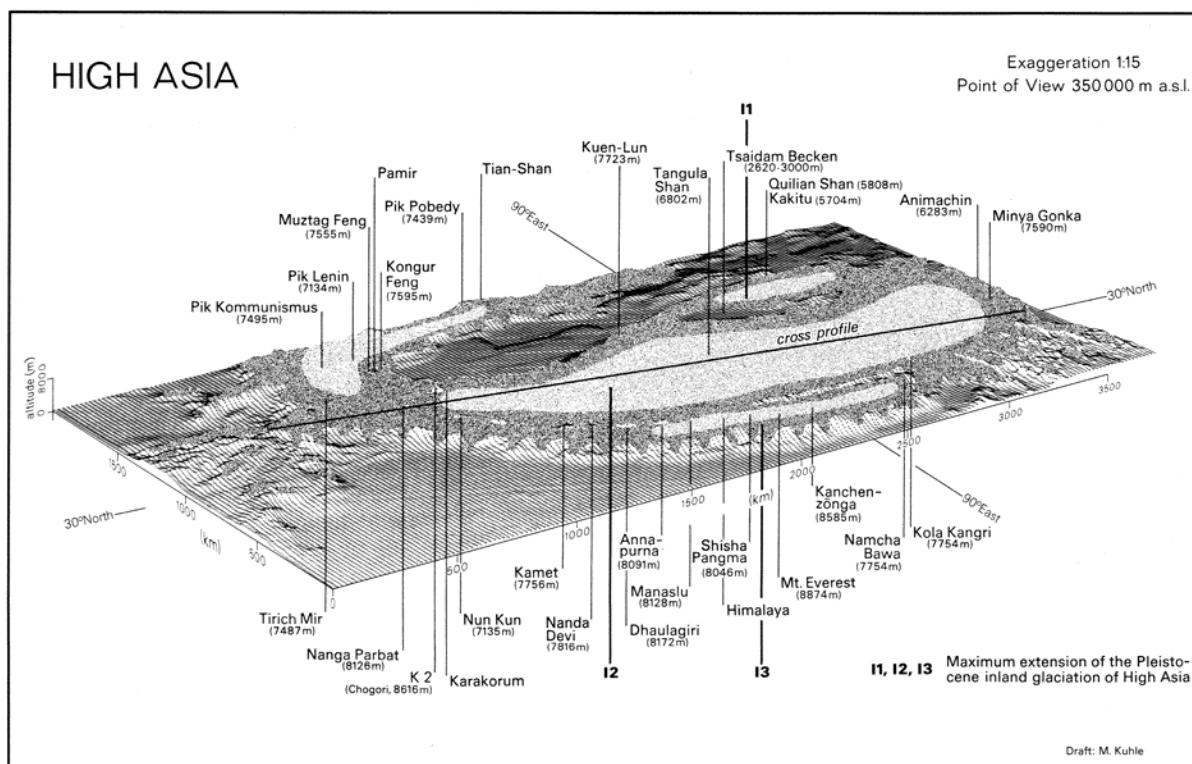
FIGURE 2. (Top) Reconstructed 2.4 million km² ice sheet, or ice stream network, covering the Tibetan plateau (Kuhle (1980, 1982a, 1982c, 1985, 1987a,b, 1988c,d, 1990d, 1991a,b,1993, 1994, 1995b, 996a,b, 1997, 1998, 1999, 2001, 2003, 2004) with three centres I1, I2, I3. Only peaks higher than 6000 m rise above the ice surface.(Bottom) Cross profile of the central ice sheet from Hindu Kush in the west to Minya Gonka in the east.

Magnetic susceptibility and biotite composition of granitoids of Amritpur and adjoining regions, Kumaun Lesser Himalaya

Santosh Kumar*, Brajesh Singh, CC Joshi and Abhishek Pandey

Department of Geology, Kumaun University, Nainital 263 002, Uttaranchal, INDIA

* To whom correspondence should be addressed. E-mail: skyadavan@yahoo.com

Felsic magmatism in Amritpur and adjoining localities of Kumaun Lesser Himalaya is represented by Palaeoproterozoic (~1890 Ma) Bt-Ms granitoids and quartz feldspar porphyries, referred to as Amritpur granitoids (AG) and Amritpur porphyry (AP) respectively. The AG are porphyritic and equigranular as well, and extend from Suraijula (west) to Barhoan (east) in the Nainital district of Kumaun Lesser Himalaya. The Main Boundary Thrust (MBT) forms the southern boundary of AG, and quartzite-metabasalts association is exposed in the north. The equigranular variety of AG, referred to as Amritpur leucogranite (ALG) dominates over porphyritic ones, and is medium- to coarse-grained, hypidiomorphic, mainly composed of K-feldspar (perthite), quartz and plagioclase (sericite). Muscovite is present associated with biotite but varies in proportion ranging from rare to noticeable amount. The magnetic susceptibility (MS) measurements of AP and AG were carried out in the field on smooth rock surfaces using hand-held SM–20 magnetic susceptibility meter. The obtained MS value (SI unit) was further corrected according to the degree of the rock-surface unevenness. Primary biotites from ALG were analyzed by wavelength dispersive electron-probe microanalysis. Ferrous and ferric iron from total iron (FeO) of biotite was estimated following charge-balance procedures.

The MS values of AP vary from 0.399 to 0.912×10^{-3} SI unit with an average of 0.528×10^{-3} SI (N=17), which typically represent ilmenite series ($\chi \leq 3.0 \times 10^{-3}$ SI) granite (Ishihara 1977). Medium-grained ALG measures relatively lesser MS values ($\chi = 0.003-0.148 \times 10^{-3}$ SI) with an average of 0.062×10^{-3} SI (N=55) compared to coarse-grained ALG which vary from 0.025 to 0.195×10^{-3} SI with an average MS of 0.117×10^{-3} SI (N=18), both being related to ilmenite series granite. Coarse-grained gneissic AG, exposed at places, record the MS values ranging from 0.295 to 0.527×10^{-3} SI with an average MS value of 0.379×10^{-3} SI (N=26). Porphyritic AG, an older lithounit, are xenolith-bearing and xenolith-free, and their MS values range from 0.368 to 0.629×10^{-3} SI and from 0.142 to 0.247×10^{-3} SI with average MS of 0.522×10^{-3} SI (N=10) and 0.190×10^{-3} SI (N=10) respectively. The observed MS variations of porphyritic AG appear related with xenolith incorporation, which might have slightly oxidized the porphyritic AG. The MS values of AP and AG including the ALG typically correspond to ilmenite series granites, and the noted MS variations may be related with their differing contents of ferromagnesian minerals, ilmenite and textural variations. The AG including the ALG are typically peraluminous (S-type) consistent with their nature similar to ilmenite series granites. About 60% of whole-rock data (N=13) of AP (Gupta et al. 1994; Nautiyal and Rawat 1990) are metaluminous (I-type) despite of their exclusively ilmenite series nature. In Japan nearly all the ilmenite series are I-type, and it has been observed that magnetite-/ilmenite-series classification is not exactly equivalent to the I-/S-type classification in terms of alumina saturation index (ASI).

The ALG biotites have ΣX variation between 1.02 and 1.25 atoms in their structural formulae, which are dominantly
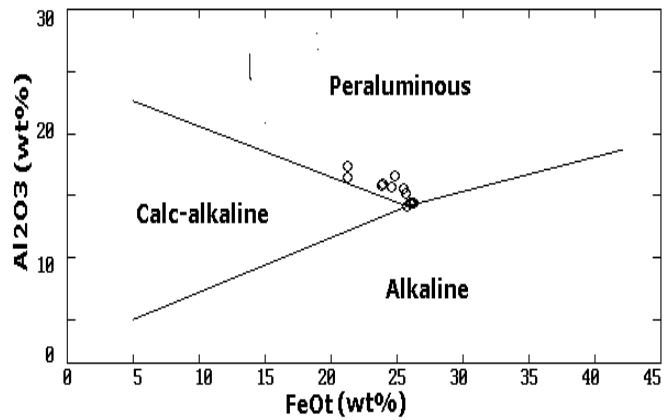
FIGURE 1. Bivariate Al_2O_3 vs. FeO^t plot for biotite(o) hosted in ALG. Biotites from ALG mostly plot in the field of biotites crystallizing in peraluminous (S-type) felsic magma. Fields are taken from Abdel-Rahman (1994)

contributed by potassium. The observed ΣX values more than one in ALG biotites may be due to the replacement of K by the elements Ba, Rb and Cs. Biotites of ALG plot into the field of primary biotite crystallized in felsic magma but scatter at and above the Ni-NiO buffer. However, presence of ilmenite and substantially low MS values ($0.003-0.157 \times 10^{-3}$ SI) of ALG suggest the prevalence of elevated reducing conditions during the evolution of ALG magma. The ALG melt was further reduced at emplacement level as evident by the presence of graphite pods and patches hosted in the ALG near the contact with country-rocks. The biotites of ALG are ferri-biotites showing enrichment in siderophyllite component, which is commonly available in crustally-derived felsic melt. The ALG biotites in terms of MgO-FeO^t-Al_2O_3 components show the compositional similarity with the biotites unaccompanied with ferromagnesian minerals, which further suggest their crystallization in crustally-derived felsic magma. The FeO^t/MgO ratio of biotite from ALG varies from 2.93 to 4.94 with an average of 4.00 suggesting the nature of host ALG magma similar to peraluminous (S-type) melt (Abdel-Rahman 1994). Biotites in ALG magma exhibit a negative $FeO-Al_2O_3$ correlation (**Figure 1**) suggesting dominance of 3Fe~2Al substitution in producing Al-rich biotites, but the substitution of 3Mg~2Al mostly vital in calc-alkaline and peraluminous magma system cannot be unambiguously inferred.

Japanese and many other granitoids are emperically divided into magnetite and ilmenite series granites using bulk Fe_2O_3 (wt%) / FeO (wt%) ratio of 0.5 at SiO_2 content of 70 wt%; Fe_2O_3/FeO > 0.5 magnetite series, Fe_2O_3/FeO < 0.5 ilmenite series (Ishihara 1979). Bulk Fe_2O_3/FeO ratio of AP (N=13) indicates proportion of 6:7 for magnetite to ilmenite-series in the silica

range of 59.82 to 75.37wt%, suggesting that ilmenite series more-or-less equals the magnetite series for AP. On the other hand Fe_2O_3/FeO ratio of AG (N=17) varies from 0.01 to 0.18 except one sample (Fe_2O_3/FeO =0.87) in the SiO_2 range of 67.08 to 78.74 wt %, which indicates that most AG are ilmenite series granites and are in accordance with the observed MS values. Ilmenite series nature of AG is consistent with their peraluminous (S-type) nature, whereas AP represents both peraluminous (S-type) and metaluminous (I-type) as well. Biotite compositions from ALG suggest their evolution and stability in peraluminous (S-type) felsic melt, and hence it can be concluded that the ALG magma is essentially derived by the partial melting of crustal protolith (metapelite), which subsequently evolved under reducing environment most likely prevailed during pre-Himalayan syntectonic orogeny.

References

Abdel-Rahman, AM. 1994. Nature of biotites from alkaline, calc-alkaline and peraluminous magmas. *J Petrol* **35**: 525-541

Gupta LN, Himanshu Ghildiyal and HS Chawla. 1994. Petrochemistry and tectonic environment of granites and porphyries of Amritpur-Ramgarh areas, Lesser Himalaya, Uttar Pradesh. *J Himalayan Geol* **5**: 103-116

Ishihara S. 1977. The magnetite-series and ilmenite-series granitic rocks. *Min Geol* **27**: 293-305

Ishihara S. 1979. Lateral variation of magnetic susceptibility of the Japanese granitoids. *J Geol Soc Japan* **85**: 509-523

Nautiyal SP and RS Rawat. 1990. Nature and preliminary petrochemistry of the Amritpur granites, Nainital district, Kumaun Himalaya, U.P., India. *J Himalayan Geol* **1**: 199-208

Variations of paleoclimate and paleoenvironment during the last 40 kyr recorded in clay minerals in the Kathmandu Basin sediments

Yoshihiro Kuwahara†*, Mukunda Raj Paudel†, Takeshi Maki†, Rie Fujii‡ and Harutaka Sakai†

†*Department of Evolution of Earth Environments, Graduate School of Social and Cultural Studies, Ropponmatsu, Fukuoka 810-8560, JAPAN*
‡*Depatment of Chemistry, Faculty of Science, Okayama University of Scinece, Ridaicho1-1, Okayama 700-0005, JAPAN*

* *To whom correspondence should be addressed. E-mail: ykuwa@rrc.kyushu-u.ac.jp*

The Asian monsoon system and its evolution are known to be closely linked to the Himalayan-Tibetan orogen. The Kathmandu Basin is the best target for clarifying the variability of the Asian monsoon climate and its linkage to the uplifting of the Himalayan-Tibetan orogen, since it is located on the southern slopes of the central Himalayas and filled with thick sediments from late Pliocene to Quaternary (Sakai 2001). Unfortunately, previous studies could not critically and completely resolve on the paleoclimatic and paleoenvironmental changes in the Kathmandu Basin because of samples from discontinuous surface exposures.

Our group has proceeded on a Japan-Nepal collaborative project "Paleo-Kathemandu Lake (PKL) Project". In the project, we have carried out core drilling within the Kathmandu Basin and have investigated the cores and surface exposures from various viewpoints and methods. The reconstruction of paleoclimatic and paleoenvirnmental variations recorded in the Kathmandu Basin sediments is one of many purposes of our project. We have already reported the results of fossil pollen analysis and characteristics of sediments for a drilled core sample obtained from the Kathmandu Basin and surface geological survey in the southern part of the Kathmandu Basin.

Clay minerals represent useful markers of successive climates, since they formed through weathering or hydrolysis processes during successive periods of the geological history and basically express the intensity of weathering or hydrolysis in the land masses adjacent to sedimentary basin. The information provided from such clay minerals fundamentally integrates the combined effects of temperature and precipitation. Detrital clay minerals can also be used as tracers of sediment transport processes, dispersal and provenance. Clay minerals in the Kathmandu Basin sediments do contain good information on the paleoclimate and paleoenvironment in this area, because they are directly formed through the weathering or hydrolysis process only from the parent minerals, feldspars and micas, in both gneiss and granite of the Shivapuri injection complex and weakly metamorphic rocks of the Phulchauki Group.

In order to reconstruct the paleoclimatic and paleoenvironmental changes during the last 40 kyr recorded in the Kathmandu Basin, we examined the estimation of the amount of the clay size fraction, the relative amounts of individual clay minerals, and the crystallinity of illite in the drill-core sediments by using the decomposition procedure of X-ray diffraction (XRD) patterns and the mineral reference intensity (MIF) method. In this paper, we report the paleoclimatic and paleoenvironmental information in the Kathmandu Basin deduced from the clay mineral data.

For clay mineral analysis, we used core sediment samples collected at 10 cm interval between 7 m and 40 m in depth of the RB core, which was drilled at Rabibhawan in the western central part of the Kathmandu Basin and is 218 m long (Sakai et al. 2001). The topmost part of the RB core from 7 m to 12.15 m in depth is generally composed of medium-to very coarse-grained micaceous granitic sand. The core sediments between 12.15 m and 40 m in depth are organic black or dark gray mud called "Kalimati Clay". A ^{14}C age of the Kalimati clay at 38.3 m in depth of the RB core is 44690±360 yr. B.P. and the mean sedimentation rate between 7 m and 40 m in depth of the RB core is about 900 mm/kyr.

The clay fraction under 2µm was separated from each sediment sample by gravity sedimentation. Then, about 200 mg of this fraction was collected by the Millipore® filter transfer method to provide an optimal orientation. The thickness of a clay cake formed on the filter is over 15 mg/cm², which is adequate for XRD quantitative analysis. The clay cake was then transferred onto a glass slide. Both air-dried (AD) and ethylene glycol solvated (EG) preparations were done for each sample. The EG preparation was carried out to expose the sample to the vapor of the reagent in desiccator over 8 hr at 60°C.

All XRD data were collected on a Rigaku X-ray Diffractometer RINT 2100V, using CuKα radiation monochromatized by a curved graphite crystal in a step of 0.02° with a step-counting time of 4 seconds. The decomposition of the obtained XRD patterns was performed with an Apple Power Macintosh computer and a program XRD MacDiff, according to Lanson (1997) and Kuwahara et al. (2001). The crystallinity of illite and the relative amounts of clay minerals in the Kathmandu Basin sediments were estimated by the decomposition data and the MIF method using a program NEWMOD.

The variations of the two illite crystallinity indices, Lanson index (LI) and modified Lanson index (MLI) for the upper part of the RB core are in harmony with the pollen analysis results of the same samples. The increasing hydrolysis condition expected from the results of illite crystallinity indices corresponds to the pollen zone in which some pollen as warm and wet climate indicators increase, while the decreasing hydrolysis condition corresponded to the pollen zone showing the increase of pollen as cold and dry climate indicators.

However, the variations of the illite crystallinity indices and the amount of the clay size fraction show roughly mirror image of that of the smectite/illite ratio. In the Kathmandu basin sediments, illite is the main constituent of the clay size fraction and the amount of smectite is very low relative to the other clay minerals (**Figure 1**). Therefore, the smectite/illite ratio depends strongly on the amount of illite. It is predicted that, in the Paleo-Kathmadu Basin, the weathering of mica formed illitic minerals but did not advance up to the ample formation of smectite even under wet climate, because of the rapid erosion of the parent rocks and rapid transport of sediments.

The variation of the hydrolysis condition inferred from the illite crystallinity indices were congruous with the variation of δ^{18}O GISP2. These results show that the major climatic variations
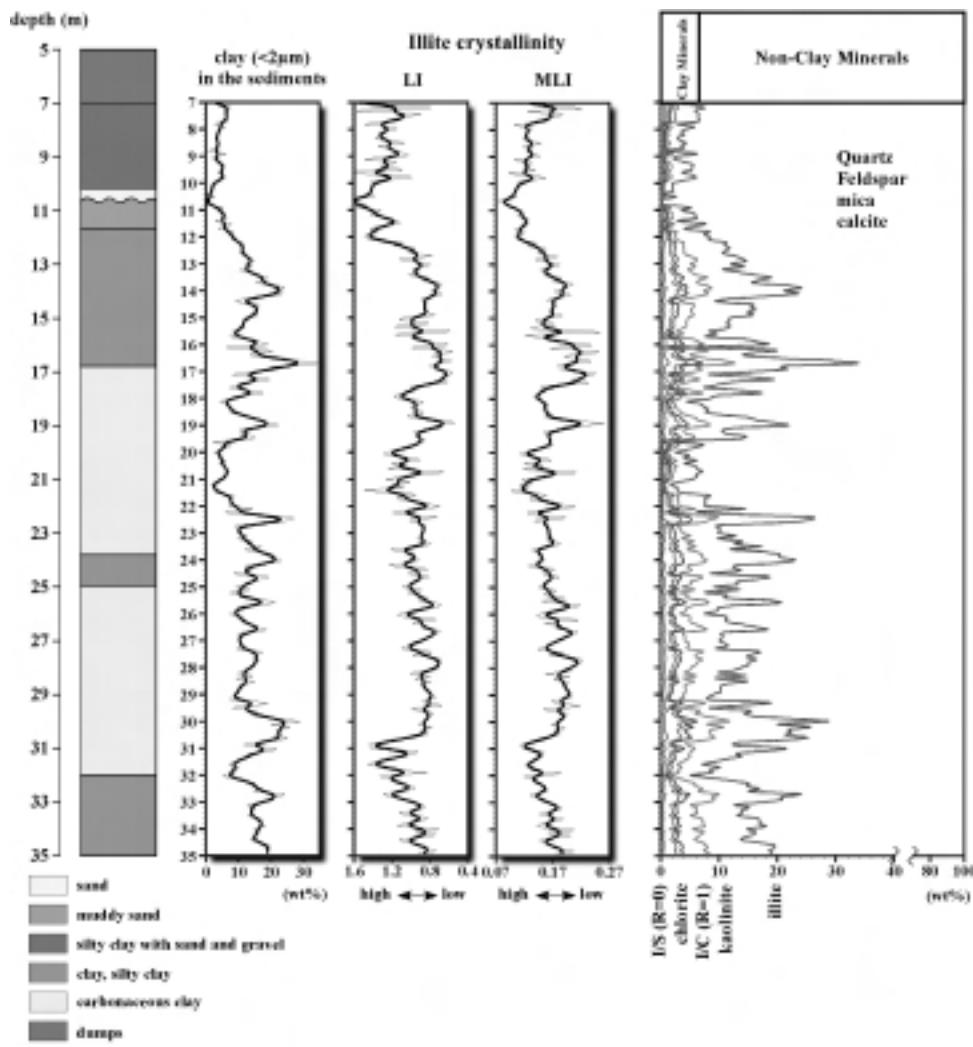
FIGURE 1. Variation curves of clay amount in the sediments, Lanson index (LI), modified Lanson index (MLI), and amount of each clay mineral in the sediments from 7 m to 35 m depth of RB-core

in the Kathmandu Basin during the last 40 kyr were closely related to global climate.

The sedimentation rate of the upper part (~40 m in depth) of the RB core tends to vary, depending on the dry-wet condition in the Kathmandu basin. Under dry climate expected from the results of clay mineral analysis, the sedimentation rate is estimated to be 300~800 mm/kyr, while that under wet climate runs to ~4700 mm/kyr, at least five times faster than that under dry climate. It is, therefore, clear that the supply of sediments into Paleo-Kathmandu Lake was strongly controlled by precipitation at least during the last 40 kyr, just like strong seasonal variation in water and suspended sediment discharge of the combined Ganges-Brahmaputra-Meghna River system under present Indian monsoon climate (Islam et al. 2002).

References

Islam MR, SF Begum, Y Yamaguchi and K Ogawa. 2002. Distribution of suspended sediment in the coastal sea off the Ganges-Brahmaputra River mouth: observation from TM data. *J Marine Systems* **32**: 307-321

Kuwahara Y, R Fujii, H Sakai, and Y Masudome. 2001. Measurment of crystallinity and relative amount of clay minerals in the Kathmandu Basin sediments by decomposition of XRD patterns (profile fitting). *J Nepal Geological Society (Sp. Issue)* **25**: 71-80

Lanson B. 1997. Decomposition of experimental X-ray diffraction patterns (profile fitting): A convenient way to study clay minerals. *Clays and Clay Minerals* **45**: 132-146

Sakai H. 2001. The Kathmandu Basin: an archive of Himalayan uplift and past monsoon climate. *J Nepal Geological Society (Sp.Issue)* **25**: 1-8

Sakai H, R Fujii, Y Kuwahara, BN Upreti, and SD Shrestha. 2001. Core drilling of the basin-fill sediments in the Kathmandu Valley for palaeoclimatic study: preliminary results. *J Nepal Geological Society (Sp. Issue)* **25**: 9-18

e-Os dating of the porphyry copper deposits in southern Gangdese metallogenic belt, Tibet

Shengrong Li†*, Wenjun Qu‡, Wanming Yuan§, Jun Deng†, Zhengqian Hou¶ and Andao Du‡

† Key Laboratory of Lithospheric Tectonics and Lithoprobing Technology, China University of Geosciences, Ministry of Education, China, Beijing, 100083, CHINA
‡China National Research Center of Geoanalysis, Beijing 100037, CHINA
§Institute of Mineral Resources, Chinese Academy of Geological Sciences, Beijing 100037, CHINA
¶ Institute of High Energy Physics, Chinese Academy of Sciences, Beijing 100080, CHINA

* To whom correspondence should be addressed. E-mail: lisr@cugb.edu.cn

The southern Gangdese block of Tibet is well characterized by its widely distributed magmatic rocks, especially granitic rocks. Many geologists have made lots of surveys and published a number of papers about the tectonics and geological history of the block. However, significance of granitoid-related copper mineralization was not recognized until recently. The porphyry copper deposits were discovered in the central portion of the southern Gangdese block. The representative deposits include the Chongjiang, Tinggong and Dabu porphyry copper deposits in the region between Rikazi and Lhasa. The ore minerals of the copper deposits are spatially related two kinds of granitoid rocks, including porphyritic granodiorite and granodioritic porphyry. The porphyritic granodiorite occurs as a batholith, with the granodioritic porphyry intruded as dikes. The porphyritic granodiorite is much similar to the regional granitoid rocks both in texture and in composition, which is known as the product of plate collision period (60-30 Ma). The granodioritic porphyry is much later with an isotopic age of 17.1 Ma (Geological Survey of Tibet, unpublished), and recognized as the product of deducting and rifting of Gangdese block. Which one of the two kinds of granitoid rocks is metallogenically related to the copper mineralization has been argued among the researchers for a long time. Due to the large difference between the granitoid rocks ages, dating the copper mineralization would be helpful for determination of the source rock, and for further regional porphyry copper targeting. Re-Os dating of molybdenite has been recognized to be a reliable tool (Suzuki 1993), and widely used in age studies of various ore deposits (McCandless and Ruiz 1993; Santosh 1994). Re-Os dating was also used in investigation of the Ni-Mo-Pt bearing black rock series (Li 2003). In this study, the Re-Os isotopes of ore mineral molybdenite is analysed to determine the source rock for the copper mineralization in southern Gangdese block.

Molybdenite occurs mainly as disseminations and occasionally as lumps in the mineralized in both porphyritic granodiorite and granodioritic porphyry. A total of 9 molybdenite samples were collected from the Chongjiang, Tinggong and Dabu porphyry copper deposits. Re-Os dating measurements were conducted at the China National Research Center of Geoanalysis, by Wenjun Qu and Gang Yang in 2002. To separate Re and Os, aqua regia was used to digest the samples in a Carius tube, then Re was extracted with acetone, and Os was purified by distilling. The measurements were made with the VG PQ EXCELL ICP-MS mass spectrometer. The blank chemistry procedure was employed with assumptions of 0.02 ng common Re and 0.003 ng common Os. Detailed method description was given by Du (2001).

The results of the measurements are shown in **Table 1.** The numbers in brackets are the 2σ level uncertainties, where for Re and Os isotopes, it includes the demarcating errors of diluent, ICP-MS measurement errors and calibration errors of mass fractional distillation as well as the weighing errors of diluent and samples. The errors for model ages include not only the errors mentioned above, but also the 1.02% overall uncertainty. The model ages (t) are calculated with the following formula:

TABLE 1. Concentrations of Re and Os isotopes and model ages of molybdenites from southern Gangdese porphyry copper deposits

Sample No.	Mine	Sample Weight(g)	Re(μg/g)	^{187}Re(μg/g)	^{187}Os(ng/g)	Model Age(Ma)
CJ-18	Chongjiang	0.00806	223.0(2.3)	140.2(1.4)	32.41(0.24)	13.88(0.21)
TG-a	Tinggong	0.00821	266.5(3.0)	167.5(1.9)	41.74(0.36)	14.96(0.25)
TG-b	Tinggong	0.00835	252.6(2.4)	158.8(1.5)	40.01(0.35)	15.13(0.24)
DB-a	Dabu	0.00707	466.6(5.2)	293.3(3.3)	69.10(0.52)	14.14(0.23)
DB-b	Dabu	0.00505	422.4(4.3)	265.5(2.7)	63.80(0.47)	14.42(0.23)
DB-c	Dabu	0.00450	424.7(4.4)	267.0(2.7)	63.45(0.49)	14.27(0.23)
DB-d	Dabu	0.00478	430.9(4.5)	270.8(2.8)	64.25(0.51)	14.24(0.23)
DB-e	Dabu	0.00957	252.6(2.5)	158.8(1.5)	37.60(0.32)	14.21(0.23)
DB-f	Dabu	0.00673	361.3(3.7)	227.1(2.3)	54.02(0.41)	14.28(0.23)
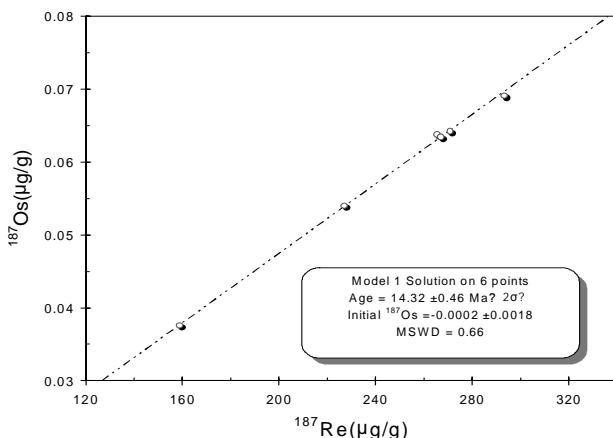
FIGURE 1. ^{187}Re-^{187}Os Isochron for the molybdenite from Dabu porphyry copper deposit

FIGURE 2. ^{187}Re-^{187}Os Isochron for molybdenite from Chongjiang, Tinggong and Dabu porphyry copper deposits

$$ t = \frac{1}{\lambda} \left[\ln \left(1 + \frac{^{187}Os}{^{187}Re} \right) \right] $$

where, λ (^{187}Re decay constant) = 1.666×10^{-11} yr^{-1}.

The Re-Os dating results demonstrate that the molybdenites of the three porphyry copper deposits have almost the same model age of 14Ma. The ^{187}Re-^{187}Os isochron diagrams of molybdenites from Dabu and all the three deposits, plotted with ISOPLOT software, indicate that their isochron ages are 14.32±0.46 Ma for Dabu porphyry copper deposit (**Figure 1**), 1.5% and 1.0% are taken as the relative errors for ^{187}Re and ^{187}Os, respectively) and 14.0±1.0Ma for all the Chongjiang, Tinggong and Dabu porphyry copper deposits (**Figure 2**, 2.5% and 1.5% are taken as the relative errors for ^{187}Re and ^{187}Os, respectively). The points plotted from Chongjiang and Tinggong data are roughly on the isochron line defined by the 6 points plotted from Dabu data.

The Re-Os isotope data clearly indicate that tectonically porphyry copper mineralization in the central region of south Gangdese block occurred in the rifting-deduction environment after the closure of the Yarlung Zangbo Tethys and the consequent orogeny. The porphyry copper mineralization was genetically related to the small-scaled post-collision granitoid rocks. In the Chongjiang, Tinggong and Dabu porphyry deposits, the copper mineralization is genetically related to the granodiorite porphyry dykes.

References

Suzuki K, Lu Q, Shimizu H, Masuda A. 1993. Reliable Re-Os age for molybdenite. *Geochimica et Cosmochimica Acta* **57**(7): 1625-1628

McCandless TE, Ruiz J. 1993. Rhenium-osmium evidence for regional mineralization in southwestern North America. *Science* **261**(5126): 1282-1286

Santosh M, Suzuki K, Masuda A. 1994. Re-Os dating of molybdenites from southern India; implication for Pan-African metallogeny. *Journal of the Geological Society of India* **43**(5): 585-590

Li SR, Xiao QY, Shen JF, Sun L, Liu B, Yan BK and Jiang YH. 2003. Rhenium-osmium isotope constraints on the age and source of the platinum mineralization in the Lower Cambrian black rock series of Hunan-Guizhou Provinces,China. *Science in China (Series D)* **46**(9): 919-927

Du AD, Wang SX, Sun DZ, Zhao DM, Liu DY. 2001. Precise Re-Os dating of molybdenite using Carius tube, NTIMS and ICPMS. In: Mineral deposits at the beginning of the 21st century. Proceedings of the Biennial SGA Meeting. 6; P 405-407. Society for Geology Applied to Mineral Deposits (SGA), International.

The basaltic volcanic rocks in the Tuyon Basin, NW China: Petrogenesis and tectonic implications

Tao Liang*, Zhaohua Luo, Shan Ke, Li Li, Wentao Li and Huaming Zhan

School of Earth and Mineral Resources, China University of Geoscience, Beijing, 100083, CHINA

* To whom correspondence should be addressed. E-mail: tao_liang0212@hotmail.com

The Tuyon basin is located near the crossing of the Tien Shan orogenic belt, the Western Kunlun fold system and the Tarim-Alashan blocks. The crossing of two lithospheric scale fault, the Talas-Ferghana dextral strike-slip fault and the NE extended South Tien Shan strike-slip fault, is just at the southern margin of the Tuyon basin. Therefore, many geoscientists all over the world have been attracted to petrogenesis of the Cenozoic basaltic volcanic rocks in the Tuyon basin and their tectonic implications. According to previous researches, the basalts emplaced within the Tuyon basin are of two units, the lower basalts and the upper basalts, aged 120~110 Ma and 70.4~36.6 Ma respectively. All these basalts are classified as alkali series, enriched in potassium, and considered as a result of a small plume probably rooted at a shallow level in the asthenosphere.

Our new works on the igneous rocks in the Tuyon basin suggest that the so-called lower basalts are preserved as a series of cone dikes, which are emplaced in Jurassic-Lower Cretaceous sedimentary rocks; the upper basalts are formed as a series of volcanic eruptions, including calderas, ring dikes, necks and volcanic cones. For example, there are three volcanic cones in the line between the Kuvt cone and Bilebluk cone. We have discovered basaltic intrusive units in Jurassic sandstone and conglomerate strata. The basaltic extrusive units have the same occurrence with the early Cretaceous sediments, but uncomfortably overlain by the Paleogene sedimentary rocks. Therefore, the Tuyon basin is a compound volcanic basin, including series of volcanic eruptions with lavas and subvolcanic rocks, rather than it has two-layer structure consisted of two igneous units. Our investigations indicate that the basaltic rocks are mainly of dark gray, massive structure and porphyritic texture. The basaltic extrusive rocks are developed as columnar joint structure, vesicular structure and amygdaloidal structure. Most of volcanic rocks within Tuyon basin contain phenocrysts such as olivine, clinopyroxene and plagioclase, and occasionally phlogopite, amphibole and apatite. Olivine belongs to chrysolite circled by fine-grained aggregate of magnetite and talc. Most of olivine phenocrysts have been altered into iddingsite and talc. The clinopyroxene mainly belongs to augite, which characterize hourglass structure and zoned texture. The plagioclase phenocrysts have more content of anorthite. They are mainly andesine and occasional labradorite, but rare in zoned texture. The matrix minerals are clinopyroxene, plagioclase, magnetite and volcanic glass, and mainly formed tholeiitic texture, occasionally intergranular texture and vitrophyric. Therefore, the Cenozoic volcanic rocks in the Tuyon basin show characteristics of alkali series, and suggest that the region may was at extensional condition.

In the Arhesaiordy volcanic-sedimentary sequences there are five basaltic sills intruded into the Jurassic sedimentary deposits. Many megacrysts have been found in the lowest basaltic layer, such as augite, phlogopite, amphibole and anorthoclasite. From the same layer we have collected lots of the deep-seated xenoliths including peridotite, granulite, pyroxenite, gneiss and so on. In the other four layers, the number of megacrysts and deep-seated xenoliths has been decreased quickly. There are also lots of deep-seated xenoliths in the Tasgeler caldera. Therefore, basaltic magma has the characteristics of rapid ascent. Consequently, the basaltic volcanic rocks in the Tuyon basin are formed direct from primary magma, which is rare affected by fractional crystallization.

As mentioned above, basaltic volcanic rocks in the Tuyon basin are not likely to be the products of two tectonic stages, and the previous K-Ar and ^{40}Ar/^{39}Ar geochronology reports seem questionable. For the tectonic condition, the thrusts and nappe structures in the north margin of the Tarim basin indicate that the local lithosphere is in compressional condition. Therefore, it is difficult to explain the petrogenesis by mechanism of a small mantle plume or rifting. At the same time, the paleomagnetic evidences indicate that the Tuyon massif and Tarim block have united during Triassic and they drifted northward together, but Tuyon massif has rotated clockwise about 10° relative to Tarim block during the Late Cretaceous. Therefore, we suggest that basaltic magma process should response to the rotation tectonic event and all of the rocks may represent a single igneous event. The block rotation is partial tectonic activity and induced by huge strike-slip faults during the process of the continental collision between India and Asia. The evidence is that the mantle-derived igneous rocks are limited to the vicinity of the crossings of the huge strike-slip faults.

Introduction to recent advances in regional geological mapping (1:250, 000) and new results from southern Qinghai-Tibet Plateau

Wang Liquan*, Zhu Dicheng and Pan Guitang

Chengdu Institute of Geology and Mineral Resources, Chengdu, 610082, CHINA

* To whom correspondence should be addressed. E-mail: cdwliquan@cgs.gov.cn

A large volume of new geological data has been obtained in the process of new round of geological surveys (at a scale of 1:250, 000) and other geoscientific studies in southern Qinghai-Tibet Plateau (Wang et al. 2004). The new results and achievements provide stable bases that are beneficial for understanding the principles governing the geological processes and verifying them in the Qinghai-Tibet Plateau. Significant data on the spatio-temporal distribution of the regional primary junction belts (suture zones) and faults also serve as the base for basic geological information required to establish a workable geotectonic framework for Qinghai-Tibet Plateau.

The discovery of high-pressure granulites and lots of data on isotope chronology of Precambrian metamorphic rocks offer new insights to discuss the formation mechanism and exhumation process of the metamorphic basement in the southern Tibet. Findings of new strata and confirmation of already known strata containing abundant fossils provide new evidences to establish a regional stratigraphic system that will be used for geological classification and comparison. Likewise, discovery of some magmatic rock types and isotope-based age data on them enable to reconstruct the process of evolution and also propose a spatio- temporal framework for the magmatic rocks. Newly discovered unconformities and sedimentary facies or the verification of existing ones together with the associated geological information are fundamental for the analysis of sedimentary basin and for the paleogeographic reconstruction of tectonic lithofacies. The results and progresses in Quaternary geological mapping at regional scale and also in studying the neotectonic movements will be useful for deciphering the history of uplift of Plateau, the changes in the paleoenvironments and also the development of lakes in the geological past. Additional progress in finding the relics of ancient human activity, deciphering zoological environments and also studying the geology of regions of touristic importance has been made. These will be definitely valuable for research on zoological environment and ancient human civilization of Qinghai-Tibet Plateau and also for regional economic development. Besides these discoveries, new information on mineralization gained through the regional geological surveys will serve as guidelines for undertaking necessary action to explore and develop the mineral resources and also for appraisal of important metallogenic regions and belts in Qinghai-Tibet Plateau.

Reference

Wang L, Z Di-cheng and P Gui-tang. 2004. Primary Results and Progress of Regional Geological Survey (1:250, 000): the South of Qinghai-Tibet Plateau. *Geological Bulletin of China*, 23(6), in press (in Chinese with English abstract)

Geochemical and SHRIMP U-Pb zircon chronological constraints on the Magam-mixing event in eastern Kunlun orogenic belt, China

Chengdong Liu‡* , Xuanxue Mo†, Zhaohua Luo†, Xuehui Yu†, Shuwei Li† and Xin Zhao†

†China University of Geosciences, Beijing, 100083, CHINA
‡East China Institute of Technology, Fuzhou city, Jiangxi province, 344000, CHINA

* To whom correspondence should be addressed. E-mail: chdliu@ecit.edu.cn /edliu@ecgi.jx.cn

A spectacular east-west extending granitoid belt in the Eastern Kunlun Orogeny, China is about 800 km long by 40~80 km wide and composed of many complex plutons, which contain abundant mafic microgranular enclaves (MME). The late Paleozoic- early Mesozoic granites are prevelent in the granitoid belt. As one of the typical plutons, Yugelu pluton with an area of about 100 km² situated at about 30 km southeast from Xiangride town of Qinghai province.

The pluton constitutes a magma series that ranges from hornblende-gabbro, diorite, granodiorite to monzogranite, and minor syenogranite etc.with dominance of granodiorite. MME are widely distributed in granodiorite and are only a few in others. The abundance of MME in the granites of Yuegelu pluton in the most felsic body is less than 0.5%, whereas in the most mafic one is up to 10%. Most MME are well-defined and have a sharp contact with diffused boundary. The enclave sizes range from less than 1 cm to more than 2 m in diameter, a few even up to 5 m, but most of them are in the range of 10 to 50 cm. The various shapes of MME, such as spheroidal, ellipsoidal, banded, wedge-shaped and irregular ones are commonly observed and show the streamlined shape with the features of rheology. These features provide a convincing evidence that they result from magma mingling (Chengdong Liu et al. 2002).

All MME show igneous texture, and are commonly porphyritic , with plagioclase, hornblende and biotite occurring both as phenocrysts and in the groundmass. Flow structures are occasionally developed with hornblendes underling linear flow structure. Structure of this type may result from plastic flowage under high-temperature conditions (Didier et al. 1991). Moreover, quenched rims, acicular apatites, irregular overgrowth of plagioclase, mantled quartz ocelli have frequently been seen within them. All of these evidences imply that MME are formed by magma mingling process (Vernon 1983).

The mineral assemblage of MME is plagioclase, hornblende, quartz, and subordinate biotite and K-feldspar. Accessory phases include zircon, titanite, apatite, magnetite, ilmenite and hematite. Plagioclases range widely from An8 to An87, but most from An35 to An55. Analyses of amphiboles by EPMA reveal that the enclaves have mainly magnesia-hornblende compositions, with ratio of Mg/(Mg +Fe) between 0.48 and 0.50, similar to those found in their host rocks.

Major, REE and trace elements were investigated in the Central Laboratory of Hubei Geological Bureau using conventional chemical analysis techniques, ICP and atomic absorption spectrometry respectively. Major element abundances in MME indicate that they are mostly intermediate in terms of SiO_2 content from 52.13% to 62.4%. Together with their host rocks, they belong to calc-alkaline, weakly peraluminous series, reflecting a subduction environment. Abundances of many elements of rocks show good linear variation on Harker diagrams, which indicate magama mixing origin (Chappell 1996).

ΣREE of MME are from 111.87 to 197.03 ppm, and those of their host rocks range more widely from 66.68 to 226.85 ppm. Moreover, ΣREE abundances of MME are slightly higher than their host rocks. Chondrite-normalized REE patterns for MME are generally similar to those of the host granites. Both have a LREE enrichment ($(La/Yb)_N$=1.04-34.80) and a slight negative Eu-anomaly.

The trace elements in both MME and their host granites are characterized by a slightly high abundance of Rb, Th, Zr, Y and low Ba, Nb, Sr, Ti. This feature reflects that MME and their host granites are in one hybrid series.

Isotope data of Sm, Nd, Rb and Sr were determined by VG-354 in Solid Isotope Laboratory of Institute of Geology and Geophysics Chinese Academy of Sciences. Isotopic data from MME have initial $^{87}Sr/^{86}Sr$ from 0.70859 to 0.70956, and those of their host granites are from 0.70144 to 0.70972; and εNd in MME from –4.5 to –9.2, and in host rocks from -5 to -6.2.These data are roughly similar.

Single-grain zircon U-Pb dating for MME, host granodiorite, and related hornblende-gabbro have been conducted in Beijing SHRIMP Center by using SHRIMP II and yielded 241±5Ma, 242±6Ma and 239±6Ma of ages, respectively. The results indicate that the three types of rocks were formed almost in the same event.

All these data imply that the granites have the origin of magma mixing. The mixing/mingling event between the crust- and mantle-derived magmas prevailed in the early-middle Triassic epoch in Eastern Kunlun orogeny. And the granitoid host rock and hornblende-gabbro may approximately represent the acid and basic end-members of the mixing with the ratio of about 70% and 30% estimated by SiO_2, respectively. MME are the incompletely mixed clots of the basic magma injected into the acid magma. Consequently, the injection and reaction of mantle mass and energy into/with the crust play an important role in the origin of granites and the vertical growth of the crust.

References

Chengdong Liu et al. 2002.Characteristics and origin of mafic microgranular enclaves in Yuegelu granitic pluton in Eastern Kunlun. Geol Bull China. 739-744

Didier J and B Barbarin. 1991. Enclaves and Granite Petrology. Elsevier. Amsterdam. 625p

Vernon RH 1983. Restite, xenoliths and microgranitoid enclaves in granites. J Proc R Soc N S W 77– 103

Chappell BW. 1996. Magma mixing and the production of compositional variation within granite suites: evidence from the granites of southeastern Australia. J Petrol. p 449– 470

Compston W et al. 1992. Zircon U-P ages of early Cabbrian time-scale. J Geol Soc 171-184

Geology of the eastern Himalayan syntaxis

Yan Liu†*, Zsolt Berner‡, Hans-Joachim Massonne§ and Xuchang Xiao†

†Institute of Geology, Chinese Academy of Geological Sciences, Beijing, 100037, CHINA
‡Institut für Mineralogie und Geochemie, Universität Karlsruhe, Kaiserstraße 12, D-76128 Karlsruhe, GERMANY
§Institut für Mineralogie und Kristallchemie, Universität Stuttgart, Azenbergstr. 18, D-70174 Stuttgart, GERMANY

* To whom correspondence should be addressed. E-mail: yanliu0315@yahoo.com.cn

Before the middle of the nineties, the eastern Himalayan syntaxis was one of the least-known segments of the Himalayas. According to studies several years ago, the eastern Himalayan syntaxis consists of three tectonic units: Gangdise, Yarlung Zangbo, and Himalayan units (Liu and Zhong 1997, Burg et al. 1998). The Gangdise unit consisting of granitoids, migmatites and amphibolite-facies rocks, commonly covered by Palaeozoic and Mesozoic sediments, is separated from the Himalayan unit by the Yarlung Zangbo unit, a mylonitic zone with lenses of metabasites and serpentinites. The basic-ultrabasic lenses of the Yarlung Zangbo unit suggest that the boundary between the Gangdise and the Himalayan units is an eastern extension of the Indus - Yarlung Zangbo suture, which was folded around the eastern Himalayan syntaxis. Recent detailed field mapping has revealed that the Himalayan unit is made up of North Col greenschist to amphibolite facies complex, Greater Himalayan Crystallines, upper Lesser Himalayan Crystallines and lower Lesser Himalayan Crystallines from north to south (**Figure 1**). The dominant mineral assemblage of the North Col complex is plagioclase+quartz+biotite+chlorite+epidote±muscovite, but at the bottom of the complex staurolite+kyanite+K-feldspar+muscovite+quartz+epidote±garnet occur. The latter assemblage is different to that at the bottom of the North Col formation of the central Himalayas. A ductile normal fault referred as STD1 here separates the North Col complex from the Greater Himalayan crystallines below. Strongly deformed granites occur between the STD1 and the top of the Greater Himalayan Crystallines. The Greater Himalayan Crystallines are marked here by the assemblages garnet+prismatic sillimanite+K-feldspar+antiperthite or plagioclase. Spinel+albite+biotite or spinel+cordierite±orthopyroxene form retrograde coronas around sillimanite and garnet. The prismatic sillimanite had been argued to replace early kyanite at elevated temperature, indicating that the Greater Himalayan Crystallines experienced high-pressure metamorphism (Liu and Zhong 1997). The Greater Himalayan Crystallines were thrust over the upper Lesser Himalayan Crystallines consisting generally of amphibolitic gneisses, sillimanite gneisses, granitic gneisses and marble by a ductile thrust system which is referred to as the MCT1. Further south, another ductile thrust system, named as the MCT2, separates the upper Lesser Himalayan Crystallines from the lower Lesser Himalayan Crystallines consisting generally of quartzite, calcschist, limestone, metapsammite and muscovite phyllite (**Figure 1**).

A distinctive feature of the Greater Himalayan Crystallines is the occurrence of numerous dykes of various compositions and different ages along the foliation of granulite facies gneisses. Three rock types can be distinguished. One type is related to carbonate dykes with fine-grained dark 'chilled' margins from several millimeters to centimeters in thickness and extensive metasomatic and/or contact alteration halos. Large dolomitic dykes commonly contain irregular-shaped xenoliths of granulitic gneiss, which seem to have been separated from source rocks nearby. Spatial relationships of carbonate-rich dykes were observed in the field. These field characteristics resemble those of typically igneous dykes and of mantle-derived carbonatites documented in numerous publications (e.g., Le Bas 1981, Tuttle and Gittins 1966). These are also considered as clear indication for an igneous origin of such carbonate dykes. A second rock type is characterized by MgO-rich ultramafic rocks, which occur as small dyke-like bodies in the granulitic terrain or as ball-shaped inclusions in diorite dykes. The third group of rocks is related to biotite-bearing diorites.

Geochemically, the carbonate-rich dykes differ significantly from mantle-derived carbonatites. The dykes are poor in REEs, Ba, Sr, U, Th, Nb, F and P and their $^{87}Sr/^{86}Sr$, $^{143}Nd/^{144}Nd$, $\delta^{18}O$ (relative to V-SMOW) and $\delta^{13}C$ (relative to V-PDB) values range from 0.709 to 0.712, 0.5117 to 0.5121, +8‰ to +24.4‰, and +0.80 ‰ to +3.55‰, respectively. These values are similar to those of many sedimentary carbonates. We suggest that the carbonate dykes were formed by remobilized melts that originated as partial melts from sedimentary carbonates at crustal levels. Structural analyses have shown that the hot Greater Himalayan Crystallines were extruded from beneath southern Tibet via ductile channel flow to overlie the limestone/marble-bearing Lesser Himalayan Crystallines. Remobilization of limestones below the Greater Himalayan Crystallines was probably triggered by stacking of the hot Greater Himalayan Crystallines including interaction of fluids enriched in H_2O and poor in CO_2 probably from the lower crust or even the Earth's mantle. In turn, remobilized carbonate melts could contribute to the exhumation of the Greater Himalayan Crystallines. According to K-Ar and Ar-Ar data obtained on amphibole and mica from the carbonate dykes, this event started during the late Neogene.

References

Burg JP, P Nievergelt, F Oberli, D Seward, P Davy, , JC Maurin, Z Diao and M Meier. 1998. The Namche-Barwa syntaxis: evidence for exhumation related to compressional crustal folding. *J Asian Earth Sciences* **16**: 239-252

Liu Y and D Zhong. 1997. Petrology of high-pressure granulite from the eastern Himalayan syntaxis. *J Met Geol* **15**: 451-466

LeBas M J. 1981. Carbonatite magmas. *Min Mag* **44**: 133-140

Tuttle O F and J Gittins. 1966. *Carbonatites*, New York, Wiley, 591 p
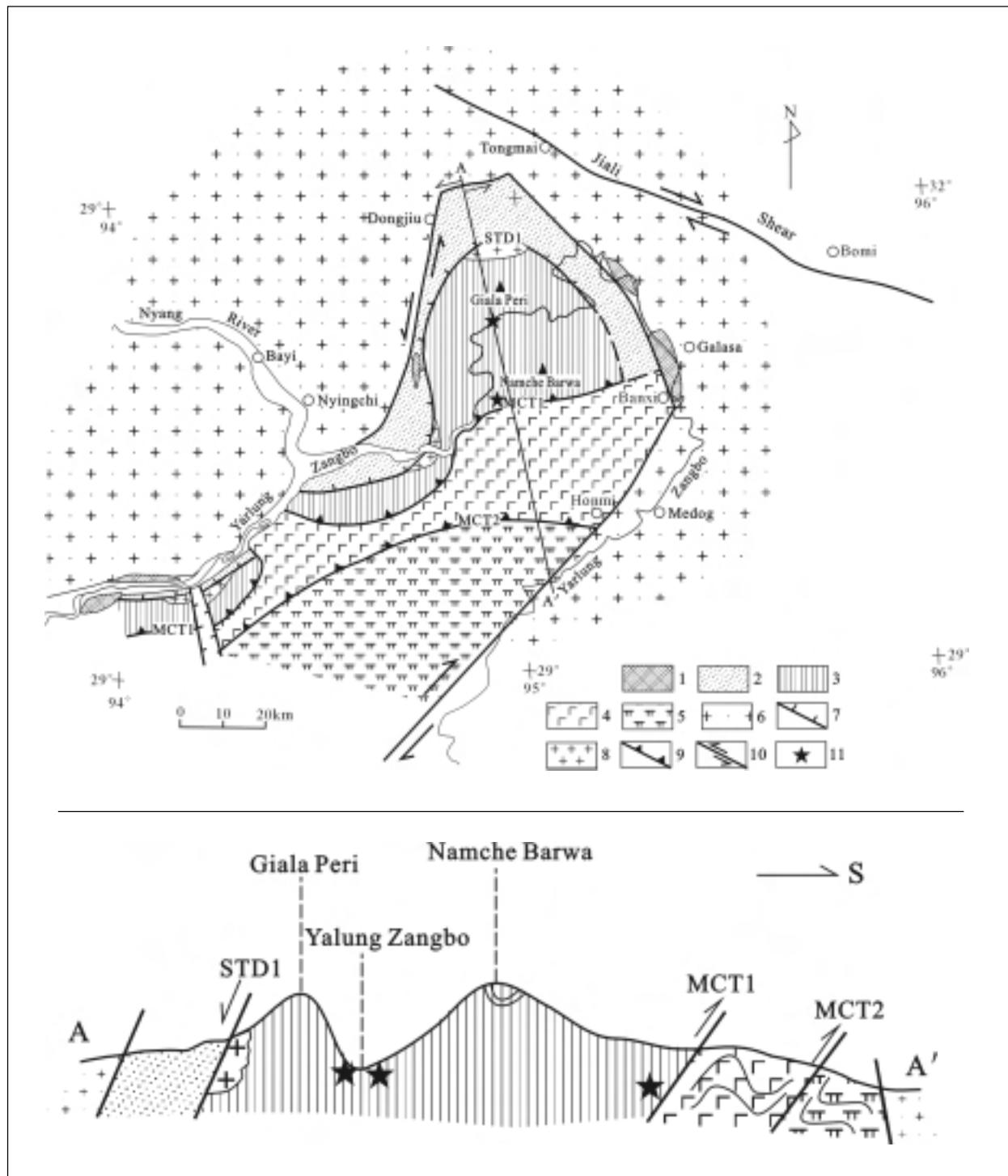
FIGURE 1. Top: Geological sketch map of the eastern Himalayan syntaxis (Liu and Zhong 1997, Burg et al. 1998 and our own observations). Bottom: Geological section. 1, Yarlung Zangbo unit. 2, North Col greenschist to amphibolite facies complex. 3, Greater Himalayan Crystallines. 4, Upper Lesser Himalayan Crystallines. 5, Lower Lesser Himalayan Crystallines. 6, Gangdise unit. 7, Normal fault. 8, Strongly deformed granites. 9, Thrusts. 10, Strike-slip fault. 11, Dyke swarm.

Geochronology and the initiation of Altyn Fault, western China

Yongjiang Liu†§*, Franz Neubauer‡, Johann Genser‡, Xiaohong Ge†, Akira Takasu§ and Sihua Yuan†

†College of Earth Sciences, Jilin University, Jianshe Str. 2199, Changchun 130061, Jilin, CHINA
‡Institute of Geology and Paleontology, Salzburg University, Salzburg, A-5020, AUSTRIA
§Department of Geoscience, Faculty of Science and Engineering, Shimane University, Matsue 690, JAPAN

* To whom correspondence should be addressed. E-mail: yjliu@mail.edu.cn

The samples of Proterozoic and Early Paleozoic metasediments, Caledonian mylonitized granite and Jurassic metasedimentary rocks were collected in Aksay-Dangjin Pass and Geshi fault-valley. Biotite, muscovite, hornblende and K-feldspar were dated by $^{40}Ar/$ ^{39}Ar method in the Isotopic Dating Laboratory-ARGONAUT with a laser fusion $^{40}Ar/^{39}Ar$ dating system in the Institute of Geology and Paleontology, Salzburg University, Austria. Several age groups were obtained. Biotites of the Early-Middle Jurassic samples from Geshi fault-valley yield an isochron age of 92±2.7 Ma. In Aksay-Dangjin Pass profile, samples away from the middle shear zone of the Altyn fault belt yield two plateau age groups in the range of 461-445.2 Ma and 414.9-342.8 Ma. But the samples of deformed granitic gneiss from northern belt give two plateau age groups of 178.4-137.5 Ma and 89.2±1.6 Ma, while the sample from middle shear zone of Altyn fault belt yields two plateau ages of 36.4 Ma and 26.3 Ma.

The age groups of 461-445.2 Ma and 414.9-342.8 Ma represent the tectono-thermal events that had been recorded in the rocks that were displaced by Altyn strike-slip fault in late Ordovician-Early Silurian and Devonian respectively. These two age groups should be related to the closures of Northern and Southern Qilian Oceans, not to the activities of Altyn fault. The ages of 178.4-137.5 Ma are interpreted as the active ages of Altyn fault in the Middle-Late Jurassic-Early Cretaceous, and should be related to the accretion of Lhasa Block to the north. The age groups of 92±2.7-89.2±1.6 Ma and 26.3-36.4 Ma suggest the strike-slip movements with strong metamorphism of greenschist facies along the Altyn fault in the Late Jurassic and Late Eocene. These tectonic thermal events occurred in most areas of northern Tibet Plateau and should be the response of the collision between Indian and Eurasian continents along the north margin. The study shows that the Altyn fault is characterized by multiple pulse-style activities under the tectonic setting of convergence between Indian and Eurasian continents.

Recently there are several suggestions or ideas about the initiation of the Altyn strike-slip fault. By $^{40}Ar/^{39}Ar$ dating method the oldest age, which we have obtained from the syntectonic-growing minerals in the Altyn fault belt, is 178.4 Ma. This suggests that the initiation of the strike-slip movement along the Altyn fault is about Middle Jurassic. Li et al. (2001) reported a zircon age of 223-226 Ma by SHRIMP method from the deformed rocks within the Altyn fault belt, which is interpreted as the initiation age of the strike-slip movement along the Altyn fault. Yue et al. (2001) argued that the initiation age of the strike-slip movement is Oligocene according to the offset of the Altyn fault, which is estimated by the distance of Oligocene sediments in Xorkol basin and Subei basin.

There are many reports of the estimated offset along the Altyn strike-slip fault belt by using different markers of different ages. **Table 1** lists some representative reports in recent years. These results show that the maximum offset is about 350-400 km. The results are consistent although the offsets were estimated by different markers of Proterozoic and Early-Middle Jurassic. This suggests that the strike-slip movement should start from Middle Jurassic or a little later. If it started before Middle Jurassic, the offset estimated from the Proterozoic marker should be more than the maximum offset (350-400 km).

Based on the investigation of the Cenozoic sediments in Xorkol basin in the north of Altyn Mountains, Yue et al. (2001) described that the pebbles in the Oligocene sediments are similar to that in the Subei basin in Northern Qilian, and do not contain high-grade metamorphic rocks and granites on the SE side of Xorkol basin. Therefore, they deduced that high grade metamorphic pebbles in Shanggancaigou and Xiayoushasan Formations should come from the Northern Qilian Mountains. They concluded that the Xorkol basin should be connected with Subei basin during Oligocene, and the offset of Altyn strike-slip fault is 380 ± 60 km with the initiation in Oligocene. In fact, according to our field investigations, there are many outcrops of granites and high grade metamorphic rocks of Dakendaban

TABLE 1. List of reported offsets of the Altyn strike-slip fault

| Reference | Offset and age of displaced marker | | | |
	Proterozoic	Early-Middle Jurassic	Middle Jurassic	Middle-Late Cenozoic
Ge et al., 1999	350-400 km			
Cui et al., 1997	350-400 km			
Che et al., 1998	350-400 km			
Zhang et al., 2001a	350-400 km			
Sobel et al., 2001		350 +/- 100 km		
Ritts et al., 2000			400 +/- 60 km	
Zhang et al., 2001b				80-100 km

Group to the SE of Xorkol basin from Dangjinshan to Datongshan. We argue that the pebbles in the Oligocene sediments in Xorkol basin might not be eroded from the Northern Qilian Mountains but from Dangjinshan-Datongshan, which might be originally derived from the Northern Qilian, but dragged or/and displaced by Altyn strike-slip fault from the Northern Qilian to Dangjinshan-Datongshan before they were eroded. Furthermore, the pebbles could be transported for quite a long distance from source to the destinated basin, and also eroded and deposited while the source rocks are displaced. Therefore, it is not reliable to use pebbly sediments as a marker to estimate offset of the Altyn strike-slip fault. Zhang et al. (2001b) reported that the offset of the Altyn fault is 80-100 km after Late Tertiary based on the studies of the displaced Late Tertiary sediments in Xorkol basin. The report of Zhang et al. (2001b) does not support the model of Yue et al. (2001).

The evidences of offsets estimated by different markers of different ages and the ages of isotopic dating suggest a Middle Jurassic (178.4 Ma) initiation of the Altyn strike-slip fault.

References

Ritts BD and U Biffi. 2000. Magnitude of post-Middle Jurassic (bajocian) displacement on the Altyn Tagh fault, NW China. *Geol Soc Amer Bull* **112**: 61-74

Sobel ER, N Arnaud, M Jolivet, BD Ritts and M Brunel. 2001. Jurassic to Cenozoic exhumation history of the Altyn Tagh range, NW China constrained by 40Ar/39Ar and apatite fission track thermochronology. *Geol Soc Amer Bull* **194**:

Yue Y, BD Ritts and SA Graham. 2001. Initiation and long-term slip history of the Altyn Tagh fault.Int *Geol Rev* **43(12)**:1087-1093

Zhang J., Z Zhang, Z Xu, et al. 2001a. Petrology and geochronology of eclogites from the western segment of the Altyn Tagh, northwestern China. *Lithos* **56**: 187-206

Zhang Y, Z Chen and N Yang. 2001b. New geological evidence for late cenozoic left-lateral displacement along the Altyn Tagh fault. *Geoscience* **15(1)**: 8-12

Oligo-Miocene evolution of the Tuotuohe Basin (headwaters of the Yangtze River) and its significance for the uplift history of the central Tibetan Plateau

Zhifei Liu† *, Chengshan Wang‡§ , Xixi Zhao¶, Wei Jin‡, Haisheng Yi‡, Yong Li‡ and Yalin Li‡

† Laboratory of Marine Geology, Tongji University, Shanghai 200092, CHINA
‡ State Key Laboratory of Oil and Gas Reservoir Geology and Exploitation, Chengdu University of Technology, Chengdu 610059, CHINA
§ China Univesity of Geosciences, Beijing 100083, CHINA
¶ Institute of Tectonics and Earth Sciences Department, University of California, Santa Cruz, CA 95064, USA

* To whom correspondence should be addressed. E-mail: lzhifei@online.sh.cn, Fax: +86-21 6598 8808

The central part of the Tibetan Plateau between the Kunlun and Tanggula ranges provides unique Eocene-Oligocene sediments in the Fenghuoshan Basin of northern part of the Hoh Xil Basin to recognize the early uplift history of Tibet (Liu et al. 2001, 2003; Wang et al. 2002). The Fenghuoshan Mountain region to the south of Jinsha River Suture Zone was recommended as Eocene Tibet and northern part to the Jinsha Suture Zone as Oligo-Miocene Tibet (Tapponnier et al. 2001). However, previous studies have failed to discover any continuous Oligocene to Miocene sequence that precludes our understanding of early evolution history of the central Tibetan Plateau, because a regional discordance developed between the overlying Early Miocene grey limestone of the the Wudaoliang Group and the underlying Eocene-Oligocene grey-violet sandstone, mudstone, and conglomerate complex of the Fenghuoshan and Yaxicuo groups (Liu and Wang 2001; Wang et al. 2002). Our recent fieldwork during summers of 2002 and 2003 in the Tuotuohe Basin as the southern part of the Hoh Xil Basin, about 120 km northward of Tanggula Pass, however, discovered a well-outcropped Oligo-Miocene section.

The Tongtianhe section (N33º55'45", E92º37'13") in the southeastern part of the Tuotuohe Basin, situated in the modern headwaters region of the Yangtze River, consists of the underlying fan-delta-fluvial Fenghuoshan Group sandstone and conglomerate, the middle part of fluvial-lacustrine Yaxicuo Group sandstone and mudstone (~2192 m thick), and the overlying lacustrine Wudaoliang Group limestone (~200 m thick). The Fenghuoshan and Yaxicuo groups were paleomagnetically dated in the Fenghuoshan Basin as Eocene-Early Oligocene (51-30 Ma) with an age of 31.3 Ma for the boundary of the two groups (Liu et al. 2003). In this Tuotuohe Basin, because of poor-outcropped Fenghuoshan Group, our measurements started from the boundary of the Fenghuoshan and Yaxicuo groups upwards to finish at the top of the Wudaoliang Group for a total thickness of 2392 m. 380 individually-oriented paleomagnetic samples, spaced at 125m stratigraphic intervals, were collected from the Tongtianhe section. Progressive thermal and alternating field demagnetization experiments were conducted by a 2G cryogenic magnetometer at the Paleomagnetic Laboratory of the University of California, Santa Cruz (UCSC). On the basis of distinct magnetic reversal zones with a reference of Cande and Kent (1995) and biostratigraphic data, this section is paleomagnetically dated as 31.3-21.8 Ma (Early Oligocene-Early Miocene), i.e. the Yaxicuo

Group as 31.3-23.8 Ma and the Wudaoliang Group as 23.8-21.8 Ma. This result fits very well the boundary age of 31.3 Ma for the Fenghuoshan and Yaxicuo groupswhich was earlier recognized in the Fenghuoshan Basin (Liu et al. 2003).

Our comprehensive basin analysis along with the new paleomagnetic data from the Tongtianhe section suggests that the basin could have been formed as a foreland basin and undergoing an (Eocene?)-Oligocene accelerated subsidence mainly with fan-delta-fluvial to fluvial-lacustrine environments. During the Oligocene, provenance analysis and predominant paleocurrents with northeasterly directions from the Yaxicuo Group suggest the uplift process of the Tanggula Mountain orogenas a major source area of the Yaxicuo Group clastics. The average sediment accumulation rate is 29.2 cm/ka for the Yaxicuo Group. However, during Early Miocene, a relative stable lacustrine environment with a low accumulation rate of about 10 cm/ka developed in the Tuotuohe Basin indicating a peneplanation process accompanying an interior water system in central Tibet. Thus, geomorphic conditions strongly suggest the Yangtze River was not established in central Tibet until after the Wudaoliang Group formation, i.e. 21.8 Ma. This work is advancing our understanding of the Oligo-Miocene tectonic-sedimentary events recorded in the central Tibetan Plateau, which have a direct relationship to the early uplift of Tibet and to the evolution of the Yangtze River water system.

References

Cande SC and DV Kent. 1995. Revised calibration of the geomagnetic polarity time-scale for the Late Cretaceous and Cenozoic. J Geophys Res 100: 6093-6095

Liu Z and C Wang. 2001. Facies analysis and depositional systems of Cenozoic sediments in the Hoh Xil basin, northern Tibet. Sedim Geol 140 (3-4): 251-270

Liu Z, C Wang and H Yi. 2001. Evolution and mass-balance in the Cenozoic Hoh Xil basin, northern Tibet. J Sedim Res 71 (6): 971-984

Liu Z, X Zhao, C Wang, S Liu and H Yi. 2003. Magnetostratigraphy of Tertiary sediments from the Hoh Xil Basin: implications for the Cenozoic tectonic history of the Tibetan plateau. Geophys J Inter 154: 233-252

Tapponnier P, Z Xu, F Roger, B Meyer, N Arnaud, G Wittlinger and J Yang, 2001. Oblique stepwise rise and growth of the Tibet Plateau. Science 294: 1671-1677.

Wang C, Z Liu, H Yi, S Liu and X Zhao. 2002. Tertiary crustal shortening and peneplanation in the Hoh Xil region: implications for the tectonic history of the northern Tibetan plateau. J Asian Earth Sci 20 (3): 211-223

Paleovegetation and paleoclimate in the Kathmandu Valley and Lake Baikal during the Late Quaternary

Takeshi Maki† *, Rie Fujii‡, Hajime Umeda§, Harutaka Sakai†, Yoshitaka Hase§ and Koji Shichi¶

† Department of Earth Sciences, Kyushu University, JAPAN
‡ Faculty of Science, Okayama University of Science, Okayama, JAPAN
§ Department of Earth Sciences, Faculty of Science, Kumamoto University, JAPAN
¶ Tohoku Research Center of Forestry and Forest Products Research Institute, Morioka, JAPAN

* To whom correspondence should be addressed. E-mail: cs302048@scs.kyushu-u.ac.jp

The Lake Baikal sediment is one of the best archives which records the Late Quaternary paleoclimatic changes at high-latitude inland of Asian continent. On the other hand, basin-fill sediment of the Kathmandu Valley is ideal for studying the history of Indian monsoon activities. We tried to reconstruct paleovegetation and paleoclimate changes in both regions during Late Quaternary based on palynological studies.

Samples and pollen record of Lake Baikal

We carried out pollen analysis on the BDP99 core, which is 300 m long and taken from Posolskaya Bank in Lake Baikal by the Baikal Drilling Project. The upper part of the core consists of diatomaceous silty clay, and lower part is mainly silty clay (Williams et al. 2001). We took samples at 40 cm interval from 0 to 120 m depth. The pollen assemblage is characterized by dominance of *Pinus*, *Artemisia* and Gramineae. The percentage of forest-tree taxa, such as *Pinus*, *Alnus* and *Betula* shows high value during a period when the total amount of pollen grains are large. The percentages of grassland taxa such as *Artemisia*, Chenopodiaceae shows high value during a period when the total amount of pollen grains are small.

The amount of pollen grains are noticeably large between 14-21 m, 34-42 m, 50.5-52 m, and below 61 m. These intervals are interpreted to indicate dense vegetation during warm periods, and they are correlated to marine oxygen isotope stages (MIS) 5, MIS 7, MIS 9 and MIS 11, respectively.

Samples and pollen record of Kathumandu Valley

A continuous 218-m-long core (RB core) was obtained in the western part of the Kathumandu Valley by Paleo-Kathmandu Lake Project in 2000. The RB core is lithologically divided into three parts: basal sand and gravel dominant beds of 38 m, 170 m-thick muddy lacustrine beds and overlying fluvial sandy beds. We took samples at 1 m interval from 218 to 30 m, and at 10 cm interval from 30 to 0 m in depth. Based on the paleomagnetic study, the RB core covers in age from ca. 750 to 10 kyr.

The pollen assemblage of the RB core is characterized by dominance of *Quercus* and *Pinus*. *Picea* and *Castanopsis* occasionally increase during short periods. *Alnus* and Gramineae show cyclic repetition of increase and decrease.

We recognized nine cycles of warm – wet and cold – dry period during ca. 750 kyr, based on the following changes of relative abundance of five genera: *Quercus*, *Castanopsis* as warm climate, *Pinus* as cold climate, *Alnus* as wet climate, and Gramineae as dry climate. The fluctuation of percentage of total arboreal pollen indicates cyclic climatic changes, which correspond to MIS 5-19.

On the basis of two climatic records in Lake Baikal and Kathmandu Valley, we discuss regional differences of vegetational responses to glacial/interglacial climate changes in representative areas in Asia. Furthermore, we refer to environmental changes during the mid- Pleistocene transition.

Organic geochemical study of continuous lacustrine sediments obtained from Kathmandu Valley, central Himalaya: interpretation of paleoenvironmental changes in the late Quaternary using bulk organic matter analyses

Mami Mampuku†*, Toshiro Yamanaka†, Harutaka Sakai†, Rie Fujii‡, Takeshi Maki†, Masao Uchida§, Hideo Sakai¶, Wataru Yahagi¶ and Hiroaki Tsutsumi#

†Department of Earth Sciences, Kyushu University, 4-2-1, Ropponmatsu, Fukuoka 810-8560, JAPAN
‡Faculty of Science, Okayama University of Science, Ridai-cho, Okayama 700-0005, JAPAN
§Japan Agency for Marine-Earth science and Technology, 2-15, Natsushima, Yokosuka 237-0061, JAPAN
¶ Department of Earth Sciences, Toyama University, 3190, Gohuku, Toyama 930-8555, JAPAN
# Faculty of Environmental and Symbiotic Sciences, Kumamoto Prefectural University, Kumamoto 862-8502, JAPAN

* To whom correspondence should be addressed. E-mail: cs202052@scs.kyushu-u.ac.jp

The climate of East and South Asia is under strong control of monsoonal climatic system. The Asian monsoon climate has been developed with the uplift of the Himalaya-Tibet orogen since the collision of Indian subcontinent with Asian continent. The timing of initiation of the monsoon and related important tectonic events have been reported, but a problem how monsoon has changed in the past, particularly in glacial-interglacial period in Quaternary, is still uncertain. It is important to clarify changes of paleomonsoon climate on land, and it would contribute to understand present monsoon climate and to estimate future monsoon climate.

The Kathmandu Valley is an intermontane basin, located on the southern slope of the central Himalaya under direct influence of Indian monsoon. The valley is filled with thick lacustrine and fluvial sediments of the late Pliocene to Quaternary. Therefore, it is expected that these sediments record a long-term paleoenvironmental changes in this region. Fujii and Sakai (2002) reported that seven cycles of warm-and-wet and cold-and-dry climate were recognized since 0.9 Ma, which reflect global glacial-interglacial cycles. However, in that study there were several problems: the samples were not continuous and ages were not directly determined. Therefore, we carried out core drilling for academic purpose in the Kathmandu Valley, and could have obtained 218 m-long drill-core. In this study, we analyzed sediment core (RB core) obtained at Rabibhawan in the western central part of the Kathmandu Valley. The RB core is composed mainly of continuous muddy lacustrine sediments. The sediments are rich in organic matter, and yield many fragments of plants and animals.

Organic components preserved in lacustrine sediments were originated in terrestrial plants and aquatic organism. Variety and productivity of the organisms are controlled by environmental factors such as temperature and precipitation. Therefore, it is important to study organic matter in lacustrine sediments, in order to reconstruct paleoenvironmental changes.

In this study, we carried out analyses of total organic carbon (TOC), total nitrogen (TN) and isotopic composition of bulk organic matter ($\delta^{13}C$) in the Paleo-Kathmandu Lake sediments and reconstructed paleoenvironment in the Kathmandu Valley during the late Quaternary. This is the first organic geochemical report of paleoenvironmental and paleoclimatic study in this region.

The sediment samples were analyzed at 1 m intervals from 10 m to 180 m below the surface. At depth of 83-89 m, samples were absent due to sand bed.

Vertical profiles of the TOC concentrations, TOC/TN ratios (C/N ratios) and $\delta^{13}C$ values in sediment are shown in **Figure 1**. The TOC concentrations range from 2 to 7 % and C/N ratios change between 7 and 20. The $\delta^{13}C$ values of total organic carbon change between -29 to -20 ‰ with the averaged value of -24 ‰, and change periodically. The TOC concentration and C/N ratio also change periodically and their oscillations correlate well. The $\delta^{13}C$ values were inversely correlated with the TOC concentrations and C/N ratios.

Based on the cyclic changes of $\delta^{13}C$ values, the muddy section of the core was divided into fourteen zones. In the zones, showing high $\delta^{13}C$ and low TOC and C/N ratio, it is inferred that the proportion of C4 plants of total organic matter was increased, while the proportion of the terrigenous organic matter to the total organic matter was decrease. The paleoenvironment of these zones indicates that C4 plants are predominant in land, and grasses proliferated in this area. In the other zones with the low $\delta^{13}C$, it is infered that the terrigenous organic matter was increased and the contribution of C4 plants was not significant. Accordingly, the paleoenvironment of the low $\delta^{13}C$ zones reveal that C4 plant was expelled, and arboreal plants were vigorous.
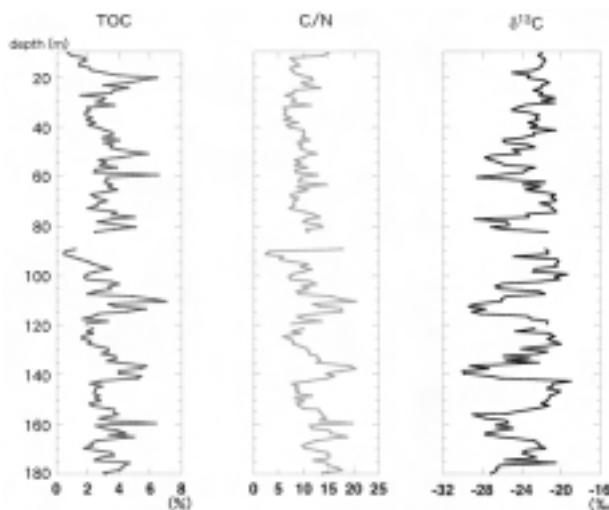
FIGURE 1. TOC concentrations, C/N weight ratios and $\delta^{13}C$ values in RB core from Kathmandu Valley, Nepal

The previous studies using Kathmandu basin sediments proposed that a dry and wet climate prevailed during the glacials and interglacials in Kathmandu area, respectively. In addition, it is commonly known that C4 plant an advantage over C3 plant in the arid climate except in the high latitude area. From these facts, it is concluded that the high $\delta^{13}C$ zones corresponded with cold and arid climate; therefore, the cyclic changes of the $\delta^{13}C$, TOC and C/N ratio reflect the paleoclimate changes, i.e., repetition of cold-arid and warm-humid climate. ^{14}C dating and paleomagnetic studies suggest that the age of the core was about 0.68 Ma-12Ka.

The present zonation with the estimated time-scale was compared to the SPECMAP stack. As a result, it is found that the cyclic changes in the paleoclimate in Kathmandu area are in good agreement with the global climate changes represented by the ice volume changes during the late Quaternary. Therefore, we conclude that paleoclimatic changes during at least 0.7 Ma in Kathmandu area were influenced mainly by the glacial-interglacial cycles and Paleo-Kathmandu Lake sediments have a high potential to provide a high-quality and high-resolution record of the Quaternary monsoonal climatic changes in the continental interior of South Asia.

References

Fujii R and H Sakai. 2002. Paleoclimatic changes during the last 2.5 myr recorded in the Kathmandu Basin, Central Nepal Himalayas. *Journal of Asian Earth Science* **20**: 255-266

Assessment of risk and vulnerability of water induced disaster: A case study of Tinau Watershed, western Nepal

Indra N Manandhar†* and Keshav P Poudel‡

† Central Department of Geography, Tribhuvan University, Kirtipur, Kathmandu, NEPAL
‡ Central Department of Education Geography, Tribhuvan University, Kirtipur, Kathmandu, NEPAL

* To whom correspondence should be addressed. E-mail: cdg@wlink.com.np, eyeyen@wlink.com.np

The Himalayas as a whole is tectonically very active and geomorphologically very unstable. It is highly vulnerable to water induced disasters like soil erosion, landslides, floods, glacial lake outburst flood etc due to its high relief, steep slopes, active geology, and intense monsoon rainfall. Moreover, rapid growth of population and consequent changes in land use and land cover, development of infrastructures and man-induced changes in runoff are also responsible for increased events of landslide and flood hazards. The loss of life and properties from these hazards has been increasing. The livelihood options of the people have been threatening. There is urgent need to develop and implement disaster management activities in order to reduce the loss of life and properties and sustain development activities in this area. An assessment of hazard, risk and vulnerability and its mapping could provide basis for the development of effective disaster management activities. It is in this context, an attempt was made to identify different types of water induced disasters and map and assess its risk and vulnerability. Tinau watershed was selected for this study. Tinau watershed with the total area of 234 sq km lies in Palpa district in western Nepal. The elevation ranges from 330 m at the confluence of Tinau river and Jhumsa khola (stream) to 1893 m at Ghustung Lekh.

Both the secondary and primary information have been used. Aerial photographs taken in 1996 were interpreted with field verification in order to identify the areas prone to different types of water induced disasters. Local people were consulted and interviewed to gather information for risk and vulnerability assessment. The field-work was carried out in September 2003. A total of eleven parameters like lithological units, lineaments, slope gradient, slope shape, slope aspects, relative relief, drainage density, water table and drainage condition, land use, vegetation cover, and distance from the road were used for landslide and flood hazard mapping. These information were derived from available analog maps such as toposheets, land system, land utilization, land capability prepared in the past with modification after field verification. GIS tool was used to analyse above mentioned parameters and prepare hazard, risk and vulnerability maps. Hazard areas were categorized into three groups according to the probability of occurrence of hazards such as high, moderate and low.

The landslide hazard map shows that about 17.6 % land lie in the high hazard zone and 36.7 % area in the moderate hazard zone In terms of flood hazard zone 11.5% of the land falls under the high and moderately high hazard zone and 4.7 % of land falls under the moderate hazard zone. As reported by focus group discussion out of 6716 households in the watershed, 2327 households are exposed to hazards of different types. Mostly affected people form river bank cutting, channel shifting and flood in this area are poor landless tenant families. The damage of road due to landslide is common. During the past three years the total value of Highway repair after the damage by landslide was Rs. 714,400.

Attempt was also made to evaluate disaster mitigation and management activities carried out in the watershed. The strategies adopted by household to minimize the risk of landslide, flood and other geomorphic hazards include evacuation from hazard area to other area, construction of small structure to control rive bank cutting and landslide, retaining wall, and tree plantation. The strategies adopted by other GOs and NGOs are mostly post disaster measures and relief distribution. The failure of past relief and post disaster management activities shows the lack of participation of local people in the entire processes. There is a lack of local level institutions/organizations responsible for disaster preparedness. Efforts should be made to create awareness among the local people, involve them in the entire processes of disaster preparedness. The response and recovery capacity of local people at present to cope with landslide and flood disasters which are common in the watershed is very low due to mass poverty, illiteracy, low level of off-farm activities and poor service facilities such as health. In this context, it is necessary to improve response and recovery capacity of local people through provision of education, training, off-farm employment opportunities and infrastructural services. Emphasis should also be given to develop construction standards for building and other infrastructures and regular monitoring and maintenance of already constructed infrastructures.

Early warning system has not yet been developed. Keeping in view the lead-time of flooding between highland and lowland areas, it is essential to develop a mechanism of community-based warning system. The magnitude of landslide, debris flow, and flood events can be reduced if strong conservation measures are implemented.

This study shows that the GIS and remote sensing tools can fruitfully be used for landslide and flood hazard and risk assessment. The risks indicated by the combination of vulnerability maps (based on population, economic value of the property, and infrastructure) with hazard maps could be useful in prioritizing areas for the implementation of disaster preparedness plans and mitigation measures.

Re-interpretation of progressive metamorphism, facies series, P-T-t path and exhumation model for the collisional orogenic belts

Shigenori Maruyama

Department of Earth and Planetary Sciences, Tokyo Institute of Technology, Tokyo 152-8551, JAPAN

For correspondence. E-mail: smaruyam@geo.titech.ac.jp

Recent discovery of ultra-high pressure (UHP) mineralogy, and descriptions of geology, petrology, geochronology and geochemistry of the Phanerozoic collisional orogens have changed the basic concepts of metamorphic facies series, P-T-time path, progressive metamorphism, Barrovian-type metamorphism and tectonic model.

The Himalayan orogen has served as a world standard for the collisional orogenic belt for a long time, characterized by Barrovian-type metamorphism (intermediate-P type metamorphism within the stability field of plagioclase), tectonic overlapping of double-continental crust, and thermal relaxation with buoyant unroofing (England and Thompson 1984). Recent discovery of coesite-bearing eclogite in the western Himalaya and eclogites from the central to eastern Himalaya can not be explained by the previous models. In the followings, summarizing the new constraints on orogenic process, I try to explain the collision orogeny including Himalaya.

(1) Major structure as a sandwiched subhorizontal tectonic slice: a thin tectonic slice with P-T maximum at structural intermediate. The UHP-HP unit is a few km thick slice cut on the top and bottom by normal and reverse faults, respectively. It is separated from the underlying and overlying low-grade or low-P metamorphic rocks.

(2) The underlying unit is thermally metamorphosed to form andalusite-sillimanite metamorphic rocks in some cases by the hot tectonic intrusion of UHP-HP rocks.

(3) Metamorphic facies series ranges from greenschist/blueschist transition or blueschist, through epidote-amphibolite, quartz- and zoisite-eclogite, to dry eclogite facies with a sharp kink point, indicating anti-clockwise P-T path in the case of the highest-P and –T belt.

(4) The P-T-time path calculated by inclusion mineralogy in garnet combined with zoned garnet compositional profile shows the same P-T path with the metamorphic facies series.

(5) Extensive hydration at mid-crustal level obliterated the pre-existing UHP-HP mineralogy, except mineral inclusions in garnet, zircon and omphacite.

(6) Zoned zircons with UHP-HP minerals mantled by late-stage hydration with Barrovian minerals are dated as ca. 30 m.y. older from that of hydration stage at rim, indicating a slow tectonic exhumation.

(7) The mountain-building stage is not related to the exhumation of UHP-HP rocks to the mid-crustal level. The mountain-building, in the case of Himalaya, started at 9 Ma, ca. 16 m.y. after the Barrovian hydration at mid-crustal level.

(8) Combining above constraints, a tectonic extrusion model is the most probable process (Maruyama 1990, Maruyama et al. 1994, Maruyama et al. 1996). (9) Previous interpretation (e.g., England and Thompson 1984) of progressive metamorphism, facies series, P-T-t path are all quite different from those summarized here.

Most of present mineralogy exhibits the late-stage crustal metamorphism due to extensive hydration underneath. The role of water must be re-evaluated to mask the progressive nature of metamorphism during subduction.

References

England PC and AG Thompson. 1984. Pressure-Temperature-time path of regional metamorphism. *I. Jour. Petrology* **25**: 894-928

Maruyama S. 1990. Denudation process of high-pressure metamorphic belt. Abst. 97th Ann. Meeting Geol. Soc. Japan. 484p

Maruyama S, JG Liou and RY Zhang. 1994. Tectonic evolution of the ultrahigh-pressure (UHP) and high-pressure (HP) metamorphic belts from central China. *The Island Arc* **3**: 112-121

Maruyama S, JG Liou and M Terabayashi. 1996. Blueschists and eclogites of the world and their exhumation. *Intern Geol Rev* **38**: 485-594

Latest Jurassic-earliest Cretaceous radiolarian fauna from the Xialu Chert in the Yarlung Zangbo Suture Zone, Southern Tibet: Comparison with coeval western Pacific radiolarian faunas and paleoceanographic implications

Atsushi Matsuoka† *, Qun Yang‡ and Masahiko Takei§

† Department of Geology, Faculty of Science, Niigata University, Niigata 950-2181, JAPAN
‡ Nanjing Institute of Geology and Palaeontology, Academia Sinica, Nanjing 210008, CHINA
§ Graduate School, Niigata University, Niigata 950-2181, JAPAN

* To whom correspondence should be addressed. E-mail: matsuoka@geo.sc.niigata-u.ac.jp

Triassic, Jurassic and Cretaceous radiolarian faunas have been reported recently from pelagic sediments in the Yarlung Zangbo Suture Zone, southern Tibet (Matsuoka et al. 2001, 2002; Wang et al. 2002, Ziabrev et al. 2004). These micropaleontological data can contribute not only to geotectonic history but also to paleoceanographic reconstruction. The Xialu Chert is distributed in the south of Xigatze along the southern margin of the Yarlung Zangbo Suture Zone and represents deep marine sediments between the Indian Block and Lhasa Block. This paper presents a full assemblage of a latest Jurassic (Tithonian)-earliest Cretaceous (Berriasian) fauna of the *Pseudodictyomitra carpatica* (KR 1) Zone (Matsuoka 1995a) in the Xialu Chert and compares it with coeval radiolarian faunas in the western Pacific regions. This paper discusses the depositional site of the Xialu Chert from a paleobiogeographic point of view.

KR 1 radiolarian fauna in the Xialu Chert (Xialu fauna) is composed of about 100 species. Abundant species include *Cinguloturris cylindra* Kemkin and Rudenko, *Emiluvia chica* Foreman, *Eucyrtidiellum pyramis* (Aita), *Loopus nuda* (Schaaf), *Pseudodictyomitra carpatica* (Lozyniak), *Sethocapsa*(?) *subcrassitestata* Aita, *Sethocapsa*(?) *ritteni* (Tan), *Stichocapsa praepulchella* Hori, *Svinitzium pseudopuga* Dumitrica, *Tethysetta dhimenaensis* (Baumgartner), *Tethysetta usotanensis* (Tumanda), and *Tethysetta boesii* (Parona). Dominant genera include *Archaeodictyomitra*, *Hemicryptocapsa*, *Xitus*, and *Zhamoidellum*. The genera *Mirifusus*, *Podobursa*, *Podocapsa*, *Ristola*, and *Syringocapsa* are rare. The *Vallupus* group is absent and *Pantanellium* is not common.

Northern hemisphere Middle-latitude coeval radiolarian faunas are found in the Torinosu Group and its equivalent formations in Southwest Japan. Common species between the Xialu and Torinosu faunas are *Eucyrtidiellum pyramis* (Aita), *Protunuma japonicus* Matsuoka and Yao, *Sethocapsa*(?) *subcrassitestata* Aita, and *Solenotryma*(?) *ichikawai* Matsuoka and Yao. They were originally described as new species from the Torinosu Group. Other common species include *Cinguloturris cylindra* Kemkin and Rudenko, *Emiluvia chica* Foreman, *Loopus nuda* (Schaaf), *Pseudodictyomitra carpatica* (Lozyniak), *Svinitzium pseudopuga* Dumitrica, *Tethysetta boesii* (Parona), and *Tethysetta dhimenaensis* (Baumgartner).

A low-latitude earliest Cretaceous (Berriasian) fauna was reported in a rock sample from the Mariana Trench. The Mariana fauna contains about 400 species and represents the most diversified radiolarian fauna among the Berriasian radiolarian faunas in the world. Dominant genera are *Archaeodictyomitra*, *Hemicryptocapsa*, *Loopus*, *Napora*, *Neorelumbra*, *Obesacapsula*, *Podobursa*, *Praecaneta*, *Pseudodictyomitra*, *Saitoum*, *Sethocapsa*, *Svinizium*, *Tethysetta*, *Williriedellum*, *Xitus*, and *Zhamoidellum*. One of the distinctive features of the Mariana fauna is to contain abundant pantanellid taxa including the *Vallupus* group. In spite of diversified nature of the Mariana fauna, species belonging to the genus *Eucyrtidiellum*, common both in the Xialu and Torinosu faunas, have not been found so far. The genera *Cinguloturris*, *Miriusus*, *Ristola*, and *Solenotryma* are rare.

The faunal comparison among southern Tibet and western Pacific regions revealed that the Xialu fauna is similar to northern hemisphere middle-latitude assemblages represented by the Torinosu fauna. On the other hand, the Xialu fauna is less similar to low-latitude (tropical) assemblages represented by the Mariana fauna. This indicates that the Xialu fauna is regarded as a representative of southern hemisphere middle-latitude faunas. The depositional site of the Xialu Chert in the KR 1 time was outside of the *Vallupus* Territory (Matsuoka 1995b) which is a tropical radiolarian realm in the Late Jurassic-early Cretaceous time. A mirror-image provincialism to the equator in radiolarian faunas is reconstructed for the Tethys-Pacific Ocean in the latest Jurassic-earliest Cretaceous time.

References

Matsuoka A. 1995a. Late Jurassic tropical Radiolaria: *Vallupus* and its related forms. *Palaeogeography, Palaeoclimatology, Palaeoecology* **119**: 359-69

Matsuoka A. 1995b. Jurassic and Lower Cretaceous radiolarian zonation in Japan and in the western Pacific. *The Island Arc* **4**: 140-53

Matsuoka A, K Kobayashi, T Nagahashi, Q Yang, Y Wang and Q Zeng. 2001. Early Middle Jurassic (Aalenian) radiolarian fauna from the Xialu chert in the Yarlung Zangbo Suture Zone, southern Tibet. In: Metcalfe I, JMB Smith, M Morwood and IAA Davidson (eds.) *Faunal and floral migrations and evolution in SE Asia-Australasia.* Balkema, Swets & Zeitlinger Publishers. p 105-10

Matsuoka A, Q Yang, K Kobayashi, M Takei, T Nagahashi, Q Zeng. and Y Wang. 2002. Jurassic-Cretaceous radiolarian biostratigraphy and sedimentary environments of the Ceno-Tethys: records from the Xialu chert in the Yarlung Zangbo Suture Zone, southern Tibet. *Jour Asian Earth Science* **20**: 277-87

Wang Y, Q Yang, A Matsuoka, K Kobayashi, T Nagahashi and Q Zeng. 2002. Triassic radiolarians from the Yarlung Zangbo Suture Zone in the Jinlu area, Zetang County, southern Tibet. *Acta Micropalaeont Sinica* **19**: 215-27

Ziabrev SV, JC Aitchison, AV Abrajevitch, Bandengzhu, AM Davis and H Luo. 2004. Bainang Terrane, Yarlung-Tsangpo suture, southern Tibet (Xizang, China): a record of intra-Neotethyan subduction-accretion processes preserved on the roof of the world. *Journal of the Geological Society* **161**: 523-38

Trace element compositions of rocks and minerals from the Chilas Igneous Complex, Kohistan, northern Pakistan

Masumi U Mikoshiba† *, Yutaka Takahashi† , Kazuya Kubo† , Yuhei Takahashi† , Allah B Kausar‡ and Tahseenullah Khan‡

† *Institute of Geoscience, Geological Survey of Japan, AIST, 1-1-1, Higashi, Tsukuba 305-8567, JAPAN*
‡ *Geoscience Laboratory, Geological Survey of Pakistan, Chak Shahzad, P.O. Box 1461, Islamabad, PAKISTAN*

* *To whom correspondence should be addressed. E-mail: masumi-mikoshiba@aist.go.jp*

The Kohistan terrane in the western Himalayan region is considered as a Cretaceous island-arc sequence sandwiched between the Asian and Indian continental crusts. It is a 300-km-long plutonic body that extends parallel to the general trend of the Kohistan terrane. Rocks of this complex are petrographically and compositionally similar to plutonic xenoliths found in island arcs (Khan et al. 1989). We report geochemical data of rocks and minerals in the Chilas Complex and discuss the melt compositions and magmatism in middle to lower arc crust.

The Chilas Complex is well exposed along the Indus and Swat Rivers. Most of the complex consists of generally homogeneous gabbronorite, pyroxene diorite and pyroxene quartz diorite, and these are called as the Main facies rocks. Some of the rocks were re-equilibrated under granulite facies conditions at 750-850 °C and 6-8 kbar (Swat valley, Jan and Howie 1980).

Rocks with layered structure are also found in the Chilas Complex, which often occur in km-scale masses. Some of the masses are abundant in peridotites associated with layered gabbroic rocks (ultramafic-mafic association), which are deduced to be crystal accumulates. One of the bodies of the ultramafic-mafic association, Thak body just to the east of Chilas town, shows excellent outcrops. This body is included in the Main facies rocks, and consists of cyclic units of layered cumulate rocks, which is classified into olivine-dominant cumulate (dunite-wehrlite), plagioclase-dominant cumulate (troctolite-gabbronorite) and pyroxene-dominant cumulate (websterite-clinopyroxenite). Hornblende and spinel are often included in the rocks. Mg values of the pyroxenes and An content of plagioclase are high in these cumulative rocks, but systematic change of major chemical composition of the minerals are not recognized through the Thak body. In addition, one gabbronorite mass along the Indus River (Basehri body) is characterized by well-developed rhythmic layering, and most of the layers were overturned. The Basehri body is intruded by the Main facies rocks, which is considered as crystal cumulate from the magma of the Main facies.

Main facies rocks of the Chilas Complex have the characteristics of subduction-related calc-alkaline magmas with depletion of Nb relative to other incompatible elements (Khan et al. 1989). The concentrations of K_2O, Y, Zr, Th and rare earth elements (REE) in the Main facies rocks are positively correlative with SiO_2 content. In the chondrite-normalized diagram, the light REE are enriched relative to heavy REE in the rocks, and the REE patterns are slightly concave upward. The chemical variation of the most of the Main facies rocks can be explained by a weak segregation of melt and early-formed crystals composed of plagioclase, clinopyroxene and orthopyroxene.

The major element compositions of the rocks from the Thak body show the wide variation reflecting accumulation of early-stage crystals. Rocks are generally poor in REE and other incompatible elements, implying the separation of the melt and crystals are effective. Even the gabbroic rocks without olivine are still poor in REE and other incompatible elements relative to the Main facies rocks. REE concentrations of the layered rocks of the Basehri body are generally lower than those of the Main facies rocks.

For characterization of magmas of these layered rocks, trace element compositions of clinopyroxene and plagioclase are determined by ICP-MS after mineral separation. Clinopyroxene fractions from wehrlite and websterite, and whole-rock sample of clinopyroxenite in the Thak body have REE, Ba, Nb, Sr and Zr concentrations similar to each other. The clinopyroxenite and the clinopyroxene from websterite have weak negative Eu anomaly and REE concentrations slightly higher than the clinopyroxene from wehrlite. The clinopyroxene from a plagioclase-rich part of the layered gabbronorite of the Basehri body shows the REE concentrations 3-5 times higher than clinopyroxenes from the Thak body, with clear negative Eu anomaly. Plagioclase fractions from a troctolite in the Thak body and from the plagioclase-rich rock of the Basehri body have REE concentrations with positive Eu anomalies, and they have similar Sr concentrations although the plagioclase from the troctolite are poor in most of the incompatible elements.

The melts calculated from the clinopyroxenes of the pyroxene- and olivine-dominant cumulates in the Thak body are enriched in light REE relative to heavy REE, showing chemical characteristics closer to calc-alkaline or high-alumina basalt magmas in island arcs rather than depleted island-arc tholeiites. The calculated melts have REE, Sr and Zr concentrations similar to the Main facies rocks. The melts calculated from the plagioclase fractions have Sr, Ba and Rb concentrations similar to the Main facies rocks. These data suggest a possibility that the original magmas of the cumulates of the Thak body and the magma of the Main facies were derived from common or similar source materials, in spite of large petrographic variations. Trace element abundances in clinopyroxene and plagioclase from the Basehri body may have been affected by subsolidus equilibration, and also affected by a small amount of trapped melt.

References

Jan MQ and RA Howie. 1980. Ortho- and clinopyroxene from pyroxene granulites of Swat, Kohistan, northern Pakistan. *Mineral Mag* **43**: 715-728

Khan MA, MQ Jan, BF Windley, J Tarney and MF Thirlwall. 1989. The Chilas Mafic-Ultramafic Igneous Complex; The root of the Kohistan Island Arc in the Himalaya of northern Pakistan. *Geol Soc Amer Spec Paper* **232**: 75-94

Garnet response diamond pressure metamorphism from Tso-Morari region, Ladakh, India

Barun K Mukherjee* and Himanshu K Sachan

Wadia Institute of Himalayan Geology, DehraDun-248 001, INDIA

* To whom correspondence should be addressed. E-mail: mukherjeebarun@ yahoo.co.in

....

Garnet is most promising container for the metamorphic event. The significance of garnets from metamorphic rocks as container of primary mineral inclusion and its uniqueness due to act as pressure vessels is noticed in coesite-eclogite by giving Diamond pressure or facies metamorphism (UHP) in the Tso-Morari Region. The Tso-Morari dome in eastern Ladakh stretches 500 Km^2 NW to SE. The dome is surrounded by Indus suture zone rocks to the north by Zildat detachment fault and south by low-grade sedimentary rocks. Structurally, the lowest rocks exposed in the complex are Puga Gneisses within that boudinaged eclogite have unidirectional pattern, which is parallel to the foliation of host gneisses.

The Tso-Morari eclogites hosted by peletic and paragneisses, occur as two types- massive, dark-coloured type and crystalline light-coloured type. The fresh crystalline type eclogites are coarser (>500 micron in size), having biminerallic component of garnet and clinopyroxene. The hexagonal to octahedral garnet porphyry contains inclusions of carbonates including magnesite, calcite/aragonite, dolomite, phengite, paragonite, kyanite, magnesiostaurolite, rutile and silica phases like quartz, coesite etc.

The garnet consisting essentially of almandine-pyrope-grossular solid solution were in the alm~67-42%, pyr~8-35%, gros~4-25%, whereas spessrtine component always being less than 5%, and usually less than 1%. The reversible pattern of Mg/Mn exhibits increase of Mg and decrease of Mn and Ca, from core to rim support strong prograde zonation, except the outer rim of garnet showing retrograde pattern due to exchange of Fe/Mg during cooling and exhumation. Furthermore the mantle portion is rich in pyrope and grossular, which marked and favoured the maximum pressure zone within the garnet porhyroblast.

The inclusions phase assemblages markedly noticed by quartz coesite, magnesite-quartz-talc, kyanite-paragonite-jadeite component in pyroxene, magnesiostaurolite-pyrope-kyanite, talc-staurolite-kyanite-pyrope, coesite -dolomite-diopside, coesite-magnesite-enstatite etc. within the garnet as in hetrogenity.

A peak and prograde P-T estimation by sequential geothermobarometry of UHP metamorphic rocks of TMC region documented by the presence of Mg-Qz-Tlc is stable in the range of T~ 400-600 °C and P~ 4-28 kbar, Pg-Ky-Jd is stable at 440-650 °C and P~13-22 kbar whereas Tlc-St-Ky-Py in which, the Mg-rich staurolite(Fe/Mg in tetrahedral coordination) could be high pressure phase in T>700 °C, P>25 kbar and it remains stable in the diamond facies i.e., >30 kbar ~800 °C favoured Fe/Mg in octahedral coordination side in case of staurolite. These assemblages are supposed to grow during the growth of core and inner mantle of garnet porphyry. The peak stage assemblages Co-Dol-Di, polycrystalline coesite associated with kyanite-eclogite yielded T~820 °C and 34-39kbar has been restricted in the outer mantle and inner rim portion of garnet porphyry moderately within the limit of diamond formation pressure. Nevethless there has no record of diamond crystallization even though the system under diamond facies metamorphism.

The possible stabilization for diamond requires C host mineral with cold subduction of geotherm about ~7 °C/Km at depth ~120 Km, i.e., deep subduction. Since such condition are essential transient during decompression of such long way back on surface, virtually no chance to survive through tectonic processes. One possibility for the survival of mantle pressure or diamond formation, recite enough stationary period, when the system in peak stage, as in the form of inclusion and armoring in the mechanically strong, pressure container like garnet and zircon.

Karakoram and NW Himalayan shear zones: Deciphering their micro- and macrotectonics using mineral fish

Soumyajit Mukherjee* and Arvind K Jain

Department of Earth Sciences, Indian Institute of Technology Roorkee, Roorkee 247667, Uttaranchal, INDIA

* To whom correspondence should be addressed. E-mail: msoumyajit@yahoo.com

Sheared metamorphic belts of Karakoram and northwest Himalaya such as the Karakoram Metamorphic Belt (KMB), the Tso Morari Crystallines (TMC) and the Himalayan Metamorphic Belt (HMB) reveal top-to-southwest overthrust sense of ductile shearing as the first order structures, which are produced during the main Himalayan D_2 deformation event (Jain et al. 2002). These belts reveal mica fishes and similar fish-shaped single grains and aggregates of amphibole, feldspar, staurolite, recrystallized quartz, calcite, epidote, sillimanite, apatite and garnet, and therefore a non-genetic term 'mineral fish' can be used to describe such generally asymmetric sheared objects. Mineral fish has been classified morphologically into single and composite types, both of which have been subdivided into 13 varieties (In this classification, three basic shapes of the mineral fish are considered: sigmoid, parallelogram and lenticular. These basic fish shapes can further be modified by fish mouth(s) and secondary shearing. The overall shape asymmetry of mineral fishes and its angular relationship to the C-plane is the most reliable primary shear sense indicator. On the other hand, orientation of its cleavage traces with respect to the C-plane, if any, is *not* always indicative of true sense of shearing. Stair stepping of fish tail(s) and deflected tip(s) of any fish variety, and the snake fish itself, are indicative of secondary shear sense. Mineral fish of any mineral species become the most abundant shear structures in combination with the C-planes, and keeping the above restrictions in mind, these become the most important structures in deciphering the sense of ductile shearing. Different minerals may acquire, and multiply into, the same fish shape by entirely different mechanisms. For single mineral fishes, such mechanisms are simple shear, pulling of the grain corners involving sequential change from sigmoidal- to elongated sigmoidal fish with decreasing aspect ratio R and inclination α, fracturing in any direction, boudinaging at the gaining corners, and pressure solution concomitant to shearing at the loosing corners of the evolving mineral fish. Material lost from the loosing corners of the single mineral fish by pressure solution might migrate and deposit at its gaining corners. Thus, while a pair of corners undergoes smoothening, the other observes extension and recrystallization of mineral.

Study of mineral fishes from the XZ thin-sections of the Karakoram- and northwest Himalayan shear zone rocks reveal consistent top-to-SW sense of ductile shearing within the Higher Himalayan Crystallines (HHC), and also shear sense reversal (SSR), which is characterized by relic and rare mineral fishes from the Himalayan shear zones of different tectonic belts: the Zanskar Shear Zone (ZSZ), and from the Tso-Morari Crystallines (TMC). There, the SSR is defined as 180° switch in the sense of shearing and does not include rare antithetic shearing, which is associated and at high angle to the primary shear plane. In the ZSZ and the TMC, the SSR has been observed on micro-scale in the following ways: (i) Type-4 mineral fish (one mineral fish cutting the other and pointing 180° difference in the sense of shear from the other); and (ii) two single mineral fishes, with same or different sub-varieties, pointing opposite shear sense. Such pairs of mineral fishes are either bounded by the same pair of C-planes, or of different pairs, which are sub-parallel to each other. In both the ZSZ and the TMC, the earlier C-planes were reactivated as the shear planes for the retro shear. However, the difference in SSR in these two tectonic scenarios is that while in the ZSZ, top-to-SW sense is the relic shear sense, and top-to-NE as the most dominant one, in the TMC opposite is the case. Observed SSR in the ZSZ and uniform shear sense in the HHC is in accordance with the proposed 'combined ductile shear and channel flow model' for the Higher Himalayan Shear Zone (HHSZ) exhumation by Mukherjee and Jain (2003). On the other hand, rare but clear-cut occurrence of mineral fishes giving top-to-NE shear sense from the TMC is a new observation, and interestingly, such SSR has not yet been reported from the field (e.g., Jain et al., 2003). Relic top-to-NE sense of shear within the TMC might be due to the shear induced crustal burial at about 90km, which resulted in its ultra-high pressure metamorphism.

References

Jain AK, S Singh and RM Manickavasagam. 2002. Himalayan Collisional Tectonics. *Gondwana Res Group* Mem **7**, Field Science Publishers. Hashimoto. 119p

Jain AK, S Singh, RM Manickavasagam, M Joshi and PK Verma. 2003. HIMPROBE Programme: Integrated Studies on Geology, Petrology, Geochronology and Geophysics of the Trans-Himalaya and Karakoram. *Mem Geol Soc India* **53**: 1-56

Mukherjee S and AK Jain. 2003. Exhumation Patterns within the Higher Himalayan Shear Zone (HHSZ)- a Combined Ductile shear and Channel Flow Model. *Abst Vol 2-4 April. 18th Himalaya-Karakoram-Tibet Workshop. Monte Verita, Ascona, Switzerland.* 83-86

The lower crustal Dasu Tonalite and its implications for the formation-reformation-exhumation history of the Kohistan arc crust

Takashi Nakajima† *, IS Williams‡ , H Hyodo§ , K Miyazaki† , Y Kono¶, AB Kausar#, SR Khan# and T Shirahase†

†Institute of Geoscience, Geological Survey of Japan, AIST Central-7, 1-1-1 Higashi, Tsukuba, 305-8567, JAPAN
‡Research School of Earth Sciences, Australian National University, Canberra, ACT 0200, AUSTRALIA
§Geochronological Laboratory, Okayama University of Science, Ridai-cho, Okayama 700-0005, JAPAN
¶ Graduate School of Environment and Information Sciences, Yokohama National University, Tokiwadai, Yokohama, 240-8501, JAPAN
# Geoscience Laboratory, Geological Survey of Pakistan, Shazad Town, Islamabad, PAKISTAN

* To whom correspondence should be addressed. E-mail: tngeoch.nakajima@aist.go.jp

....

Geological outline of the Kohistan block

The Kohistan block in northern Pakistan represents an exposed crustal cross section to near-MOHO depths of an ancient island arc which became sandwiched between the Eurasian and Indian continents. The Kohistan lower crust is composed of three geological units: south to north, ultramafic rocks and mafic granulites (Jijal Complex), banded amphibolite (Kamila Amphibolite) and a gabbronorite and ultramafic association (Chilas Complex). These units are geologically continuous, with no major tectonic breaks between them. The Kohistan block is tilted to the north due to uplift by subduction of the Indian continent from the south. Tonalite sheets intruding the lower crustal sequence of the Kohistan block provide key information on the dynamic history of the Kohistan arc crust.

Dasu Tonalite in the lower crustal sequence

A silicic melt pod which first appears in garnet pyroxenite of the Jijal Complex develops into granitic rock in the overlying Kamila Amphibolite. In the upper part of the Kamila Amphibolite it expands into kilometer-sized tonalite sheets, the Dasu Tonalite. The Dasu Tonalite is a weakly foliated epidote-garnet-muscovite-biotite-hornblende tonalite. It was emplaced as sheet-like bodies of various sizes layer-parallel to the structure of the host banded amphibolite, suggesting syn-tectonic intrusion. Based on geothermobarometry on the amphibolite, the tonalite is estimated to have been intrtruded at 20–30 km depth (Yoshino et al. 1998), implying that it was generated and emplaced into the lower crust of the Kohistan arc. This conclusion is consistent with the presence of magmatic epidotes in the Dasu Tonalite, an indicator of high-pressure crystallization.

Juvenile granitic magma in the lower crust

The Dasu Tonalite is extremely poor in K_2O (0.6–0.9 wt% at 65–70% SiO_2) and Rb (18–28 ppm), indicating that it contains no recycled upper crust. It is also depleted in Zr, Y, Th and Nb compared to common arc granitoids of similar SiO_2 content, such as the Cretaceous Circum-Pacific granitoids. The initial $^{87}Sr/^{86}Sr$ ratio of the tonalite is low, 0.7037–0.7038, similar to the lower crustal rocks of the Kohistan block and within the range of felsic rocks from the oceanic Izu-Bonin arc (Taylor and Nesbitt 1998). These features suggest that the Dasu Tonalite formed from juvenile granitic magma generated from mantle-derived lower crustal mafic components without interaction with the Indian craton, which presumably now tectonically underlies the Kohistan block.

Geochronology and tectonic implications

Two samples of Dasu Tonalite have given a SHRIMP zircon U-Pb age of 98 Ma. The euhedral shape of the zircon grains and absence of overgrowth or resorption textures in cathodoluminescence indicate a simple magmatic history starting at 98 Ma, with no secondary thermal event. The $^{40}Ar/^{39}Ar$ biotite age of the tonalite is 70 Ma. The 28 m.y. discrepancy between the two geochronometers is interpreted as a measure of the deep crustal residence time of the Dasu Tonalite. Tonalite magma generated and crystallized at 98 Ma probably remained at lower crustal temperatures of about 700–800°C (as indicated by geothermometry on the intercalated Kamila amphibolite) before cooling to ca. 300ÚC at 70 Ma, possibly when the Kohistan block was tilted, uplifted and exhumed due to the collision of India.

Dynamic processes in the Kohistan lower crust

The isotopic ages reported on the Kamila amphibolite and Chilas gabbro complex are remarkably scattered. Although this might be due in part to variation in the quality of the data, some of the scatter might also reflect a protracted emplacement and cooling history for these rocks. A long deep-crustal residence time could cause petrological reformation and isotopic re-equilibration after the igneous crystallization of the gabbros and conversion of those rocks to amphibolites. At least the upper half of the Kamila amphibolite consists of hydrated and recrystallized gabbro and gabbronorite equivalents of the Chilas complex (Yamamoto 1993). This interpretation is supported by the ubiquitous amphibolites in the Chilas complex. It would be reasonable to assume that the huge volume of the Chilas gabbro and gabbronorite was not produced in a single magmatic pulse, but formed by successive injections of mafic magma over a considerable period of time. This would have produced a mosaic of rocks frozen at various stages of the dynamic process from igneous crystallization to amphibolitization, which is what we now see.

References

Taylor RN and RW Nesbitt. 1998. Isotopic characteristics of subduction fluids in an intra-oceanic setting, Izu-Bonin Arc, Japan. Earth Plan Sci Lett 164: 79-98

Yamamoto H. 1993. Contrasting metamorphic P-T-time paths of the Kohistan granulites and tectonics of the western Himalayas. J Geol Soc London 150: 843-56

Yoshino T, H Yamamoto, T Okudaira and M Toriumi. 1998. Crustal thickening of the lower crust of the Kohistan arc (N. Pakistan) deduced from Al zoning in clinopyroxene and plagioclase. J Metamorph Geol 16: 729-48

Ion microprobe U-Pb ages of the Khunjerab granodiorite and some granitoids from Karakoram, Pakistan

Masatsugu Ogasawara† *, Tahseenullah Khan‡, Firdous Khan‡, Noriko Kita† and Yuichi Morishita†

† *Geological Survey of Japan/AIST, Tukuba Central 7, Tsukuba, 305-8567, JAPAN*
‡ *Geological Survey of Pakistan, Islamabad, PAKISTAN*

* *To whom correspondence should be addressed. E-mail:masa.ogasawara@aist.go.jp*

The Karakoram block was located at the southern margin of Asian continent before the Late Cretaceous amalgamation of the Kohistan block to Asia. The northward subduction of the ocean under the Asian continent was considered to form Early Cretaceous continental arc magmatism in the Karakoram block. The Karakoram Batholith is a major granitic body in the Karakoram block, extending from Baltoro to Chitral regions. However, several smaller granitic bodies are present to north of the Karakoram Batholith, which comprise the Khunjerab-Tirich Mir granite belt. Ogasawara et al. (1992) investigated several granitoids of this belt in the Khunjerab valley. They reported hornblende and biotite K-Ar ages of the granitoids. As the Karakoram block received continued tectonic activity since the Cretaceous to Cenozoic, the K-Ar ages may not provide clear timing of the primary igneous events. Some U-Pb zircon ages are available for the Karakoram Batholith, however, the U-Pb ages for the granitic rocks in the Khunjerab-Tirich Mir granite belt are limited (Hildebrand et al. 2001). It is important to have precise U-Pb zircon ages of the granitic rocks to understand timing of igneous activities and related tectonism of the region. Thus objectives of this study are (1) to provide precise timing of the igneous activity and (2) to search for the inherited core of the zircon and its age to understand source rock characteristics of the granitoids.

The Khunjerab granodiorite occurs around the Khunjerab Pass 60 km north of the Karakoram batholith, mainly along the northern side of the Khunjerab valley. Small outcrop of the granodiorite is found 10 km west of the Khunjerab Pass along the Karakoram Highway, and a sample was collected for the analysis from this outcrop. North Sost pluton is found in a 3.8 km section along the Karakoram Highway in the Khunjerab valley, 8 km north of Sost. Although outcrops of the granitoids are limited in the Khunjerab valley, the granitoids are exposed extensively to the north of the Misgar, west of the Khunjerab valley. This pluton is also evaluated in this study. However, the granitoids contain very small amount of zircon grains.

A high resolution ion microprobe (Cameca ims 1270) at the Geological Survey of Japan was used to obtain U-Pb zircon ages. Primary ion beam was about 25 micron diameter with intensity of 2 nA. Mass resolution was set at about 5000. A standard used for the U/Pb calibration is AS-3 from Duluth complex. Zircons were separated with magnetic and heavy liquids methods. Abundant zircon grains were obtained from the Khunjerab granodiorite. Typical size of the zircons from the granodiorite ranges 200 to 400 micron meters in length. Those grains show weak oscillatory zoning, however, inherited core is not common.

$^{206}Pb/^{238}U$ ages of the zircons range from 107 to 120 Ma, with mean value of 112 Ma. Further ion microprobe analysis will be perform to obtain statistically more precise age and to search inherited core of zircons from the Khunjerab granodiorite.

Ogasawara et al. (1992) obtained K-Ar hornblende and biotite ages, 107±5 Ma and 96.9±4.8 Ma, respectively. Zircons were separated from the same sample for the K-Ar dating. Treloar et al. (1989) presented two K-Ar biotite ages of 105±5 Ma and 107±5 Ma for the Khunjerab granodiorite. The biotite age of Ogasawara et al. (1992) is 10 million years younger than the ages obtained by the Treloar et al. (1989). As the sample for the dating has been collected from a small granodiorite dyke present 10 km west of the Khunjerab Pass, the granodiorite dyke may have slightly younger age than the main body of the pluton due to rapid cooling. The hornblende age of Ogasawara et al. (1992) is identical to the biotite ages presented by Treloar et al. (1989). Hornblende has a higher closure temperature of about 500 °C, and it is considerably higher than that of biotite (about 300 °C). Although no hornblende K-Ar data of the samples analyzed for biotite ages have been presented by Treloar et al. (1989), the granodiorites analyzed by Treloar et al. (1989) might have slightly older crystallization age than 107 Ma. The new zircon U-Pb ages are slightly older than the K-Ar ages. The mean U-Pb age (112 Ma) is considered as magmatic crystallization age of the granodiorite. This U-Pb age is consistent with slightly younger K-Ar ages as the hornblende and biotite K-Ar are considered to be cooling ages.

The new U-Pb age of the Khunjerab granodiorite suggests presence of continental arc magmatism along the southern margin of the Asian continent at about 110 Ma. Rb-Sr whole rock age of the Tirich Mir granite show similar age to the Khunjerab granodiorite. The Early Cretaceous continental arc magmatism took place in regional scale along the southern margin of the Asian continent.

References
Hildebrand PR, SR Noble, MP Searle, DJ Waters and RR Parrish. 2001. Old origin for an active mountain range: geology and geochronology of the eastern Hindu Kush, Pakistan. *Geol Soc Am Bull* **113**(5): 625-39
Ogasawara M, Y Watanabe, F Khan, T Khan, MSZ Khan and SA Khan. 1992. Late Cretaceous igneous activity and tectonism of the Karakoram block in the Khunjerab Valley, Northern Pakistan. In: Ahmed R and AM Sheikh (eds) *Geology in South Asia-I*. Proceedings of the First South Asia Geological Congress. p 203-7.
Treloar PJ, DC Rex, PG Guise, MP Coward, MP Searle, BF Windley, MG Peterson, MQ Jan and IW Luff. 1989. K-Ar and Ar-Ar geochronology of the Himalayan collision in NW Pakistan: constraints on the timing of suturing, deformation, metamorphism and uplift. *Tectonics* **8**: 881-909

Magnetic polarity stratigraphy of Siwalik Group sediments in Nepal: Diachronous lithostratigraphy and isochronous carbon isotope shift

Tank P Ojha† *, Robert F Butler‡ , Jay Quade‡ and Peter G DeCelles‡

† Himalayan Experience Kathmandu, NEPAL
‡ Department of Geosciences, University of Arizona, Tucson, AZ, USA

* To whom correspondence should be addressed. E-mail: luju@wlink.com.np

The middle Miocene-Pliocene Siwalik Group was deposited in the Himalayan foreland in response to uplift and erosion in the Himalayan fold-thrust belt (Zeitler1985, Hodges and Silverberg 1988, DeCelles et al 1998). Thermal demagnetization experiments demonstrate that laminated (probably paludal) siltstones yield paleomagnetic data useful for tectonic and magnetostratigraphic studies, whereas other lithologies yield data of questionable reliability (Ojha et al. 2000). Magnetostratigraphic data were acquired from 297 sites within a 4200-m thick section of Siwalik deposits at Surai Khola (27.8°N; 82.7°E). The observed sequence of polarity zones correlates with the geomagnetic polarity time scale (GPTS) from chron C5n to chron C2n. This geochronologic calibration indicates that the lower-middle Siwalik lithostratigraphic boundary at Surai Khola occurs at 7.5 Ma, using the GPTS of Cande and Kent (1995). This boundary is characterized by an abrupt increase in the thickness of coarse-grained channel sandstones and other sedimentological indicators of increased wetness of the floodplain. The cause of the change in depositional character at the lower-middle Siwalik boundary could be either tectonic (an increase in subsidence rate) or paleoclimatic (Cerling et al. 1997, Quade et al. 1995, Harrison et al. 1993). Data from other sites in the Nepal foreland, however, suggest that the change is highly diachronous, probably ruling out the paleoclimatic explanation (Hoorn et al. 2000, Quade et al. 1995, 1997). At Muksar Khola (26.9°N; 86.4°E), 111 paleomagnetic sites from a 2600-m thick section define a polarity zonation that correlates with the GPTS from chron C4An to chron C3n. At this locality, the lower-middle Siwalik lithostratigraphic boundary occurs at 8.8 Ma. Previously published results from Bakiya Khola (27.1°N; 85.2°E) indicate that this section was deposited from chron C5n to chron C3n and the lower-middle Siwalik lithostratigraphic boundary occurs at 9.2 Ma. The lithostratigraphic lower-middle Siwalik boundary is thus time transgressive by at least 1.7 Ma. along strike in the Himalayan foreland of Nepal. On the other hand, at Surai, Muksar, and Bakiya kholas, a shift in $\delta^{13}C$ in paleosol carbonate occurs within chron C3Ar at ~6.8 Ma, indicating that the carbon isotopic shift is isochronous. This isotopic shift has also been observed in Siwalik Group sediments of Pakistan (where the isotope shift appears to commence slightly earlier) and oceanic deposits of the Bengal Fan (Cerling et al 1993, France-Lanord and Derry 1994). The shift in carbon isotopes is interpreted as an ecological transition from dominantly C_3 plants (trees) to dominantly C_4 plants (grasses).

References

Cande SC, and DV Kent. 1995. Revised calibration of the geomagnetic polarity timescale for the Late Cretaceous and Cenozoic. *J Geoph Res* **100**: 6093-6095

Gerling TE, Y Wang and J Quade. 1993. Expansion of C4 ecosystems as an indicator of Global ecological change in the Late Miocene. *Nature* **361**: 344-345

Cerling TE, JM Harris, BJ MacFadden, MG Leakey, J Quade, V Eisenmann and JR Ehleringer. 1997. Global vegetation change through the Miocene/Pliocene boundary. *Nature* **389**: 153-158

DeCelles PG, GE Gehrels, J Quade and TP Ojha. 1998. Eocene-Early Miocene Foreland Basin Development and the history of Himalayan thrusting, Far Western and central Nepal. *Tectonics* **17**(5): 741-765

DeCelles PG, GE Gehrels, J Quade, TP Ojha, PA Kapp and BN Upreti. 1997. Neogene foreland basin deposits, erosional unroofing, and the kinematic history of the Himalayan fold-thrust belt, western Nepal. *Geol Soc Amer Bul*: **110**:21. p. 2

France-Lanord C and LA Derry. 1994. $\delta^{13}C$ of organic carbon in Bengal fan, source evolution and transport of C3 and C4 plant carbon to marine sediment. *Geochimica et Cosmochimica Acta* **58**:4809-4814

Harrison TM, P Copeland, SA Hall, J Quade, S Burner, TP Ojha and WSF Kidd. 1993. Isotopic preservation of Himalayan/Tibet uplift, denudation, and climatic Histories of two molasse deposits. *J Geol* **100**: 157-173

Hodges KV and DS Silverberg. 1988. Thermal evolution of the Greater Himalaya, Garhwal, India. *Tectonics* **7**: 583-600

Hoorn C, TP Ojha and J Quade. 2000. Palynological evidence for vegetation development and climatic change in the Sub-Himalayan Zone (Neogene, Central Nepal) *Palaeogeogr Palaeoclim Palaeoeco* **163**: 133-161

Ojha TP, RF Butler, J.Quade, PG DeCelles, D Richards and BN Upreti. 2000. Magnetic polarity stratigraphy of Siwalik Group sediments of Khutia Khola Kailali, farwesterrn Nepal. *Geol Soc Amer Bull* **112**: 424-434

Quade J, JML Cater, TP Ojha, J Adam, and TM Harrison. 1995. Late Miocene environmental change in Nepal and the northern Indian subcontinent: Stable isotopic evidence from paleosols. *Geol Soc Amer Bul*, **107**: 1381-1397

Quade J, L Roe, PG DeCelles and TP Ojha. 1997. Neogen $^{87}Sr/^{86}Sr$ record of lowland Himalayan rivers determined by carbonate, not silicate weathering. *Science* **276**: 1828-1831

Quade J, TE Cerling and JR Bowman. 1989. Development of Asian monsoon revealed by marked ecological shift during latest Miocene in northern Pakistan. *Nature* **342**: 163-166

Zeitler PK. 1985. Cooling history of the NW Himalayas, Pakistan. *Tectonics* **4**: 127-151

Geochemical study of the Dwar Khola dolerite (1.7 Ga) in the Siwalik belt, central Nepal

Yuji Orihashi†*，Harutaka Sakai‡ and Yutaka Takigami§

†Earthquake Research Institute, the University of Tokyo, Bunko, Tokyo, 113-0032 JAPAN
‡Department of Earth Science, Kyushu University, Ropponmatsu, Fukuoka, 810-8560 JAPAN
§Kanto Gakuen University, Ohta, Gunma, 373-8515 JAPAN

* To whom correspondence should be addressed. E-mail:oripachi@eri.u-tokyo.ac.jp

The Siwalik belt in central Nepal has been regarded as an accretionary prism mainly composed of the Middle Miocene to Pliocene molasse eroded out from the Himalaya (e.g., Jhonson et al. 1985). Recently, many dolerite sills showing 1.68 Ga [40]Ar/[39]Ar age (Takigami et al. 2002) and the Mid-Proterozoic orthoquartzite and quartzose sandstone beds intruded by the sills were found in the Siwalik belt of the Dwar Khola area (Sakai et al. 2000). Existence of these "exotic" rocks in the belt was suggested that detachment and accretion of crustal materials stripped from the Indian shield might take place in the frontal range of a continental-continental collision orogen (Sakai et al. 2000).

The Dwar Khola dolerite has a maximum thickness of about 400 m and is more than 6 km long in the section, and show less effects of metamorphism and alteration. Plagioclase and clinopyroxene in the dolerite are commonly fresh and the igneous textures are well-preserved in spite of the Mid-Proterozoic rocks. Due to this, Gautam et al. (1996) have inferred that the dolerite sills might have intruded into the Siwalik belt during Eocene to early Oligocene on the basis of their occurrence and paleomagnetic data. Moreover, they have pointed out that the whole rock composition has similar signature to the continental flood basalt (CFB) (e.g., Deccan Traps, Karoo and Parana basalts) but it has still remained unsolved why the CFB volcanism might occur in the frontal area of the Himalaya. In this study, major and trace elements and Nd isotope compositions of 11 samples for the Dwar Khola dolerite were determined. Using these data, we discuss petrogenesis of the Dwar Khola dolerite as well as origin and formation age of the Proterozoic mafic rocks in the Lesser
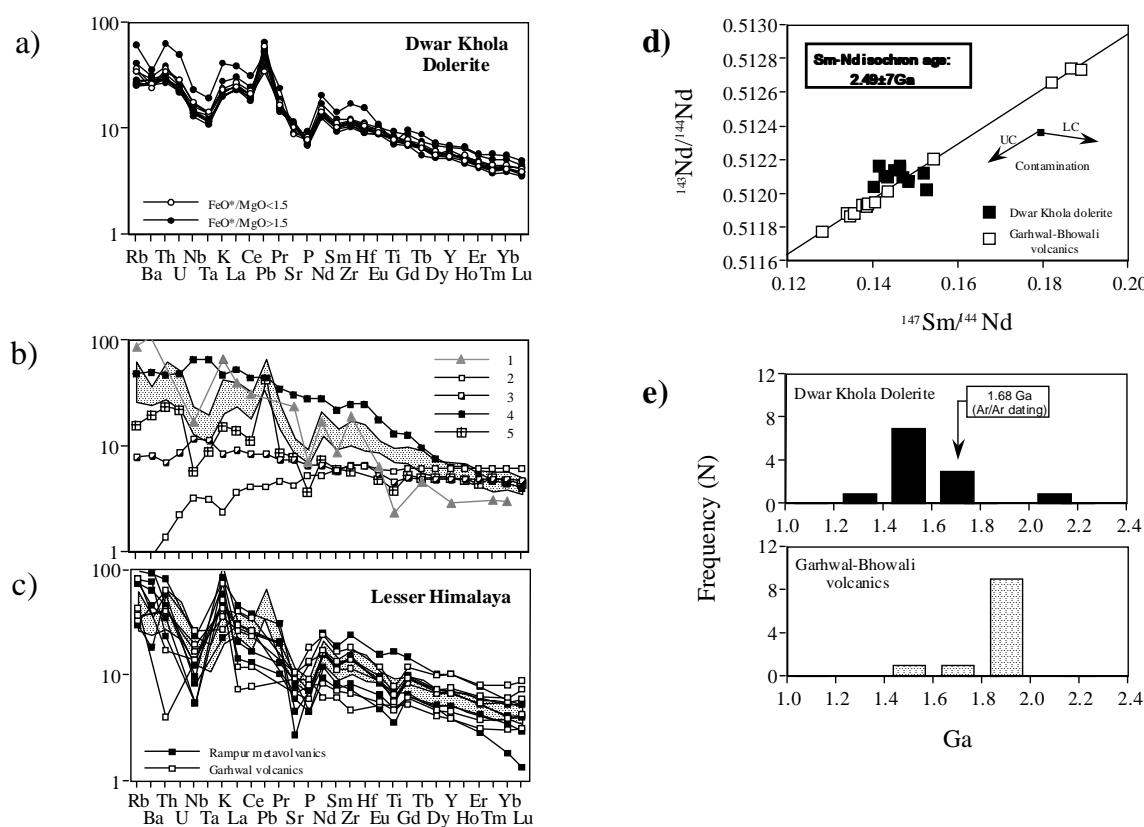
FIGURE 1. Spiderdiagrams normalized to primordial mantle value of a) the Dwar Khola dolerite (this study), b) 1: Proterozoic crust (Weaver and Tarney 1985), 2: N-MORB, 3: E-MORB, 4: OIB (Sun and McDonough 1989), 5: Deccan Traps (Mahoney et al. 2000), c) Rampur volcanics (Bhat and Le Fort 1992) and Garhwal volcanics (Ahmad and Tarney 1991) in the Himalaya belt, and d) Whole rock Sm-Nd isochron age of the Garhwal-Bhowali volcanics (Bhat et al. 1998) with the plots of the the Dwar Khola dolerite and d) Frequencys of Nd model ages of the Dwar Khola dolerite (this study) and Bhowali volcanics (Bhat et al. 1998)

Himalaya, reported by the previous studies (e.g., Ahmad and Tarney 1991, Bhat et al. 1998).

11 samples of the Dwar Khola dolerite extensively obtained from the different thrust-sheets showed very narrow variation in major and trace element abundances, i.e., 49.49–53.41 wt% in SiO_2, 5.36–7.36 wt% in MgO, 2.73–3.73 wt% in K_2O+Na_2O, 1.58–2.04 wt% in TiO_2 and 188–245 ppm in Sr, and there was no regional variation among them. On the MFA diagram, all samples indicated typical tholeiitic differentiation trend, and on FeO*/$MgO–TiO_2$ diagram, they plot within intermediate area of both MORBs and OIBs. Also, spiderdiagram patterns of the Dwar Khola dolerite normalized to primordial mantle roughly showed it to be enriched in the whole spectrum of incompatible elements relative to N-MORB and plot within the middle of both OIB and E-MORB (**Figures 1a, b**), which is consistent with those of major element signature. Moreover, these patterns displayed a marked trough at Nb, Ta, P and Sr and enrichment at Pb, indicating close similarities to those in CFBs (e.g., Wilson 1989), and particularly much closer to those in Deccan Traps. Cox and Hawkesworth (1985) suggested that such a Nb and Ta trough at the pattern in CFBs might reflect the consequence of crustal contamination but the process is likely to be much more complicated on the Deccan Traps. Peng et al. (1994) concluded that two stages of mixing among T-MORB like mantle plume source, enriched lithospheric mantle, lower and upper crustal materials were required to explain the multi-isotope variation on the southwestern Deccan Traps: first stage was performed between T-MORB like mantle plume source and lithospheric mantle or amphibolite-grade lower crust with radiogenic Sr, Nd and Pb isotopic signatures, and the second stage occurred between the products of variable amounts of first stage mixing and several different upper crustal materials with relatively low Pb isotopic signature to the lithospheric mantle and/or lower crust. Geochemical characteristics for the Dwar Khola dolerite obtained in this study is likely to be explained by the first stage mixing process rather than simple contamination of the Proterozoic upper or middle crustal material. Compared to the other Proterozoic volcanics in the Himalayan belt (e.g., Rampur and Garhwal volcanics; Bhat and Le Fort 1992, Ahmad and Tarney 1991), the spiderdiagram patterns roughly displayed the similarity to those of the Dwar Khola dolerite (**Figure 1c**).

Due to the drawback, the Dwar Khola dolerite is suggested to be mainly produced by a mantle plume activity although they are more or less affected by variable degrees of crustal contamination. This means that it is convenient to put their sources as CHUR value in calculating Nd model age. The Nd model ages for the Dwar Khola dolerite showed a range from 1310 Ma to 2110 Ma of which average (N=11) was 1600±200 Ma (SD). This result agrees with $^{40}Ar/^{39}Ar$ age of 1674±74 Ma (Takigami et al. 2002) within the range of error. Whole rock Sm-Nd isochron age of the Garhwal-Bhowali volcanics determined by Bhat et al.

(1998) yields an age of 2.51±0.08 Ga. However, this isochron age seems to be an "errorchron" caused by two component mixing between different initial Nd isotope ratios due to significantly wide range of $^{147}Sm/^{144}Nd$ value (0.1271 to 0.1883) among the basaltic rocks (**Figure 1d**). On the other hand, the Nd modal age for the Garhwal-Bhowali volcanics recalculated using CHUR value ranges from 1538 Ma to 1903 Ma, expect for three samples showing more than 0.18 in $^{147}Sm/^{144}Nd$ ratio. The average yields an age of 1820±100 Ma, which is consistent with those of the Dwar Khola dolerite (**Figure 1e**). These lead to the hypothesis that the Proterozoic metavaolcanic rocks in the Himalaya belt of the thrust sheets should be taken away from a surface of Indian shield, like the Dwar Khola dolerite.

References

Ahmad T and J Tarney. 1991. Geochemistry and petrogenesis of Garhwal volcanics: implications for evolution of the north Indian lithosphere. *Precam Res* **50**: 69-88

Bhat MI and P Le Fort. 1992. Sm-Nd age and petrogenesis of Rampur metavolcanic rocks, NW Himalayas: late Archaean relics in the Himalayan belt. *Precam Res* **56**: 191-210

Bhat MI, S Claesson, AK Dubey and K Pande. 1998. Sm-Nd age of the Garhwal-Bhowali volcanics, western Himalayas: vestiges of the late Archaean Rampur flood basalt province of the northern Indian craton. *Precam Res* **87**: 217-231

Cox KG and CJ Hawkesworth. 1984. Relative contributions of crust and mantle to flood basalt magmatism, Mahabaleshwar area, Deccan Traps. *Phil Trans R Soc Lond* **A310**: 627-641

Gautam P, BN Upreti and K Arita. 1995. Paleomagnetism and petrochemistry of the Dowar Khola volcanics, central Nepal sub Himalaya. *Jour Nepal Geol Soc* **11**: 179-195

Jhonson NM, J Stix, L Tauxe, PL Cerveny and RAK Tahirkheli. 1985. Paleomagnetic chronology, fluvial processes and tectonic implications of the Siwalik deposits near Chinji vallage, Pakistan. *J Geol* **93**: 27-40

Mahobey JJ, HC Sheth, D Chandrasekharam and ZX Peng. 2000. Geochemistry of flood basalts of the Toranmal section, northern Deccan Traps, India: implications for regional Deccan stratigraphy. *J Petrol* **41**: 1099-1120

Peng ZX, J Mahoney, P Hooper, C Harris and J Beane. 1994. A role for lower continental crust in flood basalt genesis? Isotopic and incompatible element study of the lower six formations of the western Deccan Traps. *Gechim Cosmochim Acta* **58**: 267-288

Sakai H, Y Takigami, BN Upreti and DP Adhikary. 2000. Thrust package of 1.68Ga Indian supra-crustal rocks in the Miocene Siwalik Belt, Central Nepal Himalayas. *Earth Sci Frontiers* **7**(supple):64-66; China Univ. of Geoscience (Beijing)

Sun SS and WF McDonough. 1989. Chemical and isotopic systematics of oceanic basalts: Implications for mantle composition and processes, *In Saunders AD and MJ Norry eds. Magmatism in the Ocean Basins. Geol Soc Spec Publ*, **42**: 313-345

Takigami Y, H Sakai and Y Orihashi. 2002. 1.5-1.7 Ga rocks discovered from the Lesser Himalaya and Siwalik belt: ^{40}Ar-^{39}Ar ages and their significances in the evolution of the Himalayan orogen. *Gechim Cosmochim Acta* **66** (S1):A762

Weaver BL and J Tarney. 1985. Major and trace element composition of the continental lithosphere. *In Pollack HN and VR Murthy eds. Structure and evolution of the continental lithosphere. Pergamon Oxford.* 39-68

Biostratigraphy and biogeography of the Tethyan Cambrian sequences of the Zanskar Ladakh Himalaya and of associated regions

Suraj K Parcha

Wadia Institute of Himalayan Geology, 33 - Gen. Mahadeo Singh Road, Dehra Dun -248 001, INDIA

For correspondence, E-mail: parcha_1@rediffmail.com, parchask@wihg.res.in

The Cambrian sections studied so far exhibit 4 km thick and apparently conformable successions of Neoproterozoic and Cambrian strata in Zanskar - Spiti basins. The Cambrian sediments of this area are generally fossiliferous comprising trilobites, trace fossils, hylothids, cystoids, archaeocythid and brachiopod, etc. In parts of Zanskar – Spiti and Kashmir region rich trilobite fauna is collected from the Cambrian successions. The trilobites constitute the most significant group of fossils, which are useful not only for the delimination of various biozones but also for the reconstruction of the Cambrian paleogeography of the region.

The Zanskar basin together with a part of the Spiti basin forms not only the largest succession of the Tethyan sequences in the Himalaya, but also exposes one of the best developed sections. The complete successions of rocks ranging in age from Precambrian to Eocene are exposed in the Zanskar area of Ladakh Himalaya. The Cambrian sediments in this basin are exposed in Tangzee yogma, Tangzee Kogma, Kuru, Purni – Phuktul, Kurgiakh sections of the Suru valley and Karsha section of the Zanskar valley.

On the basis of the faunal studies of icnofossils and on polymerid as well as agnostid trilobites, various faunal assemblage zones have been worked out from these sections.

The Himalayan Cambrian successions were whitherto considered to be deficient in agnostid trilobites. During recent years a variety of agnostid taxa have been reported from the Cambrian succession of the Zanskar basin. Agnostids constitute the most important index fossils for the global correlation of Cambrian successions. In the Zanskar Himalayan belt, the agnostid fauna is well preserved in the Middle Cambrian succession of Tangzee-Kuru- Purni-Phuktul and in the Kurgiakh sections of Lingti and Suru valleys. Preliminary studies reveal the presence of *Baltagnostus, Clavagnostus, Peronopsis, Hypagnostus, Diplagnostus, Lejopyge* and *Goniagnostus* a characteristic taxa of Hsuchuangian to Changhian stages of the Middle Cambrian.

In Spiti valley the agnostid fauna collected from the Parahio section (Parcha 1999) is represented only by *Peronopsis* and *Baltagnostus,* which indicates the Hsuchuangian stage of Middle. However, the agnostid fauna is not as widely present as in the Zanskar and Kashmir regions.

The record of *Diplagnostus* from Zanskar (Whittington 1986) and from northwestern part of Kashmir (Shah et al. 1995) is significant because it marks the boundary between the Middle and Late Cambrian. In the Zanskar basin, the *Diplagnostus* is also found associated with *Lejopyge*, which is more significant in order to establish the Changhian – Kushanian (Late Middle Cambrian- early Late Cambrian) boundary in this region. *Diplagnostus* is known to occur in the *Lejopyge laevigata* Zone in Australia. In the Yangliugang Group of Chiangan Belt in Sweden it extends from South Korea across southwestern China into North Vietnam. In North America *Diplagnostus* has been reported from the *Lejopyge laevigata* Zone which characterizes the latest Middle Cambrian. In the Lingti valley of the Zanskar area the presence of *Lejopyge* sp. is also of stratigraphic importance as it underlies the characteristic early Late Cambrian faunal elements. In the Magam section of Kashmir the *Diplagnostus* occurs at the top of the *Shahaspis (=Bolaspidella)* Zone of Jell and Hughes (1997), that is overlain by the *Damesella* Zone, which contains characteristic faunal elements of Changhian early Late Cambrian age. The genus *Damesella* is also reported from the Kushanian stage in China, the Tiantzun Formation in Korea and from *Agnostus pisiformis* Zone of the Outwood Formation in Britain.

The agnostid fauna reported from Kashmir and Zanskar regions occurs more or less at the same stratigraphic levels as in Australia, China, Kazakhstan, Sweden and North America. Therefore, it is useful in demarcating the intrasystem boundaries within the Himalayan Cambrian successions of Zanskar and Kashmir and also for the global correlation.

In almost all well preserved Cambrian successions of the world most of the workers find the Middle – Late Cambrian boundary in between *Lejopyge laevigata* Zone and *Agnostus pisiformis* biostratigraphic Zone. In Kashmir as well as Zanskar basins, therefore, this boundary can be marked on the basis of the occurrence of genus *Diplagnostus* in association with *Lejopyge.* In the Spiti region however, these agnostids have not been reported so far.

The trilobite fauna of the Himalayan Cambrian successions ranges from Early Cambrian (Templetonian) stage to early Late Cambrian (Mindyallan) stages of Australia. The Early Cambrian fauna is well preserved both in the Lesser as well as Tethyan Himalayan successions. Whereas, the Middle to early Late Cambrian fauna so far is known from the Tethys Himalayan successions of Zanskar – Spiti, Kashmir, and Bhutan. The proposed biostratigraphic zonation is based on the trilobite fauna collected so far from these regions. The trilobite fauna studied so far do not indicate any significant environmental change during the Cambrian period. So far no fossils have been reported from the upper part of Late Cambrian, whereas, latest part of Late Cambrian is marked by an angular unconformity in the Zanskar – Spiti region and by the facies variation in Kashmir.

References

Jell, PA and NC Hughes. 1997. Himalayan Cambrian trilobites. *Spec Papers in Paleontology* **58**: 113

Parcha, SK. 1999. Cambrian biostratigraphy in the Tethyan sequences of the Spiti Valley, Himachal Himalaya, India. *Newsletters Stratigraphy* **37**(3): 177-190

Shah, SK, SK Parcha and AK Raina.1995. Additional agnostids from the Middle Cambrian of Kashmir. *J Geol Soc India* **45**: 217-227

Whittington, HB. 1986. Late Middle Cambrian trilobites from Zanskar, Ladakh, northern India. *Rivista Italiana dil Paleontologiae Stratigrafia* **92**: 171-188

Implication of mylonitic microstructures and apatite fission track dating studies for the geotectonic evolution of the Chiplakot Crystalline Belt, Kumaon Himalaya, India

Ramesh C Patel† *, Y Kumar†, N Lal† and A Kumar‡

†Department of Earth Sciences, Kurukshetra University, Kurukshetra-136119, INDIA
‡D. A. V. College, Ambala City, Ambala (Haryana), INDIA

* To whom correspondence should be addressed. E- mail: patelramesh_chandra@rediffmail.com

In Kumaon Himalaya, the Higher Himalayan Crystalline (HHC) extends southward over the Lesser Himalayan meta-sedimentary zone (LHSZ) and forms several nappes: the Chiplakot Crystalline Belt (CCB), Askot, Almora, Lansdown, Champawat and Chamoli-Baijnath nappes (Valdiya 1980, Srivastava and Mitra 1994, 1996). The Main Central Thrust (MCT) underlies these allochthons, but it is named differently at the base of different nappes. Out of these nappes, the CCB is a unique one having special tectonic setting. The CCB mainly consists of lower amphibolite to green schist facies of mylonitised biotite gneiss and porphyroblastic augen gneiss with bands of amphibolite. It occurs within the LHSZ and is bounded by both NE-dipping South Chiplakot Thrust (SCT) at the base and the North Chiplakot Thrust (NCT) at the top. The NCT and the SCT are interpreted as the part of the MCT along which the CCB is rooted within the HHC zone and emplaced over the LHSZ (Valdiya 1980). Despite intensive study of the structural and tectonic evolution of the HHC sequence, but no significant study has been made so far to understand the geotectonic evolution of the CCB.

Geological setting and structural analysis of the CCB and its surrounding rocks reveal a large N-vergent overturned isoclinal synformal folding of the CCB. The dominant penetrative fabric in the CCB reflects the ductile stage exhumation of the CCB along the core of the fold as top-to-SW shear zone (Kumar and Patel in press). This shearing was responsible for differential palaeo-topography across the CCB.

The fabric and minor structures that reveal the geometric and kinematic evolution of this shear zone are described, analyzed and presented in detail. Incipient fabrics and structures are developed in the whole CCB but more intensely developed toward middle of the CCB. Kinematic indicators confirm consistent top-to-SW shearing along this zone. Microstructural analysis of the constituent minerals demonstrates that deformation mechanism is not uniform throughout the CCB but varies from the boundaries toward the middle of the CCB. Quantitative analysis of grain-scale geometries across the CCB reveals that the deformation is spatial and temporally concentrated along the middle zone of the belt. We interpret the middle of the CCB as the central part of the broad shear zone along which the upper part of the CCB is thrust over the basal part of the CCB. The shear zone is developed through the axial zone of the overturned isoclinal synformal fold and then progressively developed outwards by further superposition of shear and flattening strain during which time the whole CCB became a broad shear zone.

The Apatite Fission Track (AFT) dating of the CCB and the HHC rocks shows differential exhumation history. The results indicate that the HHC forming the hanging wall of the MCT cooled below the closing temperature of apatite FT at 1.65 ± 0.18 Ma. The FT apatite ages of the CCB along Kali-Darma valleys are older than the HHC but appear to fall in two distinct groups. In the northern part of the CCB the weighted mean of FT apatite age is 9.60 ± 0.14 Ma while in the southern part it is 14.10 ± 0.07 Ma. It confirms that the differential paleotopography caused by top-to-SW thrusting at the middle of the CCB played major role for different erosive denudation and hence exhumation of the CCB. It also appears that the HHC has exhumed rapidly than the CCB due to repeated reactivation of the MCT coupled with rapid erosive denudation.

The widespread presence of extensional structures indicates that extension was not limited to localized deformation, but affected the whole CCB and overprints the contractional Himalayan deformation. The extensional deformation was related to tectonic loading and uplift of the Himalaya (Patel et al. 1993).

References

Kumar, Y and RC Patel. in press. Deformation mechanisms in the Chiplakot Crystalline Belt (CCB) along Kali-Gori Valleys (Kumaon), NW-Himalaya. *J Geol Soc India*

Patel, RC, S Sandeep, A Asokan, RM Manickavasagam and AK Jain. 1993. Extensional tectonics in the Himalayan orogen Zanskar, NW India. In PJ Treolar, and MP Searle (eds.) *Himalayan Tectonics*. Geol Soc London Spec Publ **74**: 445-59

Srivastava, P and G Mitra. 1994. Thrust geometries and deep structure of the outer and lesser Himalaya, Kumaon and Garhwal (India): Implications for the evolution of the Himalayan fold-and-thrust belt. *Tectonics* **13**: 89-109

Srivastava, P and G Mitra. 1996. Deformation mechanism and inverted thermal profile in the North Almora Thrust mylonite zone, Kumaon Lesser Himalaya, India. *J Struct Geol* **18**: 27-39

Valdiya, KS. 1980. *Geology of the Kumaun Lesser Himalaya*: Dehra Dun, India. Wadia Institute of Himalayan Geology, 291p

Late Pleistocene vegetation from the Thimi Formation, Kathmandu Valley, Nepal

Khum N Paudayal

Central Department of Geology, Tribhuvan University, Kirtipur, Kathmandu, NEPAL

For correspondence, E-mail: knpaudayal@wlink.com.np

The Thimi Formation is characterized by alternation of fine to medium-grained sand, silt, silty clay and clay, deposited by distal fluvial system. Radiocarbon ages of two wood samples from middle part of the section (13 m from the top) and from the basal part (21 m from the top) are found to be $41,700 \pm \frac{5600}{3200}$ and >37,900 yrs BP, respectively. Altogether 40 samples were taken

FIGURE 1. Zonation of vegetation in the Central Midlands of Nepal (K=Kathmandu)
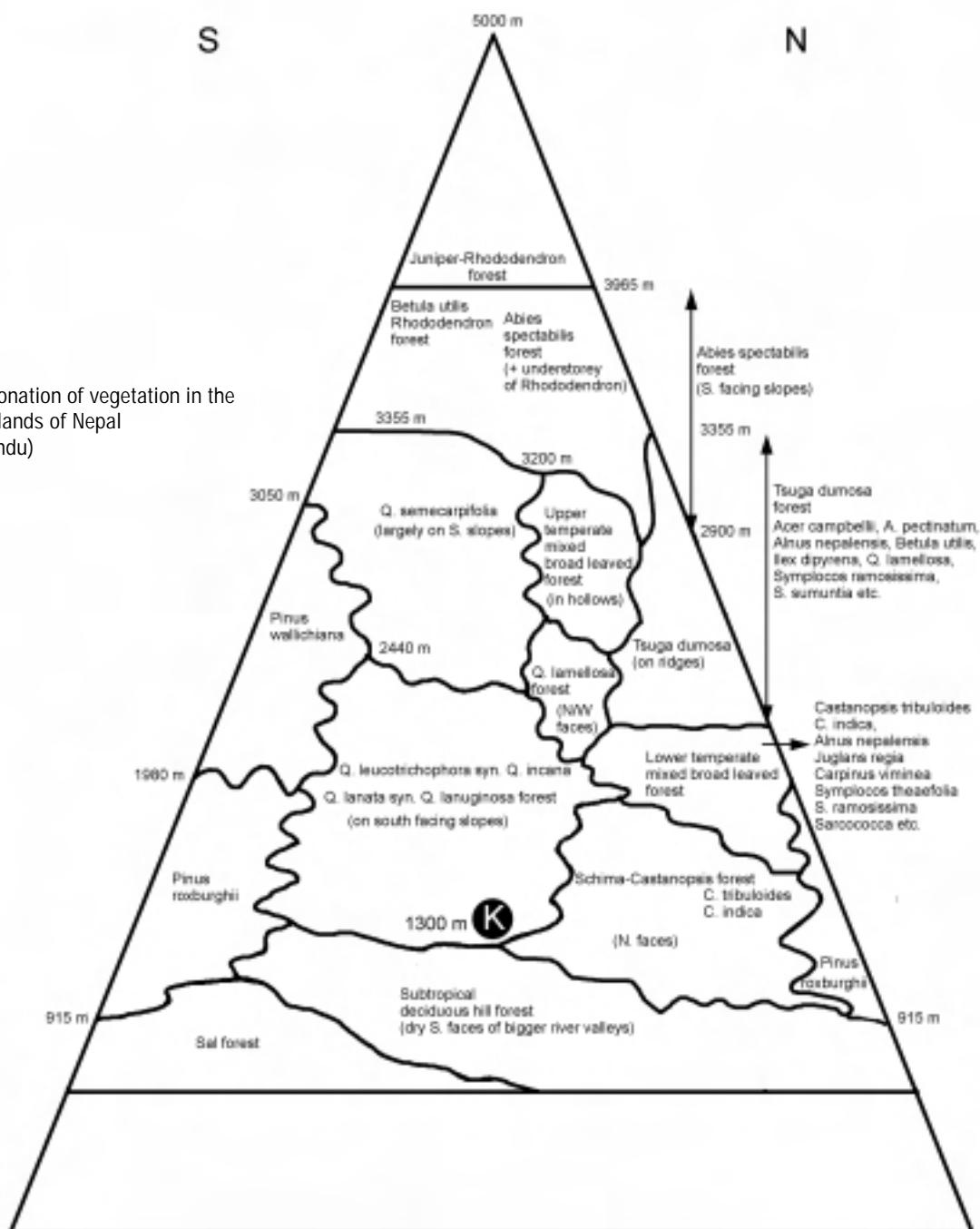
from 23 m thick type section of the Thimi Formation for palynological study. The pollen display only minor fluctuations in their assemblages without having any major break (**Figures 1 and 2**). On the basis of these minor changes this section is divided into seven pollen zones. The small-scale changes from one pollen zone to another can be explained as ''cold'', ''fairly cold'' or ''moderately warm'' climatic conditions. For example the presence of *Castanopsis* together with high amounts of *Quercus* and small amounts of *Abies* and *Picea* can be assigned to a moderately warm climate. This is followed by an increase in *Pinus, Picea, Abies* and *Tsuga* along with the contemporaneous decrease of *Castanopsis* and *Quercus* indicating a colder climate. In general the pollen assemblages of the Thimi Formation are dominated by cold elements such as *Pinus wallichiana* and different *Quercus*

species that grow in the warm to cool temperate zone of Nepal. This is confirmed by high percentages of Poaceae and other herbaceous plants with very little woody angiosperms. Gymnosperms such as *Pinus wallichiana* (along with *Abies spectabilis, Tsuga dumosa* and *Picea smithiana*) were the dominant over the woody angiosperms (*Quercus lanata, Q. lamellosa* and *Q. leucotrichophora* and *Q. semecarpifolia*). An attempt was made to quantify the climatic change by plotting the present altitudinal ranges of all available pollen taxa from a single horizon. It would appear that the vegetation in the Kathmandu Valley shifted to a lower altitude by approximately 1000 m during the late Pleistocene. If we allow for a temperature lapse rate of 0.6 °C/100 m in the Nepal Himalayas this must indicate a lowering of the temperature by 6 to 7 °C.
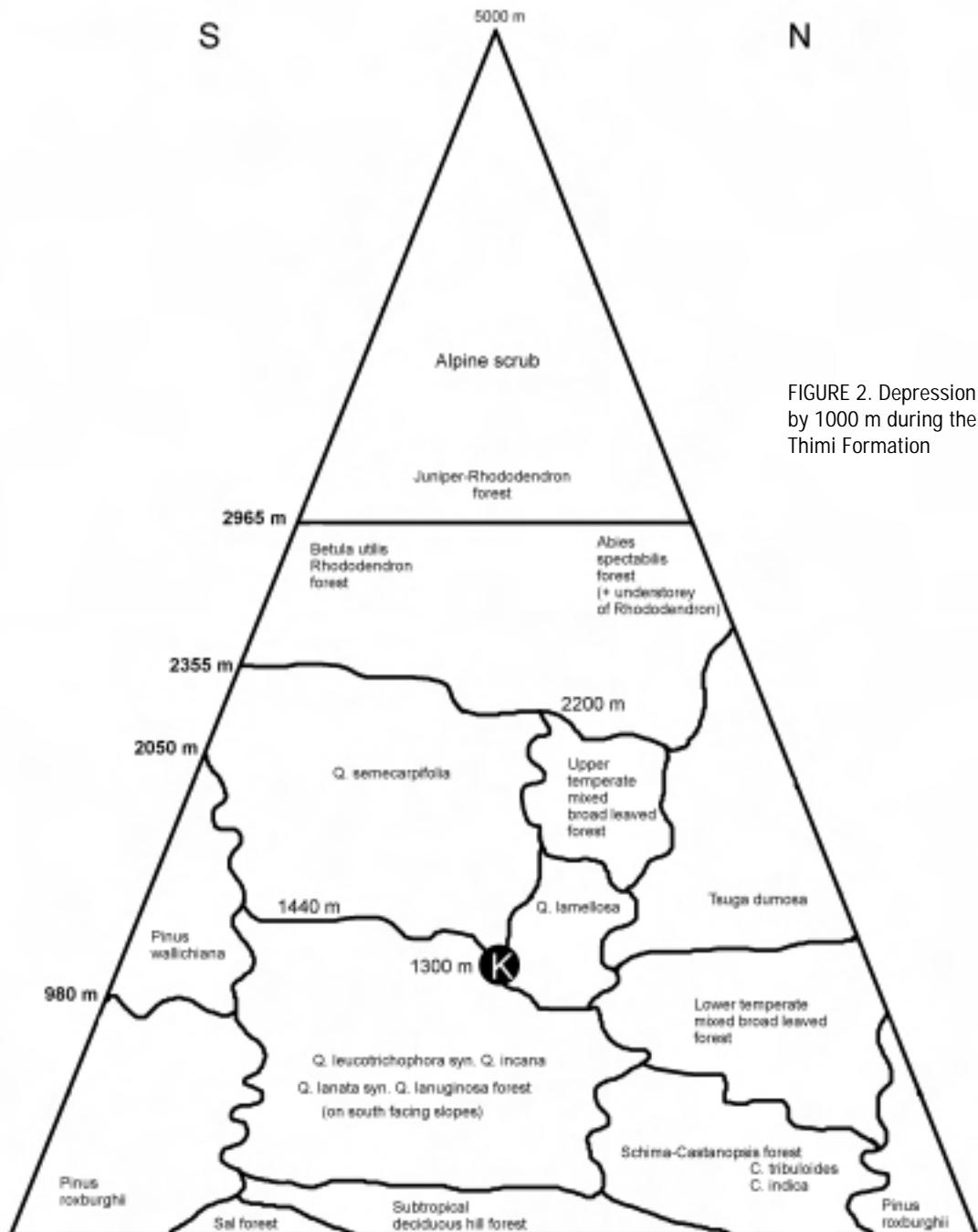
FIGURE 2. Depression of vegetation by 1000 m during the time of the Thimi Formation

The b-spacing values of white mica from low-grade metapelites of central Nepal Lesser Himalaya and their tectono-metamorphic implications

Lalu P Paudel‡* and Kazunori Arita†

†Department of Earth and Planetary Sciences, Graduate School of Science, Hokkaido University, Kita 10, Nishi 8, Sapporo
 060-0810, JAPAN
‡Permanent address: Central Department of Geology, Tribhuvan University, Kirtipur, Kathmandu, NEPAL

 * To whom correspondence should be addressed. E-mail: lalupaudel67@yahoo.com, lalu@wlink.com.np

Although, enormous P-T data have been constrained from higher-grade rocks of the central Himalayan region (Hodges et al. 1988), P-T data from lower-grade rocks of the Lesser Himalaya are still lacking. In the low-grade metamorphic terrain, the recrystallization of rocks is often not immediately obvious because of the fine-grained character, apparent irregularity in the metamorphism, and only partial recrystallization with preservation of many relict features of the protoliths. Owing to this reason, palaeopressure estimation by thermodynamic calculations is not possible.

White micas are among the most abundant phyllosilicates in low-grade metamorphic rocks. The Tschermak substitution $[(Mg, Fe^{2+})^{vi} Si^{iv} = Al^{vi} Al^{iv}]$ between the ideal muscovite and celadonite end-members, which controls the chemistry of phengites, is thought to be particularly sensitive to pressure at low-temperature conditions and serves as a qualitative geobarometer (Guidotti and Sassi 1986). Although, the b-spacing values of white micas have been widely used to estimate the palaeopressure in low-grade terrains all over the world, its application in the Himalaya is relatively rare. In the present study, we present the b-spacing values of white mica across Pokhara-Butwal road and Kali Gandaki valley sections of the Lesser Himalaya in central Nepal, and discuss their tectono-metamorphic implications.

Geological setting

The Lesser Himalaya in the Pokhara area is divided into four tectonic units from south to north: Parautochthon with Palpa Klippe lying between the Main Boundary Thrust (MBT) and the Bari Gad-Kali Gandaki Fault (BKF), Thrust Sheet I (TS I) situated between the BKF and the Phalebas Thrust, Thrust Sheet II (TS II) bounded by the Phalebas Thrust and the Lower MCT, and the MCT zone bounded by the Lower MCT and the Upper MCT, respectively. The Lesser Himalaya mostly comprises low-grade metamorphic rocks such as slates, phyllites, quartzites, and dolomites (Nawakot Complex) of the Precambrian age. The Nawakot Complex rocks are unconformably overlain by the Gondwana and post-Gondwana sedimentary rocks (Tansen Group) in the Parautochthon (Sakai 1983). Metamorphic grade gradually changes from diagenesis to lower anchizone in the Parautochthon to upper anchizone in the TS I, epizone in the TS II and garnet zone in the MCT zone (Paudel 2000).

Sampling and analytical techniques

A total of 320 pelitic rocks with unique assemblage "Mica+Chl+Ab+Qtz" (Chl-zone) and lacking detrital white mica were used to measure b-spacing values. A few samples from the northern part of the TS II are from Bt-zone and samples from the MCT zone belong to Grt-zone. Measurement was done on $<2\mu m$ powder fraction of each sample.

Diffractometer setting was constant for all the samples (Rigaku Geigerflex diffractometer, Cu cathode, Ni filter, 35 kv tube voltage, 20 mA current, time constant=2 sec, scatter slit=1°, receiving slit=0.3 mm, divergence slit=1°). The 63-59.5° 2θ range was scanned at 0.25 2è/min, and b was determined from (060) peak (approx. 61.5° 2θ) using the (211) quartz reflection (approx. 60° 2θ) as an internal standard. Mean b-spacing values were calculated from five repeated measurements for each sample.

Results and implications

The relationship between the b-spacing values with the composition of white mica was accessed by compositional analysis of white mica in the same samples. A fairly good positive linear correlation was found between the two (**Figure 1**). This indicates that the b-spacing values serve as indirect measures of phengite content of white mica in the Lesser Himalaya and hence the pressure condition.

The plots of b-spacing values versus the whole rock compositions show no marked correlation indicating that the b-spacing values are sensitive to P-T condition rather than the bulk rock composition. The intensity and shape of the $CuK_{\alpha 1}$ XRD traces of white mica (060+331) peak gradually change from south (close to the MBT) to north (close to the MCT). Many of the samples from the Tansen Group, Palpa Klippe, Parautochthon, and the TS I show bifurcated or very wide, blunt and asymmetric (060+331) peaks, which are interpreted to be due to the presence of bimodal white mica compositions crystallized at different thermal events (polymetamorphic events, Paudel and Arita 2000).

The b-spacing values vary from 8.970Å to 9.060Å in the study area. The average b-spacing values are relatively smaller in the Tansen Group $(X_{26}=8.993\pm0.033Å)$ compared to those of the Parautochthon $(X_{60}=9.029\pm0.01Å)$ and the Palpa Klippe $(X_{20}=9.039\pm0.005Å)$. Average b-spacing values from the TS I $(X_{109}=9.041\pm0.011Å)$ are also similar to those of the Parautocthon and the Palpa Klippe. The b-spacing values sharply drop across the Phalebas Thrust. The average b-spacing values for the TS II and the MCt zone are $(X_{82}=9.016\pm0.012Å)$ and $(X_{20}=9.001\pm0.011Å)$, respectively.

The b-spacing value increase with depth to the south of the Phalebas Thrust, i.e., higher values for older units. It shows that the rocks attained peak pressure when they were at normal stratigraphic position. Therefore, older units experienced higher pressure due to thicker overload. However, it is interesting to note that the trend of b-spacing values is reversed to the north of the Phalebas Thrust, i.e., lower values for older units. It is argued that the decrease in b-spacing values is the result of thermal dephengitization of the white mica due to higher temperature condition in the northern part of the Lesser Himalaya.

A cumulative frequency plot of the total data of each tectonic unit from the present area **(Figure 2)** shows that the TS I, Parautochthon, and the Palpa Klippe have b-spacing values comparable to those of the Eastern Alps and Otago metamorphic belts suggesting a typical Barrovian-type (intermediate-P) metamorphism. On the other hand the MCT zone, TS II and the Tansen Group have b-spacing values similar to that of the Bosost, N. New Hampshire and Ryoke metamorphic belts. The Tansen Group occupies the shallowest position in the stratigraphic sequence. Therefore, the lower b-spacing values from the Tansen Group are likely due to low-P metamorphic condition.

Using the P-T-b grid of Guidotti and Sassi (1986), the approximate palaeopressures have been estimated to be about 4 kbars for the TS II , TS I and Parautochthon. The estimated pressures give approximate burial depths of 15 km assuming an average bulk density of $2.60\,gm\,cm^{-3}$ for the metasediments. Thus, the estimate of the average background geothermal gradient at the time of peak metamorphism would be 27°C/km for the TS II (using peak T=400 °C given by illite crystallinity; Paudel 2000), 22°C/km for the rest of the area to the south of the Phalebas Thrust (using peak T=325 °C given by IC).

The P-T structure for the Neohimalayan metamorphism revealed from b-spacing values can be explained in relation to the thrust tectonics, i. e., overthrusting of the hot Higher Himalayan rocks over the cold Lesser Himalayan (Le Fort 1975, Arita 1983). Lower geothermal gradient and lesser thickness of overburden during peak metamorphism in the southern part (frontal part of the orogen) of the Lesser Himalaya may be the reflection of cool and thin leading edge of the MCT.

References

Arita K.1983. Origin of the inverted metamorphism of the Lower Himalayas, central Nepal. *Tectonophysics* **95**: 43-60

Guidotti CV and FP Sassi. 1986. Classification and correlation of metamorphic facies series by means of muscovite b_0 data from low-grade metapelites. *Neues Jahrb Mineral Abhand* **153**: 363-380

Hodges KV, MS Hubbard and DS Silverberg. 1988. Metamorphic constraints on the thermal evolution of the central Himalayan orogen. *Philosophical Trans Royal Soc London* **A326**: 257-280

Le Fort P. 1975. Himalaya: the collided range. Present knowledge of the continental arc. *Am J Sci* **275A**: 1-44

Paudel LP and K Arita. 2000. Tectonic and polymetamorphic history of the Lesser Himalaya in central Nepal. *J Asian Earth Sci* **18**: 561-584

Paudel LP. 2000. *Geological and petrological studies of the central Nepal Himalaya with special reference to tectono-thermal evolution and inverted metamorphism in the Lesser Himalaya*. PhD Dissertation (submitted to the Hokkaido Univertisy, Japan), 155 p

Sakai H. 1983. Geology of the Tansen Group of the Lesser Himalaya in Nepal: *Memoirs of the Faculty of Science, Kyushu University, Series D, Geology* **25**: 27-74.

Sassi FP and A Scolari. 1974. The b value of the potassic white micas as a barometric indicator in low-grade metamorphism of pelitic schists. *Contrib Mineral Petrol* **45**: 143-152
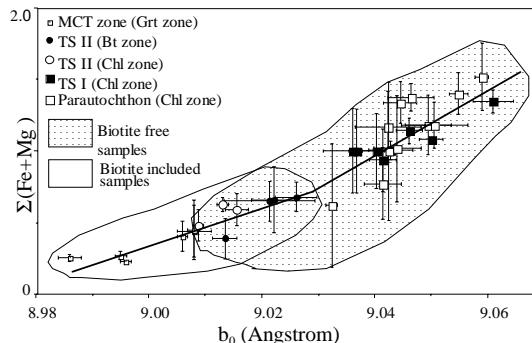
FIGURE 1. Plots of phengite content (Fe+Mg) versus the b-spacing values of white micas from the Tansen-Pokhara section. The two show good correlation (r=7.2) in the area
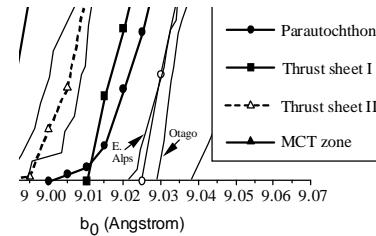
FIGURE 2. Cumulative frequency curves of b-spacing values for different tectonic units in the Lesser Himalaya. Cumulative frequency curves for the other orogenic belts are after Sassi and Scolari (1974)
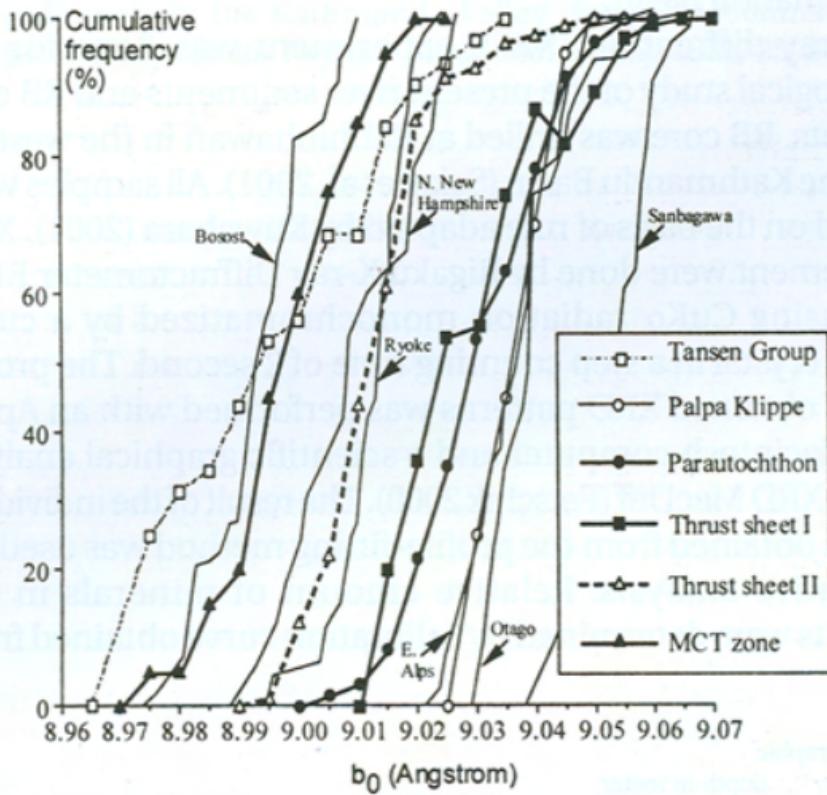
FIGURE 2. Cumulative frequency curves of b-spacing values for different tectonic units in the Lesser Himalaya. Cumulative frequency curves for the other orogenic belts are after Sassi and Scolari (1974)

Changes in mineral composition and depositional environments recorded in the present and past basin-fill sediments of the Kathmandu Valley, central Nepal

Mukunda Raj Paudel*, Yoshihiro Kuwahara and Harutaka Sakai

Department of Earth Sciences, Graduate School of Social and Cultural Studies, Kyushu University, Ropponmatsu, Fukuoka 810-8560, JAPAN

* To whom correspondence should be addressed. E-mail: cs500032@scs.kyushu-u.ac.jp

Surface and drill core sediments from the Kathmandu Basin were investigated to decipher their capability to record changes in the mineral composition and depositional environment. Spatial distribution of mineral assemblages in the terrigenous sand and mud reflects different provenance of the past and present basin filled sediments. Bulk mineral assemblages in the modern sediments are controlled by supply of terrigenous detritus from the source rocks in the adjacent surrounding mountains. This suggests the occurrence of granitic and gneiss source in the north and metasediments in the eastern, western and southern part of the Kathmandu Basin.

X-ray diffraction (XRD) experiment was done for the mineralogical study of the present river sediments and RB core sediments. RB core was drilled at Rabhibhawan in the western part of the Kathmandu Basin (Sakai et al. 2001). All samples were prepared on the basis of rule adapted by Kuwahara (2001). XRD measurement were done by Rigaku X-ray Diffractometer RINT 2100V, using CuKα radiation monochromatized by a curve graphite crystal in a step counting time of 2 second. The profile fitting of obtained XRD patterns was performed with an Apple Power Macintosh computer and a scientific graphical analysis program XRD MacDiff (Petschik 2000). The result of the individual minerals obtained from the profile-fitting method was used for quantitative analysis. Relative amount of minerals in the sediments were determined by calibration curve obtained from integrated intensity ratio of the standard mineral to internal standard zincite.

X-ray diffraction (XRD) analysis of greater than 2 mm fraction of the present river sediments from the Kathmandu Basin shows quartz, K-feldspar, plagioclase and mica to be the dominant bulk minerals (accounting over 80%). It shows the presence of low amounts of chlorite and calcite. Chlorite is relatively higher in the northern part than the east, west and south. Based on the study done, the mineral assemblages of the present river sediments within the Kathmandu Valley are divided into two groups. The first group is rich in mica, poor in quartz and has presence of K-feldspar, plagioclase and chlorite in all samples. This group of mineral originated from Shivapuri Lekh of the granite and gneiss complex. The second group is rich in quartz and poor in mica and has presence of plagioclase, K-feldspar and very poor chlorite. This group probably originated from metasediments in the eastern, western and southern part of the Kathmandu Valley. Some samples of this group also contain very low percentage of calcite (less than 5 %).

Mineral assemblages in the RB core sediments from 7 to 40 m depth indicate the same as those encountered in the present river sediments. XRD-analysis of the greater than 2 mm fraction shows the presence of quartz (10-60%), K-feldspar (2-37%), plagioclase (2-8%), mica (4-19%), chlorite (2-14%) and calcite (0-18%). Relatively high percentages of these minerals are
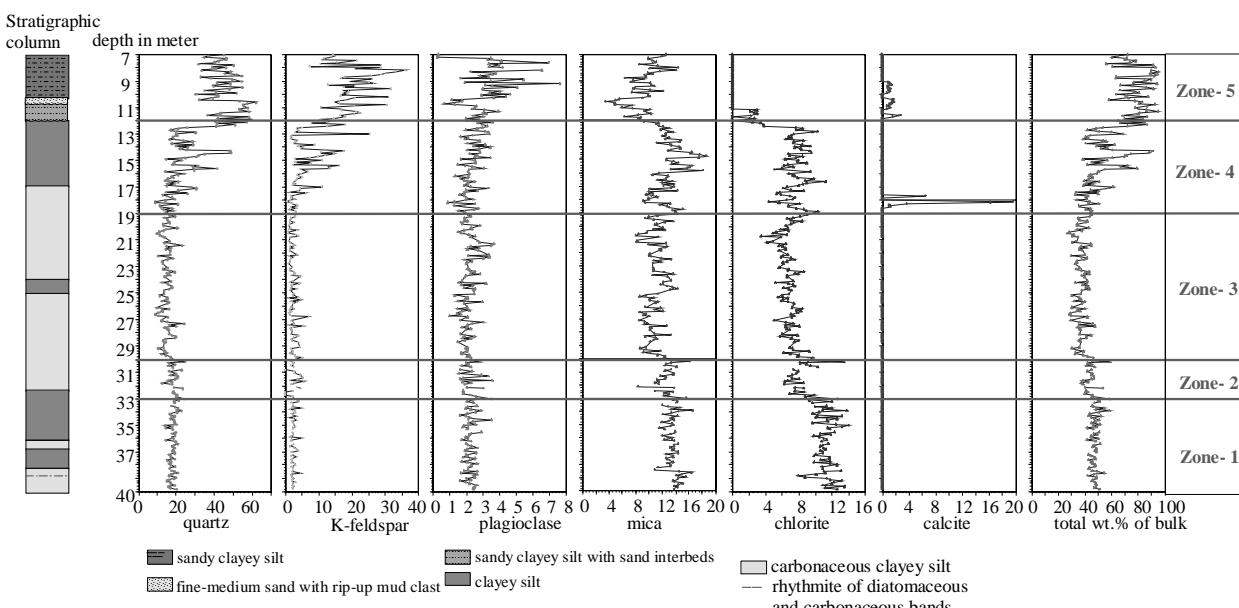

FIGURE 1. Mineralogical variation in the RB core up to 40 m depth

detected above the 13 m depth. The trends in amount between quartz, feldspar and mica are opposite, quartz and feldspar increase when mica decreases. The trend between chlorite and mica is parallel.

On the basis of the variation of these minerals with depth, we divided the RB core sediments into five mineral zones (**Figure 1**). Zone-1 (40-33 m) is rich in chlorite and with quartz and mica higher than in zone-3. Zone-2 (33-30 m) is rich in chlorite with decreased total amount of the minerals. Zone-3 (30-19 m) has the lowest total amount of all minerals poor in quartz and mica. Zone-4 (19-12 m) has increased whole mineral composition. Zone-5 (12-7 m) has increased quartz and feldspar (highest value), with the total amount twice as much as in other zones.

Changes of the mineral composition of the present river sediment with respect to different directions show the provenance of the sediments to be not just one particular direction. Moreover, relatively higher percentage of chlorite in the northern part of the sediments might indicate the source rock contains higher percentage of mica. South, east and west of the Kathmandu Basin contain the carbonate rocks. However, very few percentage of carbonate minerals are detected from this site, which indicate that the carbonate minerals are dissolved within the present river.

RB drill core is located near to the Phulchoki Group of metasediments. The present river sediments flowing from metasediment zones have very low amount of chlorite. However, sediments of the RB core contain chlorite minerals, which are similar to the granitic and gneiss source of the Shivapuri Lekh. Variation of the mineral content in the zone 4 and 5 of RB core above 13m depth are larger than the zone below 13 m depth, particularly, quartz, K-feldspar and mica. Similarly, different amount of mineralogical variation obtained from the drill-well JW-3 in the central part of the Kathmandu Basin (Fujii and Kuwahara 2001). Hence, such mineralogical variation with respect to the depth in the drill core sediments indicates the depositional environmental changes at the time of deposition.

References

Fujii R, Y Kuwahara and H Sakai. 2001. Mineral composition changes recorded in the sediments from a 284-m-long drill-well in central part of the Kathmandu Basin, Nepal. *J Nepal Geol Soc (Sp issue)* **25**:63-69

Kuwahara Y, R Fujii, Y Masudome and H Sakai. 2001. Measurement of Crystallinity and relative amount of clay mineral in the Kathmandu Basin sediments by decomposition of XRD pattern (profile fitting). *J Nepal Geol Soc (Sp.Issue)* **25**:71-80

Lanson B.1997. Decomposition of experimental X-ray diffraction pattern (Profile fitting); A convenient way to study clay minerals. *Clay and clay Miner* **45**:132-146

Petschick R. 2000. MacDiffVer.4.2.3, Manual Geologisch-Palaontologisches Institute Johann Wolfgang Goethe Universitat Frankfurt Main senckenberganlage 32-34, 60054 Frankfurt am Main, Germany. 58 p

Sakai H, R Fujii and Y Kuwahara. 2001. Core drilling of the basin-fill sediments in the Kathmandu Valley for paleaeoclimatic study: preliminary results, Nepal. *J Nepal Geol Soc (Sp issue)* **25**: 9-18

Cooling in down-slope peat ecosystems due to accelerated glacial melting in Higher Himalaya, India

Netajirao R Phadtare†*, Rajendra K Pant†, Kathleen Ruhland‡ and John P Smol‡

†*Wadia Institute of Himalayan Geology, PO Box 74, Dehra Dun - 248 001, INDIA*
‡*Paleoecological Environmental Assessment and Research Laboratory (PEARL), Department of Biology, Queen's University, Kingston, ON K7L 3N6, CANADA*

* *To whom correspondence should be addressed. E-mail: nrphadtare@rediffmail.com*

High-resolution paleoclimate data and numerous instrumental records report that, at higher elevations, Himalayan temperatures over the last ca. 100 years have been rising (Liu and Chen 2000, Thompson et al. 2000). However, many instrumental records from various lower elevation localities are reporting cooler temperatures in recent decades (Balling 2001). This recent cooling trend is not only opposite to the global warming trend but also with the accelerated retreat of the Himalayan glaciers. The effect that warming conditions and melting glaciers have on down-slope ecosystems has not been fully explored. Here we present compelling evidence that, over the last 200 years, accelerated glacier retreat and increased melt waters have played a central role in changing the ecology (and perhaps local climate) of down-slope sites.

The Pinder Valley (~30°50' - 30°52' N, 78°47' - 78°51'E) of the Kumaon Higher Himalaya, receives precipitation from the Asian monsoon predominantly during the summer but also during winter seasons. The valley climate is also influenced by hanging glaciers (viz. Sunder Dunga, Pindari, and Kaphni), situated along the valley head. An ~ 125-cm thick peat deposit situated in oak dominated mixed evergreen forest 2650-m altitude, was trenched and continuously sampled at 2-cm intervals. Well-dated multi-proxy paleoclimate record (pollen, diatoms, phytoliths, % organic matter, and magnetic susceptibility) from this peat sequence revealed past ca. 3500-year high-resolution climate history of the area.

At the beginning of the peat sequence (ca. 3500 to ca. 3300 cal yr BP), the pollen assemblage was almost exclusively represented by conifers suggesting that the regional climate was cool and wet. A sudden increase in the dominance of grass, alder (*Alnus nepalensis*) and brown oak (*Quercus semecarpifolia*) pollen at ca. 3300 cal yr BP indicates an abrupt climatic shift towards drier conditions that continued until ca 2300 cal yr BP. The increase in silver fir (*Abies pindrow*) and other conifers [Himalayan spruce (*Picea smithiana*) and blue pine (*Pinus wallichiana*)] at the expanse of grasses, and the first appearance of diatoms ca. 2300 cal yr BP mark the end of the dry period. The progressive decrease in grass pollen for the following ~200 years reveals the improved wetness of climate until ca. 2100 cal yr BP. Variations in our proxy indicators throughout the remainder of the peat sequence suggest a stepwise increase in wetness until the present.

A major shift in all of the proxy indicators at ca. 680 cal yr BP (~ 1320 AD) indicates an increase in SW monsoon at 1300 AD, evidence of which is widespread throughout the Asian monsoon region (Morrill et al. 2003). Around this time the once dominant *Fragilaria* diatoms abruptly diminished to trace abundances, *Navicula minima* appeared for the first time in the record in relatively high abundances, and epiphytic diatom taxa became more prominent.

Circa 1580 to 1730 AD, a substantial cooling was inferred with a reduction to trace levels of the epiphytic proportion of the diatom assemblage and the strong re-appearance of *Fragilaria* species to abundances of 80 – 90%, not seen before or afterwards in the peat profile. A comparison of the last ~400 years of the peat record with reconstructed spring temperature trend derived from a series of 12 Himalayan tree-ring chronologies (Yadav and Singh 2002) is consistent with our proxy-based inferences from ca. 1600 AD onwards.

The high rate of glacier melting over the last few centuries in the Himalayan mountains is a clear demonstration of a warming climate. Our data show that increased glacial melt-waters under this warmer climatic scenario has had a substantial impact on down-slope ecosystems. It appears that the glacial retreats are consistent with the global climate scenario but the resulting melt waters are having localized to regional cooling effects at lower elevation sites over the last few decades.

References

Balling JC Jr. 2001. *World Climate Report*. Available online at www.greeningearthsociety.org/human.htm

Liu X and B Chen. 2000. Climatic warming in the Tibetan Plateau during recent decades. *International Journal of Climatology* **20**: 1729-1742

Morrill C, JT Overpeck and JE Cole. 2003. A synthesis of abrupt changes in the Asian summer monsoon since the last deglaciation. *The Holocene* **13**: 465-476

Thompson LG, T Yao, E Mosley-Thompson, ME Davis, KA Henderson and PN Lin. 2000. A high-resolution millennial record of the South Asian Monsoon from Himalayan ice cores. *Science* **289**: 1916-1919

Yadav RR and J Singh. 2002. Tree-ring-based spring temperature patterns over the past four centuries in Western Himalaya. *Quaternary Research* **57**: 299-305

Tectono-metamorphic evolution of the far-Eastern Nepal Himalaya

Santa M Rai† *, H Sakai‡, Bishal N Upreti†, Yutaka Takigami§, Subesh Ghimire¶, Dibya R Koirala†, Tej P Gautam#, Desh R Sonyok|| and Chandra P Poudel†

† Department of Geology, Tri-Chandra College, Tribhuvan University, Ghantaghar, Kathmandu, NEPAL
‡ Department of Earth Sciences, Kyushu University, Ropponmatsu, Fukuoka, 810-8560, JAPAN
§ Kanto Gakuen University, Ohta-shi, Gunma, 373-8515, JAPAN
¶ Institute of Seismology and Volcanology, Hokkaido University, Sapporo, JAPAN
 # Institute of Environmental Studies, The University of Tokyo, Tokyo, 113-8656, JAPAN
|| Department of Civil and Structural Engineering, Kyushu University, Hakozaki, Fukuoka 812-8581, JAPAN

* To whom correspondence should be addressed. E-mail: santamanrai@yahoo.com

In far-Eastern Nepal, the Lesser Himalayan Sequence (LHS) exposed in the Taplejung Window and in frontal belt between the Main Boundary Thrust (MBT) and the southern extension of the Main Central Thrust (MCT) comprises greenschist to amphibolite facies rocks such as phyllite, schist, metasandstone, quartzite, amphibolite, marble and augen gneiss of granitic origin (Ulleri-type augen gneiss) (Rai et al. 2001). Two-mica granite bodies have intruded the phyllite and quartzite in the lower section of the Taplejung Window (Upreti et al. 2003). The $^{40}Ar/^{39}Ar$ muscovite plateau age from the granite of the LHS in the Taplejung Window was found to be 1.5 Ga (Upreti et al. 2002). Further analyses of the rocks yielded 1.5-1.6 Ga $^{40}Ar/^{39}Ar$ muscovite age spectrum of same granite indicating the pattern of degassing of Ar gas, at 960-1300 °C (about 88% 39 K). This result indicates that the granitic rocks have undergone weak metamorphism and the magmatic age must be older than 1.6 Ga (Takigami et al. 2002). The thrust sheet comprising the Higher Himalayan Crystallines (HHC) and forming the hanging wall of the MCT exposed around the window, and which has traveled far south reaching very close to the MBT, consists of amphibolite facies rocks, such as garnet-kyanite-sillimanite banded gneiss, calcic gneiss, granitic gneiss, and quartzite with incipient traces of mobilization in the upper section.

The area is affected mainly by two deformational episodes: (1) syn-MCT metamorphic deformation and (2) post-MCT metamorphic deformation. The syn-MCT metamorphic deformation is represented by S-C structure preserved in phyllite, schist, and augen gneiss indicating the top-to south shearing sense and NNE trending mineral lineation marked by mica and kyanite, related to the direction of the movement along the MCT. The post-MCT metamorphic deformation is well marked by the formation of Taplejung Window, Tamor River anticlinal dome, new generation foliations, longitudinal folds and extensional features, during the southward propagation of the MCT. In the northern part of the Taplejung window of LHS and HHC, the rocks dip towards north-northeastwards while in the southern part, the rocks dip towards south. The rocks dip due east in the eastern part. The window is thus a large dome shaped anticline, known as Tamor Khola Dome (Schelling and Arita 1991). In the southern part of the frontal belt near to MBT, the rocks of LHS and HHC dip towards north.

At least two metamorphic episodes are observed in the region. The phyllite and quartzite of the LHS exhibit a relict, pre-MCT isotropic fabric (deformed granoblastic mosoic), incorporated by prominent anisotropic fabric imposed during the syn-MCT metamorphism. The syn-MCT metamorphism is marked by the inverted metamorphic zonation with well-characterized Barrovian type isograds in the footwall of the MCT. The isograd in the LHS gradually decreases from garnet to the chlorite in the lower section. The kyanite isograd is achieved above the MCT and the silliminaite appears towards the upper section of the HHC. 16 to 25 Ma $^{40}Ar/^{39}Ar$ muscovite ages from the augen gneiss (Ulleri-type augen gneiss) of the LHS in the Taplejung Window clearly belong to the Neo-Himalayan metamorphic event or syn-MCT metamorphic episode. The chlorite crystals in the HHC gneiss are obliquely oriented with respect to the main foliation, and the conversion of the garnet to chlorite suggests the incipient of the retrogressive metamorphic event occurred during the post-MCT metamorphic deformation. The pressure-temperature conditions of the LHS and HHC rocks are not calculated.

The tectono-metamorphic evolution of the LHS and the HHC can be summarized as follows: The pre-MCT phase is characterized by prograde regional metamorphism. The syn-MCT phase resulting from the movement along the MCT gave rise to the inverted metamorphic event. The movement along the MCT exhumed the metamorphic rocks of HHC to the mid crustal level. During the continued movement along the MCT, a domal uplift resulted into the Tamor River domal anticline, and the HHC thrust sheet moved southwards over the LHS to reach near the MBT. This domal structure and the development of the longitudinal folds in the HHC may be related to the southward propagation of the MCT. Finally, the tectonic uplift and intense denudation resulted into deep incision of the rocks of HHC, and the rocks of LHS exposed forming the Taplejung Window during the post-MCT deformation.

References

Rai SM, BN Upreti and H Sakai. 2001. Geology, structure and metamorphism of the Taplejung Window and frontal belt, Eastern Nepal. *J Nepal Geol Soc* **24**: 26-28

Schelling D and K Arita. 1991. Thrust tectonics, crustal shortening, and the structure of the far eastern Nepal. *Tectonics* **10**(5): 851-862

Takigami Y, H Sakai and Y Orihashi, Y. 2002. 1.5-1.7 Ga rocks discovered from the Lesser Himalaya and Siwalik belt; $^{40}Ar/^{39}Ar$ ages and their significances in the evolution of the Himalayan orogen. *Geochim Cosmoch Acta* **7**: p 39-40

Upreti BN, Y Takigami, SM Rai and H Sakai. 2002. 1.5 Ga granite from the Lesser Himalayan Sequence. Abst H-K-T Int sem Sikkim India

Upreti BN, SM Rai, H Sakai, DR Koirala and Y Takigami. 2003. Early Proterozoic granite of the Taplejung Window, far eastern Lesser Nepal Himalaya. *J Nepal Geol Soc* **28**: 9-18

The Rare Earth Element geochemistry of Mesoproterozoic clastic sedimentary rocks from the Rautgara Formation, Lesser Himalaya: Implications for provenance, mineralogical control and weathering

SA Rashid

Department of Geology, AMU, Aligarh - 20200, INDIA

For correspondence, E-mail: rashidamu@hotmail.com

The geochemical studies of clastic sedimentary rocks have attracted attention of several scientists in the world primarily to understand their source rock compositions, paleoclimatic conditions, tectonic setting and in turn to examine the nature and composition of the upper crust through time (Bhatia 1985, Taylor and McLennan 1985, Condie 1993, McLennan et al. 2000). Damta Group (consisting of Chakrata Fm and Rautgara Fm) which is considered to be the oldest and best-preserved supracrustal pelite-quartzite successions in the inner carbonate belt of the Lesser Himalaya (Valdiya 1998) is best suited for this kind of studies. The Mesoproterozoic clastic sedimentary rocks, comprising pelites and quartzites from the Rautgara Formation in and around Rudraprayag, Garhwal region, Uttaranchal, Lesser Himalaya, have been analysed for major and trace elements including Rare Earth Elements (REEs) to evaluate their provenance and weathering history. Except few studies (Bhat and Ghosh 2001, Rashid 2002) the sedimentary geochemistry is almost unattended in the Himalayas despite their occurrence as most abundant rock type. In this context any work from the Himalaya may be considered as a significant contribution towards understanding the Precambrian upper crustal composition in the Himalayan region.

The pelitic rocks from the Rautgara Fm are characterised by moderate SiO_2 and Al_2O_3 contents and show consistent REE patterns with LREE (light REE) enriched and HREE (heavy REE) depleted patterns (La_N/Yb_N=7.4– 10.3). The total REE abundances are high (up to 266 ppm) with large negative Eu-anomalies (Eu/Eu^*=0.57 to 0.64). The REE characteristics of the Rautgara pelites compare very well with the average post-Archean REE patterns of European Shales (ES), Post Archean Shales from Australia (PAAS) and North American Shale Composite (NASC). Except high SiO_2 contents, the other major and trace element concentrations are significantly low in the associated quartzites. Although the quartzites contain low REE abundances (up to 41 ppm) their patterns including negative Eu anomalies are akin to pelites, suggesting that both the rock types be derived from

similar source. The Chemical Index of Alteration (CIA) and A-CN-K plot (Nesbitt and Young 1984) indicates that moderate chemical weathering has taken place in the source region of the Rautgara rocks. The linear correlation coefficients between Al_2O_3, K_2O, TiO_2 and total REE reveal that the accessory minerals (mainly Ti-bearing phases) have hosted the REEs (Taylor and McLennan 1985, Condie 1993).

The evolved felsic composition of the rocks probably related to widespread acidic igneous activity in the source. Besides the provenance, the sedimentary REE patterns seem to have been affected by sedimentary environment also. The paleocurrent studies in the area (Valdiya 1998) indicate that the granitoid rocks from the Aravalli mountain belt and Bundelkhand massif have supplied detritus to the Lesser Himalayan Rautgara sedimentary basin.

References

Bhat MI and SK Ghosh. 2001. Geochemistry of the 2.51 Ga old Rampur group pelites, western Himalayas: implications for their provenance and weathering. *Precambrian Research* **108**: 1-16

Bhatia MR. 1985. Rare earth element geochemistry of Australian Paleozoic graywackes and mudrocks: Provenance and tectonic control. *Sedimentary Geology* **45**: 97-113

Condie KC. 1993. Chemical composition and evolution of the upper continental crust: contrasting results from surface samples and shales. *Chemical Geology* **104**: 1-37

McLennan SM, A Simonetti and SL Goldstein. 2000. Nd and Pb isotopic evidence for provenance and post-depositional alteration of the Paleoproterozoic Huronian Supergroup, Canada. *Precambrian Research* **102**: 263-278

Nesbitt HW and GM Young. 1984. Prediction of some weathering trends of plutonic and volcanic rocks based on thermodynamics and kinetic considerations. *Geochim et Cosmochim Acta* **48**: 1523-1534

Rashid SA. 2002. Geochemical Characteristics of Mesoproterozoic Clastic Sedimentary rocks from the Chakrata Formation, Lesser Himalaya: implications for crustal evolution and weathering history in the Himalaya. *Journal of Asian Earth Sciences* **21**: 285-295

Taylor SR and SM McLennan. 1985. *The continental crust: its composition and Evolution*. Blackwell, Oxford

Valdiya KS. 1998. *Dynamic Himalaya*. Universities Press, Hyderabad

Slow mass movement in the Kangchenjunga Area, Eastern Nepal Himalaya

Dhananjay Regmi* and Teiji Watanabe

Graduate School of Environmental Earth Science, Hokkaido University, Sapporo 060-0810, JAPAN

* To whom correspondence should be addressed. E-mail: regumi@ees.hokudai.ac.jp

Solifluction collectively represents slow mass wasting processes associated with freeze-thaw action (Ballantyne and Harris 1994, French 1996). Solifluction operates slowly, in general, at a rate of at most 1 m year^{-1}. Solifluction, nevertheless, contributes greatly to the evolution of mountain landscapes because of its widespread coverage on mountain slopes. Beside large coverage of periglacial environment, no efforts have yet been made in the cold region of the Nepal Himalaya, which is characterized by high relief, steep slope, and concentrated monsoon precipitation. This study attempts to quantify the rate and depth of displacement of the solifluction lobe in the uppermost part of the Ghunsa valley in the Kangchenjunga area **(Figure 1)**.

The accumulated displacement was measured using non-electric probe, i.e., glass fiber tubes at sites A and B **(Figure 1)** from 7 November 1998 to 26 November 2001. Soil auger, 1-m long and 13 mm in diameter was used to make a hole in the ground. The fiber tube in one side was tied with a small nut-bolt to prevent from uplifting by frost heaving. The side with nut-bolt was placed downward and inserted inside the ground with the help of steel pipe. The remaining gap was filled with fine soil. To obtain the displacement rate, the ground was excavated after two years and

carefully scratched from one side of the fiber tube leaving another side sticking with the ground.

An improved strain probe method (Yamada and Kurashige 1996) was used to monitor continuous soil displacement from 1 December 2001 to 21 September 2002 at site B. An automatic data logger (KADEC-U of KONA System Co.), which stores data at intervals of one hour, was connected to the strain probe.

In addition, ground temperatures and soil moisture were monitored in order to understand the solifluction process. Ground temperatures of the solifluction lobes were monitored at three different depths of 6, 12 and 18 cm using data loggers (Thermo Recorder TR-52 of T & D Co.) from 24 April 2001 to 21 September 2002. Furthermore, the year-round ground temperature data taken on the mid-slope at 5433 m in altitude were used to show the general ground thermal condition. The soil moisture was measured only for 22 days from 19 April to 11 May, 2002. Soil moisture was measured by a soil moisture sensor (Theta Probe Type ML2x of Delta -T Devices Ltd) with ± 1% accuracy. Rain gauge was installed on the mid-slope at 5235 m in altitude from 21 April to 22 September, 2002 **(Figure 1)**. Precipitation data were recorded in a logger (HOBO Event of

FIGURE 1. Location of the study area
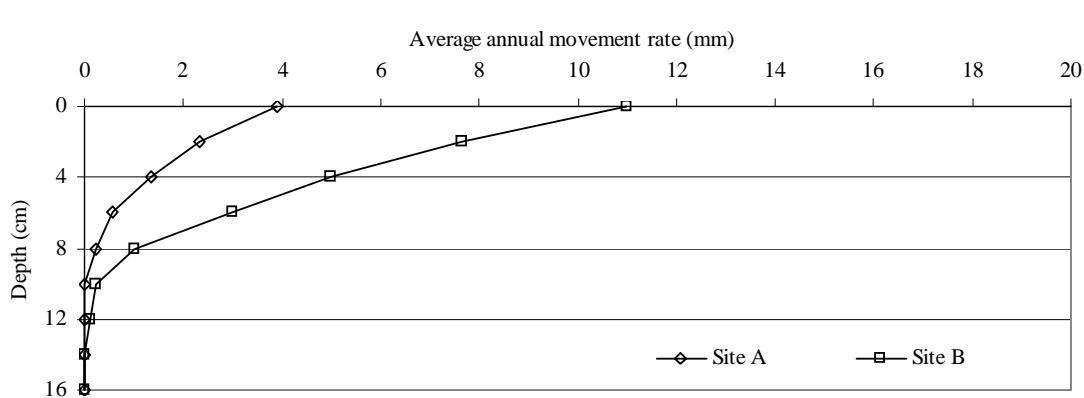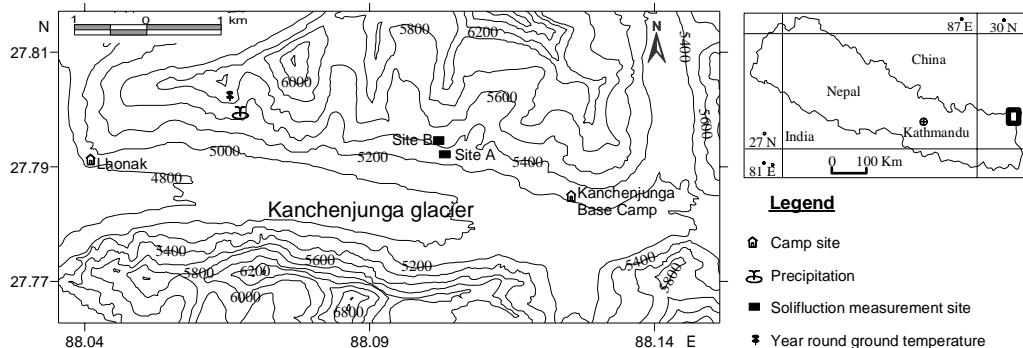
FIGURE 2. Average annual accumulated displacement rate of solifluction lobe at sites A and B
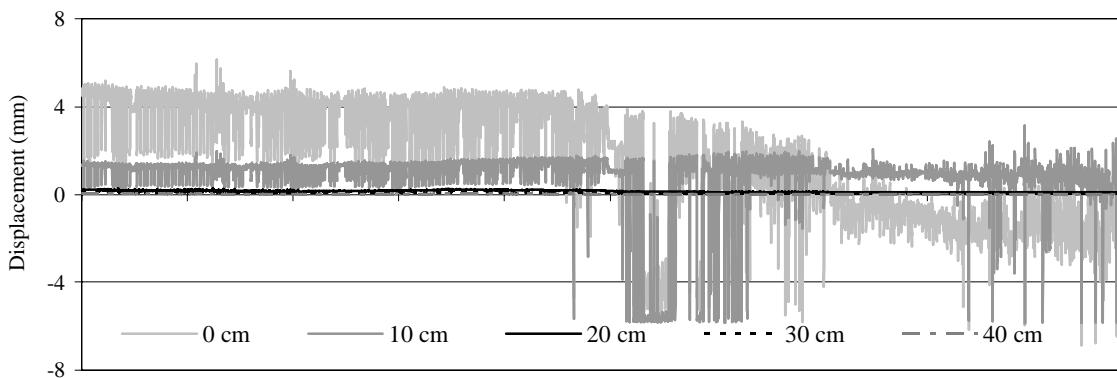
FIGURE 3. Displacement of soil at 0 cm, 10 cm, 20 cm, 30 cm and 40 cm depth from 1 December 2001 to 21 September 2002 at 5408 m (site B)

Onset Computer Co.) connected to a standard tipping-bucket rain collector.

The average movement rate of the glass fiber tubes at 5412 - 5414 m altitude with slope angle of 31° was about 11 mm/year, which was almost three times larger than that observed at 5322 - 5325 m with 22° slope angle (**Figure 2**). There was no significant difference in the depths which caused displacement at both sites. The continuous displacement near the ground surface at 5414 m shows permanent downslope movement from the middle of June. It may be attributed to high moisture supply in soil derived from precipitation. The amplitude of the displacement cycle was the largest at the ground surface, decreasing with increasing depth: the amplitude at and below 20 cm in depth is virtually zero (**Figure 3**). Although the soil moisture rises at each depth after precipitation events, the soil moisture content in general is very low. The low moisture content and the absence of freeze-thaw during monsoon period may be major factors leading to the slow rate of downslope displacement in this area.

References

Ballantyne CK and C Harris. 1994. *The Periglaciation of Great Britain*. Cambridge University Press, Cambridge. 325 p

French HM. 1996. *The Periglacial Environment*, 2nd ed. Longman, Essex. 309 p

Yamada S and Y Kurashige. 1996. Improvement of strain probe method for soil creep measurement. *Transactions Japanese Geomorphological Union* **17**: 29-38

Contrasting Pressure – Temperature Evolution of Pelitic Schists, Gneisses and Eclogites in Kaghan-Naran Valley, Pakistan Himalaya

Hafiz U Rehman†§ *, Hiroshi Yamamoto† , Yoshiyuki Kaneko‡ and AB Kausar§

†Department of Earth and Environmental Sciences, Kagoshima University, Kagoshima 890-0065, JAPAN
‡Graduate School of Environment and Information Sciences, Yokohama National University, Yokohama 240-8501, JAPAN
§Geoscience Laboratory, Geological Survey of Pakistan, Shahzad Town, Islamabad, PAKISTAN

* To whom correspondence should be addressed. E-mail: gsehafez@moon.sci.kagoshima-u.ac.jp

A classical example of Barrovian type metamorphic sequence is observed in pelitic schists, gneisses and eclogites from Balakot in the southwest to Babusar Pass in the northeast, Kaghan – Naran Valley, Pakistan Himalaya. This sequence comprises the first appearance of chlorite followed by biotite, garnet, staurolite, kyanite and sillimanite. Based on mineral chemistry, pressure – temperature conditions of garnet, staurolite, kyanite zones and eclogites in kyanite zone were estimated as 6.2 – 6.9 kbar and 420 – 478 °C; 7.1 – 8.3 kbar and 558 – 605 °C; 12.8 – 14.6 kbar and 658 – 700 °C; and 27 – 32 kbar and 727 – 799 °C respectively (**Figure 1**).

Based on detailed field survey in the study area and petrography, the previously called basement and cover sequence of Higher Himalayan sequence from the structural bottom to top is recently classified into three tectonic units referred herein as unit I, II and III (this study). Unit I mainly comprises the basement sequence and has a tectonic contact with the Main Central Thrust to the southwest. This unit mainly consists of pelitic schists and gneisses. Unit II representing ultrahigh-pressure (UHP) metamorphism, is sandwiched in between units I and III. It constitutes the lower cover having pelitic schists; gneisses; felsic gneisses, calcareous gneisses/marbles and eclogites, while unit III is uppermost part of the cover sequence and has a tectonic juxtaposition with low grade Tethyan metasediments locally and Main Mantle Thrust in particular to the northeast. It is also comprised of low grade pelitic gneisses.

Presence of coesite relics in clinopyroxene from eclogites and as inclusions in zircon in gneisses from Higher Himalayan crystalline rocks (unit II) gives evidence of deep continental subduction. Geothermal interpolations from petrological data and presence of coesite proves the hypothesis that deep continental subduction occurred when Indian plate collided with Asian plate sandwiching Kohistan Arc approximately at 53 Ma with the closure of Tethys. At the collision boundary marked by Main Mantle Thrust, continental rocks along with oceanic crust subducted beneath Kohistan Arc reaching about 100 ± 10 km depth.

Tectonic setup and relative P – T conditions (**Figure 2a, b**) interprets that the grade of metamorphism in Higher Himalayan sequence increased towards north close to the subduction front. Ultrahigh-pressure metamorphism took place in unit II when it reached to a considerable depth sufficient for the development of coesite. At this event the felsic/pelitic rocks metamorphosed to UHP gneisses and basaltic sills and flows metamorphosed to eclogites. The UHP rocks underwent medium-pressure Barrovian metamorphism during their exhumation stage. SHRIMP data for zircon core and rims from the felsic gneisses of unit II close to eclogite body yields the protolith age as of 253-170 Ma and UHP metamorphic age as 46.2 ± 0.7 Ma (Kaneko et al. 2003). Petrologic and P – T data indicate that these rocks exhumed to earth surface from depths of up to about 90~110 km evidenced by coesite retrogression to quartz and omphacite to amphibole in eclogites.
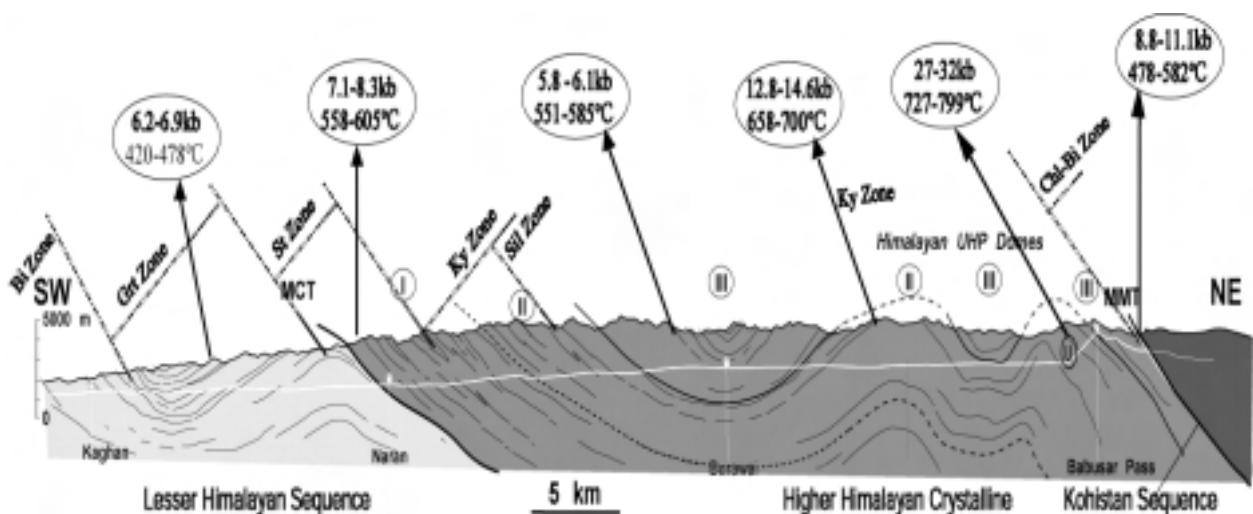
FIGURE 1. Cross section map of Kaghan – Naran Valley showing Thermobaric structure with P – T data for Grt, St, Ky zone of Unit I, II and III. Ⓤ shows UHP rocks locality.
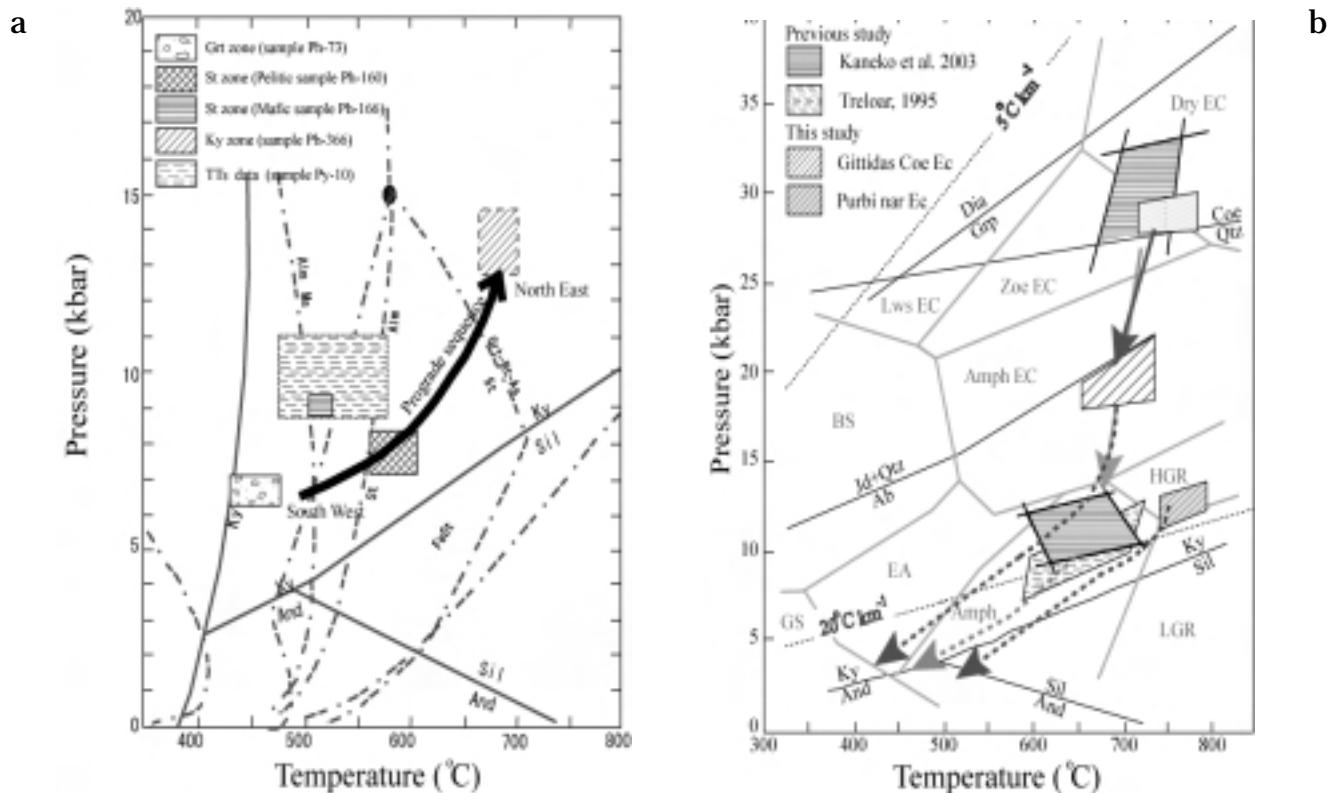
FIGURE 2. (a) Pressure-Temperature plot from gr, st, st-ky zones of pelitic rocks and from Tethyan metasediments in the Kaghan valley. P-T conditions are obtained from Thermocalc software (Powell and Holland 1988). P-T grids for petrogenic phases, stability fields for biotite, garnet, staurolite and aluminosilicates, and reaction curves are adopted from KFASH System of Spear and Cheney (1989). (b) Pressure-Temperature plot of the Kaghan UHP rocks calculated from the average P-T conditions of Thermocalc software after Powell and Holland (1994). The P-T conditions of Kaghan gneiss (Treloar 1995) and (Kaneko et al. 2003) are shown for comparison.

References

Kaneko Y, I Katayama, H Yamamoto, K Misawa, M Ishikawa, HU Rehman AB Kausar and K Shiraishi. 2003. Timing of Himalayan ultrahigh-pressure metamorphism: sinking rate and subduction angle of the Indian continental crust beneath Asia. *J Metam Geol* **21** (6): p 589-99

Powell R and TJB Holland. 1988. An internally consistent dataset with uncertainties and correlations. III. Application methods, worked examples and computer program. *J Metam Geol* **l6**: 173-204

Powell R and TJB Holland. 1994. Optimal geothermometry and geobarometry. *Amer Miner* **79**: 120-133

Spear FS and JT Cheney. 1989. A petrogenitic grid for pelitic schists in the system SiO2-Al2O3-FeO-MgO-K2O-H2O. *Contrib Miner Petrol* **101**: 149-164

Treloar PJ. 1995. Pressure-temperature-time paths and the relationship between collision, deformation and metamorphism in the north-west Himalaya. *Geol Jour* **30**: 333-348

Paleomagnetic study of the Late Jurassic formations in Northern Qaidam basin and tectonic implications

Shoumai Ren‡*, Zhenyu Yang†, Zhiming Sun† and Junling Pei†

†Institute of Geomechanics, Chinese Academy of Geological Sciences, Beijing, 100081, CHINA
‡Strategic Research Center for Oil and Gas Resources, Ministry of Land & Resources, Beijing, 100034, CHINA

* To whom correspondence should be addressed. E-mail: realshaw@vip.sina.com

According to the paleomagnetic study from the Upper Jurassic red beds along the Altyn Tagh Fault, some researchers suggest that the Jurassic blocks in the Altyn Tagh Fault show significant relative clockwise rotation with respect to Tarim basin (16.2°±11.2°), but they also point out whether this rotation was representative of the whole Qaidam basin or was of a local character (Halim et al. 2003). In order to understand the tectonic evolution of the Qaidam basin in Late Jurassic and to confirm this rotation, we carried out the paleomagnetic study on the Upper Jurassic red and brown mudstones collected at seven sites near the Lulehe profile (38.15° N, 94.69° N) in the northern Qaidam basin. Thermal demagnetization up to 685 °C shows both low- and high- temperature components (LTC and HTC, respectively). LTC lie close to the recent geomagnetic field and seem to be a recent overprint. The HTC, carried principally by haematite and presenting a sole reverse polarity, passed the fold test at the 95 per cent confidence level. The palaeomagnetic pole calculated from the tilt-corrected six sites mean direction (D_s = 216.6°, I_s = -20.4°, α_{95} = 14.0°) is situated at 47.2° N, 215.1° E (dp/dm =7.7/14.7). The comparison of this result with coeval paleomagnetic poles from the western Qaidam basin (50.1° N, 198.0° E, dp/dm=5.0/8.6) reveals no obvious rotation (5.4°±13.1°) during Late Jurassic. This study also suggests that the Qaidam basin was likely one block and could have rotated as a whole in the Late Jurassic. The differences of palaeolatitude (8.2°), while the present location is similar, perhaps is the result that the Altyn Tagh Faults, which were strike-slipping as left-lateral since the Late Mesozoic (Liu et al. 2001). Comparing this study to the coetaneous palaeomagnetic poles from Tarim, the North China Block and the Eurasia (Table 1), the results suggest that northward convergence of the Qaidam block exists with respect to Tarim (14.3°±13.3°) since Late Jurassic, unlike the previous literature (4.5°±8.2°). A significant relative clockwise rotation of the Lulehe area with respect to Tarim basin seem to have occurred (11.1°±13.9°) without doubt. The overall NS convergence absorbed between Qaidam basin and Eurasia is 29.0°±14.0°, whereas that absorbed between the Qaidam and the NCB is 17.1°±12.2°. As mentioned in the previous literatures, we also think that the latter value is the result of the India-Asia collision, but the magnitude of convergence is not known.

References

Halim N, Y Chen and JP Cogné. 2003. A first palaeomagnetic study of Jurassic formations from the Qaidam basin, Northeastern Tibet, China-tectonic implications. *Geophys J Int* **153**: 20-26

Liu YJ, HW Ye, XH Ge, W Chen, JL Liu, SHM Ren and HX Pan. 2001. Laser probe ^{40}Ar/^{39}Ar dating of mica on the deformed rocks from Altyn Fault and its tectonic implications, western China. *Chinese Science Bulletin* **46**(4): 322-325

Gilder S and V Courtillot. 1997. Timing of the North-South China collision from New Middle to Late Mesozoic palaeomagnetic data from the North China Block. *J Geophys Res* **102**: 17713-27

Li YP, ZK Zhang, M McWilliams, R Sharps, YJ Zhai, YA Li, Q Li and A Cox. 1988. Mesozoic palaeomagnetic results of the Tarim craton: tertiary relative motion between China and Siberia. *Geophys Res Lett* **15**: 217-20

Besse J and V Courtillot. 1991. Revised and synthetic apparent polar wander path of the African, Eurasian, North American and Indian plates, and the ture polar wander since 200 Ma. *J Geophys Res* **96**: 4029-50

TABLE 1. Selected palaeopoles used for comparisons

Block	Age	Lat.	Long.	λp	ϕp	$p\lambda$	A_{95} (dp/dm)	Reference
Eurasia	140Ma	-	-	71.6	173	-	10.4	Besse & Courtillot, 1991
Qaidam(Huatugou)	J_3	38.46	90.75	50.1	198.0	19.2	5.0/8.6	Halim et al., 2003
Qaidam(Lulehe)	J_3	38.15	94.69	47.2	215.1	10.5	7.7/14.7	This study
North China	J_3	31.6	116.0	74.4	222.8	26.0	5.9	Gilder & Courtillot, 1997
Tarim	J_3 to K_1	42.0	81.6	64.6	208.9	24.3	9.0	Li et al.1988

Timing of synconvergent extension in NW Himalaya: New geochronological constraints from the Gianbul dome (SE Zanskar)

Martin Robyr† *, James M Mattinson‡ and Bradley R Hacker‡

† Institut of Mineralogy and Geochemistry, University of Lausanne,CH-1015 Lausanne, SWITZERLAND
‡ Geological Sciences, University of California, Santa Barbara, CA 93106-9630, USA

* To whom correspondence should be addressed. E-mail: martin.robyr@img.unil.ch

High-grade metamorphic rocks of the High Himalayan Crystalline Zone (HHCZ) of Zanskar are exposed as a 50 km large dome along the Miyar and Gianbul valleys in the NW Himalaya of India. This Gianbul dome is cored by migmatitic paragneiss formed at peak conditions of 800°C and 8 kbar. This migmatitic core is symmetrically surrounded by rocks of the sillimanite, kyanite ± staurolite, garnet, biotite, and chlorite mineral zones. The structural and metamorphic data from the Miyar-Gianbul Valley section reveal that the tectono-metamorphic evolution of the HHCZ in SE Zanskar is associated with a polyphase tectonic history involving converging nappe structures superimposed by opposite-directed extensional structures (Dèzes et al. 1999, Steck et al.1999, Robyr et al. 2002). The first tectonic event corresponds to an early phase of crustal thickening related to NE-directed movements. This phase most likely took place during Early to Middle Eocene, and it led to the creation of Shikar Beh nappe, thrusting toward the NE along the Miyar Thrust and responsible for the prograde metamorphic field gradient in the southern limb of the dome (Steck et al. 1999, Robyr et al. 2002). Beneath the Miyar Thrust, partial melting, related to this initial phase, occurred at temperatures between 750 and 850°C. In the northern limb of the dome, the Barrovian prograde metamorphism is the consequence of a second tectonic phase, associated with the SW-directed thrusting of the Nyimaling-Tsarap nappe. During this phase, some of the paragneiss were migmatized as a consequence of temperature up to ca. 800°C at depth down to ca.40 km (Dèzes et al. 1999, Robyr et al. 2002). Geochronological data reveal that this SW-directed phase occurred between Middle Eocene and Late Oligocene (Vance and Harris 1999, Schlup et al. 2003). Following these crustal thickening events, exhumation and doming of the HHCZ high-grade rocks were controlled by extension along the north-dipping Zanskar Shear Zone, in the frontal part of the Nyimaling-Tsarap nappe, as well as by extension along the south-dipping Khanjar Shear Zone, in the southern limb of the Gianbul dome. Rapid synconvergence extension along both of these detachments induced a nearly isothermal decompression, resulting in a high-temperature/low-pressure metamorphic overprint.

New geochronological dating of monazites from various migmatites in the footwall of the Khanjar Shear Zone indicates that these rocks cooled below T=725 °C at 26.6 Ma. On the other hand, geochronological dating of monazites from an undeformed leucogranitic dyke cross-cutting the extensional structures of the Kanjar Shear Zone reveals ages between 19.9 and 23.6 Ma. These results consequently indicate that ductile shearing along the Khanjar Shear Zone ended by 23.6 Ma and that extension most likely initiated shortly before 26.6 Ma. In the Gianbul Valley, geochronological results from various leucogranitic plutons and dykes in the footwall of the Zanskar Shear Zone indicates that partial melting on the NE-half of the Gianbul dome occurred between 19.8 Ma and 22.2 Ma (Dèzes et al. 1999). Partial melting in this part of the Himalayan range is collectively interpreted as

the consequence of the rapid exhumation of the high grade metamorphic rocks along the Zanskar Shear Zone, in good agreement with the isothermal decompression revealed by the P-T data. On basis of these observations, it is commonly assumed that the onset of extension along the Zanskar Shear Zone was not significantly older than 22.2 Ma. However, structural analysis and geometric modelling indicate that the exhumation of the migmatitic Gianbul dome occurred contemporaneously along both the Khanjar Shear Zone and the Zanskar Shear Zone, mainly because of the lack of a major thrust between the two extensional shear zones. It consequently appears that the extension along the Zanskar Shear Zone has to begin shortly before 26.6 Ma. This age is in good agreement with the data from the northernmost part of the HHCZ of Zanskar where Vance and Harris (1999) indicate a rapid decompression in the HHCZ rocks of 4kbar at 25 Ma and where Inger (1998) demonstrates that ductile deformation along the Zanskar Shear Zone was ongoing at 26 Ma.

The petrographic and quantitative P-T results for the Miyar section and for the Gianbul section provide information about the depth of burial of the studied samples, as well as about the thermal structure during the tectonic evolution of a complete transect across the Gianbul dome. On the other hand, the mapping and structural analysis of this transect constrain its kinematic evolution. These various data, together with the geochronological constraints, can be combined to propose a semi-quantitative reconstruction of the tectono-metamorphic evolution across the Gianbul dome (**Figure 1**).

During the first opposite-directed crustal thickening phases, the HHCZ high grade rocks were subducted down to ca.30 km depth, where temperature up to 850°C triggered partial melting. As a consequence, the relatively high buoyancy of these low-dense and low-viscous migmatites counteracted the downward pulling forces exerted by the still subsiding lithosphere. From that moment, the migmatitic rocks of the HHCZ of Zanskar were squeezed by the compressive forces exerted by the ongoing collision and the backstop represented by the sedimentary series of the Tethyan Himalaya. The presence of two major thrust zones directly above this migmatitic zone induced a weakness in the upper crust facilitating the exhumation of these high-grade low-viscosity migmatites. As a consequence, high grade rocks of the HHCZ of Zanskar have been forced to extrude in this part of the range, and eventually "pierced" through the Tethyan sedimentary cover as a large-scale dome structure. Once the onset of extension along these detachements is triggered, decompression drives partial melting, leading to the development of positive feedback between melting and decompression, and thus enhancing the rapid exhumation of these migmatites. Following this initial doming phase, further extension along the Zanskar Shear Zone associated with combined thrusting along the Main Central Thrust led to tectonically-controlled ductile extrusion of the HHCZ toward SW.

References

Dèzes P, JC Vannay, A Steck, F Bussy and M Cosca. 1999. Synorogenic extension: quantitative constraints on the age and displacement of the Zanskar Shear Zone (NW Himalayas). *Geol Soc Amer Bull* 111: 364-374

Inger S. 1998. Timing of an extensional detachment during convergent orogeny: New Rb-Sr geochronological data from the Zanskar shear zone, northwestern Himalaya: *Geology* 26: 223–226

Robyr M, JC Vannay, JL Epard and A Steck. 2002. Thrusting, extension, and doming during the polyphase tectonometamorphic evolution of the High Himalayan Crystalline Zone in NW India. *J Asian Earth Sci* 21: 221–239

Schlup M, A Carter, M Cosca and A Steck. 2003. Exhumation history of eastern Ladakh revealed by 40Ar/39Ar and fission-track ages: the Indus River–Tso Morari transect, NW Himalaya. *J Geol Soc London* 160: 385–399

Steck A, JL Epard and M Robyr. 1999. The NE-directed Shikar Beh Nappe: A major structure of the Higher Himalaya. *Eclogae geol Helvetiae* 92: 239-250

Vance D and N Harris. 1999. Timing of prograde metamorphism in the Zanskar Himalaya. *Geology* 27: 395-398
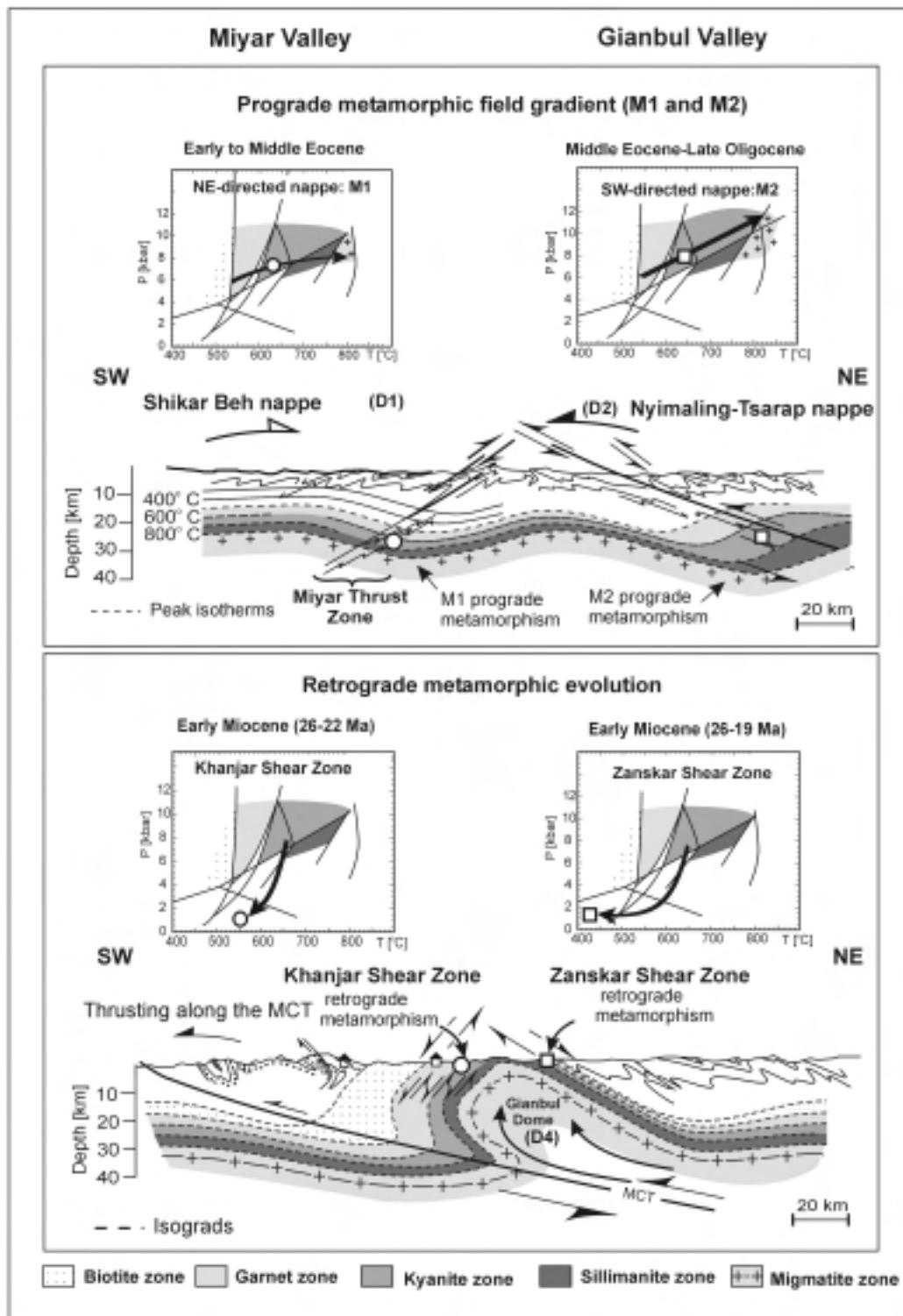
FIGURE 1. Semi-quantitative reconstruction of tectono-metamorphic evolution of the Gianbul dome

The importance of nummulites and assilina in the correlation of middle and upper Eocene rocks

Ghazala Roohi* and SRH Baqri

Earth Sciences Division, Pakistan Museum of Natural History (PMNH), Garden Avenue, Shakarparian, Islamabad, PAKISTAN

* To whom the correspondence should be addressed. E-mail: roohighazala@yahoo.com

The abundance and identification of the fossil forams was investigated in the Kohat Formation (U. Eocene), Kuldana Formation (U. Eocene) and the Chorgali Formation (M. Eocene) exposed in Kala Chitta and Margalla Ranges and representing the unstable and fluctuating environments of the vanishing Tethys Sea during the collision of the Indian and Eurasian subcontinents. The Kohat Formation and Kuldana Formation are missing further south towards the Salt Range where the marls and argillaceous limestones of the Chorgali Formation are unconformibly overlain by the continental sediments of Rawalpindi Group of Miocene age. The limestones and marls of the oldest Chorgali Formation and youngest Kohat Formation represent marine environments with abundant fossil forams and other marine fauna, while the red shales and sandstones sandwiches Kuldana Formation display continental environments with vertebrate fossils of mammals and reptiles. The Kuldana Formation also occasionally displays thin bands of limestones/marls, representing the unstable environmental conditions.

The detailed studies of fossils forams in these formations indicate the presence of mostly nummulites and assilina. The nummulites are abundant and dominant in the Chorgali Formation and in band intercalated with the continental sediment of the Kuldana Formation while assilina are subordinate. On the other hand, the assilina are dominant in the Kohat Formation with subordinate nummulites.

The fossil forams found in the Eocene rocks exposed in Kala Chitta Range, Margalla Range and Salt Range were compared and correlated with the forams found in the top beds of the Kirthar Formation, exposed further south at a distance of more than 1000 km, at Kotdiji , Khairpur and Rohri in the Sindh Province of Pakistan. The abundant limestone abundantly in Kirthar Formation display mostly with some assilina. It is most likely that the nummulites beds at the top of Kirthar Formation represent the same environment and time as the Chorgali and Kuldana Formations exposed in the north and younger beds at the top of Kirthar Formation are equivalent to Kohat Formation were eroded away during uplifting in the Oligocene times.

The deep process of the collision structure in northern Tibet revealed from investigation of the deep seismic profiles

Gao Rui*, Li Qiusheng, Guan Ye, Li Pengwu and Bai Jin

Institute of Geology, Chinese Academy of Geological Sciences, Beijing 100037, CHINA

* *To whom correspondence should be addressed. E-mail: gaorui@cags.net.cn*

In recent years, the crust and upper mantle structure of the northern Tibetan plateau has already attracted wide attention from geologists throughout the world. The collision generates not only in the southern Tibetan plateau but also in the northern part. The Tarim basin as a continental block not only has been obstructing the collision from the Indian continent, but also may have been subducting beneath the Tibetan plateau and generating collision, but the scale and deep process have not been fully understood yet. Therefore, probing the deep structure of the collision boundary in the northern Tibetan plateau is of special significance to comprehend the deep process of the intra-continent deformation caused by collision.

Since 1993, deep geophysical investigations have been carried out along the northern margin of Tibet across the basin-and-range conjectures. They include several deep seismic reflection profiles, wide-angle reflection and refraction profiles as well as broadband regional observation. They revealed the lithospheric structure of the northern margin of the Tibetan plateau at different tectonic layers. Some profiles and interpretations in detail will be discussing in this paper.

(1) The reflection image of the southward Tarim block subduction at a steep angle was found both in the West Kunlun (Gao et al. 2000) and Qilian profiles (Gao et al. 1995, 1999). In the Altyn profile, the shearing at a lithosphere scale constrains the subduction of the Tarim crust beneath the Tibetan plateau, but the Tarim mantle has already subducted beneath the plateau (Gao et al. 2001).

(2) Many groups of stronger reflections, dipping northwards under the west Kunlun Mts. and southwards under the southern margin of the Tarim basin, constitute the evidence for the collision between the Tarim basin and the Tibetan plateau (Gao et al. 2000, Kao et al. 2001). The image of reflection structure reveals the V-shaped basin-and-range coupling relationship between the west Kunlun Mts. and the Tarim basin on a lithosphere scale.

It should be particularly pointed out that a face-to-face collision pattern has not been found under the lithosphere of Tibetan plateau before. Based on the comparison of the face-to-face compression model with the deep seismic reflection profile of the Indian continent subduction beneath the southern Tibet and the seismic research of subduction residuals of the Tethys oceanic crust found under Yarlungzangbo suture, the authors consider that the north-dipping reflection under the west Kunlun Mts. should be caused by the subduction of the continental lithosphere. Although it cannot be determined whether it comes from India or Eurasia, a continental lithosphere is thrusting northwards along this thrust fault.

(3) The deep process of the normal collision and deformation are different from that of oblique collision. West Kunlun and the Qilian Mts. are both located at the position of collision and deformation, where the lithosphere of the Tarim is subducting southwards. Because West Kunlun is relatively close to the Indian plate, the Tarim lithosphere collided with the north-subducting Indian lithosphere under West Kunlun as the former subducted southwards for a short distance. The Altyn Mts. featuring oblique collision and deformation constrains the deep subduction of the Tarim crust beneath the Tibetan plateau because of strike-slipping and shearing of the lithosphere. However, in the mantle lid, low-angle south inclining reflections may reflect that the Tarim mantle has already subducted beneath the Tibetan plateau and resulted in detachment structure at the bottom of the crust. This may be the deep effect of the oblique collision.

(4) In the west Kunlun-Tarim and Qilian profiles, a thrust deformation zone has developed for about 50 km from the piedmont to the basins. And in the Altyn–Tarim profile, the deformation zone is about 120 km in width. This may be related to the angle of subduction and collision. In the Himalayan, the thrust deformation zone is about 200 km in width (Chen et al. 1999). The Indian plate is subducting along the MBT at a low angle. Therefore, deep processes of the collision deformation are different between the northern margin and southern margin of the Tibetan plateau.

References

Chen WP, CY Chen and JL Nabelek. 1999. Present-day deformation of the Qaidam basin with implications for intra-continental tectonics. *Tectonophysics* **305**: 165-181

Gao R, X Cheng and Q Ding. 1995. Preliminary Geodynamic Model of Golmud—Ejin Qi. *Geoscience Transect, Acta Geophysica Sinica (in Chinese)* **38** (II): 3-14

Gao R, X Cheng and Q Ding. 1999. Lithospheric structure and geodynamic model of the Golmud-Ejin transect in northern Tibet. *Geol. Society of America Special Paper* **328**: 9-17

Gao R, D Huang and D Lu. 2000. Deep seismic reflection profile across Juncture zone between Tarim basin and west Kunlun Mountain. *Science Bulletin* **45**(17): 1874-1849

Gao R, P Li, Q Li, Y Guan, D Shi, X Kong and H Liu. 2001. Deep process of the collision and deformation on the northern margin of the Tibetan plateau: Revelation from investigation of the deep seismic profiles. *Science in China* **44**(D): 71-78

Kao H, R Gao, RJ Rau, S Danian, R Chen, Y Guan and TW Francis. 2001. Seismic image of the Tarim basin and its collision with Tibet. *Geology* **29**(7): 575-578

Discussion on the dynamic system of China continent in Mesozoic-Cenozoic

Qiu Ruizhao†*, Zhou Su‡, Deng Jinfu‡, Xiao Qinghui§ , Cai Zhiyong¶ and Liu Cui‡

†Institute of Geology, Chinese Academy of Geological Sciences, Beijing 100037, CHINA
‡China University of Geosciences, Beijing, 100083, CHINA
§Information Center of Ministry of Land and Resources, Beijing, 100812, CHINA
¶ Guangzhou Institute of Geochemistry, Chinese Academy of Sciences, Guangzhou 510640, CHINA

* To whom correspondence should be addressed. E-mail: qiuruizhao@21cn.com

The lithosphere thinning and "Mesozoic metallogenic explosion" in east China was one one of the most noticeable scientific issues in recent decade. Regarding to its dynamic background, various view points have been proposed by the geologists both at home and abroad, and have become a hot spot to be widely concerned (Deng et al. 1996, Zhou et al. 2004). As a matter of fact, the granitic belt in Mesozoic and volcanic belt in Cenozoic running through different tectonic units in east China indicate that the process of compressive orogenic mechanism in Mesozoic and extensional rifting mechanism in Cenozoic actually are the common mechanisms that east China has faced. But what does it control or which geodynamic system does it belong to? The recent geological study on the Qinghai-Tibetan Plateau provides the important evidences to discuss it. Based on the comparison of the tectono-magmatic events and properties in Qinghai-Tibet Plateau and east China, the dynamic system of China continent in Mesozoic-Cenozoic has been discussed in this paper.

The same continental block is controlled by the same geodynamic-system. In the history of the formation of China continent, after Triassic the China continental blocks had been pieced together to form an entity; it should be controlled by the unified geodynamic system.

On the view of geological event sequences, the most important Mesozoic geological event of China continent was the development of Tethyan Ocean developed in the west and orogenic belt in east. Based on the study of ophiolite and granite in Qinghai-Tibetan Plateau, the geological event sequences and set up are shown in **Table 1**. It illustrates the process of Qinghai-Tibetan Tethyan Oceans in west China, represented by Bangong-Nujiang and Yarlung Zangpo, were opened simultaneously at

TABLE 1. tectonic evolution stages of Tethyan in Western Qinghai-Tibet Plateau

Stage	Epoch	Geological events	Bangonghu-Nujiang ophiolite belt	Yarlung Zangpo ophiolite belt
Ocean opened and developed	About J_1	Super plume activity	Oceanic basin opening gabbro magmatism(191+/-22Ma)	Oceanic basin opening gabbro magmatism(>180Ma) T_{DM} age of Nd isotopic is 180—220Ma
Oceanic-crust subduction	J_2-J_3(?)	Oceanic crust subduction	Metamorphic amphibolite is 179Ma in Dongqiao IAT volcanism is 140—167Ma boninite exposed in Dingqing and Shiquanhe	MORB, IAT volcanic boninite exposed in Rikeze IAT volcanism is less than 170Ma SSZ ophiolite
	K_1	Abundance Oceanic-crust subduction	Arc-igneous assemblages in North Gangdaze which relative with subduction and collision is 75-139Ma SSZ ophiolite O-type adakite	Arc-igneous assemblages in South Gangdaze which relative with subduction and collision is 65—110Ma
Collision	the end of K_1 to K_2	Collision & subduction	Arc-continent collision between Qiangtang and arc-island of North Gangdeze igneous assemblages which relative with collision distributing in North Gangdeze	Continuous subduction O-type adakite SSZ ophiolite with the on the active edge-arc of continent
	By the end of K_2	Collision between Gangdeze block and India continent	Intrusive rock and lava of post-collision	The bottom age of volcanic lava in Linzhou basin is about 65Ma Peak ages of granite distributing in South Gandeze is 40—65Ma
Post-collision	E-N	Subduction of intra-continent		Intrusive rock and lava of post-collision

early Jurassic under the reaction of super-plume on the platform setting in late Paleozoic Era. After that Tethyan Ocean had surpassed the stages of oceanic development, oceanic-crust subduction (Bangong-Nujiang $J_2 \rightarrow K_1$ and Yarlung Zangpo J_2(?) $\rightarrow K_2$) and collision (the collision of arc-continent in Bangong-Nujiang by the end of K_1; the collision of India-Asia plates in Yarlung Zangpo in K_2/E ($\approx$ 65 Ma, Zhou et al. 2004)).

However, in east China the Yanshanian compressive orogenic belt was developed. The recently determined Tectono-magmatic events (Deng et al. 2004) indicate that North China has surpassed a whole orogenic cycle of preliminary stage in J_1 and early stage in J_2 of orogeny $\rightarrow$ peak orogenic stage in $J_3 \rightarrow$ late orogenic stage in $K_1^1 \rightarrow$ post-orogenic stage in K_1^2; among them, thickening continental crust took place in J_1–J_2, and then the lithosphere was de-rooted at large-acreage after J_3. The most violent period of magmatic activities was in J_3-K_1^1, which was homologous with large-scale metallogeny of 130– 110 Ma and (120±10) Ma peak period (mostly range in 80– 160 Ma) of crust-mantle interaction. The key turning times of tectono-system from extrusion to extension was 140-150 Ma in North China, the time when thickness of lithosphere thinned in East-north China was 145 Ma, and the beginning time of lithosphere extension was 146 Ma indicated east China was really controlled by the same geodynamic system and has gone through the same orogenic process. The geological event sequences of orogenic movement in J-K period in North China are correspondent with Western

Tethyan evolution stages. Considering the deep process in J-K period, the development and evolution of Tethyan oceans in west China was a token of hot mantle-flow upwards with the process of extension with lithosphere thinning as a whole; while the compressive orogenic belt developed in east China was a token of cold mantle-flow downwards with the converging process of lithosphere and thickening as a whole.

In Cenozoic period, volcanic activities of 65– 25 Ma and <16 Ma in Qing Hai-Tibetan Plateau are also corresponding to the volcanic gyrations of Paleogene Period and Neogene-Quaternary Period in east China (**Table 2**); While on the deep process, the Qinghai-Tibetan Plateau entered the stage of post-collision and plateau uplifting after the collision of Europe-Asia plates at about 65Ma with the lithosphere converging and thickening, and the recycled crustal rocks had led to the down-going of cold mantle-flow; in east China the continental rifting was developed to form rift basin, marginal sea such as south-China Sea, Japanese sea with the lithosphere thinning by extensional mechanism, which is the token of a hot mantle-flow ascending upwards.

The comparison of the geological events in deep and shallow levels of the west and east China reveals that the time of both was simultaneous and their properties were compensating each other. So the China continent was controlled by a unified geodynamic system since Indosinian, *i.e.* the lithosphere/asthenosphere system (**Figure 1**), which just as what Deng (1996) has pointed out. Tomography geophysics reveals that the
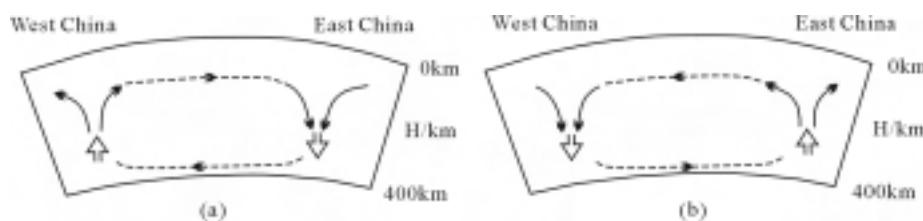

FIGURE 1. Sketch map showing the mantle convective beneath the China continet(after Deng et al. 1996) (a)Mesozoic (b)Cenozoic

TABLE 2. Volcanic events compareing between Qinhai-Tibet Plateau and North China

Volcanism correlative to the continental collision in Qinghai Tibetan Plateau	Volcanism correlative to the continental rifting in east China
（Ⅰ）volcanic erupting in Paleocene period	
Volcanism in Linzizong area is 63~39Ma Volcanism in Qiangtang area is 39~27Ma Muscovite-biotite-granite in south Gandeze is 35~23Ma	Rift basins and their volvanism in east China is 56~24Ma Japan Sea open in parallel in Paleocene period volcano arc in north-east Japan is 30~23Ma oceanic subduction belt is changed to steep ≥30 degree
（Ⅱ）late-Qligocene Epoch to early Miocene Epoch: volcanism stop	
Ground uplift, corroded and level planar formed (late Qligocene Epoch to early Miocene Epoch >15Ma)	basin reversed, corraded and level planar formed in North China in 24~16Ma Japan Sea opened at sector in 21~14 Ma
（Ⅲ）volcanic erupting in late teriary-fourthly	
Volcanism of Gangdeze is 16~10 Ma Volcanism in Kekexili is 15~8 Ma Volcanism in west Kunlun is 4.6~0.2 Ma Volcanism in west Qingling is 15~8 Ma	Rift basins and their volvanism in east China is 16~0.04 Ma Basalt erupting in Datong of Shanxi Province is 0.89~0.23 Ma Siliconic lava erupting is 0.5~0.04 Ma Volvano erupting in South-west Janpan Sea from Miocene Epoch to Pleistocene.

asthenosphere is ubiquitous at the depth of 400 km– 250 km under the China continent(Zhongxian Huang et al. 2003), which might be the link to connect the mantle convection under the China continent and the geological event sequences in west and east China. Since most of the granitic belts and the volcanic belts in east China are with NNE strikes as a whole, no doubt, which imply that the Pacific plate had also played an important role. Therefore, it comes to us that the China continent was controlled by a unified geodynamic system in Mesozoic-Cenozoic, and the granitic belt in Mesozoic, volcanic belt in Cenozoic of East China was the combined result of the systematic changing of lithosphere/ asthenosphere in China continent and the subduction of the Pacific plate.

References

Deng JF, HL Zhao, XX Mo and ZH Luo. 1996. *Continental Root-Plume Tectonics of China– Key to the Continental Dynamics.* Beijing: Geological Publishing House. 110-86

Deng JF, S Su and X Mo. 2004. The Sequence of Magmatic-Tectonic Events and Orogenic processes of the Yanshan Belt, North China. *Acta Geologica Snica* (for 32IGC, in the press)

Zhou S and X Mo. 2004. ^{40}Ar-^{39}Ar dating of Cenozoic Linzizong volcanic rocks from Linzhou Basin, Tibet and the geological implication. *Chinese Science Bulletin (in press).*

Zhongxian H, S Wei and P Yanju. 2003. Rayleigh wave tomography of China and adjacent regions. *Journal of Geophsical Research* **108**(B2, 2073): 1-10

Maximum extent of the Paleo-Kathmandu Lake in the late Pleistocene on the basis of piedmont gentle slope formation and lacustrine distribution in the Kathmandu basin, Nepal

Kiyoshi Saijo†* and Kazuo Kimura‡

†Division of Social Studies Education, Miyagi University of Education, Sendai 980-0845, Japan
‡Department of Social Science Study, Naruto University of Education, Naruto 772-8502, Japan

* To whom correspondence should be addressed. E-mail: saijo@staff.miyakyo-u.ac.jp

The Kathmandu basin is an intradeep located in the southern slope of the Nepal Himalaya. The basin, surrounded by ridges hanging around 2000 m asl, extends between the altitudes of 1200 and 1400 m asl and is filled by a thick sequence of lacustrine sediments deposited in the Paleo-Kathmandu lake during the Pliocene and Pleistocene. Several terrace surfaces, which occupy the basin floor, have been formed in response to the disappearance of the Paleo-Kathmandu lake, that was drained due to southerly erosion by the Bagmati river. This paper attempts to estimate the age and paleogeography in which the Paleo-Kathmandu lake was maximized and drained in terms of geomorphological investigation of the marginal area of the basin. In particular, characteristics of piedmont gentle slopes, lacustrine distribution, and the relationship between them are examined.

The piedmont gentle slope is well developed at the junction of the basin floor and the surrounding mountains. The piedmont gentle slope, dipping 7 to 15 degree towards the basin, shows a smooth surface with a slightly concave or almost linear vertical section. This slope coincides with alluvial and talus cones by Yoshida and Igarashi (1984), colluvial slope by Saijo (1991), and alluvial cone by Sakai et al. (2001). The piedmont gentle slope successively changes into the Gokarna surface in the direction of the basin in many places, and fades into narrow valleys in the back slopes. Surficial part (mostly less than 10 m deep) of the piedmont gentle slope is composed mainly of poorly sorted subrounded/subangular gravel or coarse sand with angular gravel. These sediments, tentatively called piedmont gentle slope deposit in this paper, are regarded as being of colluvial or fluvial origin. On the basis of their morphological characteristics and geomorphic settin integrated with the piedmont gentle slope deposit, it was determined that the piedmont gentle slope had been formed by debris supplied from the surrounding mountain slopes.

The organic clayey sediments were found at both northern and southern margins of the basin, and the piedmont gentle slope deposit overlies or interfingers with them. It is estimated, therefore, that these organic clayey sediments are considered to be lacustrine deposited near the shoreline of the lake at the foothills in a rising trend of lake level. Such deposits are recognized up to an altitude of between 1420 and 1440 m asl Several radiocarbon dates obtained from these lacustrine indicate that the uppermost part of them was deposited between 37100 and 29200 yr B.P. We can therefore conclude that the maximum level of the Paleo-Kathmandu lake reached at least 1420 to 1440 m asl and the lake occupied almost all of the basin around 30000 yr B.P. Judging from the relationship between the piedmont gentle slope deposit and the lacustrine, the debris derived from the surrounding mountains was frequently transported and flowed into the lake.

These estimates suggest a possibility that the Paleo-Kathmandu lake was drained not by the Bagmati river but another river. However, the cols on the divide of the surrounding mountains occur at the altitudes between 1465 and 1500 m asl. If we ignore tectonic movement, it is apparent that the altitudes of the cols were higher than the estimated maximum level of the Paleo-Kathmandu lake. In addition, the red weathered bedrocks are observed in topsoil of the cols on the divide. This also suggests that those cols were not covered by the lake water and overflow from the cols did not occur. It is estimated that the drainage of the lake by the Bagmati river occurred just after 30000 yr BP and the lake has been gradually reduced. The Gokarna surface emerged in conjunction with the drainage of the lake. Supply of the debris from the surrounding mountains continued even after the recession of the lake and resulted in the piedmont gentle slope formation.

References

Yoshida M and Y Igarashi. 1984. Neogene to Quaternary lacustrine sediments in the Kathmandu Valley, Nepal. *J Nepal Geol Soc* **4**: 73-100

Saijo K. 1991. Slope evolution since latest Pleistocene time on the north slope of Chandragiri, Kathmandu valley in the middle mountains of Nepal. *Science Reports of the Tohoku University, 7th Series (Geography)* **41**: 23-40

Sakai T, AP Gajurel, H Tabata and BN Upreti. 2001. Small amplitude lake level fluctuations recorded in aggrading delta deposits of the lower parts of the Thimi and Gokarna Formations (upper Pleistocene), Kathmandu Valley. *J Nepal Geol Soc* **25**: 43-51

Middle to late Pleistocene climatic and depositional environmental changes recorded in the drilled core of lacustrine sediments in the Kathmandu Valley, central Nepal

Harutaka Sakai and Members of Paleo-Kathmandu Lake Drilling Project

Department of Earth Sciences, Kyushu University, Ropponmatsu, Fukuoka, 810-8560, JAPAN

For correspondence, E-mail: hsake@rc.kyushu-u.ac.jp

Since October 2000, we have undertaken core-drilling for pure academic purposes at Kathmandu, Nepal, in order to clarify the continuous paleoclimatic records in the southern slope of the Himalaya and to reconstruct the depositional environmental changes of the ancient lake in Kathmandu (Paleo-Kathmandu Lake) during the last one million years. In this project, we also aimed to clarify the uplift history of the Himalaya and its linkage to paleoclimatic and paleo-environmental changes. We could have penetrated black muddy lacustrine sediments, called the Kalimati Formation, at western central part of the valley (RB core at Rabibhawan) in 2000 (Sakai et al 2001) and southern part of the valley (CP core at Champi and JK core at Jorkhu) in 2003 (**Figures 1 and 2**). We also could have penetrated the lower part of the fanglomerate, called Itaiti Formation and underlying Lukundol Formation which shows marginal lacustrine facies comprising of fluvial and swamp deposits in 2001 (Sakai 2001a).

The longest core drilled at Rabibhawan is 218 m in length and ranges in age from about 700 ka to 10 ka on the base of
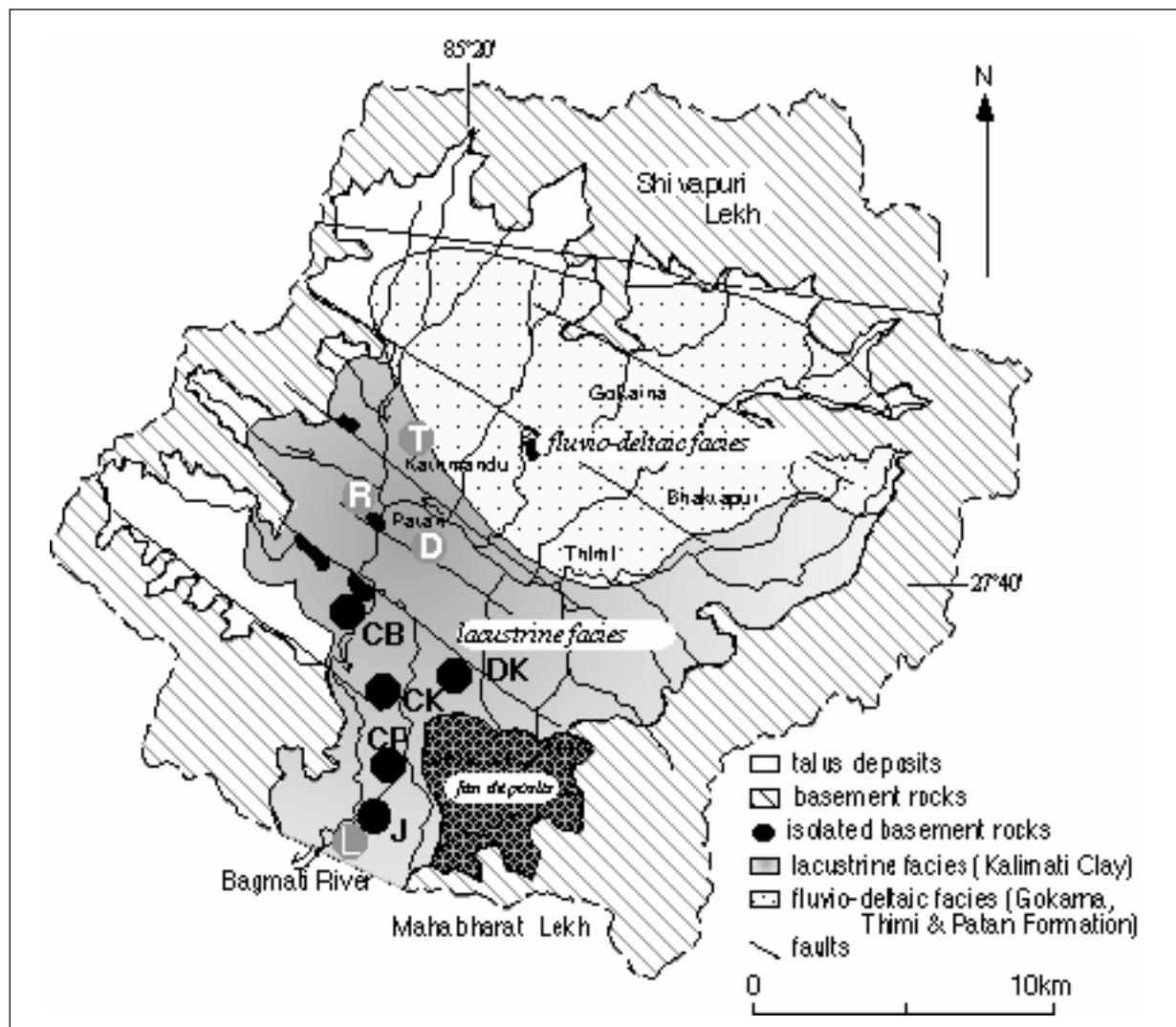

FIGURE 1. Geological outline map of the Kathmandu basin and location of drill-well by Paleo-Kathmandu Lake drilling project. Drilling was carried out in 2000 at T (Tri-Chandra Campus), R(Rabibhawan), D(Disaster Prevention Technical Center at Pulchawk). Drill sites in 2003 are CK (Chayasikot), DK (Dhapakel), CP (Champi) and J (Jorkhu). L: lukundol, CB (Chobal).

paleomagnetic study and AMS 14C dating. Judging from the paleo-magnitic and sedimentological studies of the core from the Lukundol and Itaithi Formation, muddy lacustrine sediments seems to have started their deposition at about 1 Ma. The sedimentaion rate of the muddy lacustrine sediments in the lower to middle parts is eastimated to be 0.2 mm/y, and that of the upper part is about 0.6 mm/y due to smaller compaction.

Surface geological survey in the southern part of the valley and sedimentological study of cores from the Lukundol area suggest that the lake was born by damimg up of the Proto-Bagmati river caused by debris flows and following deposition of fanglomerate originated from the Mahabharat Range (frontal range of the Nepal Himalaya) which has started its uplift at about 1 Ma (Sakai et al. 2002).

Three drilled cores at western central part of the valley commonly show that the lacustrine sediments, at 9 to 12 m deep, were eroded by river at about 12 ka. The draining out of the lake-water is likely to be triggered by earthquake, which caused by activation of earthquake fault like as Danuwargaun fault cutting the basin-fill sediments at the southern margin of the valley (Sakai 2001b). In the northern and eastern part of the basin, the muddy lacustrine sediments are covered with thick sandy lacustrine delta deposits, Gokarna and Thimi Formation, more than 80 m thick **(Figure 1)**.

Only one sand bed of 6 m thick is interbedded with muddy lacustrine deposits of RB core. It is attributed to an event bed formed by some tectonic or sedimentological event, because there is no depositional gap between the under- and overlying beds.

$\delta^{13}C$ value of organic lacustrine mud shows at least seven time fluctuation ranging from −30 to −19 ‰. A fluctuation diagram of pollen assemblage shows similar pattern to that of $\delta^{13}C$ value, and indicated that pollens of cold and dry climate increased when $\delta^{13}C$ has high value. It suggests that grasses including C4 plants expanded their distribution during the glacial period. Total organic carbon (TOC) and carbon/ nitrogen ration (T/N) shows inversed correlation with $\delta^{13}C$, and pollen concentration has good correlation with TOC and C/N. It implies that TOC and pollen concentration were controlled by land plants vegetated in the valley slope. When it was warm and wet climate, C3 land plants seem to have expanded their distribution.

Pollen concentration, total valves of diatom and C/N ratio before ca. 350 ka shows larger amplitude and larger value than those after 300 ka. During the middle Pleitocene from ca. 650 to 350 ka, frequency of diatom valves is characterized by monodominance of *Cyclotella* sp 1 and sp 2. These curious incidents are likely to be related to MIS stage 11 problem.

(Refer to papers by Fujii and Maki on the pollen analysis. On the geochemical study, refer to a paper by Mammpuku. A paper presented by Hayashi discusses on the environmental changes based on fossil diatom. The paleo-environmental changes are also discussed by Kuwahara on the basis of study on the clay minerals.)

References

Sakai H (ed). 2001. *Himalayan Uplift and Paleoclimatic Changes in Central Nepal.* J Nepal Geol.ogical Society (Special Issue) **25**: 155 p

Sakai H, R Fujii and Y Kuwahara. 2002. Changes in the depositional system of the Paleo-Kathmandu Lake caused by uplift of the Nepal Lesser Himalayas. *J Asian Earth Sciences* **20**: 267-276
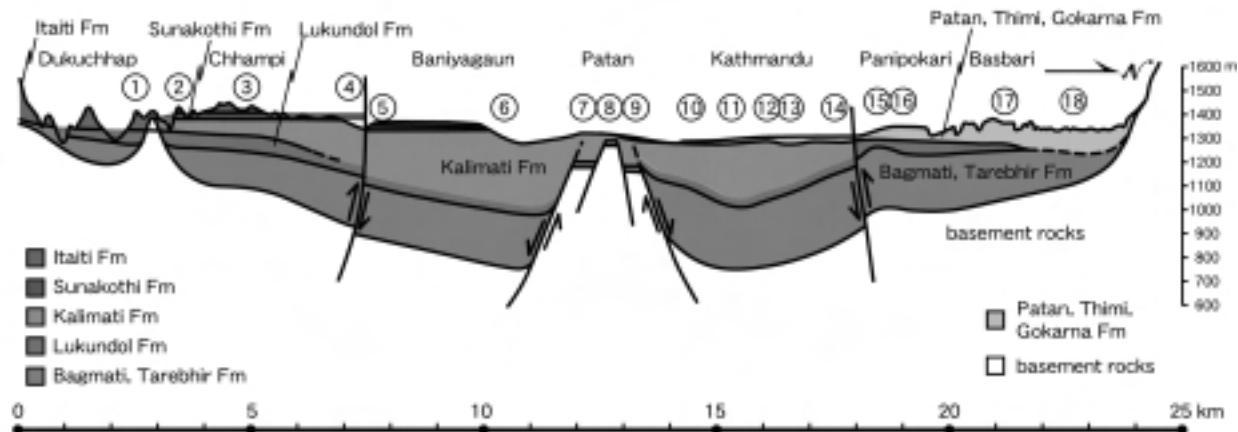
FIGURE 2. Geological cross-section of the Kathmandu Basin based on drill-core data and surface geological survey. No. 1~18: previous drill sites

Delta formations associated with high-frequency (annual?) lake-level fluctuations: An example from the uppermost Pleistocene Gokarna Formation, Kathmandu Valley, Nepal

T Sakai†*, AP Gajurel‡, H Tabata§ and BN Upreti‡

† Department of Geoscience, Shimane University, Matsue, Shimane 690-8504, JAPAN
‡ Department of Geology, Tri-Chandra Collage, Tribhuvan University, Ghantaghar, Kathmandu, NEPAL
§ Gifu Academy of Forest Science and Culture, Mino, Gifu 501-3714, JAPAN

* To whom correspondence should be addressed. E-mail: sake@riko.shimane-u.ac.jp

The Kathmandu Valley, one of the intermontane basins in the lesser Himalayan Belt, is filled with fluvio-lacustrine deposits dating from the Pliocene. After 5 ka BP, sediments in the central part of the basin occur as depositional terraces (Patan, Thimi and Gokarna terraces), the formation of which has been interpreted as being related to lake-level changes (Yoshida et al. 1984). The uppermost Pleistocene Gokarna Formation, which forms the Gokarna Terrace, has been interpreted as forming in conjunction with long-term lake-level rises associated with basin plugging and lake-level falls caused by lake water out-bursts at the basin outlet (Sakai et al. 2000). This formation is composed of small stacked Gilbert-Type delta successions, the thickness of each is up to 10 m. Small-scale, high-frequency lake-level fluctuation is especially recorded in the delta front deposits of the lower part of the formation that accumulated between ca. 50-35 ka. Based on the large number of fluctuations seen even in small outcrops, Sakai et al. (2001) inferred that these high frequency cycles were formed by annual lake-level changes. Our recent work has detected at least 21 cycles in a 40-m wide outcrop. Previous work was limited to the delta front, and broad scale stratigraphic architecture associated with the short-term fluctuations was thus unclear. Here we describe lateral facies changes of delta deposits formed in association with short-term lake-level changes and discuss their processes of formation.

Two types of delta deposits, juxtaposed in the same stratigraphic horizon, were identified in the lower part of the Gokarna Formation. Delta front deposits of the first type (type 1) are represented by 0.5-3 m thick, tabular cross-stratified sand and silt beds. The silt beds are continuous with prodelta deposits. Most of the silt beds pinch out near the top of the delta front, but some extend beyond the delta front and cover the delta plain sand beds deposited prior to the silt beds. Delta plain deposits of this type are characterized by lenticular, epsilon cross-stratified fluvial channel fill sand and silt beds and flood plain silt beds. Silt beds in the channel fill deposits continue into the surrounding flood plain silt beds in many cases. Delta front deposits of the second type (type 2) are characterized by thick, steeply dipping (ca. 30º) foreset sand beds. Thicknesses commonly reach 5-10 m. Small sand wedges (up to 1 m thick and 2-3 m wide) are frequently attached to the lower part of the foreset slope, and small gullies are developed in the upper part. The wedges contain tabular cross-stratification, are flat-topped, and are covered by thin trough cross-stratified fluvial channel fill deposits which are, in turn, overlain by delta front deposits prograded after sand wedge formation. In some delta front sand beds, inclined foreset beds tend to be flat to the up-dip direction and grade into trough cross-stratified sand beds with sheet-like geometry (up to 1 m thick), which are of braided stream origin.

The interbedded silt beds in the type 1 delta front deposits that continue from the prodelta and extend onto the delta plain deposits and those in the fluvial channel fill deposits spreading into the surrounding flood plain deposits suggest that they accumulated when the delta plain was inundated and delta progradation occurred during lake-level lowstand. The attached small delta wedges in the type 2 delta front topped by fluvial channels represent temporary deltas formed when lake level fell. This also indicates that type 2 delta progradation occurred mainly during lake-level highstand. Transition from delta front to braided stream deposits on the delta plain indicates some of the type 2 delta deposits accumulated during lake-level rise, when sediment accumulation on the delta plain was synchronized with lake-level rise. The differences in level of the tops of the delta front deposits and those of the attached sand wedges show that the amplitude of lake-level fluctuations was 6 m at most (average ca. 3 m). Changes in fluvial style from meandering (type 1) to braided streams (type 2) can be explained by alternating, possibly annual, wet and dry periods. In the lowstand phase (dry period), meandering streams0could develop due to lower water discharge. During lake-level rise (i.e. wet period), larger water discharge together with enhanced sediment supply could then produce braided streams.

The high-frequency lake-level fluctuation described above does not occur in the upper part of the Gokarna Formation. One possible explanation for the absence of cyclicity in this part of the succession is that the lake could then have been more extensive: if lakes are wider, larger volumes of water are required to produce fluctuations in level. Climate change is another possibility. Our age measurements show that the upper part of the Gokarna Formation was deposited at about 17 ka BP, indicating that accumulation occurred around the last glacial maximum. Both climate change and more extensive lake area may thus contribute to the absence of sediment cycles in the upper part of the Gokarna Formation.

References

Sakai T, AP Gajurel, H Tabata and BN Upreti. 2001. Small amplitude lake level fluctuations recorded in aggrading deltaic deposits of the lower parts of the Upper Pleistocene Thimi and Gokarna formations, Kathmandu Valley, Nepal. *J Nepal Geol Soc* **25**: 43-51

Sakai T, T Takagawa, AP Gajurel and H Tabata. 2000. Reconstruction of depositional environment and paleoclimate change from the Quaternary basin fill succession of the Kathmandu Valley, Nepal. Int Workshop Himalayan Uplift Climate Change. Program and Abstract, 27-31

Yoshida M and Igarashi Y. 1984. Neogene to Quaternary lacustrine sediments in the Kathmandu Valley, Nepal. *J Nepal Geol Soc* **4**:73-100

Temporal variation of glacial lakes since 1976 in the Great Himalayas revealed by satellite imageries

Nariyuki Sato† , Takayuki Shiraiwa‡ and Tomomi Yamada‡ *

† *Graduate School of Environmental Earth Science, Hokkaido University, Sapporo, JAPAN*
‡ *Institute of Low Temperature Science, Hokkaido University, Sapporo, JAPAN*

* *To whom correspondence should be addressed. E-mail: langmaljp@yahoo.co.jp*

The supra-glacial lakes are abundantly formed on the glacier tongues of debris-covered valley glaciers especially in the eastern Great Himalayas, which may be as a result of global warming. The lakes have frequently burst and hazardous floods have happened, since the lakes are dammed by an unstable moraine formed in the Little Ice Age (Yamada 1998). The flood is called Glacier Lake Outburst Flood (GLOF). The GLOF is a new face of the natural disaster newly arising in the Himalayas in the later half of 20th century and has been a serious problem for the socio-economical development of Himalayan countries such as Nepal, India, Bhutan and China.

Is the lake still newly born? How much are the lakes expanding? By using Landsat MSS and ETM imageries, respectively taken in 1976 and 2000/2001/2002, temporal variation of the lakes during 24 to 26 years are investigated in the northern and southern slopes of the Great Himalayas spreading over the longitude between 85º15′ and 91º00′ E. To examine the regional characteristics in the temporal variation of the lakes, the northern and southern slopes are divided into three sub-regions by River Arun running from Tibet to Nepal and River Kangpu from Tibet to Sikkim. Thus the covered area are divided into six sub-regions, which are called North-West (NW), North-Center (NC) and North-East (NE), which sub-regions belong Tibet, and South-West (SW, belonging eastern Nepal), South-Center (SC, eastern Nepal to western Sikkim) and South-East (SE, eastern Sikkim and Bhutan). The moraine-dammed glacier lakes more than 0.01 km²

in area are extracted from the imageries due to the limitation of the special resolution.

The numbers and area of the glacier lakes in each sub-region in 1976 and 2000s are shown in **Table 1**. Those of new lakes formed after 1976 are also shown in the Table. It is characterized that the total glacier area in the northern slope (Tibetan side) is larger than that in the southern slope, while the total number in the northern slope is less than that in southern slope, because the size of valley glaciers in the northern slope is remarkably larger than that in the southern slope. The number of present glacier lakes is totally 539 with the area of 122.46 km², which includes the count of new lakes formed after 1976. Total expansion area of the lakes amounts to be 37.47 km², including the total area of 10.25 km² for 35 lakes newly formed. Especially, the lakes in Bhutan (sub-region SE) have developed more than two times in the area, while 1.35 times on an average in the other sub-regions. As a result of examining the reasons of lake expansion in terms of global warming and the inclination of topography, where glaciers are situated, no clear relation is found in the global warming, but in the topography: The gentler an inclination of topography is, the more the glacial lakes develop.

Reference
Yamada T 1998. *Glacier lake and its outburst flood in the Nepal Himalaya.* Data Center for Glacier Research, Japanese Society of Snow and ice. Monograph No. 1. 96p

Table 1: Number and area of the glacier lakes in 1976 and 2000s, and also those of new lakes formed after 1976, in each sub-region.

Sub-region	1976		2000s		formed after 1976	
	Number	Area (km²)	Number	Area (km²)	Number of New Lake	Area of New Lake (km²)
NW	54	24.62	61	33.02	7	0.22
NC	70	15.29	90	20.76	20	1.86
NE	56	17.70	72	22.46	16	0.93
SW	89	11.47	121	17.83	32	1.15
SC	59	6.15	78	8.43	19	1.07
SE	82	9.76	117	19.96	35	5.02
Total	410	84.99	539	122.46	129	10.25

20 Ma of lateral mass transfer around the western Himalayan syntaxis

Eva Schill† * and William E Holt‡

† Institute of Geophysics, ETH Zürich, Hönggerberg HPP O14, CH-8093 Zürich, SWITZERLAND
‡ Department of Geoscience, State University of New York at Stony Brook, USA

* To whom correspondence should be addressed. E-mail: schill@mag.ig.erdw.ethz.ch

The thermodynamic evolution of an orogen can be subdivided into three stages depending on the relative rates of energy accumulation and dissipation. The first stage is mainly driven by plate tectonic forces and results in vertical thickening of the lithosphere. The present vertical thickening trajectory has been mapped using stress tensor inversion of earthquakes and runs from the western syntaxis via Tien Shan and NE Tibet to the eastern syntaxis (Schill et al. 2004a). After this first phase of energy accumulation, interplay of accumulative and dissipative processes dominates the second stage (Hodges et al. 2001). During the third stage the dominance of energy dissipation leads to the degradation of the orogen. The absolute deformation caused by one of these tectonic regimes depends among others on its temporal activity.

The regional configuration of forces in the India-Asia collision zone is characterized by a rotational compressional system caused by the counterclockwise indentation of the Indian plate (Patriat and Achache 1984) and a related extensional regime represented by the eastward extrusion of the Tibetan plateau (Tapponnier and Molnar 1977). In the frontal part of the collision zone, the Himalayan mountain belt, crustal thickening and potential energy dissipation are in equilibrium over time (Hodges et al. 2001). The frontal extrusion developed near the Oligocene to Miocene boundary and is limited by the South Tibetan detachment system (STDS) to the north and the Main Central Thrust (MCT) to the south (Hodges et al. 1996), while crustal thickening occurs mainly at the southern front of the Himalayan arc south of the MCT. To the north the former distal shelf of the Indian plate, the Tethyan Himalayas, represents the transition between the frontal and the E-W extrusion of the upper crust of the Tibetan plateau in the central and eastern part of the orogen. In this transition zone and further to the N in southern Tibet a dichotomy of the tectonic regime is indicate, e.g., by paleomagnetic data (Schill et al. 2004b, Schill et al. 2001) and the distribution of boiling springs (Hochstein and Regenauer-Lieb, 1998). Both information set reveal extrusion features in the central and eastern part indicated by the a large right lateral shear zone in the transition zone (Schill et al. 2004b) and a slip line solution for the observed heat lines (Hochstein and Regenauer-Lieb 1998). Around the western syntaxis stress tensor inversion (Schill et al. 2004a) and paleomagnetic investigation (Klootwijk et al. 1985) indicate a compressional regime with oroclinal bending around the syntaxis. The tectonic regimes are separated by the Karakoram fault. Both, Neogene tectono-morphologic evolution and geothermal data reveal that the present tectonic setting in southern Tibet and the Himalayas with frontal and lateral extrusion has been operational for about 10-20 Ma (Hodges et al. 2001, Hochstein and Regenauer-Lieb 1998).

From a thermodynamic point of view, oroclinal bending can be considered as lateral mass transfer without influence on the potential energy budget of the collision zone. Since no vertical thickening is involved, oroclinal bending is attributed to the second stage of orogeny. In order to investigate the transition between the first and second stage in the compressional part of the collision zone, we present a compilation of present rotation rates deduced from GPS measurements and the late-orogenic rotation pattern since 40-50 Ma deduced from paleomagnetic results. The evaluation of different correlations between both provides new constraints on the stability and the onset of oroclinal bending.

The Quaternary to present rotation pattern in the India-Asia collision is deduced from a joint inversion of Quaternary strain rates and 238 GPS velocities for a self-consistent velocity field (Holt et al. 2000). For equidimensional crustal blocks rotation rates can be calculated after Lamb (1987). This rotation pattern is characterized by counterclockwise and clockwise rotation rates of up to 10^{-16} rad/sec west and east of the Nanga Parbat Haramosh syntaxis, respectively.

The post-collisional rotation pattern is best represented by secondary remanence directions carried mainly by pyrrhotite with remanence acquisition ages between 50 and 40 Ma (Schill et al. 2002, Schill et al. 2001, Klootwijk et al. 1983). The acquisition age of secondary pyrrhotite remanences with a Curie temperature of ~325 °C and a formation temperature of >200 °C to 350 °C is deduced from $^{40}K/^{39}Ar$ and $^{40}Ar/^{39}Ar$ cooling ages with a closing temperature of about 300 °C and dated to 40 to 50 Ma. The paleo-rotation pattern in the Tethyan Himalayas in respect to the Eurasian plate is dominated by clockwise rotations W of the Nanga Parbat-Haramosh syntaxis. To the E, the counterclockwise rotation of NW Kashmir is supported by the Pliocence rotations in the Peshwar basin (Burbank and Tahirkheli 1985). This rotation pattern in conjunction with the rotations south of the Tethyan Himalayas (Klootwijk et al. 1985) pinpoints oroclinal bending around the western syntaxis. The remanence acquisition age provides the maximum age of rotations due to oroclinal bending. The consistency of the paleo-rotation pattern with the present rotation directions deduced from GPS measurements points to a long term stability of the rotation processes.

Linear extrapolation of the rotation rates from Quaternary strain rates and GPS measurements to the remanence acquisition time describe a linear correlation with the observed paleomagnetic rotations with a coefficient of determination of $R^2=0.60$. Since the age of remanence acquisition represents a maximum age for oroclinal bending, the rotation patterns of paleomagnetic results and GPS measurements have been calculated for different ages in 5 to 10 Ma steps between the remanence acquisition age and 5 Ma. At 20 Ma the correlation between the expected rotations from GPS measurements and the paleomagnetic rotations reveal a linear fit with a gradient a=1. Assuming a stable rotation velocity, this gradient indicates that the oroclinal bending related rotations initiated 20 Ma ago. The fact that the linear fit runs approximately through the origin minimizes the influence of earlier rotation processes on the absolute rotational motion. This implies that the onset of lateral mass displacement occurred at about 20 Ma, which can be considered the transition age from the first to the second stage of orogeny in the compressional part of the collision zone. The timing of onset of oroclinal bending is consistent with the right-

lateral motion at the southern end of the Karakoram fault since about 23 Ma (Lacassin et al. 2004) and the onset of doming in the Nanga Parbat-Haramosh massif in the Miocene (Schneider et al. 2001).

The inferred age of transition between stage 1 and 2 of orogeny of about 20 Ma is a Himalayan-wide event, which is reflected in onset of frontal extrusion and oroclinal bending in the extensional and compressional part of the orogen, respectively.

References

Burbank DW and RAK Tahirkheli. 1985. The magnetostratigraphy, fission trackdating, and stratigraphic evolution of the Peshawar intermontane basin, northern Pakistan. *Geol Soc Am Bull* **96**: 539-552

Hochstein MP and K Regenauer-Lieb. 1998. Heat generation associated with collision of two plates: the Himalayan geothermal belt. *J Volc Geotherm Res* **83**: 75-92

Hodges KV, JM Hurtado and KX Whipple. 2001. Southward extrusion of Tibetan crust and its effects on Himalayan tectonics. *Tectonics* **20**: 799-809

Hodges KV, RR Parrish and MP Searle. 1996. Tectonic evolution of the central Annapurna range, Nepalese Himalayas. *Tectonics* **15**: 1264-1291

Holt W.E., N Chamont-Rooke, X LePichon, AJ Haines, B Shen-Tu and J Ren. 2000. Velocity field in Asia inferred from Quaternary fault slip rates and Global Positioning System observations. *J Geophys Res* **105**(B8): 19185-19209

Klootwijk CT, PJ Conaghan and CM Powell. 1985. The Himalayan Arc: large-scale continental subduction, oroclinal bending and back-arc spreading. *Earth Planet Sci Lett* **75**: 167-183

Klootwijk CT, SK Shah, J Gergan, M. Sharma, B Tirkey and BK Gupta. 1983. A palaeomagnetic reconnaissance of Kashmir, northwestern Himalaya, India. *Earth Planet Sci Lett* **63**: 305-324

Lamb SH. 1987. A model for tectonic rotations about vertical axis. *Earth Planet Sci Lett* **84**: 75-86

Lacassin R, F Valli, N Arnaud, PH Leloup, JL Paquette, L Haibing, P Tapponnier, M-L Chevalier, S Guillot, G Maheo and X Zhiqin. 2004. Large-scale geometry, offset and kinematic evolution of the Karakorum fault, Tibet. *Earth Planet Sci Lett* **219**: 255-269

Patriat P and J Achache. 1984. India-Eurasia collision chronology has implications for crustal shortening and driving mechanism of plates. *Nature* **311**: 615-621

Schill E, S Wiemer and K Regenauer-Lieb. 2004a. Imprint of India in the Asian crust: large scale variation in earthquake-size distribution. *Geophysic Res Abstracts EUG General Assembly*, Nice

Schill E, E Appel, C Crouzet, P Gautam, F Wehland and M Staiger, 2004b. Oroclinal bending and regional significant clockwise rotations in the Himalayan arc - constraints from secondary pyrrhotite remanences. In: Weil A and A Sussmann (eds), *Orogenic curvature*, Geological Society of America Special Paper, in press

Schill E, E Appel, O Zeh, VK Singh and P Gautam. 2001. Coupling of late-orogenic tectonics and secondary pyrrhotite remanences: towards a separation of different rotation processes and quantification of rotational underthrusting in the western Himalaya (northern India). *Tectonophys* **337**: 1-21

Schill E, C Crouzet, P Gautam, VK Singh and E Appel. 2002. Where did rotational shortening occur in the Himalayas? - Inferences from palaeomagnetic remagnetisations, *Earth Planet Sci Lett* **203**: 45-57

Schneider DA, PK Zeitler, WSF Kidd and MA Edwards. 2001. Geochronologic constraints on the tectonic evolution and exhumation of Nanga Parbat, western Himalaya syntaxis, revisited. *J Geology* **109**: 563-583

Tapponnier P. and P. Molnar. 1977. Active faulting and tectonics in China, *J Geophys Res* **82**: 2905-2930

Occurrence of manganese ores in different tectonic settings in the NW Himalayas, Pakistan

Mohammad T Shah

National Centre of Excellence in Geology, University of Peshawar, Peshawar, PAKISTAN

For correspondence, E-mail: tahir_shah56@yahoo.com

In Pakistan, the occurrences of manganese ores have been reported in the Hazara area of North West Frontier Province, Kuram, Bajaur and North Waziristan agencies and the Lasbela-Khuzdar regions of Baluchistan. This study is mainly focused on the comparison of mineralogy and geochemistry of the manganese ores of Hazara and North Waziristan areas of Pakistan. The former occurs in the continental while the latter occurs in the ophiolitic sequences. In Hazara area, the ferromanganese ores are present in three localities (i.e., Kakul, Galdanian and Chura Gali) near Abbottabad within the Hazira Formation of the Kalachitta-Margala thrust belt of the NW Himalayas of the Indo-Pakistan plate. The Hazira formation of Cambrian age is a relatively thin unit (up to 150 m thick) of reddish-brown ferruginous siltstone, with variable amounts of clay, shale, ferromanganese ores, phosphorite and barite. It has a conformable lower contact with the Abbottabad Formation (Cambrian) and an unconformable upper contact with the Samana Suk limestone (Jurassic). In Waziristan area, the manganese ores occur in two localities (i.e., Saidgi and Barazai) within the Waziristan ophiolite complex, which is located along the western margin of the Indian plate in the north-western part of Pakistan. These ores, both banded and massive in nature, are hosted by metachert and generally overlying the meta-volcanics.

Mineralogicaly, the ferromanganese ores of Hazara area are divided into Kakul-Galdanian and Chura Gali ores. The Kakul-Galdanian ores contain relatively more hematite and less Mn-Fe phases such as bixbyite, partridgeite, hollandite, pyrolusite and bruinite than those of Chura Gali. Bixbyite and partridgeite are the dominant Mn-bearing phases in these ores. Among the gangue minerals iron-rich clay, alumino-phosphate minerals, apatite, barite and glauconite are present in variable amount in both the ore types. The textural behavior of the ore phases suggests recrystallization and remobilization during greenschist facies metamorphism. The Waziristan ores are dominantly composed of braunite with lesser amount of bixbyite and pyrolusite. Hematite occurs as additional minor phase in the ores of Shuidar area. Cryptocrystalline quartz is the only silicate phase occurring in these ores.

Chemically, composition of the Hazara ores differs from those of the Waziristan. In Hazara ores, Mn/Fe ratio is highly variable and ranges from 0.46 to 5.25. These ores exhibit a line of descent from LREE to HREE with a small positive Ce anomaly. Their ΣREE is higher than the hydrothermal Mn deposits and lower than the hydrogenous crust. The Waziristan ores are having Mn/Fe ratio in the range of 3 to 755. Their Major and trace elements data as well as the REE pattern, showing deep negative Ce anomaly, is typical of the submarine hydrothermal manganese ores. The petrochemical characteristics suggest that the ferromanganese ores of Hazara area have originated by a mixed hydrothermal-hydrogenetic source in shallow water or continental shelf environment due to the upwelling of anoxic deep seated water while the Waziristan manganese ores were formed along the sea-floor spreading centers within the Neo-Tethys Ocean and were later obducted as part of the ophiolite complex.

Geodynamics of Chamba Nappe, western Himalaya

BK Sharma*, AM Bhola and CS Dubey

Department of Geology, University of Delhi, Delhi, Delhi-110007, INDIA

* To whom correspondence should be addressed. bksharma@du.ac.in

Chamba Nappe is a SW-directed thrust sheet, which is composed of the Tethyan Sequence and was exhumed by thrusting along the Chamba thrust that is equivalent to the Panjal Thrust or the Main Central Thrust (MCT) over the Lesser Himalaya Sequence. Internal deformation within Chamba nappe is responsible for a large amount of crustal thickening and shortening (Sharma and Bhola 2004). The Chamba nappe is folded by regional scale fold *viz* the Chamba-Bharmaur syncline, Tandi syncline and Tisa anticline (Frank 1995, Sharma et al. 2003, Thakur 1998) and is the result of southwestward propagation of cover rocks on their basement (HHC) due to topographic uplift. The southward propagating thrust system also led to the development of major folds DF_1, DF_2 and minor DF_3 folds in a single progressive deformation.

DF_1 is the main compression phase, which corresponds to early SW-directed movements associated with the formation of the Chamba Nappe. Deformation associated with DF_2 phase propagated gradually from the Indus Suture Zone towards the SW as the Indian plate was progressively subducted below Asia along the Indus Suture Zone. DF_3 last phase is marked by kink-band formation as a result of brittle deformation in the slate/phyllites sequence due to amplification of Chamba nappe.

These deformations resulted with the southwestward-directed exhumation of the Tethyan Himalayan Sequence over the Higher Himalayan Crystalline. The southwestward propagation of the Chamba Nappe also affected the basal series of the Tethys Himalaya, which will ultimately form the High Himalayan Crystalline Sequence. In initial stage, mainly Proterozoic, basal series were still welded to the Tethys Himalaya, but as deformation proceeded, and as the Tethys Himalaya formed an increasingly thick stack of rocks, the lower part of the Tethys Himalaya became ductile enough to accommodate the compressive deformation through ductile shearing (Robyr et al. 2002). From that time onwards, the compressive forces were essentially concentrated along a ductile shear zone at the base of the Chamba nappe. Movements along Panjal thrust/Chamba thrust (MCT-1) zone contributed to the further underthrusting and metamorphism of the basal proterozoic series, which leads to the ultimate metamorphic differentiation between the Tethys Himalaya and the High Himalayan Crystalline Sequence.

References

Frank W, B Grasemann, P Guntli and C Miller. 1995. Geological map of the Kishtwar, Chamba and Kullu region, NW Himalaya, India. *Jahrbuch der Geologischen Bundesanstalt* **138**: 299-308

Robyr M, JC Vannaya, JL Epardb and Steck. 2002. Thrusting, extension, and doming during the polyphase tectonometamorphic evolution of the High Himalayan Crystalline Zone in NW India. *Jour Asian Earth Sci* **21**: 221–239

Sharma BK, AM Bhola and AE Scheidegger. 2003. Neotectonic activity in the Chamba nappe of the Himachal Himalaya: Jointing control of the drainage patterns. *Jour Geol Soc India* **61**: 159-169

Sharma BK and AM Bhola. 2004. Microstructures of co-axially folded vein segments and crenulation cleavage: Evidence for dissolution phenomena in the Chamba thrust sheet, Western Himalayas. *Episodes (in press)*

Thakur VC. 1998. Structure of the Chamba nappe and position of the Main Central Thrust in Kashmir Himalaya. *J Asian Earth Sci* **16** (2-3): 269-282

Geochemistry of biotite, muscovite and tourmaline from Early Palaeozoic granitoids of Kinnaur district, Higher Himachal Himalaya

Brajesh Singh* and Santosh Kumar

Department of Geology, Kumaun University, Nainital 263 002, Uttaranchal, INDIA

* To whom correspondence should be addressed. E-mail: bsinghng69@yahoo.co.in

Felsic magmatism exposed between Rakcham and Akpa regions is represented by Rakcham and Akpa granitoids in Kinnaur district collectively referred to as the Early Palaeozoic granitoids (EPG). Kwatra et al. (1999) have assigned Rb-Sr isochron age of 453±9 Ma with initial Sr isotopic ratio ($^{87}Sr/^{86}Sr$) of 0.737±0.002 for the granitoids of Rakcham area and 477±29 Ma with this ratio of 0.7206±0.00235 for the granitoids of Akpa region, which suggest episodic nature of Early Palaeozoic felsic magmatism derived from crustal protoliths. The EPG intrudes the granite gneiss (GGn) of the Central Crystalline Zone in the southern part of Higher Himachal Himalaya. The EPG and GGn belong to the Vaikrita Group, and are intruded by tourmaline bearing leucogranite (TLg) of Haimanta Group. The EPG are medium-to coarse-grained, porphyritic and bear qtz+Kfs+plag+bt+ms±zr ± ap±tur assemblage. Tourmaline mostly occurs in TLg as veins, pods and lenses but has also been found hosted in the EPG.

Modal mineralogy of EPG corresponds to monzogranite and granodiorite and suggests their nature typically as two-mica (biotite>muscovite) leucomonzogranite (*s.s.*) formed by partial fusion of crustal components. Based on mineral assemblages, occurrence of metasedimentary enclaves (xenoliths of country rocks or deeper lithology or restite from source), associated skarn-type tungsten mineralization and geochemical characters (SiO_2= 69.26-74.43 wt%, TiO_2= 0.02-0.64 wt%, Al_2O_3=13.09-16.78 wt%, K_2O = 2.55-6.93 wt%, CaO = 0.51-3.17 wt%, K_2O/Na_2O = 0.83-2.73, molar A/CNK = 0.93-1.33, CIPW corundum 0.17 to 4.29 wt%, Av. Sr = 208 ppm), the EPG can be characterized as peraluminous (S-type) granitoids derived by anatexis of fusible major constituents of sedimentary protoliths (Chappell and White 1974). Electron-probed compositions of biotite, muscovite and tourmaline from EPG have been extensively studied to understand nature of the host magma type and physical conditions of mineral evolution.

FIGURE 1. Bivariate Al_2O_3 vs. FeO^t plot for biotite (o) hosted in EPG. Biotites from EPG mostly plot in the field of biotites crystallized into peraluminous (S-type) felsic magma. Fields are after Abdel-Rahman (1994)

Biotites from EPG are ferri-biotites, and have shown chemical affinity with biotites coexisting with muscovite and aluminosilicates. Biotite compositions largely depend upon the nature of host magmas (anorogenic alkaline, peraluminous including collisional S-type, or calc-alkaline subduction-related including metaluminous I-type; Abdel-Rahman 1994). In terms of MgO, Al_2O_3 and FeO^t contents, most biotites from EPG appear crystallized and equilibrated in the peraluminous (S-type) granite melts derived by melting of crustal source (**Figure 1**). Few biotites however show affinity with biotites of calc-alkaline nature, which may be secondary in nature due to slight change in composition of EPG melts or as a result of magma mixing/assimilation. Most EPG biotites tightly cluster on bivariate MgO-FeO plot but to a certain extent few biotites have shown Mg – Fe substitution. Although the Mg – Fe substitution is less significant in biotites of peraluminous rocks because the biotites in peraluminous melts are significantly depleted in Mg compared to those of calc-alkaline suites. Overall the EPG biotites exhibit pronounced 3(Mg, Fe) – 2Al substitution, which were mostly buffered at NNO. However, a few EPG biotites being enriched into oxyannite component, at and above HM buffer, appear secondary in nature because of subsolidus modification. The EPG biotites (Fe/Fe+Mg = 0.53-0.76) buffered at NNO were projected onto experimental biotite equilibria at 2070 bars (Wones and Eugster, 1965), which suggest their evolution under reducing condition ($fO_2 = 10^{-13.50}$– 10^{-16} bar) in a temperature range of 820 °C - 700 °C. The observed reducing trends of biotite evolution in EPG melts are consistent with the magnetic susceptibility (MS) values (χ = 0.016 to 0.187 SI, N = 104) of EPG similar to ilmenite series granites, which most likely prevailed during melting (intrinsic to source region) and/ or subsequent fractional crystallization events.
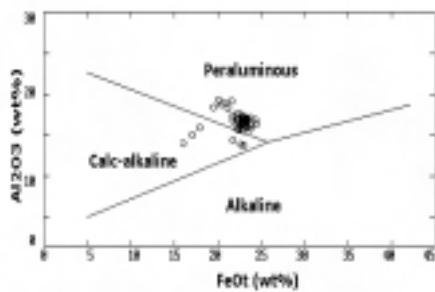

FIGURE 2. Fe (tot)–Al–Mg ternary plot for tourmalines of EPG (□) and TLg (o). Fields 1- Li-rich granitoid pegmatites and aplites; 2- Li-poor granitoids and their associated pegmatites and aplites; 3- Fe^{3+} rich quartz-tourmaline rocks (hydrothermally altered granites); 4- metapelites and metapsammites coexisting with an Al-saturating phase; 5- metapelites and metapsammites not coexisting with an Al-saturating phase; 6- Fe^{3+} rich quartz-tourmaline rocks, calc-silicate rocks, and metapelites, 7- Low-Ca metaultramafics and Cr, V-rich metasediments and, 8- metacarbonates and meta-pyroxenites (after Henry and Guidotti 1985).

The EPG muscovites (Fe/Fe+Mg = 0.41-0.69) coexist with biotites, and are primary in nature containing mostly celadonitic and paragonitic components. They can be classified as Li-Al mica group representing lithian muscovite, lepidolite and zinnwaldite, which were evolved under differentiating peraluminous (S-type) EPG melts. It has been observed that some structural features of dioctahedral and trioctahedral micas from peraluminous granitoids could be related to the crystal forming conditions (Benincasa et al. 2003).

The EPG muscovites exhibit celadonite-like substitution involving octahedral site where Al^{3+} is mainly substituted by Fe and Mg^{2+} and minor amount of Ti^{4+}. Since Ti^{4+} content of EPG muscovite varies from 0.02-0.09 apfu, and therefore it is likely that both Fe and Mg^{2+} substitute for Al^{3+}. However ferro-celadonite substitution in EPG muscovite appear prevalent where the layer-charge neutrality is mainly accounted by exchange mechanism $^{[4]}Si\ ^{[4]}Al^{3+}_{-1}\ ^{[6]}Fe^{2+}\ ^{[6]}Al^{3+}_{-1}$. The observed substitution relations in EPG muscovite are common to most muscovites crystallized in peraluminous rocks observed elsewhere. The observed substitution relations in EPG muscovite are common to most muscovites crystallized in peraluminous rocks observed elsewhere.

Tourmaline compositions from EPG and TLg are indistinguishable, and mostly belong to alkali group based on occupancy of principal constituents at X-site. In terms of schorl (Fe-rich) – dravite (Mg-rich) and elbaite (Al+Li-rich) end-members, the tourmalines of EPG and TLg have shown affinity of their crystallization in Li-poor granitoids and associated pegmatites and aplites (**Figure 2**), being enriched into elbaite components. Equivocal tourmaline compositions of EPG and TLg point to a likely process that the tourmalines were impregnated locally into the remobilized EPG during TLg emplacement as a result of Himalayan orogenesis.

References

Abdel-Rahman AM. 1994. Nature of biotites from alkaline, calc-alkaline and peraluminous magmas. *J Petrol* **35**: 525-541

Benincasa E, MF Brigatti, L Poppi and FB Barredo. 2003. Crystal chemistry of dioctahedral micas from peraluminous granites: the Pedrobernardo pluton (Central Spain). *Europ J Mineral* **15**: 543-550

Chappell BW and AJR White. 1974. Two contrasting granite types. Pacific *Geology* **8**: 173-174

Henry DJ and CV Guidotti. 1985. Tourmaline as a petrogenetic indicator mineral: an example from the staurolite-grade metapelites of NW Maine. *Amer Mineral* **70**: 1-15

Kwatra SK, Sandeep Singh, VP Singh, RK Sharma, Bimal Rai and Naval Kishor. 1999. Geochemical and geochronological characteristics of the Early Palaeozoic granitoids from Sutlej-Baspa Valleys, Himachal Himalayas. In: Jain AK and RM Manickavasagam (eds), *Geodynamics of the Himalaya.* Gondwana Res Group Mem **6**: 145-158

Wones DR and HP Eugster. 1965. Stability of biotite: experiment, theory and application. *Amer Mineral* **50**: 1228-1272

Geology and evaluation of hydrocarbon prospects of Tethyan sediments in Spiti Valley, Spiti and Zanskar, Himanchal Pradesh

Jagmohan Singh*, S Mahanti and Kamla Singh

*Keshava Deva Malaviya Institute of Petroleum Exploration, Oil and Natural Gas Corporation Limited, Dehra Dun-248001, INDIA
Present address: RGL, WO, ONGC, Baroda-390007, Gujrat, INDIA*

* To whom correspondence should be addressed. E-mail: jagmohansingh@hotmail.com

The Tethyan sediments in the Spiti Basin stretch from Pir Panjal in the south to the Zanskar Range in the north. The Tethyan sediments lie within the Higher Himalayan Physiographic Zone. Since such huge thicknesses of sediments are deposited in this area, it is anticipated by the geologists that favourable conditions might have prevailed for the generation and accumulation of hydrocarbon in the Tethyan sediments. It has been continuous endeavour of ONGC to explore and enhance hydrocarbon reserves from all Indian sedimentary basins including the category IV and frontier basins. Seismic data acquisition and geological modelling have been carried out for Lesser Himalayas and even parametric, structural, or wild cat wells have been drilled and one such well is under drilling at Sundernagar. The Tethyan part being inaccessible has not been subjected to detailed geological modelling.

Mesozoic sequences from Kibber Gate Tashegang and Lidang Domal traverses have been subjected to sedimentological, Palaeontological, Palynological and source rock investigations to reconstruct microfacies, biochronostratigraphy, depositional environment, and organic matter maturation. The petrographic study of the Mesozoic Tethyan sediments exposed along the selected traverses shows occurrence of Kioto Limestone, Spiti Shale, Giumal Sandstone, Tashegang Limestone and Chikkim Limestone formations. The Kioto Limestone is highly sparitised and has poor porosity. The Giumal Sandstone consists of glauconitic sands which are well indurated and have very poor intergranular porosity. The porosity is further reduced by calcite cementation. Similarly, the Tashegang Limestone is also highly sparitised and has poor porosity. Spiti shale is dark grey, black, carbonaceous, occasionally oxidised in nature.

Brachiopod fauna supportive of Lower Carboniferous age has been recorded from Lipak Formation and Ordovician - Silurian fauna from Takche Formation. Cephalopods supportive of Oxfordian - Callovian age have been recovered from Spiti Shale. Lilang Group has yielded rare Cephalopods of Triassic - Jurassic age. On the basis of FAD of *Riguadella filamentosa* and *Egmontodinium torynum* Late Bathonian to Late Tithonian age has been suggested to Spiti Formation. On the basis of FAD of *E. cinctum* and *Batioladinium micropodum*, Late Tithonian to Early Valanginian age has been suggested to Tashegang Formation. On the basis of FAD of *B. micropodum* the base of Giumal Formation is dated as Early Valanginian. The absolute pollen frequency (APF) value of the palynofloral assemblage from Spiti Formation suggests inner neritic to marginal marine environment of deposition, while palynoflora from Tashegang Formation indicate marginal marine to lagoonal environment and Giumal Formation was laid under marginal marine conditions. The Organic matter recorded from the studied samples shows Humic-Wood (H-W) to Humic-Sapropelic-Wood (HS-W) to Humic-Sapropelic-Charcoal (HS-C) facies.

The organic matter studies have indicated TAI value from 3 to 3.5 which is suggestive of thermally matured sediments. In general geochemical studies on all the samples have indicated poor hydrocarbon generation potential with very low TOC except for carbonaceous shales having indicated >1% TOC. S2 is very low in many organic rich samples probably due to weathering affects. So an entirely different picture can be anticipated in the subsurface. T max data is not reliable as S2 is low hence no maturity estimate could be made.

Tale of two migmatites and leucogranite generation within the Himalayan Collisional Zone: Evidences from SHRIMP U-Pb zircon ages from Higher Himalayan Metamorphic Belt and Trans-Himalayan Karakoram Metamorphic Belt, India

Sandeep Singh† *, Mark E Barley‡ and AK Jain†

†Department of Earth Sciences, Indian Institute of Technology, Roorkee - 247 667, INDIA
‡Centre for Global Metalogeny, School of Earth and Geographical Science, The University of Western Australia, 35 Stirling Highway, Crawley, WA 6009, AUSTRALIA

* To whom correspondence should be addressed. E-mail: sandpfes@iitr.ernet.in

Continental collisional tectonics in the Himalaya has been caused due to interaction between the Indian and the Eurasian Plates and has resulted in coalescing of these plates in the Himalayan and Karakoram mountains. One of the phenomena characterizing these regions is the presence of collisional-related magmatism, both within the Indian as well as Eurasian Plates. This collisional-related magmatism represents (i) crustal anatectic melting due to fluid migration during intracontinental thrusting, (ii) decompressional-controlled dehydration melting or (iii) vapour-absent muscovite dehydration melting of metamorphic rocks. These bodies are characterized by tourmaline-beraing leucogranite (TBL) and have been emplaced in a very short span between 24 and 19 Ma, as evident from the Higher Himalayan Crystallines of the western sector in Zanskar to Nepal and Bhutan. Their crystallization ages are much younger than the peak Himalayan metamorphism in Zanskar (37-28 Ma), Garhwal (44-26 Ma), Annapurna in Nepal (36 Ma), the Everest region in Nepal (32-23 Ma) and Bhutan (36-34 Ma). This gap between the timing of Eocene-Oligocene Himalayan metamorphism and generation of the Himalayan leucogranite ~20 has remained unexplained.

Both the Higher Himalayan Metamorphic Belt and Karakoram Metamorphic Belt are marked by intense migmatization, partial melting, *in situ* emplacement of various granitoids within sillimanite – K-feldspar bearing metapelite. The Higher Himalayan Metamorphic Belt has evolved in a 15-20 km thick, southwest-vergent ductile shear zone. Along the Bhagirathi valley, western Garhwal these are made up of two distinct packages. The lower package of the Bhatwari Group is separated from the upper Harsil Group by the Vaikrita Thrust and is thrust over the Lesser Himalayan sedimentary zone along the Main central Thrust (MCT). In the middle of the Harsil Group, sillimanite-kyanite-mica schist and gneiss pass gradually into stromatic- and diatexite-type migmatites. These have a melt fraction ranging from 20% to more than 50%, with clear presence of leucosome containing a few garnet porphyroblasts. The rocks that develop in migmatite are mica schist and gneisses and contain biotite, muscovite, quartz, k-feldspar, garnet, kyanite and a small amount of sillimanite. No post-tectonic garnet is observed. Biotite predominates over muscovite, which occurs in negligible amounts. Kyanite is well developed along the main foliation with mica, although a few kyanite and large muscovite crystals have grown across the main foliation, indicating their post-tectonic growth to the main deformation. Kyanite undergoes extensive retrogression to muscovite. Sillimanite needles are developed along the main foliation, as well as along the extensional foliation, and also along garnet margins. The presence of kyanite-garnet- oligoclase-biotite-sillimanite-muscovite assemblage and absence of staurolite in mica schist suggest that the HMB has undergone sillimanite-muscovite grade of middle amphibolite facies metamorphism. P-T calculations using garnet-biotite-muscovite-plagioclase-sillimanite/kyanite-quartz assemblage give $757\pm8°C$ for garnet core and $700\pm10°C$ and 8.9 to 10.7kb for garnet rim confirming sillimanite- muscovite grade metamorphism. Evidence for this is also provided by near-flat normal Mn and Fe garnet zoning. Garnet rims from samples above the Vaikrita Thrust, along the valley, give lower temperatures and pressures of $640\pm13°C$ and 8.7kb, indicating cooling during exhumation. P-T conditions of the surrounding country rocks indicate that they were in the kyanite zone, close to the dehydration-melting curve of muscovite and biotite.

The Karakoram Metamorphic Complex (KMC) represents deformation and extensive metamorphism of the southern edge of Eurasian Plate. It is characterized by intense penetrative ductile shearing as the most prominent deformation phenomenon, having top-to-SW sense of displacement, as has been deciphered from numerous shear criteria. It is superposed by an extensive phase of extensional tectonics, associated with the exhumed Karakoram metamorphics. The northwestern margin of the KMC is marked by the Tangste Shear Zone and characterized by structures indicating dextral transpressional regime. Metamorphism varies from biotite grade in the north to middle greenschist to sillimanite-muscovite grade of middle amphibolite facies condition towards south. In the middle amphibolite facies zone, mica gneiss has undergone prolofic migmatization and melting which led to the generation of *in situ* and injection granite – the Pangong Injection Complex. The P-T data from this belt indicates that upper greenschist facies rocks have undergone temperature- pressure of about 450-500°C and 6.00 kb, whereas in the highest sillimanite-muscovite grade of middle amphibolite facies in the zone of migmatization and melting, this belt seems to have reached a maximum temperature and pressure of about 700°C and 8.6kb.

U-Pb SHRIMP dating of zircons along with cathodo-luminescence (CL) imaging of metasediments, migmatites, biotite granite and *in situ* melt of collisional-related tourmaline-bearing leucogranite (TBL) have been performed along the Bhagirathi valley (Indian Plate) and Tangtse Gorge (Eurasian Plate). Zircons from these rocks are of varied shape varying from few tens of µm to ~400 µm. CL patterns of zircon grains reveal a distinctive core of apparent igneous origin and metamorphic overgrowth with faint oscillatory zoning related to the Himalayan orogeny. Zircons from *in situ* melt of the TBL along the Bhagirathi valley indicate three distinct patterns: clear rims, spongy middle

portions and older cores. U-Pb zircon age data from the Bhagirathi valley indicate that the intrusion of felsic TBL took place at the peak metamorphism of the Himalayan orogeny with an episodic influx of fluid between 46 Ma and 20 Ma causing the growth zircons. However, data from Tangtse Gorge indicate an age of 19 Ma from the zircon rim and contemporaneous plug of the 20 Ma Darbuk Granite. U-Pb age data from both the sectors indicate that intrusion of felsic collision-related TBL are contemporary with each other and have formed at the peak metamorphism of the Himalayan orogeny.

Cenozoic structural and metamorphic evolution and geological map and sections of the NW Indian Himalaya

Albrecht Steck

Institut de Minéralogie et Géochimie, Université de Lausanne, BFSH-2, CH-1015 Lausanne, SWITZERLAND

For correspondence, E-mail: albrecht.steck@img.unil.ch

A multidisciplinary geological study of the Mandi–Leh transect through the NW Indian Himalaya has been performed since 25 years by geologists from Lausanne: Aymon Baud, Vincent Baudraz, Hugo Bucher, François Bussy, Mike Cosca, Pierre Dèzes, Jean-Luc Epard, Arthur Escher, Matthieu Girard, Henri Masson, Martin Robyr, Micha Schlup, Laurent Spring, Albrecht Steck, Edgar Stutz, Philippe Thélin, Jean-Claude Vannay and Martin Wyss (References in Steck 2003). These systematic investigations have turned this region into one of the best known geological cross section of the Himalayan range. The outcrops are easily accessible at low altitude (1000- 6000 m). The Barrovian regional metamorphic overprint increases from unmetamorphic to amphibolite facies. These favourable conditions offer the opportunity to recognise the pre-

Himalayan stratigraphy, to decipher the structural and metamorphic history in great detail, to study the mechanisms of nappe formation, and to propose original models for the formation of the Cenozoic Himalayan range.

The palinspastic section of the N Indian passive margin before the formation of the Himalayan range is characterised by a continuous stratigraphic column of Proterozoic to Paleocene sediments, which are cross-cut by Ordovician, Carboniferous and Permian normal faults and magmatic rocks. A low angle unconformity at the base of the Ordovician Thaple conglomerates recorded a Kaledonian extensional tectonic event, which includes a block rotation. No Palaeozoic or Mesozoic compressional structures are recognised. The Himalayan range was formed during the Cenozoic continental
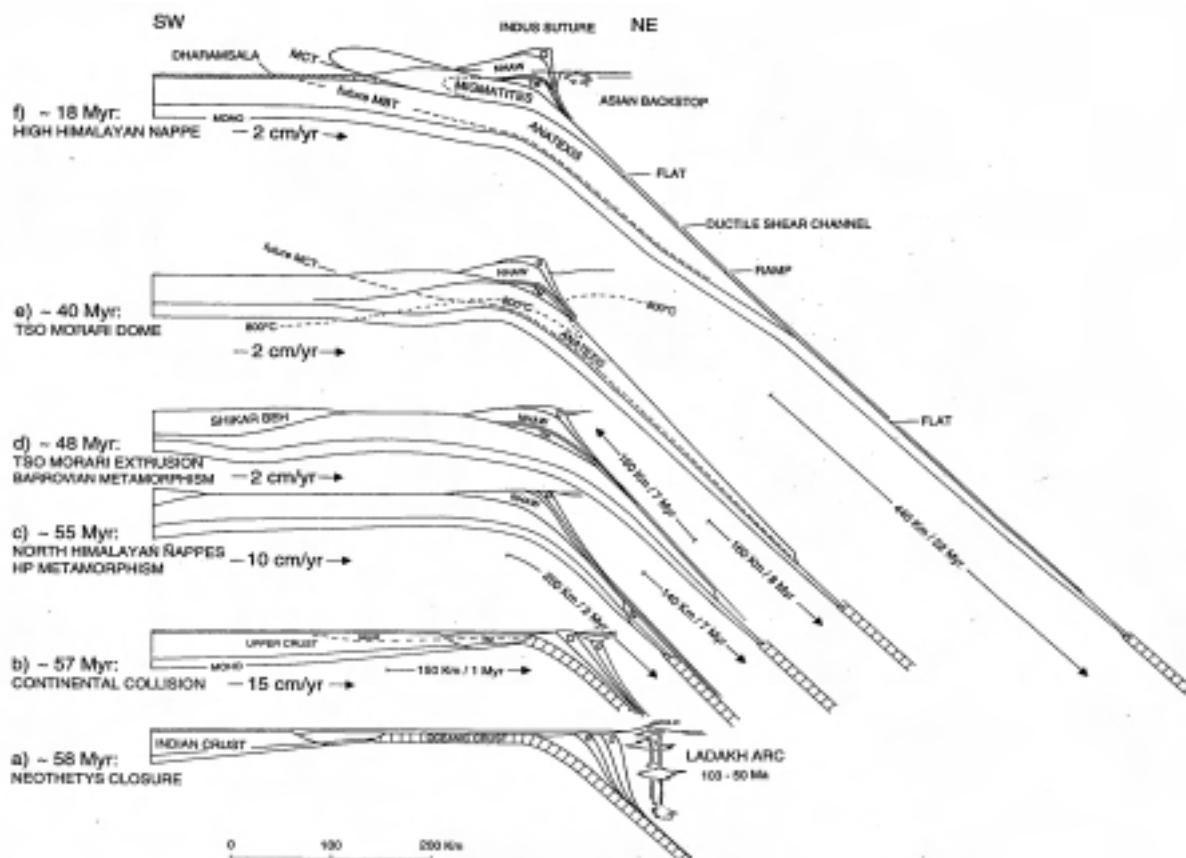
FIGURE 1. Development of the Cenozoic North and High Himalayan nappes (a) – (f). The proposed model is constrained by stratigraphic, structural, thermo-barometric, radiometric, data and rock physics considerations (J De Sigoyer et al. 2000, K Honegger et al. 1982, BK Mukherjee and HK Sachan 2001, RF Weinberg and WJ Dunlap 2000, A Steck 2003 and DL Turcotte and G Schubert 1982). Note that the unknown convergence velocity is assumed to decrease from a value of ~15 cm/yr before continental collision to a value of ~2 cm/yr during the Eocene and Miocene Himalayan range formation.

collision by underthrusting of India below Asia by a typical succession of orogenic structures.

From N to S, and hence from generally older to younger tectonic units, the following main tectonic domains are distinguished (Steck 2003):

1) The Late Cretaceous and Paleocene Transhimalayan batholith and the Indus suture zone are composed of the 103-50 Ma Ladakh arc magmatism (Honegger et al. 1982, Weinberg and Dunlap 2000), the accretion of the Dras-Nindam arc, the accretion and later obduction of the Spongtang immature island arc which formed the southern active border of Asia, and forearc sediment deposition. The Transhimalayan batholith, together with the Asian mantle wedge, represent the Asian backstop for the Himalayan range.

2) The Late Cretaceous-Neogene sediments of the Indus Group are deposited first in a forearc basin of the Ladakh batholith and then in an intermontane molasse basin, after the Early Eocene continental collision.

3) The Shikar Beh nappe is an intracontinental NE-verging structure in the High Himalaya, of an unknown post-Liassic, probably late Palaeocene to Eocene age.

4) The SW-directed North Himalayan nappe stack was created in Eocene time, along with the high pressure Tso Morari nappe, by ductile detachment of the Upper Proterozoic-Early Eocene upper Indian crust during its underthrusting below Asia. The deformational structures of the North Himalayan Nappes confirm the thrust model of E Argand (1916): The imbricate structure of the nappe fronts are related to ductile shear zones in the root of the nappes. The Tso Morari nappe is composed of the mylonitic 479 Ma (Steck 2003) Tso Morari granite which is crosscut by eclogitised mafic dikes. It has been extruded, pushed by buoyancy forces, after its burial to a depths of over 90 km (crystallisation of coesite) some 55 Ma ago (De Sigoyer et al. 2000, Mukherjee and Sachan 2001). High water pressure in the zone of underthrusting derived from dehydration reactions in the subducted oceanic serpentinites may have assisted the Tso Morari granite mylonite detachment and buoyant extrusion by ductile flow and hydrofracturing.

5) The High Himalayan nappe or "Crystalline nappe", composed of Upper Proterozoic-Early Eocene was created in Eocene-Miocene time. The zone of dry intracrustal melting below the North Himalayan range and the Shikar Beh nappe stack determined the future position of the Main Central thrust at the base of the High Himalayan nappe. During under thrusting of the Indian lithosphere, the ductile and light upper Indian crust has been sheared off and extruded, pushed by buoyancy and compressional forces in the zone of plate collision (channel flow, Turcotte and Schubert 1982). The 22
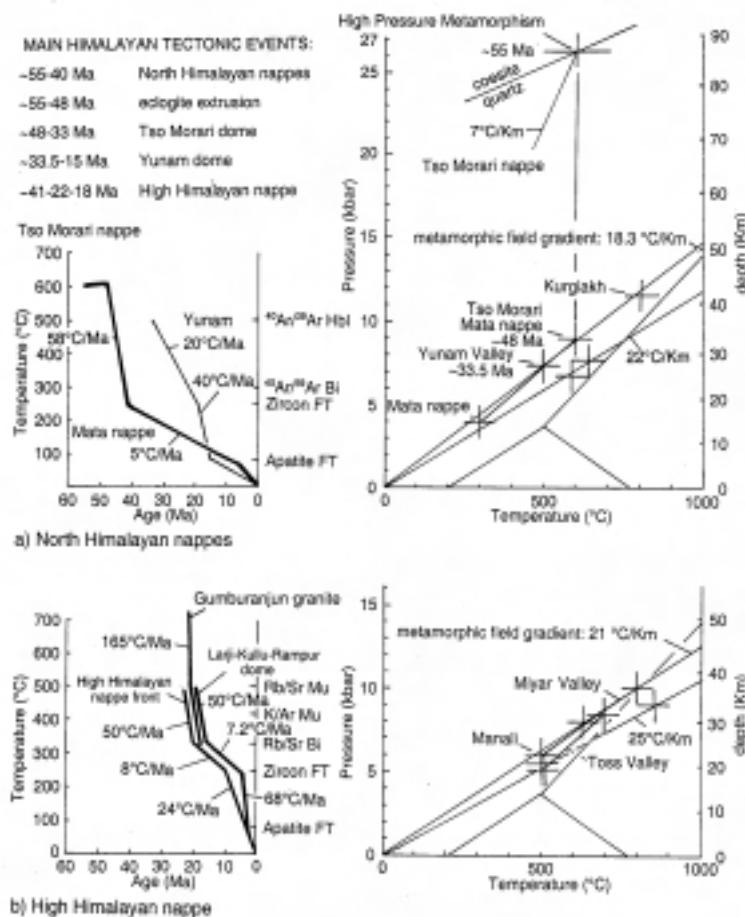

FIGURE 2. Pressure-temperaure-time paths of the North and High Himalayan nappes. The fieldgradients of the Barrovian type orogenic metamorphism increase from 18–22 °C/km in the Eocene North Himalayan nappes to 21–25 °C/km in the Oligo-Miocene High Himalayan nappe (Epard et al. 1995, Sigoyer 2000, Dèzes et al 1999, Robyr et al. 2002, Schlup et al. 2003, Vannay and Grasemann 1998, Wyss et al. 1999, ref. in A Steck 2003).

Ma Gumburanjun leucogranite, intruding the Zanskar extensional shear zone, testifie of the adiabatic muscowite dry melting in the preexisting prograde migmatites during the final extrusion of the High Himalaya nappe (Dèzes et al. 1999 in A Steck 2003).

6) The Lower Crystalline nappe, composed of lower Proterozoic rocks is characterised by an inverted metamorphic zonation similar to the High Himalayan nappe.

7) The Lesser Himalayan nappes, with formation of the deep-seated intracrustal Main Boundary Thrust, are formed from the late Miocene to the present, probably by a mechanism similar to the High Himalayan nappe formation.

8) Thin-skinned nappe structures that detach the up to 9 km thick Miocene to present Subhimalayan Molasse sediments of the Himalayan foredeep, characterise the Subhimalayan thrust which is related to the Active Himalayan thrust at the base of the present Himalayan accretionary wedge.

References

Argand E. 1916. Sur l'arc des Alpes occidentales. *Eclogae geol Helv* **14**: 145-191

De Sigoyer J, V Chavagnac, J Blichert-Toft, IM Villa, P Luais, S Guillot, M Cosca and G Mascle. 2000. Dating the Indian continental subduction and collisional thickening in the northwest Himalaya: Multichronology of the Tso Morari eclogites. *Geology* **28**: 487-490

England PC and TJB Holland. 1979. Archimedes and the Tauern eclogites: the role of buoyancy in the preservation of exotic eclogitic blocks. *EPSL* **44**: 287-294

Honeger K, V Dietrich, W Frank, A Gansser, M Thoeni and V Trommsdorff. 1982. Magmatism and metamorphism in the Ladakh Himalayas (the Indus-Tsangpo suture zone). *Earth planet Sci Lett* **60**: 253-292

Mukherjee BK and HK Sachan. 2001. Discovery of coesite from Indian Himalaya: A record of ultra-high pressure metamorphism in Indian continental crust. *Current Science* **81**: 1358-1361

Steck A. 2003. Geology of the NW Indian Himalaya. *Eclogae Geol Helv* **96**: 147-196

Weinberg RF and WJ Dunlap. 2000. Growth and Deformation of the Ladakh batholith, Northwest Himalayas: Implication for timimg of continental collision and origin of calc-acaline batholiths. *J Geol* **108**: 303-320

Turcotte DL and G Schubert. 1982. *Geodynamics.* John Wiley & Sons New York. 450 p

On the Himalayan Uplift and Himalayan Corridors

Hideo Tabata

Gifu Academy of Forest Science and Culture, Mino 501-3714, JAPAN

For correspondence, E-mail: tabata@forest.ac.jp

It is necessary to review studies carried out in the Himalayas from the interdisciplinary viewpoints for a comprehensive understanding of some features of Himalayan vegetation and the patterns of distribution of some plants, especially in connection with the Himalayan orogeny.

Himalayan corridors

Kitamura (1955) postulated that the temperate zone of the southern side of the Great Himalayas represented a corridor through which Sino-Japanese plants migrated westwards, and named it the Himalayan corridor. However, he did not pay much attention to the eastward distribution of Mediterranean elements through the corridor and extended the Sino-Japanese region up to Afghanistan by drawing the Himalayan corridor (Kitamura, 1957).

The southern slopes in the Himalayas are generally drier than the northern slopes. In the case of the Great Himalayas, however, the south-facing slope is moister than the north facing one. Therefore, there are two corridors along the Outer and Lesser Himalayas respectively, on the south facing slopes and on the north facing slopes, and the Great Himalayas provide a corridor on its southern slope. The northern side of the Great Himalayas can not act as a corridor due to its dryness.

The eastern elements extended their distribution range westwards through the moister corridor and the western elements migrated eastwards through the drier corridor. However, for example, wet sal (*Shorea robusta*) forest occurring on the south-facing slopes of the Siwalik range in Central Nepal can not survive on the south facing slopes in the western Siwaliks. It moves to the north-facing slope and it is replaced by the dry hill sal forest in the west Siwalik range. The dry hill sal forest gives place to the subtropical decidous hill forest dominated by *Anogeissus latifolia* in the west Siwalik. The deciduous hill forest dominated by *Anogeissus latifolia* is replaced by the subtropical scrub composed of *Olea cuspidata*, *Dodonea viscosa* etc. in the further west. On the north-facing slope, the wet Sal forest replaces *Castanopsis indica- Schima wallichiana* forest in the west Siwalik where the dryness caused by the increase of mediterraneity of climate is prevailing. The Siwalik range provides corridors on the south and north sides of the range for the eastward migration of western elements and westward distribution of eastern elements. In the Lesser Himalayas, *Quercus lanuginosa-Q. incana* forest is replaced by *Q. incana* forest in West Nepal, and *Q. incana* forest occurs on the all exposures in West Nepal and Kumaon region in India and then it is confined to the northern side of the Lesser Himalayas westwards. *Cedrus deodara* forest replaces *Q. incana* forest on the southern slopes of the western Lesser Himalayas where *Q. incana* forest move to the northern side. The Himalayan corridors are twisted in this way.

Historical sketch of Himalayan corridors

Prakash (1978) and Awasthi (1982) reported that the tropical forests covered the Siwalik area before its uplift in the lower Miocene. The first record of the Mediterranean elements in the Himalayan area was found above the sterile deposits indicating the uplifting of the main Himalayan ridge in the middle Miocene. This suggests that a simple Himalayan corridor was formed on the southern side of the main range in the upper Miocene. The prototype of Himalayan corridors was formed by the uplift of Outer and Lesser Himalayas.

Guo *et al* (1976) reported that the macrofossils and pollen of many temperate tree species (*Betula*, *Alnus*, *Carpinus*, *Magnolia*, *Cedrus*, *Abies*, *Picea*, *Sabina*, *Lespedeza* etc.) were found from the deposits of the last Interglacial period (Kangbula Interglacial). They concluded that the Great Himalayas experienced abrupt and a large-scale uplift during the last Glacial period.

Stainton (1972, 1977) recognized that there are two kinds of distributional gaps of Himalayan plants: one is the East Nepal-Sikkim Gap and the other is the Sino-West Himalaya Gap. *Actaea spicata*, *Lonicera quinquelocularis*, *L. webbiana*, *Plectranthus rugosus*, *Ribes alpestre*, *R. emodense*, *Sorbaria tomentosa*, *Viburnum cotinifolium* etc. show the former type of distribution gap. Although Stainton reasonably discussed about discontinuity in the distribution of the former by the specialty of wet climate and the lack of the medium-dry habitats in East Nepal and Sikkim, and the reoccurrence of drier conditions in Bhutan, he could not elucidate the latter discontinuity. *Acer caesium*, *Cotinus coggygria*, *Olea ferruginea*, *Quercus dilatata*, *Incarvillea arguta*, *Clematis grata* etc. have the latter discontinuity pattern.

I have discussed this big distribution gap in connection with the Himalayan uplift (Tabata, 1988, 1998). Chinese scientists showed that many temperate trees including *Cedrus*, one of western elements, occurred on the northern side of the Great Himalayas in the last Interglacial. It means the presence of the Himalayan corridor through which the western elements, preferring drier conditions, migrated eastwards up to the southwestern part of China during the last Interglacial period. The corridor on the northern side disappeared after the abrupt and drastic uplift during the last Glacial period and the big discontinuity of distribution range of plants, which were separated in West Himalayas and Southwest China, was formed by this kind of event in the Great Himalayan area during the last Glacial period.

There is another evidence to show the existence of the Himalayan corridor on the northern side of the Great Himalayas. The palynological study (Yoshida *et al.*, 1984) showed that *Abies*, *Picea*, *Larix*, *Tsuga* and *Pinus* were found together with *Quercus*, *Keteleeria*, *Myrica*, *Podocarpus*, *Sapium* etc. from the Tetang Formation in Thakkhola (the upper stream area of the present Kaligandaki river). It is especially important that the occurrence of *Keteleeria* was confirmed from the Tetang Formation. *Keteleeria* is a warm temperate, sometimes subtropical, conifer which is now confined to the southern China though it was distributed from Asia to Europe in the Miocene. This suggests that the Himalayan corridor on the northern side of the Great Himalayas existed in the lower Neogene. The Annapurna-Dhaulagiri mountains were high enough for the growth of *Picea* and *Abies*, and the altitude of

the mountains is estimated to be between 3500 m and a little bit higher than 4000 m asl. It is estimated from the presence of temperate and cold temperate trees that the Annapurna-Dhaulagiri mountains were not so high as to block the monsoon and the moist air reached up to Thakkhola area where the dry climate is prevailing and no forests are available now.

References

Awasthi N. 1982. Tertiary plant megafossils from the Himalaya-a review. *The Palaeobot* **30** : 254-267.

Guo X. 1976. Quaternary Interglacial Period and Palaeoclimate in the Zhumulangma Region. In: *Zhumulangma Region Scientific Report.* Beijing: Science Publishers. p 63-78

Kitamura S. 1955. Flowering plants and ferns. In: Kihara H (ed), *Fauna and flora of Nepal Himalaya.* Kyoto: Fauna and Flora Research Society. p 73-290

Kitamura S. 1957. *Colored Illustrations of Herbacious plants of Japan I. Osaka*: Hoikusha Pub. (in Japanese)

Prakash U. 1978. Some more fossil woods from the Lower Siwalik beds of Himachal Pradesh, India. *Him Geol* **8**: 61-81.

Stainton JDA. 1972. *Forest of Nepal.* London: John Murray.

Stainton JDA. 1977. Some problems of Himalayan plant distribution. *Colloques internationaux du C.N.R.S.* **268**: 99-102

Tabata H. 1988. On the Himalayan corridor. *Acta Phytotax Geobot* **39**: 13-24 (in Japanese with English summary)

Tabata H. 1998. Himalayan Uplift, Plant Corridors and the Past Climate. *Himalayan Geol* **19** (2):61-63

Yoshida M, Igarashi Y, Arita K, Hayashi D and Sharma T. 1984. Magnetostratigraphic and pollen analytic studies of the Takmar series, Nepal Himalayas. *J Nepal Geol Sci* **4**: 101-120

Geometric evolution of a plate interface-branch fault system: Its effect on tectonics in Himalaya

Youichiro Takada† * and Mitsuhiro Matsu'ura‡

† *Division of Earth and Planetary Sciences, Hokkaido University, N10 W8, Sapporo 060-0810, JAPAN*
‡ *Department of Earth and Planetary Science, University of Tokyo, Hongo 7-3-1, Bunkyo-ku, Tokyo 113-0033, JAPAN*

* *To whom correspondence should be addressed. E-mail: ytakada@ep.sci.hokudai.ac.jp*

The Himalayas is a tectonically very active region where rapid crustal uplift due to the collision of India and Eurasia is still going on. The present-day convergence rate between the Indian and Eurasian plates has been estimated as 50 mm/yr. About 40 % of the total convergence rate is consumed at the collision boundary along the Himalayas by subduction of the Indian plate beneath the Eurasian plate. The rest of 60% is consumed by internal deformation of the Eurasian plate.

In such a tectonic framework, we first construct a kinematic model for steady subduction of the Indian plate beneath the Eurasian plate on the basis of elastic dislocation theory. The crust and mantle structure is modeled by an elastic surface layer overlying a Maxwellian viscoelastic half-space, and the kinematic interaction between the adjacent plates is represented by the increase of tangential displacement discontinuity (dislocation) across the plate interface. With this plate subduction model Takada and Matsu'ura (2004) computed the present uplift rates of the Himalayas due to steady slip along the India–Eurasia plate interface (detachment) with a large-scale ramp beneath the high Himalayas. The computed results are in accord with observed free-air gravity anomalies, river terrace uplifts, and geodetic data for level changes. The computational analysis of internal deformation fields by Takada (2002) showed that the steady slip along the ramp of the plate interface is the essential cause of the present-day rapid uplift of the high Himalayas. This means that the crustal deformation process strongly depends on the geometrical structure of the plate interface.

In the India-Eurasia collision zone the plate interface is associated with a series of under-thrusting branch faults, called the Main Central Thrust (MCT), the Main Boundary Thrust (MBT) and the Main Frontal Thrust (MFT) (e.g., Schelling and Arita 1991). The slip motion along these under-thrusting branch faults has also caused the long-term crustal deformation in the Himalaya. An important point is that the geometry of the fault system will be changed because of the internal deformation caused by slip on the fault system itself. Thus, it is necessary to reveal this feedback mechanism to understand the topographic evolution process of the Himalaya.

In this study, considering the changes in fault geometry with time caused by internal deformation, we developed a simulation algorithm for the geometric evolution of the fault system. Through numerical simulations we revealed the fundamental properties of geometric evolution of faults. When the plate interface is sufficiently smooth everywhere, there is no significant change in fault geometry. When the plate interface has a ramp, remarkable changes in fault geometry occur. The ramp moves horizontally toward the hanging wall side at a half of the plate convergence rate. The offset of the ramp decreases with time. These characteristics are strongly reflected on the surface uplift pattern. When the plate interface has an under-thrusting branch fault, we can find the accelerative increase in dip-angle of the branch fault and also the development of a ramp-and-flat structure on the plate interface around the branching point. Since the branch fault with a steeper dip-angle is harder to consume the horizontal convergence, we may conclude that the increase in dip-angle results in the cessation of slip along the branch fault at last. The shallower the depth of the branching point is, the faster the rate of increase in dip-angle of the branch fault is. It means that the branch fault with a shallow branching point can not produce the large-scale mountain range, because large amount of slip can not be accommodated by the branch fault.

Incorporating the mechanism of geometric fault evolution into geological knowledge, we propose a scenario on the tectonic evolution of the Himalayas in the last 30 Myr. The tectonic evolution may be divided into three stages. From 30 Ma to 15 Ma, the Main Central Thrust (MCT) with a deep branching point has been active, and produced very high mountain ranges. After the stop of the MCT activity, the produced high mountain ranges has been gradually eroded with time. From about 10 Ma the Main Boundary Thrust (MBT) with a shallow branching point became active instead of the MCT, and produced middle-class mountain ranges. At present, the thrust motion along the MBT has not continued at many locations (Nakata et al. 1990; Mugnier et al. 1994). During the last several million years, the steady slip along the ramp of the plate interface raised the high Himalayas at the place where once the MCT had raised the high mountain ranges.

References

Schelling D and K Arita. 1991. Thrust tectonics, crustal shortening, and the structure of the far-eastern Nepal Himalaya. *Tectonics* **10**(5): 851-862

Mugnier JL, P Huyghe, E Chalaron and G Mascle. 1994. Recent movements along the Main Boundary Thrust of the Himalayas: normal faulting in an over-critical thrust wedge? *Tectonophysics* **238**(1-4): 199-215

Nakata T, K Otsuki and SH Khan. 1990. Active faults, stress field, and plate motion along the Indo-Eurasian plate boundary. *Tectonophysics* **181**(1-4): 83-95

Takada Y. 2002. Theoretical studies on crustal deformation in the India-Eurasia collision zone. Ph.D. Thesis, University of Tokyo

Takada Y and M Matsu'ura. 2004. A unified interpretation of vertical movement in Himalaya and horizontal deformation in Tibet on the basis of elastic and viscoelastic dislocation theory. *Tectonophysics* (in press)

Geochemical modeling of the Chilas Complex in the Kohistan Terrane, northern Pakistan

Yutaka Takahashi† *, Masumi U Mikoshiba† , Yuhei Takahashi† , Allah Bakhsh Kausar‡ , Tahseenullah Khan‡ and Kazuya Kubo†

† *Geological Survey of Japan, 1-1-1 Higashi, Tsukuba, Ibaraki 305-8567, JAPAN*
‡ *Geoscience Laboratory, Geological Survey of Pakistan, Chak Shazad, P. O. Box 1461, Islamabad, PAKISTAN*

* *To whom correspondence should be addressed. E-mail: takahashi-yutaka@aist.go.jp*

The Kohistan Terrane in the western Himalaya of northern Pakistan, is regarded as a tilted island arc type crust sandwiched between the Asian and Indian continental crusts (Coward et al. 1982). The Kohistan Island Arc is bounded on the south by Main Mantle Thrust (MMT), and on the north by Northern Suture (or Main Karakoram Thrust, MKT), and can be divided into some geological units. The Chilas Complex is a huge basic intrusion about 50 km wide and elongates 300 km almost parallel to the MMT and MKT. It has been interpreted as the magma chamber root zone of the Kohistan Island Arc (Khan et al. 1989). The Chilas Complex is composed mainly of gabbronorite and several masses of ultramafic-mafic association (UMA) (Jan et al. 1984). The UMA is composed mainly of olivine (with or without clinopyroxene) cumulate (dunite, wehlrite) and plagioclase-clinopyroxene-orthopyroxene cumulates (two pyroxene gabbro), with minor amount of clinopyroxene-orthopyroxene cumulate (pyroxenite) and clinopyroxene cumulate (clinopyroxinite).

Bulk chemical compositions of major elements for the gabbronorite of the Chilas Complex plotted on the ternary AFM diagram are suitable to island arc non-cumulate, and those for the UMA are suitable to island arc cumulate (Beard 1986). Major element geochemistries of the gabbronorite and the UMA, plotted on the variation diagrams of $100MgO/(MgO+FeO)$ versus oxides, are explained by cumulate and non-cumulate model.

Chondrite normalized rare earth elements (REE) for the gabbronorite of the Chilas Complex show light rare earth element (LREE) enriched patterns, which are typical for island arc type basalt. In the case of UMA, contents of REE are relatively low. This is concordant to their cumulate characters, because REE are basically incompatible especially in the case of basic magma (Hanson 1980). On the spidergram, the LIL elements are enriched and Nb and Sr show negative and positive anomalies, respectively for the gabbronorites of the Chilas Complex. These are geochemical characters of island arc type basalt. In the case of UMA, contents of these trace elements are relatively low, and high field strength (HFS) elements such as P, Zr and Ti are relatively depleted. These features are suitable to their cumulate characters.

References

Beard JS. 1986. Characteristic mineralogy of arc-related cumulate gabbros: implications for the tectonic setting of gabbroic plutons and for andesite genesis. *Geology* **14**: 848-851

Coward MP, MQ Jan, D Rex, J Tarney, M Thirlwall and BF Windley. 1982. Structural evolution of a crustal section in the western Himalaya. *Nature* **295**: 22-24

Hanson GN. 1980. Rare earth elements in petrogenetic studies of igneous systems. *Ann Rev Earth Planet Sci* **8**: 371-406

Jan MQ, MUK Khattak, MK Parvez and BF Windley. 1984. The Chilas stratiform complex: field and mineralogical aspects. *Geol Bull Univ Peshawar* **17**: 153-169

Khan MA, MQ Jan, BF Windley, J Tarney and MF Thirlwall. 1989. The Chilas Mafic-Ultramafic Igneous Complex; The root of the Kohistan Island Arc in the Himalaya of northern Pakistan. *Geol Soc Am Sp Paper* **232**: 75-94

40Ar-39Ar dating of Proterozoic basaltic and granitic rocks in the Nepal Himalaya and their comparison with those in Singbhum area, peninsular India

Yutaka Takigami†*, Harutaka Sakai‡, Yuji Orihashi§ and Kazumi Yokoyama¶

† Kanto Gakuen Uniersity, Gunma, 373-8515, JAPAN
‡ Department of Earth Sciences, Kyu-shu University, Fukuoka,810-8560, JAPAN
§ Earthquake Research Institute, University of Tokyo, Tokyo, 113-0032, JAPAN
¶ Department of Geology and Petrology, the National Science Museum, Tokyo, 169-0073, JAPAN

* To whom correspondence should be addressed. E-mail: ytakigam@rkanto-gakuen.ac.jp

Although origin of the metamorphic rocks in the Lesser and Higher Himalaya are believed to be Proterozoic sedimentary and igeneous rocks, there are a few reports of dating of Proterozoic age. We have reported the Middle Proterozoic 40Ar-39Ar ages of about 1.5-1.7 Ga for the Dowar Khola Dolerite from the Siwalik Belt of Sub-Himalaya and the Kabeli Khola Granite in the Lesser Himalaya, both in Nepal (Sakai et al. 2000, Takigami et al. 2002a, 2002b) (**Figure 1**). In this paper, we deal with several age data of both Proterozoic rocks and their country rocks, and discuss on the process how these rocks were incorporated into the Himalaya on the basis of field research and new age data on the Singbhum Complex in peninsular India.
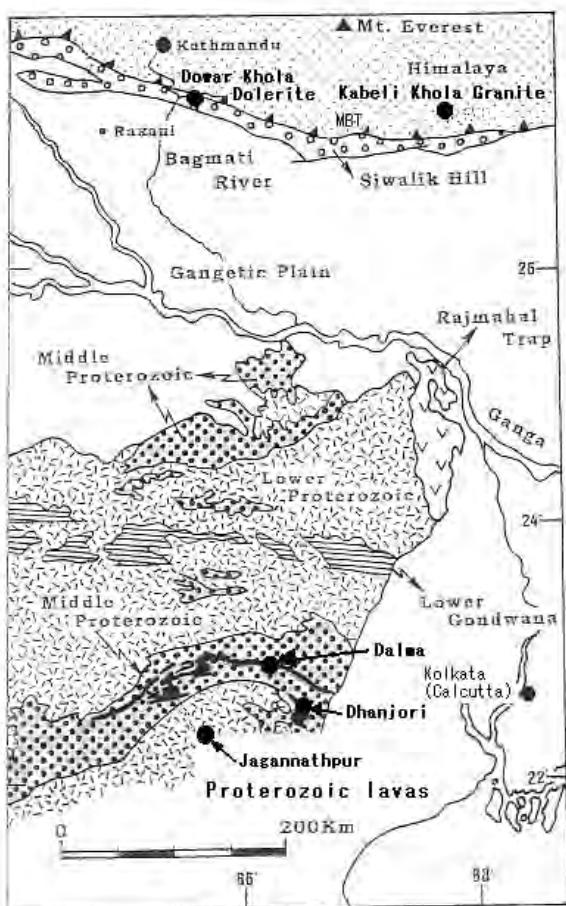

FIGURE 1. Locality map of Dowar Khola Dolerite, Kabeli Khola Granite and correlative Proterozoic lavas in Singbhum area , peninsula India

The Bagmati Group and Dowar Khola Dolerite are distributed in the Siwalik hill about 30 km SE from Kathmandu (**Figure 1**) and are composed of aeolian and lacustrine beds, and dolerite sills, respectively. A thin slice of the Siwalik Group is tectonically sandwiched in the thrust sheets of schuppen zone. The 40Ar-39Ar ages of dolerite are 1741±11 Ma and 1679±4 Ma which are plateau-like ages of 800-1100 °C(about 50-60% 39K) (**Figure 2**). Detrital muscovite separated from micaceous shale of the lacustrine beds shows a 40Ar-39Ar plateau age of 1744±9 Ma (about 98% 39Ar). Moreover, U-Pb chime age of detrital monazite separated from quartzite and Nd-Sm model age for the dolerite show their ages of 1.75-1.8 Ga and 1.6+-0.2 Ga, respectively. These results demonstrate that the dolerite is about 1.7 Ga and detrital grains of the group were supplied from granitic rocks of about 1.8 Ga.

The Kabeli Khola Granite is distributed in the Lesser Himalaya, 115 km SE from Mt. Everest (**Figure 1**). The granite body exposes in the tectonic window of the crystalline nappe, called as Taplejung Window. Ages of 960-1300C (about 86% 39K) are 1.59-1.68 Ga, although 40Ar-39Ar age spectrum of muscovite from the Kabeli Khola Granite in the center of the window indicates the pattern of degassing of Ar (**Figure 3**). This result indicates that the rock has never undergone metamorphism higher than about 350 °C and the original age is older than 1.68 Ga. Moreover, 40Ar-39Ar age at 1200 °C for muscovite from augen gneiss, to the north of Kabeli Khola Granite, is about 1.42 Ga. As Ar gas has been considered to be degassed from the feature of age spectrum, the original age of this muscovite may be older than 1.42 Ga.

In peninsular India, 400-500 km to the south of the Bagmati Group, there are Proterozoic lavas (Dalma, Dhanjori and Jagarnathpur lavas) extending large area (**Figure 1**). K-Ar ages of these lavas were reported to be about 1.6Ga and Rb-Sr age of gabbro intruded into the Dalma lava is 1.6 Ga. Accordingly, the age of these lavas are considered to be 1.5-1.6 Ga (Acharyya 2003). Judging from the occurrence of doleritic rocks and quartzose sandstone from a drill-well at Raxaul to the south of Siwalik hill (**Figure 1**) and seismic profile of the Gangetic Plain, the Dowar Khola Dolerite and the Bagmati Group are considered to have been scraped from supra-continental rocks of subducting Indian subcontinent and accreted to the Asian continent as an accretionary prism. The Kabeli Khola Granite and its cogenetic granitic rocks are likely to be converted into augen gneiss like as Ulleri augen gneiss after strong deformation by advancement of metamorphic nappe.

We had a chance to investigate the Dalma, Dhanjori and Jagarnathpur Lavas and Singbhum Granite in 2003, and collected their samples for the purpose of 40Ar-39Ar dating, Rb-Sr dating, Nd-Sm dating and geochemical studies. In this paper, we would like to refer to some preliminary 40Ar-39Ar dating results.
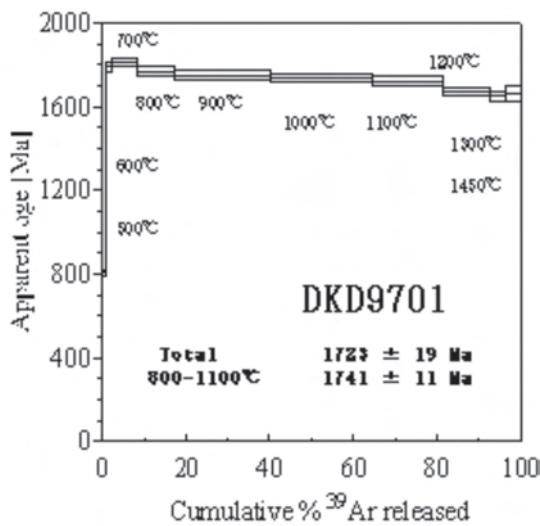
FIGURE 2. Age spectrum of ^{40}Ar-^{39}Ar dating for Dowar Khola Dolerite
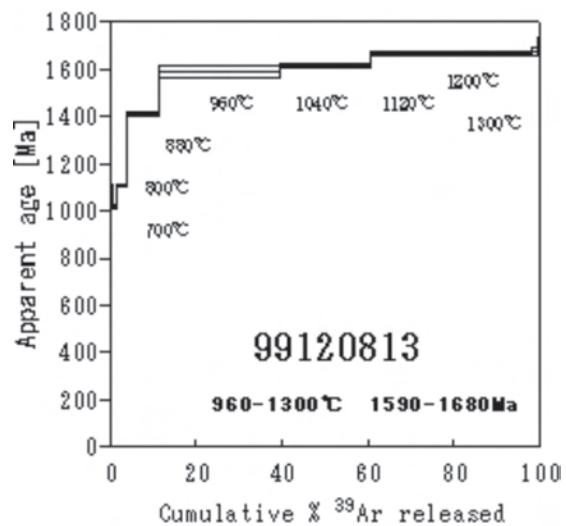
FIGURE 3. Age spectrum of ^{40}Ar-^{39}Ar dating for Kabeli Khola Granite

References

Acharyya SK. 2003. The nature of Mesoproterozoic central India tectonic zone with exhumed and reworked older granulites. *Gondwana Res* **6** (2):197-214

Sakai H, Y Takigami, BN Upreti and DP Adhikary. 2000. Thrust package of 1.68 Ga Indian supra-crustal rocks in the Miocene Siwalik Belt, Central Nepal Himalayas. *Earth Sci. Frontiers* **7** (supple): 64-66; China Univ. of Geoscience (Beijing)

Takigami Y, H Sakai and Y Orihashi. 2002a. 1.5-1.7 Ga rocks discovered from the Lesser Himalaya and Siwalik belt: ^{40}Ar-^{39}Ar ages and their significances in the evolution of the Himalayan orogen. *Gechim. Cosmochim. Acta* **66** (S1):A762

Takigami Y, H Sakai and Y Orihashi. 2002b. 1.5-1.7 Ga non-metamorphosed igneous rocks from the Lesser Himalaya and Siwalik belt: ^{40}Ar-^{39}Ar ages and an example of accretionary prism at the continent-continent collision. In: *International symposium on the amalgamation of Precambrian blocks and the role of the Paleozoic orogens in Asia*; 2002 Sep 5-7; Sapporo. Abstract no pp116. 98 p

Clay mineralogy and implication for palaeoenvironment of Patala Formation in Salt Range, Lesser Himalayas, Pakistan

Shahina Tariq†* and SRH Baqri‡

† *Institute Earth and Envirnomental Science, Bahria University, Islamabad, PAKISTAN*
‡ *Pakistan Museum of Natural History, Islamabad, PAKISTAN*

* *To whom correspondence should be addressed. E-mail: Shahinatariq@yahoo.com*

In Potwar basin the shaly part of the Patala Formation of Paleocene age stretches from the Salt Range in the southeast to Kala-Chitta Range in northwest. The paleoenvironment of the Potwar basin is interpreted by the diagenetic and sedimentational control of clay minerals in the basin. The clay mineralogy displays kaolonite, illite, with minor mixed layer of illite/ montmorillinte clay minerals and occasional chrlorite. It is inferred that the kaolinite/illite and chlorite minerals are the detrital clay minerals, brought into the depositional basin due to erosion of the source rocks exposed in the southeast of partly diagenetic origin. The clay mineral compositions from the southeast to northwest show that kaolinite decreases while illite and chlorite increase. The decrease of kaolinite in Kala-Chitta Range is most likely due to sedimental/depositional control. The course-grained kaolinite was abundantly deposited in fresh to brackish water conditions in shallow parts of the basin while the conditions changed towards northwest from shallow marine to brackish causing less transportation into deeper parts of the basin. The fine grained illite and chlorite mineral were transported and deposited in abundance in the deeper parts of the basin. No significant variation is observed in mixed-layer clay mineral. The crystallinity indices of kaolinite and illite show an increase in Salt Range where as they decrease in Kala-Chitta Range. The decrease in crystallinity of clay mineral in conjunction with kaolinite deposition patterns, prove the transportation, and deepening of the depositional basin from southeast to northwest.

Late quaternary Neotectonic evolution of dun in Garhwal Sub Himalaya

VC Thakur*, AK Pandey and N Suresh

Wadia Institute of Himalayan Geology, Dehra Dun, INDIA

* To whom correspondence should be addressed. E-mail: bindu_ddn@sancharnet.in

Dehra Dun is 80 km long 20 km wide valley within the Siwalik foreland basin of Garhwal Sub-Himalaya, bounded by the frontal Siwalik range to its south and the Lesser Himalayan Mussoorie range to its north. The base of the Mussoorie range is demarcated by the Main Boundary Thrust (MBT) that brings the late Proterozoic-Cambrian sequence of Lesser Himalaya to override the Siwaliks. To the south a sudden topographic rise of the frontal Siwalik range from the alluvial plain marks the Himalayan Frontal Thrust (HFT) that separates tectonically the Siwalik Group strata from the Holocene to recent alluvial sediments. In his pioneering work, Nakata (1972) recognized four levels of geomorphic surfaces. In Dun the Siwalik Group strata are folded and eroded, and are overlain by 100-300 m thick Dun gravels. The post-Siwalik Dun gravels are lithostratigraphically classified into four units: Unit A, Unit B and Unit C in northern part and Unit D in southern part of Dun. Based on earlier published OSL dates (Singh et al. 2001), the assigned ages are: > 40 Ka for Unit A, 29 Ka-22 Ka for Unit B and 10 Ka and younger for Unit C.

In northern part of Dun the Siwalik Group strata are exposed in two different tectono-geomorphic framework: the dissected Siwalik and the pedimented Siwalik, the former has uplifted topography with isolated cover of Dun gravels whereas the later are exposed in entrenched stream sections overlain by thick cover of Dun gravels. The dissected and uplifted Siwalik constitutes the hanging-wall and the pedimented siwalik forms the foot-wall of the Santaurgarh Thrust (ST). The Unit A of Dun gravels, occurring as tilted beds dipping NE 15°-45° to horizontal and overlying the eroded and steeply dipping Siwalik, represent synorogenic deposition related to growth of the Santaurgarh anticline. The Santaurgarh anticline, an overturned fold, facing south with steeply to moderately dipping limbs was developed as fault-propagated fold over the ST. In the frontal Siwalik range Mohand anticline was developed as fault-bend fold over the HFT. The Mohand anticline is an upright and asymmetric fold with steep dipping forelimb and gentle dipping to horizontal back limb. On the range front the strath terraces occur at ~20 m elevation, and the Siwalik strata dipping NE 30° over the older alluvium are exposed in a trench. These observations indicate active displacement ongoing in Holocene time. South of the HFT, ~15 km wide piedmont zone is uplifted to 10-15 m elevation as evidenced by remains of uplifted topography, entrenched streams and a topographic rise from flood plain towards the HFT. The uplift of piedmont zone is attributed to a blind fault emerging as imbricate of the southward propagating HFT. Based on earlier published OSL dates and our newly obtained OSL dates, age constraint is placed on the tectonic events. The HFT was initiated during interval between 500 ka and 100 ka. The ST was initiated post- 500 ka and continued its activity as young as post- 40 ka. The Bhauwala Thrust and Majhaun Fault were developed between 29 ka and 22 ka, and the Asan Fault post-dated 10 ka. The upliftment of the piedmont zone post-dated 5 ka and probably coseismic.

References

Nakata, T. 1972. *Geomorphic history and crustal movements of the foothills of the Himalaya.* Report of Tohoku University, Japan, 7th Series (Geography), 2, 39-177

Singh, AK, B Prakash, R Mahindra, JK Thomas and AK Singhvi. 2001. Quaternary alluvial fan sedimentation in the Dehradun valley piggy back basin, NW Himalaya: Tectonic and Paleoclimatic implications. *Basin Res* 13: 449-471

Paleohydrological reconstruction of molasses sediments from the Siwalik Group along Surai Khola section, West Nepal Himalaya

Prakash D Ulak

Department of Geology, Tribhuvan University, Kathmandu, NEPAL

For correspondence, E-mail: pdulak@wlink.com.np

The Siwalik Group is limited by the Main Boundary Thrust (MBT) to the north from the Lesser Himalaya and the Main Frontal Thrust (MFT) or equivalent to the Frontal Churia Thrust (FCT) to the south from Indo-Gangetic Plains. About six kilometres thick Neogene molassic mudstone, sandstone and conglomerate of the Siwalik Group is accumulated along the Surai Khola area in west Nepal in the southern frontal area of the Himalaya. The group comprises many fining-upward successions on a scale from several to tens of metres, but is a coarsening-upward succession as a whole.

Eight representative facies associations have been mainly recognized on the basis of the grain size of sandstone and assemblage of sedimentary structures in this sequence. These facies associations are intimately related to each lithological unit (Nakayama and Ulak 1999). According to them, the Bankas Formation and the Jungli Khola Member of the Chor Khola Formation are correlated to the Lower Siwaliks and are products of fine-grained meandering fluvial system. The Shivgarhi Member of the Chor Khola Formation and lower part of the Surai Khola Formation are correlatable to the Middle Siwaliks and, are deposited by the flood flow-dominated meandering fluvial system and sandy meandering fluvial system whereas the middle and upper parts of the Surai Khola Formation (Middle Siwalik) is produced by the braided fluvial system. The Dobata Formation (Upper Siwaliks) is represented of the product of anastomosed fluvial system. The lower and upper parts of the Dhan Khola Formation (Upper Siwaliks) are deposited by the gravelly braided fluvial system and debris flow-dominated braided fluvial system.

Nakayama and Ulak (1999) recognised five stages during the deposition of the Siwalik Group. They concluded the evolutional pattern of 6 stages which are from meandering system (stage 1), flood flow-dominated meandering system (stage 2), sandy braided system (stage 3), anastomosed system (stage 4), gravelly braided system (stage 5), and debris flow dominated braided system (stage 6). They inferred that three of the five stages are controlled by thrust activities; the onset of the deposition of the Siwalik Group by the Main Central Thrust (MCT), the gravelly facies of the lower part of the Dhan Khola Formation (Upper Siwaliks) by the Main Boundary Thrust (MBT), and the debris facies of the upper part of the Dhan Khola Formation (Upper Siwaliks) by the Central Churia Thrust (CCT) is equivalent to the Main Dun Thrust (MDT).

The paleohydrology and its evolutional change of the group along have been estimated using grain size of the sediment and thickness of fining-upward successions. Samples for grain size analysis were collected from the bottoms of the fining-upward cycles on a scale from several to tens of metres. The bottom of the fining-upward cycle is suitable sampling position for paleohydrological estimation. Forty-eight samples are obtained from twenty-two sections. Thin section and sieving methods are used for grain analyses because the consolidation of samples widely varied from strongly lithified to loosely packed. Both methods are explained in Tucker (1988). More than 200 of longest apparent grain dimension were measured in one section, and determined the mean of dimension, 50% dimension, and 95% of dimension, as mean diameter, median diameter, and 95% of grain size distribution, respectively.

Thickness between the top of bedload beds and sampling horizon is used for paleoflow depth. Most of the samples were obtained from the bottoms of the fining-upward cycles, so that bedload thickness is frequently concordant with flow depth. This is the extended application of the bankfull flow estimation in meandering channel (Ethridge and Schumm 1978, Bridge 1978). The estimation method in this study covers with both sandy and gravelly sediments, and also applicable to the outcrops with the limited lateral-dimension.

Paleovelocity varies from 0.17 m/s to 3.28 m/s stratigraphic upward, paleochannel gradient, and paleodischarge changes from 10^{-6} to 10^{-3} m/m and 10^{1} to 10^{4} m³. The paleohydrology shows an increase in flow velocity, channel slope gradient, and paleodischarge in stratigraphic younger sequences and suggests gradually change in fluvial system during the deposition of the Siwalik Group. Relation between gradually change in the evolution of the fluvial system and the progressively increasing in paleohydrological parameters from older to younger of the stratigraphic position along the Surai Khola section, the Siwalik Group has shown coincidence.

The changes of paleohydrology reflect the southward propagation of thrust. Two drastic paleohydrological changes in this study is coincide with the inception stage 4 and stage 5. That is, paleohydrological values change must reflect the southward progradation of thrust activities.

The Siwalik Group indicated the coarsening-upward as a whole, which has been simply considered to reflect the upliftment Himalaya. However, this study indicates that the Siwalik sedimentation has also to be considered in the viewpoint of the proximity from the thrust-formed piedmont line.

References

Nakayama K and PD Ulak. 1999. Evolution of fluvial style in the Siwalik Group in the foothills of the Nepal Himalaya. *Sedim Geol* **125**: 205-224

Tucker M. 1988. *Techniques in Sedimentology*. Oxford: Blackwell, 394 p.

Ethridge FG and SH Schumm. 1978. Reconstructing paleochannel morphologic and flow characteristics: methodology, limitations and assessment. In: Miall AD (ed), *Fluvial Sedimentology*. Canadian Soc Petrol Geol Mem **5**: 703-721

Bridge JS. 1978. Paleohydraulic interpretation using mathematical models of contemporary flow and sedimentation meandering channels. In: Miall AD (ed), *Fluvial Sedimentology*. Canadian Soc Petrol Geol Mem **5**: 723-742

Role of primary to re-equilibrated fluids during P-T evolution from Nagthat Siliciclastic of Lesser Himalaya, India

Priti Verma* and Rajesh Sharma

Wadia Institute of Himalayan Geology, Dehradun, INDIA

* To whom correspondence should be addressed. E-mail: preity_ver@yahoo.com

Tiny droplets, the fluid inclusions (FI) or the paleofluids that represents the mother fluid system existed during the growth of the host crystal with subsequent geological events. Fluid inclusion studies have been carried out to define PVTX properties of the basinal fluids and their participation in the evolution of the rocks. H_2O-NaCl, H_2O-CO_2-NaCl, CO_2 type fluid phases are noticed in the rocks of Lesser Himalayan sedimentary terrane. The distribution pattern of these inclusions varies as primary, secondary and re-equilibrated type of fluid phases that reveals the depositional history and post–deformational events. Primary FI trapped during the crystallization of the host mineral are the representative of early fluid trapped before deformation and recrystallisation. The post–deformational event directed variable P-T conditions in the system. The internal pressure inside the inclusions exceeds the confining pressure which may result into partial or complete change in the shape of the cavity with disturbing the original fluid content. The development of the requilibration textures such as C – shape, annular ring, decreptation clusters, stretching signifies high internal pressure > confining pressure. Sudden fall in pressure at constant temperature generates high internal overpressure inside the inclusion cavity that follows the isothermal decompression path.

Proterozoic Nagthat formation of Lesser Himalaya is exceptionally arenitic in nature showing the presence of two different generatons of quartz i.e. primary detrital and recrystallised ones. The majority of homogeneous H_2O-NaCl are present in both type of crystallization but H_2O-CO_2-NaCl heterogeneous FI are exclusively present in detrital quartz grains. Primary biphase aqueous inclusions cover 70 to 90 volume percent of liquid with a contemporary vapor phase and are mostly isolated in appearance but sometimes random pattern of distribution are also noticed in detrital quartz grains. Tiny monophase aqueous inclusions are frequently noticed in recyrtallised type of quartz grains. The first melting temperature of primary saline aqueous inclusions indicate the presence of H_2O-NaCl fluid with homogenization temperature of 121 to 232°C and salinity in the range of 3.8 to 11.1 wt% NaCl.

Fluid immiscibility representing the heterogeneous trapping of H_2O-NaCl, H_2O-CO_2-NaCl, CO_2 aqueous and carbonic phase is noticed in subrounded detrital quartz. The eutectic temperature of these inclusions at –56.6 °C confirms the presence of pure CO_2 in inclusions and their complete homogenization ranges between –1 to –2 °C denoting the density of 0.9 gm/cm³. Such type of primary CO_2 entrapment is predicted to have been originated from protolith of the sandstone during quartz crystallization phase.

The suturing of crystal or mineral due to post–depositional deformation events consequence the growth of fluid inclusions in linear fashion, which crosscuts the grain boundary. These linear arrays of different generations, sometimes crosscutting each other, represent two stages of deformation. Two different sets of microfractures are filled with monophase and biphase aqueous inclusion of less than 5 micron in size. Each successive trapping of inclusion trail can establish a good chronological record. The
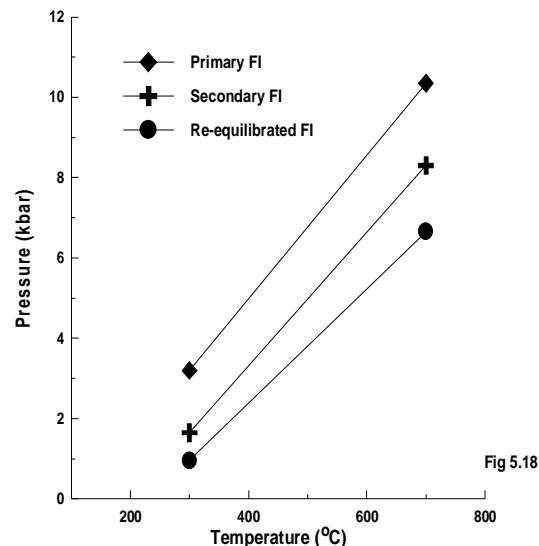

FIGURE 1. Isochors for Nagthat formation of Lesser Himalaya, India

most recent trail developed in the process is considered to be the youngest which can reveal the youngest activity prevailed after deposition. The homogenization of these secondary inclusions in quartz varies in the range of 198 to 232 °C with salinity between 2 to 14.5 wt% NaCl.

The re-qulibration of primary fluid due to high internal pressure>confining pressure develops several features like stretching of the inclusion cavity, their migration, satellite inclusion cavities etc in the quartz grains showing varied degree of recrystallisation. The homogenization temperature of these inclusions ranges between 187.5 to 235°C and salinity between 2 to 8.4 wt% NaCl.

The mineral relationship and fluid role support two stages of diagenesis i.e. locomorphic stage showing >80% quartz and low concentration of altered minerals such as sericite, chlorite and other clay minerals and phyllomorphic with the development of physillites and pressure shadows, suggested two periodic episodes of diagenesis below 250 °C.

The P-T estimation of these rocks can be done by measuring total homogenization temperature and estimated pressure; the isochore (iso- Th line) of different fluid phase's i.e. primary, secondary and re-equilibrated inclusions can reveal the evolution of the rock in the sedimentary basin. The P-T interpretation for Nagthat formation siliciclastic is plotted in **Figure 1**, which shows the iso-Th lines for primary, secondary and re-equilibrated fluids in succession and reveals:

~ Transportation of the sediments from the source and its deposition in the basin supported by carbonic FI
~ External deformation of rock and suturing of mineral and growth of secondary fluid inclusions
~ Re-equilibration of primary fluid during intense deformation.

Northeastward growth and uplift of the Tibetan Plateau: Tectonic-sedimentary evolution insights from Cenozoic Hoh Xil, Qaidam and Hexi Corridor basins

Chengshan Wang†‡*, Zhifei Liu§ and Lidong Zhu†

† State Key Laboratory of Oil and Gas Reservoir Geology and Exploitation, Chengdu University of Technology, Chengdu 610059, CHINA
‡ China Univesity of Geosciences, Beijing 100083, CHINA
§ Laboratory of Marine Geology, Tongji University, Shanghai 200092, CHINA

* To whom correspondence should be addressed. E-mail: wcs@cdut.edu.cn

The northeastward growth of the Tibetan Plateau was addressed as a major uplift process of Northeast Tibet, deduced mainly from the Qaidam, Gonghe-Guide, and Hexi Corridor basins (Métivier et al. 1998; Pares et al. 2003). These studies contributed to a significant in understanding of the crustal thickening and oblique stepwise rise of Plio-Quaternary Tibet (Meyer et al. 1998; Tapponnier et al. 2001). But sedimentary basins in central Tibet still remain less studied because of harsh conditions for fieldwork. The Hoh Xil Basin, as the largest Cenozoic sedimentary basin in the hinterland of Tibetan Plateau, is situated in central Tibet between Kunlun and Tanggula ranges (Liu et al. 2001). From Hoh Xil Basin in central Tibet northeastwards to the Qaidam Basin in Northeast Tibet, and to the Hexi Corridor Basin at the northeast edge of Tibet, the Tibetan Plateau consists mainly of basin-ridge tectonic-sedimentary system with about six north-south trending latitude ranges, i.e. the Hoh Xil, Qaidam, and Hexi Corridor basins with the Kunlun and Qilian ranges between them. Our study focuses on the tectonic and sedimentary evolution of the basin-ridge system to contribute the understanding of the uplift history of the Tibetan Plateau.

The Hoh Xil Basin exposes 5823 m thick Cenozoic sediments, which were paleomagnetically dated as the Eocene-Early Oligocene (51.0-31.3 Ma) Fenghuoshan Group in the lower part and the Early Oligocene (31.3-30.1 Ma) Yaxicuo Group in the upper part (Liu et al., 2003), with the Early Miocene Wudaoliang on the top. The basin was formed first as a strike-slip/extensional basin and remained during the 51.0-47.0 Ma period. Then during 47.0-30.1 Ma, the basin developed as a foreland basin with the Tanggula range as its major clastic provenance that contributed depocenter in the basin to shift northeastwards. In the Early Miocene, the basin-widely-distributed Wudaoliang limestone suggests the Hoh Xil Basin to be a relatively stable intermontane basin (Wang et al., 2002). The Qaidam Basin is situated between the Kunlun range in the south and the Qilian range in the north with an amount of >15000 m thick Cenozoic sediments. Following previous studies, we reconstruct the tectonic-sedimentary history as: the extensional basin stage (65-46 Ma) with brown-violet conglomerate and sandstone upward-fining sequence; the foreland basin stage (46-2.45 Ma) with a southeast-east distribution pattern of sub-basins that obviously have a direct relationship with the activity of the Altyn Tagh Fault; the intermontane basin stage (2.45-0 Ma) with basin-wide-distributed clastic sediments. The Hexi Corridor Basin was formed under the Altyn Tagh Fault activity as a strike-slip basin started from 37.7 Ma. During 30.3-0.13 Ma period, with the movement of the Qilian orogen, the basin depocenter shifted southwards to the mountain edge that indicates the formation of a foreland basin. From 0.13 Ma, the basin has evolved into an intermontane basin with a less than 100 m thick sediments.

The three Cenozoic sedimentary basins have a similar tectonic-sedimentary history, i.e. first as strike-slip/extensional basin, then as foreland basin, and last as intermontane basin. The evolution of their foreland basin stage indicates a northeastward shift of the orogenic uplift from 47.0-30.1 Ma in central Tibet (the Tanggula range), to 46-2.45 Ma in Northeast Tibet (the Kunlun range), and to 30.3-0.13 Ma in the northeast edge of Tibet (Qilian range). At the same time, each basinal depocenter also shift northeastwards with predominant northeastward paleocurrents. The tectonic-sedimentary evolution of the series of Cenozoic sedimentary basins strongly suggests the northeastward growth and uplift process of the Tibetan Plateau started from Eocene to present.

References

Liu Z, C Wang and H Yi. 2001. Evolution and mass-balance in the Cenozoic Hoh Xil basin, northern Tibet. *J Sedim Res* **71** (6): 971-984

Liu Z, X Zhao, C Wang, S Liu and H Yi. 2003. Magnetostratigraphy of Tertiary sediments from the Hoh Xil Basin: implications for the Cenozoic tectonic history of the Tibetan plateau. *Geophys J Int* **154**: 233-252

Métivier F, Y Gaudemer, P Tapponnier and B Meyer. 1998. Northeastward growth of the Tibet plateau deduced from balanced reconstruction of two depositional areas: the Qaidam and Hexi Corridor basins, China. *Tectonics* **17** (6): 823-842

Meyer B, P Tapponnier, L Bourjot, F Métivier, Y Gaudemer, G Peltzer, G Shunmin and C Zhitai, 1998. Crustal thickening in Gansu-Qinghai, lithospheric mantle subduction, and oblique, strike-slip controlled growth of the Tibet Plateau. *Geophys J Int* **135**: 1-47

Pares JM, RV der Voo, WR Downs, M Yan and X Fang, 2003. Northeastward growth and uplift of the Tibetan Plateau: Magnetostratigraphic insights from the Guide Basin. *J Geophy Res* **108**: 10.1029/2001JB001349

Tapponnier P, Z Xu, F Roger, B Meyer, N Arnaud, G Wittlinger and J Yang. 2001. Oblique stepwise rise and growth of the Tibet Plateau. *Science* **294**: 1671-1677

Wang C, Z Liu, H Yi, S Liu and X Zhao, 2002. Tertiary crustal shortening and peneplanation in the Hoh Xil region: implications for the tectonic history of the northern Tibetan plateau. *J Asian Earth Sci* **20** (3): 211-223

SHRIMP U-Pb zircon geochronology of the High Himalayan rocks in the Nyalam region, Tibet

Yanbin Wang*, Dunyi Liu and Yan Liu

Beijing SHRIMP Lab, Institute of Geology, Chinese Academy of Geological Sciences, No.26, Baaiwanzhuang Rd, Beijing, 100037, CHINA

* To whom correspondence should be addressed. E-mail: yanbinw@cags.net.cn

U-Pb age patterns of individual detrital zircons are a potentially powerful tool for constraining metasedimentary provenance. Each zircon grain has a characteristic age reflecting its genesis, and the overall population of detrital zircons represents the spectrum of primary zircon-bearing source rocks, including detritus derived from a number of sedimentary cycles (Cawood et al. 1999).

The complex of sillimanite-, kayanite- and garnet-bearing gneiss, calc-silicates and augen gneiss in Nyalam High Himalaya are intruded by granitoids. The garnet-sillimanite paragneisses have experienced an early Paleozoic metamorphism (Gehrel et al. 2003) and Tertiary metamorphism. The source of metasedimentary rocks of the Nyalam High Himalaya zone has been studied using SHRIMP ion microprobe at Beijing SHRIMP Lab, Chinese Academy of Geological Sciences.

SHRIMP U/Pb age data from the metasedimentary rocks of the High Himalayan terranes in South Tibet range from ca.23 Ma to 3221 Ma. The U-Pb data allow grouping of the zircons into five major age components with the exception of Cenozoic ages (**Figure 1**). (1) Archean grains with a maximum age frequency between 3221 and 2509 Ma, (2) Paleoproterozoic grains ranging from 2453 to 1631 Ma, (3) Mesoproterozoic to early Neoproterozoic grains ranging in age between 1530 Ma and 944 Ma, (4) Neoproterozoic grains ranging between 852 and 540 Ma, and (5) Pan-African ages (543-443 Ma).

Potential source regions for the detrital zircons occur within the Gondwana terranes: zircons of Archean age correspond to the age of rock unit formed during major a mgmatic and tectonothermal pulses in the Bhandara Craton or Singhbum craton, zircons with paleo-Mesoproterozoic ages reflect tectonic or magmatic events related to or older than the assembly of India

(Catlos et al. 2002). Neoproterozoic zircons may have been derived from Lesser Himalayan rocks or the Indian craton (Myrow et al. 2003). Pan-African zircons are the Pan-African orogen event along the Himalayan orogenic belts. The U-Pb age data suggest the sedimentary sources of the studied gneisses in the northern part of the Indian plate.

During Late Precambrian and the Palaeozoic, the Gondwanian India bounded to the north by the Cimmerian Super terranes, was part of Gondwana and was separated from Eurasia by the Paleotethys Ocean. During the periods, the northern part of India was affected by a Pan-African event, Numerous granitic intrusions dated at around 500Ma are attributed to this event. The Pan-African event is marked by an unconformity between Ordovician continental conglometrates and the underlying Cambrian marine sediments (Zhu Tongxin et al. 2003). The Pan-African event form a wide belt stretching from the Alps over the Arabic peninsula, Africa, India, Australia and down to Antarctica. These evidences suggests the presence of the Pan-African orogenic event in the Himalaya. It is tempting to correlate the early Palaeozoic thermal event with a late extensional stage of the long-lasting Pan-African orogenic events, which ended with the formation of the Gondwana supercontinent.

The protolith age of the High Himalayan metamorphic rocks is generally regarded to be Precambrian to early Paleozoic. It seems plausible that the High Himalayan metamorphic rocks represent a minimum depositional rage at ~500 Ma. Our data show strong similarities to previously published spectra for the Greater Himalayan zone, Lesser Himalayan zone and Tethyan Himalayan zone (Parrish et al. 1996; DeCelles et al. 2000; Myrow et al. 2003). Detrital zircon spectra from the High Himalayan range is as young as 500 Ma, so the High Himalaya and Tethyan Himalaya were deposited contemporaneously.
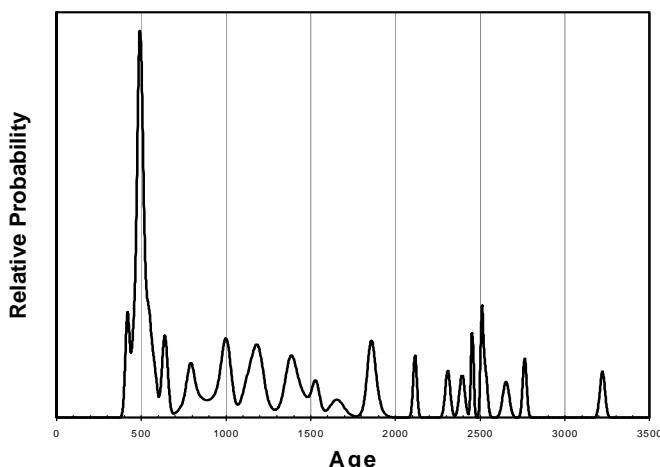
FIGURE 1. Detrital zircon age spectra from Nyalam High Himalaya (Sample NY93-1)

References

Catlos EJ, TN Harrision and CE Manning . 2003. Records of the evolutionof the Himalayan orogen from in situ Th-Pb ion microprobe dating of monazite: Eastern Nepal and western Garhwal: *J Asian Earth Sci* **20**: 459-479

Cawood PA, AA Nemchin, , A Leverenz, A Saeed and PF Balance.1999. U/Pb dating of detrital zircons:Implications for the provenance record of Gondwana margin terranes. *Geol Soc Amer Bull* **111**(8)**:** 1107-1119

DeCelles PG, GE Gehrels, J.Quade, BN Lareau and MS Spurlin.2000. Tectonic implications of U-Pb zircon ages of the Himalalyan orogenic belt in Nepal: *Science* **288**: 497-499

Gehrels GE, PG DeCelles and A Martin. 2003. Initiation of the Himalayan orogen as an Early Paleozoic thin-skinned thrust belt: *GSA Today* **13**: 4-9

Myrow PM, NC Hughes and TS Paulsen. 2003. Integrated tectonostratigraphic analysis of the Himalaya and implications for its tectonic reconstruction: *Earth Planet Sci Lett* **192**: 433-441

Parrish RR and KV Hodges. 1996. Isotopic constraints on the age and provenance of the Lesser and Greater Himalayan sequences, Nepalese Himalaya*: Geol Soc Amer Bull* **108**: 904-911

Zhu Tongxin, A Wang and Zhouguangfu. 2003. The discovery of Early Ordovician continental conglomerates in the Himalayan region. *Geol: Bull China* **22**(5)**:** 367-368

SHRIMP zircon ages of orthogneiss from EW-trending gneissic domes in Southern Tibet: Their tectonic implications

Yu Wang* and Wencan Liu

Geologic Laboratories Center and Department of Geology, China University of Geosciences, Beijing 100083, CHINA

* To whom correspondence should be addressed. E-mail: wangyu196601@sohu.com

The north Himalayan gneissic domes consist of several metamorphic and plutonic culminations that extend ~650-700 km in east-west direction. These orthogneissic domes are mantled by high-grade metamorphic rocks (Lee et al. 2000, 2004; Burchfiel et al. 1992), and in turn, are mantled by low-grade metamorphic to unmetamorphosed rocks. Five zircon SHRIMP samples, collected from the E-W trending gneissic domes, present similar ages on the western part of domes at 37-28 Ma and none of these ages on the eastern part correspond to rim of single grain. The core of the single grain yielded similar age of ~530-480 Ma. Besides, CL photographys also reveal different features for those five samples.

Kangmar Dome
Two samples contain zircons that exhibit sector zoning and well-defined low-U cores. Most crystals have intermediate U rims. Core and rim analyses of single zircons give identical ages. Of the 22 analyses, most of them fall within a single group that spreads slightly along the Concordia and constitute a coherent group, yielding a mean ^{206}Pb/^{238}U age of ~530-520 Ma. This weighted mean age is interpreted to be the crystallizing age of zircon, which can be referred to constrain the age of the orthogneiss, its former granite.

Mabja Dome
Thirteen analyses on 12 zircon grains or fragments were performed. Of these, 13 analyses constitute no coherent group, but yield a weighted mean ^{206}Pb/^{238}U age of ~502 Ma (8 data). This weighted mean age is interpreted to be the crystallizing age of zircon. Most of zircons from these samples bear oscillatory zoning, and crystallized during the magmatic event in which the granite formed.

Lagri-Kangri Dome
Twentyeight analyses on 25 zircon grains or fragments were performed whose ages range from ~36 Ma to ~500 Ma. These are from modified oscillatory-zoned zircon with the lower Th/U ratios.These yield younger ages of ~36-37 Ma. These ages can represent the timing related to a metamorphic event.
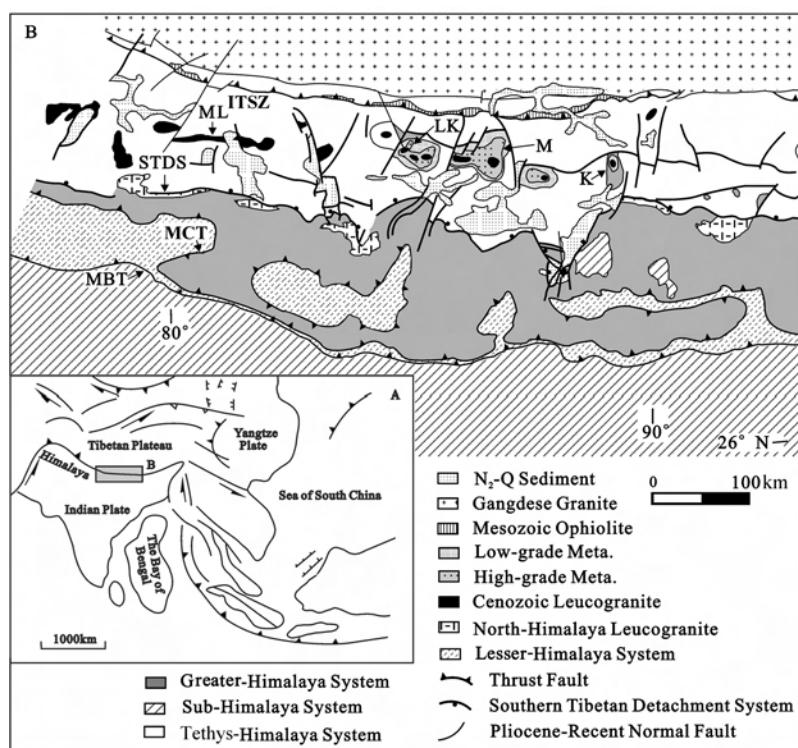
FIGURE 1. Regional tectonic setting of E-W-trending gneissic domes in southern Tibet. Abbreviations are as follows: K-Kangmar, M-Mabja, LK-Lagri-Kangri, ML-Malashan, ITSZ- Indus-Tsangpo Suture Zone, STDS-southern Tibetan Detchment System, MCT-Main Central Thrust fault, MBT-Main Boundary Thrust fault

Malashan Dome

Sixteen zircon grains or fragments were analysedwith ages ranging from ~28 Ma to ~500 Ma. Those having modified oscillatory-zoned zircon with the lower Th/U ratios yield younger ages of ~25-37 Ma. These ages can represent the timing related to a metamorphic event.

For samples from Malashan and Lagri-Kangri, both the cores and rims have different U and Th contents. The rims have much lower Th/U ratios (<0.01), than the cores (Th/U ratios >0.1-1). We interpret the oscillatory-zoned zircon as primary zircon inherited from the parent granite rocks, similar to samples from Kangmar and Mabja. The rims of zircons of some grains suggest formation of new zircon overgrowths during amphibole facies metamorphism.

Tectonic Interpretation and Discussion

The southern Tibetan gneissic-domes are petrographically, geochemically and structurally similar to each other. Most of zircon grains from east, i.e. Mabja and Kangmar appear to be homogeneous in zoning patterns. These features, together with their high Th/U ratios, indicate an igneous origin. This study does not support the viewpoint that the gneissic domes are the injection or the diapir of the Cenozoic magmatic event. Our study confirms that these gneissic domes had igneous precursors formed during Neoproterozoic time (as Pan-African thermal event). The young ages recorded initial formation of the E-W-trending gneissic domes, as well as the metamorphism of the southern Tibet. Moreover, this age can be referred as the peak time of crustal thickening in southern Tibet followed with the collision between Indian and Asian plates in the early Cenozoic time. This also indicates that the metamorphism is not at same time as the formation of the STDS, and also not at the same time as the injection of the leucogranite in southern Tibet. At the same time, this event also resulted in the re-metamorphism of the middle-lower crustal rocks.

Zircon features, Th/U ratios and ages indicate that these have different evolution or experienced various geologic events from east to west along this gneissic dome belt. Which kinds of mechanism or geologic events result in the differential ages of orthogneissic zircons, although they were covered by similar high-grade metamorphic rocks—by differential exhumation, uplift or adjoining of the fluid—remains speculative.

References

Burchfiel BC, ZL Chen, KV Hodges, YP Liu, LH Royden, CR Deng and JN Xu. 1992. The south Tibetan detachment system, Himalayan orogen: extension contemporaneous with and parallel to shortening in a collisional mountain belt. *GSA Special Paper* **269**: 1-41

Lee J, BR Hacker, WS Dinklage, Y Wang, P Gans, A Calvert, JL Wan, W Chen, AE Blythe and W McCleland. 2000. Evolution of the Kangmar dome, southern Tibet: structural, petrologic, and thermochronologic constraints. *Tectonics* **19**: 872-895

Lee J, BR Hacker and Y Wang. in press. Evolution of north Himalayan gneiss domes: structural and metamorphic studies in Mabja Dome, southern Tibet. *J Struct Geol*

Calcrete crust formation on the lateral moraine of Batura glacier, Northern Pakistan

Tetsuya Waragai

Department of Geography, Nihon University, Sakurajyosui Setagaya-ku Tokyo, 156-8550, JAPAN

For correspondence. E-mail: waragai@chs.nihon-u.ac.jp

Calcrete crusts, which are cementing gravels, are observed on the surface of lateral moraine on the circumference of the Batura glacier, northwestern Karakoram Mountains. Although calcretes generally develop from arid and semi-arid environments with an annual precipitation of 500 mm or less, they are also found in cold climatic regions such as permafrost environments (Swett 1974, Lauriol and Clark 1999). It is thought that the calcrete crust formation in cold environments is involved in carbonate dissolution on the permafrost table and calcite production near ground surfaces, which are derived from the temperature-induced solubility differential of calcium carbonate ($CaCO_3$). With regard to geochronological studies, calcrete and calcic soils can provide accurate dating and useful paleoenvironmental information by stable isotope analysis using ^{14}C, $^{230}Th/U$ and $\delta^{18}O$ (e.g., Sharp et al. 2003). This study considers the formation processes of the calcrete crusts in the cold environment around Batura glacier terminals through their mineralogical and chemical compositions and ^{14}C dating by an accelerator mass spectrometry (AMS).

In the study area (**Figure 1**), the Batura, Pasu and Ghulkin glaciers are going down to around the altitude of 2,500 m of glacier terminals from mountain peaks exceeding 7,000 m such as Batura peak I (7,794 m asl). There are distributed Pasu limestone and Pasu slate of the Palaeozoic, and granodiorites composed of Hunza plutonic complex of the Cretaceous around the Batura glacier terminals (Crawford and Searle, 1993). On the other hand, according to Waragai (1998, 1999) who carried out air temperature measurements at the lateral moraine located in the Batura glacier snout from July 1994 to July 1996, maximum and minimum temperatures were 43.7 and -13.7 degrees C, respectively. Annual average precipitation in Gilgit (1,490 m), located about 70km south of the study site, is 131.6 mm.
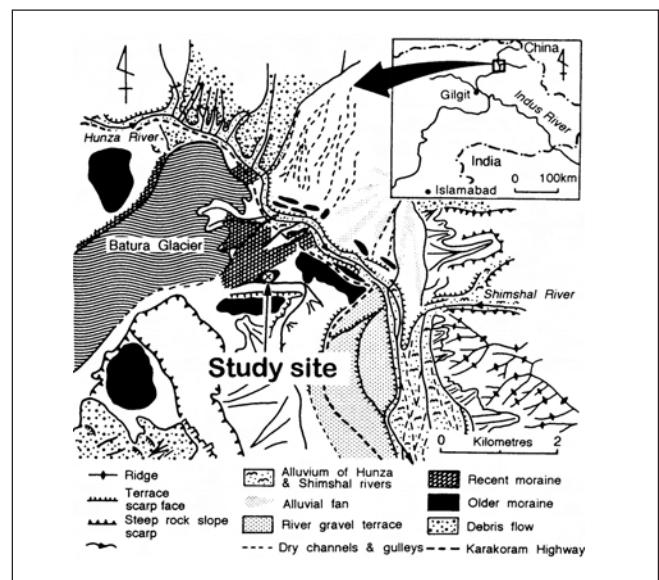
FIGURE 1. Location of a study site and geomorphological map at Batura glacier snout

Description of the calcrete crust

The calcrete crust develops on the ground surface (about 2,700 m) of the lateral moraine's ridge that was probably formed in the Batura glacial stage (Owen et al. 2002). Analysis was carried out for pebble calcretes (**Plate 1**) that accumulate on the ground under a granodiorite boulder (3.0x2.5x1.5 m^3) near the ridge of the lateral moraine. This sample, highly indurated, is composed

PLATE 1. Pebble calcretes formed under a boulder
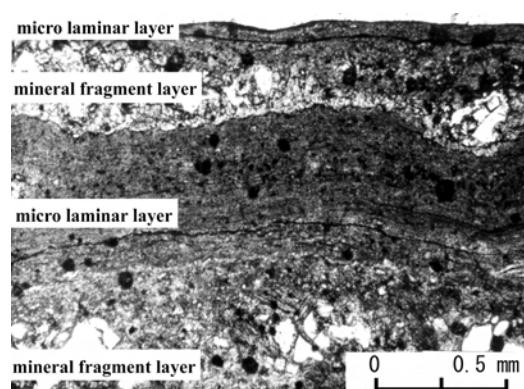
PLATE 2. The outermost layer of the calcrete crust showing laminar structure
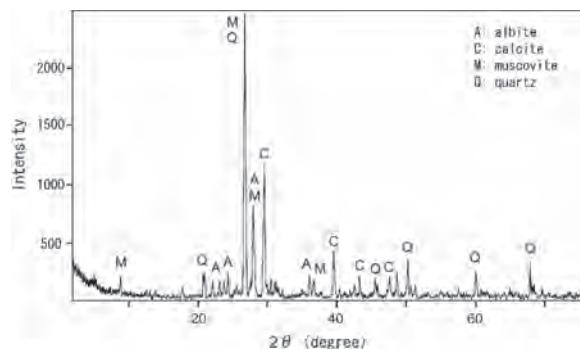
FIGURE 2. An X-ray diffraction pattern of the outermost layer of the calcrete crust

FIGURE 3. Ca and HCO_3 concentration of some glacier ice and waters

of pebbles and porous cementing materials as a matrix. Cements overlapped on pebbles form a micro-relief reflecting the surface morphology of pebbles and are cream in colour.

In order to investigate the structure of the calcrete crust, a sample was prepared, which was cut from the surface to a depth of about 2 cm, and a thin section was made. The microscopic structure from the surface of the crust to a depth of 1.5 mm is shown in **Plate 2**. According to the plate, the calcrete crust can be distinguished into mineral fragment layers and micro laminar layers developing by turns. The mineral fragment layer consists of some rounded mineral grains with a maximum diameter of 0.2 mm. Since the mineral fragment layer tends to place large particles in a lower part, it is recognized that this layer shows a slight grading bedding structure. Thus the boundary between upper parts of the mineral fragment layer and the lower parts of the micro laminar layer is relatively conformable. However, the micro laminar layer obviously borders the mineral fragment layer at its upper part. This shows that the outermost part of the calcrete crust has several sequences of layers joining both layers together.

1) Mineralogical and chemistry compositions

The mineralogical composition of the outermost part of the calcrete crust was examined with X-ray diffractometer (XRD). Quartz, albite, muscovite, and calcite crystals were identified (**Figure 2**). This result indicates that the mineral fragment layer shown in **Plate 2** is composed of quartz, albite, and muscovite crystals, while the micro laminar layer consists of calcite ($CaCO_3$).

Since the micro laminar layer is characterized by a striped pattern, the chemical composition for micro spots (quantitative point analysis) and element distribution (qualitative mapping analysis) for this layer was examined by electron-probe microanalysis (EPMA). A polished specimen, which was extracted from the surface to a depth of 2 cm, was used for these analyses. As a result of the qualitative mapping analysis for an analysed area of about 650 μm^2, it was revealed that a high concentration of Ca was present compared with Mg, Al, and Si in the micro laminar layer. In addition, it was surmised that the laminar structure reflects the difference of Ca concentration. Quantitative analysis for a spot (3 μm in diameter) showed about 60 % of CaO and about one percent of MgO. Total major element composition for the micro laminar layer was about 63 % by weight, and the remaining about 37 % was estimated to be H_2O content.

2) ^{14}C age of the calcrete crust

Since the outermost part of the calcrete crust dominantly consists
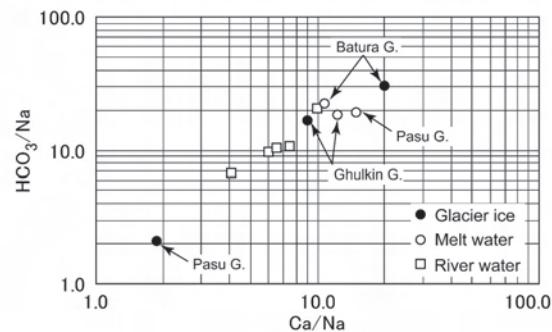
of calcium carbonates ($CaCO_3$), ^{14}C age by AMS was measured at the Institute of Geological & Nuclear Sciences Limited, New Zealand. An outermost thin layer of the calcrete crust was carefully removed with tweezers, then the carbon compound subjected to acid treatments was extracted from the outermost portion. The result of the measurement was the specimen indicated 7,358±57 yBP (NZA9243, $\delta^{13}C$=6.7‰).

Conclusion

According to Owen et al. (2002) who carried out the cosmogenic radionuclide (CRN) age determination for boulders on moraines around the present study site, the Batura glacial stage to which glaciers advanced is placed to 9.0-10.8 ka (yBP). This Batura glacial stage corresponds to the glacial advance period which is widely accepted in the Himalaya and Karakoram mountains between late Pleistocene and early Holocene (8 – 11 ka). The age for the outermost portion of the crust in this study (7,358 ± 57 yr) clearly places it in the later age of the Batura glacial stage. It is considered that the calcrete crust was formed under the warm climate when the Batura glacier was retreating about 7,000 years ago.

Meanwhile, the chemical reaction in connection with formation of calcite ($CaCO_3$) which is the dominant ingredient of calcrete crusts, is described as follows:

$$Ca^{2+}+2HCO_3^- \rightarrow CaCO_3+CO_2+H_2O$$
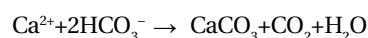
Precipitation of the carbonates due to supersaturation mainly results from the evaporation and freezing of water, decreases in CO_2 partial pressure, CO_2 degassing, and biological activities. Since Pasu limestone is widely distributed around Batura glacier terminals, the presence of high Ca^{2+} is supposed in groundwater and surface water around the study area. Results of chemical analysis by the Ion Chromatography analyser demonstrate that the glacier ice and melt water of the Batura glacier have a high concentration of Ca^{2+} and HCO_3^- (**Figure 3**). Particularly, cold climatic environments during glacial stages are effective in formation of $CaCO_3$, because $CaCO_3$ is more soluble at lower temperatures. The climatic warming following the glacial stage may have accelerated $CaCO_3$ precipitation accompanied by decreases in CO_2 partial pressure from the glacial ice pressurized. It is concluded that the calcrete crusts precipitated by decreases in CO_2 partial pressure and evaporation of water including high concentration of Ca^{2+} under the climatic warming at the place between moraines and glacial ice bodies.

References

Crawford MB and MP Searle. 1993. Collision-related granitoid magmatism and crustal structure of the Hunza Karakoram, North Pakistan. In: Treloar PJ and MP Searle (eds), *Himalayan Tectonics*. London: Geological Society Special Publication. No. 74, p 53-68

Lauriol B and I Clark. 1999. Fissure calcretes in the arctic: a paleohydrologic indicator. *Applied Geochemistry* **14**: 775-85

Owen LA, RC Finkel, MW Caffee and L Gualtieri. 2002. Timing of multiple late Quaternary glaciations in the Hunza Valley, Karakoram Mountains, northern Pakistan: Difined by cosmogenic radionuclide dating of moraines. *Geol Soc Amer Bull* **114**: 593-604

Sharp WD, KR Ludwig, OA Chadwick, R Amundson and LL Glaser. 2003. Dating fluvial terraces by ^{230}Th/U on pedogenic carbonate, Wind river basin, Wyoming. *Quaternary Research* **59**: 139-50

Swett K. 1974. Calcrete crusts in an arctic permafrost environment. *Amer Jour Sci* **274**: 1059-63

Waragai T. 1998. Effects of rock surface temperature on exfoliation, rock varnish, and lichens on a boulder in the Hunza Valley, Karakoram mountains, Pakistan. *Arct Alp Res* **30**: 184-92

Waragai T. 1999. Weathering processes in rock surface in the Hunza Valley, Karakoram, North Pakistan. *Z Geomorph N.F. Suppl.-Bd.*, **119**: 119-36

Active landslides on the lateral moraines in the Kanchanjunga Conservation Area, eastern Nepal Himalaya

Teiji Watanabe†* and Naohiro Nakamura‡

† Graduate School of Environmental Earth Science, Hokkaido University, Sapporo, JAPAN
‡ Asahidake Visitor Center, Daisetsuzan National Park, Higashikawa, JAPAN

* To whom correspondence should be addressed. E-mail: twata@spa.att.ne.jp

This study identified the present development of landslide on the Holocene moraines (4,760-5,200 m) in the Kanchanjunga (Kangchenjunga) Conservation Area, eastern Nepal, which may result in disasters in future.

A tension crack with ca. 100 m in length runs parallel to the moraine ridge on the debris flow deposits (5050 m) between the lateral moraine and mountain slope near Pangpema Base Camp. On the right bank of the Kanchanjunga Glacier, ground surface of the sliding blocks, moraines, mountain slope, and other deposits such as debris flow deposits are almost completely covered by *Kobresia*. On the other hand, the landslide scars show the fresh outcrops without vegetation. Such landslide scars ranging from 1 m to 70 m in relative height are developed in a few rows on the right bank around the Kanchanjunga Glacier, and continuously extend for about 7.2 km although at some places they are not clear.

The interpretation of the air photographs taken in 1980 and field survey in 1989 clearly demonstrated that the landslides on the lateral moraines of the Kanchanjunga Glacier at the altitudes near the lower limit of the present permafrost (4,755 m: Ishikawa et al. 2001) have been created and enlarged between the two years. In the oblique air photographs taken in 1982, only one remarkable landslide scar can be seen on the lateral moraines near Lhonak and on the terminal moraine of the tributary glacier near Pangpema Base Camp. During the field survey in 1998, multiple landslide scars were observed at each site. This means that new landslides began to occur in this decade, especially in Pangpema and Lhonak. These new landslide scars are also identified in the 1992 air photographs.

With the help of the studies on the glacial chronology study (e.g., Asahi and Watanabe 2000), the surface level of the former Kanchanjunga Glacier was estimated: the glacial ice of approximately 100 m thick melted in the past century. This estimate is also supported by an old photograph of the Jannu Glacier, some 9 km to the south, which is published in the book, "Round Kangchengjunga", by Freshfield (1903). Therefore, unloading by rapid deglaciation might be a cause of the landslide although deglaciation alone cannot explain the development of the landslides.

We applied electrical resistivity soundings to detect the existence of the permafrost. No clear existence, however, was confirmed with possible small bodies of the permafrost. The landslides may have been developed during the final stage of the permafrost melting.

Many fresh and small cracks on the moraine surface indicate that the landslides are enlarging even today. This enlargement could cause hazards when the area is developed: the landslides occur on major trails and camping site. In the New Zealand Alps, mountain trails and recreation huts have been moved or demolished as a result of landslides on lateral moraines (Blair 1994). Because the similar features are observed in other Himalayan regions as well, monitoring landslides at higher altitudes should be a priority concern.

References

Asahi K and T Watanabe. 2000. Past and recent glacier fluctuations in Kanchanjunga Himal, Nepal. *J Nepal Geoll Soc* **22**: 481-490

Blair RWJr. 1994. Moraine and valley wall collapse due to rapid deglaciation in Mount Cook National Park, New Zealand. *Mountain Res Devel* **14**: 347-358

Freshfield DW.1903. *Round Kangchenjunga*. Republished in 1979, Ratha Pustak Bhandar. 373 p

Ishikawa M, T Watanabe and N Nakamura. 2001. Genetic differences of rock glaciers and the discontinuous mountain permafrost zone in Kanchanjunga Himal, eastern Nepal. *Permafrost and Periglacial Processes* **12**: 243-253

Watanabe T, N Nakamura and NR Khanal. 2000. Mountain hazards in the Kanchanjunga area, eastern Nepal: landslides developed on lateral moraines. *J Nepal Geol Soc* **22**: 525-532

Early aged ophiolites in the Qinghai-Tibet plateau and their tectonic implications

Xiao Xuchang*, Wang Jun and Zhang Zhaochong

Institute of Geology, Chinese Academy of Geological Sciences, Beijing, PO Box 100037, CHINA

* To whom correspondence should be addressed. E-mail: xxchng@ public.bta.net.cn, xxchng@geochina.cn

The Precambrian ophiolites, the oldest ophiolites, have attracted the studies from many geologists in recent decades (Li et al. 1997, 2001; Scarrow et al. 2001, Colombo et al. 2001), because the Pre-Cambrian ophiolites are relevant to the evolution of plate tectonics in the early period of the earth. This paper reveals two definite Pre-Cambrian ophiolites, named "Aoyougou Ophiolite", in the northeast and "Kudi Ophiolite" in the northwest of the Qinghai-Tibet plateau; the former lies near the intersection of 39°5' North latitude and 98°15' East longitude, the latter lies at the intersection of 77°10' East longitude and 36°45' North latitude.

Assemblage, age and tectonic implications of the Aoyougou ophiolite
The Aoyougou ophiolite occurred along the southern margin of northern Qilian orogen and is always associated with the late-early Proterozoic sediments containing stromatolites. It consists of serpentinite (mainly serpentinized harzburgite), gabbro, diabase dikes, basaltic rocks associated of pillow lavas and red-banded siliceous rocks, and has been dismembered, formed thrust slab intercalated with the Proterozoic sediments, but in some places, it is noteworthy that the upper part of the ophiolite, the basalt with pillow structure was overlain by the Proterozoic limestone or dolomitic limestone containing the Stromatolites (Hian-hua Li et al. 1997), the *Colonnella* sp. and the *Kussiella* sp. (Li et al. 1997) . The diabase dikes from the ophiolite were samples for the SHRIMP U-Pb zircon geochronology and give the ages of 1777±28Ma (Zhang et al. 2001). It is most probably the earliest ophiolite in China.

Samples from the Aoyougou ophiolite were analysed for major, trace and rare elements, showing that the SiO_2 contents of diabase and lavas range from 45.60% to 52.83% and TiO_2 from 1.42% to 3.22%, resembling to those of MORB and OIB. The diagrams of SiO2 vs. Nb/Y and ΣFeO vs. $\Sigma FeO/MgO$ indicate that all basaltic rocks belong to tholeiite series. Low MgO, Cr and Ni contents and Mg value of the basaltic rocks suggest that they might not be the primary magmas melted directly from mantle sources, but the evolved magmas after fractional crystallization of olivine, Cr-spinel in magma chamber. A tentative Zr/Y vs Zr diagram for basalts shows that the Aoyougou ophiolite might have formed in a small oceanic basin with slow spreading rate.

Assemblage, age and tectonic implications of the Kudi ophiolite
The upper part of the ophiolite comprises a thick series of basaltic rocks with pillow structure intercalated of thin bedded reddish siliceous rock, intruded by mafic dikes, which are well exposed along the road, the lower part mainly consists of the gabbro associated with gabbro-diorite and tonalite, the peridotite and dunite which occur at the top of the mountain.

There are much debate concerning the age of the Kudi-ophiolite in last few years in geological circle at home and abroad, so the highlight of this presentation is to report the reasonable isotopic age of 510±4 Ma (U-Pb ratio in zircon) for the gabbro-diorite, operated at the advanced and most powerful dating technique, the SHRIMP II (Beijing SHRIMP Center, Institute of Geology, CAGS). The Sm/Nd isochron age for the ultramafic rock is 651±53Ma (Ding et al. 1996).

The radiolaris from the siliceous rocks associated with the upper part of basaltic rocks are *Entactinia* sp and *Spumellaria* sp. ascribed to the Early Paleozoic (Zhou 1998).

On the basis of geochemical studies including major, trace and rare-earth elements data suggest oceanic basin (mainly the MORB) affinities for the major part of basaltic rocks.

Both the geochemical and geochronological data integrating with the geological setting suggest that the Kudi-ophiolite might have formed in an archipelago ocean which developed in the northwestern margin of the Tibet plateau during the Late-Proterozoic. It was not a vast ocean, the so-called Protero-Tethys, but a multi-island-ocean-basin which was subducted and closed probably during the early Paleozoic.

References

Colombo CG et al. 2001. Neoproterozoic ocean in the Ribeira belt (SE. Brazil), Episodes, V. 24 No. 4, p 245-252

Ding Daogui et al. 1996. The western Kunlun orogen belt and basin, Geol. Publishing house, Beijing, China

Hian-hua Li et al. 1997. Geochemical and Sm-Nd isotopic study of Neoproterozoic ophiiolites from SE. China, *Precambrian Research* **8881**(1997): 129-144

Scarrow JH et al. 2001. The late Neoproterozoic Enganepe ophiolite,Polar Urals,Russia: An extension of the Cadomian arc? *Precambrian Research* **81**(1997) 129-144

Xiao Xuchang et al. 1978. A study of the ancient ophiolite in the Qilian Mtns. NW. *China, Acta Geol. Sinica* **52**: 281-295

Zhang Zhaochong et al. 2001. SHRIMP dating of the Aoyougou ophiolite in the Qilian Mtns. And its geological significance, *Acta Petrologica Sinica* **17**(2) 222-226

Zhou Hui et al.1998. Discovery of the early Paleozoic Radiolarias in the ophiolite Melange zone at Kudi, W. Kunlun Mtns. and its tectonic implications,Chinese Science Bulletin, **43**(22): 248-251

Evolution of Mustang Graben, Tibet Himalayas, due to eastward extrusion of Tibet Plateau in and after the Last Glacial Age

Hiroshi Yagi†*, Hideaki Maemoku‡, Yasuhiro Kumahara‡, Takashi Nakata‡ and Vishnu Dangol§

† Lab. Geography, Yamagata University, Kojirakawa, Yamagata, 990-8560, JAPAN
‡ Institute of Geography, Hiroshima Universitys, JAPAN
§ Institute of Geology, Trichandra Campus, Trivbhan University, NEPAL

* To whom correspondence should be addressed. E-mail: yagi@kescriv.kj.yamagata-u.ac.jp

Mustang Graben is a NS trending longitudinal depression located in Tibet Himalayan Zone just behind the Higher Himalayas of Nepal (**Figure 1**). Its height is 3,000 to 4,000 m asl. surrounded by Tibetan Himalayas of which summit level is 5,000 to 7,000 m asl. Its width and length are less than ten kilometers and more than fifty kilometers, respectively. Kali Gandaki River originates from the uppermost course of the Mustang valley and flows through the valley. The river joins to the Ganga, forming the deepest transverse valley across the Higher Himalayas in the world. Development of such a graben in Tibetan Plateau is attributed to EW tensile stress field resulted from eastward extrusion of the Tibetan Plateau (Molnar and Tapponier 1975). There are some chronological studies on Takkhola Formation, burring Mustang Graben, and studies on relation between upheaval of Himalaya Range and deposition of Takkhola Formation (Yoshida et al. 1984). Hurtado et al. (2001) reports neotectonics of the Takkhola Graben. There are, however, no detail studies based on a field research in the upper Mustang about the most recent active faulting such as deformation of fluvial terraces and glacial landforms developed in the late Pleistocene or Holocene.

The authors (Yagi, Maemoku and Dangol) carried out a field study in the upper Mustang valley up to the border between Nepal and Tibet in Sept. 2002. This study also depends on elaborate interpretation of aerial photographs on scale of 1/50,000 over the Mustang Graben with special reference to terrace classification and active faults.

Fluvio-glacial terraces as time markers

Kali Gandaki River is an entrenched valley with more than 12 levels of terraces. The terraces are outwash plains continuing from moraine, fans and fluvial terraces. Development of those terraces was caused by complex of detritus supply due to glaciation, hydrological and tectonic conditions in this valley in the late Pleistocene and Holocene. There are some previous studies on geomorphological history along the Kali Gandaki River in the lower course from Kagbeni (Iwata et al. 1982, Iwata 1984, Hasegawa and Sasaki 1998, Hurtado et al. 2001).

This study tentatively classified those terraces into three groups; Higher terrace group, Middle terrace group and Lower terrace group, respectively. They are correlated as follows; Higher terrace group: MIS 4-3, Middle terrace group: MIS 2 and Lower terrace group: MIS 1, respectively, on the basis of their continuity along Kali Gandaki River, relative chronological level of terraces and radio carbon data obtained from terrace deposits (Iwata 1984, Hasegawa and Sasaki 1998, Hurtado et al. 2001). The higher terrace group is at least older than 22,770 yrs BP (Hasegawa & Sasaki 1998). This study also reports new radio carbon data from the Lowest terrace (L II) of 2,605 Cal BP just near Lo Mantang. Elder terraces are distributed in the lower course side around Jomoson, and younger terraces are distributed in the upper course side over the study area. Such chronological feature implies glaciation in the Holocene age in the upper Mustang area.
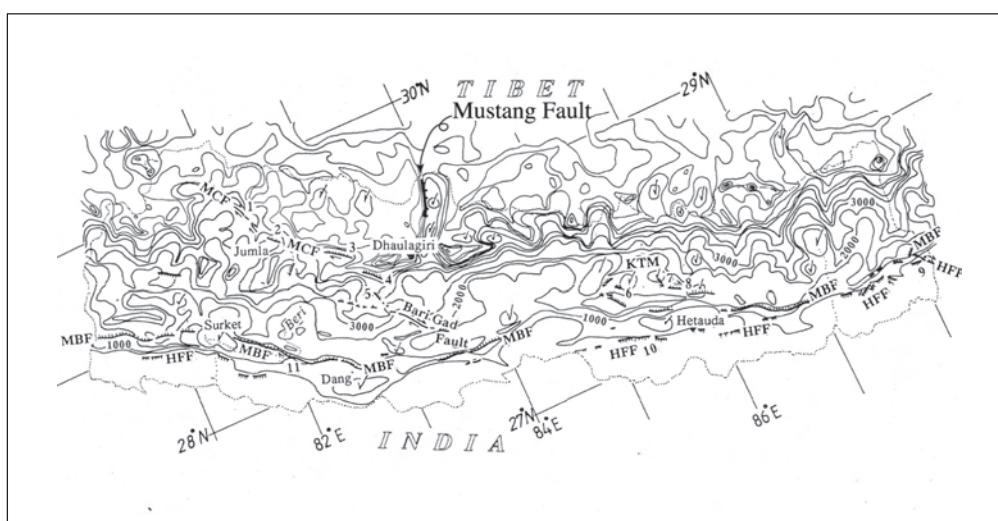
FIGURE 1. Location of Mustang Graben and distribution of active faults in the Nepal Himalayas
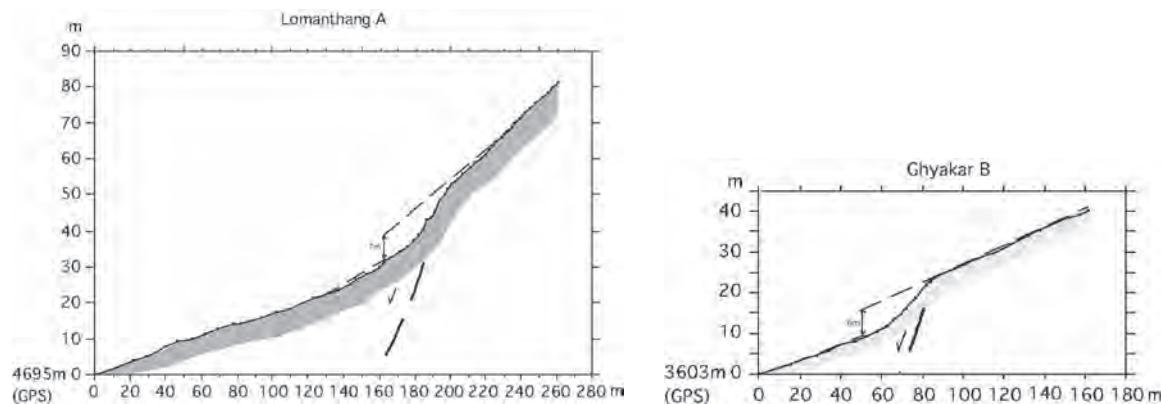
FIGURE 2. Geomorphological profiles of deformed fan surfaces due to active faulting

Mustang Fault

Distinct topographic contrast occurs along a foot line between the Graben and the surrounding mountains of Tibet Himalaya. Moraines and fan surface of outwash plain origin have been sometimes interrupted their geomorphological continuity by low relief scarplets perpendicular or oblique to the surfaces declination, where the foot line crosses the recent geomorphological surfaces. The scarplets usually occur on the Middle and Lower terrace groups and face to east **(Figure 2)**. They are traceable along the western foot line as long as fifty kilometers, though they occur sometimes fragmentarily. Such phenomena imply that these scarplets were caused by active faulting in and after the last Glacial Age. The authors call this active fault as Mustang Fault. Outcrop at left bank of the Ghilunpa Khola shows active faulting of river terrace deposits, dipping down to the east by high angle fault of 70 - 80 degrees. Consequently, sense of Mustang Fault is normal, down-throwing to the east. Lateral displacement of the topographic surface is not found, though Hurtado et al. (2001) describes the fault (Dangardzong fault) is a dextral strike slip in sense.

The authors surveyed tectonic deformation of topographic surfaces where fault scarps are clear. The highest profiles are obtained at 4,700 m asl. near the border. Dislocation of the surfaces ranges from 3.5 to 7 m. Vertical slip rate is higher in the north compared with that in southern part of the Graben. Valley side fault of normal sense is also found in the Thakkhola formation, Plio-Pleistocene sediments, near Dhakmar village in central part of the Graben. Deformation of the Thakkhola formation is more than fifty meters. These phenomena indicate that Mustang Graben has been formed by a tensile stress field of EW direction after Pliocene and evolved until Holocene. Extrusion of Tibet affects the Tibet Himalayan zone and has been continuing throughout the late Pleistocene to the Holocene.

References

Molnar P and P Tapponier. 1975. Cenozoic tectonics of Asia: Effects of a continental collision. *Science* **189**: p 419-426

Yoshida M, Y Igarashi, K Arita, D Hayashi and T Sharma. 1984. Magnetostratigraphic and pollen analytic studies of the Takmar series, Nepal Himalayas. *Journal of Nepal Geological Society (Special issue)* **4**: 101-20

Hurtado JM, KV Hodges and KX Whipple. 2001. Neotectonics of the Thakkhola graben and implications for recent activity on the South Tibetan fault system in the central Nepal Himalaya. *GSA Bulletin* **113**(2): 222-40

Iwata S. 1984. Geomorphology of the thakkhola-Muktinath region, central Nepal, and its late Quaternary history. *Geographical Report of Tokyo Metropolitan Univ* **19**: 25-42

Hasegawa Y and A Sasaki. 1998. Radio carbon data bearing on a lateral moraine distributed at Pandha Khola, a tributary of Kaligandaki River, Nepal Himalaya, *Quaterly J Geography*. **50**(3): 220-21 (in Japanese)

Digital sandbox modelling of Indian collision to Eurasia

Yasuhiro Yamada†*, Atsushi Tanaka‡ and Toshi Matsuoka†

† Department of Civil and Earth Resources Engineering, Kyoto University, JAPAN
‡ Sumiko, JAPAN

* To whom correspondence should be addressed. E-mail: yama@electra.kumst.kyoto-u.ac.jp

Summary

Discrete Element Method (DEM) is a powerful tool as a digital sandbox simulator to numerically reproduce fault related structures and to analyse the deformation quantitatively. Similar to analogue sandbox experiments, DEM approximates the geologic body as an assembly of particles that can properly simulate the brittle behaviour of the upper crust. We examined the collision process of the Indian sub-continent to the Eurasian Plate by using the DEM. The simulations reproduced the deformation geometry similar to published analogue experiments. Velocity and stresses of each particle extracted from the simulation were quite unstable showing a characteristic feature of the brittle behaviour of the upper crust. A comparison of these results with GPS and in-situ stress data of the eastern Asia suggests that the ductile deformation of the lower crust and mantle may have major roles to control the real deformation. The results also suggest that Tapponnier's tectonic model may have a strong boundary effect, particularly to the stress field within the model.

FIGURE. 1 Basic idea of the DEM. The given external forces define the motion of each particle.

Introduction

In order to analyse deformation processes of geologic structures, analogue physical experiments have been performed for a century. In particular, experiments using granular materials (dry quartz sand, micro glass beads, etc.) can properly scale the brittle behaviour of the upper crust, and have been successfully applied to various sedimentary basins, especially by the petroleum exploration industry. Recent techniques such as 'sandbox experiments' utilise Newtonian fluids as well, and the combinations of these two materials allow us to examine a great variety of deformation styles. The knowledge obtained from these experiments has been employed to understand structural development processes and also to predict possible future deformations. The experiments have also been contributing to determine the design of data acquisition of geophysical measurements, the parameters of data processing, and geological interpretations.

Since the material of the sandbox experiments is an assembly of grains, the deformation can be simulated with a numerical technique, the Discrete Element Method (DEM). We believe that DEM can replace at least partly the role of the sandbox experiments and can be applied to various scales of tectonic deformations (Yamada and Matsuoka 2004). This paper presents some results of this simulation which has been applied to the Indian collision to the Eurasia.

DEM simulation

DEM assumes the geologic body to be a particle assembly (**Figure 1**). The method requires two steps in calculation cycle to simulate the deformation: the first step to evaluate interaction forces for every particle, and the second step to move these particles according to numerical integration following the Newton's equation of motion for the given external forces. The interaction forces can be evaluated from force-displacement law (Cundall
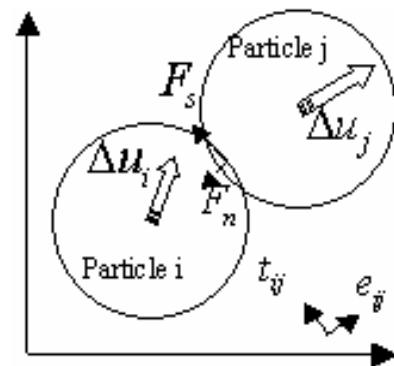
and Strack 1979). One of the significant advantages of DEM is that velocity and stresses can be extracted from each particle during deformation. When applied to real geology, these can be compared with GPS and in-situ stress/seismicity data.

Analogue Models

Lithospheric deformation process of the Indian collision to Eurasia has been investigated by a series of analogue physical experiments (Davy and Cobbold 1988, Tapponnier et al. 1982). Basic assumptions of these experiments included 1) rigid Indian continent, 2) deformable Eurasian Plate, 3) constrained northern and western margins of the experiments, and 4) unconstrained southern and eastern margins.

Simulation Results

We have conducted a series of DEM simulations following the same assumptions as those of the analogue experiments above to see the deformation styles and the velocity/stress fields of each particle. In all simulations, particle size was randomized to avoid potential weak planes due to the 'perfect' initial packing arrangement by a homogeneous size of the particle. The collision produced progressive development of fault systems, which propagated from the left corner of the indenter to the unconstrained right margin. The outline of the right-hand-side of the particle assembly is broadened to overcome the space problem due to the collision. During the deformation, velocity distribution within the assembly is quite unstable and easily changed the magnitude as well. The region in front of the indenter, however, has no systematic direction, suggesting that the region is highly fragmented. The normal stress distribution suggests that fragmented blocks in the east of the indenter are not highly compressed and this may correspond to the boundary condition of the unconstrained right margin. The normal stress

in the particles is not homogeneous and some chain-like structures of high stresses are formed from the indenter to the constrained walls. The tangential stress diagram shows that the collision produced a broad sinistral shear band in the particles.

Comparison with Experiments/GPS/In-situ Stress Field

DEM results produced faulting types similar to the analogue experiments. The faults initiated at the left corner of the indenter and propagated to the right margin of the particle assembly. In the frontal region of the indenter, the layers were thinned in the DEM instead of the thrust faults produced in the experiments. The velocity distributions of the particles are quite unstable during the deformation and commonly showed unsystematic variations, whereas GPS vectors are generally continuous from the collision front. This may suggest that the ductile deformation of the lower crust is a significant control of the Indian collision. The normal stresses of the DEM particles are generally directed to the fixed end-walls and are hardly compared with the real directions of the maximum horizontal compressional stresses.

Conclusions

DEM simulation results are correlated well with the analogue experiments, and also with natural deformations including GPS and in-situ stress data. Therefore, the method can be a useful digital simulator to analyse natural geologic deformations qualitatively

References

Cundall PA and ODL Strack. 1979. A discrete numerical model for granular assemblies. *Geotechnique* **29:** 47-65

Davy P and PR Cobbold. 1988. Indentation tectonics in nature and experiment. 1. Experiments scaled for gravity. *Bull Geol Instit Uppsala* NS **14:** 129-141

Tapponnier P, G Peltzer, R Armijo, A-Y Le Dain, and P Cobbold. 1982. Propagating extrusion tectonics in Asia: new insights from simple experiments with plasticine. *Geology* **10:** 611-616

Yamada Y and T Matsuoka. 2004. Digital Sandbox Modelling using Discrete Element Method (DEM): Applications to Fault Tectonics. In: Sorkhabi R and Y Tsuji (eds), *Faults and Petroleum Traps*. Amer Assoc Petrol Geol Mem, in press

Lateral variations along the Main Central Thrust in the central Nepal Himalayas: The evidence from chemical maps of garnet

Haruka Yamaguchi†* and Kazunori Arita‡

† *Institute for Frontier Research on Earth Evolution (IFREE), Japan Agency of Marine Science and Technology (JAMSTEC), Showa-cho 3173-25, Kanazawa-ku, Yokohama, 236-0001, JAPAN*
‡ *Division of Earth and Planetary Sciences, Graduate school of Science, Hokkaido University, Kita-10 Nishi-8, Sapporo, 060-0810, JAPAN*

* *To whom correspondence should be addressed. E-mail: harukay@jamstec.go.jp*

Chemical maps of garnet are the key to understand the tectonometamorphic evolution of the metamorphic rocks. They provide useful information on element distribution, diffusion, and mechanical truncation of crystal. In the Himalayas, studies on ultra-high pressure rocks denudated along the Main Central Thrust (MCT) revealed the great displacement along this intracontinental shear zone. Pêcher (1989) suggested the difference in thickness of hangingwall as a result of large erosion along the thrust, and Macfarlane (1993) discussed the various thermal structures within the hangingwall. However, lateral variations in footwall have been poorly investigated although inverted thermal gradient has been often discussed. In order to clarify the variation of tectonometamophic events along the MCT, garnet crystals within pelitic rocks were investigated in detail.

In the central Nepal Himalayas, Annapurna area and Kathmandu nappe are suitable to study these variations. Estimated metamorphic temperatures just above the MCT are different in two areas: 600-700 °C in Annapurna area (Kaneko et al. 1995) and 550-600 °C in Kathmandu nappe (Johnson et al. 2001). These variations are interpreted as different positions within hangingwall; Kathmandu nappe corresponds to frontal zone whereas Annapurna area to root zone.

Microstructures of garnet in the Annapurna area and Kathmandu nappe are almost the same, characterized by tripartite growth: 1) core with spiral inclusion, 2) mantle with/without non-arranged inclusion which is asymmetrically truncated at rim and 3) re-overgrown rim. On the other hand, chemical zonings of garnet are slightly different in two areas. In the both areas, constant decrease of Mn from center to mantle and high Mn rim is observed, but Mg zoning at rim show opposite pattern, decrease in Annapurna area whereas increase in Kathmandu nappe.

The exact P-T paths have been deduced by Gibbs method, inverse differential calculation using garnet growth zoning and mineral assemblages in the rock. Results show clockwise P-T path from center to mantle part, which is adiabatic compression (dP = 0.2-0.3 GPa, dT = 30 °C) followed by heating (dT = 30°C). P-T condition at rim show different path in each area, decompression cooling (dP = 0.2 GPa, dT = 30 °C) in the Annapurna area and decompression heating (dP = 0.3 GPa, dT = 50 °C) in the Kathmandu nappe.

Comprehensively, two shearing evidences of spiral trail at core and asymmetrical truncation between mantle and rim may be referred to as underthrusting and exhumation, for their adiabatic compression and decompression paths. Evidences also show the cooling at root zone (Annapurna area) and heating at frontal nappe (Kathmandu nappe) after the exhumation, which suggest that rapid denudation occurred at hangingwall of root zone whereas heating from hangingwall continued at the front zone.

References

Pêcher A. 1989. The metamorphism in the central Himalaya. *J Metamorph Geology* **7**(1): 31-41

Macfarlane AM. 1993. Chronology of tectonic events in the crystalline core of the Himalaya, Langtang National Park, central Nepal. *Tectonics* **12**(4): 1004-25

Kaneko, Y. 1995. Thermal structure in the Annapurna region, central Nepal Himalaya: implication for the inverted metamophism. *J Min and Econ Geol* **90**: 143-154

Johnson MRW, GJH Oliver, RR Parrish and SP Johnson. 2001. Synthrusting metamorphism, cooling, and erosion of the Himalayan Kathmandu Complex, Nepal. *Tectonics*, **20**(3): p. 394-415

Imbricate structure of Luobusa ophiolite, southern Tibet

Hiroshi Yamamoto†*, S Yamamoto‡, Y Kaneko§, M Terabayashi¶, T Komiya‡, Ikuo Katayama‡ and T Iizuka‡

† Department of Earth and Environmental Sciences, Kagoshima University, Kagoshima 890-0065, JAPAN
‡ Department of Earth and Planetary Science, Tokyo Institute of Technology, Meguro, Tokyo 152-8851, JAPAN
§ National Institute of Advanced Industrial Science and Technology, Geological Survey of Japan, Tsukuba 305-8567, JAPAN
¶ Department of Safety Systems Construction Engineering, Kagawa University, Takamatsu 761-0396, JAPAN

* To whom correspondence should be addressed. E-mail:hyam@sci.kagoshima-u.ac.jp

Cretaceous ophiolite sequences lie in the Indus-Yarlung Zangbo suture zone (IYSZ), which separates the Indian Subcontinent from the Lhasa Terrane (e.g. Allegre et al. 1984). A large ophiolite sequence, called the Luobusa ophiolite is about 200 km east-southeast of Lhasa in southern Tibet. The ophiolite extends 43 km in east–west and its exposure is about 70 km^2 (Zhou et al. 1996). The Luobusa ophiolite consists of mantle peridotite (harzburgite and dunite) and a melange zone, which contains pyroxenite, gabbro, pillowed basalt and chert. Podiform bodies of chromitite are sporadically distributed in harzburgite. The podiform chromitite has received much attention because it contains "unusual mineral assemblage" which includes diamond and octahedral serpentine (Bai et al. 1993 2002, Yamamoto et al. 2003). Previous studies of the Luobusa ophiolite have concentrated on petrology and mineralogy of mantle peridotite. However, the mechanism by which the mantle peridotite were emplaced has not been made clear. The difficulty in tectonic interpretation arises from the limited scope of structural data. In this study we analyzed deformation structures in the boundary zones of the ophiolite to decipher the emplacement process of the Luobusa ophiolite through the suturing of Asia and India.

The northern edge of Luobusa ophiolite in the study area has a fault contact with the Tertiary Luobusa Formation composed of molasse-type deposits. To the south the ophiolite sequence has a fault contact with the Triassic flysch-type sedimentary rocks. The northern and the southern boundaries dip gently to the south. Mesoscopic structures were observed on outcrop surfaces which are nearly perpendicular to the foliation and nearly parallel to the lineation. Microscopic observations were made on polished slabs and thin sections of oriented samples taken from the shear zones near to the top and bottom boundaries of the Luobusa ophiolite. The slabs and thin sections were made on the section perpendicular to the foliation and parallel to the mineral lineation.

A serpentine melange zone, which lies along the northern margin of ophiolite sequence occupies the structural bottom of Luobusa ophiolite. The serpentine melange zone contains lenses of gabbroic rocks, pillow lavas and Cretaceous marine sedimentary rocks. These rocks occur as blocks in a partly serpentinized ultramafic matrix. Individual lithologies are irregularly distributed and the serpentinite matrix is intensively deformed. In the outcrops and oriented samples sets of subparallel shear bands and minor shear zones occur in the serpentinite. The shear bands are oblique to foliation in serpentinite and are regarded as "C'-type shear bands" (**Figure 1**). Consistent top-to-the-north displacements are observed at three localities in the serpentine melange zone.

FIGURE 1. Sheared serpentinite near to the bottom of Luobusa ophiolite. The attitude of foliation is N20°W, 34°S and striation on the surface of sheared fragment of peridotite trends N13°W. Broken lines indicate C'-type shear bands (N80°E, 31°N) suggesting top-to-the-north displacement. Scale bar on the bottom is 10 cm.
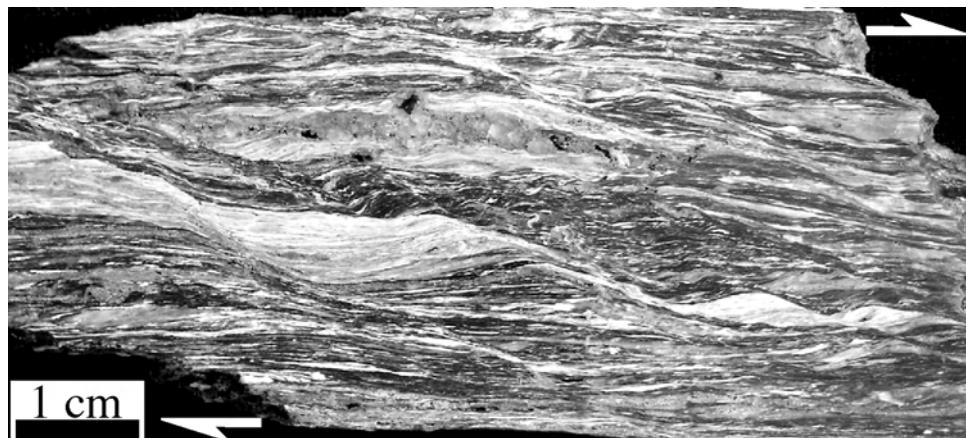
FIGURE 2. Polished surface of sheared phyllite in Triassic sedimentary rocks near to the top of mantle peridotite. C'-type shear bands displacing compositional layering indicate top-to-the-northeast displacement. The attitude of foliation is N74°W, 54°S and the trend of mineral lineation is N46°E.
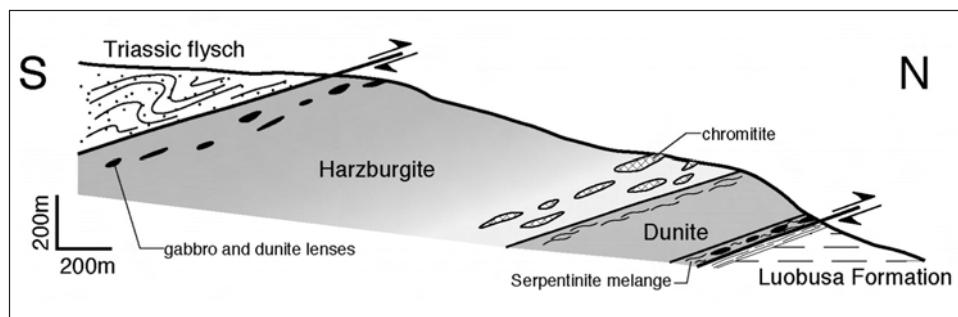
FIGURE 3. Cross-section across the Luobusa ophiolite. Arrows indicate relative motions along shear zones in the upper and lower boundaries.

Harzburgite with dunite lenses lies in the structural upper part of the Luobusa ophiolite although the structural top is not well exposed because of the flat ground surface in the southern part of study area. Feebly metamorphosed pelitic, siliceous and calcareous rocks overlie the mantle peridotite. C'-type shear bands commonly occur in siliceous phyllite (**Figure 2**). Some quartz porphyroclasts in well-foliated micaceous phyllite are mantled by asymmetric 'tails' to form 'σ-type' porphyroclasts. Consistent top-to-the-north displacements are observed in four oriented samples from separate localities.

These observations give the following constraints on kinematics of the three rock units: (1) northward thrusting of the Luobusa ophiolite upon the Tertiary Luobusa Formation, (2) northward thrusting of the Triassic sedimentary rocks upon the Luobusa ophiolite and (3) this stack of rock units forms north vergent imbricate structure (**Figure 3**). It can be interpreted that the imbricate structure was formed due to northward

displacement of India continued after the welding of India with Asia.

References

Allegre CJ, V Courtillot, P Tapponier, A Hirn and M Mattauer. 1984. Structure and evolution of the Himalaya-Tibet orogenic belt. *Nature* **307**: 17-22

Bai W., MF Zou and PT Robinson. 1993. Possibly diamond-bearing mantle peridotite and podiform chromitites in the Luobusa and Donqiao ophiolites, Tibet. *Can J Earth Sci* **30**: 1650-59

Bai W., J Yang, Q Fang, R Shi and B Yang. 2002. Unusual minerals in the podiform chromitite of Luobusa, Tibet: Do they come from Lower mantle and how? Abstracts of the *Superplume International Workshop*, 2002 Jan 28-31; Tokyo: Tokyo Institute of Technology. p 153-57

Zhou MF, PT Robinson, J Malpas. and Z Li. 1996. Podiform Chromitites in the Luobusa Ophiolite (Southern Tibet): Implications for Melt-Rock Interaction and Chromite Segregation in the Upper Mantle. *J Petrol* **37**: 3-21

Yamamoto S., T Komiya, K Hirose and S Maruyama. 2003. Interesting Inclusions From Podiform Chromitites in Luobusa Ophiolite, Tibet. EOS Transactions of the American Geophysical Union, **84**, p F1514

Evolution of the Asian monsoon and the coupled atmosphere-ocean system in the tropics associated with the uplift of the Tibetan Plateau – A simulation with the MRI coupled atmosphere-ocean GCM

Tetsuzo Yasunari†*, Manabu Abe‡ and Akio Kitoh§

† Hydrospheric Atmospheric Research Center, Nagoya University, Nagoya, 464-8601, JAPAN
‡ Graduate school of Environmental Studies, Nagoya University, Nagoya, 464-8601, JAPAN
§ Meteorological Research Institute, Tsukuba, 305-0052, JAPAN

* To whom correspondence should be addressed. E-mail: yasunari@hyarc.nagoya-u.ac.jp

Large-scale orographies, such as the Tibetan Plateau and the Rocky mountains, play an important role to form the present global climate system (Kutzbach et al. 1993). The large-scale orography has dynamical and thermodynamical effects to the atmosphere, which in turn influences the ocean circulation through the atmosphere-ocean interaction.

Many previous studies investigated the effect of mountains on the Asian summer monsoon using atmospheric general circulation models (AGCMs), by comparing the equilibrium climate states with and without mountains (Tibetan Plateau) and that without mountains (e.g., Hahn and Manabe 1974). However, these studies could not reveal to what degree the change of mountain height affects a climate and monsoon. It can also be postulated that the effect of mountains does not necessarily change linearly with increasing mountain heights. In addition, the Asian summer monsoon has been noted to have an active role of the interannual variability of the coupled atmosphere-ocean system in the tropical Pacific through the east-west circulation (e.g., Yasunari 1990, Yasunari and Seki 1992). The coupling of the Asian summer monsoon with the tropical Pacific Ocean system may, therefore, be crucial for the formation and variability of the tropical climate. An essential issue may be to investigate to what extent and how the tropical climate system, which is a coupled system of the Pacific/Indian Oceans and the Asian monsoon, is regulated by the uplift of the Tibetan plateau and other large-scale orographies.

Thus, to understand changes of the atmosphere/ocean coupled system associated with gradual uplift of the orography, a numerical experiment was conducted using the Meteorological Research Institute (MRI) coupled atmosphere–ocean general circulation model I (CGCM-I) (Abe et al. 2003). The MRI CGCM-I is the global grid model. Horizontal resolution of atmospheric part of the CGCM is 5° in longitude and 4° in latitude, and the vertical is 15 layers. The oceanic part has nonuniform meridional resolution ranging from 0.5° to 2.0°, with a finer grid in the tropics, fixed zonal resolution of 2.5°, and 21 layers vertically.

In this experiment six runs were performed, with six different elevations of the global mountains. That is, 0, 20, 40, 60, 80, and 100% of the present standard mountain height, were set for each run, which is called M0, M2, M4, M6, M8, and M, respectively. The continent-ocean distribution is the same in all runs. All the runs were integrated for 50 years, separately, and the data for the last 30 years (year 21 to 50) were used in our analyses.

An active convection region extends with mountain uplift to form a moist climate in South and East Asia. Monsoon circulation such as low-level westerly, and upper-level anticyclonic circulation, is also enhanced with uplift of the Tibetan Plateau. The increase in precipitation, and the enhancement of southwesterly, in the later stages of the uplift of the Tibetan Plateau, appear only over India and the south and southeastern slope of the Tibetan Plateau. Over the coastal region of Southeast and East Asia, where the maximum precipitation appears in M0, precipitation decreases gradually with uplift of the Tibetan Plateau, and the southwesterly in the later stages becomes weaker. The intensity of the Indian, Southeast Asian, and East Asian monsoon was investigated with indices, which are defined by area mean precipitation. The Indian monsoon becomes strong gradually with mountain uplift; particularly, in the later stages, the remarkable enhancement is found. The intensity of the South Asian monsoon is the strongest in M4. Thus, in the later stages of uplift the Tibetan Plateau, it becomes weaker in association with the northwestward migration of the convective activity. Although the East Asian monsoon is enhanced gradually with uplift of the Tibetan plateau, the enhancement in the earlier stages is larger than that in the later stages. In the equatorial Indian Ocean, sea surface temperature (SST) also increases with uplift of the Tibetan plateau, resulting in the increase in precipitation.

A pool of warm SSTs appears in the western Pacific as the Tibetan Plateau grows up, although SSTs in the tropical Pacific decrease as a whole. In addition, easterly winds at low levels over the equatorial Pacific strengthen as the Tibetan plateau rise. The enhanced easterlies alter surface heat flux and ocean dynamics, changing the water temperature field in the upper Pacific Ocean. Water temperatures between the surface and 300 m in the western Pacific increase because upwelling is suppressed and the thermocline deepens. Water temperatures in the eastern Pacific decrease and the thermocline rises. Therefore, the east-west gradient of water temperature in the Pacific is enhanced for cases with mountain heights of 80% and 100% of the standard mountain height. An increase in diabatic heating over South Asia, as height of the Tibetan Plateau increases, causes sea level pressure (SLP) to decline over the Indian Ocean, and enhances upper atmospheric divergence over the eastern hemisphere. Consequently, the east-west circulation over the Indian and Pacific Oceans strengthens as the Tibetan plateau become taller. Probably, the east-west circulation is also enhanced by changes in convective activity associated with SST changes. The coupled general circulation model (GCM) results show that uplift of the Tibetan Plateau significantly affects the tropical atmospheric and oceanic climate, changing the east-west circulation and altering the evolution of the Asian summer monsoon (Abe et al. 2004).

References

Abe M, A Kitoh and T Yasunari. 2003. An evolution of the Asian summer monsoon associated with mountain uplift –simulation with the MRI atmosphere-ocean coupled GCM-. *J Meteor Soc Japan* **81**: 909-33

Abe M, T Yasunari and A Kitoh. 2004. Effects of large-scale orography on the coupled atmosphere-ocean system in the tropical Indian and Pacific oceans in boreal summer. *J Meteor Soc Japan* **82**: 745-59

Hahn DG and S Manabe. 1975. The role of mountains in the south Asian monsoon circulation. *J Atmos Sci* **77**: 1515-41

Kutzbach JE, WL Prell and WF Ruddiman.1993. Sensitivity of Eurasian climate to surface uplift of the Tibetan plateau. *J Geology* **101**: 177-190

Yasunari T. 1990: Impact of Indian monsoon on the coupled atmosphere/ocean system in the tropical Pacific. *Meteorology and Atmospheric Physics* **44**: 29-41.

Yasunari T and Y Seki. 1992: Role of the Asian monsoon on the interannual variability of the global climate system. *J Meteor Soc Japan* **70**: 177-189

Structural framework of the westernmost Arunachal Himalaya, NE India

An Yin†*, Thomas K Kelty‡, CS Dubey§, GE Gehrels¶, Q Chou†, Marty Grove† and Oscar Lovera†

† Department of Earth and Space Sciences and Institute of Geophysics and Planetary Physics, University of California, Los Angeles,
 CA 90095-1567, USA
‡ Department of Geological Sciences, California State University, Long Beach, California 90840-3902, USA
§ Department of Geology, University of Delhi, Delhi 110007, India
¶ Department of Geosciences, University of Arizona, Tucson, Arizona 85721, USA

* To whom correspondence should be addressed. E-mail: yin@ess.ucla.edu

A 150-km long NW-SE traverse was mapped from Bhalukpong to Zimithang in the westernmost Arunachal Himalaya of NE India. From south to north major structures involving Cenozoic strata include the Main Frontal Thrust (MFT) placing the Plio-Pleistocene Kimin and Subansiri Formations (= upper Siwalik Sequence) over recent alluvial deposits, the Bhalukpong thrust within the Kimin-Subansiri strata, and the Tipi thrust juxtaposing the Miocene Dafla Formation (= Dumri Formation and lower Siwalik Group in Nepal) over the Kimin-Subanriri strata. The Main Boundary Thrust (MBT) juxtaposes Permian strata over the Dafla Formation. Both units are folded and locally develop penetrative cleavage transposing bedding. The Permian strata are in turn thrust under Proterozoic Bomdila gneiss (= Uleri gneiss in Nepal). The Bomdila gneiss is extensively mylonitized and interlayered with minor schist and phyllite belonging to the Lesser Himalayan Sequence. The gneiss is structurally repeated by five major NW-dipping thrusts, which may have accommodated a significant amount of crustal shortening in the Cenozoic. Except in one place, the mylonitic Bomdila gneiss exhibits kinematic indicators dominantly suggesting top-SE sense of shear. The age of mylonitic deformation is unknown.

The Main Central Thrust (MCT) is exposed near Dirang between Bhalukpong to Zimithang. The fault zone is ~100-300 m thick and consists of highly folded quartzite, phyllite, calc-silicate schist and kyanite-bearing leucosome veins. All folds trend N5-45°W and verge variably to the SE and NE. Because the folds are perpendicular to the local NE-striking trace of the MCT and subparallel to stretching lineation trending N10-20°W in the MCT zone, we suggest that these folds are A-type parallel to thrust transport direction (i.e., top-SE). Neither mylonite nor mylonitic gneisses was observed within and directly above the MCT zone. Immediately above the MCT near Dirang is biotite-garnet gneiss with rare and small leucosome veins; some are folded while others severely sheared. The high-grade gneiss is part of the Greater Himalayan Crystalline Complex (GHC). Up-section from the MCT zone, the number and size of deformed and undeformed leucogranites increase. They are typically exposed as 5-50 m thick sills parallel to the regional foliation. However, locally, undeformed leucogranites also cut the foliation. Associated with the large quantity of leucogranites upsection from the MCT is the appearance of sillimenite, indicating upward increase in metamorphic grades within the GHC as noted in Nepal.

A tectonic window is observed near Lumpla about 65 km northwest of Dirang. There a warped low-angle fault places biotite-garnet gneiss over a quartzite unit that is interbedded with phyllite. The fault exhibits a 3-5 m thick fine-grained gouge zone. Striations and weakly developed stretching lineation in footwall phyllite trend S40-50°E. According to the existing regional tectonic map, the quartzite unit belongs to the Lumpla Formation that has been regarded as part of the Tethyan Himalayan Sequence (THS) resting on top of the GHC. Our field observations show that the Lumpla Formation in fact is structurally below the GHC juxtaposed by a low-angle fault. The fault, which we refer to as the Lumpla thrust, is offset between 5 and 200 meters by multiple closely spaced east-dipping normal faults. The cross-cutting relationship suggests that motion on the Lumpla thrust predates regional east-west extension.

The hanging-wall and footwall units across the Lumpla thrust are remarkably similar to those across the frontal trace of the MCT near Dirang. Correlating these lithologic units leads us to propose that the Lumpla thrust is a tectonic window of the MCT, which implies that the MCT has a minimum displacement of 65 km in its SE transport direction. To test this hypothesis, we conducted U-Pb dating of detrital zircon from the quartzite units below the Lumpla window and the MCT in Dirang. The analysis was preformed at University of Arizona. We dated 100 zircon grains from each sample, with both samples yielding similar $^{207}Pb/^{206}Pb$ age distribution ranging from ~950 Ma to ~2960 Ma. For both samples there are two prominent clusters at 1400 Ma and 1700 Ma, respectively. These age distributions are very different from typical detrital zircon ages of the THS that usually contains a Cambro-Ordovician age pulse (~510-480 Ma). We have also performed two types of statistical tests to determine if the two samples are statistically differentiable in terms of their zircon age populations. The analyses strongly indicate that the two samples share the same zircon age distribution. The recognition of a MCT tectonic window inside the eastern Himalaya suggests that (1) the MCT is broadly folded, a case widely recognized elsewhere and has been reported particularly in Bhutan by Indian geologists, and (2) the thickness of the GHC is much less than previously thought (i.e., < 5-7 km instead of > 15 km) when projecting the South Tibet Detachment (STD) klippes above the GHC in nearby easternmost Bhutan.

About 20 km north of the Lumpla window a top-SE mylonitic shear zone (>200 m) is observed near Zimithang within the GHC. This shear zone, located about 10 km south of the India-China border and about 5-7 km east of India-Bhutan border, places mylonitic augen gneiss over both non-mylonitic augen gneiss and quartzo-feldspathic gneiss. Its position and trend correspond well with the projected trace of the Kakhtang Thrust mapped in Bhutan. The latter has been interpreted to be an out-of-sequence thrust younger than motion on the MCT. Geochronologic, thermochronologic, petrological analyses of the metamorphic and leucogranite samples collected from the Bhalukpong-Zimithang traverse are currently being analyzed. These data will be presented in the meeting together with a new tectonic reconstruction of the eastern Himalaya and southeastern Tibet.

Relationship between the Higher Himalayan Crystalline and Tethyan Sediments in the Kali Gandaki area, western Central Nepal: South Tibetan Detachment revisited

Masaru Yoshida†‡*, Sant M Rai†, Ananta P Gajurel†, Tara N Bhattarai† and Bishal N Upreti†

† Department of Geology, Tri-Chandra Campus, Tribhuvan University, Kathmandu, NEPAL
‡ Gondwana Institute for Geology and Environment, Hashimoto, JAPAN

* To whom correspondence should be addressed. E-mail: gondwana@wlink.com.np/gondwana@orion.ocn.ne.jp

During our recent fieldwork in Kali Gandaki valley in western-central Nepal, we observed a definite intrusive relationship between the augen gneiss of the Higher Himalayan Crystalline Sequence (HHCS, Formation III of Le Fort 1975) and the base of the Tethyan Sedimentary Sequence (TSS). Hagen (1968) also reported beautiful outcrops of the similar relationship from Namun range east of the Annapurna Range.

This means that the observed contact between the HHCS and TSS is the intrusive, exemplified by the intrusion of the augen gneiss unit between the remaining part of HHCS and the overlying TSS. Between the TSS and underlying HHCS, a north-dipping normal fault system has been reported from various parts of the Himalayan Orogen from Kashmir to Bhutan through Nepal; this fault system has been identified as the South Tibetan Detachment System (STDS) and been considered to form one of the major fault systems dividing principal geologic units in the Himalayan Orogen (e.g., Burchfiel and Royden 1985). In the Kali Gandaki area, the STDS was identified as the Annapurna Detachment by Brown and Nazarchuk (1993) and studied in detail by Godin (1999). Our small observation above conforms neither to these studies, nor even to other earlier studies, which mentioned a tectonic contact between the two (e.g., Bodenhausen and Egeler 1971, Garzanti and Frette 1991). We also observed that there is a good lithological similarity between the lower part of the TSS and the metasedimentary gneisses of the HHCS, the metasedimentary gneisses forming the lower part of the HHCS and being separated from the TSS by the intrusive augen gneiss body as mentioned above. Worth noting is that the metasedimentary gneisses are quite consistent throughout HHCS, their lithology changing gradually downwards from calcareous to psamopelitic, maintaining structural conformity throughout as pointed out in earlier studies (e.g., Gansser 1964, Stöcklin 1980). Many small reverse folds and related small structures with southerly vergence were observed, while normal sense faults and folds were rarely observed in the lower part of TSS.

Based on these lines of evidences, we suspect a continuous development of the Annapurna Detachment in the Kali Gandaki area. We also consider a possibility that the metasedimentary gneisses of the HHCS are actually the lower equivalent or a lower formation of the TSS intervened by the intrusive body of the augen gneiss. This view is in conformity with the classical observation by Le Fort (1975), and is supported by recent geochronologic data suggesting that the age of the HHCS could be in the range of 800–480 Ma (e. g., DeCelles et al. 2000). Our observations also support in part a recent proposal by Gehrels et al. (2003) who proposed Cambro-Ordovician thrusting tectonics at the base of the TSS, and pointing out a possibility of repetition of the lower formations of the TSS into the underlying HHCS. If the above are to be admitted, we may have to consider the re-definition of the Tethyan Sedimentary Sequence so that it could include all metasediments of HHCS, with the stratigraphic and structural base lying just above the MCT. This consideration leads us to re-examine the role of the STDS in the Himalayan Orogen.

References

Bodenhausen JWA and CG Egeler. 1971. On the geology of the upper Kali Gandaki Valley, Nepalese Himalayas. I. *Koninkl. Nederl. Akademie van Wetenschappen -Amsterdam, Proceedings, Ser. B* **74** (5)**:** 526-538

Brown RL and JH Nazarchuk. 1993. Annapurna detachment fault in the Greater Himalaya of central Nepal. In: Treloar, PJ and , MP Searle (eds), *Himalayan Tectonics.* Geol Soc London Sp. Pub **74:** 461-473

Burchfiel BC and LH Royden. 1985. North-south extension within the convergent Himalayan region. *Geology* **13:** 679-682.

DeCelles PG, GE Gehrels, J Quade, B LaReau, and M Spurlin. 2000. Tectonic implications of U-Pb zircon ages of the Himalayan Orogenic Belt in Nepal. *Science* **288:** 497-499.

Gansser A. 1964. *Geology of the Himalayas.* Intersci. Publ. John Wiley & Sons, London, 289 p

Gehrels GE, RG DeCelles, A Martin, TP Ojha, and G Pinhasssi. 2003. Initiation of the Himalayan Orogen as an early Paleozoic thin-skinned thrust belt. *GSA Today* **13**(9)**:** 4-9

Garzanti E and Frette. 1991. Stratigraphic succession of the Thakkhoka region (Central Nepal) – comparison with the northwestern Tethys Himalaya. *Riv It Paleont Strat* **97**(1)**:** 3-26

Godin L. 1999. Tectonic evolution of the Tethyan Sedimentary Sequence in the Annapurna area, Central Nepal Himalaya. *Ph.D. thesis, Carleton University, Ottawa,* 219 p

Hagen T. 1968. Report on the geological survey of Nepal. Volume 2: Geology of the Thakkhola. *Soc Helvetique Sci Nt Mem, Zurich* **84**(2)**:** 160 p

Le Fort P. 1975. Himalaya: the collided range. Present knowledge of the continental arc. *Amer J Sci* **275-A:** 1-44

Stöcklin J. 1980. Geology of Nepal and its regional frame. *J Geol Soc London* **137:** 1-34

Commentary on the position of higher Himalayan basement in Proterozoic Gondwanaland

Masaru Yoshida†‡* and **Bishal N Upreti**†

† *Department of Geology, Tri-Chandra Campus, Tribhuvan University, Kathmandu, NEPAL*
‡ *Gondwana Institute for Geology and Environment, Hashimoto, JAPAN*

* *To whom correspondence should be addressed. E-mail: gondwana@wlink.com.np*

Until recently the Higher Himalayan Crystalline Sequence (HHCS) was generally regarded to be the basement of the Himalayan Orogen. Our recent field work in the Kali Gandaki area of western Central Nepal showed that the HHCS is likely continuous with the overlying Tethyan Sedimentary Sequence (TSS) stratigraphically and structurally, and therefore does not form the basement of the Himalayan Orogen (Yoshida et al. 2004); a similar view was already mentioned in some earlier works (e.g., Le Fort 1975, Gehrels et al. 2003). Many workers have placed thrust or normal fault, and even unconformity between the HHCS and TSS; but based on our observation it is difficult to confirm any of these relationships. Our observation also conforms to the geochronologic work by DeCelles et al. (2000) that the HHCS is younger than ca 800 Ma and older than ca 480 Ma; this age-range naturally shows the geochronologic identity or continuation of the HHCS with the so far known base of the TSS.

Although the basement of the Himalayan Orogen is not recognized anywhere, its paleoposition can be estimated by identifying the provenance of sediment deposited on the basement. Examination of zircon U-Pb data from HHCS gneisses by DeCelles et al. (2000) showed that the ages of detritus zircons have a range of ca 800~2700 Ma with a main peak at ca 954 Ma; based on these, they suggested the provenance to be the Arabian-Nubian Shield of the East-African Orogen lying to the west of the Proterozoic Himalayan Basin (Indian coordinate within the East Gondwana assembly, e.g., Yoshida et al. 2003). Robinson et al. (2001) showed the Nd model ages of HHCS to lie between 1.36-2.29 Ga (with an exceptional age of 2.85 Ga) and εNd (0) is moderately minus (-7.6~19.9, average–13.8); their neodymium isotopic data indicate the source area to have somewhat long crustal history.

Recent compilation of geochronologic data from the Arabian-Nubian Shield (Johnson and Woldehaimanot 2003) shows zircon ages as well as neodymium model ages from the Arabian-Nubian Shield are a little too younger when compared with those of HHCS, and even bearing many positive εNd values. Although there are some exceptional data showing older neodymium model with highly minus εNd (0) values for rocks from some small areas of older crustal blocks within the Arabian-Nubian Shield, it is difficult to expect considerable amount of material supply from these blocks, since they are thought to lie, if any, below the younger geologic units and only a small amount could have exposed. Gehrels et al. (2003) recently reported somewhat older ages of detritus zircons from HHCS than those reported by DeCelles et al. (2000), showing a major peak range of ca 900-1300 Ma with a main peak of ca 1050 Ma. The wide range of Palaeoproterozoic and late Archaean zircons were also reported, although they form minor populations except those of ca 2500 Ma, which forms the second major peak. Thus, the Arabian-Nubian Shield may not constitute the source for the HHCS.

We propose the Pinjarra Orogen (Western Australia, Fitzsimons 2003) lying to the east of the ancient Himalayan basin in the Proterozoic East Gondwana assembly, to be a more possible candidate for the source area that provided material to HHCS, based on their similar geochronologic and crustal signatures and suitable location near by the Himalayan basin. The Pinjarra Orogen suffered peak metamorphism of ca 1000–1100 Ma with later granitic activity of ca 800-650 Ma and superposed by ca 550–500 Ma Pan-African deformation and metamorphism. Material of rocks in the orogen were derived from Mesoproterozoic Albany-Flaser Orogen of southwestern Australia, in which a variety of older crustal component were incorporated. The ages of rocks from the Pinjarra Orogen are quite conformable with recent zircon data from HHCS (Gehrels et al. 2003). Sporadically known Nd model ages from the Pinjarra Orogen lie between ca 1.6-2.2 Ga, with few exceptions of ca 1.1-1.6 Ga. Thus, it is most likely that the Pinjarra Orogen provided source material for the HHCS. Our conclusion does not support a recent model denoting the Pan-African assembly of East Gondwana (Pisarevsky et al. 2003) in which India and Western Australia do not juxtapose during the Neoproterozoic, but is in favour of the classical model of East Gondwana assembly through the Circum-East Antarctic Orogen of ca 1000 Ma (Yoshida et al. 2003) where Western Australia juxtaposes with northern India.

References

DeCelles PG, GE Gehrels, J Quade, B LaReau and M Spurlin. 2000. Tectonic implications of U-Pb zircon ages of the Himalayan Orogenic Belt in Nepal. *Science* **288**: 497-499

Fitzsimons ICW. 2003. Proterozoic basement provinces of southern and southwestern Australia, and their correlation with Antarctica. In: Yoshida M, BF Windley and S Dasgupta (eds), *Proterozoic East Gondwana: Supercontinent Assembly and Breakup.* Geol Soc Special Pub No. 206. Geol Soc London: 93-130

Gehrels GE, PG DeCelles, A Martin, TP Ojha and G Pinhassi. 2003. Initiation of the Himalayan Orogen as an early Paleozoic thin-skinned thrust belt. *GSA Today* **13** (9). 4-9

Johnson PR and B Woldehaimanot. 2003. Development of the Arabian-Nubian Shield: perspectives on accretion and deformation in the northern East African Orogen and the assembly of Gondwana. In: Yoshida M, BF Windley and S Dasgupta (eds), *Proterozoic East Gondwana: Supercontinent Assembly and Breakup.* Geol Soc Special Pub No. 206. Geol Soc London: 289-325.

Le Fort P. 1975. Himalaya: the collided range. Present knowledge of the continental arc. *Am Jour Sci* **275**(A): 1-44

Pisarevsky SA, MTD Wingate, CMA Powell, S Johnson and DD Evans. 2003. Models of Rodinia assembly and fragmentation. In: Yoshida M, BF Windley and S Dasgupta (eds), *Proterozoic East Gondwana: Supercontinent Assembly and Breakup.* Geol Soc Special Pub No. 206. Geol Soc London: 35-55

Robinson, D.M., DeCelles, P.G., Patchett, P.J., and Garzione, C.N., 2001, The kinematic evolution of the Nepalese Himalaya interpreted from Nd isotopes. Earth Planet Sci Lett **192**: 507-521

Yoshida M, M Santosh and HM Rajesh. 2003. Role of Pan-African events in the Circum-East Antarctic Orogen of East Gondwana: a critical overview. In: Yoshida M, BF Windley and S Dasgupta (eds), *Proterozoic East Gondwana: Supercontinent Assembly and Breakup.* Geol Soc Special Pub No. 206. Geol Soc London: 57-75.

Yoshida M, SM Rai, AP Gajurel, TN Bhattarai and BN Upreti. 2004. Relationship between the Higher Himalayan Crystalline and Tethyan Sediments in the Kali Gandaki area, western central Nepal: South Tibetan Detachment revisited. Ninth HKTW, 10-14th July 2004, Niseko (Japan), Abstracts (this volume)

The geomorphic characteristics of the Minshan Tectonic Belt along the northeast margin of the Tibetan Plateau — A DEM study

Hui ping Zhang†*, Nong Yang‡ and Shao feng Liu†

† *School of Earth Sciences and Resources, China University of Geosciences (CUGB), Beijing, PO Box 100083, CHINA*
‡ *Institute of Geomechanics, Chinese Acadamy of Gelogical Sciences (CAGS), CHINA*

* *To whom correspondence should be addressed. E-mail: beijingzhhuiping@163.com*

Topographically, the eastern Tibetan Plateau with high elevation and thick crust is bounded by Longmenshan and Minshan Ranges (Deng et al. 1994, Zhao et al. 1994a, Searle 2001), and is one of the world's most remarkable continental escarpments (Kirby et al. 2002). The topographic elevations decreased gradually from 5000-6000 m in the northeast Tibetan Plateau to 600 m in the Sichuan Basin across a horizontal distance of only 50-60 km (Zhao et al. 1994, Searle 2001, Kirby et al. 2002). Moreover, the topographic expression of the eastern margin of the Tibetan Plateau is largely more irregular and diffuse in contrast to the northern and southern margins (Kirby et al. 2002).

The Minshan Tectonic Belt (MTB), first brought forward by Deng et al. (1994), is located in the northeast margin of the Tibetan Plateau (**Figure 1**). Tectonically and geomorphically, the MTB is the right linkage between the West Qinling, the Sichuan Basin and the Tibetan Plateau. The significant faults, the Longmenshan Thrust Belt (LTB), the Minjiang Fault Zone (MFZ), the Huya Fault (HF), and important contacts are shown in **Figure 1**. The Triassic sandstone and slate located in the western flank of the MFZ and the HF are in lower erodibility compared with the pre-Mesozoic

carbonatite on the east side. Mostly influenced by the Cenozoic collision of India and Eurasia (Deng et al. 1994, Kirby 2000), the MTB experienced intense uplifting and erosion. The previous researches mostly dealt with the tectonic evolution and geomorphic characteristics of the LTB and the MFZ (Chen et al. 1994a, 1994b, 1994c, Deng et al. 1994, Zhao et al. 1994a, 1994b, Burchfiel et al. 1995, Chen and Wilson 1996), and presented many theoretic and conceptual models of the geological evolution (Chen et al. 1994b, 1994c, Deng et al. 1994). But their studies have not dealt with the general geomorphic characteristics of the MTB as a whole. Combining with Quaternary deformation information and thermochronology data such as ^{40}Ar/^{39}Ar, (U-Th)/He and FT, Dennis et al. (1994) and Kirby et al. (2000, 2002) systematically analyzed the neotectonics of the eastern margin of the Tibetan Plateau, and pointed out markedly heterogeneous denudation in late Cenozoic along the northeastern margin and the differential cooling evolution. According to the derformity style, stratigraphy distribution and geomorphic zonation, Yang et al. (2004, in press) proposed that the MTB comprises an uplifting zone clamped by two fault zones (Minjiang Fault and Huya Fault)
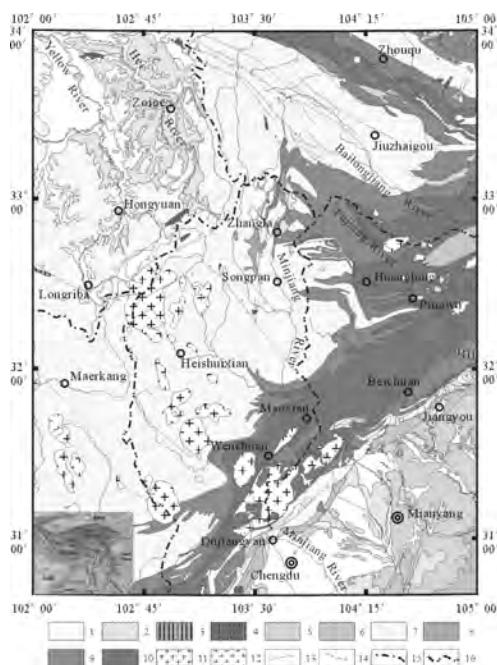
FIGURE 1. Simplified geological map of the MTB
1. Holocene, 2. Pleistocene, 3. Neocene, 4. Palaeogene, 5. Cretaceous, 6. Jurassic, 7. Triassic, 8. Permian-Triassic, 9. Paleozoic, 10. Pre-Paleozoic, 11. Mesozoic granite 12. Mesozoic and Paleozoic diorite, 13. Fault, 14. Reverse fault, 15. Main drainage divide, 16. Secondary drainage divides. See text for the further discussion
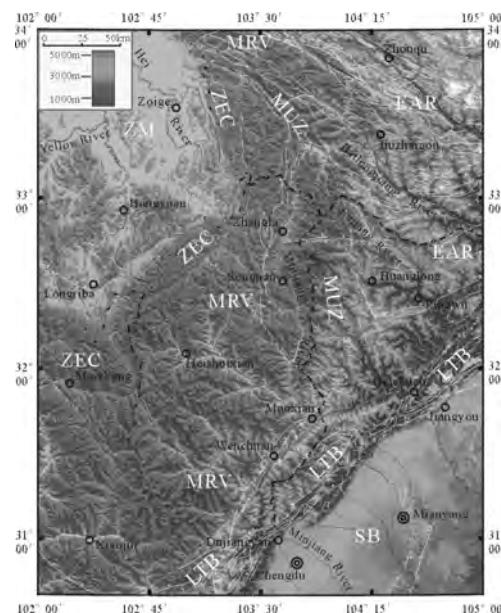
FIGURE 2. The elevation-shaded DEM of the MTB. The blue dashed lines are the boundaries of the geomorphic units. The white lines are the faults presented in Fig.1. ZM: Zoige massif, ZEC: Zoige east margin range chains, MRV: Minjiang River valley, MUZ: Minshan Uplifting Zone, EAR: East actic region, LTB: Longmenshan Thrust Belt, SB: Sichuan Basin.

and the folded zones bilaterally distributed westwards and eastwards of the uplifting zone. Accordingly, the MTB includes four geomorphic units as the ZEC, the MRV, the MUZ and the EAR **(Figure 2)**. Although Kirby et al. (2000, 2002) and Yang et al. (2004, in press) have taken cognizance of the geomorphic features along the northeast margin of the Tibetan Plateau, some aspects are still undiscussed yet, such as the drainage pattern and the mutual relations among the lithology, the structure and the topography.

Based on the digital elevation model (DEM) created by digitizing topographic contours (1:2,50,000), this study aims to analyze the geomorphic characteristics of the MTB in detail. The spatial resolution of the data used is 50 mx50 m, and the interval of contours is 100 m. The standard error of the elevation data is less than 45 m. Although the resolution of the DEM is a little modest, nevertheless, it is also useful for this study. Almost all of the procedures including visualization and data processing were done with the software MapGIS ™ 6.5 (Zondy Info-Engineering Co., Ltd. Wuhan, China).

Figure 2 shows the elevation shaded DEM overlain by the boundaries of an important contacts and the main and secondary water divides. In the northwestern flank of the study area, the elevation of the eastern Zoige massif controlled by the NE trending Longriba Fault is about 3500-3800 m, presenting itself in an annular shape. The low local relief of this region is very typical. The main drainage divide of the Huang He (Yellow River) and the Chang Jiang (Yangtze River) is about along the margin of the Zoige massif. The Hei River and other confluents flow generally north into the Yellow River, and the outcrops of the Mesozoic granites confine the drainages at the southeast. Eastward the plateau transits itself from 4000 m to 4500 m and reaches the Minjiang River Valley Zone at the elevation of about 1500-3800 m. The Minjiang River is also N-S trending like the Hei River. But unlike the later, the Minjiang River flows south to the Yangtze River, which is mostly restricted by the Cenozoic activities of the Minjiang Fault Zone in the north and of the Longmenshan Tectonic Belt in the south (Zhao et al. 1994a, 1994b). The drainage style of the Minjiang River abstracted from the **Figure 2** also can attract our attention. On the western side, there are plenty of developed confluents, and the drainage is very extensive. Meanwhile, the case on the east side of the Minjiang River is contrary to the west; there exists almost no tributaries. This drainage appearance magnificently confirms the differential uplifting of the east flank vs. the west side of the river.

Besides the above-mentioned, the most important and interesting geomorphic unit is the Minshan Uplift Zone; many studies indicate that the MUZ is clumped between the MFZ and the HF, and has experienced the intense Cenozoic tectonic uplifting (Zhou et al. 2000, Deng et al. 1994, Zhao et al. 1994b, Kirby et al. 2000). This uplifting zone is about 40-50 km wide and contains many peaks that are above 4500 m even reaching 5588

m. Note that the higher erodibility and the outcropping altitude of the carbonatite along the uplift zone, we also can infer the intense differential uplifting of the MUZ during the Cenozoic. Based on the analysis of the dislocation elevation of the existing planation surface and the strata age, Zhou et al. (2000) estimated that the mean uplifting rate of the MUZ is about 1.5 mm/a from the Quaternary, and also proposed the formation mechanism of the new rise of the Minshan block (the MUZ in our study). Southward, the MUZ joins up with the Longmenshan Tectonic Belt, and becomes an erosional escarpment adjacent to the Sichuan Basin. Together with the LTB, the topographic dominance of the MUZ makes them the northeast margin of the Tibetan Plateau.

In the east and northeast flanks of our study area, the landforms with an altitude of 1000-3000 m are members the West Qingling Orogen. The gradient of this region is greater than any other part. Topographically, the E-W geomorphic difference becomes very well marked. The drainage patterns of the Bailongjiang River and the Fujiang River of Jialingjiang Drainage are regularly flowing in the directions of NNW or near EW, obviously differing from the other west drainages such as the Minjiang River and Hei River. This geomorphic appearance represents the tectonic stress transformation from EW to NW-SE regionally.

In conclusion, the Minshan Tectonic Belt, as the northeastern margin of the Tibetan Plateau, has distinct characteristics of topography, which are in relation to the structure and the stratigraphical lithology. The drainage divide of the Yellow River and the Yangtze River is controlled mainly because of the lithological difference; however, in the Yangtze River drainage, the differential uplifting during the Cenozoic controls the patterns of the drainage networks.

References

Zhao XL, QD Deng and SF Chen. 1994a. Tectonic geomorphology of the central segment of the Longmenshan Thrust Belt, west Sichuan, Southwestern China. *Seismology and Geology* **16**(4): 422-428 (in Chinese with English abstract)

Zhao XL, QD Deng and SF Chen. 1994b. Tectonic geomorphology of the Minshan Uplift in the western Sichuan, Southwestern China. *Seismology and Geology* **16**(4): 429-439 (in Chinese with English abstract)

Chen SF, CJL Wilson, QD Deng and others 1994. Active faulting and block movement associated with large earthquakes in the Min Shan and Longmen Mountains, northeastern Tibetan Plateau. *J Geophys Res* **99**(12): 24,025-38

Burchfiel BC, Z Chen, Y Liu and others. 1995. Tectonics of the Longmen Shan and adjacent regions, central China. *Int Geol Rev* **37**: 661-735

Kirby E, KX Whipple, BC Burchfiel and others 2000. Neotectonics of the Min Shan, China: Implications for mechanisms driving Quaternary deformation along the eastern margin of the Tibetan Plateau. *GSA bulletin* **112**(3): 375-393

^{40}Ar-^{39}Ar thermochronological evidence for formation and tectonic exhumation of the northern-central segment of the Altyn Tagh Fault System in the Mesozoic, northern Tibetan Plateau

Xuemin Zhang†*, Yu Wang‡, Erchie Wang§, Qi Li¶ and Guihua Sun#

† *School of Geophysics and Information Technology, China University of Geosciences, Beijing 100083, CHINA*
‡ *Geologic Laboratories Center and Department of Geology, China University of Geosciences, Beijing 100083, CHINA*
§ *Institute of Geology and Geophysics, Chinese Academy of Science, Beijing 100029, CHINA*
¶ *Institute of Geology, China Seismological Bureau, Beijing 100029, CHINA*
# *Institute of Geology, Chinese Academy of Geological Sciences, Beijing 100037, CHINA*

* *To whom correspondence should be addressed. E-mail:* zhangxm96@sohu.com

To better constrain the probable timing of formation and evolution of the Altyn Tagh sinistral strike-slip system in the Mesozoic, a ^{40}Ar/^{39}Ar thermochronological study has been carried out in the northern-central segment of the Altyn Tagh fault system, the northern margin of Qaidam Basin and the eastern Kunlun orogenic belt (**Figure 1**). Muscovite and biotite separated from mylonite, granite, pegmatite and metamorphic rocks have been analyzed and cooling histories of the K-feldspar have been modeled. The ranges of ^{40}Ar/^{39}Ar data in the middle-early Paleozoic, early and middle-late Mesozoic time periods, indicate that the peak metamorphic event along the Altyn Tagh fault system occurred during 450-420 Ma. And at ~250-220 Ma there was sinistral strike-slip shearing. Later at 164-155 Ma and ~100-89 Ma, sinistral strike-slip deformation and rapid tectonic exhumation along the Altyn Tagh fault system took place. Structural and thermochronological evidence demonstrates that sinistral strike-slip motion of the Altyn Tagh fault system developed initially at ~250-220 Ma. After this event, multiple-stage deformation and exhumation proceeded.

The cooling histories in the northern margin of Qaidam Basin and the eastern Kunlun orogenic belt show that, similar to the northern segment of the Altyn Tagh fault system, these had experienced rapid cooling process during ~250-220 Ma (**Figure 2**). This regional tectonic and thermal cooling process indicates that the initial formation of the Altyn Tagh sinistral strike-slip fault system in the late Permian-early Mesozoic was coupled with or related to the suturing in the northern margin of the Qaidam Basin and the Kunlun orogenic belt, as well as suturing in Jinsha River suture zone between Qiangtang block and Kunlun-Bayankala geologic units. During 164-155 Ma and 100-89 Ma, cooling events along the Altyn Tagh fault system were accompanied by the closure along Bangong Lake-Nujiang suture zone, which developed differently on its eastern and western sectors during middle-late Jurassic and early Cretaceous, respectively.
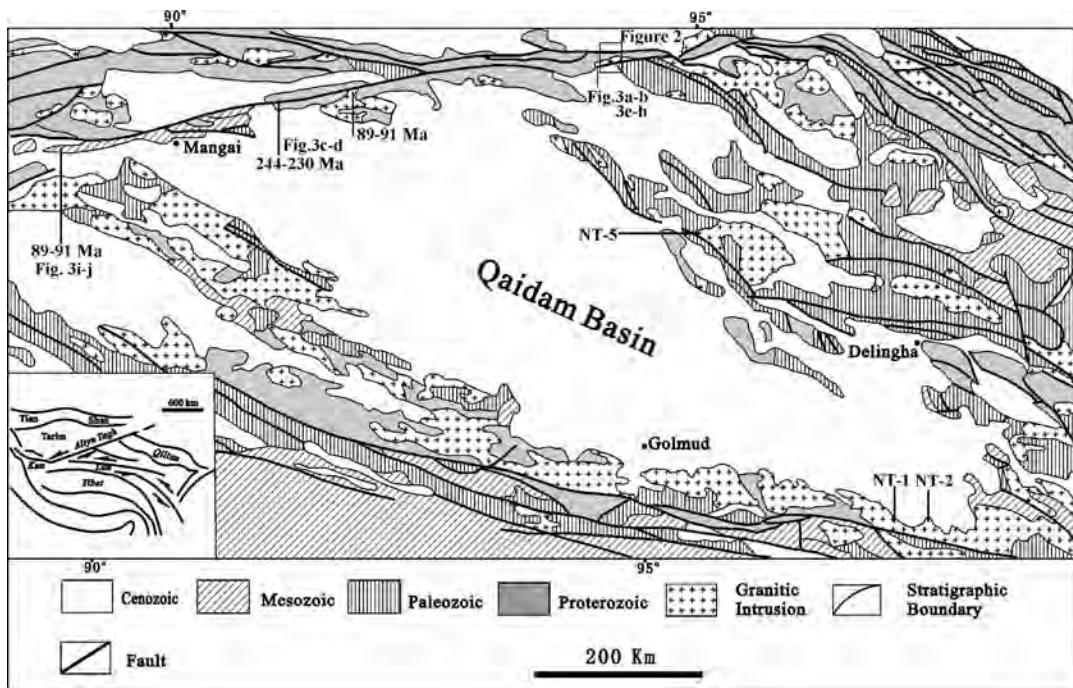
FIGURE 1. Regional geologic map of the Altyn Tagh fault system and its adjacent areas. In the figure, some sampled sites are shown (Simplified from Chen, 1990)
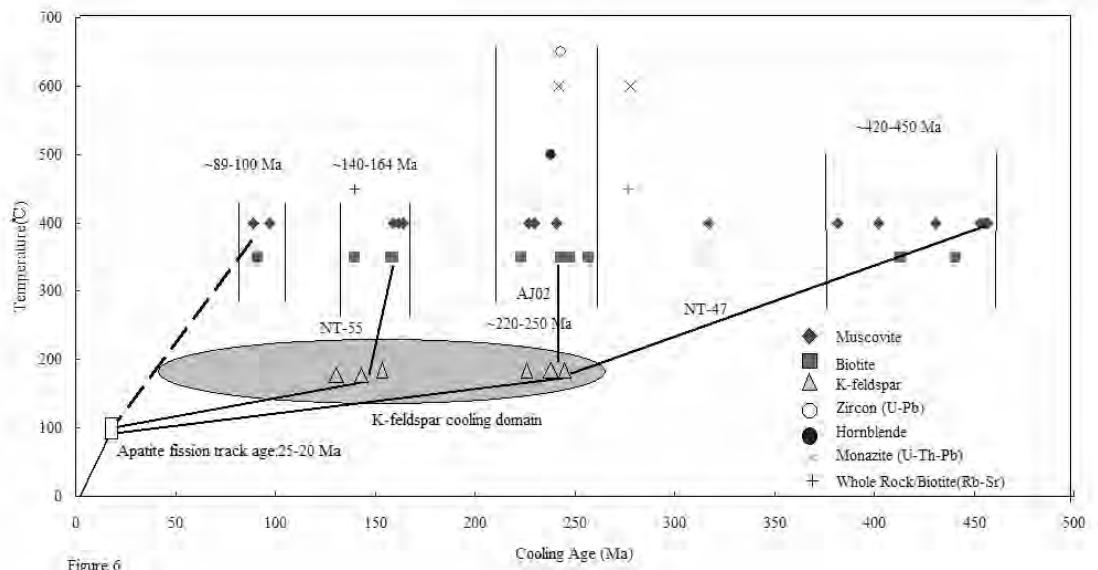
Figure 6

FIGURE 2. Analytical data and cooling diagram of age data from published and this time analysis. (Data compiled from various sources)

Geochemical characteristics and geological significance of the adakites from west Tibet

Cai Zhiyong‡ *, Qiu Ruizhao§ and Xiong Xiaoling‡

† *Guangzhou Institute of Geochemistry, Chinese Academy of Sciences, Guangzhou 510640, CHINA*
‡ *Northwestern Hubei Survey of Geology and Mineral Resources, Xiangfan, 441003, CHINA*
§ *Institute of Geology, Chinese Academy of Geological Sciences, Beijing 100037, CHINA*

* To whom correspondence should be addressed. E-mail: zhiyongcai@vip.sina.com

The occurrences of adakite or adakite-like rocks in the eastern part of the Qinghai-Tibetan region are well known (Qu et al. 2002, Hou et al. 2003). Here, we report the first occurrence of such rocks from the western part. The geochemical characteristics of adakite distributed in the west Tibet (between 88° longitudes and the western borders of China) and of less than 25 Ma in age are presented in this paper. The geological significance of the adakites is also discussed by comparing with the adakite-like rocks exposed in the east.

Samples for geochemical study were taken from 3 sites from the southern, middle and northern Gangdese plutons where the trends are generally NNE. These samples, which belong to the series of continental alkaline magmatism, have the following characteristics: relatively high SiO_2 (56.00~71.51%) and Al_2O_3 (13.04~16.85 %) and Na_2O (Na_2O/K_2O=1.2 to 2.4); high $Mg^\#$ ratios (57~64) based on petrochemistry; high Sr (420~1068 ppm); low Y (3.32~16.7 ppm). They show a REE pattern rich in light REE and abnormality in Eu (weak) and Sr (positive) compared to the standardized pattern. These geochemical characteristics are typical of adakite according to Defant and Drummond (1990) (**Figure 1**).

Considering the isotopic age of the samples as less than 25 Ma and a crustal thickness of the Tibetan crust reached to 60 km at that time based on petrologic evidence (Qiu 2002), it is suggested that the subducted oceanic crust slab was not involved in producing adakite magmas, which formed these rocks. So they probably belong to C-type adakite (Zhang et al. 2001), which were derived from the partial melting of the lower thickened crust.

Most of the plutons, which host the adakites, show with NNE trends. The direction of shortening of the crust is SN whereas the extension occurred along an EW direction. Hence, the adakites from west Tibet are probably genetically related to the development of a rift along SN direction.

It is well known that Cu deposits are closely related to adakite in China as well as abroad. Also reported are the occurrences of many copper deposits in and around the cotemporaneous adakite or adakite-like rocks in eastern part of the Qinghai-Tibetan Plateau (Qu et al. 2002, Hou et al. 2003). Therefore, the discovery of the Cenozoic adakite implies to the brilliant prospect for new copper deposits in the western part of Qinghai-Tibetan Plateau.
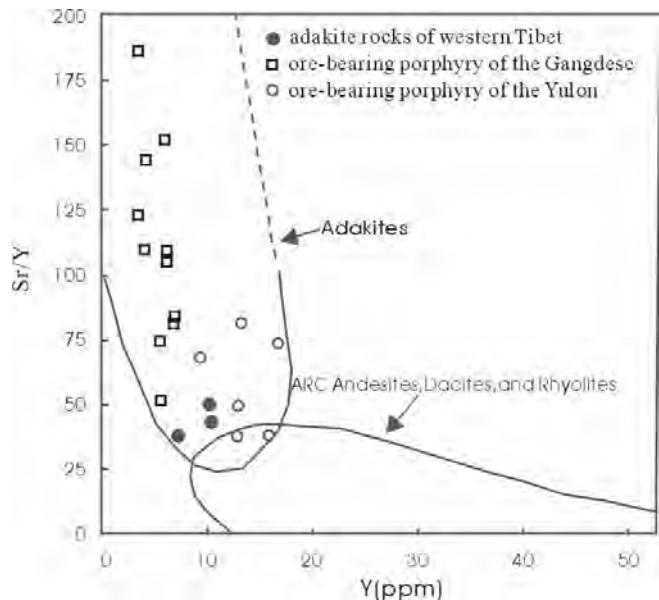
FIGURE 1. Y vs Sr/Y plot for adakite like rocks from the Tibetan plateau

References

Defant MJ and Drummond, MS. 1990. Derivation of some modern arc magmas by melting of young subduction lithosphere. *Nature* **347**: 662~665

Hou ZQ, Mo XX, and Gao YF. 2003. Adakite, a possible host rock for porphyry copper deposits: case studies of porphyry copper belts in Tibetan Plateau and in Northern Chile. *Mineral Deposits*, **1**(22): 1-12

Qiu Ruizhao. 2002. *Igneous rocks and tectonic evolution of the Neo-tethyan in the western Tibetan Plateau* [dissertation]. Beijing: China University of Geosciences: 100 p

Qu XM, Hou ZQ, and Li YG. 2002. Implications of S and Pb isotopic compositions of the Gangdise porphyry copper. *Geological bulletin of china* **21**(11): 768-776

Zhang Q, Wang Y, Qian Q, Yang JH, Wang YL, Zhao TP, Guo GJ. 2001. The chataceristics and tectonic-metallogenic significances of the Mesozoic adakitic rocks in eastern China. *Acta Petrologica Sinica* **17**: 236-244

Temporal-spatial distribution and implications of peraluminous granites in Tibet

Liao Zhongli†*, Mo Xuanxue‡, Pan Guitang†, Zhu Dicheng†, Wang Liquan†, Jiang Xinsheng† and Zhao Zhidan‡

† Chengdu Institute of Geology and Mineral Resources, Chengdu, Sichuan, 610082, CHINA
‡ China University of Geosciences, Beijing,100083, CHINA

* To whom correspondence should be addressed. E-mail: liaozl@cugb.edu.cn

There are many outcrops of peraluminous granites in Qinghai-Tibet plateau. It is an important format of stronger magmatic activity. The Himalayan and Gandise belts are the famous for research bases of peraluminous granites. In the Himalayan belt, muscovite granite provide petrological evidence that India subducted northward below the Tibetan Continent (Deng Jinfu et al. 1994). Based on summary of past research data, the goal of present paper is to study temporal-spatial distribution and basic character of peraluminous granites in Tibet, and to discuss the implication of peraluminous granites to Eurasia–India collision and the uplift of Tibetan Plateau.

The Temporal-Spatial Distributions of peraluminous granites in Tibet
The peraluminous granites in Tibet, which are approximately distributed E-W, belong to Gandise-Nyainqentanglha and Himalayan tectono-magmatic provinces. There are 58 major peraluminous granitic bodies in southern Tibet, which cover an area of about 3800 km^2 and distributed in seven belts (**Figure 1**): Baingoin-Baxoila Ling Belt, Coqen-Xainza belt, south Gandise belt, Yarlung Zangpo suture, Lhagoi Kangri belt, northern Himalayas belt and high Himalayas belt. Most of the granites occur to the south of Bangong Co-Gerze-Amdo-Nu Jiang suture and tectonically in the Gandise-Himalayas tectonic region. The intrusive bodies greatly vary in scale ranging from the minimum of less than 1 km^2 to the maximum of 1780 km^2. W-E oriented Kula Kargari granite is the biggest pluton in the studied region.

The periods of peraluminous granites
The authors analyzed 704 vended chronological data on granite during past two decades (Zhang 1981, Sorkhabi and Stump 1993) and discoverd that the magmatic activity became gradually stronger and reached peak in Miocene. The authors also revealed that the magmatic activity of peraluminous granites have similar trend (**Figure 2**).

182 chronological data of peraluminous granites (Sorkhabi and Stump 1993, Tong Jingsong, 2003) show differences in different belts, mainly in 10-20 Ma (**Figure 2**). The magmatic activities of the peraluminous granites began in the Early Jurassic and gradually reached a peak in the Miocene. The isotopic ages vary in different granite belt but are concentrated in the period between 10-20 Ma.

The granites in northern Himalayas were formed in Miocene during the late period of Himalayan orogeny. The granites in the three belts north of Yarlung Zangpo suture were formed in the Jurassic, Cretaceous, and Eocene-Miocene, respectively with different activity peak of 90-140 Ma (i.e., the Cretaceous period) in addition to the Miocene peak. Zircon U-Pb isotopic dating of two samples by SHRIMP shows that the Luoza granite formed in early Cretaceous with an age of 116±43 Ma. The upper intercepton of zircon U-Pb concordia is 2475±13 Ma, showing old basement in Gandise belt.
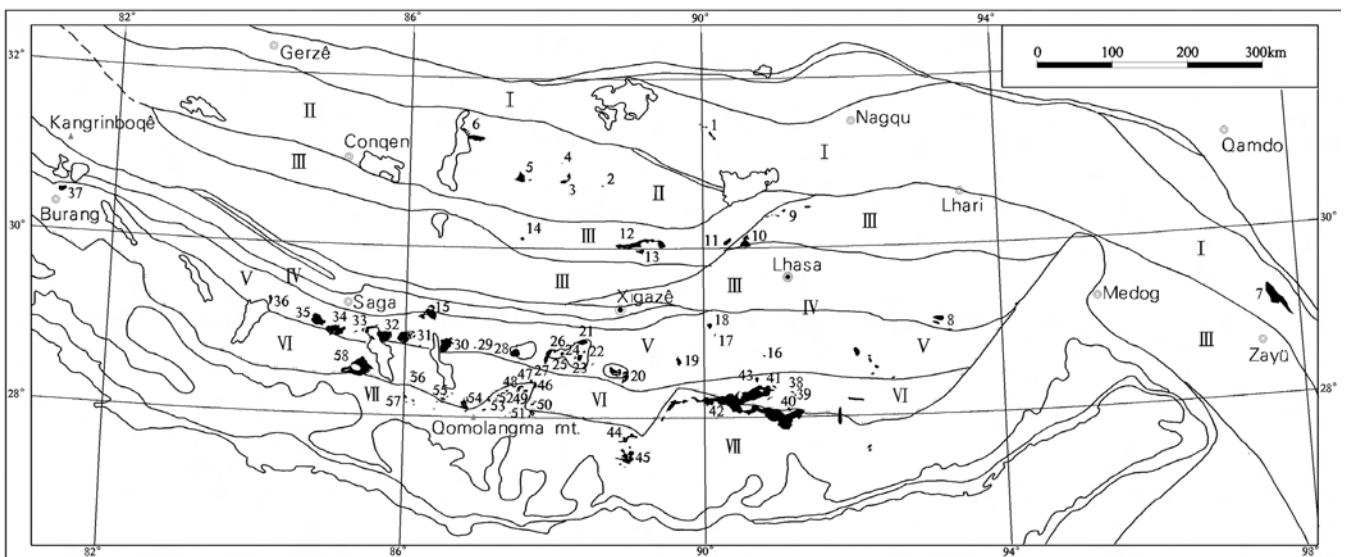
FIGURE 1. The distributions of peraluminous granites in Tibet
I- Baingoin-Baxoila Ling belt II- Coqen-Xainza belt III- South Gandise belt IV- Yarlung Zangpo suture V- Lhagoi Kangri belt VI- northern Himalayan belt VII- High Himalayan belt; 1~58 - rock number
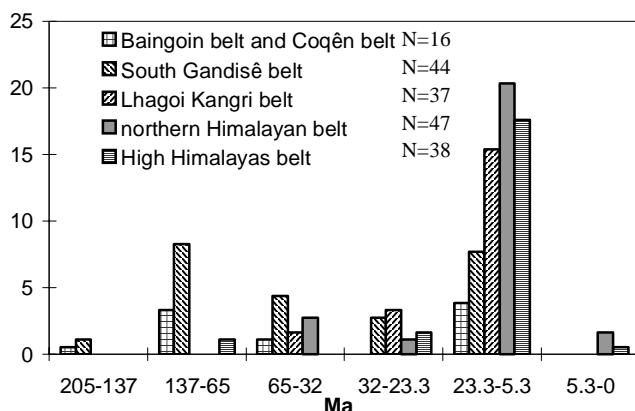
FIGURE 2. Histogram of isotope ages peraluminous granites from Tibet

FIGURE 3. Histogram of age-area for peraluminous granites from Tibet

Scale of magmatic activity

There are obvious differences in different period of magmatic activity scale. In these cases, magmatic activity was mainly concentrated in Miocene (<23.3 Ma) and in Eocene (56.5-32 Ma). The area of Miocene peraluminous granites covers 77.29% of total area of peraluminous granites from Tibet (**Figure 3**).

Implications

In Tibet, study of peraluminous granites was affluent in research contents about Eurasia-India collision and the uplift of Tibetan Plateau. And it provides petrological evidence that India subducted beneath the Tibetan continent.

Despite the fact that the study become serious about the present lithospheric structure and facts were constantly discovered, some basic characteristics are to be accepted by everyone (Mo et al. 1995): (1) generally, the earth's crust of Qinghai-Tibet plateau is very deep (in average of about 70 km), and the lithosphere was comparatively thin (in average of about 150 km); (2) obvious differences in the lithosphere structure exist in Qinghai-Tibet plateau everywhere (inhomogeneity); and (3) it shows low velocity layer inside crust southward from Nyainqentanglha, north Tibet ubiquity crust and mantle mix belt. The present lithosphere structure of Qinghai-Tibet plateau is the final result of integrated geological, geophysical, geochemical processes. Based on this case, we can discuss the magmatic event of Tibet peraluminous granites which will contribute to the form and evolution of Qinghai-Tibet plateau.

Since 200 Ma, the activity of peraluminous granites become gradually stronger, and is mainly concentrated in 3 peaks: 137-96 Ma, 65-32 Ma and 20-10 Ma. It is comparable to 3 peaks of volcanic activities: 115-75 Ma, 60-50 Ma and <20 Ma. The first and the second tectonic-magmatic events are concentrated in Gandise belt, and form a volcano-granitic basement of more than 2000 km length and 300000 km^2 area. Gandise belt was the center of magmatic activity and hot center of Qinghai-Tibet plateau in this period. The third tectonic-magmatic event brings on peraluminous granites because of inner crust movement and regulate in Himalaya. The three magmatic events correspond to three tectonic events: subduction of Neotethyan ocean, India-Eurasia collsion and intracontinental subduction and plateau uplift.
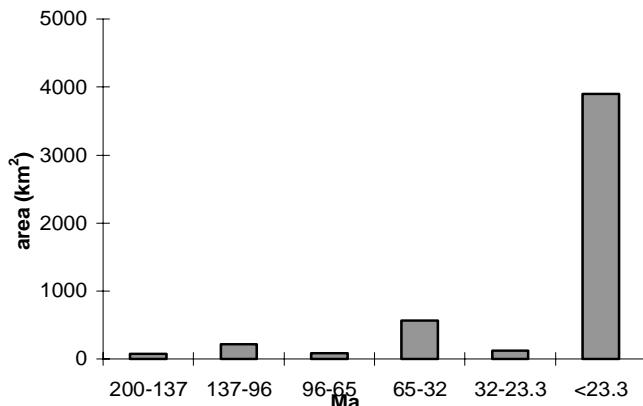
The characteristics of lithosphere tectonic evolution can be reflected by the petrological and geochemical feature of the south Tibetan peraluminous granite as follows: the peraluminous granite in Late Triassic and Early Jurassic (208-157 Ma) may be the result of the early subduction event of the Bangong co - Nujiang Ocean; the granite in the Late Jurassic-Early Cretaceous(157-97 Ma) represents the subduction and collisional event of the Bangong co-Nujiang Ocean; the granite in Late Cretaceous(97-65 Ma) represents the initial subduction and collision of Yarlung Zangpo Ocean; the granite in Eocene(65-40 Ma) represents the main collision stage, when the Yarlung Zangpo belt was still under the stage of subduction-collision, forming a serial of crust source granite. Oligocene and Miocene indicate violent intracontinental subduction stage and form a series of thrust slipend ductile shear zones. Since Miocene, the quick thinning of plateau lithosphere and delamination occurred followed by thickening of the lithosphere and the crust.

References

Deng J, Zhao H, Lai S et al. 1994. Generation of muscovite/two-mica granite and intracontinental subduction. *Earth Science – Journal of China University of Geosciences* **19**(2): 139-147 (in Chinese with English abstract)

Mo X, Zhao C, Guo T et al. 1995. Some problems study for tectonic evolution and magmatic hot event in Qinghai-Tibet plateau. Unpublished internal report (in Chinese)

Zhang Y, Dai T and Hong A. 1981. Isotopic geochronology of granitoid rocks in southern Tibet plateau. *Geochimica* **1981** (1) : 8-18 (in Chinese with English abstract)

Sorkhabi RB and E Stump. 1993. Rise of the Himalaya: A Geochronologic Approach. *GSA Today* **3**(4): 87-92

Tong J, Zhong H, Xia J et al. 2003. Geochemical features and tectonic setting of peraluminous granite in the Lhozagarea. southern Tibet. *Geological bulletin of China* **22**(5): 308-318 (in Chinese with English abstract)

Geochronology on Cenozoic volcanic rocks of a profile Linzhou Basin, Tibet, China and their geological implications

Su Zhou‡ *, Xuanxue Mo‡, Guochen Dong‡, Zhidan Zhao‡, Ruizhao Qiu§, Tieying Guo‡ and Liangliang Wang‡

† Key Laboratory of Lithospheric Tectonics Deep-level process and Exploration Ministry of Education, PR CHINA
‡ China University of Geosciences (Beijing), 100083, PR CHINA
§ Institute of Geology, Chinese Academy of Geological Sciences, Beijing, 100037, PR CHINA

* To whom correspondence should be addressed. E-mail: zhousu@cugb.edu.cn

Linzizong volcanic rocks are widely distributed in the Gangdese-Nyainqentanglha tectono-magmatic belt of Tibet. They contain plenty of information on the closure of the Neotethyan Ocean and the subsequent intracontinental collision. Much research on stratigraphic sequences and geochronology has been conducted, and has helped in understanding the volcanic series of Linzizong and southern Tibet. It has also provided a sound foundation for the present study. Thus far, the formation ages of Linzizong volcanic rocks and other rock units in them are still controversial. While some results indicated that they formed in Late Cretaceous (Liu 1993; Bureau of Geology and Mineral Resources of Xizang Autonomous Region 1993), others suggested that they formed in Paleo-Eocene. Moreover, although numerous radiochronological results have been published (Wang et al. 1990), these results were not associated with in-situ stratigraphical study. Therefore, it is difficult to correlate geochronological data with stratigraphical units and, consequently, a complete geochronology framework of this region is yet to be established.

Linzhou volcanic-sedimentary basin is the main site of Linzizong volcanic rocks with good exposure of interlayered volcanic- sedimentary sections and a clear unconformity with the underlying rock units. Most previous work on Mesozoic and Cenozoic volcanic rocks along the Gangdese-Nyainqentanglha belt has been cross-referenced with Linzhou Basin. Hence, Linzhou volcanic-sedimentary basin is critical for establishing the geochronology framework of Linzizong volcanic rocks and other volcanic rocks along the Gangdese-Nyainqentanglha belt. Detailed petrological and geochemical studies suggested that the characteristics of magmas, types of tectono-magmatism, as well as the geodynamic environments of Linzizong volcanic rocks have changed through time. The Dianzhong Formation in the lower part mainly consists of medium potassium calc-alkaline and metaluminous volcanic rocks, whereas the Nianbo and Pana Formations in the middle and upper parts mainly consist of K-rich calc-alkaline to shoshonitic rocks, indicating the process of gradual crustal thickening. Trace and rare earth element geochemistry shows dual characters of continental margin-and intra-continental volcanic rocks. From the lower part to the upper part, the arc signature became weaker, and the intra-continental signature became more prominent. The Pana Formation at the latest stage was indistinguishable from the typical post-collision volcanic rocks of Tibetan plateau. Nd-Sr-Pb isotopes of these late stage rocks indicate isotopic mixing between the subducted oceanic crust and oceanic lithospheric mantle and between the continental crust and sub-continental lithospheric mantle. That is, there may be interaction between mantle and crust as well as between oceanic and continental mantle indicating transitional geodynamic settings from subduction regime of Neo-Tethyan ocean to that of continental collision. Thus Linzizong volcanic rocks may record the termination of subduction, the onset and the end of collision, and the initiation of the post-collisional

stage,which is coupled with the collision between the Indian and Asian continents.

The purpose of this work is to clarify the geochronological framework of the Linzizong volcanic rocks and to integrate the geochronological data with stratigraphical studies in order to shed light on the tectono-magmatism related to the major collision event between the Indian- Asian continents. We carried out systematic $^{40}Ar/^{39}Ar$ geochronlogical dating of the volcanic rocks from all three formations in Linzizong series and the dyke rocks intruded in them. In order to define the precise time for the end of the regional angular unconformity, samples from Maqu profile are also collected and dated.

Linzhou volcanic basin is in the eastern part of Gangdese in Tibetan Plateau, about 60 km northeast of Lhasa. The basin is of an irregular elliptical form trending approximately E-W, and covers an area of about 230 km². Within the basin the Linzizong volcanic series occurs annularly with their strata flatly dipping northwards, generally between 20° and 25°. The volcanic sequences consist of Dianzhong, Nianbo and Pana Formations upwards in the column. Dianzhong Formation is primarily distributed in the south of the basin and consists of andesite, dacites, trachy-andesite flows and pyroclastic rocks. The rhyolitic pyroclastic rocks in the lower part (southwest part of the region) is about 800-meter thick, constituting several rhythmic eruption cycles. Pebbles of the basal conglomerate of various thicknesses are likely from the underlying Shexing Formation. The Nianbo Formation is zonally distributed in the central part of the basin, and is comprised of thin-bedded limestone and rhyolitic tuff. The thickness of Nianbo and Shexing Formations covaries inversely eastwards. Thin limestone layers are thickened eastward from Xiagunba, whereas the number of rhyolitic tuff layers and layer thickness increase westwards. In the eastern part of the basin, there are abundant andesite, shoshonite and relevant pyroclastic rock assemblages in the upper part of Nianbo Formation with uabergine pelite at the summit. The Pana Formation mainly cropped out in the north part of the basin and is in elliptic shape in the center, consisting of a set of thick acidic ignimbrite layers. In the upper part volcanic rocks are interbeded with fluvial and lacustrine sediments. The Pana Formation was truncated by Ranmojiang Fault in the north. The contact relationship between the formations in the Linzizong series ranges from parallel unconformity to slightly angular unconformity.

On the basis of detailed geological investigation, especially the study of stratigraphical sequences, seven volcanic rock samples were collected from the series from the bottom to near the top. In addition, a sample was collected from a dyke intruding into the Linzizong volcanic rocks in the western part of the basin.

Samples were wrapped in Cd shielding to absorb slow neutrons and then irradiated in the 49-2 Fast Neutron Nuclear Reactor at Institute of Nuclear Energy of China with an irradiation standard ZBH-25 (t = 133.2 Ma) for 8 hours and received a total

of 1.86×10^{17} fast neutrons per cm^2. Incremental step-heating analysis was performed at Micromass 5400 static vacuum mass spectrometer in the Geochronology Laboratory at China University of Geoscience (Beijing). Heating of a sample to release argon was achieved using a resistance furnace. The released gas was purified using Titanium sponge furnace at 800 °C, and let into the extraction line where it was continuously purified using the Ti-furnace (which can be switched off to let it cool) and two Sorb-AC getters (one operated at 400 °C and the other at room temperature) to remove active gases for another 20 min. The purified gas was let into the mass spectrometer and measured in turn on the trap with a current of 200 µA and an accelerating voltage of 4.5 kV. Measured mass peak intensities were corrected for mass discrimination, radioactive decays of ^{37}Ar, and interfering isotopes from neutron reactions on K and Ca using the formulas in McDougall and Harrison (1999). The correction factors were, $^{36}Ar/^{37}Ar(Ca)=0.0002398$, $^{39}Ar/^{37}Ar(Ca)=0.0008$, $^{40}Ar/^{39}Ar(K)=0.004782$. The ^{40}Ar blank was $2\text{-}5 \times 10^{-10} cm^3 STP$ at 1500 °C. Determination of the background and careful checking of the peak position were routinely performed. Correction for mass discrimination was based on multiple measurements of atmosphere. The apparent age for each gas extraction was calculated using the decay constant of 5.543×10^{-10} yr^{-1} and assuming an initial $^{40}Ar/^{39}Ar$ value of 295.5. A 2% uncertainty was assigned to the apparent age, reflecting the propagated error in all correction factors and the J parameter Classical age spectra were plotted against the cumulative ^{39}Ar fraction and isochron ages were calculated using the ISOPLOT program provided by Dr K. Ludwig of the Berkeley Geochronology Center, USA.

From one sample from Nianbo Formation, and four samples each from Dianzhong and Pana Formations, a simple age sequence for Linzizong volcanic activities can be summarized as follows: Dianzhong Formation formed at 64.43 Ma to ca.60 Ma, Pana Formation at 48.73 Ma to 43.93 Ma, with Nianbo Formation in between the two formations. The age of 54 Ma for sample N-9 in Nianbo Formation agrees with the evidence of Paleocene-Eocene fossils of *Amnicola sp., Bythinia sp.,* Ostracods: *Homocucypris cyprinortus(Heterocypris), Syclocypris sp., Cyprisotus., Cyprois sp., Sinocypris sp.* in the Formation . The age spectrum of the K-feldspar separate from rhyolitic dyke in Pana Formation is 51.6±2.6 Ma.

All of these show that (i) the age and duration of Linzizong volcanics are well constrined to be between 40-65 Ma, and (ii) the establishment of a geochronology framework on the Linzizong volcanic rocks at Linzhou basin would serve as a reference for understanding regional volcanic rocks.

Linzizong volcanic activities are synchronous with the dominant phase of the Gangdese pluton (65-40 Ma). One explanation is that both were due to the magmatic response to the Indo-Asian collision. There are great differences in sedimentary facies, tectonic deformation and structural styles across the unconformity. The Linzizong volcanic series are characterized by continental sedimentary facies with steady flat-lying strata, the Shexing Formation is characterized by marine facies and complicated folding structures, reflecting the super-position of multiple tectonic activities. All these features are indicative of a major geotectonic event for this unconformity. The lowermost time limit of Linzizong volcanic rocks roughly coincides with the beginning of the collision between Indian and Asian continents at ~K/T boundary (~65 Ma) as argued from stratigraphy, paleontology as well as paleomagnetism studies (Ding 2003). Therefore, we argue that Linzizong volcanic activities are initiated by the collision.

References

Liu HF. 1993. Division of Linzizong vo1canic series and its geochronology in Lhasa area. *Xizang Geology* **2**:59-69

Bureau of Geology and Mineral Resources of Xizang Autonomous Region. 1993. *People's Republic of China Ministry of Geology and mineral resources geological memoirs— Regional Geology of Xizang (Tibet)*. Beijing: Geological Publishing House. P 237-463

Wang S. 1990. Volcanic rocks in central-southern Xizang. In: Liu GH et al. (eds), *Geological Memoirs,Series 3. No.11 Tectonic Evolution of the lithosphere of the Himalayas. Metamorphics and igneous rocks in Xizang(Tibet)*, Beijing: Geological Publishing House. p 199-239

McDougall I and TM Harrison. 1999. *Geochronology and thermochronology by the $^{40}Ar/^{39}Ar$ method*. New York Oxford: Oxford University Press, p 16-93

Ding L. 2003. Paleocene deep-water sediments and radiolarian faunas: Implications for evolution of Yarlung-Zangbo foreland basin, southern Tibet. *Science in China Series D***46**(1): 84-96

Author Index

Volume 2, Issue 4

NOTE: The author with a figure in boldface type is the principal author in the indicated page.